Instytut Farmakologii
im. Jerzego Maja
Polskiej Akademii Nauk

mgr inż. Anna Solarz-Andrzejewska

The role of the blood-brain barrier, inflammation and endoplasmic reticulum stress in the mechanisms of susceptibility and resilience to early-life stress

Rola bariery-krew mózg, procesów zapalnych i stresu siateczki śródplazmatycznej w mechanizmach podatności bądź oporności na stres we wczesnym okresie życia

Praca doktorska wykonana w Zakładzie Farmakologii,
w Pracowni Farmakologii i Biostruktury Mózgu
Instytutu Farmakologii im. Jerzego Maja Polskiej Akademii Nauk

Promotor:

Dr hab. Agnieszka Chocyk

Kraków, 2023

Badania opisane w niniejszej pracy doktorskiej zostały zrealizowane w ramach funduszy pochodzących z:

1. projektu badawczego Preludium 12 finansowanego przez Narodowe Centrum Nauki (2016/23/N/NZ4/01148) pt. „Wpływ stresu we wczesnym okresie życia na dojrzewanie i przepuszczalność bariery krew-mózg oraz aktywację procesów neurozapalnych w rozwoju ontogenetycznym" kierowanego przez mgr. inż Annę Solarz-Andrzejewską

2. projektu badawczego Opus 13 finansowanego przez Narodowe Centrum Nauki (2017/25/B/NZ7/00174) pt. „Rola stresu retikulum endoplazmatycznego w patomechanizmach dysfunkcji kory przedczołowej wywołanej stresem we wczesnym okresie życia oraz w mechanizmach działania fluoksetyny u dzieci i młodzieży" kierowanego przez dr hab. Agnieszkę Chocyk

3. działalności statutowej Pracowni Farmakologii i Biostruktury Mózgu

Chciałam podziękować wszystkim osobom, które przyczyniły się do powstania niniejszej rozprawy doktorskiej:

Dr hab. Agnieszce Chocyk
za bycie mentorem, dzieleniem się swoimi umiejętnościami, wiedzą i doświadczeniem, a także cierpliwość, życzliwość, zrozumienie oraz czas poświęcony nie tylko przy tworzeniu tej rozprawy, ale też w codziennej pracy

Ś.p. prof. dr hab. Krzysztofowi Wędzonemu i Prof. dr hab. Marzenie Maćkowiak
za możliwość realizowania badań w Pracowni Farmakologii i Biostruktury Mózgu

Iwonce Majcher-Maślanka oraz Asi Kryst
za przyjaźń, wsparcie, zaangażowanie i nieocenioną pomoc

Życzliwym mi osobom, w szczególności Przemkowi Dankowi oraz koleżankom i kolegom z Zespołu PFiBM za wszelką pomoc, wsparcie i przyjazną atmosferę

Bartkowi, Rodzicom, Rodzeństwu i Przyjaciołom za to, że zawsze jesteście przy mnie

Pracę doktorską dedykuję Mojej Mamie

Spis treści

1. Spis artykułów naukowych stanowiących podstawę rozprawy doktorskiej

1. **Solarz, A.**, Majcher-Maslanka, I., Chocyk, A. (2021a) Effects of early-life stress and sex on blood-brain barrier permeability and integrity in juvenile and adult rats. *Developmental Neurobiology*, 81, 861-876.

   IF= 3.1, MNiSW= 100

2. **Solarz, A.**, Majcher-Maślanka, I., Kryst, J., Chocyk, A. (2023) Early-life stress affects peripheral, blood-brain barrier, and brain responses to immune challenge in juvenile and adult rats. *Brain, behavior, and immunity*, 108, 1-15.

   IF= 15.1, MNiSW= 140

3. **Solarz, A.**, Majcher-Maslanka, I., Kryst, J., Chocyk, A. (2021b) A search for biomarkers of early-life stress-related psychopathology: focus on 70-kDa heat shock proteins. *Neuroscience*, 463, 238-253.

   IF= 3.7, MNiSW= 140

4. **Solarz-Andrzejewska, A.**, Majcher-Maślanka, I., Kryst, J., Chocyk, A. (2023) Modulation of the endoplasmic reticulum stress and unfolded protein response mitigates the behavioral effects of early-life stress. *Pharmacological reports*, 75, 293-319.

   IF= 4.4, MNiSW= 140

2. Spis najważniejszych skrótów

AD – choroba Alzheimera (ang. *Alzheimer's disease*)

AFR – warunki standardowe hodowli (grupa kontrolna) (ang. *animal facility rearing*)

AIF1 – allogeniczny czynnik zapalny 1 (ang. *allograft inflammatory factor 1*)

ANOVA – analiza wariancji (*ang. analysis of variance*)

AQP – akwaporyny (ang. *aquaporins*)

ATF6 – aktywujący czynnik transkrypcyjny 6 (ang. *activating transcription factor* 6)

BBB – bariera krew-mózg (ang. *blood-brain barrier*)

BCL2 – (ang. *B-cell CLL/Lymphoma 2*)

BEC – komórki śródbłonka naczyń krwionośnych mózgu (ang. *brain endothelial cells*)

CG1 – kora obręczy 1

CHOP – białko homologiczne C/EBP (ang. *C/EBP homologous protein*)

CLDN – klaudyny (ang. *claudins*)

DAB – 3,3'-diaminobenzydyna

DAMP - wzorce molekularne związane z uszkodzeniem (ang. *damage-associated molecular patterns*)

DMSO – dimetylosulfotlenek

dSTR – grzbietowe prążkowie (ang. *dorsal striatum*)

EBA – antygen (marker) bariery krew-mózg (ang. *endothelial barrier antigen*)

eIF2α – eukariotyczny czynnik inicjacji translacji 2α (ang. *eukaryotic translation initiation factor 2α*)

ELS – stres we wczesnym okresie życia (ang. *early-life stress*)

ER – siateczka śródplazmatyczna, retikulum endoplazmatyczne

ERAD – degradacja związana z ER (ang. *ER-associated degradation*)

GC – glikokortykoidy (ang. *glucocorticoids*)

GLUT-1 – transporter glukozy typu 1

GR – receptory glikortykoidowe (ang. *glucocorticoid receptor*)

GRP78 – białko regulowane glukozą 78 kDA (ang. *glucose-regulated protein 78*)

HP – hipokamp

HPA – oś podwzgórze-przysadka-nadnercza (ang. *hypothalamic-pituitary-adrenal*)

HSP – białka szoku cieplnego (ang. *heat shock proteins*)

HSP70 – HSP o masie 70 kDa

ICAM1 – cząsteczka adhezji międzykomórkowej - 1 (ang. *intercellular adhesion molecule 1*)

IHC – immunohistochemia

IL – interleukiny

ILC – kora infralimbiczna

IRE1α – enzym 1α zależny od inozytolu (ang. *inositol-requiring enzyme 1 α*)

ITGAM – integryna α M (ang. *integrin subunit α M*)

LPS – lipopolisacharyd

LTP – długotrwałe wzmocnienie synaptyczne (ang. *long-term potentiation*)

mPFC – przyśrodkowa kora przedczołowa (ang. *medial prefrontal cortex*)

MR – receptor mineralokortykoidowy (ang. *mineralocorticoid receptor*)

MS – separacja potomstwa od matki (ang. *maternal separation*)

NaF – sól sodowa fluoresceiny

OCLN – okludyny (ang. *ocludins*)

OUN – ośrodkowy układ nerwowy

PAMP – wzorce molekularne związane z patogenami (ang. *pathogen-associated molecular patterns*)

PD – choroba Parkinsona (ang. *Parkinson's disease*)

PERK – kinaza ER (ang. *protein kinase R-like ER kinase*)

PGP – glikoproteina P (ang. *P-glycoprotein*)

PLC – kora przedlimbiczna

PND – dzień po narodzinach (ang. *postnatal day*)

SAL – salubrinal

SD – odchylenie standardowe

TJP – białka złącz ścisłych

TJ – złącza ścisłe (ang. *tight junctions*)

TLR – receptory toll-podobne (ang. *toll-like receptors*)

TNFα – czynnik martwicy nowotworów α (ang. *tumor necrosis factor α*)

UPR – odpowiedź na nieprawidłowo zwinięte białka (ang. *unfolded protein response*)

VEH – rozpuszczalnik (ang. *vehicle*)

XBP1 – czynnik transkrypcyjny XBP1 (ang. *X-box binding protein-1*)

3. Streszczenie w języku polskim

Dane klinicznie wskazują, że stres we wczesnym okresie życia (ELS) może zwiększać ryzyko wystąpienia problemów ze zdrowiem fizycznym i psychicznym w późniejszym życiu. Wśród powyższych problemów zdrowotnych wyróżnia się szczególnie depresję, zaburzenia lękowe i poznawcze oraz zespół metaboliczny. Wspólnym mianownikiem w etiologii i progresji tych chorób mogą być zaburzenia procesów zapalnych, funkcji bariery krew-mózg (BBB) i proteostazy.

Pomimo rosnącej wiedzy o wpływie ELS na dojrzewanie i funkcjonowanie mózgu, mechanizmy leżące u podstaw podatności bądź oporności na jego działanie w dalszym ciągu nie są dobrze poznane. Niniejsza rozprawa doktorska, bazująca na zwierzęcym modelu ELS, tj. procedurze separacji potomstwa od matki (MS) u szczurów, miała na celu pogłębienie wiedzy w tym zakresie, szczególnie w kontekście udziału BBB, neurozapalenia i stresu komórkowego w biologii ELS.

W pierwszej kolejności badano wpływ MS na dojrzewanie i integralność BBB u szczurów obu płci w różnych okresach rozwoju. Kolejnym aspektem badań było sprawdzenie czy i jak doświadczenie MS determinuje przebieg późniejszej odpowiedzi zapalnej wywołanej jednorazowym podaniem lipopolisacharydu (LPS). W następnej części rozprawy doktorskiej, badano udział stresu komórkowego w mechanizmach podatności lub oporności na ELS. W tym celu analizowano wpływ MS na ekspresję białek szoku cieplnego o masie 70 kDa (HSP70), markerów stresu siateczki śródplazmatycznej (ER) i odpowiedzi na nieprawidłowo zwinięte białka (UPR) w mózgu. Następnym krokiem było zastosowanie wielokrotnych podań inhibitora stresu ER, salubrinalu (SAL), we wczesnym okresie postnatalnym, do oceny zaangażowania tego procesu w powstawanie zaburzeń dojrzewania przyśrodkowej kory przedczołowej (mPFC) oraz kształtowanie zachowań zwierząt poddanych MS.

Przeprowadzone badania wykazały różnice rozwojowe i płciowe w funkcjonowaniu BBB szczura w warunkach podstawowych i w obliczu zapalenia. Zaobserwowano, że BBB uszczelnia się wraz z wiekiem, a jej przepuszczalność i integralność są zależne od płci. Ponadto, w przypadku wielu badanych parametrów związanych z przepuszczalnością BBB i ekspresją kluczowych elementów odpowiedzialnych za utrzymanie jej homeostazy, MS nie wywołała jednoznacznie

negatywnych skutków, a jej wpływ był zależny od wieku, regionu mózgu i płci. Niemniej jednak młode samce wykazywały większą wrażliwość na działanie ELS.

Następnie, badania wykazały, że MS w sposób zależny od płci moduluje przebieg odpowiedzi neurozapalnej wywołanej podaniem LPS. U młodych samców poddanych procedurze MS obserwowano nasilenie tej odpowiedzi, natomiast u samic - brak wpływu MS lub wręcz osłabienie reakcji zapalnej, szczególnie w okresie dorosłości.

W kolejnym etapie badań stwierdzono długotrwałą nadekspresję HSPA1B i HSPA5 we krwi i mózgu, której towarzyszyły zaburzenia plastyczności synaptycznej i zmniejszona lękliwość u dorosłych samców poddanych MS. Na tej podstawie wskazano białka rodziny HSP70 jako potencjalnych kandydatów na biomarkery ELS.

Analiza ekspresji markerów stresu ER, UPR i apoptozy w mPFC nie wykazała silnego wpływu MS na te procesy w badanych okresach rozwoju. Niemniej jednak, modulacja powyższych procesów poprzez podania SAL i/lub jego rozpuszczalnika zapobiegała lub łagodziła niektóre skutki MS na poziomie biochemicznym i behawioralnym.

Uzyskane wyniki wskazują, że regulacja funkcji BBB, procesów zapalnych oraz stresu komórkowego podczas dojrzewania mózgu może odgrywać ważną rolę w mechanizmach podatności lub oporności na działanie ELS. Podkreślają one także potrzebę prowadzenia dalszych badań, rozszerzonych o inne układy narządów, w celu kompleksowego zrozumienia wpływu ELS na zdrowie psychiczne i fizyczne oraz znalezienia uniwersalnych biomarkerów, które ułatwiłyby diagnostykę zaburzeń związanych z ELS.

4. Streszczenie w języku angielskim

Clinical data indicate that early-life stress (ELS) may increase the risk of physical and mental health problems later in life. The above-mentioned health conditions include particularly depression, anxiety disorders, cognitive impairments, as well as, a metabolic syndrome. The common thread in etiology and progression of these disorders can be disturbances in the inflammatory processes, blood-brain barrier (BBB) function and proteostasis.

Despite the expanding knowledge about the impact of ELS on brain maturation and function, the mechanisms underlying the susceptibility or resilience to its effects remain insufficiently understood. The present doctoral dissertation was aimed to broaden the knowledge in this subject, particularly in terms of the engagement of the BBB, neuroinflammation and cellular stress in the biology of ELS, modeled by the maternal separation (MS) paradigm in rats.

First, the effects of MS on the BBB maturation and integrity was studied in both sexes at different developmental stages. The second goal was to examine whether MS determines the subsequent inflammatory response induced by acute lipopolysaccharide (LPS) administration. In the next part of the doctoral dissertation, the involvement of cellular stress in the mechanisms of susceptibility or resilience to ELS was investigated. In this regards, the impact of MS on the expression of 70-kDa heat shock proteins (HSP70), endoplasmic reticulum (ER) stress and unfolded protein response (UPR) markers in the brain were analyzed. Finally, repeated early-life administration of ER stress inhibitor, salubrinal (SAL), was used to assess the involvement of this process in MS-induced dysfunction of the medial prefrontal cortex (mPFC) maturation and rat behavior.

The studies revealed developmental and sex differences in BBB functioning in rats in basal conditions and under an inflammation. Developmental sealing of the BBB was observed and sex differences in BBB permeability and integrity. Additionally, MS did not have a clear negative impact on many of the studied BBB permeability- and homeostasis-related parameters, and observed effects were age-, brain region- and sex-dependent. Nevertheless, juvenile males were more sensitive to ELS.

Next, the research showed that MS in a sex-dependent manner modulated LPS-induced neuroinflammatory response. In juvenile males subjected to MS, this response was enhanced, while in females, not changed by MS or even blunted, especially in adulthood.

The subsequent studies revealed a long lasting overexpression of HSPA1B and HSPA5 in the blood and brain with concomitant impairments in synaptic plasticity and reduced anxiety in adult males subjected to MS. Based on these findings, HSP70 family members were proposed as potential candidates for ELS biomarkers.

Analysis of the expression of ER stress, UPR and apoptosis markers in the mPFC did not show a strong impact of MS at the studied developmental stages. Nevertheless, SAL and/or its vehicle administration prevented or blunted some of the MS effects at biochemical and behavioral levels.

The results indicate that the regulation of BBB function, inflammatory processes and cellular stress responses during brain maturation may play an important role in the mechanisms of susceptibility or resilience to ELS. Moreover, they highlight the need to expand the research to multiorgan approach to better understand the complex effects of ELS on mental and physical health and to find universal biomarkers facilitating diagnostics for ELS-related diseases.

5. Wprowadzenie

5.1 Stres we wczesnym okresie życia – wpływ na zdrowie psychiczne i fizyczne

Współcześnie, stres często postrzegany jest jako zaburzenie homeostazy organizmu, występujące na skutek działania wewnętrznych oraz zewnętrznych czynników, tzw. stresorów, wywołujących wielosystemową odpowiedź (Packard i wsp., 2016). Niemniej jednak stres (reakcja stresowa) to reakcja przystosowawcza (adaptacyjna) służąca przetrwaniu i radzeniu sobie w różnych warunkach środowiska. Aktywowana jest ona dwiema ścieżkami. W odpowiedzi na stresor, najszybciej aktywowana jest ścieżka układu współczulno-nadnerczowego (reakcja: walcz lub uciekaj), prowadząca do uwolnienia adrenaliny i noradrenaliny z rdzenia nadnerczy (Packard i wsp., 2016). Po pewnym czasie może dochodzić także do aktywacji drugiej ścieżki, tj. osi podwzgórze-przysadka-nadnercza (ang. *hypothalamic-pituitary-adrenal*, HPA), skutkującej uwolnieniem kortykoliberyny *(*ang. *corticotropin-releasing hormone*, CRH) z podwzgórza do przysadki. Następnie, CRH stymuluje przysadkę do sekrecji kortykotropiny (ang. *adrenocorticotropic hormone,* ACTH), co w konsekwencji prowadzi do syntezy i uwolnienia glikokortykoidów (ang. *glucocorticoids*, GC) (kortyzolu u ludzi, a kortykosteronu u zwierząt) z kory nadnerczy oraz wzrostu GC w osoczu (Pechtel i Pizzagalli, 2011; Teixeira i wsp., 2020). Na poziomie komórkowym GC wiążą się do receptorów glikortykoidowych (ang. *glucocorticoid receptor*, GR) i mineralokortykoidowych (ang. *mineralocorticoid receptor*, MR) zlokalizowanych w cytoplazmie. Po utworzeniu aktywnego kompleksu receptory przechodzą do jądra komórkowego, gdzie pełnią funkcję czynników transkrypcyjnych regulujących ekspresję genów, stąd nazywane są receptorami jądrowymi. (Pechtel i Pizzagalli, 2011; Joëls i wsp., 2012; Joëls i wsp., 2018). W ten sposób GC mogą wywoływać przejściowe bądź trwałe (epigenetyczne) zmiany w funkcjonowaniu organizmu. Wykazano również zdolność GC do szybkiego, niegenomowego działania poprzez receptory GR i MR zlokalizowane w błonie i aktywujące ścieżki sygnalizacji wewnątrzkomórkowej (Joëls i wsp., 2018).

W warunkach fizjologicznych GC hamują zwrotnie oś HPA, kończąc tym samym odpowiedź na stres (Teixeira i wsp., 2020). Jednak chroniczna ekspozycja na bodźce stresowe może prowadzić do zmian w reaktywności osi HPA, fluktuacji poziomu GC w surowicy i tym samym do negatywnych skutków dla zdrowia. Doświadczenie tego typu stresu we wczesnym okresie życia (ang. *early-life* stress, ELS), w którym dojrzewający

organizm jest wyjątkowo wrażliwy na działanie czynników środowiskowych, może nieść ze sobą szczególnie groźne konsekwencje i wywierać długotrwałe, wielopoziomowe efekty związane z programowaniem epigenetycznym (Smith i Pollak, 2020).

ELS wywiera znaczący wpływ na rozwój mózgu dziecka i stanowi jeden z ważniejszych czynników ryzyka wystąpienia chorób psychicznych i zaburzeń kognitywnych (Barlow i wsp., 2007; Teicher i wsp., 2022). Dostępne dane kliniczne wskazują, że ELS odpowiada za 30% populacyjnego ryzyka wystąpienia zaburzeń lękowych, 45% zaburzeń psychicznych wieku dziecięcego, 54% depresji, 64% uzależnień od narkotyków(Teicher i wsp., 2022). Co więcej, doświadczenie ELS zwiększa również ryzyko wystąpienia przewlekłych problemów ze zdrowiem fizycznym w życiu dorosłym, takich jak choroby układu krążenia, zespół metaboliczny i cukrzyca (Loria i wsp., 2014; Su i wsp., 2015; Murphy i wsp., 2017; Noteboom i wsp., 2021).

Poznanie mechanizmów i konsekwencji ELS w dużej mierze jest możliwe dzięki zwierzęcym modelom ELS. Modelowanie ELS opiera się na wprowadzeniu czynnika stresowego w określonym okresie rozwojowym, stąd wyróżniamy modele stresu w okresie prenatalnym, neonatalnym oraz młodzieńczym (Cirulli i wsp., 2009; Malinovskaya i wsp., 2018) (Pryce i wsp., 2002). Do szczególnie popularnych i szeroko stosowanych modeli ELS i zaburzeń psychicznych człowieka, charakteryzujących się dużą trafnością teoretyczną, należy separacja osesków gryzoni od matki (ang. *maternal separation*, MS). MS jest najczęściej przeprowadzana w dwóch pierwszych tygodniach życia szczurów/myszy, w wielu wariantach od jednorazowej (24-godzinnej) po wielokrotną (1-6 godzin dziennie) (Pryce i wsp., 2002; Cirulli i wsp., 2009; Vetulani, 2013; Italia i wsp., 2020).

Modele zwierzęce dostarczyły już sporej wiedzy o molekularnych epigenetycznych mechanizmach leżących u podstaw ELS (Malinovskaya i wsp., 2018). Co więcej, obserwuje się w nich, podobnie jak w klinice, nasilenie odpowiedzi na podanie substancji psychostymulujących (Kessler i wsp., 2010; Brenhouse i wsp., 2013; Danese i Lewis, 2017), a także wpływ ELS na zachowania lękowe i depresyjne (Chocyk i wsp., 2010; Brenhouse i wsp., 2013; Chocyk i wsp., 2013; Chocyk i wsp., 2015; Danese i Lewis, 2017; Majcher-Maslanka i wsp., 2019). Nasz zespół od wielu lat prowadzi własne badania nad biologią ELS, wykorzystując procedurę wielokrotnej MS (3 godziny dziennie, od 1 do 14 dnia po urodzeniu). Wykazaliśmy, m.in., że MS zaburza neurorozwojową apoptozę w śródmózgowiu i przyśrodkowej korze przedczołowej (ang. *medial prefrontal cortex*, mPFC), a także plastyczność synaptyczną w mPFC (Chocyk i wsp., 2011a; Chocyk i wsp.,

2013; Majcher-Maslanka i wsp., 2019) oraz, że nasila zachowania lękowe u adolescentów i trwale wpływa na procesy pamięci o zdarzeniach awersyjnych (Chocyk i wsp., 2014; Majcher-Maslanka i wsp., 2019). Ponadto inni badacze wykazali, iż ELS nasilał związane z wiekiem zaburzenia funkcji poznawczych (Martisova i wsp., 2013; Loi i wsp., 2017) oraz zaburzenia behawioralne i neurochemiczne w zwierzęcych modelach choroby Alzheimera (AD) i Parkinsona (PD) (Barlow i wsp., 2007; Mabandla i Russell, 2010; Martisova i wsp., 2013; Hoeijmakers i wsp., 2017). Potwierdzono również, że u gryzoni ELS jawi się jako niezależny czynnik ryzyka rozwoju zaburzeń metabolicznych (nietolerancja glukozy, cukrzyca typu drugiego) (Ilchmann-Diounou i wsp., 2019) oraz patologii układu sercowo-naczyniowego (Loria i wsp., 2013; Loria i wsp., 2014; Ho i wsp., 2016).

Chociaż potwierdzono, że doświadczenie ELS może mieć silny wpływ na rozwijający się organizm, to nie u wszystkich jednostek obserwuje się negatywne konsekwencje ELS. Coraz częściej uważa się, że ELS może indukować specyficzne adaptacje fenotypowe (Teicher i wsp., 2020; Teicher i wsp., 2022). Dlatego obecnie intensywnie poszukuje się potencjalnych mechanizmów, determinujących skuteczną kompensację zmian wywołanych przez stres.

Powstały różne hipotezy opisujące zjawiska leżące u podstaw podatności i oporności na stres. Pierwsza z nich to koncepcja skumulowanych efektów stresu (ang. *stress accumulation*), która zakłada, że jeśli gromadzące się w ciągu życia jednostki stresujące zdarzenia przekroczą pewien próg, to wzrasta ryzyko rozwoju choroby u osobników z nieadekwatnymi zdolnościami adaptacyjnymi (McEwen, 1998). Z kolei, hipoteza dopasowania/niedopasowania (ang. *match/mismatch*) zakłada, że ELS wywołuje zmiany adaptacyjne w odpowiedzi na warunki środowiska, mogące przygotować jednostkę do podobnych warunków w późniejszym okresie życia. Jeżeli warunki w życiu późniejszym będą podobne do wczesnożyciowych (ang. *match*), to organizm dysponuje strategiami aktywnego radzenia sobie ze zdarzeniami awersyjnymi, co w rezultacie może prowadzić do oporności na choroby. Natomiast, rozbieżność jakościowa pomiędzy wczesnymi i późniejszymi warunkami życia (ang. *mismatch*), zwiększa szanse na rozwój choroby (podatność) (Andersen i Teicher, 2004; Gluckman i wsp., 2005). Powstała także hipoteza trzech uderzeń (ang. *three-hit concept)*, która w założeniach integruje genetyczne predyspozycje jednostki (pierwszy czynnik) z ekspozycją na czynniki środowiskowe we wczesnym okresie życia (drugi czynnik), co determinuje powstanie określonego fenotypu, który z kolei w odpowiedzi na wyzwania w późniejszym życiu (trzeci czynnik) skutkuje

zwiększoną podatnością bądź opornością na choroby (Nederhof i Schmidt, 2012; Daskalakis i wsp., 2013).

5.2 Komórkowa odpowiedź stresowa: stres siateczki śródplazmatycznej i odpowiedź na niepoprawnie zwinięte białka

W celu zapewnienia sobie przetrwania, organizm ma zdolność do reagowania na zmiany warunków środowiskowych. Reakcje organizmu na bodźce stresowe są regulowane i realizowane również na poziomie komórkowym (komórkowa reakcja stresowa). W toku ewolucji komórki wykształciły mechanizmy adaptacyjne, które przywracają homeostazę i tym samym promują przeżycie (Özbey i wsp., 2021). Stresory aktywują specyficzne dla organelli komórkowe odpowiedzi stresowe, takie jak cytozolowa odpowiedź białek szoku cieplnego (ang. *heat shock proteins,* HSP), stres siateczki śródplazmatycznej (ER) oraz odpowiedź na nieprawidłowo zwinięte białka (ang. *unfolded protein response,* UPR) ER i mitochondrialna, a także zintegrowana odpowiedź na stres (Özbey i wsp., 2021; Diaz-Hung i Hetz, 2022). W wyniku aktywacji tych szlaków generowane są specyficzne sygnały wysyłane do cytozolu i jądra komórkowego, gdzie wpływają na ekspresję genów, a tym samym biosyntezę białek i metabolizm energetyczny (Özbey i wsp., 2021). Procesy komórkowej odpowiedzi na stres są ewolucyjnie konserwatywne i odgrywają ważną rolę w utrzymaniu homeostazy komórkowej, w tym również proteostazy (Özbey i wsp., 2021). Proteostaza to homeostaza białek, która jest możliwa dzięki szeregowi skoordynowanych procesów zachodzących głównie w ER i polegających na syntezie, kontroli jakości i rozmieszczenia białek (Bengesser i wsp., 2016; Muneer i Shamsher Khan, 2019). Utrzymanie proteostazy jest kluczowe dla właściwego funkcjonowania komórki i wspiera jej przeżycie. Stres komórkowy spowodowany np. niedotlenieniem, niedoborem składników odżywczych, hiperglikemią, hiperlipidemią, zaburzeniami równowagi redoks i gospodarki jonów wapnia lub ogólnym wzrostem syntezy białek, może prowadzić do gromadzenia nieprawidłowo zwiniętych białek i zaburzeń proteostazy. Najczęściej aktywowane są wtedy procesy naprawcze, takie jak stres ER oraz UPR (Kitamura, 2013).

Stres ER jest wykrywany przez trzy białka transbłonowe ER, działające jak przekaźniki sygnału: (1) enzym 1α zależny od inozytolu (ang. *inositol-requiring enzyme 1 α,* IRE1α), (2) kinazę ER (ang. *protein kinase R-like ER kinase,* PERK) i (3) aktywujący

czynnik transkrypcyjny 6 (ang. *activating transcription factor* 6, ATF6) (Bengesser i wsp., 2016; Muneer i Shamsher Khan, 2019) (Ryc. 1). W warunkach podstawowych białka te są ujemnie regulowane przez białko regulowane glukozą 78 kDA (ang. *glucose-regulated protein 78*, GRP78) znane też jako białko HSPA5, należy bowiem do rodziny białek opiekuńczych HSP o masie 70 kDa (HSP70). (Bengesser i wsp., 2016; Muneer i Shamsher Khan, 2019). Jednak po nagromadzeniu niezwiniętych lub niepoprawnie zwiniętych białek, GRP78 odłącza się od białek-przekaźników sygnału, umożliwiając aktywację trzech różnych ścieżek UPR. Po pierwsze, aktywacji polegającej na dimeryzacji i autofosforylacji przy treoninie 980 ulega PERK, co z kolei prowadzi do fosforylacji i inaktywacji eukariotycznego czynnika inicjacji translacji 2α (ang. *eukaryotic translation initiation factor 2α,* eIF2α). W rezultacie dochodzi do zahamowania globalnej translacji i ostatecznie do zmniejszenia całkowitej ilości wydzielanych białek w świetle ER (Bengesser i wsp., 2016; Muneer i Shamsher Khan, 2019) (Ryc. 1). Zachowana zostaje jednak translacja specyficznych białek, np. tych związanych z przebiegiem UPR. Kolejny przekaźnik, IREα, na skutek dimeryzacji i autofosforylacji na serynie 724, nabiera aktywności endonukleazy i katalizuje splicing mRNA XBP1 (ang. *X-box binding protein-1*) (Ryc. 1). Powstałe w wyniku tego procesu białko XBP1 jest wysoce aktywnym czynnikiem regulującym ekspresję genów zaangażowanych w UPR (np. kodujących białka opiekuńcze) i degradację związaną z ER (ang. *ER-associated degradation*, ERAD) (Bengesser i wsp., 2016; Muneer i Shamsher Khan, 2019) (Ryc. 1). W rezultacie nasileniu ulegają procesy fałdowania białek bądź degradacji i eliminacji tych nieprawidłowo zwiniętych, co zapobiega ich gromadzeniu i wspomaga przywrócenie proteostazy (Bengesser i wsp., 2016; Muneer i Shamsher Khan, 2019). Trzeci przekaźnik stresu ER, ATF6, ulega translokacji do aparatu Golgiego, gdzie poprzez cięcie ulega aktywacji. Powstałe aktywne cząsteczki ATF6 uwalniane są do cytozolu (Ryc. 1), a następnie przechodzą do jądra, gdzie również pełnią funkcję czynników transkrypcyjnych, regulujących ekspresję genów związanych z przebiegiem UPR (Bengesser i wsp., 2016; Muneer i Shamsher Khan, 2019).

Celem opisanych powyżej procesów jest zwiększanie szans na przeżycie komórki. Jednak w przypadku, gdy stres komórkowy przewyższa możliwości adaptacyjne UPR, inicjowana jest śmierć komórki poprzez proapoptotyczne komponenty tego szlaku. Wtedy, eIF2α poprzez selektywną stymulację translacji ATF4 (Ryc. 1) indukuje aktywację białka homologicznego C/EBP (ang. *C/EBP homologous protein*, CHOP), będącego czynnikiem transkrypcyjnym bezpośrednio hamującym ekspresję czynnika antyapoptotycznego BCL2

(ang. *B-cell CLL/Lymphoma 2*) (Bengesser i wsp., 2016; Muneer i Shamsher Khan, 2019).

Procesy stresu ER i UPR są powszechne, zachodzą w większości typów komórek i tkanek. Dynamiczna regulacja tych procesów pośrednio decyduje o losie komórki, o jej przeżyciu lub śmierci, przez co może wpływać na prawidłowy rozwój i dojrzewanie poszczególnych narządów i układów we wczesnym okresie życia oraz na ich funkcjonowanie w życiu dorosłym. W trakcie dojrzewania mózgu stres ER i UPR mogą determinować przebieg takich procesów jak neurogeneza i neurorozwojowa apoptoza. Warto w tym miejscu wspomnieć, że UPR jest również silnym regulatorem procesów zapalnych na obwodzie i w mózgu. Ponadto zrównoważone procesy stresu ER odpowiadają za prawidłowe funkcjonowanie bariery krew-mózg (ang. *blood-brain barrier*, BBB), stojącej na straży homeostazy w ośrodkowym układzie nerwowym (OUN) (Perner i Krüger, 2022).

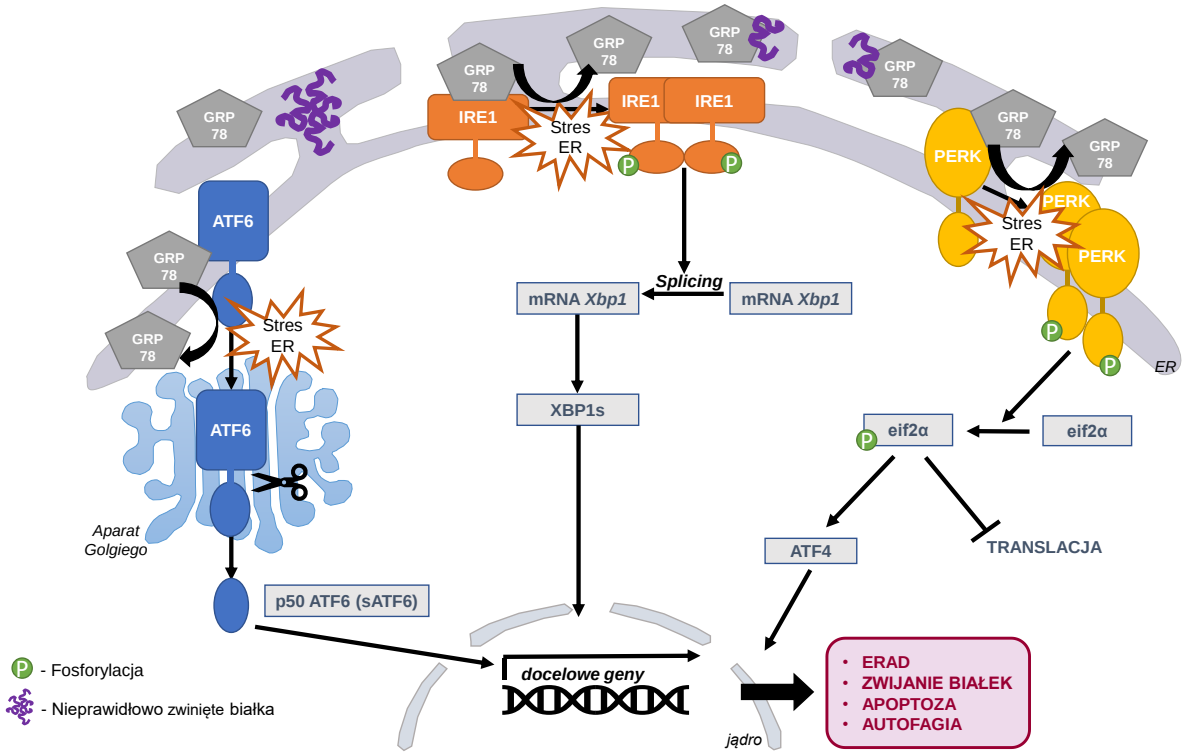

Ryc. 1. Schemat przedstawiający aktywację ścieżek odpowiedzi na nieprawidłowo zwinięte białka (UPR). Skróty: ATF4 - aktywujący czynnik transkrypcyjny 4; ATF6 - aktywujący czynnik transkrypcyjny 6; eIF2α – eukariotyczny czynnik inicjacji translacji 2α; ER – siateczka śródplazmatyczna; ERAD – degradacja związana z ER; GRP78 – białko regulowane glukozą 78 kDA; IRE1α – enzym zależny od inozytolu 1α; PERK – kinaza siateczki ER; XBP1 – *X-box binding protein-1*.

Zaburzenia procesów stresu ER i UPR wiązane są patofizjologią wielu chorób, np. nowotworów, cukrzycy, arteriosklerozy czy chorób neurodegeneracyjnych (Tabas, 2010; Chaudhari i wsp., 2014). Badania w modelach zwierzęcych wykazały, że zarówno ostry, jak i chroniczny stres w życiu dorosłym nasila ekspresję markerów stresu ER i UPR oraz aktywację szlaków UPR (Jangra i wsp., 2017; Tang i wsp., 2018; Li i wsp., 2019). Jednakże wpływ ELS i rola tych procesów w dojrzewaniu organizmu (w tym mózgu) we wczesnym okresie życia pozostaje wciąż niewystarczająco poznana i przebadana, szczególnie w kontekście etiologii różnych chorób.

W ostatnim czasie procesy stresu ER i UPR zaczęto postrzegać jako mediatory między- i wewnątrzgatunkowej zmienności w odpowiedzi na różne warunki środowiskowe (Yap i wsp., 2021). Wykazano, że stopień intensywności odpowiedzi stresu ER jest dziedziczny i istnieją indywidualne różnice fenotypowe w UPR, zarówno u ludzi, jak i zwierząt. Sugeruje to, że fenotypy odpowiedzi stresu ER i UPR mogą podlegać naturalnej selekcji i przez to kształtować mechanizmy podatności i oporności na działanie stresorów czy rozwój chorób (Yap i wsp., 2021).

5.3 Bariera krew-mózg a stres

Powszechnie BBB uważana jest za fizyczną i funkcjonalną granicę pomiędzy parenchymą mózgu a krążeniem ogólnoustrojowym, kontrolującą napływ i wypływ substancji biologicznych, zapewniających prawidłowe funkcjonowanie i homeostazę OUN (Hawkins i Davis, 2005; Brzezinska K. , 2012). BBB jest też pierwszą linią ochrony, zapobiegającą przedostawaniu się do mózgu potencjalnie szkodliwych czynników, takich jak patogeny, toksyny oraz obwodowe komórki układu odpornościowego (Abbott i wsp., 2010). BBB zbudowana jest z komórek śródbłonka naczyń krwionośnych mózgu (ang, *brain endothelial cells*, BEC), błony podstawnej, perycytów i zakończeń wypustek astrocytów, tzw. stopek astrocytarnych. Powyższe składowe BBB wraz ze zlokalizowanymi w pobliżu naczyń komórkami mikrogleju i neuronami tworzą tzw. jednostkę nerwowo-naczyniową (ang. *neurovascular unit,* NVU) (Abbott i wsp., 2010; Alvarez i wsp., 2013) (Ryc. 2).

Wybiórcza przepuszczalność i ochronna funkcja BBB jest możliwa m.in. dzięki unikalnemu fenotypowi BEC (Hawkins i Davis, 2005; Abbott i wsp., 2010). Ściany naczyń w OUN tworzy pojedyncza warstwa BEC pozbawiona fenestracji (okienek), o zwiększonej

gęstości mitochondriów i minimalnej aktywności pinocytarnej. Pomiędzy BEC występują wysokooporowe połączenia obejmujące szczelinę międzykomórkową, tzw. złącza ścisłe (ang. *tight junctions*, TJ) oraz połączenia przylegające (ang. *adherens junctions*), które zapewniają wzajemne, ścisłe przyleganie BEC i gwarantują ograniczony transport parakomórkowy (Ryc. 2). TJ to kompleksy białek, których głównymi składowymi są transbłonowe okludyny (ang. *ocludins*, OCLN) i klaudyny (ang. *claudins*, CLDN), które łączą się z cytoszkieletem poprzez cytoplazmatyczne białka kompleksu *zonula occludens* (ZO) i cingulinę (Abbott i wsp., 2010) (Ryc. 2). W rodzinie CLDN to głównie CLDN 3 i 5 zasługują na szczególną uwagę, ponieważ zaburzenie ich funkcji w kompleksie TJ może wpływać na integralności BBB (Abbott i wsp., 2010).

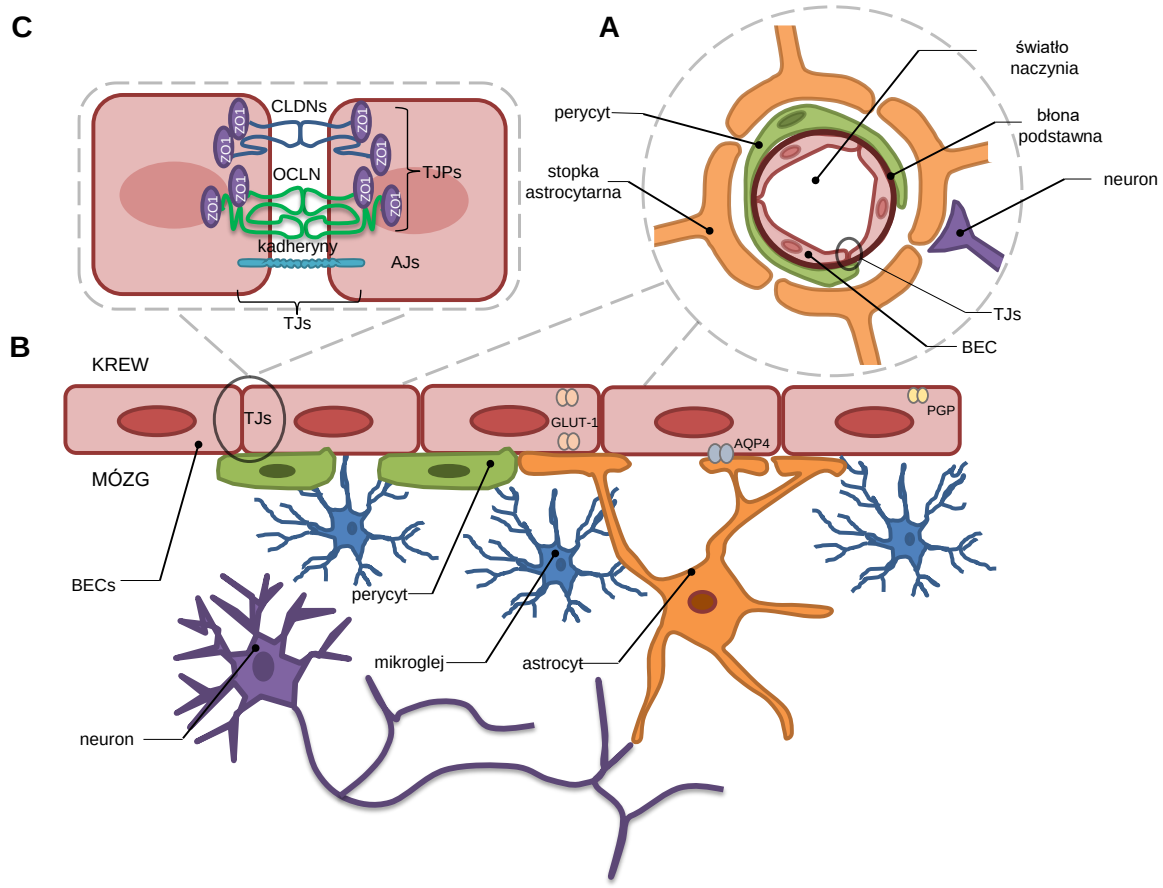

Ryc. 2. Schemat budowy bariery krew-mózg. (**A**) Bariera krew-mózg – przekrój poprzeczny przez naczynie. (**B**) Interakcje komórkowe na poziomie jednostki nerwowo-naczyniowej. (**C**) Schemat przestrzeni między komórkami śródbłonka naczyń – budowa złącz ścisłych. Skróty: AJs – połączenia przylegające; AQP4 – akwaporyna 4; BEC – komórki śródbłonka naczyń mózgu; CLDNs – klaudyny; GLUT-1 – transporter glukozy typu 1; OCLN – okuldyna; PGP – glikoproteina P; TJs – złącza ścisłe, TJPs – białka złącz ścisłych; ZO1 – *zonula occludens 1*.

BBB ma niską pasywną przepuszczalność dla metabolitów i niezbędnych składników odżywczych rozpuszczalnych w wodzie. Na drodze prostej dyfuzji do OUN przedostają się gazy, związki rozpuszczalne w lipidach czy peptydy o masie 400 – 800 Da (Abbott i wsp., 2010; Brzezinska K. , 2012). Ważną rolę w zachowaniu niezależnej homeostazy OUN odgrywa zatem aktywny transport jonów oraz białka transportowe BBB, takie jak np. transporter glukozy typu GLUT-1, glikoproteina P (ang. *P-glycoprotein, PGP*) czy specyficzne kanały wodne, akwaporyny (AQP) (głównie AQP 4 obecna na stopkach astrocytarnych) (Zheng i wsp., 2010; Brzezinska K. , 2012; Alvarez i wsp., 2013).

Ze względu na skomplikowaną, wielopoziomową budowę i dynamiczne funkcjonowanie BBB, procesy jej rozwoju i dojrzewania są sekwencyjne i przebiegają zgodnie z dobrze zdefiniowanym programem morfogenetycznym (Krause i wsp., 2002; Brzezinska K. , 2012). U ludzi BBB rozpoczyna rozwój w życiu płodowym, ale funkcjonalność osiąga dopiero pół roku po narodzinach (Brzezinska K. , 2012). Gryzonie przychodzą na świat stosunkowo nierozwinięte, dlatego wiele mechanizmów w obrębie BBB dojrzewa i nabiera pełnej funkcjonalności dopiero w okresie około- lub poporodowym (Krause i wsp., 2002; Abbott i wsp., 2010). Ramy czasowe kształtowania się BBB są zbliżone do angiogenezy, której największe nasilenie u szczura przypada pomiędzy 3 a 5 dniem po narodzinach (Krause i wsp., 2002; Blanchette i Daneman, 2015). Tworzeniu funkcjonalnej sieci TJ pomiędzy BEC towarzyszy nasilona ekspresja GLUT-1, co powoduje, że jest on stosowany jako marker dojrzewania tych komórek w mózgu (Zheng i wsp., 2010). Z kolei, obserwowany w trzecim tygodniu po urodzeniu duży wzrost ekspresji PGP, wskazuje na przedłużony rozwój BBB u gryzoni (Daneman i wsp., 2010; Ek i wsp., 2010). Co więcej, we wczesnym okresie postnatalnym gęstość naczyń odpowiada lokalnym funkcjom obszarów korowych, co sugeruje ścisły związek między ich równoczesnym i wydłużonym rozwojem (Caley i Maxwell, 1970; Krause i wsp., 2002). Ponadto zarówno na rozwój mózgu w tym okresie, jak i na rozwój BBB, może wpływać także kształtujący się układ odpornościowy oraz interakcje neuroimmunologiczne (Danese i Lewis, 2017; Brenhouse i wsp., 2019). Zatem niekorzystne czynniki środowiskowe, działające we wczesnym okresie życia (np. stres), mogą potencjalnie interferować jednocześnie z dojrzewaniem mózgu i BBB.

Do oceny integralności BBB w modelach zwierzęcych służy szereg technik. Jedną z podstawowych jest pomiar przepuszczalności BBB dla endogennych białek osocza lub egzogennych znaczników o różnej masie cząsteczkowej (Kaya i Ahishali, 2011; Brzezinska K. , 2012; Sun i wsp., 2021). Do pierwszej z grup możemy zaliczyć albuminę

(69 kDa), immunoglobuliny klasy G (150 kDa), fibronektynę (200 kDa) oraz fibrynogen (340 kDa), jednak znacznym ograniczeniem ich stosowania są wahania stężenia tych białek we krwi, wynikające z zaburzeń homeostazy spowodowanych badanymi stanami chorobowymi. Egzogenne znaczniki w mniejszym stopniu podlegają takim fluktuacjom (Brzezinska K. , 2012). Spośród nich możemy wyróżnić te, które wiążą się do endogennej albuminy, np. peroksydaza chrzanowa (40 kDa), dekstran (70 kDa) czy błękit Evansa (950 Da) (Kaya i Ahishali, 2011; Brzezinska K. , 2012; Sun i wsp., 2021) oraz te o niskiej masie cząsteczkowej (i niskim powinowactwie do białek), takie jak sól sodowa fluoresceiny (NaF) (376 Da) i znakowana radioligandem sacharoza (342 kDa). Obecność znacznika w przestrzeni pozanaczyniowej wykrywa się m.in. za pomocą metod immunochemicznych *in situ* lub spektrofotometrycznych i spektrofluorymetrycznych, umożliwiających ilościowy pomiar znacznika w badanej tkance (Kaya i Ahishali, 2011; Sun i wsp., 2021). Innymi technikami oceniającymi integralność BBB są badania morfologiczne i ultrastrukturalne mające na celu identyfikację i ocenę stanu poszczególnych składowych BBB (immunohistochemia (IHC), mikroskopia) oraz badania ilościowe ekspresji genów i białek budujących BBB, np. białek TJ (TJP), czy transporterów BBB.

Coraz częściej zaburzenia funkcjonowania BBB uznawane są za brakujące ogniwo, będące ważną przyczyną pojawienia się zaburzeń homeostazy, zarówno w młodym, jak i starzejącym się mózgu (Stolp i Dziegielewska, 2009; Erickson i Banks, 2013; Winkler i wsp., 2015; Arora i wsp., 2019). Dysfunkcje BBB występują w patofizjologii wielu chorób, takich jak np. stwardnienie rozsiane, udar, padaczka (Profaci i wsp., 2020), czy choroby neurodegeneracyjne. Obecnie, coraz więcej dowodów wskazuje również na zmiany w funkcjonowania BBB jako potencjalny patomechanizm stresu (Menard i wsp., 2017; Greene i wsp., 2020; Kamintsky i wsp., 2020). Badania prowadzone w zwierzęcych modelach ostrego i przewlekłego stresu, ujawniają potencjalne zaburzenia BBB (Hanin, 1996; Santha i wsp., 2015; Menard i wsp., 2017; Kamintsky i wsp., 2020; Welcome i Mastorakis, 2020; Wu i wsp., 2022). Większość tych badań wykazała wywołany stresem fenotyp prodepresyjny, przy równocześnie zwiększonej przepuszczalność BBB w regionach mózgu zaangażowanych w odpowiedź na stres (Hanin, 1996; Santha i wsp., 2015; Wu i wsp., 2022). Zmianom tym często towarzyszyły zaburzenia poziomu określonych komponentów BBB, w szczególności: spadek ekspresji TJP – CLDN 5 (Menard i wsp., 2017; Dion-Albert i wsp., 2022b; Wu i wsp., 2022) i OCLN (Santha i wsp., 2015), zmiany ekspresji białka AQP 4 (Xu i wsp., 2019; Taler i wsp., 2021), a także poziomu GLUT-1 (Santha i wsp., 2015; Welcome i Mastorakis, 2020). Dotychczas

bardzo nieliczne badania podjęły tematykę zaburzeń BBB w modelach zwierzęcych ELS. Co więcej, dostępne dane ograniczają się jedynie do oceny przepuszczalności BBB (Gomez-Gonzalez i Escobar, 2009; Carlessi i wsp., 2022). Z badań tych wynika, że procedura MS może powodować wzrost przepuszczalności BBB w korze nowej, hipokampie (HP) i jądrze podstawnym szczurów (Gomez-Gonzalez i Escobar, 2009; Carlessi i wsp., 2022). Choć we wspomnianych badaniach wykorzystano zarówno samce, jak i samice w różnym wieku (Gomez-Gonzalez i Escobar, 2009; Carlessi i wsp., 2022) to wciąż brakuje szerszego, kompleksowego spojrzenia na różnice międzypłciowe i rozwojowe, opartego o dane dotyczące wpływu ELS także na ultrastrukturę TJ czy ekspresję genów/białek budujących BBB.

5.4 Procesy neurozapalne a stres

Zadaniem układu odpornościowego jest rozpoznawanie i ochrona organizmu przed wirusami, bakteriami i innymi cząstkami zakaźnymi (Brenhouse i wsp., 2019). W odpowiedzi na zakażenie i uszkodzenie tkanek, układ odpornościowy indukuje wrodzoną reakcję obronną, zwaną reakcją zapalną. Jeśli toczy się ona w obrębie OUN, mówimy wtedy o neurozapaleniu. Układ odpornościowy i OUN kształtują się w okresie prenatalnym, ale ich rozwój i dojrzewanie trwają nieprzerwanie przez wczesny okres postnatalny, aż do adolescencji (Brydges i Reddaway, 2020). Już w okresie prenatalnym, komórki immunokompetentne, które wyposażone są w mechanizmy wrodzonej (nieswoistej) odporności komórkowej, uczestniczą w odpowiedzi zapalnej (Brenhouse i wsp., 2019). Większość wrodzonej kompetencji immunologicznej OUN pochodzi od mikrogleju, który stanowi 10-15% wszystkich komórek OUN. Komórki te różnicują się z prymitywnych makrofagów w woreczku żółtkowym i kolonizują embrionalną tkankę nerwową (E 10.5 – 17.5 u gryzoni), gdzie dojrzewają, aby następnie spełniać podstawowy nadzór immunologiczny w OUN (Brydges i Reddaway, 2020; Dudek i wsp., 2021).

Patogeny w organizmie są odróżniane od cząstek gospodarza, dzięki obecności w swojej budowie charakterystycznych, powtarzalnych wzorców molekularnych tzw. wzorców molekularnych związanych z patogenami (ang. *pathogen-associated molecular patterns*, PAMP). Należą do nich najczęściej składniki ścian komórkowych bakterii (glikany, glikokoniugaty) oraz endotoksyny, znajdujące się w zewnętrznych błonach komórkowych bakterii Gram-ujemnych (np. lipopolisacharyd, LPS) (Brenhouse i wsp., 2019; Perner i Krüger, 2022). PAMP są rozpoznawane przez wysoce konserwatywne

receptory rozpoznające wzorce (ang. *pattern recognition receptors*, PRR), takie jak np. receptory toll-podobne (ang. *toll-like receptors*, TLR), obecne na powierzchni komórek, czy receptory cytozolowe (np. kompleksy białek inflamasomu) (Brenhouse i wsp., 2019; Perner i Krüger, 2022). TLR są obecne na różnych typach komórek odpornościowych ssaków. Ich ekspresję w OUN wykazano na neuronach, mikrogleju, astrocytach oraz BEC (Serna-Rodríguez i wsp., 2022). Do TLR obecnych w mózgu należą TLR od 1 do 9, jednak ze względu na szeroki profil dystrybucji i aktywacji w stanach fizjologicznych i patologicznych, szczególną rolę w OUN odgrywają TLR 2 i 4 (Trotta i wsp., 2014; Serna-Rodríguez i wsp., 2022). W wyniku rozpoznania PAMP dochodzi do synergistycznej aktywacji receptorów TLR i kompleksu inflamasomu i w konsekwencji uwalniane są mediatory reakcji zapalnej, tj. cytokiny prozapalne (interleukina 1β (IL-1β), IL-6, czynnik martwicy nowotworów (ang. *tumor necrosis factor α*, TNFα)), chemokiny (CCL2, CCL5, CXCL1), reaktywne formy tlenu (ROS) czy przekaźniki (NO, prostaglandyny) (Figueroa-Hall i wsp., 2020; Yang i wsp., 2020). Uwalnianie mediatorów zapalnych to jeden z podstawowych objawów toczącego się zapalenia, a mikroglej jest jedną z pierwszych populacji komórek w mózgu, która reaguje na sygnały zagrożenia. Indukcja neurozapalenia związana jest z morfologicznymi i funkcjonalnymi zmianami tych komórek, dzięki którym osiągają stan umożliwiający sekrecję cząstek prozapalnych i fagocytozę (da Fonseca i wsp., 2014). Obok mikrogleju, również astrocyty, BEC, perycyty, a nawet neurony mogą być źródłem mediatorów zapalnych w OUN.

Warto podkreślić, że do aktywacji wrodzonej odpowiedzi komórkowej z udziałem receptorów TLR nie dochodzi jedynie w obecności patogenów. TLR2, TLR4 i TLR9, mogą bowiem rozpoznawać również tzw. wzorce molekularne związane z uszkodzeniem (ang. *damage-associated molecular patterns*, DAMP) (Franklin i wsp., 2018; Serna-Rodríguez i wsp., 2022). DAMP, zwane również alarminami, sygnalizują endogenne zagrożenie, stres i/lub śmierć komórek. Należą do nich m.in.: HSP, białka S100, fibrynogen, ATP czy kwas moczowy (Perner i Krüger, 2022; Serna-Rodríguez i wsp., 2022). Aktywacja TLR z udziałem DAMP prowadzi do indukcji tzw. sterylnego zapalenia.

Jak już wspomniano, dzięki BBB mózg jest do pewnego stopnia chroniony przed patogenami oraz procesami zapalnymi toczącym się na obwodzie. BBB jest pierwszą linią obrony, która ogranicza napływ obwodowych komórek układu odpornościowego i cząstek zapalnych (Varatharaj i Galea, 2017). Jednakże postępujące procesy zapalne stopniowo mogą prowadzić do naruszenia poszczególnych elementów składowych BBB. Początkowo, pod wpływem Il-1β i TNFα, dochodzi do aktywacji BEC, co wiąże się ze

wzrostem ekspresji cząsteczek adhezji komórkowej w tych komórkach, szczególnie cząsteczek adhezji międzykomórkowej 1 (ang. *intercellular adhesion molecule 1*, ICAM1). Wzrost ekspresji ICAM1 na powierzchni BEC ułatwia ich interakcję z integrynami obecnymi na obwodowych komórkach odpornościowych prowadząc do ich rekrutacji i rolowania (da Fonseca i wsp., 2014; Varatharaj i Galea, 2017; Brenhouse i wsp., 2019). Równocześnie, w wyniku działania mediatorów prozapalnych, może dochodzić do naruszenia struktury TJ i zmian w ekspresji CLDN5 i OCLN, ZO-1 (Varatharaj i Galea, 2017; Brenhouse i wsp., 2019; Peng i wsp., 2021). Tym zaburzeniom w obrębie BBB może towarzyszyć migracja komórek odpornościowych drogą parakomórkową, czyli pomiędzy komórkami BEC, do przestrzeni okołonaczyniowej i finalnie do parenchymy mózgu (Varatharaj i Galea, 2017; Brenhouse i wsp., 2019; Peng i wsp., 2021). Co ważne, w stanie neurozapalenia migracja komórek odpornościowych do mózgu może zachodzić także drogą transkomórkową, czyli przez BEC (Varatharaj i Galea, 2017; Mapunda i wsp., 2022), a funkcje TJ mogą ulegać zmianie, pomimo iż ich struktura pozostaje nienaruszona (Papadopoulos i wsp., 1999; da Fonseca i wsp., 2014; Varatharaj i Galea, 2017). Należy wspomnieć, że istnieją także inne drogi komunikacji pomiędzy układem odpornościowym i mediatorami zapalnymi a układem nerwowym, należą do nich obszary pozbawione BBB, tj. splot naczyniówkowy i narządy okołokomorowe oraz aktywacja nerwu błędnego i jąder pnia mózgu (Dudek i wsp., 2021; Mapunda i wsp., 2022).

Powszechnie uważa się, że stres i GC osłabiają odporność i działają przeciwzapalnie (Baxter i Forsham, 1972). Dane literaturowe pokazują jednak, że stres, zwłaszcza przewlekły, powoduje wzrost poziomu cytokin prozapalnych (IL-1β, TNFα i IL-6) w surowicy, co moduluje odpowiedź zapalną w OUN i tym samym wpływa na funkcjonowanie mózgu (Franklin i wsp., 2018). Co więcej, chroniczny stres może wpływać uwrażliwiająco na przebieg odpowiedzi układu odpornościowego w przyszłości (Franklin i wsp., 2018; Serna-Rodríguez i wsp., 2022). Ważnym mechanizmem działania stresu na układ odpornościowy, może być indukcja „sterylnego zapalenia" (Serna-Rodríguez i wsp., 2022). Wiadomo bowiem, że psychologiczny stres powoduje uwolnienie i wzrost poziomu DAMP (np. białek HSP, S100) w przestrzeni zewnątrzkomórkowej, które przez wiązanie z TLR4 na komórkach immunokompetentnych promują odpowiedź prozapalną (Serna-Rodríguez i wsp., 2022). W warunkach podstawowych procesy te mają na celu utrzymanie homeostazy, jednak wywołane przewlekłym stresem, mogą przyczyniać się do aktywacji procesów patologicznych w OUN (Serna-Rodríguez i wsp., 2022).

Chociaż wielu badaczy w ostatniej dekadzie podjęło próbę wykazania wpływu ELS na przebieg reakcji zapalnej w modelach zwierzęcych, to uzyskane wyniki wciąż pozostają niejednoznaczne. Ta niespójność może wynikać z kwestii metodologicznych, takich jak różnorodność stosowanych modeli ELS, badanych markerów zapalnych czy koncepcji eksperymentalnych (np. wiek badanych zwierząt) (Brenhouse i wsp., 2019; Dutcher i wsp., 2020). Choć wykazano, że ELS może ogólnie zaburzać aktywację mikrogleju i poziom cząstek prozapalnych w mózgu, to nie zaobserwowano jednoznacznego, długoterminowego wpływu ELS na ekspresję cytokin w tkankach obwodowych, czy na przebieg procesów neurozapalnych (Dutcher i wsp., 2020). Jednakże w obliczu działania kolejnego czynnika środowiskowego w późniejszym okresie życia (stres, infekcja), zwierzęta poddane ELS często wykazywały nasiloną reakcją prozapalną (Roque i wsp., 2016; Catale i wsp., 2020; Dutcher i wsp., 2020).

5.5 Modulacja procesów zapalnych, stresu ER i funkcji BBB przez chroniczny stres – wspólny mianownik w patofizjologii i / lub progresji chorób psychicznych i neurodegeneracyjnych?

Jak już wspomniano, przewlekły stres, w tym ELS, jest ważnym czynnikiem w etiologii zaburzeń nastroju i lęku. Jest również wiązany z patofizjologią i progresją innych chorób psychicznych oraz neurodegeneracyjnych (Danese i Lewis, 2017; Hoeijmakers i wsp., 2017; Brenhouse i wsp., 2019). Równocześnie chroniczny stres jest silnym modulatorem procesów zapalnych, a obecnie depresję, schizofrenię oraz AD i PD postrzega się również jako choroby o podłożu zapalnym (Stolp i Dziegielewska, 2009; Erickson i Banks, 2013; Danese i Lewis, 2017; Hoeijmakers i wsp., 2017; Brenhouse i wsp., 2019; Dutcher i wsp., 2020; Dudek i wsp., 2021).

Dane kliniczne dostarczają dowodów łączących podatność na stres z nasiloną odpowiedzią prozapalną, a u pacjentów z depresją obserwuje się podwyższony poziom obwodowych cytokin, TNFα, Il-16 i IL-1β (Maes i wsp., 1995; Dowlati i wsp., 2010; Dudek i wsp., 2021). W przypadku dużej depresji podwyższonym parametrom prozapalnym towarzyszy wzrost liczby obwodowych leukocytów, monocytów i neutrofili (Maes i wsp., 1992; Dudek i wsp., 2021) oraz nasilona ekspresja chemokiny CCL2 w mózgu (Torres-Platas i wsp., 2014). Udokumentowany związek między markerami zapalnymi a indywidualnymi objawami depresyjnymi, takimi jak zmęczenie czy

dysfunkcje poznawcze, wskazuje na zaangażowanie procesów zapalnych w patogenezę depresji (Miller i wsp., 2009). Podwyższone poziomy cytokin prozapalnych w surowicy, płynie mózgowo-rdzeniowym i w mózgu są wykrywane również u pacjentów cierpiących na AD i PD (Voet i wsp., 2019; Fernández i wsp., 2021). Ponadto wykazano prozapalną aktywację komórek mikrogleju otaczających blaszki β-amyloidu w mózgu pacjentów z AD (Voet i wsp., 2019).

Stres i procesy zapalne mogą wpływać na funkcjonowanie BBB (Erickson i Banks, 2013; da Fonseca i wsp., 2014; Disdier i Stonestreet, 2019; Dudek i wsp., 2021). Dysfunkcje BBB obserwowane są w przypadku wielu chorób, w tym w AD, PD oraz depresji i schizofrenii (Stolp i Dziegielewska, 2009; Winkler i wsp., 2015; Disdier i Stonestreet, 2019; Greene i wsp., 2020; Kamintsky i wsp., 2020; Profaci i wsp., 2020). W przypadku chorób neurodegeneracyjnych zaburzenia w obrębie BBB mogą poprzedzać lub nasilać postęp choroby, jednak stopień zaangażowania i zaawansowania tych zaburzeń, stanowi obszar wciąż rozwijających się badań (Stolp i Dziegielewska, 2009; Winkler i wsp., 2015; Disdier i Stonestreet, 2019; Greene i wsp., 2020; Profaci i wsp., 2020; Dion-Albert i wsp., 2022a). W płynie mózgowo-rdzeniowym pacjentów z neurodegeneracjami, obserwuje się podniesiony poziom albumin (Stolp i Dziegielewska, 2009; Profaci i wsp., 2020) oraz zdiagnozowane metodą rezonansu magnetycznego zaburzenia przepuszczalności BBB (Stolp i Dziegielewska, 2009; Profaci i wsp., 2020). Badania *post mortem* potwierdzają dysfunkcje BBB. U pacjentów z AD obserwuje się nadmierne gromadzenie się albuminy, immunoglobuliny czy fibrynogenu (szczególnie w obszarach mózgu bogatych w blaszki β-amyloidu) (Stolp i Dziegielewska, 2009; Profaci i wsp., 2020), a także zaburzenia funkcji ważnych komponentów BBB, np. TJ czy perycytów (Profaci i wsp., 2020). Z kolei, analiza histologiczna próbek istoty czarnej pochodzących od pacjentów z PD wykazała m.in. zmiany grubości oraz gęstości naczyń krwionośnych (Faucheux i wsp., 1999).

Rola zaburzeń funkcji BBB w patofizjologii chorób psychicznych jest zdecydowanie mniej przebadana, ale obecnie taka koncepcja zaczyna cieszyć się coraz większą popularnością wśród badaczy (Menard i wsp., 2017; Greene i wsp., 2020; Kamintsky i wsp., 2020; Dudek i wsp., 2021; Dion-Albert i wsp., 2022a). Zaburzenia ekspresji TJP, głównie CLDN5, wykazano *post mortem* w spektrum zaburzeń psychicznych, z najbardziej wyraźnymi efektami u pacjentów ze zdiagnozowaną depresją i schizofrenią (Menard i wsp., 2017; Dudek i wsp., 2020; Greene i wsp., 2020; Dion-Albert i wsp., 2022b). Co więcej, u pacjentów z depresją obserwowano także wzrost

przepuszczalności BBB. Udowodniły to badania wykorzystujące pomiar poziomu obwodowego markera zaburzeń szczelności BBB - białka S100β (Gulen i wsp., 2016) i obrazowanie rezonansem magnetycznym (Kamintsky i wsp., 2020).

Szczegółowe mechanizmy leżące u podstaw dysfunkcji BBB i nasilenia procesów zapalnych, obserwowanych w zaburzeniach psychicznych i neurodegeneracyjnych, wciąż wymagają poznania. Ważną rolę mogą potencjalnie odgrywać tu procesy stresu komórkowego, w tym odpowiedź HSP, stres ER i UPR (Fernández i wsp., 2021; Diaz-Hung i Hetz, 2022; Serna-Rodríguez i wsp., 2022). Wzrost obwodowego poziomu DAMP obserwuje się u pacjentów cierpiących na zaburzenia nastroju, lękowe i choroby neurodegeneracyjne (Kakiuchi i wsp., 2005; Stertz i wsp., 2015; Franklin i wsp., 2018; Bauer i Teixeira, 2021; Serna-Rodríguez i wsp., 2022). Przykładem może być białko HSPA1B, należące do rodziny HSP70, które zostało zidentyfikowane jako potencjalny obwodowy marker zaburzeń lękowych (Le-Niculescu i wsp., 2011; Yang i wsp., 2013). Badania wskazują również na związek polimorfizmu genu HSPA1B z próbami samobójczymi u pacjentów cierpiących na schizofrenię (Kakiuchi i wsp., 2005). Dodatkowo funkcjonalny polimorfizm genu HSPA5 (GRP 78) i XBP1 jest potencjalnie związany z chorobą afektywną dwubiegunową w populacji Japończyków (Le-Niculescu i wsp., 2011; Yang i wsp., 2013). U pacjentów cierpiących na depresję, wykazano zaburzoną ekspresję genów i mRNA markerów stresu ER i UPR w leukocytach (HSPA5, CHOP, XBP1) oraz w korze czołowej i skroniowej (HSPA5, GRP94, ATF4) (Bown i wsp., 2000; Kakiuchi i wsp., 2005; Nevell i wsp., 2014; Yoshino i Dwivedi, 2020). Z kolei, analiza *post mortem* mózgów pacjentów cierpiących na AD, PD i stwardnienie rozsiane ujawniła podniesiony poziom markerów UPR - CHOP, HSPA5, PERK, P-eIF2α, P-IRE1 i XBP1, szczególnie w mikrogleju (Hoozemans i wsp., 2007; Mháille i wsp., 2008; Cunnea i wsp., 2011; McMahon i wsp., 2012; Wheeler i wsp., 2019).

Przedstawione powyżej dane literaturowe pozwalają wysnuć hipotezę, że modulacja procesów zapalnych, stresu ER i funkcji BBB przez chroniczny stres może być wspólnym mianownikiem w patofizjologii i / lub progresji chorób psychicznych i neurodegeneracyjnych. Choć wiadomo, że doświadczenie ELS, może zwiększać ryzyko wystąpienia zarówno zaburzeń nastroju, jak i chorób neurodegeneracyjnych (Stolp i Dziegielewska, 2009), to wiedza na temat wpływu ELS na procesy potencjalnie, wiążące się z patofizjologią tych chorób, takie jak zapalenie, UPR i funkcje BBB jest wciąż niewielka i niekompletna (Gomez-Gonzalez i Escobar, 2009; Brydges i Reddaway, 2020; Carlessi i wsp., 2022). Szczególnie ograniczona jest wiedza dotycząca zależnych od płci

różnic we wspominanych procesach, a jak wiadomo w obrazie klinicznym i w częstości występowania zaburzeń psychicznych i chorób neurodegeneracyjnych, bardzo widoczne są różnice płciowe (Pinares-Garcia i wsp., 2018).

6. Cel badań

Dane epidemiologiczne wskazują, że choroby psychiczne i neurodegeneracyjne, obok schorzeń sercowo-naczyniowych i nowotworowych oraz cukrzycy, są jedną z głównych przyczyn niepełnosprawności na świecie. Wiele czynników środowiskowych, działających na wczesnym etapie życia osobnika, takich jak np. ELS czy infekcje, może zwiększać ryzyko wystąpienia wymienionych problemów zdrowotnych w późniejszym okresie życia. Obecnie coraz częściej przewlekłe procesy zapalne, stres ER oraz, w przypadku schorzeń OUN, dysfunkcje BBB postrzegane są jako wspólny mianownik związany z etiologią i progresją wspomnianych schorzeń.

Choć badania ostatnich dekad przyczyniły się do zwiększenia wiedzy o wpływie ELS na dojrzewanie i funkcjonowanie mózgu, wciąż poszukuje się pierwotnych mechanizmów, leżących u podstaw podatności bądź oporności na ELS i zaburzenia przezeń wywołane. Szczególnie mało poznany jest udział BBB, procesów zapalnych i stresu komórkowego w biologii ELS i modulacji tych procesów przez czynniki związane z płcią. Skłoniło nas to do podjęcia badań nad rozszerzeniem wiedzy w tym właśnie zakresie, które zaowocowały cyklem publikacji składających się na niniejszą rozprawę doktorską. Badania przeprowadzono w modelu ELS opartym o procedurę MS u szczurów. Wyznaczono w nich następujące cele badawcze:

I. Zbadanie wpływu MS na dojrzewanie i integralność BBB u szczurów obu płci na różnym etapie rozwoju (publikacja 1, wyniki uzupełniające nieopublikowane) (Ryc. 3).
   W ramach tego celu zmierzono:

A. przepuszczalność BBB w mPFC, grzbietowym prążkowiu (*dorsal striatum*, dSTR) i HP
B. ekspresję mRNA TJP i transporterów BBB w mPFC, dSTR i HP
C. gęstość naczyń wykazujących ekspresję markera BBB w mPFC, dSTR i HP (wyniki uzupełniające nieopublikowane)
D. poziom wybranych markerów stanu zapalnego i zaburzeń integralności BBB w surowicy

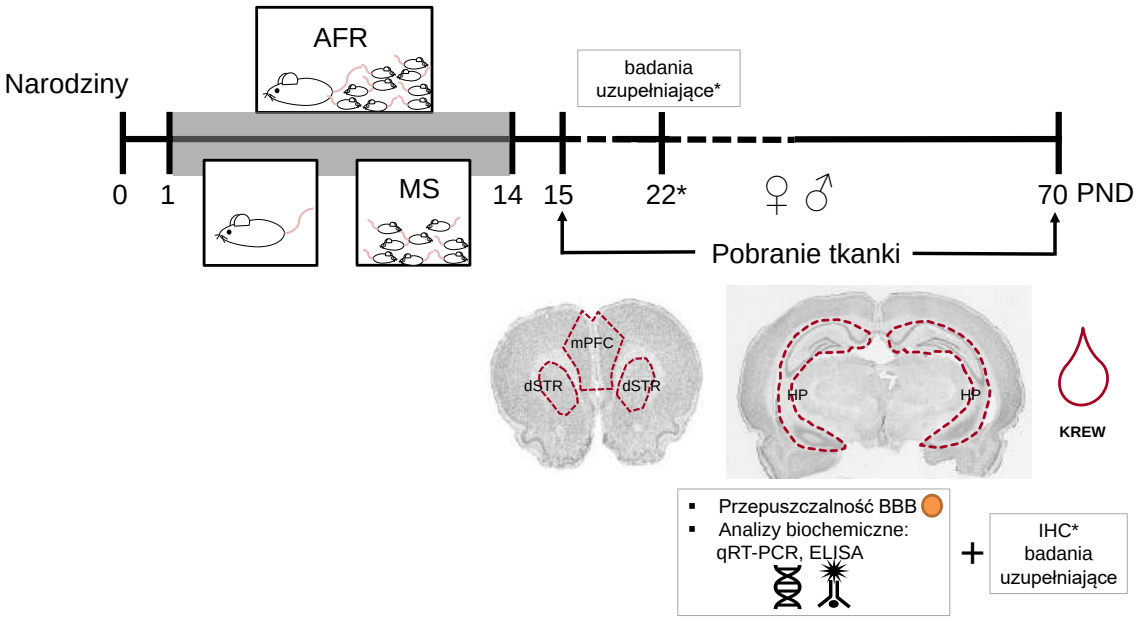

Ryc. 3. Cel I - Schemat eksperymentu. Mikrofotografie prezentują przekroje mózgu szczura z zaznaczonymi regionami wybranymi do analiz. Skróty: AFR - warunki standardowe hodowli (grupa kontrolna), BBB - bariera krew-mózg, dSTR - grzbietowe prążkowie, HP - hipokamp, IHC - immunohistochemia, mPFC - przyśrodkowa kora przedczołowa, MS - separacja od matki, PND - dzień po narodzinach.

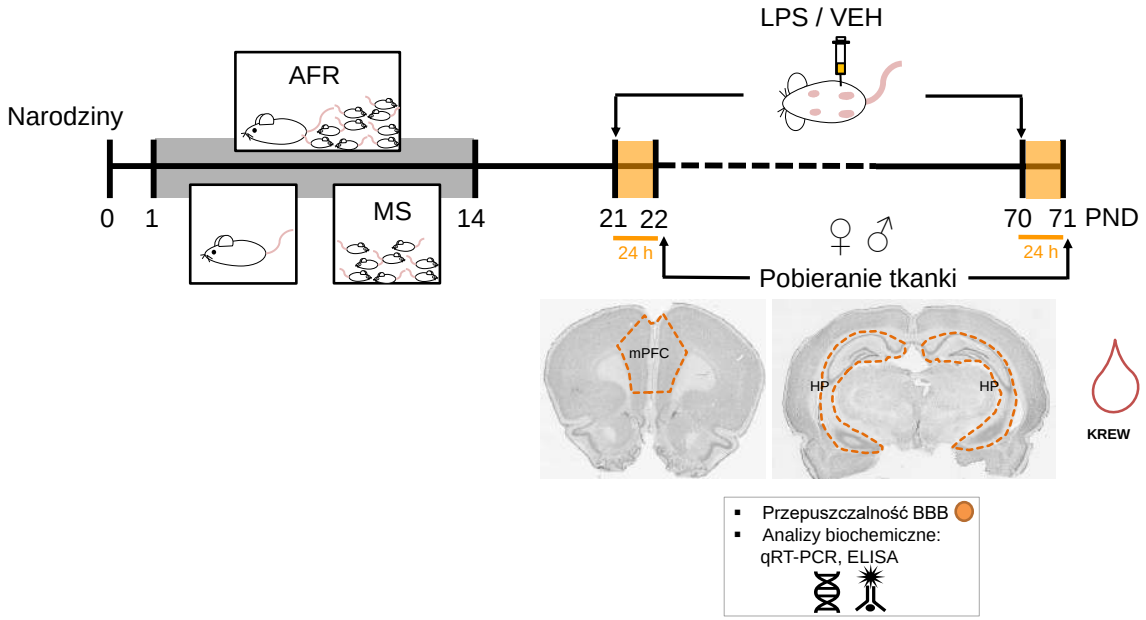

Ryc. 4. Cel II - Schemat eksperymentu. Mikrofotografie prezentują przekroje mózgu szczura z zaznaczonymi regionami wybranymi do analiz. Skróty: AFR - warunki standardowe hodowli (grupa kontrolna), BBB - bariera krew-mózg, HP - hipokamp, IHC - immunohistochemia, LPS - lipopolisacharyd, mPFC - przyśrodkowa kora przedczołowa, MS - separacja od matki, PND - dzień po narodzinach, VEH - rozpuszczalnik.

II. Zbadanie, czy doświadczenie MS wpływa na przebieg reakcji zapalnej w późniejszym okresie życia modelowanej podaniem LPS zwierzętom obu płci w 21 i 70 dniu po urodzeniu (ang. *postnatal day*, PND) (publikacja 2) (Ryc. 4). W trakcie realizacji tego celu zbadano:

A. poziom wybranych markerów odpowiedzi zapalnej w surowicy, mPFC i HP
B. przepuszczalność BBB i ekspresję mRNA TJP w mPFC i HP

III. Sprawdzenie, czy MS moduluje ekspresję białek rodziny HSP70 na różnych etapach rozwoju – poszukiwanie mózgowego i obwodowego biomarkera ELS (publikacja 3) (Ryc. 5). Realizując ten cel, zbadano:

A. ekspresję mRNA i białek HSPA5 i HSPA1B w mPFC i HP zwierząt (samców) w PND 15, 26 i 70
B. ekspresję mRNA HSPA5 i HSPA1B we krwi obwodowej wyżej wspomnianych zwierząt
C. procesy długotrwałego wzmocnienia synaptycznego (LTP) w mPFC i HP (PND 70)
D. zachowanie zwierząt w testach oceniających lęk, anhedonię, strategię radzenia sobie ze stresem oraz procesy bramkowania sensomotorycznego (PND 70)

IV. Zbadanie roli stresu ER i UPR w mechanizmach podatności bądź oporności na ELS u samców (publikacja 4) (Ryc. 6). W ramach tego celu zbadano:

A. wpływ MS i podań inhibitora stresu ER, salubrinalu (SAL), na ekspresję markerów UPR i apoptozy w mPFC zwierząt w PND 15, 26 i 70
B. wpływ MS i SAL na liczbę komórek nerwowych i glejowych w mPFC (PND 26 i 70)
C. wpływ MS i SAL na zachowanie zwierząt w testach oceniających lęk, pamięć o zdarzeniach awersyjnych, anhedonię i odpowiedź na podanie substancji psychostymulującej (PND 26 i 70)

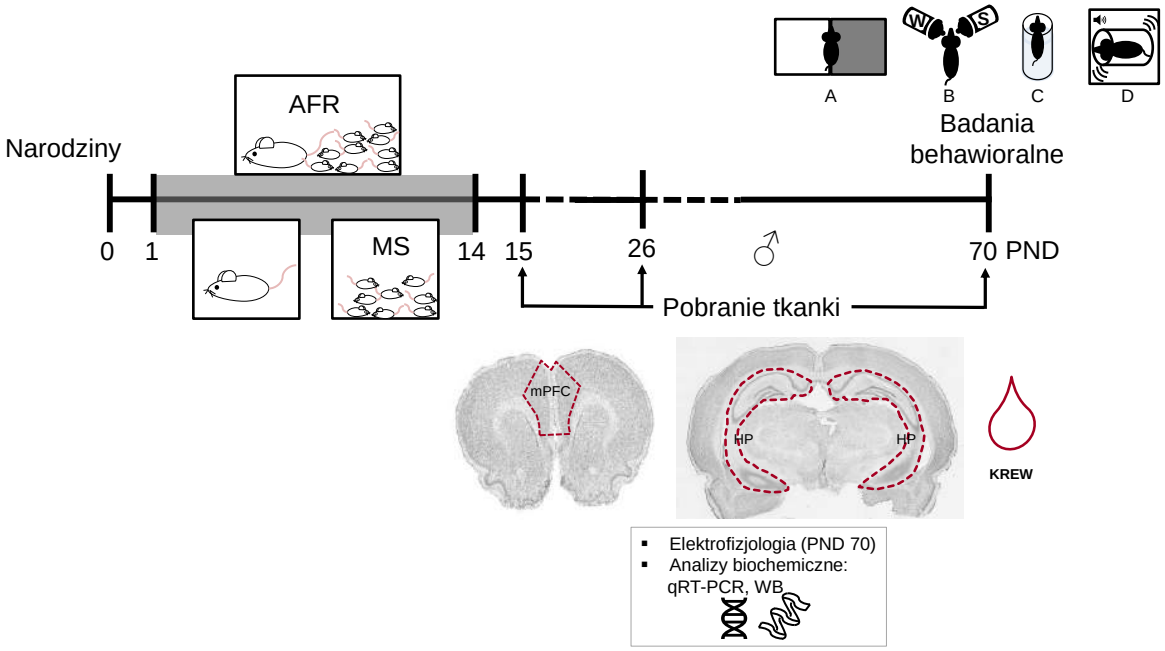

Ryc. 5. Cel III - Schemat eksperymentu. Mikrofotografie prezentują przekroje mózgu szczura z zaznaczonymi regionami wybranymi do analiz. **(A-D)** - Zastosowane testy behawioralne: **A)** test jasnego/ciemnego pudełka, **B)** test preferencji sacharozy, **C)** test wymuszonego pływania, **D)** ocena bramkowania sensomotorycznego. Skróty: AFR - warunki standardowe hodowli (grupa kontrolna), HP - hipokamp, mPFC - przyśrodkowa kora przedczołowa, MS - separacja od matki, PND - dzień po narodzinach, WB - Western blot.

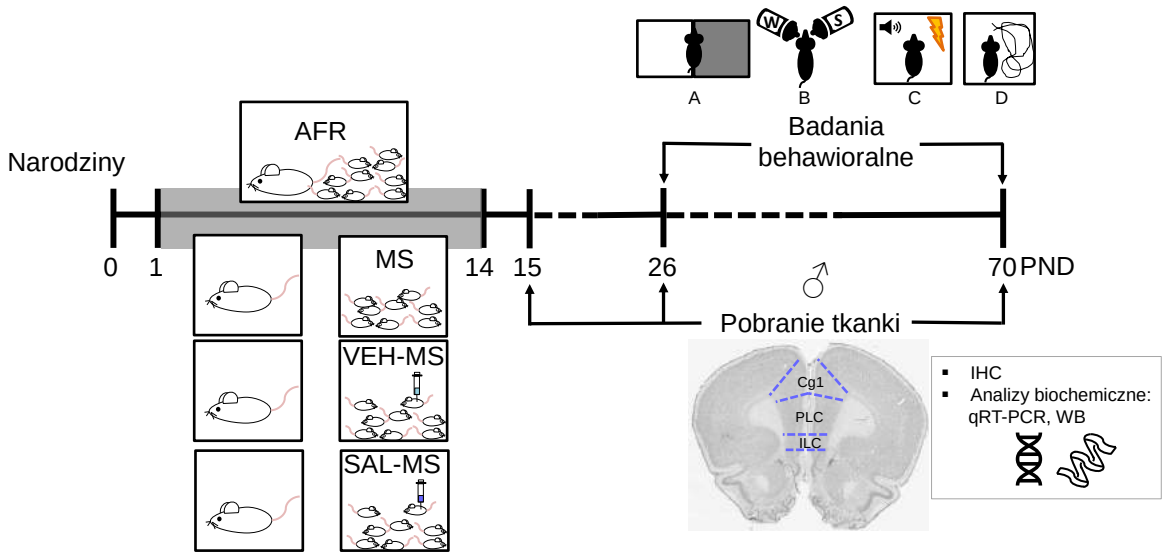

Ryc. 6. Cel IV - Schemat eksperymentu. Mikrofotografia prezentuje przekrój mózgu szczura z zaznaczonymi regionami przyśrodkowej kory przedczołowej wybranymi do analiz. **(A-D)** - Zastosowane testy behawioralne: **A)** test jasnego/ciemnego pudełka, **B)** test preferencji sacharozy, **C)** warunkowanie strachu, **D)** aktywność lokomotoryczna. Skróty: AFR - warunki standardowe hodowli (grupa kontrolna), Cg1 - kora obręczy 1, IHC - immunohistochemia, ILC - kora infralimbiczna, MS - separacja od matki, PLC - kora przedlimbiczna, PND - dzień po narodzinach, SAL - salubrinal, VEH - rozpuszczalnik, WB - Western blot.

7. Badania uzupełniające

7.1 Metodyka

7.1.1 Zwierzęta

Wszystkie procedury eksperymentalne zostały zatwierdzone przez II Lokalną Komisję Etyczną ds. Doświadczeń na Zwierzętach w Krakowie (nr zgody 260/2017), a także spełniały wymagania Dyrektywy Parlamentu Europejskiego i Rady 2010/63/EU w sprawie ochrony zwierząt wykorzystywanych do celów naukowych. Jednocześnie dołożono wszelkich starań, aby zminimalizować cierpienie i liczbę wykorzystanych zwierząt. Wszystkie badania uzupełniające przeprowadzono na szczurach stada Wistar hodowanych w warunkach standardowych (ang. *animal facility rearing*, AFR) lub poddanych procedurze separacji od matki (MS). Warunki hodowli zostały szczegółowo opisane w publikacjach Solarz i wsp. (2021a,b,2023) i Solarz-Andrzejewska i wsp. (2023). Eksperymenty przeprowadzono w PND 15, PND 22 i w PND 70 u zwierząt obu płci.

7.1.2 Ilościowe oznaczenie przepuszczalności BBB

W celu ilościowej oceny przepuszczalności BBB, u szczurów w PND 22 zastosowano dootrzewnowe podanie NaF, drobnocząsteczkowego znacznika fluorescencyjnego o masie 376 Da. Zaletami tego czułego markera są: zdolność do wykazania nawet dyskretnych zmian przepuszczalności BBB i brak niespecyficznego wiązania z białkami, w przeciwieństwie do innych stosowanych w tym celu barwników. W sposób szczegółowy procedura została opisana w publikacjach Solarz i wsp. (2021a) oraz (Solarz i wsp., 2023). Zawartość barwnika fluorescencyjnego w homogenatach mPFC, dSTR i HP oznaczono spektrofluorymetrycznie, a wyniki wyrażono jako ilość NaF (µg) na gram mokrej tkanki.

7.1.3 Metody immunohistochemiczne (IHC)

W PND 15 i PND 70 zwierzęta poddano transkardialnej perfuzji w celu utrwalenia tkanki mózgowej. Szczegółowo procedura eksperymentalna została opisana w publikacji Solarz-Andrzejewska i wsp. (2023). W skrócie, przy pomocy wibratomu (VT1000S, Leica) mózgi pocięto w płaszczyźnie czołowej na 50 µm skrawki na poziomie mPFC, dSTR i HP (Bregma, odpowiednio: 3.70 do 2.20 mm, 2.20 do -0.40 mm, -1.8 do -6.04 mm), według

stereotaktycznego atlasu mózgu szczura (Paxinos G. i Watson C., 1998). Kolejność skrawków do analizy wybierano przez systematyczne, losowe pobieranie przekrojów anatomicznych wybranych regionów mózgu. Do blokowania swobodnie pływających skrawków użyto 5% roztworu koziej surowicy (1h). W eksperymencie zastosowano komercyjnie dostępne mysie przeciwciało I rzędowe klasy IgM rozpoznające marker BBB, antygen EBA (ang. *endothelial barrier antigen*) (klon SMI 71) (1:500, 48h w 4°C, 836801, Biolegend), a następnie specyficzne biotynylowane II-rzędowe przeciwciało kozie skierowane przeciw mysim IgM (1:500, 1h, BA-2020, Vector Laboratories) oraz kompleks awidyna-biotyna-peroksydaza (1:200, 1h, Vectastein ABC Kit Vector Laboratories). Końcowe barwienie IHC przeprowadzono, wykorzystując metodę 3,3'-diaminobenzydyna (DAB)-nikiel.

Cyfrowe obrazy wybarwionych skrawków uzyskano przy użyciu skanera preparatów histologicznych Aperio Leica CS2 (Leica, Niemcy) wyposażonego w obiektyw 20x/0.75 NA Plan Apo oraz kompatybilnego oprogramowania Scan Scope Console i Aperio Image Scope. Na uzyskanych obrazach zaznaczano obszary mózgu objęte analizą na podstawie anatomicznych punktów orientacyjnych i w odniesieniu do stereotaktycznego atlasu mózgu szczura (Paxinos G. i Watson C., 1998). Analizę gęstości naczyń mózgowych EBA-immunoreaktywnych (IR) w badanych strukturach wykonano w obu półkulach na wszystkich skrawkach mózgu pochodzących od danego zwierzęcia (mPFC: n = 5-9, dSTR: n = 8-10, HP: n = 7-10). Do analizy wykorzystano oprogramowanie Leica Application Suit X (LAS X) (Leica Microsystem, USA). Wszystkie analizowane obrazy zostały poddane jednakowej kalibracji, a także zastosowano jednakowe wartości zadanych parametrów, aby zapewnić maksymalnie ujednoliconą i bezstronną analizę. Dodatkowo wykorzystano funkcję oprogramowania, która umożliwia manualne usunięcie artefaktów z analizy, które nie były klasyfikowane jako naczynia i zaburzały prawidłowy obraz. W rezultacie końcowa analiza pozwoliła na oszacowanie gęstości naczyń mózgowych EBA-IR, wyrażonej jako stosunek powierzchni zajętej przez naczynia EBA-IR (w mm^2) do całkowitej powierzchni obrysowanego obszaru w obrębie badanego regionu mózgu (w mm^2).

7.1.4 Analiza statystyczna

Dane przedstawiono jako średnie arytmetyczne dla grupy ± odchylenie standardowe (SD). Analizę statystyczną danych przeprowadzono przy użyciu pakietu statystycznego

Statistica 10 (TIBCO Software Inc., USA). Na początku, zbadano zgodność rozkładu danych z rozkładem normalnym testem Shapiro-Wilka, a także jednorodność wariancji wykorzystując test Levene'a. Następnie, wyniki analizowano za pomocą dwuczynnikowej analizy wariancji (ANOVA). W przypadku oceny rozwojowych zmian w przepuszczalności BBB, jako zmienne niezależne przyjęto płeć i PND. Natomiast do analizy przepuszczalności BBB w PND 22 i gęstości naczyń EBA-IR jako zmienne niezależne zastosowano warunki hodowli (AFR vs MS) i płeć. W przypadku uzyskania znamiennej interakcji zmiennych niezależnych w ANOVA dane poddano dalszej analizie testem *post-hoc* Bonferroniego. Wartości $p < 0.05$ uznano za znamiennie różne.

7.2 Wyniki

7.2.1 Wpływ MS oraz płci na dojrzewanie i integralność BBB

7.2.1.1 Zmiany przepuszczalności BBB w rozwoju ontogenetycznym zwierząt kontrolnych

Badania dotyczące przepuszczalności BBB zamieszczone w publikacji nr 1 (Solarz i wsp., 2021a) uzupełniono o badania przeprowadzone w PND 22, czyli w okresie, w którym według danych literaturowych, BBB szczura powinna osiągnąć pełną dojrzałość funkcjonalną (Caley i Maxwell, 1970; Butt i wsp., 1990; Krause i wsp., 2002; Abbott i wsp., 2010). Analiza ilościowych zmian w przepuszczalności BBB u zwierząt kontrolnych (AFR) wykazała znamienną statystycznie interakcję pomiędzy wiekiem i płcią we wszystkich badanych strukturach mózgu (dwuczynnikowa ANOVA, Tabela 1). Szczegółowa analiza wykazała, że wraz z wiekiem BBB zmniejszała swoją przepuszczalność (uszczelnianie się BBB), co objawiało się zmniejszającą się zawartością NaF w tkance (Ryc. 7). Co ciekawe, u samców zjawisko to postępowało stopniowo pomiędzy PND 15 i PND 22 oraz PND 22 i PND 70 we wszystkich badanych strukturach mózgu (PND 15 vs PND 22: mPFC: $p < 0.001$, dSTR: $p < 0.001$, HP: $p < 0.001$, PND 22 vs 70: mPFC: $p < 0.001$, dSTR: $p < 0.001$, HP: $p = 0.0078$) (Ryc. 7). Natomiast u samic, we wszystkich strukturach z wyjątkiem dSTR, analiza wykazała znamienny spadek przepuszczalności BBB tylko pomiędzy PND 15 a PND 22 (mPFC: $p < 0.001$, HP: $p < 0.001$) (Ryc. 7). Wskazuje to na szybsze dojrzewanie BBB w mPFC i HP samic. Jednakże dSTR samic charakteryzowało się stopniowym uszczelnianiem BBB, podobnie

jak to występowało u samców (PND 15 vs PND 22: $p < 0.001$, PND 22 vs PND 70: $p < 0.022$) (Ryc. 7).

Dalsza analiza wykazała również duże różnice płciowe w przepuszczalności BBB w PND 22, gdzie u samic przepuszczalność BBB we wszystkich badanych strukturach mózgu była znacznie niższa niż u samców (mPFC: $p < 0.001$, dSTR: $p < 0.001$ HP: $p < 0.001$) (Ryc. 7)

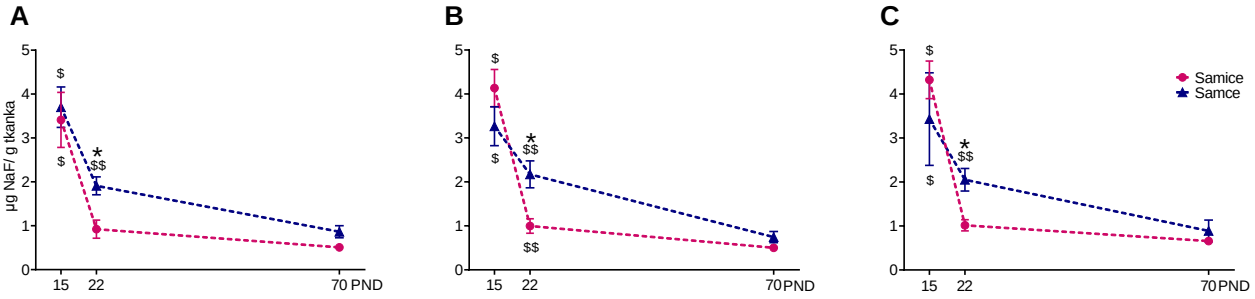

Ryc. 7. Zmiana przepuszczalności BBB w trakcie rozwoju ontogenetycznego u szczurów kontrolnych (AFR). Dane przedstawiono jako średnie arytmetyczne grup ± SD zawartości NaF w tkance mPFC (**A**), dSTR (**B**) i HP (**C**) ($n = 8$). $^{\$}p < 0.05$ vs PND 22 i PND 70, $^{\$\$}p < 0.05$ vs PND 70, $^{*}p < 0.05$ vs samice w PND 22 (dwuczynnikowa ANOVA, test *post-hoc* Bonferroniego).

Tabela 1. Wyniki dwuczynnikowej ANOVA badającej wpływ płci i wieku na przepuszczalność BBB szczurów grupy kontrolnej (AFR)

źródło zmienności	region mózgu					
	mPFC		dSTR		HP	
PND	$F_{2,42} = 298.31$	$\mathbf{p < 0.001}$	$F_{2,42} = 462.45$	$\mathbf{p < 0.001}$	$F_{2,42} = 91.56$	$\mathbf{p < 0.001}$
PŁEĆ	$F_{2,42} = 29.78$	$\mathbf{p < 0.001}$	$F_{2,42} = 4.80$	$\mathbf{p = 0.034}$	$F_{2,42} = 0.06$	$p = 0.808$
PND$_x$PŁEĆ	$F_{2,42} = 4.95$	$\mathbf{p = 0.011}$	$F_{2,42} = 48.81$	$\mathbf{p < 0.001}$	$F_{2,42} = 15.99$	$\mathbf{p < 0.001}$

Efekty istotne statystycznie oznaczono pogrubioną czcionką. Skróty: PND, dzień po narodzinach.

7.2.1.2 Wpływ MS na przepuszczalność BBB w PND 22

Interesująca dynamika uszczelniania BBB w trakcie rozwoju i zależne od płci różnice w jej przepuszczalności obserwowane w PND 22, skłoniły nas do zbadania wpływu MS na funkcje BBB w tym właśnie punkcie rozwojowym. Analiza wykazała, że jedynie w mPFC warunki hodowli znamiennie wpływały na przepuszczalność BBB (dwuczynnikowa ANOVA, Tabela 2), a mianowicie samce MS miały zwiększoną przepuszczalność BBB w mPFC w porównaniu do zwierząt kontrolnych ($p = 0.015$) (Ryc. 8). Co więcej, zarówno u zwierząt MS jak i AFR, samice wykazywały mniejszą

przepuszczalność BBB niż samce we wszystkich badanych regionach mózgu (dSTR: $p < 0.0001$ (główny efekt płci), HP: $p < 0.0001$ (główny efekt płci), mPFC: $p = 0.0002$ (AFR), $p < 0.0001$ (MS)) (Ryc. 8).

Tabela 2. Wyniki dwuczynnikowej ANOVA badającej wpływ MS i płci na przepuszczalność BBB w PND 22

źródło zmienności	region mózgu					
	mPFC		dSTR		HP	
WH	$F_{1,28} = 5.36$	**$p = 0.028$**	$F_{1,28} = 0.73$	$p = 0.399$	$F_{1,28} = 0.57$	$p = 0.458$
PŁEĆ	$F_{1,28} = 85.50$	**$p < 0.001$**	$F_{1,28} = 158.02$	**$p < 0.001$**	$F_{1,28} = 104.24$	**$p < 0.001$**
WH$_x$PŁEĆ	$F_{1,28} = 5.74$	**$p = 0.025$**	$F_{1,28} = 0.318$	$p = 0.577$	$F_{1,28} = 1.25$	$p = 0.273$

Efekty istotne statystycznie oznaczono pogrubioną czcionką.
Skróty: WH, warunki hodowli,

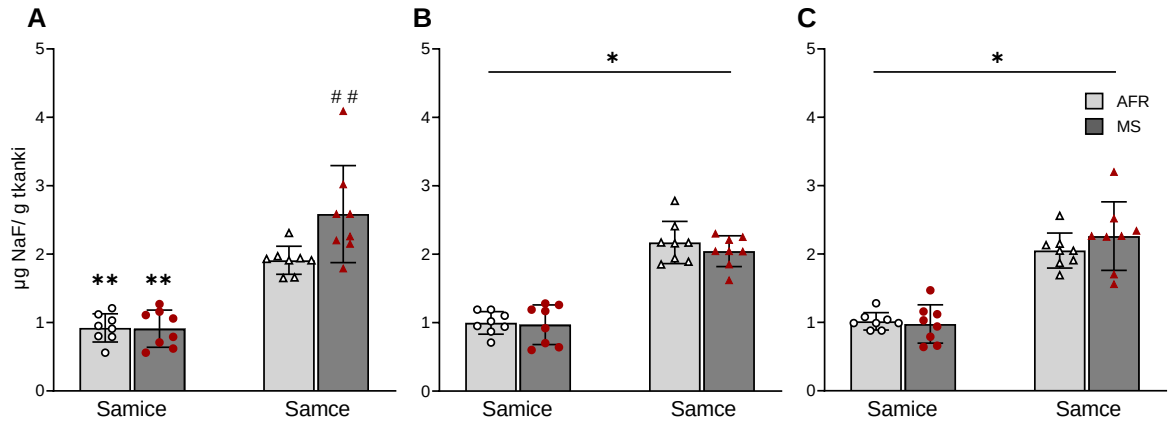

Ryc. 8. Zmiany przepuszczalności BBB zależne od MS i płci w PND 22. Dane przedstawiono jako średnie arytmetyczne grup ± SD zawartości NaF w tkance mPFC (**A**), dSTR (**B**) i HP (**C**) ($n = 8$). $^{\#\#}p < 0.05$ vs samce AFR, $^{**}p < 0.05$ vs. samce według warunków hodowli, $^{*}p < 0.05$ – główny efekt płci (dwuczynnikowa ANOVA, *post-hoc* Bonferroniego).

7.2.1.3 Wpływ MS oraz płci na gęstość naczyń wykazujących ekspresję markera BBB (EBA) w badanych strukturach mózgu szczurów w PND 15 i dorosłości (PND 70)

Wyniki zamieszczone w publikacji nr 1 (Solarz i wsp., 2021a) uzupełniono o immunohistochemiczne badanie ekspresji markera BBB, antygenu EBA, przy użyciu przeciwciał klonu SMI 71. Przeciwciała SMI 71 rozpoznają specyficznie białka śródbłonka naczyń w obszarach występowania BBB u szczura (Sternberger i wsp., 1989; Cassella i wsp., 1997; Westin i wsp., 2006). Analiza jakościowa preparatów

immunohistochemicznych wykazała słabszą EBA immunoreaktywność u młodych zwierząt w PND 15 w porównaniu z osobnikami dorosłymi w PND 70, co może odzwierciedlać stopień dojrzałości BBB w badanych grupach (Ryc. 9 i 10). Jednakże tego typu różnice mogły wyniknąć również z przyczyn metodycznych (różnice we wrażliwość tkanki młodego i dorosłego mózgu na utrwalenie i zamrażanie), dlatego dane w obrębie badanych grup wiekowych zanalizowano osobno.

Analiza statystyczna gęstości naczyń EBA-IR u zwierząt w PND 15 wykazała znamienny wpływ warunków hodowli na badany parametr w mPFC (p = 0.003) i dSTR (p = 0.008) oraz istotny wpływ płci w dSTR (p = 0.022) i HP (p = 0.027) (dwuczynnikowa ANOVA, Tabela 3). Zwierzęta MS w PND 15, ogólnie wykazywały zwiększoną gęstość naczyń EBA-IR w mPFC i dSTR (Ryc. 9). Ponadto samice charakteryzowały się większą gęstością naczyń EBA-IR w dSTR i HP niż samce (Ryc. 9).

Analiza gęstości naczyń EBA-IR u zwierząt dorosłych (PND 70) wykazała jedynie istotny statystycznie wpływ płci w HP (dwuczynnikowa ANOVA, Tabela 3). Podobnie jak w przypadku zwierząt młodych, dorosłe samice wykazywały zwiększoną gęstość naczyń EBA-IR w HP w porównaniu do samców (p = 0.012) (Ryc. 10).

Tabela 3. Wyniki dwuczynnikowej ANOVA badającej wpływ warunków hodowli (AFR vs MS) oraz płci na gęstość naczyń EBA-IR

	źródło	region mózgu					
PND	zmienności	mPFC		dSTR		HP	
15	WH	$F_{1,20}$ = 11.59	**p = 0.003**	$F_{1,20}$ = 8.69	**p = 0.008**	$F_{1,20}$ = 2.13	p = 0.160
	PŁEĆ	$F_{1,20}$ = 0.16	p = 0.696	$F_{1,20}$ = 6.16	**p = 0.022**	$F_{1,20}$ = 5.73	**p = 0.027**
	WH$_x$PŁEĆ	$F_{1,20}$ = 0.66	p = 0.427	$F_{1,20}$ = 0.96	p = 0.340	$F_{1,20}$ = 0.07	p = 0.801
70	WH	$F_{1,20}$ = 2.50	p = 0.130	$F_{1,20}$ = 0.42	p = 0.526	$F_{1,20}$ = 1.91	p = 0.182
	PŁEĆ	$F_{1,20}$ = 1.40	p = 0.250	$F_{1,20}$ = 0.74	p = 0.401	$F_{1,20}$ = 7.56	**p = 0.012**
	WH$_x$PŁEĆ	$F_{1,20}$ = 0.19	p = 0.667	$F_{1,20}$ = 1.29	p = 0.270	$F_{1,20}$ = 0.07	p = 0.790

Efekty istotne statystycznie oznaczono pogrubioną czcionką
Skróty: WH, warunki hodowli,

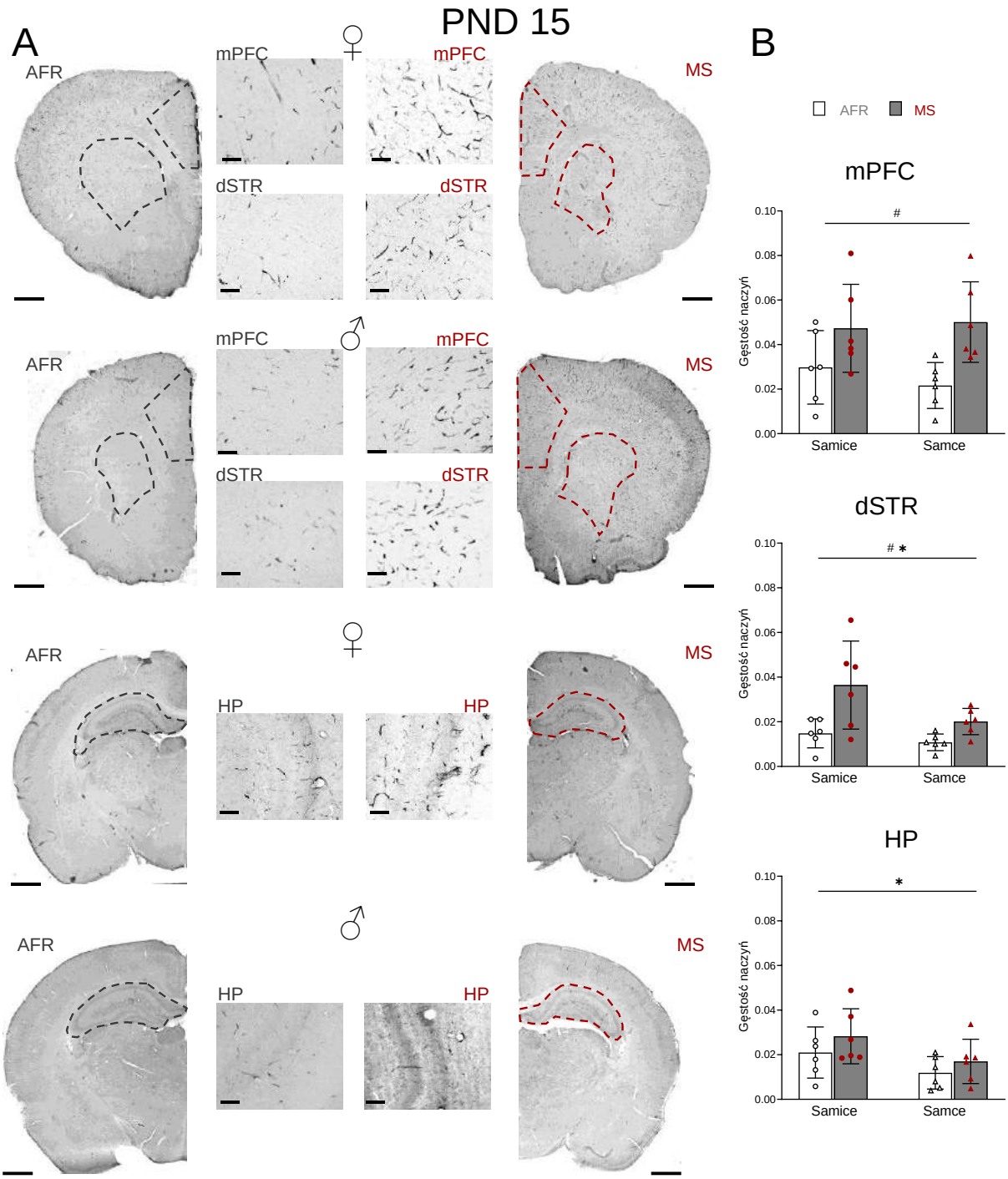

Ryc. 9. Wpływ MS oraz płci na ekspresję markera BBB (EBA) w mPFC, dSTR i HP szczurów w PND 15. (**A**) Przykładowe mikrofotografie pokazujące barwienia immunohistochemiczne z użyciem przeciwciał anty-EBA (SMI 71). Skale reprezentują odpowiednio 1 mm dla przekroju mózgu oraz 100 µm dla powiększenia danej struktury (20x) (**B**) Dane przedstawiono jako średnie arytmetyczne grup ± SD (n = 6). $^{\#}p < 0.05$ – wpływ MS, $^{*}p < 0.05$ – wpływ płci (dwuczynnikowa ANOVA). Linie odnoszą się do istotności statystycznej głównych efektów ANOVA.

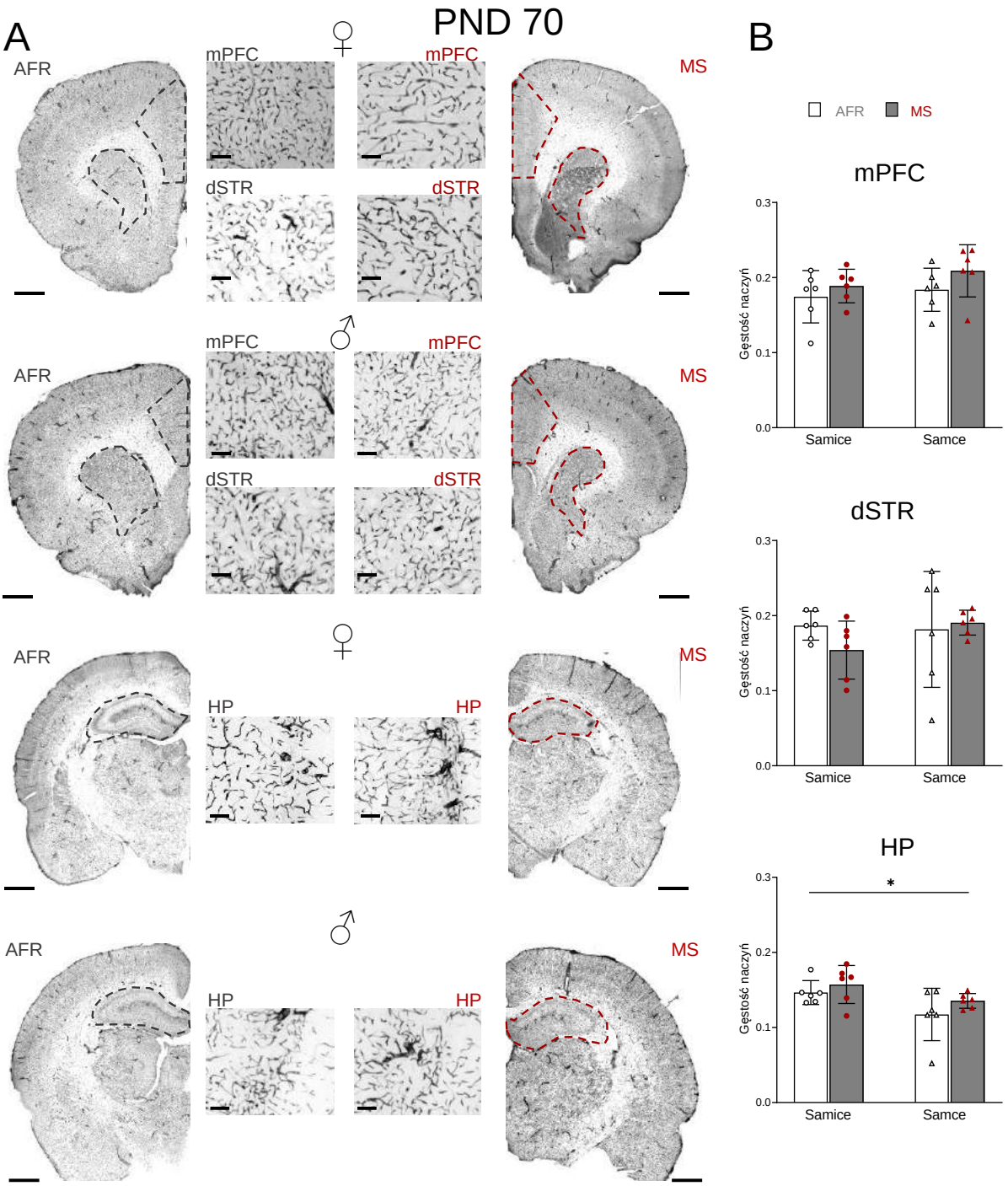

Ryc. 10. Wpływ MS oraz płci na ekspresję markera BBB (EBA) w mPFC, dSTR i HP szczurów dorosłych (PND 70). (**A**) Przykładowe mikrofotografie pokazujące barwienia immunohistochemiczne z użyciem przeciwciał anty-EBA (SMI 71). Skale reprezentują odpowiednio 1 mm dla przekroju mózgu oraz 100 µm dla powiększenia danej struktury (20x). (**B**) Dane przedstawiono jako średnie arytmetyczne grup ± SD (n = 6). $^{*}p < 0.05$ – wpływ płci (główny efekt w dwuczynnikowej ANOVA).

7.3 Podsumowanie wyników badań uzupełniających oraz wnioski płynące po ich przeprowadzeniu

- Proces rozwojowego uszczelniania się BBB przebiegał według odmiennego wzorca u samic i u samców szczurów. Samce wykazywały stopniowe uszczelnianie BBB w trakcie rozwoju, natomiast w przypadku samic, poziom przepuszczalności BBB w mPFC i HP w PND 22 osiągał już poziom typowy dla dorosłych samic. Towarzyszyły temu szczególnie duże różnice płciowe w przepuszczalności BBB we wszystkich badanych strukturach mózgu w PND 22, kiedy to samice charakteryzowały się znacznie mniejszą przepuszczalnością BBB niż samce. Taka tendencja występowała również u zwierząt MS. Ponadto, u młodocianych samic w PND 15 gęstość naczyń wykazujących ekspresję markera BBB w dSTR i HP była większa niż u samców.
  Powyższe wyniki wraz z rezultatami zawartymi w publikacji Solarz i wsp. (2023), pokazującymi już w PND 22 wyższy poziom mRNA TJP u samic w porównaniu do samców, mogą wskazywać na to, że **procesy dojrzewania BBB u samic szczura przebiegają szybciej.**

- MS powodowała u samców przejściowe zwiększenie przepuszczalności BBB w dSTR (PND 15, Solarz i wsp. (2021a)) i mPFC (PND 22, badania uzupełniające). Jednocześnie obserwowano wzrost gęstości naczyń wykazujących ekspresję markera BBB w mPFC i dSTR zwierząt MS obu płci w PND 15. Uwzględniając również wpływ MS na ekspresję mRNA *Cldn5* (zwiększenie) oraz na poziom obwodowego markera zaburzeń integralności BBB, S100β (redukcja) Solarz i wsp. (2021a), wyniki te mogą wskazywać na wczesną **aktywację mechanizmów adaptacyjnych/kompensacyjnych w obrębie BBB w odpowiedzi na ELS. Mechanizmy te wydają się bardziej skuteczne w przypadku samic.**

8. Dyskusja

8.1 Wpływ wieku i płci na przepuszczalność i strukturę BBB szczura

Kluczowe znaczenie dla zrozumienia komórkowych i molekularnych mechanizmów regulacji funkcji BBB ma identyfikacja momentu jej ostatecznego funkcjonalnego ukształtowania w trakcie rozwoju. Ze względu na stopień złożoności tego procesu i interakcji komórkowych w obrębie jednostki nerwowo-naczyniowej, moment ten jest trudny do jednoznacznego określenia. Dostępne dane literaturowe wskazują, że u gryzoni BBB osiąga dojrzałość w 3-4 tygodniu po narodzinach (Caley i Maxwell, 1970; Butt i wsp., 1990; Krause i wsp., 2002; Blanchette i Daneman, 2015), a jej przepuszczalność u dorosłych zwierząt jest niższa niż u niedojrzałych osobników (Lossinsky i wsp., 1986; Xu i Ling, 1994; Utsumi i wsp., 2000; Abbott i wsp., 2010).

W badaniach opisanych w publikacji Solarz i wsp. (2021a) stwierdzono zmniejszenie przepuszczalności BBB dla NaF między PND 15 a PND 70, co wskazuje na rozwojowe uszczelnianie BBB. Efekt ten został odzwierciedlony również we wzrastającej wraz z wiekiem ekspresji mRNA *Slc2a1* i większości badanych TJP oraz w związanej z wiekiem redukcji stężenia obwodowego markera rozszczelnienia BBB – białka S100β w surowicy. Dane przedstawione w niniejszej rozprawie są zgodne z obserwowanym w literaturze rozwojowym wzrostem poziomu transportera GLUT-1 w naczyniach mózgu gryzoni (Cornford i wsp., 1993; Vannucci, 1994) oraz z opisywaną w klinice negatywną korelacją pomiędzy wiekiem a poziomem S100β w surowicy pacjentów (Gazzolo i wsp., 2003; Thelin i wsp., 2017). Co ciekawe, badania dodatkowe zawarte w niniejszej pracy doktorskiej wykazały, że proces rozwojowego uszczelniania się BBB różni się między płciami. U samców obserwowano stopniowe uszczelnianie się BBB, natomiast samice (z wyjątkiem dSTR) już w PND 22 wykazywały poziom przepuszczalności BBB typowy dla zwierząt dorosłych. Dodatkowo, samice w PND 22 charakteryzowały się znacznie niższą przepuszczalnością BBB dla NaF w porównaniu do samców we wszystkich badanych strukturach mózgu. Warto podkreślić, że efektowi temu towarzyszył wyższy poziom mRNA *Cldn5* w mPFC i HP i *Ocln* w HP u samic w PND 22 (Solarz i wsp., 2023). Zatem stosunkowo krótki okres młodzieńczy u szczura charakteryzuje się dużą dynamiką zmian w funkcjonowaniu BBB (Krause i wsp., 2002). Ujawnione w tym okresie rozwoju różnice międzypłciowe utrzymują się aż do dorosłości, co szczególnie dobrze obrazują wyniki zamieszczone w publikacji Solarz i wsp. (2021a). Pokazują one mniejszą

przepuszczalność BBB we wszystkich badanych regionach mózgu i wyższy poziom mRNA TJP i *Slc2a1* w mPFC i dSTR (ale nie w HP) u dorosłych samic w porównaniu do samców. Podobną tendencję wskazującą na ogólnie zwiększony poziom mRNA TJP u dorosłych samic w stosunku do samców wykazano również w publikacji Solarz i wsp. (2023). W tym przypadku, różnice te dotyczyły HP. Jednakże wymienionym różnicom międzypłciowym nie towarzyszyły tym razem różnice w przepuszczalność BBB między dorosłymi samcami a samicami we wszystkich badanych obszarach mózgu. Rozbieżności między wynikami zawartymi w publikacjach Solarz i wsp. (2021a) i Solarz i wsp. (2023) mogą wynikać z zastosowania różnych schematów eksperymentalnych, kohort zwierząt oraz uwzględnienia w złożonej analizie statystycznej odmiennych czynników (wiek, podanie LPS). Warto podkreślić, że ogólne tendencje dotyczące różnic międzypłciowych na poziomie BBB utrzymywały się również w trakcie ogólnoustrojowego zapalenia wywołanego podaniem LPS w okresie młodzieńczym i dorosłości (Solarz i wsp., 2023).

Dostępne dane literaturowe wskazują na różnice płciowe w regionalnych funkcjach mózgu, zużyciu glukozy i przepływie krwi, co sugeruje, że płeć może determinować także integralność i funkcję BBB (przegląd w Oztas (1998)). Jednakże temat różnic płciowych w budowie, dojrzewaniu i funkcjonowaniu BBB jest tak naprawdę wciąż otwartą kwestią wymagającą szerszych badań (Profaci i wsp., 2020). Publikacje składające się na tę rozprawę doktorską są pierwszymi, które w tak szerokim zakresie analizują zależną od płci i wieku ekspresję genów kodujących białka związane z integralnością i funkcjonowaniem BBB wraz z jednoczesną oceną przepuszczalności BBB w różnych obszarach mózgu, co znacznie wzbogaca dostępne dane literaturowe. Uzupełnienie wyników o badania dodatkowe, pozwoliło wykazać, że BBB u samic nie tylko uszczelnia się szybciej z wiekiem, ale prawdopodobnie również szybciej dojrzewa w porównaniu do samców. Uzyskane dane wskazują bowiem, że już w PND 15, samice charakteryzowały się większą gęstością naczyń EBA-IR w dSTR i HP niż samce. EBA to marker funkcjonalny BBB (Sternberger i Sternberger, 1987; Lin i wsp., 2001), którego ekspresja w mózgu szczura istotnie wzrasta od PND 14 do PND 28, kiedy to osiąga poziom właściwy dla osobników dorosłych (Argandoña i wsp., 2005).

Zgodnie z zaobserwowanymi w przedstawionych badaniach różnicami płciowymi, nieliczne prace kliniczne pokazują, że dorosłe kobiety charakteryzują się mniejszą przepuszczalnością BBB i bariery krew-płyn mózgowo-rdzeniowy niż mężczyźni (Castellazzi i wsp., 2020; Moon i wsp., 2021). Dane sugerują, że różnice te mogą wynikać z działania hormonów płciowych (Krause 2006). Wiadomo, że estrogeny mogą wpływać

protekcyjnie na funkcje BBB, działając przez obecne w BEC receptory estrogenowe (Zuloaga i wsp., 2012) i regiony promotorowe genów, zawierające elementy odpowiedzi na estrogeny, np. w genach kodujących TJP (Greene i wsp., 2020). Co więcej, wykazano, że 17β-estradiol odwracał zaburzenia BBB u samic szczura pozbawionych jajników oraz przekraczających wiek reprodukcyjny (Saija i wsp., 1990; Shi i Simpkins, 1997; Bake i Sohrabji, 2004; Kang i wsp., 2006). Niemniej jednak należy podkreślić, że w przedstawionych w dysertacji badaniach, różnice płciowe w funkcjonowaniu BBB dostrzegalne są jeszcze przed osiągnięciem dojrzałości płciowej przez zwierzęta, co sugeruje, że różnice te mogą być związane z płcią genetyczną i programowane w trakcie prenatalnej i okołoporodowej ekspozycji na hormony steroidowe (wczesna faza różnicowania płciowego mózgu) (Ngun i wsp., 2011; Czech i wsp., 2012). Dymorfizm płciowy BBB może potencjalnie determinować stopień przenikania do mózgu określonych patogenów i czynników cytotoksycznych, ale też glukozy i różnych leków (Dudek i wsp., 2021). Może także modulować przebieg reakcji neurozapalnej (Dudek i wsp., 2021). Zatem różnice płciowe w funkcjonowaniu BBB mogą leżeć u podstaw obserwowanych w klinice różnic płciowych w podatności na niektóre choroby psychiczne i neurodegeneracyjne, a także wpływać na sposoby ich leczenia (Dudek i wsp., 2021).

8.2 Wpływ MS na przepuszczalność i integralność BBB na różnych etapach ontogenezy

Badania zawarte w niniejszej rozprawie doktorskiej nie ujawniły spójnego ani jednoznacznie negatywnego wpływu MS na funkcjonowanie BBB. Jednak można wyszczególnić pewne specyficzne, zależne od wieku, regionu mózgu i płci, efekty działania ELS na parametry związane z BBB. Wyniki przedstawione w publikacji Solarz i wsp. (2021a) oraz wyniki badań dodatkowych wykazały, że MS zwiększała przepuszczalność BBB w dSTR (PND 15) i mPFC (PND 22) u młodych samców. Efekt ten był jednak przejściowy i nie utrzymał się do dorosłości. Niespodziewanie, zaburzeniom przepuszczalności w dSTR w PND 15 nie towarzyszyły zmiany w ekspresji genów kodujących TJP. Niemniej jednak zaobserwowano wzrost poziomu mRNA *Aqp4,* potencjalnego markera funkcji BBB, którego ekspresja zwykle wzrasta w trakcie rozszczelnienia BBB, np. przy obrzęku mózgu i udarze (Xu i wsp., 2019). Co ciekawe, badania dodatkowe w PND 15 wykazały również wzrost gęstości naczyń EBA-IR w mPFC

i dSTR u zwierząt MS niezależnie od płci. Wyniki te mogą wskazywać na odmienną dynamikę dojrzewania BBB i/lub na włączenie mechanizmów adaptacyjnych czy kompensacyjnych u zwierząt poddanych ELS.

Warto podkreślić, że znacznik zastosowany do badania szczelności BBB, NaF, to mała cząstka (376 Da), wykrywana w bardzo niskich stężeniach. Zatem wykorzystana w tej pracy doktorskiej metoda oceny przepuszczalności BBB jest wysoce czuła i ujawnia nawet nieznaczne zaburzenia integralności BBB i jej przepuszczalności dla małych cząstek. Wyniki zawarte w Solarz i wsp. (2021a) sugerują, że MS wywołuje raczej dyskretne zmiany w przepuszczalności BBB, nie obserwowano bowiem wzrostu poziomu białka S100β (o masie 10 kDa) w surowicy zwierząt MS. Wręcz przeciwnie, procedura MS obniżała stężenie tego markera zaburzeń integralności BBB. Efekt ten utrzymał się do dorosłości, ale tylko u samic. Może to ponownie sugerować indukcje zmian adaptacyjnych w odpowiedzi na ELS.

Dane literaturowe wskazują, że ekspozycja zwierząt dorosłych na ostry i chroniczny stres zwiększa przepuszczalność BBB (Santha i wsp., 2015; Menard i wsp., 2017; Xu i wsp., 2019; Taler i wsp., 2021; Dion-Albert i wsp., 2022b). Nieliczne dostępne dane dotyczące wpływu ELS na funkcje BBB pokazują wzrost jej przepuszczalności dla błękitu Evansa u szczurów w różnym wieku, ale bez znacznych różnic płciowych (Gomez-Gonzalez i Escobar, 2009; Carlessi i wsp., 2022). Podobnie jak w niniejszej pracy doktorskiej, Gomez-Gonzalez i Escobar (2009) wykazali, że wzrost przepuszczalności BBB wywołany przez ELS był przejściowy i niewidoczny już w okresie adolescencji. Co ciekawe, badania zawarte w publikacji Solarz i wsp. (2023), wykonane na innej kohorcie zwierząt i w innym układzie eksperymentalnym, ujawniły nawet specyficzne zmniejszenie przepuszczalności BBB w HP dorosłych zwierząt MS obu płci.

Większość badań przeprowadzonych w zwierzęcych modelach chronicznego stresu wykazało zmniejszenie ekspresji TJP i zaburzenia poziomów GLUT-1 głównie u dorosłych zwierząt (Welcome i Mastorakis, 2020). W badaniach zawartych w tej pracy doktorskiej nie wyróżnił się jednoznaczny wzorzec zmian wywołanych przez ELS w poziomie mRNA kluczowych elementów odpowiedzialnych za funkcjonowanie BBB. Pokrótce, w dorosłości procedura MS obniżyła ekspresję *Ocln* i *Slc2a1* w dSTR (Solarz i wsp., 2021a). Co więcej, wyłącznie u samic, MS trwale zmniejszyła poziom mRNA *Cldn3* w HP i mPFC (Solarz i wsp., 2021a). Z drugiej strony, zaobserwowano również trwały wzrost ekspresji *Cldn5* w dSTR i HP u zwierząt MS (Solarz i wsp., 2021a). Co ważne,

zwiększoną ekspresją mRNA TJP, szczególnie *Cldn5,* zwierzęta MS odpowiadały także na toczący się proces zapalny (Solarz i wsp., 2023).

Spośród TJP to właśnie CLDN5 odgrywa szczególną rolę w prawidłowym funkcjonowaniu BBB już na wczesnym etapie rozwoju mózgu (Abbott i wsp., 2010; Haseloff i wsp., 2015). Dodatkowo to CLDN5 kontroluje przenikanie parakomórkowe cząstek poniżej 800 Da (Abbott i wsp., 2010; Haseloff i wsp., 2015), do których zalicza się stosowany w opisanych badaniach NaF. Co ciekawe, ostatnie doniesienia literaturowe sugerują, że modulacja ekspresji CLDN5 może leżeć u podstaw podatności i/lub oporności na stres i depresję poprzez jej zaangażowanie w przebudowę i regulację funkcji naczyń mózgowych (Menard i wsp., 2017; Pearson-Leary i wsp., 2017; Dion-Albert i wsp., 2022b). Wykazano, że chroniczny stres przedłużonej izolacji społecznej zwiększał poziom mRNA *Cldn5* w HP dorosłych zwierząt (Alshammari i wsp., 2020), podobnie jak w prezentowanych badaniach nad ELS. Ponadto indukowana nadekspresja CLDN5 w ciele migdałowatym samic poddanych izolacji społecznej w dzieciństwie hamowała zachowania lękowe (Wu i wsp., 2022). Z drugiej strony, u pacjentów chorych na depresję zaobserwowano redukcję ekspresji CLDN5 w PFC i jądrze półleżącym przegrody (Dudek i wsp., 2020; Dion-Albert i wsp., 2022b). Ponadto w zwierzęcym modelu depresji opartym o przewlekły stres (ang. *chronic defeat stress*) wykazano, że redukcja poziomu CLDN5 i zwiększona przepuszczalność BBB w jądrze półleżącym przegrody występuje jedynie u myszy o fenotypie podatnym, a nie opornym na stres (Menard i wsp., 2017; Dion-Albert i wsp., 2022b). Dodatkowo warunkowe wyciszenie ekspresji *Cldn5* wystarczyło do wywołania zachowań przypominających depresję u myszy (Menard i wsp., 2017; Dion-Albert i wsp., 2022b). Natomiast, niską ekspresję represyjnego czynnika transkrypcyjnego związanego z *Cldn5* w BEC powiązano z opornością na stres (Dudek i wsp., 2020).

Biorąc pod uwagę powyższe dane można przypuszczać, że trwały wzrost ekspresji *Cldn5* obserwowany w niniejszej pracy doktorskiej może ogólnie chronić szczury MS przed znaczną dysfunkcją BBB i leżeć u podstaw zmian adaptacyjnych o nieznanych konsekwencjach neurofizjologicznych i behawioralnych. Warto w tym miejscu wspomnieć, że wieloletnie badania naszego zespołu nad zachowaniem zwierząt poddanych MS wykazały jej, zależny od wieku i płci, wpływ na zachowania przypominające depresję i lęk i sugerują, że samce są bardziej podatne na działanie ELS (Chocyk i wsp., 2013; Chocyk i wsp., 2015; Majcher-Maslanka i wsp., 2019; Solarz i wsp., 2021b; Solarz-Andrzejewska i wsp., 2023). Z drugiej strony, procedura MS zaburzała pamięć

o zdarzeniach awersyjnych i odpowiedź na podanie substancji psychostymulujących u obu płci (Chocyk i wsp., 2011b; Chocyk i wsp., 2014).

Podsumowując, uzyskane wyniki wskazują, że w warunkach podstawowych, stosowana procedura ELS nie wywołuje jednoznacznego czy negatywnego wpływu na funkcje BBB (zwłaszcza u samic). Na podstawie dostępnej literatury można przypuszczać, że wywołane przez MS zmiany w poziomie mRNA TJP, szczególnie wzrost ekspresji *Cldn5*, mogą świadczyć o wystąpieniu pewnych kompensacji/adaptacji na poziomie BBB, które mogą potencjalnie determinować jej odpowiedź funkcjonalną na działanie różnych czynników środowiskowych w późniejszym okresie życia. Powyższą hipotezę weryfikowano wykonując badania zawarte w publikacji Solarz i wsp. (2023).

8.3 Wpływ płci i MS na przebieg odpowiedzi zapalnej

W celu modelowania ogólnoustrojowego zapalenia u zwierząt, powszechnie stosuje się podanie LPS, endotoksyny, która stymuluje wrodzoną odpowiedź komórkową, a także może zaburzać integralność BBB oraz powodować zmiany w reaktywności mikrogleju (Varatharaj i Galea, 2017; Erickson i Banks, 2018). Między innymi dzięki takiemu modelowaniu dowiedziono, że na przestrzeni życia funkcjonowanie układu odpornościowego oraz odpowiedź zapalna może różnić się między płciami (Klein i Flanagan, 2016; Dudek i wsp., 2021). Przyjmuje się, że po osiągnięciu dojrzałości płciowej obwodowa odpowiedź zapalna u samic ssaków jest silniejsza niż u samców, dzięki czemu samice szybciej usuwają patogeny z organizmu i wykazują wyższą skuteczność szczepień. Równocześnie, przyczynia się to do większej podatności na schorzenia o podłożu zapalnym i autoimmunologicznym u samic (Schwarz i Bilbo, 2012; Klein i Flanagan, 2016; Dudek i wsp., 2021). Dane dotyczące różnic płciowych w odpowiedzi zapalnej OUN są mniej jednoznaczne (Schwarz i Bilbo, 2012; Villa i wsp., 2018; Posillico i wsp., 2021), choć różnicowanie płciowe mikrogleju we wczesnym okresie życia jest potwierdzone i dotyczy procesu kolonizacji oraz morfologii i reaktywności tych komórek (Schwarz i Bilbo, 2012; Bollinger i wsp., 2016).

Badania przedstawione w niniejszej pracy doktorskiej nie wykazały jednak istotnych różnic płciowych w poziomie obwodowych cytokin prozapalnych (szczególnie w warunkach podstawowych). U dorosłych zwierząt kontrolnych (AFR) zasadniczo nie obserwowano także różnic płciowych w odpowiedzi mózgu na podanie LPS (z wyjątkiem

ekspresji *Tlr4*) (Solarz i wsp., 2023). Zaobserwowano natomiast, że intensywność odpowiedzi neurozapalnej u zwierząt AFR w PND 22 zdecydowanie różniła się między płciami. 24 h po iniekcji LPS, młode samce AFR, w odróżnieniu od samic, nie wykazywały charakterystycznego zwiększenia ekspresji mRNA markerów neurozapalenia (IL-1β, ICAM1, TLR4 i markerów mikrogleju/makrofagów) w mPFC i HP oraz w obwodowym poziomie IL-1β. Uzyskane wyniki mogą wskazywać na słabszą odpowiedź zapalną u samców w tym okresie życia. Przeprowadzenie analizy parametrów zapalenia tylko w jednym punkcie czasowym (24 godziny po podaniu LPS), uniemożliwia jednak porównanie dynamiki odpowiedzi zapalnej między płciami. Zatem nie można wykluczyć, że różnice płciowe w odpowiedzi na LPS mogą wynikać z odmiennych dla każdej z płci ram czasowych odpowiedzi zapalnej (czas indukcji i ustąpienia procesów). Może wiązać się to również z odmienną dynamiką dojrzewania układu odpornościowego między płciami, przejawiającą się np. w poziomie ekspresji *Tlr4*. TLR4 jest receptorem rozpoznającym i wiążącym LPS, obecnym w mózgu, m.in. na komórkach mikrogleju i BEC, i aktywującym wrodzoną odpowiedź komórkową i uwalnianie cytokin prozapalnych (Trotta i wsp., 2014; Serna-Rodríguez i wsp., 2022). Warto podkreślić, że w badaniach zamieszczonych w publikacji Solarz i wsp. (2023), w warunkach podstawowych (podanie VEH), obserwowano wyższy poziom mRNA *Tlr4* w mPFC i HP samic w PND 22 niż u samców. Co więcej, tylko u samic (AFR) stymulacja LPS spowodowała wzrost ekspresji tego genu w PND 22 (mPFC, HP) i dorosłości (mPFC).

U dojrzałych płciowo zwierząt hormony płciowe odgrywają znaczną rolę w modulacji układu odpornościowego (Schwarz i Bilbo, 2012; Klein i Flanagan, 2016; Dudek i wsp., 2021). Po raz kolejny jednak badania zawarte w tej rozprawie doktorskiej pokazują, że różnice płciowe, tym razem dla odpowiedzi zapalnej, pojawiają się jeszcze przed osiągnięciem dojrzałości. Dostępne dane literaturowe wskazują, że różnice te mogą kształtować się w trakcie okołoporodowej ekspozycji na hormony steroidowe i być związane z płcią genetyczną (Schwarz i Bilbo, 2012; Klein i Flanagan, 2016; Villa i wsp., 2018; Dudek i wsp., 2021).

Co szczególnie istotne, w badaniach przedstawionych w publikacji Solarz i wsp. (2023), wykazano, że doświadczenie ELS moduluje odpowiedź zapalną wywołaną przez LPS również w sposób zależny od płci. W PND 22 procedura MS nasiliła lub też wydłużyła odpowiedź neurozapalną. Zjawisko to szczególnie zauważalne było u samców i przejawiało się zwiększoną ekspresją, np. *Icam1, Tlr4*, *Aif1* i *Itgam* w HP i/lub w mPFC wybiórczo u zwierząt stresowanych, ale nie kontrolnych. Co więcej, w surowicy samców

MS w PND 22 zaobserwowano ogólnie wyższy poziom CORT. Zgodnie z danymi literaturowymi wcześniejsza ekspozycja na GC lub stres może uwrażliwić, lub predysponować do reakcji prozapalnych (Frank i wsp., 2010; Loram i wsp., 2011). W tym samym okresie życia samice MS wykazywały bardziej zróżnicowany wzór odpowiedzi na LPS niż samce, choć warto podkreślić, że u obu płci obserwowaliśmy zwiększoną przepuszczalność BBB w mPFC i HP (główny efekt warunków hodowli). Co ciekawe, w dorosłości zwierzęta poddane procedurze MS okazały się mniej wrażliwe na podanie LPS niż te z grupy AFR, co szczególnie jest widoczne u samic. Ekspresja mRNA markerów neurozapalenia, np. *Il-1β* i *Aif1* (mPFC i HP), *Icam1* (mPFC), czy *Tnfα* (HP) u stresowanych samic nie ulegała w ogóle zmianie lub była niższa od tej obserwowanej u zwierząt AFR po podaniu LPS. Wyniki te mogą świadczyć o mniejszej intensywności lub o szybszym ustąpieniu odpowiedzi zapalnej u dorosłych samic MS.

Dostępne dane literaturowe, dotyczące modulującego wpływu ELS na przebieg procesów zapalnych indukowanych w późniejszym życiu, są bardzo niejednoznaczne (Avitsur i wsp., 2013; Saavedra i wsp., 2017; Gildawie i wsp., 2020; Nicolas i wsp., 2022). Wynika to prawdopodobnie z różnic metodycznych dotyczących modelowania ELS oraz schematu podań i dawkowania LPS. Wyniki zawarte w tej rozprawie doktorskiej po raz pierwszy pokazują spójne różnice płciowe i wiekowe w odpowiedzi zwierząt MS na immunostymulację. Jednocześnie, wskazują, że sama procedura MS (MS-VEH, warunki podstawowe) nie wpływała bardzo znacząco na poziom markerów stanu zapalnego (z wyjątkiem ekspresji *Tlr4* w mózgu). Wyniki te są zgodne z dostępnymi danymi literaturowymi (Dutcher i wsp., 2020).

Co ciekawe, badania zawarte w publikacji Solarz i wsp. 2023 wykazały niższy poziom ekspresji *Tlr4* w HP samic MS-VEH niż u samic kontrolnych (AFR-VEH) niezależnie od wieku. Ponadto, pod wpływem LPS, tylko u samic kontrolnych, a nie u stresowanych, wzrastał poziom tego receptora w mPFC (PND 70 i 22) i HP (PND 22). U samców MS obserwowano odwrotną regulację. Tylko samce MS (a nie AFR) odpowiadały na podanie LPS zwiększoną ekspresją *Tlr4* w mPFC, a w HP wykazywały ogólnie wyższy poziom mRNA *Tlr4* niż kontrole. Powyższa modulacja ekspresji *Tlr4* przez MS może odpowiadać za mniejszą u samic, a większą u samców, wrażliwość na podanie LPS. Wzrost ekspresji TLR4 obserwowano w modelach przewlekłego stresu, a także *post mortem* w tkance pacjentów cierpiących na dużą depresję (Garate i wsp., 2011; Figueroa-Hall i wsp., 2020; Zhang i wsp., 2020) . Wspólnie dane te sugerują, że regulacja

ścieżek sygnałowych związanych z TLR4 może stanowić ważny mechanizm podatności i/lub oporności na stres i choroby z nim związane.

Podsumowując, wyniki zawarte w publikacji Solarz i wsp. (2023) wskazują, że ELS ma potencjał do wywoływania zależnych od płci zmian adaptacyjnych w układzie odpornościowym, które mogą determinować siłę odpowiedzi organizmu na czynnik immunostymulujący w późniejszym okresie życia. Wspomniane zmiany adaptacyjne mogą wiązać się np. z regulacją ekspresji *Tlr4*.

8.4 Zależny od płci wpływ ELS na funkcje BBB i procesy zapalne - potencjalne konsekwencje i znaczenie

Procesy rozwoju i dojrzewania w mózgu nie ustają z chwilą narodzin, lecz trwają nieprzerwanie aż do okresu wczesnej dorosłości (Danese i Lewis, 2017). Dostępne dane pokazują, że po narodzinach wraz z mózgiem dojrzewa też układ odpornościowy (Danese i Lewis, 2017; Brenhouse i wsp., 2019; Dutcher i wsp., 2020). Działanie stresorów we wczesnym okresie postnatalnym i w okresie młodzieńczym może silnie interferować z powyższymi procesami i trwale wpływać na funkcjonowanie OUN. Strukturą mózgu o szczególnie wydłużonej trajektorii rozwojowej jest mPFC. Tuż przed i w trakcie okresu dojrzewania osobniczego mPFC przechodzi gwałtowną przebudowę morfologiczną i funkcjonalną, co czyni ją wyjątkowo wrażliwą na działanie ELS (Brenhouse i wsp., 2019). Zatem, zawarte w tej rozprawie doktorskiej wyniki badań, wykazujące znamienny wpływ MS na przepuszczalność BBB i przebieg procesów zapalnych u młodych zwierząt, w PND 15 i 22 (głównie u samców), wydają się szczególnie istotne dla zrozumienia wpływu ELS na dojrzewanie mózgu (Solarz i wsp., 2021a; Solarz i wsp., 2023).

Infekcje są powszechnymi przypadłościami występującymi przez cały okres życia, jednak infekcje OUN występują częściej u dzieci niż u dorosłych i niosą ze sobą poważne konsekwencje dla rozwoju mózgu (Danese i Lewis, 2017; Teixeira i wsp., 2020; Kim i wsp., 2022). Nasilona odpowiedź neurozapalna we wczesnym okresie postnatalnym, jak ta obserwowana w PND 22 u samców poddanych procedurze MS, może skutkować zmienioną reaktywnością mikrogleju lub z niej wynikać. Dane literaturowe potwierdzają, że ELS wpływa na morfologię komórek mikrogleju i zwiększa ich reaktywność w odpowiedzi na LPS u młodych zwierząt (Saavedra i wsp., 2017; Gildawie i wsp., 2020). Komórki te nie tylko odpowiadają za mechanizmy obronne mózgu, ale też za procesy

związane z jego dojrzewaniem i plastycznością synaptyczną. Biorą bowiem udział w neurorozwojowej apoptozie i redukcji synaps, co wiąże się z rearanżacją połączeń nerwowych (Selemon, 2013; Nikodemova i wsp., 2015; Brenhouse i wsp., 2019). Zaburzone funkcjonowanie mikrogleju może zatem silnie wpływać na procesy dojrzewania mózgu, szczególnie w mPFC. Może tym samym leżeć u podstaw np. zaburzeń apoptozy neuronów i procesów LTP w mPFC zwierząt MS w okresie adolescencji obserwowanych we wcześniejszych badaniach naszego zespołu (Chocyk i wsp., 2013; Majcher-Maslanka i wsp., 2019) oraz wiązać się ze specyficznymi zaburzeniami behawioralnymi występującymi w tym modelu (Chocyk i wsp., 2013; Chocyk i wsp., 2014; Majcher-Maslanka i wsp., 2019).

Obecnie, liczne dane pochodzące zarówno z badań przedklinicznych, jak i klinicznych wskazują, że wcześniejsze doświadczenie stresu, czy ekspozycja na GC mogą uwrażliwiać, bądź przygotować układ odpornościowy na działanie czynnika immunostymulującego i przez to determinować przebieg późniejszej odpowiedzi neurozapalnej (Frank i wsp., 2016; Kelly i wsp., 2018; Barrett i wsp., 2021). Postuluje się, że zjawisko indukowanej stresem sensytyzacji odpowiedzi prozapalnej oraz zaburzenia w obrębie BBB mogą wiązać się z predyspozycją do określonych chorób psychicznych i neurodegeneracyjnych (Frank i wsp., 2016; Profaci i wsp., 2020; Dudek i wsp., 2021). Warto podkreślić, że choroby te różnią się obrazem klinicznym oraz częstością występowania w zależności od płci (Pinares-Garcia i wsp., 2018). Chociaż jak dotąd nie wykazano wyraźnych i jednoznacznych różnić płciowych w podatności na ELS w modelach zwierzęcych, to wiele danych wskazuje, że samice mogą być bardziej odporne na zaburzenia funkcji poznawczych wywołane przez ELS (Loi i wsp., 2017; Reincke i Hanganu-Opatz, 2017). Wcześniejsze prace naszego zespołu (Chocyk i wsp., 2011a; Chocyk i wsp., 2015), jak i badania zawarte w tej rozprawie doktorskiej sugerują, że samice są mniej wrażliwe na skutki MS. Szczególnie uwidoczniło się to w publikacji Solarz i wsp. (2023), gdzie odpowiedź neurozapalna wywołana stymulacją LPS u samic MS (zwłaszcza dorosłych) była słabsza i/lub ustępowała szybciej w porównaniu do samców. Jak wspomniano w poprzednim rozdziale, u podstaw różnic płciowych we wrażliwości na podanie LPS może leżeć modulacja ekspresji *Tlr4*. Warto w tym miejscu przypomnieć, że TLR4 rozpoznaje nie tylko patogeny (PAMP), ale także alarminy (DAMP), uwalniane w trakcie stresu komórkowego, czy śmierci komórek. Aktywacja TLR4 z udziałem DAMP prowadzi do indukcji tzw. sterylnego zapalenia (Franklin i wsp., 2018; Serna-Rodríguez i wsp., 2022). Liczne badania przedkliniczne i kliniczne wskazują na zaangażowanie ścieżek

sygnałowych TLR4 i sterylnego zapalenia w patofizjologię stwardnienia rozsianego, AD, udaru, ale też zaburzeń depresyjnych i lękowych (Femenia i wsp., 2018; Nie i wsp., 2018; Figueroa-Hall i wsp., 2020).

Wyniki zawarte w niniejszej rozprawie doktorskiej wskazują, że działanie kolejnego obok ELS czynnika środowiskowego ujawniło dymorfizm płciowy odpowiedzi i potencjalnie korzystniejszy fenotyp związany z adaptacją u samic poddanych MS. Należy jednak podkreślić, że u dorosłych samców nie wystąpiło nasilenie reakcji neurozapalnej w porównaniu do grupy kontrolnej. Powyższe obserwacje pozostają w zgodzie z hipotezą tzw. inokulacji (szczepienia) stresem (ang. *stress inoculation*) oraz dopasowania/niedopasowania (ang. *match/mismatch)* (Andersen i Teicher, 2004; Gluckman i wsp., 2005; Parker i wsp., 2019; Qin i wsp., 2019). Hipotezy te, w przeciwieństwie do założenia, że stres predysponuje do nasilonej odpowiedzi na kolejne wyzwania środowiskowe (akumulacja) (McEwen, 1998), zakładają, że ekspozycja na umiarkowaną ilość stresorów, szczególnie we wczesnym okresie życia, może promować strategię lepszego radzenia sobie w sytuacji narażenia na kolejne czynniki w późniejszym życiu (Andersen i Teicher, 2004; Gluckman i wsp., 2005; Parker i wsp., 2019; Qin i wsp., 2019). Z drugiej strony, w przypadku samców MS badanych w PND 22 obserwowano wyraźne nasilenie odpowiedzi w modelu infekcji (Solarz i wsp., 2023). Zatem przedstawione badania sugerują, że charakter wpływu ELS na funkcjonowanie osobnika w dużej mierze zależy od specyficznych warunków środowiskowych i stopnia rozwoju mózgu/organizmu w danym momencie życia (modulowanego dodatkowo przez czynniki związane z płcią), które to razem mogą przyczyniać się do ujawnienia konkretnego typu zmian adaptacyjnych.

8.5 Białka rodziny HSP70, stres ER i UPR – poszukiwanie mechanizmów i biomarkerów podatności bądź oporności na ELS

Kolejnym i naturalnym etapem w poszukiwaniu mechanizmów leżących u podstaw obserwowanych już wcześniej w stosowanym modelu ELS zaburzeń na poziomie biochemicznym, plastyczności synaptycznej oraz behawioralnym (Chocyk i wsp., 2011a; Chocyk i wsp., 2011b; Chocyk i wsp., 2013; Chocyk i wsp., 2014) było przeprowadzenie przesiewowych badań ekspresji genów w mPFC metodą mikromacierzy cDNA. Jak już wspomniano, mPFC, z uwagi na wydłużony rozwój, jest szczególnie wrażliwa na ELS. Ponadto jest obszarem mózgu silnie związanym z patofizjologią zaburzeń nastroju

i lękowych oraz z rozwojem uzależnień (Brenhouse i wsp., 2013; Selemon, 2013; Teicher i wsp., 2022). Badania przesiewowe wykonane w PND 15 wskazały grupę genów silnie regulowanych przez MS, kodujących białka należące do rodziny białek HSP70, to jest *Hspa1b i Hspa5* (dane nieopublikowane i niezamieszczone w pracy doktorskiej). Białka te związane są z komórkową odpowiedzią stresową, zarówno bezpośrednio jako podstawowe elementy cytozolowej odpowiedzi HSP oraz jako białka uczestniczące w odpowiedzi na stres ER i UPR (Bengesser i wsp., 2016; Perner i Krüger, 2022; Serna-Rodríguez i wsp., 2022). Dzięki zaangażowaniu w powyższe procesy mają duży wpływ na przeżywalność komórek. Białka HSP70 należą także do alarmin (zawierają DAMP) i poprzez wiązanie z receptorami TLR mediują odpowiedź zapalną (Serna-Rodríguez i wsp., 2022). Są one także zaangażowane w procesy plastyczności synaptycznej, uczenia się i pamięci (Belenichev i wsp., 2023). Co ciekawe, doniesienia literaturowe wskazują również, że HSPA5 i HSPA1B mogą być potencjalnie związane z patofizjologią zaburzeń nastroju i lękowych (Kakiuchi i wsp., 2005; Le-Niculescu i wsp., 2011; Yang i wsp., 2013). Rezultaty badań przesiewowych oraz powyższe fakty zainspirowały nas do zweryfikowania hipotezy o modulującym wpływie MS na ekspresję HSPA5 i HSPA1B w mózgu (mPFC, HP) i we krwi na różnych etapach rozwoju, w kontekście poszukiwania potencjalnych biomarkerów zmian wywołanych przez ELS.

W publikacji Solarz i wsp. (2021b) wykazano, że procedura MS spowodowała wzrost poziomu mRNA HSPA1B we krwi i mPFC zwierząt na wczesnym etapie życia (PND 15 i 26). Efekt ten zaobserwowano też w mPFC samców w okresie adolescencji (PND 35) (Majcher-Maslanka i wsp., 2019). W mPFC i HP zwierząt badanych w PND 15 wykazano również znamienny wpływ MS na ekspresję białka HSPA1A/1B (99% podobieństwa form białka 1A i 1B uniemożliwia specyficzne oznaczenie HSPA1B za pomocą przeciwciał). Zwiększony poziom białka HSPA1A/1B utrzymywał się aż do dorosłości zwierząt stresowanych, ale tylko w przypadku mPFC (Solarz i wsp., 2021b). Zaobserwowano również trwały wzrost ekspresji mRNA HSPA5 we krwi oraz białka HSPA5 w HP zwierząt MS. Nie przeprowadzono analiz korelacyjnych, jednak powyższym zmianom w ekspresji HSP70 u zwierząt stresowanych towarzyszyły zaburzenia procesów LTP w mPFC (osłabienie) i HP (nasilenie) oraz zmniejszona lękliwość w teście jasnego/ciemnego pudełka sugerująca zwiększoną impulsywność zwierząt (szukanie nowości, podejmowanie ryzyka). Co ciekawe, w transgenicznym modelu myszy z trwałą nadekspresją HSP70 obserwowano spotęgowanie LTP w HP (Ammon-Treiber i wsp., 2008). Ponadto inni autorzy również zaobserwowali, że zwiększonej ekspresja *Hspa1b* w mPFC myszy

towarzyszy redukcja lęku (Hüttenrauch i wsp., 2016), a donosowe podania egzogennych HSPA1A/1B zmniejszały niepokój i zwiększały ciekawość u starzejących się myszy (Bobkova i wsp., 2015). Zatem wyniki przedstawione w tej rozprawie doktorskiej wskazują, że białka rodziny HSP70 mogą być potencjalnymi kandydatami na biomarkery zaburzeń związanych z ELS, niemniej potwierdzenie tej hipotezy wciąż wymaga szerszych badań.

Wzrost ekspresji HSP70, szczególnie HSPA5, obserwowany u młodych i dorosłych zwierząt poddanych MS, nasuwał przypuszczenie, iż procedura ta może indukować stres ER i UPR. Aktywację stresu ER i UPR obserwowano w zwierzęcych modelach ostrego (Ishisaka i wsp., 2011; Xie i wsp., 2014) i przewlekłego stresu (Jangra i wsp., 2017; Tang i wsp., 2018; Li i wsp., 2019). Powyższe fakty zainspirowały do podjęcia szeroko zakrojonych badań, których wyniki zaprezentowano w publikacji Solarz-Andrzejewska i wsp. (2023). Badania te nie wykazały silnego i jednoznacznego wpływu procedury MS na procesy stresu ER, UPR i apoptozy w mPFC zwierząt w badanych okresach rozwojowych (PND 15, 26 i 70), choć taki wpływ obserwowano u zwierząt w okresie adolescencji (PND 35) (Majcher-Maslanka i wsp., 2019). Zatem, zmiany wywołane przez MS w mPFC w dużej mierze zależą od okresu rozwojowego, a ich ujawnienie specyficznie w okresie adolescencji wiąże się prawdopodobnie z występującą wtedy silną i dynamiczną przebudową morfologiczno-funkcjonalną mPFC (Markham i wsp., 2007; Cressman i wsp., 2010; Nikolić i wsp., 2013). Warto podkreślić, że badania zawarte w publikacji Solarz-Andrzejewska i wsp. (2023) wykazały jednak modulujący wpływ wielokrotnych podań inhibitora stresu ER (SAL) i jego rozpuszczalnika (VEH) we wczesnym okresie postnatalnym na ekspresję markerów UPR i apoptozy oraz zachowanie zwierząt MS w późniejszym wieku. SAL jest inhibitorem fosfatazy eIF2α, który wykazuje działanie antyapoptotyczne i neuroprotekcyjne, m.in. w zwierzęcych modelach chorób neurodegeneracyjnych (Saxena i wsp., 2009; Godin i wsp., 2016) i uszkodzeń mózgu (Logsdon i wsp., 2016). Analiza biochemiczna wykazała, że zarówno podania SAL, jak i VEH zapobiegały niektórym efektom wywołanym przez MS i głównie osłabiały ekspresję mRNA markerów stresu ER i UPR. Na poziomie behawioralnym podania SAL i/lub VEH prowadziły zasadniczo do łagodzenia i normalizacji zaburzeń zachowania u zwierząt MS, szczególnie, zmniejszonej lękliwości, anhedonii, zaburzeń ekspresji warunkowanego strachu oraz nasilonej aktywności lokomotorycznej indukowanej podaniem amfetaminy. Niestety, zaobserwowanie modulującego wpływu zarówno podań SAL, jak i VEH znacznie utrudniło jednoznaczną interpretację otrzymanych wyników i częściowo poddaje

w wątpliwość specyficzność biologicznego działania SAL. Szczegółowo kwestie te zostały przedyskutowane w publikacji Solarz-Andrzejewska i wsp. (2023). Dostępne dane literaturowe wskazują, że zarówno ostre, jak i przewlekłe iniekcje rozpuszczalnika, jako typowe stresory, nie pozostają obojętne, lecz mogą modulować poziom GC w surowicy oraz wpływać na zachowanie zwierząt (Lapin, 1995; Deutsch-Feldman i wsp., 2015; Freiman i wsp., 2016; Du Preez i wsp., 2020). Jak już wspomniano w poprzednim rozdziale, ekspozycja na stresory o średnim natężeniu, szczególnie we wczesnym okresie życia, może promować strategię lepszego radzenia sobie z czynnikami środowiskowymi w późniejszym życiu (szczepienie stresem) (Parker i wsp., 2019; Qin i wsp., 2019). Badania zawarte w tej rozprawie doktorskiej sugerują, że u podstaw molekularnych takiego zjawiska może leżeć modulacja procesów stresu ER i UPR. Istnieje bowiem hipoteza, że procesy te są mediatorami między- i wewnątrzgatunkowej zmienności w odpowiedzi na środowisko. Ich intensywność jest dziedziczna, podlega naturalnej selekcji i dzięki temu może kształtować mechanizmy podatności i oporności na działanie stresorów czy rozwój chorób (Yap i wsp., 2021).

W ocenie skutków podań VEH nie można pominąć potencjalnego biologicznego wpływu specyficznego rozpuszczalnika, tj. dimetylosulfotlenku (DMSO), stosowanego w przedstawionych badaniach. Nawet jeśli DMSO jest rutynowo stosowany jako rozpuszczalnik wielu substancji w badaniach podstawowych, to warto pamiętać, iż dane literaturowe pokazują zarówno pozytywny, jak i negatywny jego wpływ na funkcje mózgu (Farkas i wsp., 2004; Hanslick i wsp., 2009; Rabow i wsp., 2021).

Jak już wspomniano, białka HSP70, ale też stres ER i UPR pełnią ważną funkcję w kontroli wielu procesów w OUN, w tym w utrzymaniu proteostazy. Co więcej, ścieżki molekularne stresu komórkowego zaangażowane są także w regulację procesów zapalnych i funkcji BBB (Fernández i wsp., 2021; Diaz-Hung i Hetz, 2022; Serna-Rodríguez i wsp., 2022). Nieprawidłowości w kontroli tych procesów mogą przekładać się na zaburzenia poznawcze, motoryczne oraz szerzej psychiczne i neurodegeneracyjne (Fernández i wsp., 2021; Diaz-Hung i Hetz, 2022). Jednak odpowiedź HSP, stres ER i UPR nie są specyficzne tylko dla OUN, lecz rozpowszechnione są w większości komórek i tkanek i związane również z patofizjologią takich schorzeń jak nowotwory, cukrzyca czy miażdżyca (Kakiuchi i wsp., 2005; Chaudhari i wsp., 2014; Mohan i wsp., 2019). Badania kliniczne i epidemiologiczne wskazują, że ELS przyczynia się (często jednocześnie) do problemów ze zdrowiem zarówno psychicznym, jak i fizycznym, w tym do rozwinięcia zespołu metabolicznego prowadzącego do chorób układu krążenia i cukrzycy typu 2 (Murphy i

wsp., 2017). Wydaje się zatem, że procesy stresu ER, UPR i odpowiedź HSP mogą stanowić wspólne ścieżki molekularne i mechanizmy leżące u podstaw współwystępowania chorób psychicznych, sercowo-naczyniowych i metabolicznych u osób doświadczonych ELS. Zrozumienie powyższych mechanizmów i wskazanie związanych z nimi biomarkerów w znacznym stopniu ułatwiłoby rozwój skutecznych środków zapobiegawczych i terapeutycznych. Niemnie jednak wciąż istnieje potrzeba zakrojonych na szeroką skalę badań wielonarządowych, aby potwierdzić tę interesującą hipotezę. Co warte podkreślenia, takie badania zostały już rozpoczęte (Mariani i wsp., 2021).

9. Wnioski końcowe i znaczenie prowadzonych badań

Badania zawarte w rozprawie doktorskiej wykazały, że wpływ ELS na integralność i funkcje BBB oraz przebieg procesów zapalnych w dużej mierze zależy od regionu mózgu, płci oraz wieku zwierząt. W warunkach podstawowych procedura MS nie wywołuje jednoznacznie negatywnych zmian tych parametrów, choć samce we wczesnym okresie postnatalnym wykazują większą wrażliwość na działanie stresu niż samice. To ekspozycja na kolejny czynnik środowiskowy (infekcje) powoduje wyraźną zmianę odpowiedzi u tych zwierząt, decydując tym samym o ostatecznym charakterze wpływu ELS w danym okresie życia. Podjęcie kwestii różnic płciowych pozwoliło wykazać, że stresowane we wczesnym okresie życia samice słabiej odpowiadają na kolejny czynnik środowiskowy (LPS), co może świadczyć o aktywacji właśnie u samic specyficznych mechanizmów adaptacji i/lub oporności na stres.

Ponadto wykazano udział odpowiedzi stresu komórkowego (stresu ER, odpowiedź HSP i UPR) w patofizjologii i wrażliwości na ELS u samców.

Otrzymane wyniki wskazują, że neurobiologiczne mechanizmy kształtujące podatność/oporność na działanie ELS mogą wiązać się m.in. z regulacją: (i) ekspresji *Cldn5* i *Tlr4*, (ii) ścieżek sygnałowych TLR4, również tych związanych ze sterylnym zapaleniem indukowanym przez alarminy (np. HSP70), (iii) procesów stresu ER i UPR.

Realizacja badań składających się na tę rozprawę doktorską pozwoliła na poszerzenie wiedzy na temat ELS jako potencjalnego czynnika etiologicznego zaburzeń zdrowia fizycznego i psychicznego. Co więcej, przeprowadzone badania zaowocowały wytypowaniem kandydatów na obwodowo-mózgowe biomarkery zmian związanych

z ELS (białka z rodziny HSP70), co potencjalnie może zainspirować także innych badaczy do poszukiwania uniwersalnych biomarkerów ELS i chorób z nim związanych w różnych układach narządów, nie tylko w mózgu. Może to przyczynić się w przyszłości do wdrożenia wczesnej diagnostyki i profilaktyki klinicznej u dzieci i młodzieży doświadczonej przez ELS. Dramatycznie wzrastająca obecnie liczba diagnozowanych przypadków chorób psychicznych właśnie w tej grupie społecznej powoduje, że eliminacja zdarzeń awersyjnych we wczesnym okresie życia powinna być priorytetem społecznym i ekonomicznym. Przedstawione wyniki i publikacje mogą zatem przyczynić się również do zwiększenia społecznej wrażliwości na krzywdę dzieci oraz świadomości długotrwałych konsekwencji ELS, zarówno dla zdrowia psychicznego, jak i fizycznego.

10. Bibliografia

Abbott, N.J., Patabendige, A.A., Dolman, D.E., Yusof, S.R. & Begley, D.J. (2010) Structure and function of the blood-brain barrier. *Neurobiol Dis*, **37**, 13-25.

Alshammari, T.K., Alghamdi, H.M., Alduhailan, H.E., Saja, M.F., Alrasheed, N.M. & Alshammari, M.A. (2020) Examining the central effects of chronic stressful social isolation on rats. *Biomedical reports*, **13**, 56.

Alvarez, J.I., Katayama, T. & Prat, A. (2013) Glial influence on the blood brain barrier. *Glia*, **61**, 1939-1958.

Ammon-Treiber, S., Grecksch, G., Angelidis, C., Vezyraki, P., Höllt, V. & Becker, A. (2008) Emotional and learning behaviour in mice overexpressing heat shock protein 70. *Neurobiology of learning and memory*, **90**, 358-364.

Andersen, S.L. & Teicher, M.H. (2004) Delayed effects of early stress on hippocampal development. *Neuropsychopharmacol*, **29**, 1988-1993.

Argandoña, E.G., Bengoetxea, H. & Lafuente, J.V. (2005) Lack of experience-mediated differences in the immunohistochemical expression of blood-brain barrier markers (EBA and GluT-1) during the postnatal development of the rat visual cortex. *Brain research. Developmental brain research*, **156**, 158-166.

Arora, P., Sagar, R., Mehta, M., Pallavi, P., Sharma, S. & Mukhopadhyay, A.K. (2019) Serum S100B levels in patients with depression. *Indian journal of psychiatry*, **61**, 70-76.

Avitsur, R., Maayan, R. & Weizman, A. (2013) Neonatal stress modulates sickness behavior: Role for proinflammatory cytokines. *Journal of neuroimmunology*, **257**, 59-66.

Bake, S. & Sohrabji, F. (2004) 17beta-estradiol differentially regulates blood-brain barrier permeability in young and aging female rats. *Endocrinology*, **145**, 5471-5475.

Barlow, B.K., Cory-Slechta, D.A., Richfield, E.K. & Thiruchelvam, M. (2007) The gestational environment and Parkinson's disease: evidence for neurodevelopmental origins of a neurodegenerative disorder. *Reproductive toxicology (Elmsford, N.Y.)*, **23**, 457-470.

Barrett, T.J., Corr, E.M., van Solingen, C., Schlamp, F., Brown, E.J., Koelwyn, G.J., Lee, A.H., Shanley, L.C., Spruill, T.M., Bozal, F., de Jong, A., Newman, A.A.C., Drenkova, K., Silvestro, M., Ramkhelawon, B., Reynolds, H.R., Hochman, J.S., Nahrendorf, M., Swirski, F.K., Fisher, E.A., Berger, J.S. & Moore, K.J. (2021) Chronic stress primes innate immune responses in mice and humans. *Cell Rep*, **36**, 109595.

Bauer, M.E. & Teixeira, A.L. (2021) Neuroinflammation in Mood Disorders: Role of Regulatory Immune Cells. *Neuroimmunomodulation*, **28**, 99-107.

Baxter, J.D. & Forsham, P.H. (1972) Tissue Effects of Glucocorticoids. *Am J Med*, **53**, 573-+.

Belenichev, I.F., Aliyeva, O.G., Popazova, O.O. & Bukhtiyarova, N.V. (2023) Involvement of heat shock proteins HSP70 in the mechanisms of endogenous neuroprotection: the prospect of using HSP70 modulators. *Frontiers in cellular neuroscience*, **17**, 1131683.

Bengesser, S.A., Fuchs, R., Lackner, N., Birner, A., Reininghaus, B., Meier-Allard, N., Stracke, A., Kapfhammer, H.P., Reininghaus, E.Z. & Wallner-Liebmann, S. (2016) Endoplasmic Reticulum Stress and Bipolar Disorder - Almost Forgotten Therapeutic Drug Targets in the Unfolded Protein Response Pathway Revisited. *CNS Neurol Disord Drug Targets*, **15**, 403-413.

Blanchette, M. & Daneman, R. (2015) Formation and maintenance of the BBB. *Mechanisms of development*, **138 Pt 1**, 8-16.

Bobkova, N.V., Evgen'ev, M., Garbuz, D.G., Kulikov, A.M., Morozov, A., Samokhin, A., Velmeshev, D., Medvinskaya, N., Nesterova, I., Pollock, A. & Nudler, E. (2015) Exogenous Hsp70 delays senescence and improves cognitive function in aging mice. *Proceedings of the National Academy of Sciences of the United States of America*, **112**, 16006-16011.

Bollinger, J.L., Bergeon Burns, C.M. & Wellman, C.L. (2016) Differential effects of stress on microglial cell activation in male and female medial prefrontal cortex. *Brain, behavior, and immunity*, **52**, 88-97.

Bown, C., Wang, J.F., MacQueen, G. & Young, L.T. (2000) Increased temporal cortex ER stress proteins in depressed subjects who died by suicide. *Neuropsychopharmacol*, **22**, 327-332.

Brenhouse, H.C., Danese, A. & Grassi-Oliveira, R. (2019) Neuroimmune Impacts of Early-Life Stress on Development and Psychopathology. *Curr Top Behav Neurosci*, **43**, 423-447.

Brenhouse, H.C., Lukkes, J.L. & Andersen, S.L. (2013) Early life adversity alters the developmental profiles of addiction-related prefrontal cortex circuitry. *Brain sciences*, **3**, 143-158.

Brydges, N.M. & Reddaway, J. (2020) Neuroimmunological effects of early life experiences. *Brain Neurosci Adv*, **4**, 2398212820953706.

Brzezinska K. , Z.M. (2012) Struktura i funkcje bariery krew-mózg. *Postepy Biologii Komorki*, **39**, 87-102.

Butt, A.M., Jones, H.C. & Abbott, N.J. (1990) Electrical resistance across the blood-brain barrier in anaesthetized rats: a developmental study. *J Physiol*, **429**, 47-62.

Caley, D.W. & Maxwell, D.S. (1970) Development of the blood vessels and extracellular spaces during postnatal maturation of rat cerebral cortex. *The Journal of comparative neurology*, **138**, 31-47.

Carlessi, A.S., Botelho, M.E.M., Manosso, L.M., Borba, L.A., Maciel, L.R., Andrade, N.M., Martinello, N.S., Padilha, A.P.Z., Generoso, C.M., Bencke, C.V., de Moura, A.B., Lodetti, B.F., Collodel, A., Joaquim, L., Bonfante, S., Biehl, E., Generoso, J.S., Arent, C.O., Barichello, T., Petronilho, F., Quevedo, J. & Réus, G.Z. (2022) Sex differences on the response to antidepressants and psychobiotics following early life stress in rats. *Pharmacology, biochemistry, and behavior*, **220**, 173468.

Cassella, J.P., Lawrenson, J.G., Lawrence, L. & Firth, J.A. (1997) Differential distribution of an endothelial barrier antigen between the pial and cortical microvessels of the rat. *Brain research*, **744**, 335-338.

Castellazzi, M., Morotti, A., Tamborino, C., Alessi, F., Pilotto, S., Baldi, E., Caniatti, L.M., Trentini, A., Casetta, I., Granieri, E., Pugliatti, M., Fainardi, E. & Bellini, T. (2020) Increased age and male sex are independently associated with higher frequency of blood-cerebrospinal fluid barrier dysfunction using the albumin quotient. *Fluids Barriers CNS*, **17**, 14.

Catale, C., Gironda, S., Lo Iacono, L. & Carola, V. (2020) Microglial Function in the Effects of Early-Life Stress on Brain and Behavioral Development. *J Clin Med*, **9**.

Chaudhari, N., Talwar, P., Parimisetty, A., Lefebvre d'Hellencourt, C. & Ravanan, P. (2014) A molecular web: endoplasmic reticulum stress, inflammation, and oxidative stress. *Frontiers in cellular neuroscience*, **8**, 213.

Chocyk, A., Bobula, B., Dudys, D., Przyborowska, A., Majcher-Maslanka, I., Hess, G. & Wedzony, K. (2013) Early-life stress affects the structural and functional plasticity of the medial prefrontal cortex in adolescent rats. *Eur J Neurosci*, **38**, 2089-2107.

Chocyk, A., Dudys, D., Przyborowska, A., Mackowiak, M. & Wedzony, K. (2010) Impact of maternal separation on neural cell adhesion molecules expression in dopaminergic brain regions of juvenile, adolescent and adult rats. *Pharmacological reports : PR*, **62**, 1218-1224.

Chocyk, A., Dudys, D., Przyborowska, A., Majcher, I., Mackowiak, M. & Wedzony, K. (2011a) Maternal separation affects the number, proliferation and apoptosis of glia cells in the substantia nigra and ventral tegmental area of juvenile rats. *Neuroscience*, **173**, 1-18.

Chocyk, A., Majcher-Maslanka, I., Przyborowska, A., Mackowiak, M. & Wedzony, K. (2015) Early-life stress increases the survival of midbrain neurons during postnatal development and enhances reward-related and anxiolytic-like behaviors in a sex-dependent fashion. *Int J Dev Neurosci*, **44**, 33-47.

Chocyk, A., Przyborowska, A., Dudys, D., Majcher, I., Mackowiak, M. & Wedzony, K. (2011b) The impact of maternal separation on the number of tyrosine hydroxylase-

expressing midbrain neurons during different stages of ontogenesis. *Neuroscience*, **182**, 43-61.

Chocyk, A., Przyborowska, A., Makuch, W., Majcher-Maslanka, I., Dudys, D. & Wedzony, K. (2014) The effects of early-life adversity on fear memories in adolescent rats and their persistence into adulthood. *Behav Brain Res*, **264**, 161-172.

Cirulli, F., Francia, N., Berry, A., Aloe, L., Alleva, E. & Suomi, S.J. (2009) Early life stress as a risk factor for mental health: role of neurotrophins from rodents to non-human primates. *Neuroscience and biobehavioral reviews*, **33**, 573-585.

Cornford, E.M., Hyman, S. & Pardridge, W.M. (1993) An electron microscopic immunogold analysis of developmental up-regulation of the blood-brain barrier GLUT1 glucose transporter. *J Cereb Blood Flow Metab*, **13**, 841-854.

Cressman, V.L., Balaban, J., Steinfeld, S., Shemyakin, A., Graham, P., Parisot, N. & Moore, H. (2010) Prefrontal cortical inputs to the basal amygdala undergo pruning during late adolescence in the rat. *The Journal of comparative neurology*, **518**, 2693-2709.

Cunnea, P., Mháille, A.N., McQuaid, S., Farrell, M., McMahon, J. & FitzGerald, U. (2011) Expression profiles of endoplasmic reticulum stress-related molecules in demyelinating lesions and multiple sclerosis. *Multiple sclerosis (Houndmills, Basingstoke, England)*, **17**, 808-818.

Czech, D.P., Lee, J., Sim, H., Parish, C.L., Vilain, E. & Harley, V.R. (2012) The human testis-determining factor SRY localizes in midbrain dopamine neurons and regulates multiple components of catecholamine synthesis and metabolism. *J Neurochem*, **122**, 260-271.

da Fonseca, A.C., Matias, D., Garcia, C., Amaral, R., Geraldo, L.H., Freitas, C. & Lima, F.R. (2014) The impact of microglial activation on blood-brain barrier in brain diseases. *Frontiers in cellular neuroscience*, **8**, 362.

Daneman, R., Zhou, L., Kebede, A.A. & Barres, B.A. (2010) Pericytes are required for blood-brain barrier integrity during embryogenesis. *Nature*, **468**, 562-566.

Danese, A. & Lewis, S.J. (2017) Psychoneuroimmunology of Early-Life Stress: The Hidden Wounds of Childhood Trauma? *Neuropsychopharmacol*, **42**, 99-114.

Daskalakis, N.P., Bagot, R.C., Parker, K.J., Vinkers, C.H. & de Kloet, E.R. (2013) The three-hit concept of vulnerability and resilience: toward understanding adaptation to early-life adversity outcome. *Psychoneuroendocrinology*, **38**, 1858-1873.

Deutsch-Feldman, M., Picetti, R., Seip-Cammack, K., Zhou, Y. & Kreek, M.J. (2015) Effects of handling and vehicle injections on adrenocorticotropic and corticosterone concentrations in Sprague-Dawley compared with Lewis rats. *J Am Assoc Lab Anim Sci*, **54**, 35-39.

Diaz-Hung, M.L. & Hetz, C. (2022) Proteostasis and resilience: on the interphase between individual's and intracellular stress. *Trends Endocrinol Metab*, **33**, 305-317.

Dion-Albert, L., Bandeira Binder, L., Daigle, B., Hong-Minh, A., Lebel, M. & Menard, C. (2022a) Sex differences in the blood–brain barrier: Implications for mental health. *Frontiers in Neuroendocrinology*, **65**, 100989.

Dion-Albert, L., Cadoret, A., Doney, E., Kaufmann, F.N., Dudek, K.A., Daigle, B., Parise, L.F., Cathomas, F., Samba, N., Hudson, N., Lebel, M., Signature, C., Campbell, M., Turecki, G., Mechawar, N. & Menard, C. (2022b) Vascular and blood-brain barrier-related changes underlie stress responses and resilience in female mice and depression in human tissue. *Nat Commun*, **13**, 164.

Disdier, C. & Stonestreet, B.S. (2019) Blood–Brain Barrier *Stress: Physiology, Biochemistry, and Pathology*, pp. 325-336.

Dowlati, Y., Herrmann, N., Swardfager, W., Liu, H., Sham, L., Reim, E.K. & Lanctôt, K.L. (2010) A meta-analysis of cytokines in major depression. *Biological psychiatry*, **67**, 446-457.

Du Preez, A., Law, T., Onorato, D., Lim, Y.M., Eiben, P., Musaelyan, K., Egeland, M., Hye, A., Zunszain, P.A., Thuret, S., Pariante, C.M. & Fernandes, C. (2020) The type of stress matters: repeated injection and permanent social isolation stress in male mice have a differential effect on anxiety- and depressive-like behaviours, and associated biological alterations. *Translational psychiatry*, **10**, 325.

Dudek, K.A., Dion-Albert, L., Kaufmann, F.N., Tuck, E., Lebel, M. & Menard, C. (2021) Neurobiology of resilience in depression: immune and vascular insights from human and animal studies. *Eur J Neurosci*, **53**, 183-221.

Dudek, K.A., Dion-Albert, L., Lebel, M., LeClair, K., Labrecque, S., Tuck, E., Ferrer Perez, C., Golden, S.A., Tamminga, C. & Turecki, G. (2020) Molecular adaptations of the blood–brain barrier promote stress resilience vs. depression. *Proceedings of the National Academy of Sciences*, **117**, 3326-3336.

Dutcher, E.G., Pama, E.A.C., Lynall, M.E., Khan, S., Clatworthy, M.R., Robbins, T.W., Bullmore, E.T. & Dalley, J.W. (2020) Early-life stress and inflammation: A systematic review of a key experimental approach in rodents. *Brain Neurosci Adv*, **4**, 2398212820978049.

Ek, C.J., Wong, A., Liddelow, S.A., Johansson, P.A., Dziegielewska, K.M. & Saunders, N.R. (2010) Efflux mechanisms at the developing brain barriers: ABC-transporters in the fetal and postnatal rat. *Toxicology letters*, **197**, 51-59.

Erickson, M.A. & Banks, W.A. (2013) Blood-brain barrier dysfunction as a cause and consequence of Alzheimer's disease. *J Cereb Blood Flow Metab*, **33**, 1500-1513.

Erickson, M.A. & Banks, W.A. (2018) Neuroimmune Axes of the Blood-Brain Barriers and Blood-Brain Interfaces: Bases for Physiological Regulation, Disease States, and Pharmacological Interventions. *Pharmacological reviews*, **70**, 278-314.

Farkas, E., Institoris, A., Domoki, F., Mihaly, A., Luiten, P.G. & Bari, F. (2004) Diazoxide and dimethyl sulphoxide prevent cerebral hypoperfusion-related learning dysfunction and brain damage after carotid artery occlusion. *Brain Res*, **1008**, 252-260.

Faucheux, B.A., Bonnet, A.M., Agid, Y. & Hirsch, E.C. (1999) Blood vessels change in the mesencephalon of patients with Parkinson's disease. *Lancet (London, England)*, **353**, 981-982.

Femenia, T., Qian, Y., Arentsen, T., Forssberg, H. & Heijtz, R.D. (2018) Toll-like receptor-4 regulates anxiety-like behavior and DARPP-32 phosphorylation. *Brain Behavior and Immunity*, **69**, 273-282.

Fernández, D., Geisse, A., Bernales, J.I., Lira, A. & Osorio, F. (2021) The Unfolded Protein Response in Immune Cells as an Emerging Regulator of Neuroinflammation. *Frontiers in aging neuroscience*, **13**, 682633.

Figueroa-Hall, L.K., Paulus, M.P. & Savitz, J. (2020) Toll-Like Receptor Signaling in Depression. *Psychoneuroendocrinology*, **121**, 104843.

Frank, M.G., Miguel, Z.D., Watkins, L.R. & Maier, S.F. (2010) Prior exposure to glucocorticoids sensitizes the neuroinflammatory and peripheral inflammatory responses to E. coli lipopolysaccharide. *Brain, behavior, and immunity*, **24**, 19-30.

Frank, M.G., Weber, M.D., Watkins, L.R. & Maier, S.F. (2016) Stress-induced neuroinflammatory priming: A liability factor in the etiology of psychiatric disorders. *Neurobiol Stress*, **4**, 62-70.

Franklin, T.C., Xu, C. & Duman, R.S. (2018) Depression and sterile inflammation: Essential role of danger associated molecular patterns. *Brain, behavior, and immunity*, **72**, 2-13.

Freiman, S.V., Onufriev, M.V., Stepanichev, M.Y., Moiseeva, Y.V., Lazareva, N.A. & Gulyaeva, N.V. (2016) The stress effects of a single injection of isotonic saline solution: systemic (blood) and central (frontal cortex and dorsal and ventral hippocampus). *Neurochem J+*, **10**, 115-119.

Garate, I., Garcia-Bueno, B., Madrigal, J.L.M., Bravo, L., Berrocoso, E., Caso, J.R., Mico, J.A. & Leza, J.C. (2011) Origin and consequences of brain Toll-like receptor 4 pathway stimulation in an experimental model of depression. *Journal of neuroinflammation*, **8**.

Gazzolo, D., Michetti, F., Bruschettini, M., Marchese, N., Lituania, M., Mangraviti, S., Pedrazzi, E. & Bruschettini, P. (2003) Pediatric Concentrations of S100B Protein in Blood: Age- and Sex-related Changes. *Clinical Chemistry*, **49**, 967-970.

Gildawie, K.R., Orso, R., Peterzell, S., Thompson, V. & Brenhouse, H.C. (2020) Sex differences in prefrontal cortex microglia morphology: Impact of a two-hit model of adversity throughout development. *Neurosci Lett*, **738**, 135381.

Gluckman, P.D., Hanson, M.A. & Pinal, C. (2005) The developmental origins of adult disease. *Maternal & child nutrition*, **1**, 130-141.

Godin, J.D., Creppe, C., Laguesse, S. & Nguyen, L. (2016) Emerging Roles for the Unfolded Protein Response in the Developing Nervous System. *Trends Neurosci*, **39**, 394-404.

Gomez-Gonzalez, B. & Escobar, A. (2009) Altered functional development of the blood-brain barrier after early life stress in the rat. *Brain Res Bull*, **79**, 376-387.

Greene, C., Hanley, N. & Campbell, M. (2020) Blood-brain barrier associated tight junction disruption is a hallmark feature of major psychiatric disorders. *Translational psychiatry*, **10**, 373.

Gulen, B., Serinken, M., Eken, C., Karcioglu, O., Kucukdagli, O.T., Kilic, E., Akpinar, G., Nogay, S. & Kuh, M. (2016) Serum S100B as a Surrogate Biomarker in the Diagnoses of Burnout and Depression in Emergency Medicine Residents. *Acad Emerg Med*, **23**, 786-789.

Hanin, I. (1996) The Gulf War, stress and a leaky blood-brain barrier. *Nat Med*, **2**, 1307-1308.

Hanslick, J.L., Lau, K., Noguchi, K.K., Olney, J.W., Zorumski, C.F., Mennerick, S. & Farber, N.B. (2009) Dimethyl sulfoxide (DMSO) produces widespread apoptosis in the developing central nervous system. *Neurobiol Dis*, **34**, 1-10.

Haseloff, R.F., Dithmer, S., Winkler, L., Wolburg, H. & Blasig, I.E. (2015) Transmembrane proteins of the tight junctions at the blood-brain barrier: structural and functional aspects. *Semin Cell Dev Biol*, **38**, 16-25.

Hawkins, B.T. & Davis, T.P. (2005) The blood-brain barrier/neurovascular unit in health and disease. *Pharmacological reviews*, **57**, 173-185.

Ho, D.H., Burch, M.L., Musall, B., Musall, J.B., Hyndman, K.A. & Pollock, J.S. (2016) Early life stress in male mice induces superoxide production and endothelial dysfunction in adulthood. *American journal of physiology. Heart and circulatory physiology*, **310**, H1267-1274.

Hoeijmakers, L., Ruigrok, S.R., Amelianchik, A., Ivan, D., van Dam, A.M., Lucassen, P.J. & Korosi, A. (2017) Early-life stress lastingly alters the neuroinflammatory response to amyloid pathology in an Alzheimer's disease mouse model. *Brain, behavior, and immunity*, **63**, 160-175.

Hoozemans, J.J., van Haastert, E.S., Eikelenboom, P., de Vos, R.A., Rozemuller, J.M. & Scheper, W. (2007) Activation of the unfolded protein response in Parkinson's disease. *Biochem Biophys Res Commun*, **354**, 707-711.

Hüttenrauch, M., Salinas, G. & Wirths, O. (2016) Effects of Long-Term Environmental Enrichment on Anxiety, Memory, Hippocampal Plasticity and Overall Brain Gene Expression in C57BL6 Mice. *Front Mol Neurosci*, **9**, 62.

Ilchmann-Diounou, H., Olier, M., Lencina, C., Riba, A., Barretto, S., Nankap, M., Sommer, C., Guillou, H., Ellero-Simatos, S., Guzylack-Piriou, L., Théodorou, V. & Ménard, S. (2019) Early life stress induces type 2 diabetes-like features in ageing mice. *Brain, behavior, and immunity*, **80**, 452-463.

Ishisaka, M., Kudo, T., Shimazawa, M., Kakefuda, K., Oyagi, A., Hyakkoku, K., Tsuruma, K. & Hara, H. (2011) Restraint-Induced Expression of Endoplasmic Reticulum Stress-Related Genes in the Mouse Brain. *Pharmacology & Pharmacy*, **2**, 10-16.

Italia, M., Forastieri, C., Longaretti, A., Battaglioli, E. & Rusconi, F. (2020) Rationale, Relevance, and Limits of Stress-Induced Psychopathology in Rodents as Models for Psychiatry Research: An Introductory Overview. *Int J Mol Sci*, **21**.

Jangra, A., Sriram, C.S., Dwivedi, S., Gurjar, S.S., Hussain, M.I., Borah, P. & Lahkar, M. (2017) Sodium Phenylbutyrate and Edaravone Abrogate Chronic Restraint Stress-Induced Behavioral Deficits: Implication of Oxido-Nitrosative, Endoplasmic Reticulum Stress Cascade, and Neuroinflammation. *Cellular and molecular neurobiology*, **37**, 65-81.

Joëls, M., Karst, H. & Sarabdjitsingh, R.A. (2018) The stressed brain of humans and rodents. *Acta physiologica (Oxford, England)*, **223**, e13066.

Joëls, M., Sarabdjitsingh, R.A. & Karst, H. (2012) Unraveling the time domains of corticosteroid hormone influences on brain activity: rapid, slow, and chronic modes. *Pharmacological reviews*, **64**, 901-938.

Kakiuchi, C., Ishiwata, M., Nanko, S., Kunugi, H., Minabe, Y., Nakamura, K., Mori, N., Fujii, K., Umekage, T., Tochigi, M., Kohda, K., Sasaki, T., Yamada, K., Yoshikawa, T. & Kato, T. (2005) Functional polymorphisms of HSPA5: possible association with bipolar disorder. *Biochem Biophys Res Commun*, **336**, 1136-1143.

Kamintsky, L., Cairns, K.A., Veksler, R., Bowen, C., Beyea, S.D., Friedman, A. & Calkin, C. (2020) Blood-brain barrier imaging as a potential biomarker for bipolar disorder progression. *NeuroImage. Clinical*, **26**, 102049.

Kang, H.S., Ahn, H.S., Kang, H.J. & Gye, M.C. (2006) Effect of estrogen on the expression of occludin in ovariectomized mouse brain. *Neurosci Lett*, **402**, 30-34.

Kaya, M. & Ahishali, B. (2011) Assessment of permeability in barrier type of endothelium in brain using tracers: Evans blue, sodium fluorescein, and horseradish peroxidase. *Methods in molecular biology (Clifton, N.J.)*, **763**, 369-382.

Kelly, K.A., Michalovicz, L.T., Miller, J.V., Castranova, V., Miller, D.B. & O'Callaghan, J.P. (2018) Prior exposure to corticosterone markedly enhances and prolongs the

neuroinflammatory response to systemic challenge with LPS. *PLoS One*, **13**, e0190546.

Kessler, R.C., McLaughlin, K.A., Green, J.G., Gruber, M.J., Sampson, N.A., Zaslavsky, A.M., Aguilar-Gaxiola, S., Alhamzawi, A.O., Alonso, J., Angermeyer, M., Benjet, C., Bromet, E., Chatterji, S., de Girolamo, G., Demyttenaere, K., Fayyad, J., Florescu, S., Gal, G., Gureje, O., Haro, J.M., Hu, C.Y., Karam, E.G., Kawakami, N., Lee, S., Lepine, J.P., Ormel, J., Posada-Villa, J., Sagar, R., Tsang, A., Ustun, T.B., Vassilev, S., Viana, M.C. & Williams, D.R. (2010) Childhood adversities and adult psychopathology in the WHO World Mental Health Surveys. *Br J Psychiatry*, **197**, 378-385.

Kim, J., Erice, C., Rohlwink, U.K. & Tucker, E.W. (2022) Infections in the Developing Brain: The Role of the Neuro-Immune Axis. *Frontiers in Neurology*, **13**.

Kitamura, M. (2013) The unfolded protein response triggered by environmental factors. *Semin Immunopathol*, **35**, 259-275.

Klein, S.L. & Flanagan, K.L. (2016) Sex differences in immune responses. *Nat Rev Immunol*, **16**, 626-638.

Krause, D., Faustmann, P.M. & Dermietzel, R. (2002) Molecular Anatomy of the Blood-Brain Barrier in Development and Aging. In de Vellis, J.S. (ed) *Neuroglia in the Aging Brain*. Humana Press, Totowa, NJ, pp. 291-303.

Lapin, I.P. (1995) Only controls: effect of handling, sham injection, and intraperitoneal injection of saline on behavior of mice in an elevated plus-maze. *J Pharmacol Toxicol Methods*, **34**, 73-77.

Le-Niculescu, H., Balaraman, Y., Patel, S.D., Ayalew, M., Gupta, J., Kuczenski, R., Shekhar, A., Schork, N., Geyer, M.A. & Niculescu, A.B. (2011) Convergent functional genomics of anxiety disorders: translational identification of genes, biomarkers, pathways and mechanisms. *Translational psychiatry*, **1**, e9.

Li, M.X., Li, Q., Sun, X.J., Luo, C., Li, Y., Wang, Y.N., Chen, J., Gong, C.Z., Li, Y.J., Shi, L.P., Zheng, Y.F., Li, R.C., Huang, X.L., Xiong, Q.J. & Chen, H. (2019) Increased Homer1-mGluR5 mediates chronic stress-induced depressive-like behaviors and glutamatergic dysregulation via activation of PERK-eIF2α. *Progress in neuro-psychopharmacology & biological psychiatry*, **95**, 109682.

Lin, B., Ginsberg, M.D., Zhao, W., Alonso, O.F., Belayev, L. & Busto, R. (2001) Quantitative analysis of microvascular alterations in traumatic brain injury by endothelial barrier antigen immunohistochemistry. *Journal of neurotrauma*, **18**, 389-397.

Logsdon, A.F., Lucke-Wold, B.P., Nguyen, L., Matsumoto, R.R., Turner, R.C., Rosen, C.L. & Huber, J.D. (2016) Salubrinal reduces oxidative stress, neuroinflammation and impulsive-like behavior in a rodent model of traumatic brain injury. *Brain Res*, **1643**, 140-151.

Loi, M., Mossink, J.C., Meerhoff, G.F., Den Blaauwen, J.L., Lucassen, P.J. & Joels, M. (2017) Effects of early-life stress on cognitive function and hippocampal structure in female rodents. *Neuroscience*, **342**, 101-119.

Loram, L.C., Taylor, F.R., Strand, K.A., Frank, M.G., Sholar, P., Harrison, J.A., Maier, S.F. & Watkins, L.R. (2011) Prior exposure to glucocorticoids potentiates lipopolysaccharide induced mechanical allodynia and spinal neuroinflammation. *Brain, behavior, and immunity*, **25**, 1408-1415.

Loria, A.S., Brands, M.W., Pollock, D.M. & Pollock, J.S. (2013) Early life stress sensitizes the renal and systemic sympathetic system in rats. *American journal of physiology. Renal physiology*, **305**, F390-395.

Loria, A.S., Ho, D.H. & Pollock, J.S. (2014) A mechanistic look at the effects of adversity early in life on cardiovascular disease risk during adulthood. *Acta physiologica (Oxford, England)*, **210**, 277-287.

Lossinsky, A.S., Vorbrodt, A.W. & Wisniewski, H.M. (1986) Characterization of endothelial cell transport in the developing mouse blood-brain barrier. *Developmental neuroscience*, **8**, 61-75.

Mabandla, M.V. & Russell, V.A. (2010) Voluntary exercise reduces the neurotoxic effects of 6-hydroxydopamine in maternally separated rats. *Behav Brain Res*, **211**, 16-22.

Maes, M., Meltzer, H.Y., Bosmans, E., Bergmans, R., Vandoolaeghe, E., Ranjan, R. & Desnyder, R. (1995) Increased plasma concentrations of interleukin-6, soluble interleukin-6, soluble interleukin-2 and transferrin receptor in major depression. *Journal of affective disorders*, **34**, 301-309.

Maes, M., Van der Planken, M., Stevens, W.J., Peeters, D., DeClerck, L.S., Bridts, C.H., Schotte, C. & Cosyns, P. (1992) Leukocytosis, monocytosis and neutrophilia: hallmarks of severe depression. *Journal of psychiatric research*, **26**, 125-134.

Majcher-Maslanka, I., Solarz, A. & Chocyk, A. (2019) Maternal separation disturbs postnatal development of the medial prefrontal cortex and affects the number of neurons and glial cells in adolescent rats. *Neuroscience*, **423**, 131-147.

Malinovskaya, N.A., Morgun, A.V., Lopatina, O.L., Panina, Y.A., Volkova, V.V., Gasymly, E.L., Taranushenko, T.E. & Salmina, A.B. (2018) Early Life Stress: Consequences for the Development of the Brain. *Neuroscience and Behavioral Physiology*, **48**, 233-250.

Mapunda, J.A., Tibar, H., Regragui, W. & Engelhardt, B. (2022) How Does the Immune System Enter the Brain? *Frontiers in immunology*, **13**, 805657.

Mariani, N., Borsini, A., Cecil, C.A.M., Felix, J.F., Sebert, S., Cattaneo, A., Walton, E., Milaneschi, Y., Cochrane, G., Amid, C., Rajan, J., Giacobbe, J., Sanz, Y., Agusti, A., Sorg, T., Herault, Y., Miettunen, J., Parmar, P., Cattane, N., Jaddoe, V., Lotjonen, J., Buisan, C., Gonzalez Ballester, M.A., Piella, G., Gelpi, J.L., Lamers, F., Penninx, B., Tiemeier, H., von Tottleben, M., Thiel, R., Heil, K.F., Jarvelin, M.R., Pariante, C.,

Mansuy, I.M. & Lekadir, K. (2021) Identifying causative mechanisms linking early-life stress to psycho-cardio-metabolic multi-morbidity: The EarlyCause project. *PLoS One*, **16**, e0245475.

Markham, J.A., Morris, J.R. & Juraska, J.M. (2007) Neuron number decreases in the rat ventral, but not dorsal, medial prefrontal cortex between adolescence and adulthood. *Neuroscience*, **144**, 961-968.

Martisova, E., Aisa, B., Guerenu, G. & Ramirez, M.J. (2013) Effects of early maternal separation on biobehavioral and neuropathological markers of Alzheimer's disease in adult male rats. *Curr Alzheimer Res*, **10**, 420-432.

McEwen, B.S. (1998) Stress, adaptation, and disease. Allostasis and allostatic load. *Annals of the New York Academy of Sciences*, **840**, 33-44.

McMahon, J.M., McQuaid, S., Reynolds, R. & FitzGerald, U.F. (2012) Increased expression of ER stress- and hypoxia-associated molecules in grey matter lesions in multiple sclerosis. *Multiple sclerosis (Houndmills, Basingstoke, England)*, **18**, 1437-1447.

Menard, C., Pfau, M.L., Hodes, G.E., Kana, V., Wang, V.X., Bouchard, S., Takahashi, A., Flanigan, M.E., Aleyasin, H., LeClair, K.B., Janssen, W.G., Labonte, B., Parise, E.M., Lorsch, Z.S., Golden, S.A., Heshmati, M., Tamminga, C., Turecki, G., Campbell, M., Fayad, Z.A., Tang, C.Y., Merad, M. & Russo, S.J. (2017) Social stress induces neurovascular pathology promoting depression. *Nature neuroscience*, **20**, 1752-1760.

Mháille, A.N., McQuaid, S., Windebank, A., Cunnea, P., McMahon, J., Samali, A. & FitzGerald, U. (2008) Increased expression of endoplasmic reticulum stress-related signaling pathway molecules in multiple sclerosis lesions. *Journal of neuropathology and experimental neurology*, **67**, 200-211.

Miller, A.H., Maletic, V. & Raison, C.L. (2009) Inflammation and its discontents: the role of cytokines in the pathophysiology of major depression. *Biological psychiatry*, **65**, 732-741.

Mohan, S., R, P.R.M., Brown, L., Ayyappan, P. & G, R.K. (2019) Endoplasmic reticulum stress: A master regulator of metabolic syndrome. *Eur J Pharmacol*, **860**, 172553.

Moon, Y., Lim, C., Kim, Y. & Moon, W.J. (2021) Sex-Related Differences in Regional Blood-Brain Barrier Integrity in Non-Demented Elderly Subjects. *Int J Mol Sci*, **22**.

Muneer, A. & Shamsher Khan, R.M. (2019) Endoplasmic Reticulum Stress: Implications for Neuropsychiatric Disorders. *Chonnam medical journal*, **55**, 8-19.

Murphy, M.O., Cohn, D.M. & Loria, A.S. (2017) Developmental origins of cardiovascular disease: Impact of early life stress in humans and rodents. *Neuroscience and biobehavioral reviews*, **74**, 453-465.

Nederhof, E. & Schmidt, M.V. (2012) Mismatch or cumulative stress: toward an integrated hypothesis of programming effects. *Physiology & behavior*, **106**, 691-700.

Nevell, L., Zhang, K., Aiello, A.E., Koenen, K., Galea, S., Soliven, R., Zhang, C., Wildman, D.E. & Uddin, M. (2014) Elevated systemic expression of ER stress related genes is associated with stress-related mental disorders in the Detroit Neighborhood Health Study. *Psychoneuroendocrinology*, **43**, 62-70.

Ngun, T.C., Ghahramani, N., Sanchez, F.J., Bocklandt, S. & Vilain, E. (2011) The genetics of sex differences in brain and behavior. *Front Neuroendocrinol*, **32**, 227-246.

Nicolas, S., McGovern, A.J., Hueston, C.M., O'Mahony, S.M., Cryan, J.F., O'Leary, O.F. & Nolan, Y.M. (2022) Prior maternal separation stress alters the dendritic complexity of new hippocampal neurons and neuroinflammation in response to an inflammatory stressor in juvenile female rats. *Brain, behavior, and immunity*, **99**, 327-338.

Nie, X., Kitaoka, S., Tanaka, K., Segi-Nishida, E., Imoto, Y., Ogawa, A., Nakano, F., Tomohiro, A., Nakayama, K., Taniguchi, M., Mimori-Kiyosue, Y., Kakizuka, A., Narumiya, S. & Furuyashiki, T. (2018) The Innate Immune Receptors TLR2/4 Mediate Repeated Social Defeat Stress-Induced Social Avoidance through Prefrontal Microglial Activation. *Neuron*, **99**, 464-479 e467.

Nikodemova, M., Kimyon, R.S., De, I., Small, A.L., Collier, L.S. & Watters, J.J. (2015) Microglial numbers attain adult levels after undergoing a rapid decrease in cell number in the third postnatal week. *Journal of neuroimmunology*, **278**, 280-288.

Nikolić, M., Gardner, H.A. & Tucker, K.L. (2013) Postnatal neuronal apoptosis in the cerebral cortex: physiological and pathophysiological mechanisms. *Neuroscience*, **254**, 369-378.

Noteboom, A., Have, M.T., de Graaf, R., Beekman, A.T.F., Penninx, B. & Lamers, F. (2021) The long-lasting impact of childhood trauma on adult chronic physical disorders. *Journal of psychiatric research*, **136**, 87-94.

Özbey, N.P., Thompson, M.A. & Taylor, R.C. (2021) The regulation of animal behavior by cellular stress responses. *Experimental cell research*, **405**, 112720.

Oztas, B. (1998) Sex and blood-brain barrier. *Pharmacol Res*, **37**, 165-167.

Packard, A.E., Egan, A.E. & Ulrich-Lai, Y.M. (2016) HPA Axis Interactions with Behavioral Systems. *Compr Physiol*, **6**, 1897-1934.

Papadopoulos, M.C., Lamb, F.J., Moss, R.F., Davies, D.C., Tighe, D. & Bennett, E.D. (1999) Faecal peritonitis causes oedema and neuronal injury in pig cerebral cortex. *Clin Sci (Lond)*, **96**, 461-466.

Parker, K.J., Buckmaster, C.L., Hyde, S.A., Schatzberg, A.F. & Lyons, D.M. (2019) Nonlinear relationship between early life stress exposure and subsequent resilience in monkeys. *Sci Rep*, **9**, 16232.

Paxinos G. & Watson C. (1998) The rat brain in stereotaxic coordinates. *Academic Press.*

Pearson-Leary, J., Eacret, D., Chen, R., Takano, H., Nicholas, B. & Bhatnagar, S. (2017) Inflammation and vascular remodeling in the ventral hippocampus contributes to vulnerability to stress. *Translational psychiatry*, **7**, e1160.

Pechtel, P. & Pizzagalli, D.A. (2011) Effects of early life stress on cognitive and affective function: an integrated review of human literature. *Psychopharmacology*, **214**, 55-70.

Peng, X., Luo, Z., He, S., Zhang, L. & Li, Y. (2021) Blood-Brain Barrier Disruption by Lipopolysaccharide and Sepsis-Associated Encephalopathy. *Frontiers in cellular and infection microbiology*, **11**, 768108.

Perner, C. & Krüger, E. (2022) Endoplasmic Reticulum Stress and Its Role in Homeostasis and Immunity of Central and Peripheral Neurons. *Frontiers in immunology*, **13**, 859703.

Pinares-Garcia, P., Stratikopoulos, M., Zagato, A., Loke, H. & Lee, J. (2018) Sex: A Significant Risk Factor for Neurodevelopmental and Neurodegenerative Disorders. *Brain sciences*, **8**.

Posillico, C.K., Garcia-Hernandez, R.E. & Tronson, N.C. (2021) Sex differences and similarities in the neuroimmune response to central administration of poly I:C. *Journal of neuroinflammation*, **18**, 193.

Profaci, C.P., Munji, R.N., Pulido, R.S. & Daneman, R. (2020) The blood-brain barrier in health and disease: Important unanswered questions. *The Journal of experimental medicine*, **217**.

Pryce, C.R., Rüedi-Bettschen, D., Dettling, A.C. & Feldon, J. (2002) Early life stress: long-term physiological impact in rodents and primates. *News in physiological sciences : an international journal of physiology produced jointly by the International Union of Physiological Sciences and the American Physiological Society*, **17**, 150-155.

Qin, X., He, Y., Wang, N., Zou, J.X., Zhang, Y.M., Cao, J.L., Pan, B.X. & Zhang, W.H. (2019) Moderate maternal separation mitigates the altered synaptic transmission and neuronal activation in amygdala by chronic stress in adult mice. *Mol Brain*, **12**, 111.

Rabow, Z., Morningstar, T., Showalter, M., Heil, H., Thongphanh, K., Fan, S., Chan, J., Martinez-Cerdeno, V., Berman, R., Zagzag, D., Nudler, E., Fiehn, O. & Lechpammer, M. (2021) Exposure to DMSO during infancy alters neurochemistry, social interactions, and brain morphology in long-evans rats. *Brain Behav*, **11**, e02146.

Reincke, S.A. & Hanganu-Opatz, I.L. (2017) Early-life stress impairs recognition memory and perturbs the functional maturation of prefrontal-hippocampal-perirhinal networks. *Sci Rep*, **7**, 42042.

Roque, A., Ochoa-Zarzosa, A. & Torner, L. (2016) Maternal separation activates microglial cells and induces an inflammatory response in the hippocampus of male rat pups, independently of hypothalamic and peripheral cytokine levels. *Brain, behavior, and immunity*, **55**, 39-48.

Saavedra, L.M., Fenton Navarro, B. & Torner, L. (2017) Early Life Stress Activates Glial Cells in the Hippocampus but Attenuates Cytokine Secretion in Response to an Immune Challenge in Rat Pups. *Neuroimmunomodulation*, **24**, 242-255.

Saija, A., Princi, P., D'Amico, N., De Pasquale, R. & Costa, G. (1990) Aging and sex influence the permeability of the blood-brain barrier in the rat. *Life Sci*, **47**, 2261-2267.

Santha, P., Veszelka, S., Hoyk, Z., Meszaros, M., Walter, F.R., Toth, A.E., Kiss, L., Kincses, A., Olah, Z., Seprenyi, G., Rakhely, G., Der, A., Pakaski, M., Kalman, J., Kittel, A. & Deli, M.A. (2015) Restraint Stress-Induced Morphological Changes at the Blood-Brain Barrier in Adult Rats. *Front Mol Neurosci*, **8**, 88.

Saxena, S., Cabuy, E. & Caroni, P. (2009) A role for motoneuron subtype-selective ER stress in disease manifestations of FALS mice. *Nature neuroscience*, **12**, 627-636.

Schwarz, J.M. & Bilbo, S.D. (2012) Sex, glia, and development: interactions in health and disease. *Horm Behav*, **62**, 243-253.

Selemon, L.D. (2013) A role for synaptic plasticity in the adolescent development of executive function. *Translational psychiatry*, **3**, e238.

Serna-Rodríguez, M.F., Bernal-Vega, S., de la Barquera, J.A.O., Camacho-Morales, A. & Pérez-Maya, A.A. (2022) The role of damage associated molecular pattern molecules (DAMPs) and permeability of the blood-brain barrier in depression and neuroinflammation. *Journal of neuroimmunology*, **371**, 577951.

Shi, J. & Simpkins, J.W. (1997) 17 beta-Estradiol modulation of glucose transporter 1 expression in blood-brain barrier. *Am J Physiol*, **272**, E1016-1022.

Smith, K.E. & Pollak, S.D. (2020) Early life stress and development: potential mechanisms for adverse outcomes. *Journal of neurodevelopmental disorders*, **12**, 34.

Solarz-Andrzejewska, A., Majcher-Maślanka, I., Kryst, J. & Chocyk, A. (2023) Modulation of the endoplasmic reticulum stress and unfolded protein response mitigates the behavioral effects of early-life stress. *Pharmacological reports : PR*, **75**, 293-319.

Solarz, A., Majcher-Maslanka, I. & Chocyk, A. (2021a) Effects of early-life stress and sex on blood-brain barrier permeability and integrity in juvenile and adult rats. *Dev Neurobiol*, **81**, 861-876.

Solarz, A., Majcher-Maslanka, I., Kryst, J. & Chocyk, A. (2021b) A Search for Biomarkers of Early-life Stress-related Psychopathology: Focus on 70-kDa Heat Shock Proteins. *Neuroscience*, **463**, 238-253.

Solarz, A., Majcher-Maślanka, I., Kryst, J. & Chocyk, A. (2023) Early-life stress affects peripheral, blood-brain barrier, and brain responses to immune challenge in juvenile and adult rats. *Brain, behavior, and immunity*, **108**, 1-15.

Sternberger, N.H. & Sternberger, L.A. (1987) Blood-brain barrier protein recognized by monoclonal antibody. *Proceedings of the National Academy of Sciences of the United States of America*, **84**, 8169-8173.

Sternberger, N.H., Sternberger, L.A., Kies, M.W. & Shear, C.R. (1989) Cell surface endothelial proteins altered in experimental allergic encephalomyelitis. *Journal of neuroimmunology*, **21**, 241-248.

Stertz, L., Fries, G.R., Rosa, A.R., Kauer-Sant'anna, M., Ferrari, P., Paz, A.V., Green, C., Cunha Â, B., Dal-Pizzol, F., Gottfried, C. & Kapczinski, F. (2015) Damage-associated molecular patterns and immune activation in bipolar disorder. *Acta psychiatrica Scandinavica*, **132**, 211-217.

Stolp, H.B. & Dziegielewska, K.M. (2009) Review: Role of developmental inflammation and blood-brain barrier dysfunction in neurodevelopmental and neurodegenerative diseases. *Neuropathol Appl Neurobiol*, **35**, 132-146.

Su, S., Jimenez, M.P., Roberts, C.T. & Loucks, E.B. (2015) The role of adverse childhood experiences in cardiovascular disease risk: a review with emphasis on plausible mechanisms. *Current cardiology reports*, **17**, 88.

Sun, H.X., Hu, H.L., Liu, C.J., Sun, N.N. & Duan, C.H. (2021) Methods used for the measurement of blood-brain barrier integrity. *Metab Brain Dis*, **36**, 723-735.

Tabas, I. (2010) The role of endoplasmic reticulum stress in the progression of atherosclerosis. *Circulation research*, **107**, 839-850.

Taler, M., Aronovich, R., Henry Hornfeld, S., Dar, S., Sasson, E., Weizman, A. & Hochman, E. (2021) Regulatory effect of lithium on hippocampal blood-brain barrier integrity in a rat model of depressive-like behavior. *Bipolar disorders*, **23**, 55-65.

Tang, J., Yu, W., Chen, S., Gao, Z. & Xiao, B. (2018) Microglia Polarization and Endoplasmic Reticulum Stress in Chronic Social Defeat Stress Induced Depression Mouse. *Neurochemical research*, **43**, 985-994.

Teicher, M.H., Gordon, J.B. & Nemeroff, C.B. (2022) Recognizing the importance of childhood maltreatment as a critical factor in psychiatric diagnoses, treatment, research, prevention, and education. *Molecular psychiatry*, **27**, 1331-1338.

Teicher, M.H., Ohashi, K. & Khan, A. (2020) Additional Insights into the Relationship Between Brain Network Architecture and Susceptibility and Resilience to the

Psychiatric Sequelae of Childhood Maltreatment. *Adversity and resilience science*, **1**, 49-64.

Teixeira, A.L., Macedo, D. & Baune, B.T. (2020) *Perinatal Inflammation and Adult Psychopathology [electronic resource] : From Preclinical Models to Humans / edited by Antonio L. Teixeira, Danielle Macedo, Bernhard T. Baune*. Springer International Publishing, Cham.

Thelin, E.P., Nelson, D.W. & Bellander, B.M. (2017) A review of the clinical utility of serum S100B protein levels in the assessment of traumatic brain injury. *Acta neurochirurgica*, **159**, 209-225.

Torres-Platas, S.G., Comeau, S., Rachalski, A., Bo, G.D., Cruceanu, C., Turecki, G., Giros, B. & Mechawar, N. (2014) Morphometric characterization of microglial phenotypes in human cerebral cortex. *Journal of neuroinflammation*, **11**, 12.

Trotta, T., Porro, C., Calvello, R. & Panaro, M.A. (2014) Biological role of Toll-like receptor-4 in the brain. *Journal of neuroimmunology*, **268**, 1-12.

Utsumi, H., Chiba, H., Kamimura, Y., Osanai, M., Igarashi, Y., Tobioka, H., Mori, M. & Sawada, N. (2000) Expression of GFRalpha-1, receptor for GDNF, in rat brain capillary during postnatal development of the BBB. *Am J Physiol Cell Physiol*, **279**, C361-368.

Vannucci, S.J. (1994) Developmental expression of GLUT1 and GLUT3 glucose transporters in rat brain. *J Neurochem*, **62**, 240-246.

Varatharaj, A. & Galea, I. (2017) The blood-brain barrier in systemic inflammation. *Brain, behavior, and immunity*, **60**, 1-12.

Vetulani, J. (2013) Early maternal separation: a rodent model of depression and a prevailing human condition. *Pharmacological reports : PR*, **65**, 1451-1461.

Villa, A., Gelosa, P., Castiglioni, L., Cimino, M., Rizzi, N., Pepe, G., Lolli, F., Marcello, E., Sironi, L., Vegeto, E. & Maggi, A. (2018) Sex-Specific Features of Microglia from Adult Mice. *Cell Rep*, **23**, 3501-3511.

Voet, S., Srinivasan, S., Lamkanfi, M. & van Loo, G. (2019) Inflammasomes in neuroinflammatory and neurodegenerative diseases. *EMBO molecular medicine*, **11**.

Welcome, M.O. & Mastorakis, N.E. (2020) Stress-induced blood brain barrier disruption: Molecular mechanisms and signaling pathways. *Pharmacol Res*, **157**, 104769.

Westin, J.E., Lindgren, H.S., Gardi, J., Nyengaard, J.R., Brundin, P., Mohapel, P. & Cenci, M.A. (2006) Endothelial proliferation and increased blood-brain barrier permeability in the basal ganglia in a rat model of 3,4-dihydroxyphenyl-L-alanine-induced dyskinesia. *The Journal of neuroscience : the official journal of the Society for Neuroscience*, **26**, 9448-9461.

Wheeler, M.A., Jaronen, M., Covacu, R., Zandee, S.E.J., Scalisi, G., Rothhammer, V., Tjon, E.C., Chao, C.C., Kenison, J.E., Blain, M., Rao, V.T.S., Hewson, P., Barroso, A., Gutiérrez-Vázquez, C., Prat, A., Antel, J.P., Hauser, R. & Quintana, F.J. (2019) Environmental Control of Astrocyte Pathogenic Activities in CNS Inflammation. *Cell*, **176**, 581-596.e518.

Winkler, E.A., Nishida, Y., Sagare, A.P., Rege, S.V., Bell, R.D., Perlmutter, D., Sengillo, J.D., Hillman, S., Kong, P., Nelson, A.R., Sullivan, J.S., Zhao, Z., Meiselman, H.J., Wendy, R.B., Soto, J., Abel, E.D., Makshanoff, J., Zuniga, E., De Vivo, D.C. & Zlokovic, B.V. (2015) GLUT1 reductions exacerbate Alzheimer's disease vasculo-neuronal dysfunction and degeneration. *Nature neuroscience*, **18**, 521-530.

Wu, X., Ding, Z., Fan, T., Wang, K., Li, S., Zhao, J. & Zhu, W. (2022) Childhood social isolation causes anxiety-like behaviors via the damage of blood-brain barrier in amygdala in female mice. *Frontiers in cell and developmental biology*, **10**, 943067.

Xie, J., Han, F. & Shi, Y. (2014) The unfolded protein response is triggered in rat neurons of the dorsal raphe nucleus after single-prolonged stress. *Neurochemical research*, **39**, 741-747.

Xu, G., Li, Y., Ma, C., Wang, C., Sun, Z., Shen, Y., Liu, L., Li, S., Zhang, X. & Cong, B. (2019) Restraint Stress Induced Hyperpermeability and Damage of the Blood-Brain Barrier in the Amygdala of Adult Rats. *Front Mol Neurosci*, **12**, 32.

Xu, J. & Ling, E.A. (1994) Studies of the ultrastructure and permeability of the blood-brain barrier in the developing corpus callosum in postnatal rat brain using electron dense tracers. *J Anat*, **184 (Pt 2)**, 227-237.

Yang, J., Wise, L. & Fukuchi, K.I. (2020) TLR4 Cross-Talk With NLRP3 Inflammasome and Complement Signaling Pathways in Alzheimer's Disease. *Frontiers in immunology*, **11**, 724.

Yang, R., Daigle, B.J., Jr., Muhie, S.Y., Hammamieh, R., Jett, M., Petzold, L. & Doyle, F.J., 3rd (2013) Core modular blood and brain biomarkers in social defeat mouse model for post traumatic stress disorder. *BMC Syst Biol*, **7**, 80.

Yap, K.N., Yamada, K., Zikeli, S., Kiaris, H. & Hood, W.R. (2021) Evaluating endoplasmic reticulum stress and unfolded protein response through the lens of ecology and evolution. *Biological reviews of the Cambridge Philosophical Society*, **96**, 541-556.

Yoshino, Y. & Dwivedi, Y. (2020) Elevated expression of unfolded protein response genes in the prefrontal cortex of depressed subjects: Effect of suicide. *Journal of affective disorders*, **262**, 229-236.

Zhang, K., Lin, W., Zhang, J., Zhao, Y., Wang, X. & Zhao, M. (2020) Effect of Toll-like receptor 4 on depressive-like behaviors induced by chronic social defeat stress. *Brain Behav*, **10**, e01525.

Zheng, P.P., Romme, E., van der Spek, P.J., Dirven, C.M., Willemsen, R. & Kros, J.M. (2010) Glut1/SLC2A1 is crucial for the development of the blood-brain barrier in vivo. *Annals of neurology*, **68**, 835-844.

Zuloaga, K.L., Swift, S.N., Gonzales, R.J., Wu, T.J. & Handa, R.J. (2012) The androgen metabolite, 5α-androstane-3β,17β-diol, decreases cytokine-induced cyclooxygenase-2, vascular cell adhesion molecule-1 expression, and P-glycoprotein expression in male human brain microvascular endothelial cells. *Endocrinology*, **153**, 5949-5960.

11. Oświadczenia współautorów

Instytut Farmakologii
im. Jerzego Maja
Polskiej Akademii Nauk

Dr hab. Agnieszka Chocyk

Zakład Farmakologii
Pracownia Farmakologii i Biostruktury Mózgu
Instytut Farmakologii im. Jerzego Maja
Polskiej Akademii Nauk w Krakowie

Kraków, 30.08.2023

OŚWIADCZENIE

Oświadczam, że w pracach:

1. Solarz A, Majcher-Maślanka I, Kryst J, **Chocyk A.** A Search for Biomarkers of Early-life Stress-related Psychopathology: Focus on 70-kDa Heat Shock Proteins. Neuroscience. 2021 May 21;463:238-253

2. Solarz A, Majcher-Maślanka I, **Chocyk A.** Effects of early-life stress and sex on blood-brain barrier permeability and integrity in juvenile and adult rats. Dev Neurobiol. 2021 Oct;81(7):861-876

3. Solarz A, Majcher-Maślanka I, Kryst J, **Chocyk A.** Early-life stress affects peripheral, blood-brain barrier, and brain responses to immune challenge in juvenile and adult rats. Brain Behav Immun. 2023 Feb;108:1-15

4. Solarz-Andrzejewska A, Majcher-Maślanka I, Kryst J, **Chocyk A.** Modulation of the endoplasmic reticulum stress and unfolded protein response mitigates the behavioral effects of early-life stress. Pharmacol Rep. 2023 Apr;75(2):293-319

5. Badania dodatkowe

mój udział polegał na:

- Stworzeniu koncepcji badań
- Pomocy w pozyskaniu funduszy na realizację badań
- Uzyskaniu zgody Komisji Etycznej ds. Doświadczeń na Zwierzętach na przeprowadzenie badań (1, 4)
- Pomocy w planowaniu badań i nadzorowaniu działań w projekcie badawczym
- Pomocy w przygotowaniu zwierząt do eksperymentów i pobieraniu tkanek do analiz
- Pomocy w interpretacji i dyskusji uzyskanych wyników
- Pomocy w pisaniu i poprawie manuskryptów oraz redagowaniu odpowiedzi na recenzje

ul. Smętna 12
31-343 Kraków

e-mail: ifpan@if-pan.krakow.pl
www.if-pan.krakow.pl

tel.: +48 12 662 32 20
+48 12 662 32 05
+48 12 662 32 49
fax: +48 12 637 45 00

Instytut Farmakologii
im. Jerzego Maja
Polskiej Akademii Nauk

Wyrażam zgodę na wykorzystanie publikacji w postępowaniu doktorskim Pani Anny Solarz-Andrzejewskiej oraz oświadczam, że powyższe wyniki nie zostaną ponownie wykorzystane w innych postępowaniach o nadanie stopnia doktora lub doktora habilitowanego.

.....AChocyk.....

dr hab. Agnieszka Chocyk

ul. Smętna 12
31-343 Kraków

e-mail: ifpan@if-pan.krakow.pl
www.if-pan.krakow.pl

tel.: +48 12 662 32 20
+48 12 662 32 05
+48 12 662 32 49
fax: +48 12 637 45 00

Dr Iwona Majcher-Maślanka Kraków, 28.08.2023

OŚWIADCZENIE

Oświadczam, że w pracach:

1. Solarz A, **Majcher-Maślanka I**, Kryst J, Chocyk A. A Search for Biomarkers of Early-life Stress-related Psychopathology: Focus on 70-kDa Heat Shock Proteins. Neuroscience. 2021 May 21;463:238-253

2. Solarz A, **Majcher-Maślanka I**, Chocyk A. Effects of early-life stress and sex on blood-brain barrier permeability and integrity in juvenile and adult rats. Dev Neurobiol. 2021 Oct;81(7):861-876
3. Solarz A, **Majcher-Maślanka I**, Kryst J, Chocyk A. Early-life stress affects peripheral, blood-brain barrier, and brain responses to immune challenge in juvenile and adult rats. Brain Behav Immun. 2023 Feb;108:1-15

4. Solarz-Andrzejewska A, **Majcher-Maślanka I**, Kryst J, Chocyk A. Modulation of the endoplasmic reticulum stress and unfolded protein response mitigates the behavioral effects of early-life stress. Pharmacol Rep. 2023 Apr;75(2):293-319

5. Badania dodatkowe

mój udział polegał na:

- Pomocy w przygotowaniu zwierząt do eksperymentów, w tym na przeprowadzaniu procedury separacji od matki (1-5) oraz podań związków (4)
- Pomocy w przeprowadzeniu pomiarów przepuszczalności BBB (2, 3, 5)
- Pomocy w wykonaniu eksperymentów behawioralnych (1 , 4)
- Wykonaniu części barwień immunohistochemicznych (4, 5)
- Wykonaniu części stereologicznej analizy liczby komórek (4)

- Pomiarze i analizie ekspresji białek metodą Western błot (1, 4)
- Przeprowadzeniu i analizie pomiarów elektrofizjologicznych (1)
- Pomocy w analizie, interpretacji i dyskusji otrzymanych wyników
- Pomocy w poprawach manuskryptów po recenzjach zgodnie z sugestiami autora korespondującego i recenzentów

Wyrażam zgodę na wykorzystanie publikacji w postępowaniu doktorskim Pani Anny Solarz Andrzejewskiej oraz oświadczam, że powyższe wyniki nie zostaną ponownie wykorzystane w innych postępowaniach o nadanie stopnia doktora lub doktora habilitowanego.

Iwona Majcher-Maślanka

Dr Iwona Majcher-Maślanka

Dr Joanna Kryst Kraków, 04.08.2023

OŚWIADCZENIE

Oświadczam, że w pracach:

1. Solarz A, Majcher-Maślanka I, **Kryst J**, Chocyk A. A Search for Biomarkers of Early-life Stress-related Psychopathology: Focus on 70-kDa 1--leat Shock Proteins. Neuroscience. 2021May21;463:2

2. Solarz A, Majcher-Maślanka I, **Kryst J**, Chocyk A. Early-life stress affects peripheral, bloodbrain barrier, and brain responses to immune challenge in juvenile and adult rats. Brain Behav Immun. 2023Feb:108:

3. Solarz-Andrzejewska A, Majcher-Maślanka I, **Kryst J**, Chocyk A. Modulation of the endoplasmic reticulum stress and unfolded protein response mitigates the behavioral effects of early-life stress. Pharmacol Rep. 2023 Apr;75(2):293-319

mój udział polegał na:

- Pomocy w przygotowaniu zwierząt do eksperymentów, w tym na przeprowadzaniu procedury separacji od matki (1-3) oraz podań związków (3)
- Pomocy w wykonaniu pomiarów przepuszczalności BBB (2)
- Pomocy w przeprowadzeniu eksperymentów behawioralnych (1, 3)
- Wykonaniu i pomocy w przeprowadzeniu barwień immunohistochemicznych (3)
- Wykonaniu części stereologicznej analizy liczby komórek (3)
- Pomiarze ekspresji wybranych genów metodą RT qPCR (3)
- Pomocy w analizie, interpretacji i dyskusji otrzymanych wyników
- Wykonaniu wstępnych rycin do manuskryptu (3)
- Pomocy w poprawie manuskryptu po recenzjach zgodnie z sugestiami autora korespondującego i recenzentów (l)

Wyrażam zgodę na wykorzystanie publikacji w postępowaniu doktorskim Pani Anny Solarz Andrzejewskiej oraz oświadczam, że powyższe wyniki nie zostaną ponownie wykorzystane w innych postępowaniach o nadanie stopnia doktora lub doktora habilitowanego.

.....

Dr Joanna Kryst

Instytut Farmakologii
im. Jerzego Maja
Polskiej Akademii Nauk

Mgr inż. Anna Solarz-Andrzejewska Kraków, 30.08.2023

Zakład Farmakologii
Pracownia Farmakologii i Biostruktury Mózgu
Instytut Farmakologii im. Jerzego Maja
Polskiej Akademii Nauk w Krakowie

OŚWIADCZENIE

Oświadczam, że w pracach:

1. **Solarz A**, Majcher-Maślanka I, Kryst J, Chocyk A. A Search for Biomarkers of Early-life Stress-related Psychopathology: Focus on 70-kDa Heat Shock Proteins. Neuroscience. 2021 May 21;463:238-253

2. **Solarz A**, Majcher-Maślanka I, Chocyk A. Effects of early-life stress and sex on blood-brain barrier permeability and integrity in juvenile and adult rats. Dev Neurobiol. 2021 Oct;81(7):861-876

3. **Solarz A**, Majcher-Maślanka I, Kryst J, Chocyk A. Early-life stress affects peripheral, blood-brain barrier, and brain responses to immune challenge in juvenile and adult rats. Brain Behav Immun. 2023 Feb;108:1-15

4. **Solarz-Andrzejewska A**, Majcher-Maślanka I, Kryst J, Chocyk A. Modulation of the endoplasmic reticulum stress and unfolded protein response mitigates the behavioral effects of early-life stress. Pharmacol Rep. 2023 Apr;75(2):293-319

5. Badania dodatkowe

mój udział polegał na:

- Pomocy w pozyskaniu funduszy na realizację badań (2, 3, 5)
- Uzyskaniu zgody Komisji Etycznej ds. Doświadczeń na Zwierzętach na przeprowadzenie badań
- Planowaniu szczegółów wszystkich eksperymentów
- Przygotowaniu zwierząt do eksperymentów, w tym na przeprowadzaniu procedury separacji od matki (1-5) oraz podań związków (3, 4)
- Przeprowadzeniu pomiarów przepuszczalności BBB (2, 3, 5)
- Przeprowadzeniu barwień immuohistochemicznych (4-5)
- Wykonaniu stereologicznej analizy liczby komórek glejowych (4)
- Wykonaniu analizy gęstości naczyń w mózgu (5)

ul. Smętna 12
31-343 Kraków

e-mail: ifpan@if-pan.krakow.pl
www.if-pan.krakow.pl

tel.: +48 12 662 32 20
+48 12 662 32 05
+48 12 662 32 49
fax: +48 12 637 45 00

- Wykonaniu i pomocy przy wykonaniu eksperymentów behawioralnych (test: eksploracji jasnego / ciemnego pudełka (1, 4), preferencji sacharozy (1, 4), wymuszonego pływania (1); reakcja warunkowania strachu (4); *aktywność lokomotoryczna (4)*
- Pomiarze ekspresji wybranych białek metodą Western Blot (1, 4)
- Wykonaniu pomiarów metodą ELISA (2, 3)
- Pomiarze i analizie ekspresji genów metodą RT qPCR (1-4)
- Analizie statystycznej i wstępnej interpretacji wszystkich wyników badań
- Pomocy w dyskusji otrzymanych wyników i wyciągnięciu wniosków z przeprowadzonych badań (1-5)
- Wykonaniu większości rycin do manuskryptów (1-4)
- Pisaniu wstępnych wersji manuskryptów i pomocy w ich poprawach zgodnie z sugestiami autora korespondującego i recenzentów (1-4)

Wyrażam zgodę na wykorzystanie publikacji w postępowaniu dotyczącym mojego przewodu doktorskiego (Anna Solarz-Andrzejewska) oraz oświadczam, że powyższe wyniki nie zostaną ponownie wykorzystane w innych postępowaniach o nadanie stopnia doktora lub doktora habilitowanego.

Anna Solarz-Andrz

.....

Mgr inż. Anna Solarz-Andrzejewska

ul. Smętna 12
31-343 Kraków

e-mail: ifpan@if-pan.krakow.pl
www.if-pan.krakow.pl

tel.: +48 12 662 32 20
+48 12 662 32 05
+48 12 662 32 49
fax: +48 12 637 45 00

12. Artykuły naukowe w wersji oryginalnej

Received: 12 May 2021 | Revised: 14 July 2021 | Accepted: 16 July 2021

DOI: 10.1002/dneu.22846

RESEARCH ARTICLE

WILEY

Effects of early-life stress and sex on blood–brain barrier permeability and integrity in juvenile and adult rats

Anna Solarz | **Iwona Majcher-Maślanka** | **Agnieszka Chocyk**

Department of Pharmacology, Laboratory of Pharmacology and Brain Biostructure, Maj Institute of Pharmacology, Polish Academy of Sciences, Kraków, Poland

Correspondence
Agnieszka Chocyk, Department of Pharmacology, Laboratory of Pharmacology and Brain Biostructure, Maj Institute of Pharmacology, Polish Academy of Sciences, Smętna Street 12, 31–343 Kraków, Poland.
Email: chocyk@if-pan.krakow.pl

Funding information
National Science Centre, Poland, Grant/Award Number: 2016/23/N/NZ4/01148

Abstract

Early-life stress (ELS) is considered a relevant etiological factor for neurodegenerative and mental disorders. In the present study, we hypothesized that ELS may persistently and sex dependently influence blood–brain barrier (BBB) integrity and function during critical periods of brain development and consequently determine susceptibility to and sex-related prevalence of chronic diseases in adult life. We used the maternal separation (MS) procedure in rats to model ELS and evaluated BBB permeability and gene expression of selected tight junction (TJ) proteins, glucose transporter type 1 (*Slc2a1*) and aquaporin 4 (*Aqp4*) in the medial prefrontal cortex (mPFC), dorsal striatum (dSTR) and hippocampus of juvenile and adult rats. Serum concentrations of a peripheral marker of BBB function (S100β) and proinflammatory cytokines were also assessed. We observed developmental sealing of the BBB and sex differences in the permeability of the BBB and the mRNA expression of TJ proteins and *Slc2a1*. Adult females showed lower BBB permeability and higher levels of *Cldn3*, *Cldn5*, *Ocln*, and *Slc2a1* in the mPFC and dSTR than males. MS temporarily increased BBB permeability in the dSTR of juvenile males and affected mRNA expression of the majority of studied proteins related to BBB function in age-, region- and sex-dependent manners. Additionally, MS sex dependently decreased serum S100β levels and did not affect proinflammatory cytokine concentrations. In general, our study did not reveal a clear or strong negative effect of MS on BBB integrity. However, the results suggest that ELS may induce adaptive/maladaptive changes or compensatory mechanisms within the BBB of unknown yet consequences.

KEYWORDS

aquaporin 4, blood–brain barrier, early-life stress, glucose transporter-1, proinflammatory cytokines, S100β, tight junctions

1 | INTRODUCTION

The blood–brain barrier (BBB) plays a major role in maintaining the stable environment required for normal brain function and ensures central nervous system (CNS) homeostasis by supplying oxygen, glucose, and nutrients and protecting against peripheral neurotoxic substances, infections and immune cells (Abbott et al., 2010; Ballabh et al., 2004). The BBB provides the necessary neuronal microenvironment via efficient cooperation between endothelial cells (ECs) and other specialized cell types such as pericytes and astrocytes (Abbott et al., 2006). Equally important BBB components are tight junctions (TJs), which limit the permeability of the BBB by sealing the interendothelial space between neighboring ECs. TJs consist of transmembrane proteins, such as the junctional adhesion molecules occludin (OCLN), claudin-3

(CLDN3) and claudin-5 (CLDN5), and cytoplasmic accessory proteins such as zona occludens 1 (ZO-1) (Abbott et al., 2010; Ballabh et al., 2004; Haseloff et al., 2015). ECs also express a variety of transporter proteins to deliver essential nutrients that cannot penetrate the brain by diffusion. One of the most abundant and crucial BBB-related transporters is glucose transporter-1 (GLUT-1) (Bolz et al., 1996). The major water channel in the CNS is aquaporin-4 (AQP4), expressed in brain perivascular astrocyte processes called astrocyte endfeet (Nicchia et al., 2004; Nielsen et al., 1997).

The involvement of BBB dysfunction in the development of psychiatric and neurodegenerative disorders has been increasingly confirmed (Arora et al., 2019; Erickson & Banks, 2013; Stolp & Dziegielewska, 2009; Winkler et al., 2015). Clinical data have also indicated that stress is generally linked to the pathogenesis and progression of these diseases (Baudin et al., 2012; Danese & Lewis, 2017; Loria et al., 2014). However, a limited number of studies have connected these two phenomena as a gateway to pathology in these diseases (Menard et al., 2017; Santha et al., 2015; Sharma, 2004; Xu et al., 2019). Early-life stress (ELS) or adverse childhood experiences are known to affect brain development and may prime an organism for mental and neurological diseases in adult life (Danese & Lewis, 2017; Kessler et al., 2010; Loria et al., 2014). BBB maturation is a sequential process. Along with brain structural immaturity, the BBB is functionally immature during the prenatal and early postnatal life periods (Abbott et al., 2010; Krause et al., 2002; Stolp & Dziegielewska, 2009). During the early postnatal period, capillary density matches local functions in cortical regions, suggesting a close connection between their simultaneous developments (Caley & Maxwell, 1970; Krause et al., 2002). Thus, during the perinatal period, an adverse experience, such ELS, may affect the developmental trajectory of specific brain regions along with the BBB (Fareri & Tottenham, 2016; Gomez-Gonzalez & Escobar, 2009; Welcome & Mastorakis, 2020).

It is well known that ELS is considered a potential source of later susceptibility to Alzheimer's disease (AD) and Parkinson's disease (PD) (Andersen & Teicher, 2004; Barlow et al., 2007; Llorente et al., 2009; Martisova et al., 2013). Animal studies have revealed that adult rats exposed to ELS show intensified age-related cognitive decline (Martisova et al., 2013; Solas et al., 2010). Animal models of PD, showed that ELS exacerbates 6-hydroxydopamine-induced behavioral and neurochemical impairments (Barlow et al., 2007; Mabandla & Russell, 2010; Mpofana et al., 2016). It is also well known that ELS increases the risk of anxiety, mood disorders, and addiction (Brenhouse et al., 2013; Danese & Lewis, 2017; Kessler et al., 2010). Many animal studies, including our own previous studies, that employed the maternal separation (MS) procedure in rats to model ELS, have clearly shown that ELS affects anxiety- and depressive-like behaviors (Chocyk et al., 2013, 2010, 2015; Majcher-Maslanka et al., 2019) and the function of the medial prefrontal cortex (mPFC) and hippocampus (HP), which are brain regions highly implicated in the pathophysiology of depression and anxiety (Andersen & Teicher, 2004; Baudin et al., 2012; Chocyk et al., 2013; Llorente et al., 2009; Majcher-Maslanka et al., 2019). Therefore, if ELS is considered a relevant etiological factor in mental and neurodegenerative disorders, concomitant BBB disturbance may contribute to the neurochemical and behavioral dysfunctions observed in humans and animals subjected to early-life adversity (Fareri & Tottenham, 2016; Ganguly & Brenhouse, 2015; Stolp & Dziegielewska, 2009).

We hypothesize that during a critical period of brain maturation, ELS may affect the development and function of the BBB within brain structures engaged in the pathophysiology of neurodegenerative and mental illnesses. The impact of ELS on cellular and molecular components and BBB permeability is still largely unexplored. Moreover, knowledge of the region- and sex-dependent differences in BBB integrity and function and their potential modulation by ELS is limited. Mental and neurodegenerative diseases are known to exhibit sex differences in prevalence and clinical presentation (Pinares-Garcia et al., 2018). Therefore, the present study aims to provide an analysis of BBB integrity changes during critical time periods in rodent brain development, that is, juvenility (postnatal day [PND] 15) and adulthood (PND 70), in both male and female rats subjected to MS procedures during the first two weeks of postnatal life. Specifically, BBB permeability and the gene expression of key elements contributing to the functional maintenance of the BBB, such as CLDN3, CLDN5 and OCLD, the transporter GLUT-1 and AQP4, was studied in the mPFC, dorsal STR (dSTR), and HP. Additionally, the serum levels of peripheral markers of inflammation and/or BBB disruption, namely, proinflammatory cytokines and s100 calcium-binding protein b (S100β), were also measured. We found pronounced sex differences in the permeability of the BBB and mRNA expression of TJ proteins and *Slc2a1*. Adult females showed lower BBB permeability and higher levels of *Cldn3*, *Cldn5*, *Ocln*, and *Slc2a1* in the mPFC and dSTR than males. MS temporarily increased BBB permeability in the dSTR of juvenile males and affected mRNA expression of the majority of studied proteins related to BBB function in age-, region- and sex-dependent manners. However, our study did not reveal a clear or strong negative effect of MS on BBB integrity

2 | MATERIALS AND METHODS

2.1 | Animals

All experimental procedures were approved by the Committee for Laboratory Animal Welfare and the Ethics Committee of the Maj Institute of Pharmacology, Polish Academy of

Sciences, Krakow, and met the requirements of the Directive 2010/63/EU of the European Parliament and of the Council of 22 September 2010 on the protection of animals used for scientific purposes. All efforts were made to minimize animal suffering.

Adult male and female Wistar rats were purchased from Charles River Laboratories (Sulzfeld, Germany). All animals were housed under controlled conditions with an artificial 12-h light/dark cycle (lights on from 07:00 to 19:00), 55% ± 10 humidity, and a temperature of 22˚C ± 2. Food and tap water were freely available. The rats were mated at the Maj Institute of Pharmacology, PAS, Krakow Animal Facility. The offsprings of primiparous dams were used in this study. Before delivery, the dams were housed individually in standard plastic cages (type III H, 38 × 24 × 19 cm). The day of birth was designated as PND 0. On PND 1, the litter size was standardized to eight pups per litter (four males and four females) and the litters were assigned to one of the following rearing conditions: MS or animal facility rearing (AFR), that is, control conditions.

2.2 | MS procedure

The MS procedure was performed as previously described by Solarz et al. (2021) and Chocyk et al. (2013, 2010, 2015). Briefly, on PNDs 1-14, the dams and pups were removed from the maternity cages for 3 h (09:00−12:00) per day. The mothers were placed individually in holding cages (type III, 38 × 24 × 19 cm), while each litter was placed in a plastic container (22 × 16 × 10 cm) lined with fresh bedding material, and the containers were moved to an adjacent room and placed in an incubator that was set at a constant temperature of 34˚C, imitating the nest temperature. After separation, the pups and dams were returned to maternity cages. The AFR animals were left undisturbed with their mothers except during weekly cage cleaning, thus, reflecting a minimal amount of handling. The impact of the MS procedure on specific maternal and pup behaviors was previously described in detail by our group (Chocyk et al., 2013). The animals, excluding those examined on PND 15, were weaned on PND 22, sexed, and then randomly divided and designated to specific experimental groups. The rats were housed under controlled conditions (as described above) in standard plastic cages (type IV, 57 × 33 × 20 cm) in same-sex groups of five unrelated subjects under the same treatment protocol until adulthood (PND 70). The scheme of the experimental procedures is presented in Figure 1.

2.3 | Experimental groups

A total of 112 rats (56 males and 56 females) originating from eight AFR and eight MS litters were used in the study. To avoid litter effects, the final experimental groups consisted of subjects that originated from different litters and were unrelated ($n = 6$ for RT-qPCR, serum markers; $n = 8$ for assessment of BBB permeability). The number of animals used in the study was chosen based on pilot experiments and our previous experiences with specific experimental protocols and it guaranteed the possibility of obtaining a relevant effect size and statistically significant differences in the results.

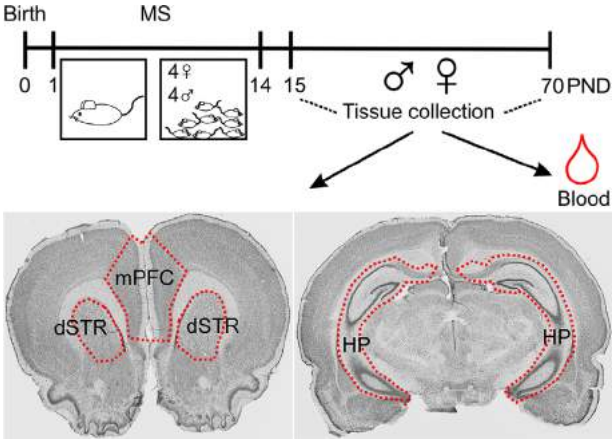

FIGURE 1 Scheme of the experimental procedures applied in the study. Lower panel: photomicrographs showing cresyl violet-stained rat brain sections with marked regions under study. Abbreviations: dSTR, dorsal striatum; MS, maternal separation; mPFC, medial prefrontal cortex; HP, hippocampus; PND, postnatal day.

2.4 | Assessment of BBB permeability

To assess BBB permeability, we used a fluorescent small-molecule tracer (376 Da), sodium fluorescein (NaF), a sensitive marker of even slight BBB breakdown and leakage. NaF does not bind to protein nonspecifically in contrast to Evans blue (961 Da, in complex with albumin), another popular marker of BBB permeability (Sun et al., 2021). In our study, we adapted the procedures previously described by Ramirez et al. (2009) and Yen et al. (2013). On PND 15 or PND 70, eight AFR and eight MS rats per age and sex group were intraperitoneally injected with 4% NaF (Merck) dissolved in 0.9% saline at a dose of 2 mL/kg. The dye was permitted to circulate for 30 min before the animals were transcardially perfused with 0.9% saline to remove the circulating dye. Thereafter, the brain tissue parenchyma containing only the extravasated dye was collected. Samples of the mPFC (including the cingulate cortex 1, prelimbic cortex, and infralimbic cortex regions) and dSTR were dissected from 1-mm thick coronal slices using a rodent brain matrix (Ted Pella, Inc., CA, USA) according to the stereotaxic atlas of the rat brain (Paxinos & Watson, 1998), whereas the HP was dissected freehand

(Figure 1). The brain tissue was weighed, homogenized (TissueLyserII, Qiagen) in a 1:3 volume of 50% trichloroacetic acid (TCA, Merck, US), and centrifuged (10,000 rpm for 10 min) and the supernatants were diluted with a 1:3 volume of 95% ethanol prior to spectrophotometric determination of NaF fluorescence (Tecan, Männedorf, Zürich, Switzerland; 440 nm excitation/525 nm emission). Fluorescent dye content was calculated using external standards and the data were expressed as the amount of NaF (μg) per gram of wet brain tissue.

2.5 | RT-qPCR

The RT-qPCR method used in this study has been previously described in detail by Solarz et al. (2021). Briefly, on PND 15 and PND 70, six AFR and six MS rats per age and sex group were sacrificed via decapitation and the brains were immediately removed from the skulls. The mPFC (including the cingulate cortex 1, prelimbic cortex, and infralimbic cortex regions) and dSTR were dissected from 1-mm thick coronal slices using a rodent brain matrix (Ted Pella Inc.), whereas the HP was dissected freehand (Figure 1). The brain tissue was quickly frozen in liquid nitrogen and stored at −80˚C for later use. Total RNA was extracted using the RNAeasy Mini Kit (Qiagen). The total RNA concentration was measured using an Eon absorbance microplate reader and Gen 5 software (BioTek, Winooski, VT, USA). RNA was reverse transcribed using a High-Capacity cDNA Reverse Transcription Kit (Thermo Fisher Scientific, MA). Quantitative real-time PCR was performed in duplicate with TaqMan® Gene Expression Assays (Thermo Fisher Scientific; Supporting information Table S1) using TaqMan™ Universal Master Mix II, no UNG (Thermo Fisher Scientific) and the QuantStudio 12K Flex System (Thermo Fisher Scientific). Real-time PCR was conducted under the following conditions: 50˚C for 2 min and 95˚C for 10 min followed by 40 cycles of 95˚C for 15 s and 60˚C for 1 min. The abundance of RNA was calculated according to the following equation: abundance $= 2^{-(\text{threshold cycle})}$. The results were normalized to glyceraldehyde-3-phosphate dehydrogenase (*Gapdh)* expression levels.

2.6 | Enzyme-linked immunosorbent assay (ELISA)

Trunk blood was collected during the decapitation procedure (see the RT-qPCR procedure). Commercially available microtubes containing a clotting activator (Sarstedt, Germany) were used for serum separation. The blood was centrifuged (10,000 × *g*, 5 min, 4 ˚C), and the serum was collected and stored in aliquots at −20˚C until the day of assay. Using commercially available ELISA kits, quantitative determination of S100β (Fine Test, China), interleukin 1 beta (IL-1β) (R&D Systems, USA), and tumor necrosis factor-alpha (TNF-α) (R&D Systems) were performed according to the manufacturers' instructions. Positive controls for each assay were provided by the manufacturers.

2.7 | Statistical analysis

Statistical analysis of the data was performed using Statistica 13.3 software (TIBCO Software Inc., USA). Initially, data were tested for normal distribution and homogeneity of variances and then analyzed by global analysis of variance (ANOVA). The majority of data were analyzed by three-way ANOVA, with PND, rearing conditions (MS vs. AFR), and sex as the independent variables. The data were analyzed individually for each brain region (or serum) and parameter studied. Regional differences in BBB permeability were assessed by one-way ANOVA separately for each developmental time and sex. When the global ANOVA resulted in statistically significant effects, the data were subdivided into significant factors and/or interactions and a lower-order statistical analysis was performed (two-way ANOVA and Bonferroni *post-hoc* test when required). The data are presented as the mean ± SD. A value of $p < 0.05$ was considered statistically significant.

3 | RESULTS

3.1 | Effects of age, sex, and MS on regional quantitative BBB permeability

The first goal of our study was to investigate the impact of PND, sex, and rearing conditions (AFR vs. MS) on BBB permeability in the mPFC, dSTR, and HP. The animals were injected with a fluorescent tracer, NaF, and its extravasated content was spectrophotometrically determined in the studied brain regions. The statistical analysis revealed an age-dependent decrease in BBB permeability in all studied brain regions (Supporting information Tables S2 and S3; Figure 2a–c).

We found that the BBB in the mPFC of females was less permeable than that in males, regardless of PND and MS (Supporting information Table S2, Figure 2a). In the dSTR and HP, sex differences were manifested in combination with PND and rearing conditions (Supporting information Tables S2 and S3; Figure 2b,c). Specifically, BBB permeability in the dSTR of AFR juvenile females was increased compared with that in AFR juvenile males (two-way ANOVA, sex × rearing conditions: $F_{1,28} = 29.30$, $p < 0.001$; *post-hoc*: $p = 0.039$) (Figure 2b). The opposite effect was observed in adults, that is, females in the AFR group showed lower BBB

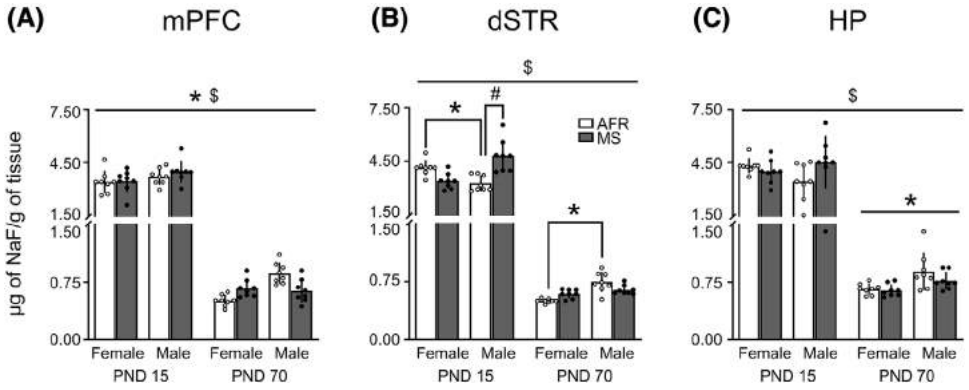

FIGURE 2 Effects of age, sex and MS on the regional brain content of extravasated NaF in the mPFC (a), dSTR (b) and HP (c). The data are presented as the mean ± SD and indicate the accumulation of NaF in the brain (in microgram per gram of wet tissue). Circles represent individual data points ($n = 8$). $^{\$}p < 0.05$: effect of PND, $^{*}p < 0.05$: effect of sex, $^{\#}p < 0.05$: effect of MS (three-way ANOVA followed by Bonferroni *post-hoc* test). Lines relate to the significance of the main effects in ANOVA and connectors indicate *post-hoc* comparisons between the specific groups. Abbreviations: AFR, animal facility rearing; dSTR, dorsal striatum; MS, maternal separation; mPFC, medial prefrontal cortex; HP, hippocampus; PND, postnatal day.

TABLE 1 Regional differences in BBB permeability in control (AFR) rats

Sex	PND	Brain region mPFC	dSTR	HP
Females	15	3.41 ± 0.63^{A}	4.13 ± 0.42^{B}	4.32 ± 0.42^{C}
	70	0.51 ± 0.08^{D}	0.50 ± 0.03^{E}	0.66 ± 0.07^{F}
Males	15	3.70 ± 0.54	3.27 ± 0.46	3.43 ± 1.25
	70	0.87 ± 0.14	0.75 ± 0.04	0.89 ± 0.08

The data indicate the accumulation of NaF tracer in the brain as microgram of NaF per gram of wet tissue (the mean ± SD, $n = 8$). A versus B: $p = 0.027$; A versus C: $p = 0.005$; D versus F: $p = 0.0002$; E versus F: $p = 0.0001$ (one-way ANOVA followed by Bonferroni *post-hoc* test). Abbreviations: AFR, animal facility rearing; BBB, blood–brain barrier; dSTR, dorsal striatum; mPFC, medial prefrontal cortex; HP, hippocampus; PND, postnatal day.

permeability in the dSTR than AFR males (two-way ANOVA, sex × rearing conditions: $F_{1,28} = 13.09$, $p = 0.001$; *post-hoc*: $p < 0.001$) (Figure 2b). In the HP, adult females, regardless of the rearing conditions, also exhibited lower BBB permeability than males (two-way ANOVA, the main effect of sex: $F_{1,28} = 12.95$, $p = 0.001$) (Figure 2c). These sex differences were not observed in the HP of juvenile rats (two-way ANOVA, the main effect of sex: $F_{1,28} = 1.16$, $p = 0.290$) (Figure 2c).

We observed that MS affected BBB permeability exclusively in the dSTR (Figure 2b). Specifically, MS sex dependently increased BBB permeability in juvenile males (*post-hoc*: $p < 0.001$), which disrupted the general sex differences observed in juveniles. In adults, MS did not influence BBB permeability in the dSTR per se; however, MS rats again did not show sex-related differences typical of the dSTR (*post-hoc:* $p = 1.00$) (Figure 2b).

Next, we focused on regional differences in BBB permeability in the control, that is, AFR rats of specific age and sex. We found that, in juvenile females, BBB permeability in both the HP and dSTR was higher than that in the mPFC ($F_{2,21} = 7.33$, $p = 0.004$, HP vs. mPFC: $p = 0.005$; dSTR vs. mPFC: $p = 0.027$; dSTR vs. HP: $p = 1.000$) (Table 1). This effect persisted to adulthood only in the case of HP. Moreover, BBB permeability in the HP of adult females was also greater than that in the dSTR ($F_{2,21} = 17.44$, $p < 0.001$, HP vs. mPFC: $p = 0.0002$; dSTR vs. mPFC: $p = 1.00$; dSTR vs. HP: $p = 0.0001$) (Table 1). In male rats, we did not observe any significant regional differences in BBB permeability (PND 15: $F_{2,21} = 0.762$, $p = 0.479$; PND 70: $F_{2,21} = 1.43$, $p = 0.262$) (Table 1).

3.2 | Effects of age, sex, and MS on the mRNA expression of TJ proteins

The integrity and permeability of the BBB is highly related to the expression and function of TJ proteins, such as OCLN and claudins, which are responsible for the structural support of TJs and physically occlude the interendothelial space (Abbott et al., 2010; Ballabh et al., 2004; Haseloff et al., 2015). Therefore, the next goal of our study was to determine how age, sex and MS could influence the expression of TJ proteins' representatives, that is, CLDN3 and CLDN5 and OCLN.

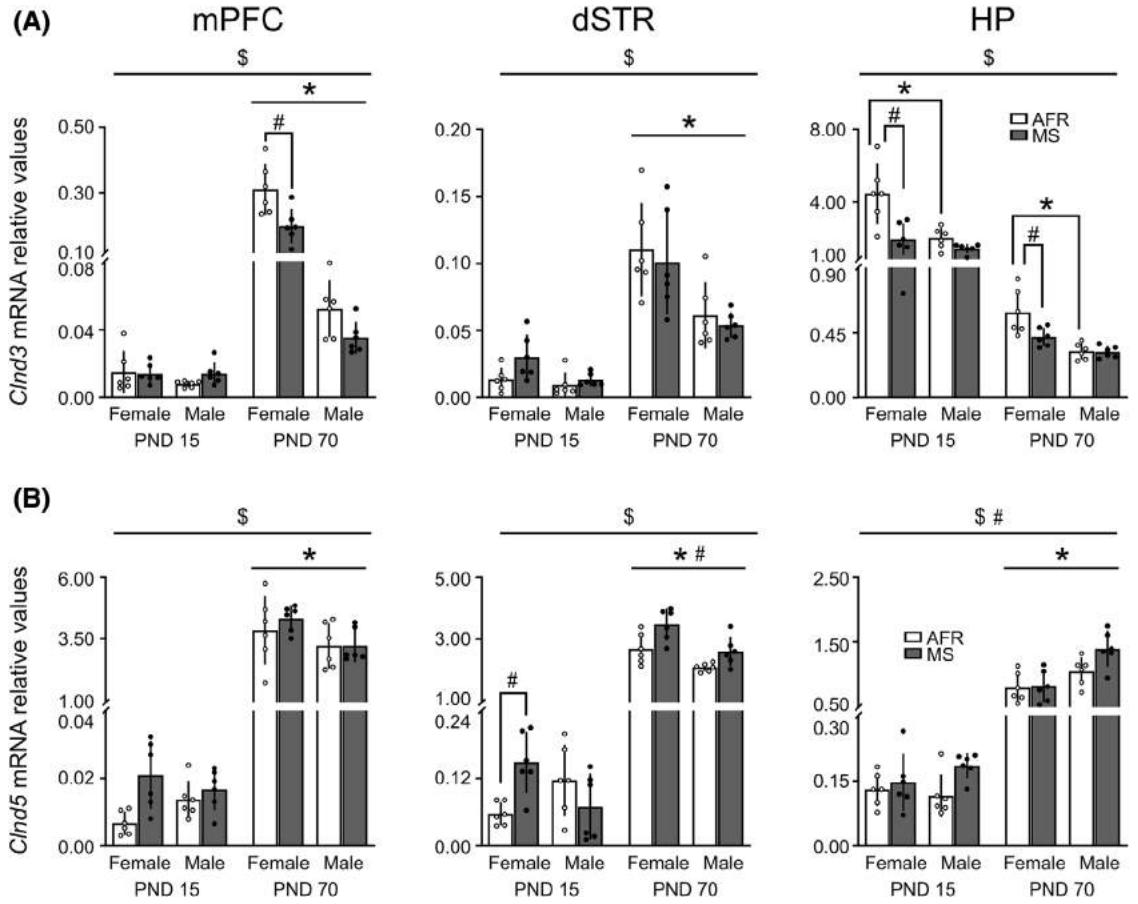

FIGURE 3 Effects of age, sex and MS on the mRNA expression of *Cldn3* (a) and *Cldn5* (b) in the mPFC (left column), dSTR (middle column) and HP (right column). The mRNA expression was determined by RT-qPCR. The data are presented as the mean ± SD and expressed as relative values of mRNA levels in arbitrary units. Circles represent individual data points ($n = 6$). $^{\$}p < 0.05$: effect of PND, $^{*}p < 0.05$: effect of sex, $^{\#}p < 0.05$: effect of MS (three-way ANOVA followed by Bonferroni *post-hoc* test). Lines relate to the significance of the main effects in ANOVA and connectors indicate *post-hoc* comparisons between the specific groups. Abbreviations are explained in legends of Figure 2 and Supporting information Table S1.

We applied RT-qPCR method to assess the mRNA levels of all studied markers of BBB integrity and function (see Section 3.3), because it is a very sensitive method, able to detect even small changes in the mRNA expression. Moreover, the persistent change in mRNA expression observed long after the cessation of MS may provide information about potential ELS-induced programming of specific genes.

We found an age-dependent increase in *Cldn3* mRNA levels in the mPFC and dSTR (Supporting information Tables S3, S4 and Figure 3a, left and middle columns). In contrast, an age-dependent decrease in *Cldn3* expression was observed in the HP (Supporting information Tables S3, S4, and Figure 3a, right column). In adulthood, *Cldn3* expression in the mPFC and dSTR was greater in females than in males regardless of the rearing conditions (mPFC: two-way ANOVA, sex × rearing conditions: $F_{1,20} = 5.78$, $p = 0.026$; *post-hoc:* $p < 0.001$; dSTR: $p < 0.001$) (Figure 3a, left and middle columns). However, in the HP, AFR but not MS females displayed higher expression of *Cldn3* mRNA than males in both the early-life period and adulthood (PND 15: two-way ANOVA, sex × rearing conditions: $F_{1,20} = 5.69$, $p = 0.027$; *post-hoc*: $p < 0.001$ and PND 70: two-way ANOVA, sex × rearing conditions: $F_{1,20} = 4.95$, $p = 0.037$; *post-hoc:* $p < 0.001$) (Figure 3a, right column). Moreover, we observed that MS induced persistent downregulation of *Cldn3* expression specifically in the HP of females (PND15: *post-hoc:* $p = 0.002$; PND70: *post-hoc:* $p = 0.026$) (Figure 3a, right column). Additionally, MS induced decrease in *Cldn3* mRNA levels was also observed in the mPFC of adult females (two-way ANOVA, sex × rearing conditions: $F_{1,20} = 5.78$; $p = 0.026$; *post-hoc*: $p = 0.004$) (Figure 3a, left column).

Next, we focused on *Cldn5* mRNA expression and observed its consistent age-dependent increase in all studied brain regions (Supporting information Tables S3, S4 and Figure 3b). Moreover, regardless of the rearing conditions,

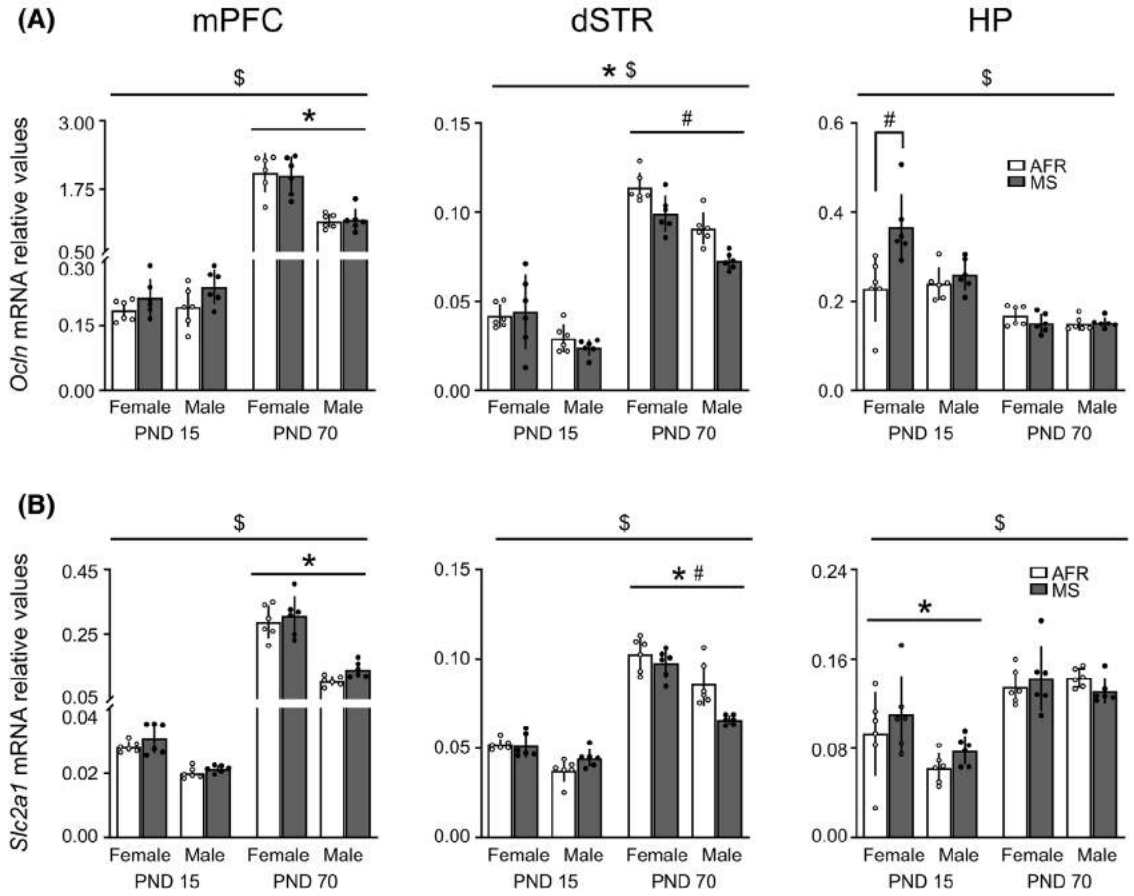

FIGURE 4 Effects of age, sex and MS on the mRNA expression of *Ocln* (a) and *Slc2a1* (b) in the mPFC (left column), dSTR (middle column) and HP (right column). The mRNA expression was determined by RT-qPCR. The data are presented as the mean ± SD and expressed as relative values of mRNA levels in arbitrary units. Circles represent individual data points ($n = 6$). $^{\$}p < 0.05$: effect of PND, $^{*}p < 0.05$: effect of sex, $^{\#}p < 0.05$: effect of MS (three-way ANOVA followed by Bonferroni *post hoc*-test). Lines relate to the significance of the main effects in ANOVA and connector indicates a *post-hoc* comparison between the specific groups. Abbreviations are explained in legends of Figure 2 and Supporting information Table S1.

adult females had higher levels of Cldn5 mRNA than males in the mPFC ($p = 0.010$) and dSTR (two-way ANOVA, the main effect of sex, $F_{1,20} = 17.22$, $p < 0.001$) (Figure 3b, left and middle column). Interestingly, the opposite sex-related effects were observed in the HP of adults ($p < 0.001$) (Figure 3b, right column). Moreover, we found that MS affected *Cldn5* mRNA expression exclusively in the dSTR and HP. Specifically, MS increased the expression of *Cldn5* mRNA in the dSTR of juvenile females (two-way ANOVA, sex × rearing conditions: $F_{1,20} = 10.64$, $p = 0.004$; *post-hoc:* $p = 0.038$) (Figure 3b, middle column). However, in adulthood, both MS females and males showed higher *Cldn5* mRNA expression than AFR rats (two-way ANOVA, the main effect of rearing conditions: $F_{1,20} = 13.40$, $p = 0.002$) (Figure 3b, middle column). In the HP, MS rats showed higher levels of *Cldn5* mRNA than AFR rats regardless of PND (Supporting information Tables S3, S4 and Figure 3b, right column).

In the case of *Ocln*, we observed an age-dependent increase in the mRNA levels in the mPFC and dSTR (Supporting information Tables S3, S4, Figure 4a, left and middle columns). In contrast, an age-dependent decrease in *Ocln* expression was observed in the HP (Supporting information Tables S3, S4 and Figure 4a, right column). Moreover, in the mPFC, adult females had higher levels of *Ocln* mRNA than males, regardless of the rearing conditions ($p < 0.001$) (Figure 4a, left column). In the dSTR, both juvenile and adult females showed higher expression of *Ocln* mRNA than males (Figure 4a, middle column). We found that MS affected *Ocln* mRNA expression specifically in the dSTR and HP. Namely, MS induced downregulation of *Ocln* mRNA levels in the dSTR of adult rats ($p = 0.002$) (Figure 4a, middle column). In the HP, MS specifically upregulated the mRNA expression of *Ocln* in MS juvenile females compared to AFR females (two-way ANOVA, sex × rearing conditions:

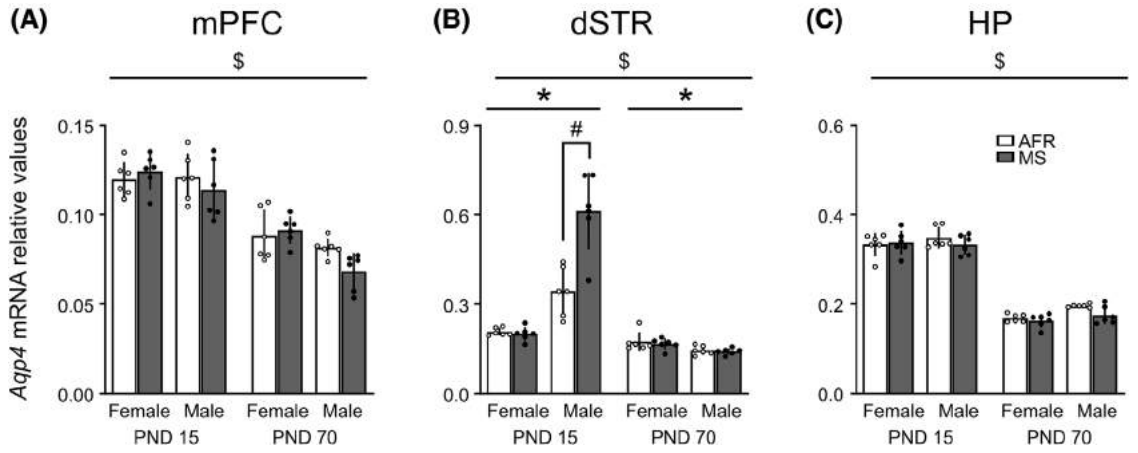

FIGURE 5 Effects of age, sex and MS on the mRNA expression of *Aqp4* in the mPFC (a), dSTR (b) and HP (c). The mRNA expression was determined by RT-qPCR. The data are presented as the mean ± SD and expressed as relative values of mRNA levels in arbitrary units. Circles represent individual data points ($n = 6$). $^{\$}p < 0.05$: effect of PND, $^{*}p < 0.05$: effect of sex, $^{\#}p < 0.05$: effect of MS (three-way ANOVA followed by Bonferroni *post-hoc* test). Lines relate to the significance of the main effects in ANOVA and connector indicates a *post-hoc* comparison between the specific groups. Abbreviations are explained in legends of Figure 2 and Supporting information Table S1.

$F_{1,20} = 5.97$, $p = 0.024$; *post-hoc*: $p = 0.004$) (Figure 4a, right column).

3.3 | Effects of age, sex, and MS on the mRNA expression of the studied BBB transporters

Glucose is the primary energy source of the brain; therefore, GLUT-1 is the most abundant and crucial BBB-related transporter (Bolz et al., 1996). GLUT-1 also plays an essential role in postnatal CNS angiogenesis (Tang et al., 2021). These facts prompted us to investigate developmental profile, sex-related differences and impact of ELS on GLUT-1 gene expression, that is, *Slc2a1* mRNA levels.

We found that consistent with the results for the mRNA expression of TJ proteins, *Slc2a1* mRNA levels increased with age in the mPFC and dSTR (Supporting information Tables S3 and S4 and Figure 4b, left and middle column). An age-dependent increase in the mRNA expression of *Slc2a1* was also observed in the HP (Supporting information Tables S3 and S4, Figure 4b, right column). Moreover, adult females showed higher mRNA levels of *Slc2a1* than males in the mPFC ($p < 0.001$) and dSTR ($p < 0.001$) (Figure 4b, left and middle column). Sex differences in *Slc2a1* expression presented similar direction trends in the HP; however, in juvenile rats ($p = 0.001$) (Figure 4b, right column). We observed that MS influenced the expression of *Slc2a1* exclusively in the dSTR. Namely, MS caused a downregulation of *Slc2a1* mRNA levels in adulthood ($p = 0.048$) (Figure 4b, middle column).

Next, we focus on the assessment of *Aqp4* expression in our experimental conditions. AQP4, as a major water channel in the CNS, is responsible for maintaining water homeostasis and considered another marker of BBB functioning (Nicchia et al., 2004; Xu et al., 2019).

We found an age-dependent decrease in *Aqp4* mRNA levels in all studied brain regions (Supporting information Tables S3, S4 and Figure 5a–c). Moreover, sex and MS affected *Aqp4* mRNA expression only in the dSTR (Figure 5b). Namely, *Aqp4* mRNA levels were lower in juvenile females than in males (two-way ANOVA, the main effect of sex: $F_{1,20} = 74.42$; $p < 0.001$), while in adults, the opposite effect was observed (two-way ANOVA, the main effect of sex: $F_{1,20} = 9.99$; $p = 0.005$) (Figure 5b). Additionally, we observed that MS upregulated *Aqp4* expression exclusively in the dSTR of juvenile males (two-way ANOVA, sex × rearing conditions: $F_{1,20} = 19.03$; $p < 0.001$; *post-hoc:* $p < 0.001$) but not in females (*post-hoc:* $p = 0.100$) (Figure 5b). To help to capture and understand the main findings of the study, we have presented a stripped-down summary of the sex- and MS-induced effects on BBB permeability and mRNA expression of proteins related to BBB functioning in Table 2 and Supporting information Figure S1.

3.4 | Effects of age, sex, and MS on serum S100*β* and proinflammatory cytokine levels

S100*β* belongs to a family of calcium-binding proteins, expressed and released mainly by astrocytes and oligodendrocytes in the brain (Thelin et al., 2017). Serum levels of S100*β* inform about BBB integrity and function

TABLE 2 Stripped-down summary of MS-induced effects on BBB permeability and mRNA expression of proteins related to BBB functioning

		mPFC		dSTR		HP	
Parameter	**PND**	**Females**	**Males**	**Females**	**Males**	**Females**	**Males**
BBB permeability	15	—	—	—	↑	—	—
	70	—	—	—	—	—	—
Cldn3 mRNA	15	—		—	—	↓	—
	70	↓	—	—	—	↓	—
Cldn5 mRNA	15	—	—	↑	—	↑	↑
	70	—	—	↑	↑	↑	↑
Ocln mRNA	15	—	—	—	—	↑	—
	70	—	—	↓	↓	—	—
Slc2a1 mRNA	15	—	—	—	—	—	—
	70	—	—	↓	↓	—	—
Aqp4 mRNA	15	—	—	—	↑	—	—
	70	—	—	—	—	—	—

BBB permeability was determined by extravasation of NaF tracer in the brain. The mRNA expression was determined by RT-qPCR. ↑ indicates an increase versus AFR rats; ↓ indicates a decrease versus AFR rats; and – indicates no difference. Abbreviations are explained in legends of Table 1 and Supporting information Table S1.

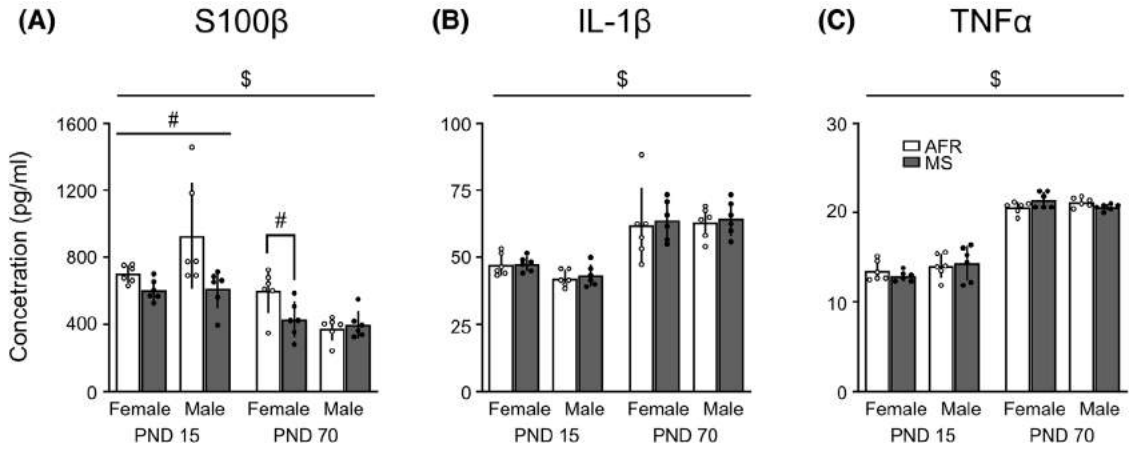

FIGURE 6 Effects of age, sex and MS on serum levels of S100β (a), IL-1β (b) and TNF-α (c). The data indicate serum concentrations of studied proteins (in pg/mL) measured by ELISA and are presented as the mean ± SD. Circles represent individual data points ($n = 6$). $^{\$}p < 0.05$: effect of PND, $^{\#}p < 0.05$: effect of MS (three-way ANOVA followed by Bonferroni *post-hoc* test). Lines relate to the significance of the main effects in ANOVA and connector indicates a *post-hoc* comparison between the specific groups. Abbreviations are explained in legend of Figure 2.

(Kanner et al., 2003). On the other hand, it is well known that increased peripheral inflammation may contribute to BBB leakage (Huang et al., 2021; Welcome & Mastorakis, 2020). Thus, both serum S100β and proinflammatory cytokines can be considered peripheral markers of BBB dysfunction and we decided to measure their levels in our study.

We found that developmental sealing of the BBB observed in our study was accompanied by an age-dependent decrease in serum S100β levels (Supporting information Tables S5 and S6, Figure 6a). Additionally, MS reduced serum S100β levels in juvenile males and females (two-way ANOVA, the main effects of the rearing conditions: $F_{1,20} = 8.52$, $p = 0.009$) (Figure 6a). A similar pattern of MS influence remained until adulthood but was limited only to females (two-way ANOVA, sex × rearing conditions: $F_{1,20} = 5.55$, $p = 0.029$; *post-hoc:* $p = 0.048$) (Figure 6a) and, thus, was not observed in males (*post-hoc:* $p = 0.100$) (Figure 6a).

Next, we focused on the measurements of serum levels of proinflammatory cytokines' representatives such as IL-1β and TNF-α. However, we found that only age influenced the concentrations of these proinflammatory cytokines (Supporting information Tables S5, S6 and Figure 6b,c). Specifically, an age-dependent increase in IL-1β and TNF-α serum levels was observed in both AFR and MS rats (Supporting information Tables S5, S6 and Figure 6b,c).

4 | DISCUSSION

The most noticeable findings of the present study are the developmental sealing of the BBB and pronounced sex differences in the permeability of the BBB and mRNA expression of TJ proteins and *Slc2a1*. Specifically, the BBB of females was less permeable than that of males, especially in adult rats. Lower BBB permeability was accompanied by higher levels of *Cldn3*, *Cldn5*, *Ocln*, and *Slc2a1* in the mPFC and dSTR of adult females. Interestingly, the HP showed slightly distinct patterns in the expression of key factors associated with BBB homeostasis. The present study also revealed that MS temporarily increased BBB permeability in the dSTR of juvenile males and affected mRNA expression of the majority of studied proteins related to BBB function. However, the MS-induced effects proved to be inconsistent regarding the change direction, brain regions, and developmental time. The most distinctive but controversial trend among MS-induced changes was observed in the dSTR of adults, in which *Ocln* and *Slc2a1* were downregulated and *Cldn5* was upregulated. However, in the HP, MS permanently increased the mRNA levels of *Cldn5*.

4.1 | Age-, sex- and region-dependent differences in BBB permeability and structure

Data from the literature indicate that the BBB is mature between postnatal weeks 3 and 4 (Butt et al., 1990; Caley & Maxwell, 1970; Krause et al., 2002) and more permeable in immature animals than in adult animals (Abbott et al., 2010; Lossinsky et al., 1986; Utsumi et al., 2000; Xu & Ling, 1994). The available data on age-related structural changes of the BBB are inconclusive (Ek et al., 2006), although most studies have shown progressive changes in BBB structure during development (Abbott et al., 2010; Bolz et al., 1996; Hirase et al., 1997; Stewart & Hayakawa, 1987). According to previous studies and our findings, the expression of GLUT-1 and OCLD increases from the second postnatal week to the adult level (Hirase et al., 1997; Krause et al., 2002; Vannucci, 1994), which correlates with sealing of the BBB during postnatal development (Butt et al., 1990; Hirase et al., 1997; Utsumi et al., 2000). In the present study, the expression of the majority of the studied TJ proteins and *Slc2a1* clearly increased with age along with a concomitant reduction in the extravasation of the NaF tracer. To the best of our knowledge, our study is the first to analyze the age-dependent mRNA expression of a broad range of proteins related to BBB integrity and function together with a concurrent assessment of BBB permeability in different brain regions and in both sexes, which greatly expands the available literature data. Additionally, we showed an age-dependent decrease in serum levels of S100β, which is a peripheral marker of BBB function (Kanner et al., 2003).

S100β is expressed mainly by astrocytes and oligodendrocytes within the brain (Thelin et al., 2017). It is present both intracellularly and extracellularly. Extracellular levels of S100β increase and are released to the periphery during severe brain pathology, for example, traumatic brain injury (Thelin et al., 2017), and in depressed and schizophrenic patients (Aleksovska et al., 2014; Arora et al., 2019; Gulen et al., 2016). Consistent with our results, clinical data also show a negative correlation between age and serum S100β concentrations and indicate sealing of the BBB during postnatal development (Gazzolo et al., 2003; Thelin et al., 2017).

Our study also showed an age-dependent increase in the serum levels of IL-1β and TNF-α, which are representatives of proinflammatory cytokines. This may reflect developmental maturation of the immune system. It is well known that early-postnatal immune cells in rodents and humans are relatively immature and show impaired innate and adaptive immune response to different stimuli, for example, lower levels of proinflammatory cytokines when compared to adults (Bogaert et al., 2009; Danese & Lewis, 2017).

Sexual dimorphism is still an open question in research on BBB structure and function (reviewed in Profaci et al., 2020). Sex differences in regional brain functions, glucose utilization, and blood flow have been observed and suggest that sex may also determine the integrity and function of the BBB (reviewed in Oztas, 1998). Our study showed that young adult females (PND 70) generally had a less permeable BBB than males, and it was accompanied by higher mRNA levels of TJ proteins and *Slc2a1* (mainly in the mPFC and dSTR). Our results are in line with recent data in humans in which females were shown to have lower blood–cerebrospinal fluid barrier permeability than males (Castellazzi et al., 2020; Parrado-Fernandez et al., 2018). Available data indicate that sex steroid hormones may play an important role in these differences (reviewed in Krause et al., 2006). First, estrogen receptors are expressed in vascular ECs (Zuloaga et al., 2012). Additionally, promoter regions of genes encoding TJ proteins contain estrogen response elements (Greene et al., 2019). Moreover, an impairment in BBB function has been observed in ovariectomized and reproductively senescent female rats and has been reversed by 17β-estradiol treatment (Bake & Sohrabji, 2004; Kang et al., 2006; Saija et al., 1990; Shi & Simpkins, 1997; Shi et al., 1997). Nevertheless, our study showed that sex-related differences also occurred in juveniles in certain cases. Thus, sex-dependent differences in BBB function may develop before puberty during the perinatal phase of sexual differentiation of the brain (Czech et al., 2012; Ngun et al., 2011). Sexual dimorphism in BBB function may contribute to the differences in the efficacy of the transport of many substances through the BBB including glucose and drugs penetrating the CNS (Dudek et al., 2021). Sex differences in BBB integrity may also determine the specific influx of pathogens and cytotoxic agents into the brain and the

neuroinflammatory response. All these factors may underlie well-known sex-related differences in the prevalence of specific mental or neurodegenerative disorders and affect their treatment (Dudek et al., 2021).

Another important question is whether the BBB presents regional heterogeneity and what underlies such heterogeneity (Profaci et al., 2020; Wilhelm et al., 2016). Recent data on humans and mice males indicate that the HP may have increased BBB permeability relative to the cortex and STR and show that it also presents the highest variability of quantitative data (Ivanidze et al., 2019; Weidman et al., 2016). Interestingly, we observed a higher BBB permeability in the HP than in the mPFC in the case of females, both juvenile and adult, but not for males. We also showed that a pattern of developmental changes in *Cldn3* and *Ocln* mRNA expression in the HP differed from that in the mPFC and dSTR. We can only speculate about potential reasons for such differences. It is worth mentioning that the HP itself shows anatomical and functional heterogeneity, with specific subregions of the HP differing in the density of microvessels (Cavaglia et al., 2001; Zhang et al., 2019). For example, the CA1 region has a low capillary density compared to the CA3 region (Cavaglia et al., 2001). In our study, we assessed the HP as a whole, which might have strongly determined the outcome of the mRNA analysis and variability of the data.

4.2 | Effect of ELS on BBB permeability and integrity

Although our study revealed that MS did not cause consistent or substantial changes in the parameters related to BBB function, we observed specific age-, region- and sex-dependent effects. The dSTR and HP were the brain regions most affected by MS in our study. The impact of MS on BBB permeability was limited to the dSTR of juvenile males. MS induced increases in BBB permeability disrupted the general sex differences observed in juveniles. In adults, MS did not significantly affect BBB permeability in the dSTR per se; however, MS rats did not show sex-related differences typical of dSTR.

Acute and chronic exposure to psychophysiological stressors has been shown to increase BBB permeability (Gomez-Gonzalez & Escobar, 2009; Hanin, 1996; Santha et al., 2015; Sharma, 2004; Welcome & Mastorakis, 2020). To the best of our knowledge, only one prior report has shown changes in BBB permeability induced by ELS (Gomez-Gonzalez & Escobar, 2009). The authors demonstrated that prenatal stress and MS increase BBB permeability in the neocortex, HP, and basal ganglia in juvenile rats and that this effect does not persist until adolescence. However, the authors of this study pooled data for male and female subjects together, thus, excluding the possibility of sex differences (Gomez-Gonzalez & Escobar, 2009).

Although the MS induced increase in BBB permeability in the dSTR was temporal, it was revealed during a critical period of postnatal brain development and may have potential detrimental consequences for juveniles and adolescents. Unexpectedly, the increased BBB permeability observed in the dSTR of MS juvenile males was not accompanied by any change in the mRNA expression of TJ proteins. However, MS enhanced *Aqp4* expression in the dSTR of juvenile males. AQP4, which is expressed in astrocytes and accumulates specifically in astrocyte end feet, is responsible for maintaining water homeostasis, especially during the second week of postnatal development (Wen et al., 1999). AQP4 is one of the key players in vasogenic edema formation and resolution (Fukuda & Badaut, 2012). Edema is accompanied by enhanced AQP4 levels and is frequently associated with BBB disruption (Fukuda & Badaut, 2012; Tomas-Camardiel et al., 2005). Therefore, a change in AQP4 expression is often considered a marker of BBB function (Xu et al., 2019). Consistent with our data, chronic restraint stress has been shown to induce hyperpermeability of the BBB in the amygdala, which is accompanied by an increase in AQP4 protein expression (Xu et al., 2019).

It is worth emphasizing that the NaF used in our study to determine BBB permeability is a very small molecule (376 Da) and detectable at very low concentrations (Sun et al., 2021). Therefore, the method applied in the present study is very sensitive and detects slight BBB breakdown. We argue that MS caused a small-scale change in BBB permeability in juvenile males that applied only to small molecules. Thus, it is not surprising that we did not observe MS induced increases in serum levels of S100β, which is another marker of BBB integrity, with a molecular weight of approximately 10 kDa. Instead, we revealed a reduction in serum S100β levels in MS juveniles that persisted to adulthood in females. It is worth emphasizing that S100β is also a marker of glial function, and levels of this glial protein in serum below control levels may indicate glial pathology within the BBB or generally in the brain (Michetti et al., 2019). A reduction in the number of glial cells or their specific markers has been frequently observed in animal models of chronic stress (including ELS) and in patients with affective disorders (Czeh et al., 2013; Rajkowska & Stockmeier, 2013). We have previously shown that MS decreased the number of S100β immunoreactive cells in the midbrain of juvenile rats (Chocyk et al., 2011). Moreover, studies have identified several extracerebral sources of S100β protein, for example, adipocytes; however, S100β released from these sources has a faster clearance than that released from the brain (Michetti et al., 2019; Thelin et al., 2017). Nevertheless, we cannot completely exclude the contribution of S100β from extracerebral sources to the S100β level measured in our study.

It is generally accepted that peripheral inflammation may contribute to BBB disruption (Huang et al., 2021; Welcome & Mastorakis, 2020). Our study revealed that the serum levels of proinflammatory cytokines were not influenced by MS. Thus, our MS procedure did not induce visible signs of inflammatory response in either juvenile or adult rats. The majority of data from the literature show that repeated MS does not affect the serum concentrations of proinflammatory cytokines, especially in basal conditions (for review, see Dutcher et al., 2020). This may result from a relative immaturity of the immune system during the MS procedure (Bogaert et al., 2009; Ortega et al., 2011). The lack of peripheral inflammation in MS rats is consistent with the small-scale changes or lack of changes in BBB permeability observed in the present study.

Available data have shown that chronic stress downregulates the expression of TJ proteins and alters GLUT-1 levels in different brain regions of adult animals (Welcome & Mastorakis, 2020). Consistent with these data, we found MS induced decreases in the mRNA expression of *Ocln* and *Slc2a1* in the dSTR of adult males and females and an enduring reduction in *Cldn3* mRNA levels in the HP and mPFC of females. Interestingly, in the dSTR and HP, these effects were accompanied by a persistent upregulation of *Cldn5* mRNA expression. CLDN5 is considered a major TJ protein, and it is functionally active at early developmental stages (Abbott et al., 2010; Haseloff et al., 2015) and controls paracellular permeation of molecules lower than 800 Da (Haseloff et al., 2015) such as NaF (376 Da) used in our study. We argue that persistent upregulation of *Cldn5* mRNA expression may generally protect MS rats from significant BBB dysfunction. Notably, for the only case in which MS induced increases in BBB permeability, such as in the dSTR of juvenile males, we did not observe upregulation of *Cldn5*.

Recent reports proposed that vascular remodeling in the brain may determine vulnerability or resilience to stress and depression (Menard et al., 2017; Pearson-Leary et al., 2017). In this respect, changes in the expression of CLDN5 are especially interesting. It has been shown that, like in our study, chronic stress in the form of prolonged social isolation increased *Cldn5* levels in the HP of adult rats (Alshammari et al., 2020). On the other hand, a reduction in CLDN5 has been observed in the nucleus accumbens of depressed patients (Dudek et al., 2020). Moreover, conditional knockdown of *Cldn5* is sufficient to produce depressive-like behavior (Menard et al., 2017). In a model of chronic social defeat stress, which is a mouse model of depression, it has been demonstrated that only stress-susceptible but not stress-resilient mice showed increased BBB permeability and reduced expression of *Cldn5* (Menard et al., 2017). Moreover, permissive epigenetic regulation of *Cldn5* expression and low endothelial expression of the repressive Cldn5-related transcription factor *foxo1* are associated with stress resilience (Dudek et al., 2020). However, these studies were solely focused on the nucleus accumbens.

We can only speculate that MS-induced changes in mRNA expression of TJ proteins, especially *Cldn5*, could be a manifestation of adaptive changes and compensatory mechanisms within the BBB that may lead to resilience of an unknown kind. Although in the present study, we did not correlate the data with the behavioral phenotype of the animals, we have previously shown that our MS adult rats did not display depressive-like behaviors (Chocyk et al., 2015; Solarz et al., 2021). However, our ELS model affects anxiety-like behaviors (Chocyk et al., 2015; Solarz et al., 2021), impairs fear memory (Chocyk et al., 2014), and enhances the locomotor response to cocaine injection in adult rats (Chocyk et al., 2011). Thus, we observe many but not all typical behavioral characteristics of ELS models.

Taken together, the results of the present study indicate that our ELS procedure did not produce a clear or strong negative effect on BBB integrity. Rather, signs of adaptation and/or resilience were observed in the MS rats. However, we cannot exclude the possibility that the ELS-induced impact on the expression of key regulators of BBB function may result in maladaptation of the BBB specifically in response to other environmental factors. Animal studies clearly show that ELS increases susceptibility to age-related cognitive decline and neurodegenerative disorders, such as AD and PD, or exacerbates the effects of brain injury (Andersen & Teicher, 2004; Barlow et al., 2007; Catale et al., 2021; Lajud et al., 2021; Llorente et al., 2009; Martisova et al., 2013). Further studies are needed to verify this interesting hypothesis.

In conclusion, we observed developmental sealing of the BBB and a less permeable BBB in females than in males. Our study revealed small-scale effects of MS on BBB permeability and mRNA expression of proteins related to BBB function. Although MS-induced effects may seem inconsistent, they could reflect adaptive/maladaptive changes within the BBB. These changes may precondition individuals who have experienced ELS and enhance their susceptibility or resilience to psychiatric and/or neurodegenerative disorders later in life.

ACKNOWLEDGMENTS

The authors thank Dr. Joanna Kryst for valuable technical assistance with MS procedure and biochemical analyses. This work was supported by a Preludium 12 Grant (2016/23/N/NZ4/01148) from the National Science Centre, Poland.

CONFLICT OF INTEREST

The authors declare no conflict of interest.

AUTHOR CONTRIBUTIONS

AC and AS conceived the original idea. AC supervised the project. AS, IMM and AC carried out the experiments and

collected the data. AS analyzed the data. All authors provided critical feedback and helped shape the research. AS wrote the manuscript with support from AC. All authors discussed the results and contributed to the final manuscript.

DATA AVAILABILITY STATEMENT

The data that support the findings of this study are available from the corresponding author upon reasonable request.

ORCID

Agnieszka Chocyk https://orcid.org/0000-0002-0589-6569

REFERENCES

Abbott, N. J., Patabendige, A. A., Dolman, D. E., Yusof, S. R., & Begley, D. J. (2010). Structure and function of the blood–brain barrier. *Neurobiology of Disease*, *37*(1), 13–25.

Abbott, N. J., Ronnback, L., & Hansson, E. (2006). Astrocyte-endothelial interactions at the blood–brain barrier. *Nature Reviews Neuroscience*, *7*(1), 41–53.

Aleksovska, K., Leoncini, E., Bonassi, S., Cesario, A., Boccia, S., & Frustaci, A. (2014). Systematic review and meta-analysis of circulating S100B blood levels in schizophrenia. *Plos One*, *9*(9), e106342.

Alshammari, T. K., Alghamdi, H. M., Alduhailan, H. E., Saja, M. F., Alrasheed, N. M., & Alshammari, M. A. (2020). Examining the central effects of chronic stressful social isolation on rats. *Biomedical Reports*, *13*(6), 56.

Andersen, S. L., & Teicher, M. H. (2004). Delayed effects of early stress on hippocampal development. *Neuropsychopharmacology*, *29*(11), 1988–1993.

Arora, P., Sagar, R., Mehta, M., Pallavi, P., Sharma, S., & Mukhopadhyay, A. K. (2019). Serum S100B levels in patients with depression. *Indian Journal of Psychiatry*, *61*(1), 70–76.

Bake, S., & Sohrabji, F. (2004). 17beta-estradiol differentially regulates blood–brain barrier permeability in young and aging female rats. *Endocrinology*, *145*(12), 5471–5475.

Ballabh, P., Braun, A., & Nedergaard, M. (2004). The blood–brain barrier: An overview: Structure, regulation, and clinical implications. *Neurobiology of Disease*, *16*(1), 1–13.

Barlow, B. K., Cory-Slechta, D. A., Richfield, E. K., & Thiruchelvam, M. (2007). The gestational environment and Parkinson's disease: Evidence for neurodevelopmental origins of a neurodegenerative disorder. *Reproductive Toxicology*, *23*(3), 457–470.

Baudin, A., Blot, K., Verney, C., Estevez, L., Santamaria, J., Gressens, P., Giros, B., Otani, S., Daugé, V., & Naudon, L. (2012). Maternal deprivation induces deficits in temporal memory and cognitive flexibility and exaggerates synaptic plasticity in the rat medial prefrontal cortex. *Neurobiology of Learning and Memory*, *98*(3), 207–214.

Bogaert, D., Weinberger, D., Thompson, C., Lipsitch, M., & Malley, R. (2009). Impaired innate and adaptive immunity to *Streptococcus pneumoniae* and its effect on colonization in an infant mouse model. *Infection and Immunity*, *77*(4), 1613–1622.

Bolz, S., Farrell, C. L., Dietz, K., & Wolburg, H. (1996). Subcellular distribution of glucose transporter (GLUT-1) during development of the blood–brain barrier in rats. *Cell and Tissue Research*, *284*(3), 355–365.

Brenhouse, H. C., Lukkes, J. L., & Andersen, S. L. (2013). Early life adversity alters the developmental profiles of addiction-related prefrontal cortex circuitry. *Brain Sciences*, *3*(1), 143–158.

Butt, A. M., Jones, H. C., & Abbott, N. J. (1990). Electrical resistance across the blood–brain barrier in anaesthetized rats: A developmental study. *Journal of Physiology*, *429*, 47–62.

Caley, D. W., & Maxwell, D. S. (1970). Development of the blood vessels and extracellular spaces during postnatal maturation of rat cerebral cortex. *Journal of Comparative Neurology*, *138*(1), 31–47.

Castellazzi, M., Morotti, A., Tamborino, C., Alessi, F., Pilotto, S., Baldi, E., Caniatti, L. M., Trentini, A., Casetta, I., Granieri, E., Pugliatti, M., Fainardi, E., & Bellini, T. (2020). Increased age and male sex are independently associated with higher frequency of blood-cerebrospinal fluid barrier dysfunction using the albumin quotient. *Fluids Barriers CNS*, *17*(1), 14.

Catale, C., Bisicchia, E., Carola, V., & Teresa Viscomi, M. (2021). Early life stress exposure worsens adult remote microglia activation, neuronal death, and functional recovery after focal brain injury. *Brain, Behavior, and Immunity*,*94*, 89—103.

Cavaglia, M., Dombrowski, S. M., Drazba, J., Vasanji, A., Bokesch, P. M., & Janigro, D. (2001). Regional variation in brain capillary density and vascular response to ischemia. *Brain Research*, *910*(1-2), 81–93.

Chocyk, A., Bobula, B., Dudys, D., Przyborowska, A., Majcher-Maslanka, I., Hess, G., & Wedzony, K. (2013). Early-life stress affects the structural and functional plasticity of the medial prefrontal cortex in adolescent rats. *European Journal of Neuroscience*, *38*(1), 2089–2107.

Chocyk, A., Dudys, D., Przyborowska, A., Mackowiak, M., & Wedzony, K. (2010). Impact of maternal separation on neural cell adhesion molecules expression in dopaminergic brain regions of juvenile, adolescent and adult rats. *Pharmacological Reports*, *62*(6), 1218–1224.

Chocyk, A., Dudys, D., Przyborowska, A., Majcher, I., Mackowiak, M., & Wedzony, K. (2011). Maternal separation affects the number, proliferation and apoptosis of glia cells in the substantia nigra and ventral tegmental area of juvenile rats. *Neuroscience*, *173*, 1–18.

Chocyk, A., Majcher-Maslanka, I., Przyborowska, A., Mackowiak, M., & Wedzony, K. (2015). Early-life stress increases the survival of midbrain neurons during postnatal development and enhances reward-related and anxiolytic-like behaviors in a sex-dependent fashion. *International Journal of Developmental Neuroscience*, *44*, 33–47.

Chocyk, A., Przyborowska, A., Makuch, W., Majcher-Maslanka, I., Dudys, D., & Wedzony, K. (2014). The effects of early-life adversity on fear memories in adolescent rats and their persistence into adulthood. *Behavioural Brain Research*, *264*, 161–172.

Czech, D. P., Lee, J., Sim, H., Parish, C. L., Vilain, E., & Harley, V. R. (2012). The human testis-determining factor SRY localizes in midbrain dopamine neurons and regulates multiple components of catecholamine synthesis and metabolism. *Journal of Neurochemistry*, *122*(2), 260–271.

Czeh, B., Fuchs, E., & Flugge, G. (2013). Altered glial plasticity in animal models for mood disorders. *Current Drug Targets*, *14*(11), 1249–1261.

Danese, A., & Lewis, S. J. (2017). Psychoneuroimmunology of early-life stress: The hidden wounds of childhood trauma? *Neuropsychopharmacology*, *42*(1), 99–114.

Dudek, K. A., Dion-Albert, L., Kaufmann, F. N., Tuck, E., Lebel, M., & Menard, C. (2021). Neurobiology of resilience in depression: Immune and vascular insights from human and animal studies. *European Journal of Neuroscience*, *53*(1), 183–221.

Dudek, K. A., Dion-Albert, L., Lebel, M., LeClair, K., Labrecque, S., Tuck, E., Perez, C. F., Golden, S. A., Tamminga, C., Turecki, G., Mechawar, N., Russo, S. J., & Menard, C. (2020). Molecular

adaptations of the blood–brain barrier promote stress resilience vs. depression. *Proceedings of the National Academy of Sciences of the United States of America*, *117*(6), 3326–3336.

Dutcher, E. G., Pama, E. A. C., Lynall, M. E., Khan, S., Clatworthy, M. R., Robbins, T. W., Bullmore, E. T., & Dalley, J. W. (2020). Early-life stress and inflammation: A systematic review of a key experimental approach in rodents. *Brain and Neuroscience Advances*, *4*, 239821282097804.

Ek, C. J., Dziegielewska, K. M., Stolp, H., & Saunders, N. R. (2006). Functional effectiveness of the blood–brain barrier to small water-soluble molecules in developing and adult opossum (*Monodelphis domestica*). *Journal of Comparative Neurology*, *496*(1), 13–26.

Erickson, M. A., & Banks, W. A. (2013). Blood–brain barrier dysfunction as a cause and consequence of Alzheimer's disease. *Journal of Cerebral Blood Flow and Metabolism*, *33*(10), 1500–1513.

Fareri, D. S., & Tottenham, N. (2016). Effects of early life stress on amygdala and striatal development. *Developmental Cognitive Neuroscience*, *19*, 233–247.

Fukuda, A. M., & Badaut, J. (2012). Aquaporin 4: A player in cerebral edema and neuroinflammation. *Journal of Neuroinflammation*, *9*, 279.

Ganguly, P., & Brenhouse, H. C. (2015). Broken or maladaptive? Altered trajectories in neuroinflammation and behavior after early life adversity. *Developmengtal Cognitive Neuroscience*, *11*, 18–30.

Gazzolo, D., Michetti, F., Bruschettini, M., Marchese, N., Lituania, M., Mangraviti, S., Pedrazzi, E., & Bruschettini, P. (2003). Pediatric concentrations of S100B protein in blood: Age- and sex-related changes. *Clinical Chemistry*, *49*(6), 967–970.

Gomez-Gonzalez, B., & Escobar, A. (2009). Altered functional development of the blood–brain barrier after early life stress in the rat. *Brain Research Bulletin*, *79*(6), 376–387.

Greene, C., Hanley, N., & Campbell, M. (2019). Claudin-5: Gatekeeper of neurological function. *Fluids and Barriers of the CNS*, *16*, 3.

Gulen, B., Serinken, M., Eken, C., Karcioglu, O., Kucukdagli, O. T., Kilic, E., Akpinar, G., Nogay, S., & Kuh, M. (2016). Serum S100B as a surrogate biomarker in the diagnoses of burnout and depression in emergency medicine residents. *Academic Emergency Medicine*, *23*(7), 786–789.

Hanin, I. (1996). The Gulf War, stress and a leaky blood–brain barrier. *Nature Medicine*, *2*(12), 1307–1308.

Haseloff, R. F., Dithmer, S., Winkler, L., Wolburg, H., & Blasig, I. E. (2015). Transmembrane proteins of the tight junctions at the blood–brain barrier: Structural and functional aspects. *Seminars in Cell & Developmental Biology*, *38*, 16–25.

Hirase, T., Staddon, J. M., Saitou, M., Ando-Akatsuka, Y., Itoh, M., Furuse, M., Fujimoto, K., Tsukita, S., & Rubin, L. L. (1997). Occludin as a possible determinant of tight junction permeability in endothelial cells. *Journal of Cell Science*, *110*(Pt 14), 1603–1613.

Huang, X. W., Hussain, B., & Chang, J. L. (2021). Peripheral inflammation and blood–brain barrier disruption: Effects and mechanisms. *CNS Neuroscience & Therapeutics*, *27*(1), 36–47.

Ivanidze, J., Mackay, M., Hoang, A., Chi, J. M., Cheng, K., Aranow, C., Volpe, B., Diamond, B., & Sanelli, P. C. (2019). Dynamic contrast-enhanced MRI reveals unique blood-brain barrier permeability characteristics in the hippocampus in the normal brain. *American Journal of Neuroradiology*, *40*(3), 408–411.

Kang, H. S., Ahn, H. S., Kang, H. J., & Gye, M. C. (2006). Effect of estrogen on the expression of occludin in ovariectomized mouse brain. *Neuroscience Letters*, *402*(1-2), 30–34.

Kanner, A. A., Marchi, N., Fazio, V., Mayberg, M. R., Koltz, M. T., Siomin, V., Stevens, G. H. J., Masaryk, T., Ayumar, B., Vogelbaum, M. A., Barnett, G. H., & Janigro, D. (2003). Serum S100beta: A non-invasive marker of blood–brain barrier function and brain lesions. *Cancer*, *97*(11), 2806–2813.

Kessler, R. C., McLaughlin, K. A., Green, J. G., Gruber, M. J., Sampson, N. A., Zaslavsky, A. M., Aguilar-Gaxiola, S., Alhamzawi, A. O., Alonso, J., Angermeyer, M., Benjet, C., Bromet, E., Chatterji, S., de Girolamo, G., Demyttenaere, K., Fayyad, J., Florescu, S., Gal, G., Gureje, O., … & Williams, D. R. (2010). Childhood adversities and adult psychopathology in the WHO World Mental Health Surveys. *British Journal of Psychiatry*, *197*(5), 378–385.

Krause, D. N., Duckles, S. P., & Pelligrino, D. A. (2006). Influence of sex steroid hormones on cerebrovascular function. *Journal of Applied Physiology (1985)*, *101*(4), 1252–1261.

Krause, D. N., Faustmann, P. M., & Dermietzel, R. (2002). Molecular anatomy of the blood-brain barrier in development and aging. In J. S. de Vellis (Ed.), *Neuroglia in the aging brain* (pp. 291–303). Humana Press.

Lajud, N., Roque, A., Cheng, J. P., Bondi, C. O., & Kline, A. E. (2021). Early life stress preceding mild pediatric traumatic brain injury increases neuroinflammation but does not exacerbate impairment of cognitive flexibility during adolescence. *Journal of Neurotrauma*, *38*(4), 411–421.

Llorente, R., Gallardo, M. L., Berzal, A. L., Prada, C., Garcia-Segura, L. M., & Viveros, M. P. (2009). Early maternal deprivation in rats induces gender-dependent effects on developing hippocampal and cerebellar cells. *International Journal of Developmental Neuroscience*, *27*(3), 233–241.

Loria, A. S., Ho, D. H., & Pollock, J. S. (2014). A mechanistic look at the effects of adversity early in life on cardiovascular disease risk during adulthood. *Acta Physiol (Oxf)*, *210*(2), 277–287.

Lossinsky, A. S., Vorbrodt, A. W., & Wisniewski, H. M. (1986). Characterization of endothelial cell transport in the developing mouse blood-brain barrier. *Developmental Neuroscience*, *8*(2), 61–75.

Mabandla, M. V., & Russell, V. A. (2010). Voluntary exercise reduces the neurotoxic effects of 6-hydroxydopamine in maternally separated rats. *Behavioural Brain Research*, *211*(1), 16–22.

Majcher-Maslanka, I., Solarz, A., & Chocyk, A. (2019). Maternal separation disturbs postnatal development of the medial prefrontal cortex and affects the number of neurons and glial cells in adolescent rats. *Neuroscience*, *423*, 131–147.

Martisova, E., Aisa, B., Guerenu, G., & Ramirez, M. J. (2013). Effects of early maternal separation on biobehavioral and neuropathological markers of Alzheimer's disease in adult male rats. *Current Alzheimer Research*, *10*(4), 420–432.

Menard, C., Pfau, M. L., Hodes, G. E., Kana, V., Wang, V. X., Bouchard, S., Takahashi, A., Flanigan, M. E., Aleyasin, H., LeClair, K. B., Janssen, W. G., Labonté, B., Parise, E. M., Lorsch, Z. S., Golden, S. A., Heshmati, M., Tamminga, C., Turecki, G., Campbell, M., & Russo, S. J. (2017). Social stress induces neurovascular pathology promoting depression. *Nature Neuroscience*, *20*(12), 1752–1760.

Michetti, F., D'Ambrosi, N., Toesca, A., Puglisi, M. A., Serrano, A., Marchese, E., Corvino, V., & Geloso, M. C. (2019). The S100B story: From biomarker to active factor in neural injury. *Journal of Neurochemistry*, *148*(2), 168–187.

Mpofana, T., Daniels, W. M., & Mabandla, M. V. (2016). Exposure to early life stress results in epigenetic changes in neurotrophic factor

gene expression in a parkinsonian rat model. *Parkinson's Disease*, *2016*, 6438783 .

Ngun, T. C., Ghahramani, N., Sanchez, F. J., Bocklandt, S., & Vilain, E. (2011). The genetics of sex differences in brain and behavior. *Frontiers in Neuroendocrinology*, *32*(2), 227–246.

Nicchia, G. P., Nico, B., Camassa, L. M., Mola, M. G., Loh, N., Dermietzel, R., Spray, D. C., Svelto, M., & Frigeri, A. (2004). The role of aquaporin-4 in the blood-brain barrier development and integrity: Studies in animal and cell culture models. *Neuroscience*, *129*(4), 935–944.

Nielsen, S., Nagelhus, E. A., Amiry-Moghaddam, M., Bourque, C., Agre, P., & Ottersen, O. P. (1997). Specialized membrane domains for water transport in glial cells: High-resolution immunogold cytochemistry of aquaporin-4 in rat brain. *Journal of Neuroscience*, *17*(1), 171–180.

Ortega, A., Jadeja, V., & Zhou, H. (2011). Postnatal development of lipopolysaccharide-induced inflammatory response in the brain. *Inflammation Research*, *60*(2), 175–185.

Oztas, B. (1998). Sex and blood-brain barrier. *Pharmacological Research*, *37*(3), 165–167.

Parrado-Fernandez, C., Blennow, K., Hansson, M., Leoni, V., Cedazo-Minguez, A., & Bjorkhem, I. (2018). Evidence for sex difference in the CSF/plasma albumin ratio in ∼20 000 patients and 335 healthy volunteers. *Journal of Cellular and Molecular Medicine*, *22*(10), 5151–5154.

Paxinos, G., & Watson, C. (1998). *The rat brain in stereotaxic coordinates*. Academic Press.

Pearson-Leary, J., Eacret, D., Chen, R., Takano, H., Nicholas, B., & Bhatnagar, S. (2017). Inflammation and vascular remodeling in the ventral hippocampus contributes to vulnerability to stress. *Translational Psychiatry*, *7*, e1160.

Pinares-Garcia, P., Stratikopoulos, M., Zagato, A., Loke, H., & Lee, J. (2018). Sex: A significant risk factor for neurodevelopmental and neurodegenerative disorders. *Brain Sciences*, *8*(8), 154, ,.

Profaci, C. P., Munji, R. N., Pulido, R. S., & Daneman, R. (2020). The blood-brain barrier in health and disease: Important unanswered questions. *Journal of Experimental Medicine*, *217*(4): e20190062.

Rajkowska, G., & Stockmeier, C. A. (2013). Astrocyte pathology in major depressive disorder: Insights from human postmortem brain tissue. *Current Drug Targets*, *14*(11), 1225–1236.

Ramirez, S. H., Potula, R., Fan, S., Eidem, T., Papugani, A., Reichenbach, N., Dykstra, H., Weksler, B. B., Romero, I. A., Couraud, P. O., & Persidsky, Y. (2009). Methamphetamine disrupts blood-brain barrier function by induction of oxidative stress in brain endothelial cells. *Journal of Cerebral Blood Flow and Metabolism*, *29*(12), 1933–1945.

Saija, A., Princi, P., D'Amico, N., De Pasquale, R., & Costa, G. (1990). Aging and sex influence the permeability of the blood-brain barrier in the rat. *Life Sciences*, *47*(24), 2261–2267.

Santha, P., Veszelka, S., Hoyk, Z., Meszaros, M., Walter, F. R., Toth, A. E., Kiss, L., Kincses, A., Oláh, Z., Seprényi, G., Rákhely, G., Dér, A., Pákáski, M., Kálmán, J., Kittel, Á., & Deli, M. A. (2015). Restraint stress-induced morphological changes at the blood-brain barrier in adult rats. *Frontiers in Molecular Neuroscience*, *8*, 88.

Sharma, H. S. (2004). Blood-brain and spinal cord barriers in stress. In H. S. Sharma (Ed.), *Blood-spinal cord and brain barriers in health and disease* (Vol., 1, pp. 231–298). Academic Press, Elsevier.

Shi, J., & Simpkins, J. W. (1997). 17 beta-Estradiol modulation of glucose transporter 1 expression in blood-brain barrier. *American Journal of Physiology*, *272*(6 Pt 1), E1016–E1022.

Shi, J., Zhang, Y. Q., & Simpkins, J. W. (1997). Effects of 17beta-estradiol on glucose transporter 1 expression and endothelial cell survival following focal ischemia in the rats. *Experimental Brain Research Experimentelle Hirnforschung Experimentation Cerebrale*, *117*(2), 200–206.

Solarz, A., Majcher-Maslanka, I., Kryst, J., & Chocyk, A. (2021). A search for biomarkers of early-life stress-related psychopathology: Focus on 70-kDa heat shock proteins. *Neuroscience*,*463*, 238-253,

Solas, M., Aisa, B., Mugueta, M. C., Del Rio, J., Tordera, R. M., & Ramirez, M. J. (2010). Interactions between age, stress and insulin on cognition: Implications for Alzheimer's disease. *Neuropsychopharmacology*, *35*(8), 1664–1673.

Stewart, P. A., & Hayakawa, E. M. (1987). Interendothelial junctional changes underlie the developmental 'tightening' of the blood-brain barrier. *Brain Research*, *32*(2), 271–281.

Stolp, H. B., & Dziegielewska, K. M. (2009). Review: Role of developmental inflammation and blood-brain barrier dysfunction in neurodevelopmental and neurodegenerative diseases. *Neuropathology and Applied Neurobiology*, *35*(2), 132–146.

Sun, H., Hu, H., Liu, C., Sun, N., & Duan, C. (2021). Methods used for the measurement of blood-brain barrier integrity. *Metabolic Brain Disease*, *36*(5), 723–735.

Tang, M., Park, S. H., Petri, S., Yu, H., Rueda, C. B., Abel, E. D., Kim, C. Y., Hillman, E. M. C., Li, F., Lee, Y., Ding, L., Jagadish, S., Frankel, W. N., De Vivo, D. C., & Monani, U. R. (2021). An early endothelial cell-specific requirement for Glut1 is revealed in Glut1 deficiency syndrome model mice. *JCI Insight*, *6*(3),.

Thelin, E. P., Nelson, D. W., & Bellander, B. M. (2017). A review of the clinical utility of serum S100B protein levels in the assessment of traumatic brain injury. *Acta Neurochirurgica*, *159*(2), 209–225.

Tomas-Camardiel, M., Venero, J. L., Herrera, A. J., De Pablos, R. M., Pintor-Toro, J. A., Machado, A., & Cano, J. (2005). Blood-brain barrier disruption highly induces aquaporin-4 mRNA and protein in perivascular and parenchymal astrocytes: Protective effect by estradiol treatment in ovariectomized animals. *Journal of Neuroscience Research*, *80*(2), 235–246.

Utsumi, H., Chiba, H., Kamimura, Y., Osanai, M., Igarashi, Y., Tobioka, H., Mori, M., & Sawada, N. (2000). Expression of GFRalpha-1, receptor for GDNF, in rat brain capillary during postnatal development of the BBB. *American Journal of Physiology. Cell Physiology*, *279*(2), C361–C368.

Vannucci, S. J. (1994). Developmental expression of GLUT1 and GLUT3 glucose transporters in rat brain. *Journal of Neurochemistry*, *62*(1), 240–246.

Weidman, E. K., Foley, C. P., Kallas, O., Dyke, J. P., Gupta, A., Giambrone, A. E., Ivanidze, J., Baradaran, H., Ballon, D. J., & Sanelli, P. C. (2016). Evaluating permeability surface-area product as a measure of blood–brain barrier permeability in a murine model. *American Journal of Neuroradiology*, *37*(7), 1267–1274.

Welcome, M. O., & Mastorakis, N. E. (2020). Stress-induced blood brain barrier disruption: Molecular mechanisms and signaling pathways. *Pharmacological Research*, *157*, 104769.

Wen, H., Nagelhus, E. A., Amiry-Moghaddam, M., Agre, P., Ottersen, O. P., & Nielsen, S. (1999). Ontogeny of water transport in rat brain: Postnatal expression of the aquaporin-4 water channel. *European Journal of Neuroscience*, *11*(3), 935–945.

Wilhelm, I., Nyul-Toth, A., Suciu, M., Hermenean, A., & Krizbai, I. A. (2016). Heterogeneity of the blood-brain barrier. *Tissue Barriers*, *4*(1), e1143544.

Winkler, E. A., Nishida, Y., Sagare, A. P., Rege, S. V., Bell, R. D., Perlmutter, D., Sengillo, J. D., Hillman, S., Kong, P., Nelson, A. R., Sullivan, J. S., Zhao, Z., Meiselman, H. J., Wenby, R. B., Soto, J., Abel, E. D., Makshanoff, J., Zuniga, E., De Vivo, D. C., & Zlokovic, B. V. (2015). GLUT1 reductions exacerbate Alzheimer's disease vasculo-neuronal dysfunction and degeneration. *Nature Neuroscience*, *18*(4), 521–530.

Xu, G., Li, Y., Ma, C., Wang, C., Sun, Z., Shen, Y., Liu, L., Li, S., Zhang, X., & Cong, B. (2019). Restraint stress induced hyperpermeability and damage of the blood-brain barrier in the amygdala of adult rats. *Frontiers in Molecular Neuroscience*, *12*, 32.

Xu, J., & Ling, E. A. (1994). Studies of the ultrastructure and permeability of the blood-brain barrier in the developing corpus callosum in postnatal rat brain using electron dense tracers. *Journal of Anatomy*, *184*(Pt 2), 227–237.

Yen, L. F., Wei, V. C., Kuo, E. Y., & Lai, T. W. (2013). Distinct patterns of cerebral extravasation by Evans blue and sodium fluorescein in rats. *Plos One*, *8*(7), e68595.

Zhang, X. C., Yin, X. Z., Zhang, J. J., Li, A. A., Gong, H., Luo, Q. M., Zhang, H. Y., Gao, Z. B., & Jiang, H. L. (2019). High-resolution mapping of brain vasculature and its impairment in the hippocampus of Alzheimer's disease mice. *National Science Review*, *6*(6), 1223–1238.

Zuloaga, K. L., Swift, S. N., Gonzales, R. J., Wu, T. J., & Handa, R. J. (2012). The androgen metabolite, 5 alpha-androstane-3 beta,17 beta-diol, decreases cytokine-induced cyclooxygenase-2, vascular cell adhesion molecule-1 expression, and p-glycoprotein expression in male human brain microvascular endothelial cells. *Endocrinology*, *153*(12), 5949–5960.

SUPPORTING INFORMATION

Additional supporting information may be found online in the Supporting Information section at the end of the article.

How to cite this article: Solarz, A., Majcher-Maślanka, I., & Chocyk, A. (2021). Effects of early-life stress and sex on blood–brain barrier permeability and integrity in juvenile and adult rats. *Developmental Neurobiology*, *81:*861–876. https://doi.org/10.1002/dneu.22846

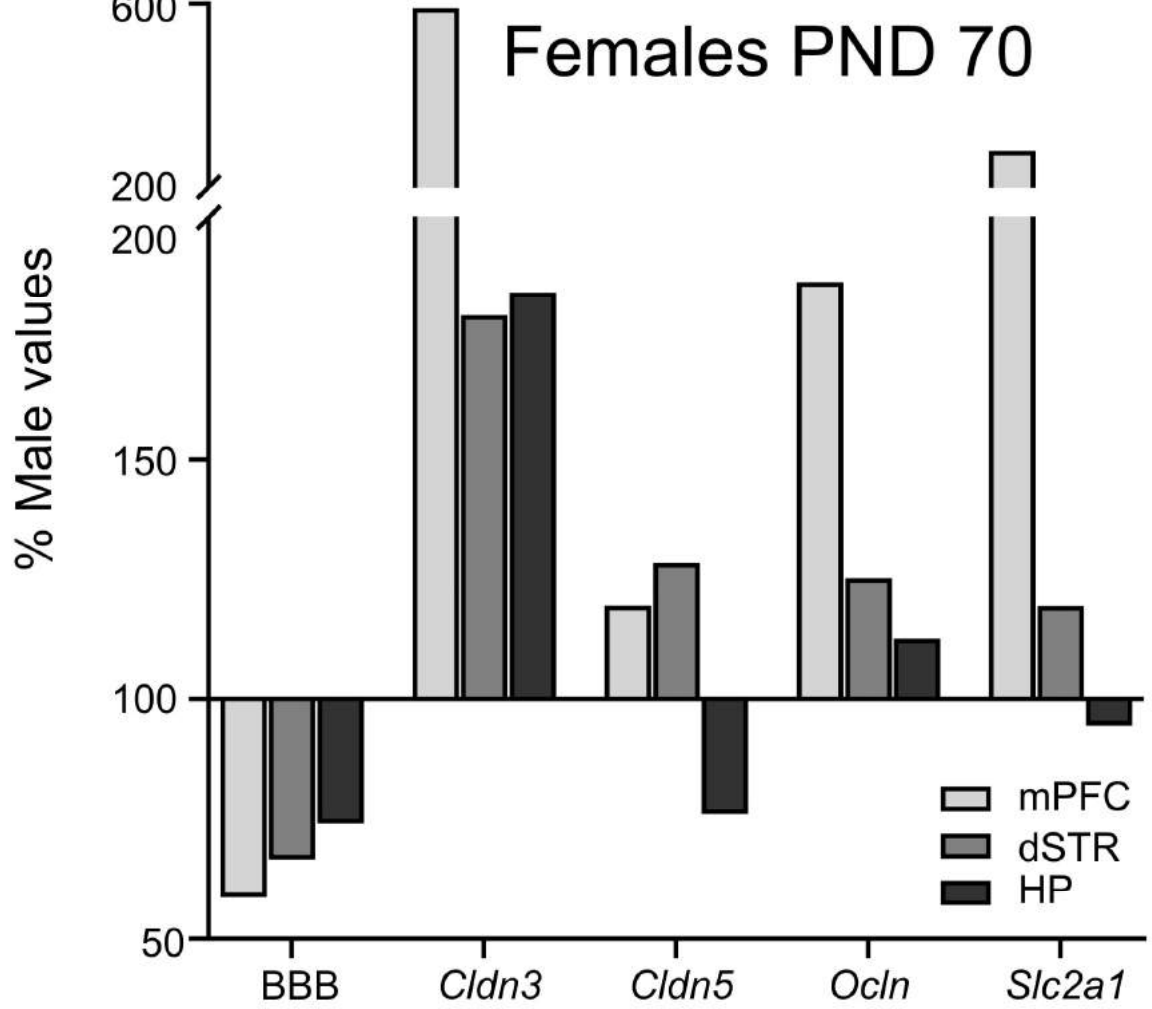

FIGURE S1. Schematic summary of sex differences in BBB permeability and mRNA expression of proteins related to the BBB structure and function in adult control rats. BBB permeability was determined by extravasation of NaF tracer in the brain. The mRNA expression was determined by RT-qPCR. The values of AFR females are expressed as a percentage of the values of AFR males. Abbreviations are explained in legends of Figure 2 and Supporting information Table S1.

Table S1. List of TaqMan® Gene Expression Assays used in the study

Gene product	Gene name	Assay ID
Claudin 3	*Cldn 3*	Rn00581751_s1
Claudin 5	*Cldn 5*	Rn01753146_s1
Occludin	*Ocln*	Rn00580064_m1
Solute Carrier Family 2 Member 1 (GLUT-1)	*Slc2a1*	Rn01417099_m1
Aquaporin 4	*Aqp4*	Rn01401327_s1
Glyceraldehyde-3-Phosphate Dehydrogenase	*Gapdh*	Rn01775763_g1

Table S2. Results of a three-way ANOVA investigating the effects age, sex and rearing conditions (RC) and their interactions on the content of extravasated NaF in the mPFC, dSTR and HP

Source of variation	Brain region					
	mPFC		dSTR		HP	
	$F_{1,56}$	p	$F_{1,56}$	p	$F_{1,56}$	p
PND	775.72	**<0.001**	823.19	**<0.001**	346.76	**<0.001**
SEX	7.36	**0.009**	0.03	0.855	0.00	0.995
RC	0.34	0.561	1.57	0.216	0.80	0.376
PNDxSEX	1.42	0.239	8.33	**0.006**	1.06	0.308
PNDxRC	0.84	0.362	3.47	0.068	1.54	0.220
SEXxRC	0.10	0.750	23.69	**<0.001**	3.51	0.066
PNDxSEXxRC	2.30	0.134	27.39	**<0.001**	4.51	**0.038**

Statistically significant effects are given in bold. Abbreviations are explained in legend of Figure 2.

Table S3. Effects of age, sex and rearing conditions on BBB permeability and mRNA expression of proteins related to BBB integrity and function in the mPFC, dSTR and HP – numerical data

Parameter	PND	RC	mPFC		dSTR		HP	
			Females	Males	Females	Males	Females	Males
BBB permea-bility	15	AFR	3.413 ± 0.628	3.701 ± 0.545	4.135 ± 0.422	3.267 ± 0.464	4.325 ± 0.430	3.429 ± 1.246
		MS	3.445 ± 0.628	3.989 ± 0.741	3.381 ± 0.438	**4.797 ± 1.074**	3.992 ± 0.667	4.523 ± 1.770
	70	AFR	0.507 ± 0.076	0.865 ± 0.139	0.499 ± 0.027	0.747 ± 0.128	0.659 ± 0.069	0.889 ± 0.247
		MS	0.667 ± 0.118	0.633 ± 0.149	0.588 ± 0.056	0.639 ± 0.058	0.640 ± 0.082	0.767 ± 0.114
Cldn3 mRNA	15	AFR	0.015 ± 0.012	0.008 ± 0.002	0.013 ± 0.005	0.009 ± 0.010	4.460 ± 1.669	2.013 ± 0.576
		MS	0.014 ± 0.006	0.014 ± 0.007	0.030 ± 0.020	0.013 ± 0.005	**1.953 ± 0.867**	1.437 ± 0.255
	70	AFR	0.311 ± 0.078	0.053 ± 0.017	0.110 ± 0.035	0.061 ± 0.025	0.595 ± 0.158	0.322 ± 0.056
		MS	**0.200 ± 0.052**	0.035 ± 0.010	0.101 ± 0.039	0.054 ± 0.009	**0.423 ± 0.065**	0.317 ± 0.041
Cldn5 mRNA	15	AFR	0.007 ±0.006	0.014 ± 0.006	0.057 ± 0.021	0.117 ± 0.064	0.130 ± 0.039	0.115 ± 0.050
		MS	0.021 ± 0.010	0.018 ± 0.006	**0.149 ± 0.055**	0.069 ± 0.059	**0.147 ± 0.066**	**0.185 ± 0.029**
	70	AFR	3.867 ± 1.376	3.237 ± 0.907	2.270 ± 0.492	2.097 ± 0.132	0.079 ± 0.023	0.104 ± 0.021
		MS	4.348 ± 0.528	3.238 ± 0.662	**3.477 ± 0.517**	**2.609 ± 0.472**	**0.081 ± 0.024**	**0.139 ± 0.028**
Ocln mRNA	15	AFR	0.185 ± 0.042	0.139 ± 0.046	0.042 ± 0.007	0.029 ± 0.008	0.229 ± 0.083	0.240 ± 0.037
		MS	0.210 ± 0.044	0.240 ± 0.040	0.044 ± 0.021	0.024 ± 0.005	**0.366 ± 0.075**	0.260 ± 0.036
	70	AFR	2.004 ± 0.376	1.071 ± 0.135	0.114 ± 0.008	0.091 ± 0.009	0.168 ± 0.022	0.149 ± 0.015
		MS	1.946 ± 0.369	1.095 ± 0.216	**0.099 ± 0.010**	**0.073 ± 0.005**	0.151 ± 0.021	0.152 ± 0.012
Slc2a1 mRNA	15	AFR	0.028 ± 0.002	0.020 ± 0.002	0.052 ± 0.003	0.038 ± 0.006	0.093 ± 0.038	0.062 ± 0.013
		MS	0.031 ± 0.005	0.021 ± 0.001	0.051 ± 0.007	0.045 ± 0.005	0.110 ± 0.034	0.078 ± 0.013
	70	AFR	0.288 ± 0.052	0.105 ± 0.014	0.103 ± 0.009	0.086 ± 0.012	0.135 ± 0.016	0.143 ± 0.008
		MS	0.307 ± 0.062	0.140 ± 0.024	**0.096 ± 0.008**	**0.066 ± 0.003**	0.142 ± 0.029	0.131 ± 0.011
Aqp4 mRNA	15	AFR	0.120 ± 0.010	0.121 ± 0.005	0.207 ± 0.082	0.342 ± 0.082	0.333 ± 0.026	0.348 ± 0.024
		MS	0.124 ± 0.010	0.114 ± 0.007	0.200 ± 0.023	**0.612 ± 0.129**	0.337 ± 0.027	0.332 ± 0.022
	70	AFR	0.088 ± 0.014	0.082 ± 0.005	0.173 ± 0.019	0.145 ± 0.015	0.169 ± 0.009	0.195 ± 0.004
		MS	0.091 ± 0.008	0.068 ± 0.010	0.166 ± 0.019	0.141 ± 0.011	0.163 ± 0.015	0.175 ± 0.020

The data are presented as the mean ± SD (n =6-8). The values concerning BBB permeability indicate the accumulation of NaF in the brain (in µg per g of wet tissue). The mRNA expression data were determined by RT-qPCR and presented as relative values of mRNA levels in arbitrary units. Statistically significant differences in MS (vs AFR) rats are given in bold (three-way ANOVA followed by Bonferroni *post hoc* test, for detailed description of statistical differences, see legends of Figure 2-5). Abbreviations are explained in legends of Figure 2 and Table S1 and S2.

Table S4. Three-way ANOVA results for the effects of age, sex and rearing conditions and their interactions on mRNA expression of BBB integrity regulators in the mPFC, dSTR and HP

Gene	Source of variation	Brain region					
		mPFC		dSTR		HP	
		$F_{1,40}$	p	$F_{1,40}$	p	$F_{1,40}$	p
Cldn3	PND	192.07	**<0.001**	104.53	**<0.001**	101.77	**<0.001**
	SEX	118.58	**<0.001**	21.06	**<0.001**	16.87	**<0.001**
	RC	9.71	**0.003**	0.02	0.880	16.06	**<0.001**
	PNDxSEX	110.87	**<0.001**	8.70	**0.005**	10.10	**0.003**
	PNDxRC	11.43	**0.002**	2.08	0.157	12.77	**0.001**
	SEXxRC	6.54	**0.014**	0.18	0.670	6.66	**0.014**
	PNDxSEXxRC	4.80	**0.034**	0.34	0.559	4.70	**0.036**
Cldn5	PND	374.06	**<0.001**	835.81	**<0.001**	295.12	**<0.001**
	SEX	5.28	**0.027**	0.07	0.797	17.97	**<0.001**
	RC	0.44	0.513	0.01	0.920	5.07	**0.030**
	PNDxSEX	5.31	**0.026**	0.03	0.872	16.02	**<0.001**
	PNDxRC	0.38	0.543	0.10	0.750	1.95	0.170
	SEXxRC	0.42	0.519	19.01	**<0.001**	3.71	0.061
	PNDxSEXxRC	0.39	0.538	13.54	**0.001**	1.94	0.171
Ocln	PND	480.43	**<0.001**	399.05	**<0.001**	88.76	**<0.001**
	SEX	52.77	**<0.001**	47.85	**<0.001**	8.06	**0.007**
	RC	0.03	0.863	9.19	**0.004**	5.03	**0.030**
	PNDxSEX	56.79	**<0.001**	2.20	0.163	2.30	0.137
	PNDxRC	0.21	0.647	6.37	**0.016**	11.69	**0.001**
	SEXxRC	0.17	0.686	0.85	0.363	0.38	0.059
	PNDxSEXxRC	0.07	0.792	0.12	0.735	7.43	**0.009**
Slc2a1	PND	444.41	**<0.001**	1967.78	**<0.001**	223.45	**<0.001**
	SEX	110.32	**<0.001**	47.56	**<0.001**	8.42	**0.006**
	RC	2.72	0.107	10.93	**0.002**	2.20	0.146
	PNDxSEX	90.08	**<0.001**	37.23	**<0.001**	7.81	**0.008**
	PNDxRC	2.03	0.162	12.41	**0.001**	2.25	0.141
	SEXxRC	0.18	0.671	5.23	**0.028**	0.00	0.959
	PNDxSEXxRC	0.26	0.616	3.10	0.086	0.01	0.917
Aqp4	PND	127.99	**<0.001**	125.54	**<0.001**	2186.29	**<0.001**
	SEX	8.62	**0.005**	56.60	**<0.001**	0.75	0.393
	RC	0.94	0.339	14.75	**<0.001**	1.07	0.306
	PNDxSEX	2.47	0.124	83.71	**<0.001**	3.44	0.071
	PNDxRC	0.36	0.554	17.46	**<0.001**	0.01	0.928
	SEXxRC	4.38	**0.043**	18.22	**<0.001**	2.72	0.107
	PNDxSEXxRC	0.14	0.708	17.33	**<0.001**	0.03	0.873

The mRNA expression was determined by RT-qPCR. Statistically significant effects are given in bold. Abbreviations are explained in legends of Table 1 and Table S1 and S2.

Table S5. Effects of age, sex and rearing conditions on circulating S100β and proinflammatory cytokines levels – numerical data

PND	RC	Serum levels					
		S100β		IL-1β		TNFα	
		Females	Males	Females	Males	Females	Males
15	AFR	702.21 ± 53.25	928.46 ± 316.62	47.28 ± 4.16	42.14 ± 3.06	13.48 ± 1.11	14.06 ± 1.36
	MS	**604.08 ± 63.60**	**612.10 ± 117.77**	47.56 ± 2.76	43.25 ± 4.05	12.89 ± 0.56	14.37 ± 1.93
70	AFR	601.00 ± 132.43	375.35 ± 71.13	61.86 ± 14.14	62.97 ± 5.72	20.57 ± 0.66	21.17 ± 0.53
	MS	**428.56 ± 108.16**	398.15 ± 82.12	63.81 ± 7.45	64.50 ± 6.47	21.40 ± 0.90	20.60 ± 0.36

The data indicate serum concentrations of studied proteins (in pg/ml) measured by ELISA (the mean ± SD, n = 6). Statistically significant differences in MS (vs AFR) rats are given in bold (three-way ANOVA followed by Bonferroni *post hoc* test, for detailed description of statistical differences, see legend of Figure 6). Abbreviations are explained in legends of Figure 2 and Table S2.

Brain, Behavior, and Immunity 108 (2023) 1–15

Contents lists available at ScienceDirect

Brain Behavior and Immunity

journal homepage: www.elsevier.com/locate/ybrbi

Full-length Article

Early-life stress affects peripheral, blood-brain barrier, and brain responses to immune challenge in juvenile and adult rats

Anna Solarz [a], Iwona Majcher-Maślanka [a], Joanna Kryst [a,b], Agnieszka Chocyk [a,*]

[a] Department of Pharmacology, Laboratory of Pharmacology and Brain Biostructure, Maj Institute of Pharmacology, Polish Academy of Sciences, 31-343 Kraków, Smętna Street 12, Poland
[b] Department of Chemistry and Biochemistry, Institute for Basics Sciences, Faculty of Physiotherapy, University of Physical Education, Jana Pawła II Av. 78, 31-571 Kraków, Poland

ARTICLE INFO

Keywords:
Maternal separation
Blood–brain barrier
Inflammation
Claudin 5
Occludin
Sex differences
LPS
Cytokines
ICAM1, Toll-like receptor 4

ABSTRACT

Early-life stress (ELS) may affect brain maturation and neuroimmune interactions and, consequently, the inflammatory response to subsequent environmental factors later in life. Recently, the coexistence of blood–brain barrier (BBB) dysfunction and inflammation has been implicated in the etiology and progression of mental and/or neurodegenerative diseases. There are sex differences in the prevalence and outcomes of these disorders. The number of studies reporting the effects of ELS and sex on BBB functioning and neuroinflammatory processes in response to immune challenge is very limited, and the data are inconsistent. In the present study, we examined whether ELS, based on the maternal separation (MS) paradigm in rats, can condition male and female subjects to subsequent lipopolysaccharide (LPS)-induced immune challenge in juvenility or adulthood. Twenty-four hours after acute LPS injection, serum proinflammatory cytokines were measured, and BBB permeability in the medial prefrontal cortex (mPFC) and hippocampus (HP) was evaluated. Additionally, the mRNA expression of neuroinflammatory markers and BBB-related genes was also studied. We found that a single LPS challenge induced a proinflammatory response both in the periphery and in the mPFC and HP and increased BBB permeability in a sex-dependent fashion. Moreover, MS enhanced the neuroinflammatory response to LPS challenge in males (especially juveniles), whereas MS females showed no difference or a blunted central response to LPS compared with control females, mainly during adulthood. These results suggest that ELS may precondition individuals to subsequent environmental factors later in life in a sex-specific manner and potentially determine their susceptibility or resilience to mental and/or neurodegenerative diseases.

1. Introduction

Brain development is an incomplete process at birth but continues postnatally into early adulthood or even later in life (Danese and Lewis, 2017). In parallel, the immune system matures, and neuroimmune interactions are established, determining brain function and behavior throughout the lifespan (Danese and Lewis, 2017; Brenhouse et al., 2019; Dutcher et al., 2020). Research shows that exposure to early-life stress (ELS) may affect the trajectories of brain maturation and thus neuroimmune interactions and, consequently, the inflammatory response to subsequent environmental factors later in life (Avitsur et al., 2013; Saavedra et al., 2017; Brenhouse et al., 2019; Brydges and Reddaway, 2020; Catale et al., 2020; Gildawie et al., 2020; Lumertz et al., 2022). It is well known that alterations in the immune response in the periphery and within the brain are involved in the pathogenesis and progression of depression, schizophrenia, Alzheimer's disease (AD) and Parkinson's disease (PD) (Stolp and Dziegielewska, 2009; Erickson and Banks, 2013; Brenhouse et al., 2019; Dutcher et al., 2020; Dudek et al., 2021). Therefore, it is believed that early-life programming of the stress/immune axis may be a potential source of later susceptibility to mental and neurodegenerative disorders with immune components (Hoeijmakers et al., 2017; Brenhouse et al., 2019; Dutcher et al., 2020). Animal

Abbreviations: AD, Alzheimer's disease; AFR, animal facility rearing; AIF-1, allograft inflammatory factor 1; BBB, blood-brain barrier; CLD5, claudin 5; CORT, corticosterone; ELS, early-life stress; HP, hippocampus; ICAM-1, intercellular adhesion molecule 1; IL-1β, interleukin 1β; ITGAM, integrin alpha M; LPS, lipopolysaccharide; mPFC, medial prefrontal cortex; MS, maternal separation; NaF, sodium fluorescein; OCLN, occludin; PD, Parkinson's disease; PND, postnatal day; RC, rearing conditions; TJ, tight junctions; TLR4, toll-like receptor 4; TNF-α, tumor necrosis factor α; VEH, vehicle.

* Corresponding author.
E-mail address: chocyk@if-pan.krakow.pl (A. Chocyk).

https://doi.org/10.1016/j.bbi.2022.11.005
Received 5 July 2022; Received in revised form 21 October 2022; Accepted 12 November 2022
Available online 15 November 2022

studies have shown that ELS may affect anxiety- and depressive-like behaviors (Chocyk et al., 2010; Chocyk et al., 2013; Chocyk et al., 2015; Loi et al., 2017; Majcher-Maslanka et al., 2019) and impair the function of the medial prefrontal cortex (mPFC) and hippocampus (HP), which are brain regions highly implicated in the pathophysiology of mental and neurodegenerative disorders (Andersen and Teicher, 2004; Baudin et al., 2012; Chocyk et al., 2013; Majcher-Maslanka et al., 2019; Brydges and Reddaway, 2020). Moreover, many studies have also demonstrated that ELS exacerbates symptoms in animal models of PD and AD and intensifies age-related cognitive impairments (Baudin et al., 2012; Hoeijmakers et al., 2017; Loi et al., 2017).

Dysfunctions at the blood–brain barrier (BBB) level are equally relevant causes of neuropathology emergence in immature and aging brains (Ballabh et al., 2004; Stolp and Dziegielewska, 2009; Erickson and Banks, 2013). Currently, the coexistence of BBB disturbances and inflammation appears to play an important role in the etiology, development and progression of neurodegenerative diseases. Although stress, including ELS, is a well-known risk factor for mental and neurodegenerative diseases (Baudin et al., 2012; Loria et al., 2014; Danese and Lewis, 2017), a limited number of studies have linked stress and BBB dysfunction as a combined cause of neuropathology (Santha et al., 2015; Menard et al., 2017; Disdier and Stonestreet, 2019; Xu et al., 2019; Dudek et al., 2020; Solarz et al., 2021a; Dion-Albert et al., 2022).

In rodents, the BBB continues to mature after birth and gradually seals, reaching adult functional levels in the juvenile period (3–4 postnatal weeks) (Caley and Maxwell, 1970; Krause et al., 2002). There is a close association between simultaneous development of the BBB and brain (Caley and Maxwell, 1970; Krause et al., 2002; Solarz et al., 2021a). Sparse research, including our recent study, showed that ELS in rodents may affect BBB function, resulting in both adaptive and maladaptive changes within the BBB, depending on sex, age and brain region, which may potentially program the response of the BBB to subsequent environmental factors, e.g., an immune challenge (Gomez-Gonzalez and Escobar, 2009; Solarz et al., 2021a).

In animal research, Gram-negative bacterial lipopolysaccharide (LPS) injection is commonly used to mimic the infection state and model systemic inflammation with concomitant BBB disruption (Singh and Jiang, 2004; Erickson and Banks, 2011; Ortega et al., 2011; Varatharaj and Galea, 2017). A limited number of animal studies have shown that ELS alters proinflammatory cytokines levels in both plasma and cerebral tissue (Avitsur et al., 2013; Saavedra et al., 2017; Catale et al., 2020; Nicolas et al., 2022) and affects the morphology, function and reactivity of neuroimmune cells, such as microglia and astrocytes, in response to subsequent LPS administration later in life (Saavedra et al., 2017; Catale et al., 2020; Gildawie et al., 2020; Nicolas et al., 2022). However, the results of these studies are quite inconsistent and do not relate to BBB functioning in response to immune challenge.

All of these facts prompted us to conduct a broad-scale study to investigate whether ELS would condition peripheral and brain inflammatory responses and BBB functioning to subsequent LPS challenge later in life. To model ELS, we applied the repeated three-hour maternal separation procedure (MS) in rats during the first two weeks of life. MS procedure is a popular and widely used model of ELS and human psychopathology with a high construct validity (Vetulani, 2013; Italia et al., 2020). Although, the specific variant of MS applied in the present study and in our previous studies can be considered as moderate stressor, it significantly affects mother–pup interactions (Chocyk et al., 2013) and in consequence brain maturation and animal behavior (Chocyk et al., 2010; Chocyk et al., 2013; Chocyk et al., 2015; Loi et al., 2017; Majcher-Maslanka et al., 2019). This time, we applied MS and subsequent acute LPS challenge in juvenile and adult rats and, 24 h later, measured the serum levels of corticosterone (CORT) and proinflammatory cytokines, i.e., interleukin 1β (IL-1β) and tumor necrosis factor α (TNF-α), and investigated the mRNA expression of a wide range of neuroinflammatory markers, i.e., IL-1β, TNF-α, intercellular adhesion molecule 1 (ICAM-1), microglial/macrophage markers and LPS recognizing toll-like receptor 4 (TLR4) in the mPFC and HP of both females and males. Moreover, BBB permeability and the expression of genes encoding tight junction (TJ) proteins contributing to the structural maintenance of the BBB, such as claudin 5 (CLD5) and occludin (OCLN), were also evaluated in the mPFC and HP in our ELS-LPS model.

2. Materials and methods

2.1. Animals

All experimental procedures were approved by the Committee for Laboratory Animal Welfare and the Ethics Committee of the Maj Institute of Pharmacology, Polish Academy of Sciences, Krakow, and met the requirements of the Directive 2010/63/EU of the European Parliament and of the Council of September 22, 2010 on the protection of animals used for scientific purposes. All efforts were made to minimize animal suffering.

Adult male and female Wistar rats were purchased from Charles River Laboratories (Sulzfeld, Germany). All animals were housed under controlled conditions with an artificial 12-h light/dark cycle (lights on from 07:00 to 19:00), 55 ± 10 % humidity, and a temperature of 22 ± 2 °C. Food and tap water were freely available. The rats were mated at the Maj Institute of Pharmacology, PAS, Krakow Animal Facility. The offspring of primiparous dams were used in this study. Before delivery, the dams were housed individually in standard plastic cages (type III H, 38 × 24 × 19 cm). The day of birth was designated as postnatal (PND) 0. On PND 1, the litter size was standardized to eight pups per litter (four males and four females), and the litters were randomly assigned to one of the following rearing conditions (RC): MS or animal facility rearing (AFR), that is, control conditions.

2.2. Maternal separation

The MS procedure was performed as previously described by Solarz et al. (2021a), Majcher-Maslanka et al. (2019) and Chocyk et al. (2010), Chocyk et al. (2013), Chocyk et al. (2015). Briefly, on PNDs 1–14, the dams and pups were removed from the maternity cages for 3 h (09:00–12:00) per day. The mothers were placed individually in holding cages (type III, 38 × 24 × 19 cm), while each litter was placed in a plastic container (22 × 16 × 10 cm) lined with fresh bedding material, and the containers were moved to an adjacent room and placed in an incubator that was set at a constant temperature of 34 °C, imitating the nest temperature. After separation, the pups and dams were returned to maternity cages. The AFR animals were left undisturbed with their mothers except during weekly cage cleaning, thus reflecting a minimal amount of handling. The pups were not cross-fostered. The impact of the MS procedure on specific maternal and pup behaviors was previously described in detail by our group (Chocyk et al., 2013). On PND 21, some of the animals were randomly assigned to experimental groups evaluated on PND 22 (in juvenility). The rest of the animals were weaned and sexed on PND 22 and randomly assigned to specific experimental groups evaluated in adulthood (PND 70). These rats were housed under controlled conditions (as described above) in standard plastic cages (type IV, 57 × 33 × 20 cm) in same-sex groups of five unrelated subjects until PND 70. The scheme of the experimental procedures is presented in Fig. 1.

2.3. Lipopolysaccharide administration

To model acute infection in juvenility or adulthood, on PND 21 or PND 70, respectively, AFR and MS male and female rats received a single intraperitoneal (i.p.) injection of LPS (1 mg/kg/1 ml), an endotoxin that is a component of the outer membrane of Gram-negative bacteria *Escherichia coli* (Sigma Aldrich, St. Louis, MO, USA) or vehicle (VEH, 0.9 % saline, 1 ml/kg i.p.). All subsequent biochemical experiments took place 24 h after acute LPS/VEH injection (Fig. 1). The LPS treatment

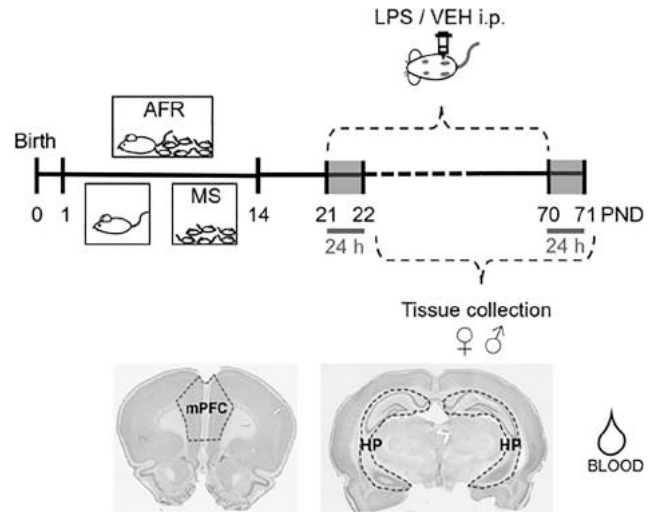

Fig. 1. Scheme of the experimental procedures applied in the study. Lower panel: photomicrographs showing cresyl violet-stained rat brain sections with the marked regions under study. Abbreviations: AFR, animal facility rearing; LPS, lipopolysaccharide; MS, maternal separation; mPFC, medial prefrontal cortex; HP, hippocampus; PND, postnatal day; VEH, vehicle.

regimen was chosen based on a pilot experiment and literature data that showed its safety for use in juvenile rats and effectiveness in inducing peripheral and central immune responses and increasing BBB permeability both a few hours and 24 h after the injection (Bay-Richter et al., 2011; Jangula and Murphy, 2013; Saavedra et al., 2017). During the period between weaning (on PND 22) and the start of the experiments in adulthood, the respective animals were subjected to handling to eliminate stress associated with the experimental procedures. The handling procedure consisted of gently grasping and picking up the animals for a short period of time to familiarize them with the experimenter and experimental procedures.

2.4. Experimental groups

A total of 192 rats (96 males and 96 females) originating from 12 AFR and 12 MS litters were used in this study. To avoid litter effects, the final experimental groups (AFR-VEH, AFR-LPS, MS-VEH and MS-LPS) consisted of subjects that originated from different litters and were unrelated ($n = 6$ for assessment of BBB permeability; $n = 6$ for serum markers; $n = 6$ for RT–qPCR). The number of animals used in the study was chosen based on pilot experiments and our previous experiences with the specific experimental protocols, and it guaranteed the possibility of obtaining a relevant effect size and statistically significant differences in the results.

2.5. Assessment of BBB permeability

The BBB permeability assessment procedure was previously described by Solarz et al. (2021a). We used a fluorescent small-molecule tracer (376 Da), sodium fluorescein (NaF), a sensitive marker of even slight BBB breakdown and leakage. NaF does not bind to proteins nonspecifically, in contrast to Evans blue (961 Da, in complex with albumin), another popular marker of BBB permeability (Sun et al., 2021). In our study, we adapted the procedures previously described by Ramirez et al. (2009) and Yen et al. (2013). On PND 22 or in adulthood, six rats per experimental group were intraperitoneally injected with 4 % NaF (Merck, US) dissolved in 0.9 % saline at a dose of 2 ml/kg. The dye was permitted to circulate for 30 min before the animals were transcardially perfused with 0.9 % saline to remove the circulating dye. Thereafter, the brain tissue parenchyma containing only the extravasated dye was collected. Samples of the mPFC (including the cingulate cortex 1, prelimbic cortex, and infralimbic cortex regions) were dissected from 1 mm thick coronal slices using a rodent brain matrix (Ted Pella, Inc., CA, USA) according to the stereotaxic atlas of the rat brain (Paxinos and Watson, 1998), whereas the HP was dissected freehand (Fig. 1). The brain tissue was weighed, homogenized (Tissue Lyser II, Qiagen) in a 1:3 vol of 50 % trichloroacetic acid (TCA, Merck, US), and centrifuged (10,000 rpm for 10 min), and the supernatants were diluted with a 1:3 vol of 95 % ethanol prior to spectrophotometric determination of the NaF fluorescence (Tecan, Männedorf, Zürich, Switzerland; 440 nm excitation/525 nm emission). The fluorescent dye content was calculated using external standards, and the data are expressed as the amount of NaF (μg) per gram of wet brain tissue.

2.6. RT–qPCR

The RT–qPCR method used in this study has been previously described in detail by Solarz et al. (2021a). Briefly, on PND 22 and in adulthood, six rats per experimental group were sacrificed via decapitation, and the brains were immediately removed from the skulls. The mPFC (including the cingulate cortex 1, prelimbic cortex, and infralimbic cortex regions) was dissected from 1 mm thick coronal slices using a rodent brain matrix (Ted Pella Inc.), whereas the HP was dissected freehand (Fig. 1). The brain tissue was quickly frozen in liquid nitrogen and stored at −80 °C until analysis. Total RNA was extracted using the RNeasy Mini Kit (Qiagen, Germany). The total RNA concentration was measured using an Eon absorbance microplate reader and Gen 5 software (BioTek, Winooski, VT, USA). RNA was reverse transcribed using a High-Capacity cDNA Reverse Transcription Kit (Thermo Fisher Scientific, MA). Quantitative real-time PCR was performed in duplicate with TaqMan® Gene Expression Assays (Thermo Fisher Scientific; Table 1) using TaqMan™ Universal Master Mix II, no UNG (Thermo Fisher Scientific) and the QuantStudio 12 K Flex System (Thermo Fisher Scientific). Real-time PCR was conducted under the following conditions: 50 °C for 2 min and 95 °C for 10 min followed by 40 cycles of 95 °C for 15 s and 60 °C for 1 min. The abundance of RNA was calculated according to the following equation: abundance $= 2^{-(\text{threshold cycle})}$. The results were normalized to glyceraldehyde-3-phosphate dehydrogenase (*Gapdh*) expression levels and underwent statistical analysis as relative values of mRNA levels.

2.7. Enzyme-linked immunosorbent assay (ELISA)

Trunk blood was collected during the decapitation procedure (see the RT–qPCR procedure). Commercially available microtubes containing a clotting activator (Sarstedt, Germany) were used for serum separation. The blood was centrifuged (10,000 × *g*, 5 min, 4 °C), and the serum was collected and stored in aliquots at −20 °C until the day of the assay. Using commercially available ELISA kits, CORT (IDS, UK), IL-1β (R&D Systems, USA) and TNF-α (R&D Systems, USA) levels were determined according to the manufacturers' instructions. Positive controls for each assay were provided by the manufacturers. Detections limits and intra assay percentage variations for ELISA assays were as follows, for CORT: 0.55 ng/ml and 5.1 %, for IL-1β: 5 pg/ml and 3.9 %,

Table 1
List of TaqMan® Gene Expression Assays used in this study.

Gene product	Gene name	Assay ID
Claudin 5	*Cld5*	Rn01753146_s1
Occludin	*Ocln*	Rn00580064_m1
Toll-like receptor 4	*Tlr4*	Rn00569848_m1
Interleukin 1β	*Il-1β*	Rn00580432_m1
Tumor necrosis factor α	*Tnfα*	Rn99999017_m1
Intercellular adhesion molecule 1	*Icam1*	Rn00564227_m1
Allograft inflammatory factor 1	*Aif1*	Rn00574125_g1
Integrin alpha M	*Itgam*	Rn00709342_m1
Glyceraldehyde-3-Phosphate Dehydrogenase	*Gapdh*	Rn99999916_s1

for TNF-α: 5.0 pg/ml and 3.8 %, respectively.

2.8. Statistical analysis

Statistical analysis of the data was performed using Statistica 13.3 software (TIBCO Software Inc., USA). Initially, the data were tested for a normal distribution and homogeneity of variances and then analyzed by three-way ANOVA, with treatment (VEH vs LPS), sex and RC (MS vs AFR) as the independent variables. The data were analyzed individually for each age and brain region (or serum) and parameter studied. When the global ANOVA resulted in statistically significant effects of the interactions between analyzed factors, a lower-order statistical analysis was performed (two-way ANOVA and/or Bonferroni *post hoc* test when required). The data are presented as the mean ± SD. A value of $p < 0.05$ was considered statistically significant.

3. Results

3.1. Effects of MS and subsequent LPS-induced immune challenge on serum corticosterone and proinflammatory cytokines levels

Fluctuations in stress marker CORT and proinflammatory cytokines serum levels due to stress or peripheral inflammation may increase BBB permeation and trigger a series of signaling events leading to the development of an inflammatory response in the brain (Singh and Jiang, 2004). Therefore, the first goal of the study was to determine whether our LPS-based model of infection was sufficient to induce symptoms of peripheral inflammation. Accordingly, we measured CORT, IL-1β, and TNF-α serum levels 24 h after LPS challenge.

Analysis of serum CORT levels in juveniles revealed a statistically significant interaction between all studied factors (three-way ANOVA, sex × LPS × RC: $p = 0.043$) (Supplemental Table 1). Further analysis showed that although LPS injection per se did not induce changes in serum CORT levels in juvenile females, the AFR-LPS group had a higher CORT level in comparison to MS-LPS females (two-way ANOVA, RC × LPS: $p = 0.004$, *post hoc:* $p = 0.014$) (Supplemental Table 2) (Fig. 2A). On the other hand, in juvenile males, LPS administration caused an increase in peripheral stress marker levels regardless of RC (two-way ANOVA, main effect of treatment: $p = 0.010$) (Supplemental Table 2) (Fig. 2A). Moreover, MS males generally showed a higher CORT level than AFR juvenile males (main effect of RC: $p = 0.003$) (Supplemental Table 2) (Fig. 2A).

LPS administration, regardless of RC, increased IL-1β serum levels in juvenile females but not males (three-way ANOVA, sex × LPS: $p = 0.002$, *post hoc:* $p < 0.001$ (females), $p = 0.829$ (males)) (Supplemental Table 1) (Fig. 2A). Additionally, LPS-injected MS juveniles, regardless of sex, had greater IL-1β levels than AFR-LPS rats (LPS × RC: $p = 0.012$, *post hoc:* $p = 0.018$) (Supplemental Table 1) (Fig. 2A).

The peripheral level of TNFα was increased by LPS regardless of sex and RC in juvenile rats (three-way ANOVA, main effect of treatment: $p < 0.001$) (Supplemental Table 1) (Fig. 2A).

In adulthood, LPS induced an elevation in CORT serum levels

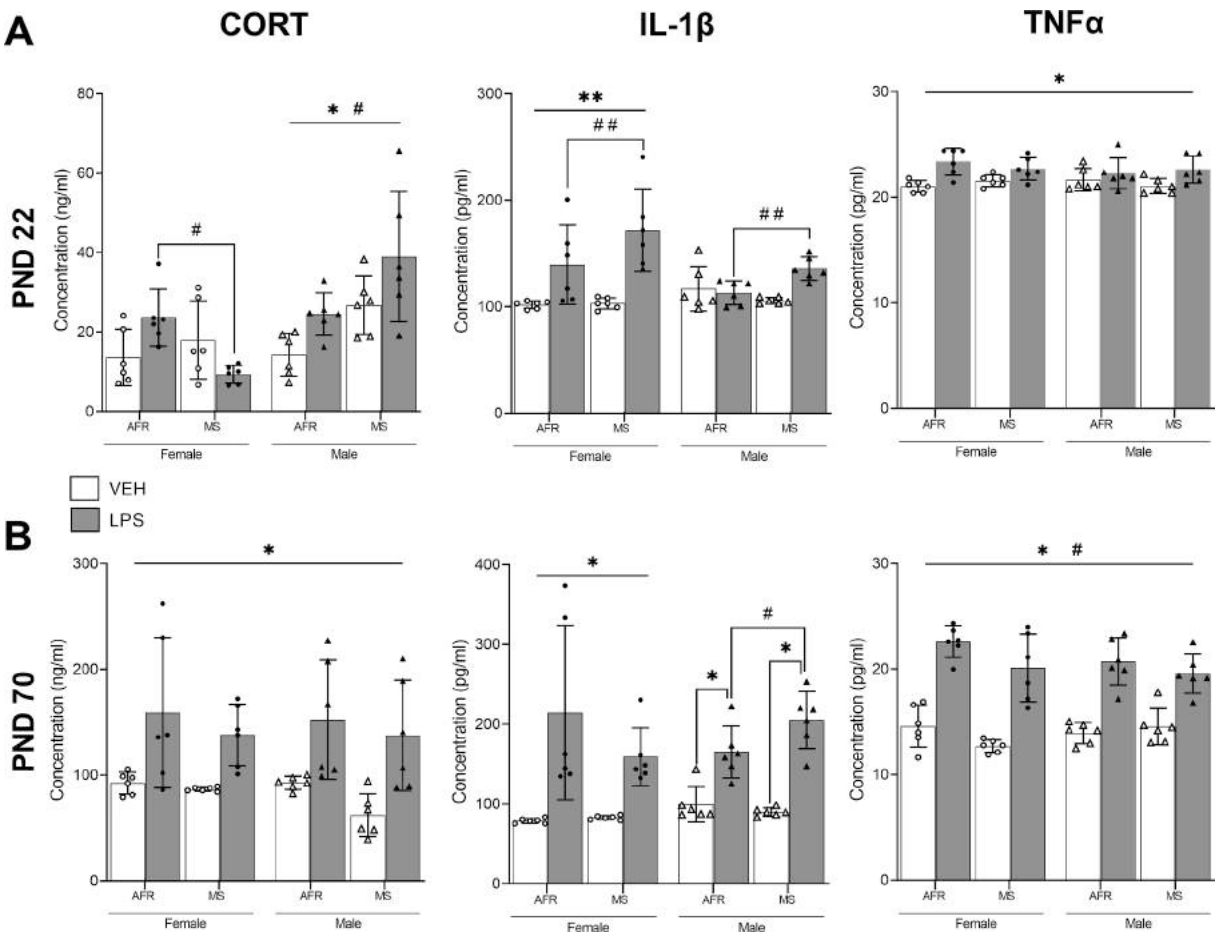

Fig. 2. The effect of MS and subsequent LPS treatment in juvenile (A) and adult rats (B) on serum levels of CORT (left column), IL-1β (middle column) and TNFα (right column). The data indicate the serum concentrations of the studied markers (in ng/ml and pg/ml) measured by ELISA and are presented as the mean ± SD. Circles and triangles represent individual data points ($n = 6$). *$p < 0.05$: the effect of treatment, #$p < 0.05$: the effect of RC. Lines with a single symbol * and # relate to the significance of the main effects in ANOVA, connectors indicate *post hoc* comparisons between the specific groups, and twin symbols ** or ## relate to the effects of significant interactions between two factors in a three-way ANOVA.

regardless of sex and MS experience (three-way ANOVA, main effect of treatment: $p < 0.001$) (Supplemental Table 1) (Fig. 2B).

On the other hand, all studied factors affected IL-1β serum levels in adults (three-way ANOVA, sex × LPS × RC: $p = 0.042$) (Supplemental Table 1) (Fig. 2B). Females showed LPS-induced elevation in IL-1β concentration regardless of RC (two-way ANOVA, main effect of treatment: $p < 0.001$) (Supplemental Table 2) (Fig. 2B). In males, both AFR and MS subjects showed an LPS-triggered increase in IL-1β levels (two-way ANOVA, RC × LPS: $p = 0.004$, *post hoc:* $p < 0.001$ (AFR), $p < 0.001$ (MS)) (Supplemental Table 2) (Fig. 2B). Additionally, this increase was intensified in the MS group compared to the AFR group ($p = 0.001$) (Fig. 2B).

The peripheral level of TNFα was increased by LPS regardless of sex and RC in adult rats (three-way ANOVA, main effect of treatment: $p < 0.001$) (Supplemental Table 1) (Fig. 2B). Additionally, MS adult rats generally showed lower TNFα serum levels than AFR rats (main effects of RC, $p = 0.032$) (Supplemental Table 1) (Fig. 2B). To help to follow the main findings of the study, the stripped-down summaries of LPS- and MS-triggered effects and sex differences in the basal levels of studied markers were presented in Tables 2, 3 and 4, respectively.

3.2. Effects of MS and subsequent LPS-induced immune challenge on the permeability and integrity of the BBB

The next goal of this study was to investigate the impact of RC (AFR vs MS) combined with LPS treatment (VEH vs LPS) on BBB permeability in the mPFC and HP during juvenility and adulthood in both sexes. For this purpose, 24 h after LPS challenge, the animals were injected with a fluorescent tracer, NaF, and its extravasated content was spectrophotometrically determined in the studied brain regions.

LPS administration to juveniles increased BBB permeability in the mPFC regardless of sex and RC (three-way ANOVA, main effect of treatment: $p < 0.001$) (Supplemental Table 3) (Fig. 3A). Moreover, BBB permeability was generally greater in MS rats (main effect of RC: $p = 0.013$) (Supplemental Table 3) (Fig. 3A). Additionally, females had lower BBB permeability than males (main effect of sex: $p < 0.001$) (Table 4) (Supplemental Table 3) (Fig. 3A). Similar sex- and RC-dependent effects on BBB permeability were also observed in the HP of juveniles (three-way ANOVA, main effects of sex: $p < 0.001$; RC: $p = 0.034$) (Supplemental Table 3) (Fig. 3A). However, LPS action was evident only in males (three-way ANOVA, sex × LPS: $p = 0.022$, *post hoc*: $p < 0.001$ (males), $p = 0.274$ (females)) (Supplemental Table 3) (Fig. 3A).

In adults, global ANOVA of the BBB permeability in the mPFC revealed only statistically significant interactions between sex and treatment ($p = 0.043$) and sex and RC ($p = 0.034$) (Supplemental Table 3) (Fig. 3B). Nevertheless, these effects were weak, and further *post hoc* analysis did not indicate significant differences between the studied groups. In the HP of adults, regardless of sex, MS-VEH rats had lower BBB permeability than AFR-VEH rats (three-way ANOVA, LPS × RC: $p = 0.010$, *post hoc:* $p = 0.010$) (Supplemental Table 3) (Fig. 3B). Moreover, only MS rats, regardless of sex, showed an LPS-induced increase in BBB permeability (*post hoc:* $p = 0.023$) (Fig. 3B).

BBB integrity and permeability depend on the expression and functioning of TJ proteins, such as CLD5 and OCLN, which provide structural support to the BBB and physically occlude the interendothelial space (Ballabh et al., 2004; Abbott et al., 2010; Haseloff et al., 2015). Therefore, the next step in our study was to assess the impact of combined MS and LPS on the level of *Cld5* and *Ocln* mRNA expression, measured by RT–qPCR.

We found that LPS administration regardless of sex increased *Cld5* expression in the mPFC of juvenile MS rats but not in AFR rats (three-way ANOVA, LPS × RC: $p = 0.011$, *post hoc*: $p < 0.001$ (MS), $p = 1.000$ (AFR)) (Supplemental Table 4) (Fig. 4A). Additionally, females generally showed greater levels of *Cld5* mRNA than males (main effect of sex: $p < 0.001$) (Table 4) (Supplemental Table 4) (Fig. 4A). A similar sex-dependent effect was observed in the HP of juveniles (three-way ANOVA, main effect of sex: $p = 0.039$) (Table 4) (Supplemental Table 4) (Fig. 4A). Moreover, in this brain region, LPS increased *Cld5* expression regardless of sex and RC (main effect of treatment: $p < 0.001$) (Supplemental Table 4) (Fig. 4A).

The same effects were observed in the case of *Ocln* expression in the HP of juveniles, i.e., a general stimulatory effect of LPS and greater mRNA levels of *Ocln* in females (three-way ANOVA, main effect of treatment: $p < 0.001$, main effect of sex: $p < 0.001$) (Supplemental Table 4) (Fig. 4A). In the mPFC of juveniles, global ANOVA of *Ocln* expression revealed a significant interaction between all examined factors (three-way ANOVA, sex × LPS × RC: $p = 0.044$) (Supplemental Table 4) (Fig. 4A). LPS treatment increased the mRNA levels of *Ocln* in both females and males (two-way ANOVA, main effect of treatment: $p <$

Table 2
Stripped-down summary of the impact of LPS-induced immune challenge on AFR rats.

Marker	Sample	Sex	PND	
			22	70
CORT	Serum	♀	0	↑
		♂	↑	↑
IL-1β	Serum	♀	↑	↑
		♂	0	↑
TNF-α	Serum	♀	↑	↑
		♂	↑	↑
Il-1β	mPFC	♀	↑	↑
		♂	0	↑
	HP	♀	↑	↑
		♂	0	↑
Tnfα	mPFC	♀	↑	↑
		♂	↑	↑
	HP	♀	↑	↑
		♂	↑	↑
Tlr4	mPFC	♀	↑	↑
		♂	0	0
	HP	♀	↑	0
		♂	0	↑
Icam1	mPFC	♀	↑	↑
		♂	↑	↑
	HP	♀	↓	↑
		♂	0	↑
Aif1	mPFC	♀	0	↑
		♂	0	↑
	HP	♀	↑	↑
		♂	↑	↑
Itgam	mPFC	♀	↑	↑
		♂	0	↑
	HP	♀	↑	↑
		♂	0	↑
NaF	mPFC	♀	↑	0
		♂	↑	0
	HP	♀	0	0
		♂	↑	0
Cld5	mPFC	♀	0	↑
		♂	0	↑
	HP	♀	↑	0
		♂	↑	0
Ocln	mPFC	♀	↑	↑
		♂	↑	↑
	HP	♀	↑	0
		♂	↑	0

LPS-triggered increase (↑), decrease (↓) or no effect of LPS (0).

Table 3
Stripped-down summary of the impact of LPS-induced immune challenge on MS rats when compared to the response observed in AFR rats.

Marker	Sample	Sex	PND	
			22	70
CORT	Serum	♀	↓	↔
		♂	↑	↔
IL-1β	Serum	♀	↑	↔
		♂	↑	↑
TNF-α	Serum	♀	↔	↓
		♂	↔	↓
Il-1β	mPFC	♀	↔	0
		♂	↔	↔
	HP	♀	↔	↓
		♂	↔	↔
Tnfα	mPFC	♀	↑	↔
		♂	↑	↔
	HP	♀	↔	0
		♂	↔	↑
Tlr4	mPFC	♀	0	0
		♂	↑	↑
	HP	♀	0	↑
		♂	↑	↑
Icam1	mPFC	♀	↓	0
		♂	↑	↔
	HP	♀	↔	↔
		♂	↑	↔
Aif1	mPFC	♀	↑	↓
		♂	↑	↓
	HP	♀	↑	0
		♂	↑	0
Itgam	mPFC	♀	↔	↓
		♂	↔	↓
	HP	♀	↓	↔
		♂	↑	↔
NaF	mPFC	♀	↑	↔
		♂	↑	↔
	HP	♀	↑	↑
		♂	↑	↑
Cld5	mPFC	♀	↑	0
		♂	↑	↑
	HP	♀	↔	↑
		♂	↔	↑
Ocln	mPFC	♀	↔	↔
		♂	↑	↔
	HP	♀	↔	↑
		♂	↔	↑

(↑) increased response to LPS when compared to AFR rats, (↓) decreased response to LPS when compared to AFR rats, (↔) no modulation of LPS-induced effects by MS, (0) no response to LPS in MS rats.

0.001 (females), $p = 0.001$ (males)) (Supplemental Table 5) (Fig. 4A). Moreover, MS males generally showed enhanced *Ocln* expression in comparison to AFR males (two-way ANOVA, main effect of RC: $p = 0.046$) (Supplemental Table 5) (Fig. 4A).

Analysis of *Cld5* mRNA levels in the mPFC of adults showed a statistically significant interaction between all studied factors (three-way ANOVA, sex × LPS × RC: $p = 0.003$) (Supplemental Table 4) (Fig. 4B). LPS treatment upregulated *Cld5* expression in the mPFC of AFR females but not in the MS females (two-way ANOVA, LPS × RC: $p < 0.001$, *post hoc:* $p < 0.001$ (AFR), $p = 0.079$ (MS)) (Supplemental Table 5) (Fig. 4B). In adult males, LPS increased *Cld5* mRNA levels regardless of RC (two-way ANOVA, main effect of treatment: $p < 0.001$) (Supplemental Table 5) (Fig. 4B). Additionally, MS males showed greater *Cld5* expression in the mPFC than AFR rats (main effect of RC: $p = 0.033$) (Supplemental Table 5) (Fig. 4B). In the HP of adults, LPS administration generally increased *Cld5* expression in MS rats but not in AFR rats (three-way ANOVA, LPS × RC: $p = 0.045$, *post hoc*: $p < 0.001$ (MS), $p = 0.005$ (AFR)) (Supplemental Table 4) (Fig. 4B). Additionally, females showed greater levels of *Cld5* mRNA than males (main effect of sex: $p < 0.001$) (Table 4) (Supplemental Table 4) (Fig. 4B).

In the case of *Ocln* expression in the mPFC of adults, global ANOVA revealed a statistically significant interaction between all examined factors (three-way ANOVA, sex × LPS × RC: $p = 0.006$) (Supplemental Table 4) (Fig. 4B). Regardless of RC, LPS treatment increased *Ocln* expression in the mPFC of both females and males (two-way ANOVA, main effect of treatment: $p < 0.001$ (females), $p = 0.001$ (males)) (Supplemental Table 5) (Fig. 4B). Additionally, basal *Ocln* mRNA levels in the mPFC of AFR-VEH females and MS-VEH females were greater than those in males (AFR: $p < 0.001$, MS: $p < 0.001$) (Table 4). In the HP of adults, LPS triggered an increase in *Ocln* expression specifically in MS subjects regardless of sex (three-way ANOVA, LPS × RC: $p = 0.010$) (Supplemental Table 4) (Fig. 4B). Additionally, *Ocln* mRNA levels in the HP of females were generally greater than those in males (three-way ANOVA, main effect of sex, $p < 0.001$) (Table 4) (Supplemental Table 4) (Fig. 4B). To help to follow the main findings of the study, the stripped-down summaries of LPS- and MS-triggered effects and sex differences in the basal levels of studied markers were presented in Tables 2, 3 and 4, respectively.

3.3. Effects of MS and subsequent LPS-induced immune challenge on the expression of Icam1 and microglial/macrophage markers Aif1 and Itgam in the brain parenchyma

Next, we investigated whether MS modulates the LPS-induced inflammatory response in the brain. Using RT–qPCR, we evaluated the mRNA expression of certain markers related to this process, such as the adhesion molecule ICAM-1 and microglial/macrophage markers AIF-1 and ITGAM.

Analysis of *Icam1* mRNA levels in the mPFC of juveniles showed a statistically significant interaction between all studied factors (three-way ANOVA, sex × LPS × RC: $p < 0.001$) (Supplemental Table 4) (Fig. 5A). In juvenile females, LPS increased *Icam1* expression in AFR rats and decreased it in MS rats (two-way ANOVA, LPS × RC: $p < 0.001$, *post hoc*: $p = 0.005$ (AFR), $p = 0.005$(MS)) (Supplemental Table 5) (Fig. 5A). Interestingly, the opposite situation was observed in the case of males, i.e., LPS reduced *Icam1* mRNA levels in AFR rats and increased its levels in MS subjects (two-way ANOVA, LPS × RC: $p < 0.001$, *post hoc*: $p = 0.024$ (AFR), $p = 0.001$ (MS)) (Supplemental Table 5) (Fig. 5A). Additionally, the basal level of *Icam1* expression in the mPFC of juvenile MS males was lower than that in AFR males (*pos hoc*: $p < 0.001$) (Fig. 5A). Moreover, the basal *Icam1* mRNA level in males was generally lower than that in females in both RC groups ($p < 0.001$ (AFR), $p < 0.001$ (MS)) (Table 4). In the HP of juveniles, global ANOVA of *Icam1* expression revealed a significant interaction between all examined factors (three-way ANOVA, sex × LPS × RC: $p = 0.002$) (Supplemental Table 4) (Fig. 5A). LPS treatment generally enhanced *Icam1* expression in the HP of juvenile females (two-way ANOVA, main effect of treatment: $p = 0.007$) (Supplemental Table 5) (Fig. 5A). In males, only the MS group showed an LPS-induced increase in *Icam1* mRNA levels (two-way ANOVA, LPS × RC: $p < 0.001$, *post hoc*: $p < 0.001$) (Supplemental Table 5) (Fig. 5A). Additionally, regardless of RC, the basal level of *Icam1* expression in the HP of juvenile females was lower than that in males ($p < 0.001$ (AFR),/ $p = 0.022$ (MS)) (Table 4).

In the case of *Aif1* expression in juveniles, statistical analysis revealed that, regardless of sex, LPS upregulated *Aif1* mRNA levels in the mPFC of MS rats but not AFR rats (three-way ANOVA, LPS × RC: $p = 0.021$, *post hoc*: $p = 0.037$ (MS), $p = 1.000$ (AFR)) (Supplemental Table 4) (Fig. 5A). In the HP, a general increase in *Aif1* expression was

Table 4
Stripped-down summary of sex differences in the basal levels of studied markers in VEH-treated rats.

Marker	Sample	PND											
		22						70					
		AFR			MS			AFR			MS		
CORT	Serum	♀	↔	♂	♀	↔	♂	♀	↔	♂	♀	↔	♂
IL-1β	Serum	♀	↔	♂	♀	↔	♂	♀	↔	♂	♀	↔	♂
TNF-α	Serum	♀	↔	♂	♀	↔	♂	♀	↔	♂	♀	↔	♂
Il-1β	mPFC	♀	↔	♂	♀	↔	♂	♀	↔	♂	♀	<	♂
	HP	♀	↔	♂	♀	↔	♂	♀	>	♂	♀	<	♂
Tnfα	mPFC	♀	↔	♂	♀	↔	♂	♀	↔	♂	♀	↔	♂
	HP	♀	↔	♂	♀	↔	♂	♀	>	♂	♀	↔	♂
Tlr4	mPFC	♀	>	♂	♀	>	♂	♀	<	♂	♀	↔	♂
	HP	♀	>	♂	♀	<	♂	♀	>	♂	♀	<	♂
Icam1	mPFC	♀	>	♂	♀	>	♂	♀	↔	♂	♀	↔	♂
	HP	♀	<	♂	♀	<	♂	♀	>	♂	♀	>	♂
Aif1	mPFC	♀	↔	♂	♀	↔	♂	♀	↔	♂	♀	↔	♂
	HP	♀	↔	♂	♀	↔	♂	♀	↔	♂	♀	↔	♂
Itgam	mPFC	♀	>	♂	♀	>	♂	♀	↔	♂	♀	↔	♂
	HP	♀	↔	♂	♀	>	♂	♀	↔	♂	♀	↔	♂
NaF	mPFC	♀	<	♂	♀	<	♂	♀	↔	♂	♀	↔	♂
	HP	♀	<	♂	♀	<	♂	♀	↔	♂	♀	↔	♂
Cld5	mPFC	♀	>	♂	♀	>	♂	♀	<	♂	♀	<	♂
	HP	♀	>	♂	♀	>	♂	♀	>	♂	♀	>	♂
Ocln	mPFC	♀	<	♂	♀	↔	♂	♀	>	♂	♀	>	♂
	HP	♀	>	♂	♀	>	♂	♀	>	♂	♀	>	♂

observed regardless of sex and RC (three-way ANOVA, main effect of treatment: $p < 0.001$) (Supplemental Table 4) (Fig. 5A). Additionally, MS rats showed greater *Aif1* mRNA levels than AFR rats (main effect of RC: $p = 0.007$) (Supplemental Table 4) (Fig. 5A).

In the mPFC of juveniles, LPS administration enhanced the expression of *Itgam* only in females, regardless of RC (three-way ANOVA, sex × LPS: $p = 0.003$, *post hoc*: $p < 0.001$) (Supplemental Table 4) (Fig. 5A). In the HP, global ANOVA revealed a statistically significant interaction between all studied factors (three-way ANOVA, sex × LPS × RC: $p = 0.002$) (Supplemental Table 4) (Fig. 5A). Both AFR and MS juvenile females showed upregulation of *Itgam* mRNA levels in the HP after LPS treatment (two-way ANOVA, LPS × RC: $p = 0.021$, *post hoc*: $p < 0.001$ (AFR), $p = 0.015$ (MS)) (Supplemental Table 5) (Fig. 5A). Moreover, the LPS-triggered increase in *Itgam* expression was significantly lower in MS females than in AFR females ($p = 0.010$) (Fig. 5A). On the other hand, in males, LPS induced *Itgam* expression only in the MS group (two-way ANOVA, LPS × RC: $p = 0.049$, *post hoc*: $p = 0.001$) (Supplemental Table 5) (Fig. 5A).

In adults, analysis of *Icam1* mRNA levels in the mPFC revealed a statistically significant interaction between all examined factors (three-way ANOVA, sex × LPS × RC: $p = 0.001$) (Supplemental Table 4) (Fig. 5B). In females, LPS enhanced *Icam1* expression only in the AFR group (two-way ANOVA, LPS × RC: $p = 0.011$, *post hoc*: $p < 0.001$ (AFR), $p = 0.168$ (MS)) (Supplemental Table 5) (Fig. 5B). In males, both MS and AFR rats showed LPS-triggered increases in *Icam1* mRNA levels (two-way ANOVA, LPS × RC: $p = 0.031$, *post hoc*: $p = 0.002$ (AFR), $p < 0.001$ (MS)) (Supplemental Table 5) (Fig. 5B). In the HP of adults, LPS treatment upregulated *Icam1* mRNA levels regardless of sex and RC (three-way ANOVA, main effect of treatment: $p < 0.001$) (Supplemental Table 4) (Fig. 5B). Additionally, adult females in general showed greater levels of *Icam1* expression in the HP than males (main effect of sex: $p < 0.001$) (Table 4) (Supplemental Table 4) (Fig. 5B).

In the case of *Aif1* expression in the mPFC of adults, analysis revealed a general stimulatory effect of LPS (three-way ANOVA, main effect of treatment: $p < 0.001$) (Supplemental Table 4) (Fig. 5B). Moreover, LPS-triggered upregulation of *Aif1* mRNA levels was lower in MS rats than in AFR rats, regardless of sex (three-way ANOVA, LPS × RC: $p = 0.002$, *post hoc*: $p < 0.001$) (Supplemental Table 4) (Fig. 5B). In the HP of adults, LPS increased *Aif1* expression only in AFR rats regardless of sex (three-way ANOVA, LPS × RC: $p < 0.001$, *post hoc:* $p < 0.001$) (Supplemental Table 4) (Fig. 5B). Additionally, MS females in general showed lower levels of *Aif1* mRNA compared to AFR females (sex × RC: $p < 0.001$, *post hoc:* $p < 0.001$) (Supplemental Table 4) (Fig. 5B).

Analysis of *Itgam* expression in adults showed a stimulatory effect of LPS regardless of sex and RC in both the mPFC and HP (three-way ANOVA, main effect of treatment: $p < 0.001$ (mPFC), $p < 0.001$ (HP)) (Supplemental Table 4) (Fig. 5B). Furthermore, the LPS-triggered increase in *Itgam* mRNA levels in the mPFC was lower in MS rats than in AFR rats, regardless of sex (LPS × RC: $p = 0.017$, *post hoc:* $p = 0.009$) (Supplemental Table 4) (Fig. 5B).

To help to follow the main findings of the study, the stripped-down summaries of LPS- and MS-triggered effects and sex differences in basal levels of studied markers were presented in Tables 2, 3 and 4, respectively.

3.4. Effects of MS and subsequent LPS-induced immune challenge on the expression of *Tlr4*, *Il-1β*, and *Tnfα* in the brain parenchyma

We continued an investigation of the central effects of LPS injection and studied the mRNA expression of the LPS-recognizing receptor TLR4 and the proinflammatory cytokines IL-1β and TNF-α, all of which are highly engaged in the inflammatory response.

Analysis of *Tlr4* mRNA levels in juveniles revealed a statistically significant interaction between all studied factors in both the mPFC and

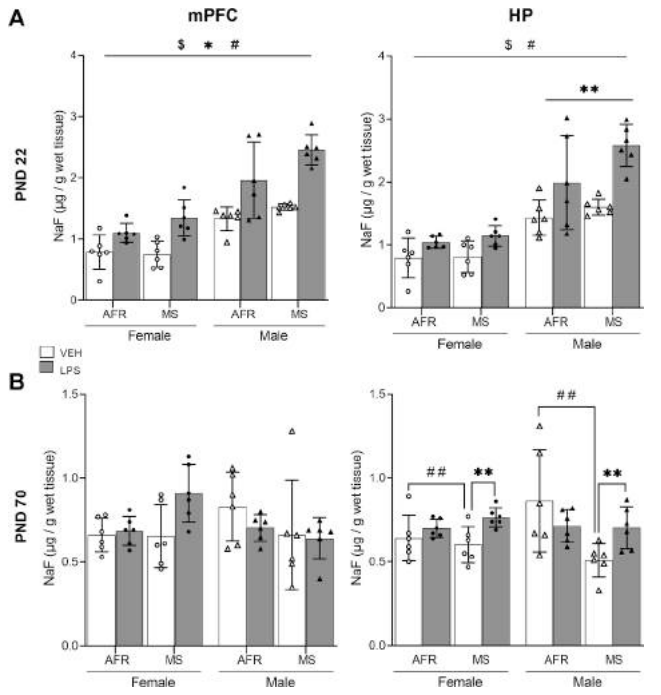

Fig. 3. The effect of MS and subsequent LPS treatment in juvenile (A) and adult rats (B) on the regional brain content of extravasated NaF in the mPFC (left column) and HP (right column). The data are presented as the mean ± SD and indicate the accumulation of NaF in the brain (in micrograms per gram of wet tissue). Circles and triangles represent individual data points ($n = 6$). $^{\$}p < 0.05$: the effect of sex, $^{*}p < 0.05$: the effect of treatment, $\#p < 0.05$: the effect of RC. Lines with a single symbol $^{\$}$ and * *or* # relate to the significance of the main effects in ANOVA, connectors indicate *post hoc* comparisons between the specific groups, and twin symbols ** or ## relate to the effects of significant interactions between two factors in a three-way ANOVA.

HP (three-way ANOVA, sex × LPS × RC: $p < 0.001$ (mPFC), $p = 0.009$ (HP)) (Supplemental Table 4) (Fig. 6A). In the mPFC, LPS triggered a significant increase in *Tlr4* expression specifically in AFR females (two-way ANOVA, LPS × RC: $p = 0.003$, *post hoc*: $p = 0.042$) (Supplemental Table 5) (Fig. 6A). In contrast, in the mPFC of juvenile males, a stimulatory effect of LPS was observed only in the case of MS rats (two-way ANOVA, LPS × RC: $p = 0.012$, *post hoc*: $p = 0.005$) (Supplemental Table 5) (Fig. 6A). Additionally, the basal *Tlr4* mRNA level in VEH-treated juvenile females was greater than that in males in both RC groups ($p < 0.001$ (AFR), $p < 0.001$ (MS)) (Table 4). In the HP of juvenile females, once again, only the AFR group showed LPS-induced enhancement in *Tlr4* expression (two-way ANOVA, LPS × RC: $p < 0.001$, *post hoc:* $p < 0.001$) (Supplemental Table 5) (Fig. 6A). Additionally, MS-VEH females showed lower basal levels of *Tlr4* mRNA than AFR-VEH females (two-way ANOVA, LPS × RC: $p < 0.001$, *post hoc:* $p = 0.001$) (Supplemental Table 5) (Fig. 6A). In the HP of males, LPS did not affect *Tlr4* expression at all (two-way ANOVA, main effect of treatment: $p = 0.469$) (Supplemental Table 5) (Fig. 6A). However, MS juvenile males generally showed greater *Tlr4* mRNA levels than AFR males (main effect of RC: $p = 0.014$) (Supplemental Table 5) (Fig. 6A). Additionally, basal *Tlr4* expression in the HP of AFR juvenile males was lower than that in females ($p = 0.007$) (Table 4) (Fig. 6A). The opposite sex-specific trend was observed in MS subjects ($p = 0.006$) (Table 4) (Fig. 6A).

In the case of *Il-1β* expression in juveniles, global ANOVA revealed a significant interaction between sex and LPS in both the mPFC ($p = 0.014$) and HP ($p = 0.018$) (Supplemental Table 4) (Fig. 6A). Only females, regardless of RC, showed an LPS-induced increase in *Il-1β* mRNA levels in both brain regions (*post hoc*: $p < 0.001$ (mPFC), $p < 0.001$ (HP)) (Fig. 6A).

LPS administration had a general stimulatory effect on *Tnfα* expression in the mPFC and HP of juveniles (three-way ANOVA, main effect of treatment: $p = 0.003$ (mPFC), $p = 0.002$ (HP)) (Supplemental Table 4) (Fig. 6A). Additionally, *Tnfα* mRNA levels in the mPFC were greater in MS rats than in AFR rats (main effect of RC: $p = 0.007$) (Supplemental Table 4) (Fig. 6A).

Analysis of *Tlr4* mRNA levels in the mPFC of adults revealed a statistically significant interaction between all examined factors and an identical pattern of changes in the expression of this gene to that observed in the mPFC of juveniles (three-way ANOVA, sex × LPS × RC: $p < 0.001$) (Supplemental Table 4) (Fig. 6B). Namely, LPS triggered a significant increase in *Tlr4* expression specifically in AFR females (two-way ANOVA, LPS × RC: $p < 0.001$, *post hoc:* $p = 0.003$) (Supplemental Table 5) (Fig. 6B). In contrast, in the mPFC of adult males, a stimulatory effect of LPS was observed only in the case of MS rats (two-way ANOVA, LPS × RC: $p = 0.031$, *post hoc:* $p = 0.006$) (Supplemental Table 5) (Fig. 6B). Additionally, AFR-VEH adult females showed lower basal *Tlr4* mRNA levels than AFR-VEH males ($p = 0.006$) (Table 4). Global ANOVA of *Tlr4* mRNA levels in the HP of adults also showed a significant interaction between all studied factors (three-way ANOVA, sex × LPS × RC: $p = 0.002$) (Supplemental Table 4) (Fig. 6B). In females, LPS administration enhanced *Tlr4* expression only in the MS group (two-way ANOVA, LPS × RC: $p = 0.016$, *post hoc:* $p = 0.024$) (Supplemental Table 5) (Fig. 6B). Additionally, MS-VEH females had lower levels of *Tlr4* mRNA in the HP than AFR-VEH adult females (*post hoc:* $p < 0.001$) (Fig. 6B). In the HP of adult males, LPS increased *Tlr4* expression regardless of RC (two-way ANOVA, main effect of treatment: $p = 0.002$) (Supplemental Table 5) (Fig. 6B). Moreover, MS males generally showed greater levels of *Tlr4* mRNA than AFR males (main effect of RC: $p = 0.036$) (Supplemental Table 5) (Fig. 6B). Further analysis revealed a lower basal level of *Tlr4* expression in the HP of AFR-VEH males than in females ($p < 0.001$) (Table 4). However, the opposite sex-specific trend was observed in MS-VEH subjects ($p < 0.001$) (Table 4) (Fig. 6B).

In the case of *Il-1β* expression in adults, statistical analysis revealed a significant interaction between all examined factors both in the mPFC and HP (three-way ANOVA, sex × LPS × RC: $p = 0.030$ (mPFC), $p = 0.017$ (HP)) (Supplemental Table 4) (Fig. 6B). In males, only a general stimulatory effect of LPS on *Il-1β* expression was observed both in the mPFC and HP (two-way ANOVA, main effect of treatment: $p < 0.001$ (mPFC), $p < 0.001$ (HP)) (Supplemental Table 5) (Fig. 6B). In the HP of females, LPS also induced enhancement in *Il-1β* expression regardless of RC (two-way ANOVA, main effect of treatment: $p < 0.001$) (Supplemental Table 5) (Fig. 6B). Additionally, MS females showed lower levels of *Il-1β* mRNA in the HP than AFR females (two-way ANOVA, main effect of RC: $p = 0.048$) (Supplemental Table 5) (Fig. 6B). Moreover, the basal expression of *Il-1β* in the HP of AFR-VEH females was higher than that in males ($p = 0.012$) (Table 4). The opposite sex-specific trend was observed in MS subjects ($p = 0.003$) (Table 4) (Fig. 6B). However, in the mPFC of adult females, LPS triggered an increase in *Il-1β* mRNA levels only in AFR females (two-way ANOVA, LPS × RC: $p = 0.012$, *post hoc*: $p < 0.001$) (Supplemental Table 5) (Fig. 6B).

Analysis of *Tnfα* expression in the mPFC of adults showed only a general stimulatory effect of LPS regardless of RC and sex (three-way ANOVA, main effect of treatment: $p = 0.012$) (Supplemental Table 4) (Fig. 6B). In the HP, statistical analysis of *Tnfα* mRNA levels revealed a significant interaction between all examined factors (three-way ANOVA, sex × LPS × RC: $p = 0.001$) (Supplemental Table 4) (Fig. 6B). In the HP of females, LPS triggered a significant increase in *Tnfα* mRNA levels specifically in AFR females (two-way ANOVA, LPS × RC: $p = 0.004$, *post hoc*: $p < 0.001$) (Supplemental Table 5) (Fig. 6B). However, in males, LPS administration increased *Tnfα* expression regardless of RC (two-way ANOVA, main effect of treatment: $p = 0.017$) (Supplemental Table 5) (Fig. 6B). Additionally, MS males showed higher levels of *Tnfα* mRNA in the HP than AFR males (two-way ANOVA, main effect of RC: $p = 0.020$) (Supplemental Table 5) (Fig. 6B). Further analysis revealed that the basal expression of *Tnfα* in the HP was lower in AFR-VEH males than in females ($p = 0.002$) (Table 4) (Fig. 6B). To help to follow the main

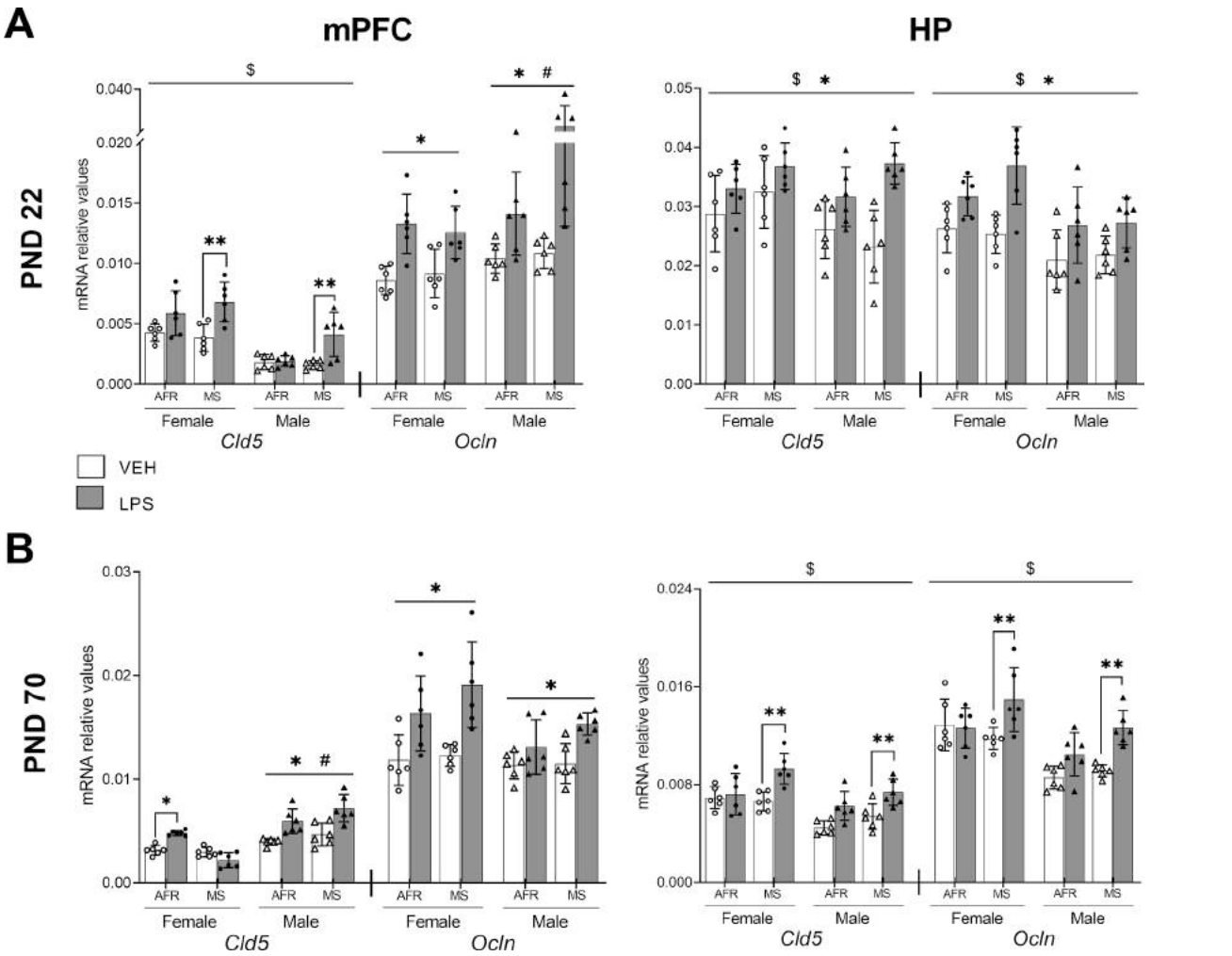

Fig. 4. The effect of MS and subsequent LPS treatment in juvenile (A) and adult rats (B) on the mRNA expression of *Cld5* and *Ocln* in the mPFC (left column) and HP (right column). The mRNA expression was determined by RT–qPCR. The data are presented as the mean ± SD and expressed as relative values of mRNA levels. Circles and triangles represent individual data points ($n = 6$). $^{\$}p < 0.05$: the effect of sex, $^{*}p < 0.05$: the effect of treatment, $\#p < 0.05$: the effect of RC. Lines with a single symbol $^{\$}$, * and # relate to the significance of the main effects in ANOVA, connectors indicate *post hoc* comparisons between the specific groups, and twin symbols ** relate to the effects of significant interactions between two factors in a three-way ANOVA. For clarity, detailed summary of sex differences in the basal levels of studied markers is presented in Table 4.

findings of the study, the stripped-down summaries of LPS- and MS-triggered effects and sex differences in basal levels of studied markers were presented in Tables 2, 3 and 4, respectively.

4. Discussion

In the present study, we investigated whether ELS based on the MS paradigm would condition peripheral, BBB, and parenchymal brain responses to subsequent environmental factors later in life, such as an immune challenge. We showed that a single LPS injection at a dose of 1 mg/kg induced a proinflammatory response both in the periphery and within brain regions, such as the mPFC and HP, in a sex-dependent fashion. Additionally, MS experience by itself exerted a sex-specific influence on the LPS-induced effects in both juvenile and adult rats. Notably, MS increased the neuroinflammatory response to LPS challenge in males during the juvenile period. However, MS females showed a blunted central response to LPS, mainly during adulthood.

4.1. LPS-induced immune challenge – general considerations and basic sex-dependent differences

In animal studies, LPS is widely used as a stimulator of the innate immune response to model systemic inflammation with concomitant BBB disruption and changes in microglial reactivity (Varatharaj and Galea, 2017; Erickson and Banks, 2018). In our study, we were specifically interested in brain inflammatory changes. Therefore, we focused on LPS-induced effects observed 24 h after an immune challenge, according to the concept that the inflammatory response in the brain initiates later and resolves more slowly than the peripheral inflammatory response (Erickson and Banks, 2011). Literature data showing late or prolonged effects of LPS treatment on inflammatory markers in the brain are very limited (Bay-Richter et al., 2011; Erickson and Banks, 2011). To the best of our knowledge, our study is the first to examine a wide range of brain inflammatory markers with simultaneous measurement of BBB permeability and peripheral inflammatory markers 24 h after an immune challenge in both males and females.

The present study generally demonstrated that systemic administration of LPS at a single dose of 1 mg/kg was sufficient to induce an inflammatory response in the periphery and brain in both juvenile and adult rats. Twenty-four hours after LPS administration, there was mainly an increase in proinflammatory cytokines levels in the serum and their mRNA levels in the brain. The pattern of LPS-induced changes in the mRNA expression of *Il-1β* and *Tnfα* in both the mPFC and HP of control (AFR) animals fully reflected that observed in the serum concentrations

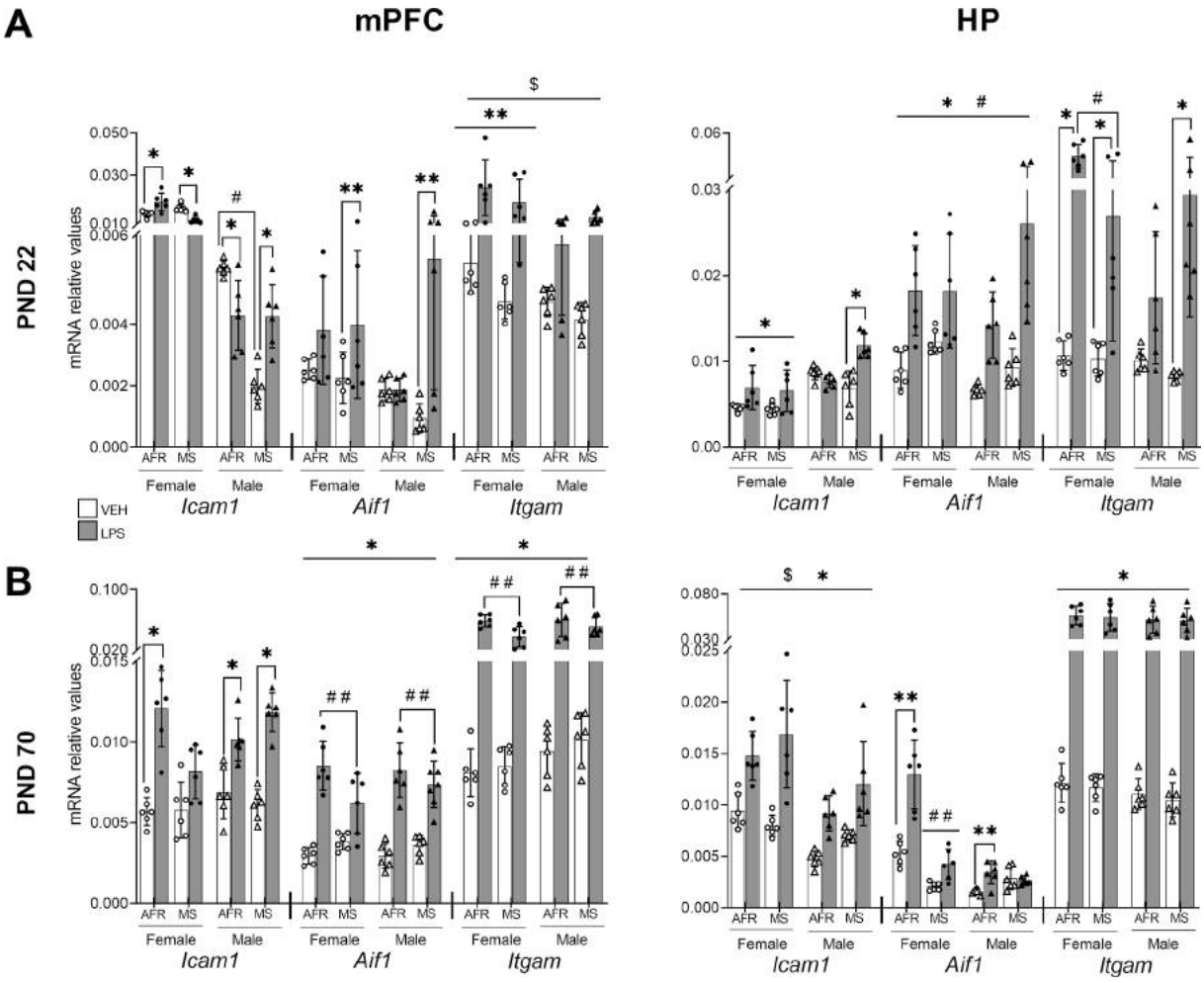

Fig. 5. The effect of MS and subsequent LPS treatment in juvenile (A) and adult rats (B) on the mRNA expression of adhesion molecule *Icam1* and microglial/macrophage markers: *Aif1* and *Itgam* in the mPFC (left column) and HP (right column). The mRNA expression was determined by RT–qPCR. The data are presented as the mean ± SD and expressed as relative values of mRNA levels. Circles and triangles represent individual data points ($n = 6$). $^{\$}p < 0.05$: the effect of sex, $^{*}p < 0.05$: the effect of treatment, $\#p < 0.05$: the effect of RC. Lines with a single symbol * and/or $, # relate to the significance of the main effects in ANOVA, connectors indicate *post hoc* comparisons between the specific groups, and twin symbols ** or ## relate to the effects of significant interactions between two factors in a three-way ANOVA. For clarity, detailed summary of sex differences in the basal levels of studied markers is presented in Table 4.

of IL-1β and TNF-α. Additionally, LPS administration generally increased the expression of *Icam1* and microglial/macrophage markers *Aif1* and *Itgam* in the brain, which may also suggest the occurrence of neuroinflammation. However, we observed sex differences in the intensities of LPS-triggered effects in both control (AFR) and MS rats.

In general, control juvenile males responded less intensely to LPS injection than juvenile females. In the case of many markers expressed in the HP and/or mPFC of control juvenile males, e.g., IL-1β, ICAM1, TLR4, and microglial/macrophage markers, LPS did not induce any changes in their mRNA expression. LPS also did not increase IL-1β serum levels in juvenile males. Against this background, MS-induced intensification of the LPS-triggered neuroinflammatory response in juvenile males was clearly visible.

Significant sex differences in the response to LPS challenge were not observed in adult AFR rats, except for *Tlr4* expression. In the mPFC, males still did not respond to LPS by upregulating the expression of this gene, in contrast to females. The opposite situation was observed in the HP. It is worth mentioning that there were some sex differences in basal levels of inflammatory markers (in VEH-injected animals), mainly in the brain. Juvenile AFR females showed greater *Tlr4* expression in the mPFC and HP than males. A similar effect was also observed in the HP of adult females together with increased levels of *Icam1*, *Il-1β,* and *Tnfα* in this brain region compared to males.

Sex differences in the immune system and immune responses over the life course are well known (Klein and Flanagan, 2016; Dudek et al., 2021). It is generally accepted that after puberty, females have more robust peripheral immune responses than males, which contribute to faster clearance of pathogens, greater vaccine efficacy, and increased susceptibility to inflammatory and autoimmune diseases in females (Schwarz and Bilbo, 2012; Klein and Flanagan, 2016; Dudek et al., 2021). Knowledge about sex differences in the central immune response is more inconclusive. Sex differences in microglial colonization, morphology, and reactivity have been reported in animal studies (Schwarz et al., 2012; Bollinger et al., 2016). Schwarz et al. (2012) showed that healthy male rats had more microglial cells in the PFC and HP in early postnatal time (PND 4) than females. This effect reversed around PND 30, when females showed a greater number of microglial cells with thicker and branched processes, which suggests their heightened basal reactivity. Similar morphological and physiological features of reactive microglia were also observed in adult females compared to males (Schwarz et al., 2012; Bollinger et al., 2016). On the other hand, transcriptome analysis of isolated microglia from the HP of adult mice revealed the opposite trend, i.e., under basal conditions, male microglia had a more inflammatory phenotype, whereas female microglia showed a neuroprotective phenotype (Villa et al., 2018). Other studies on mice demonstrated that adult males also had greater and enduring responses

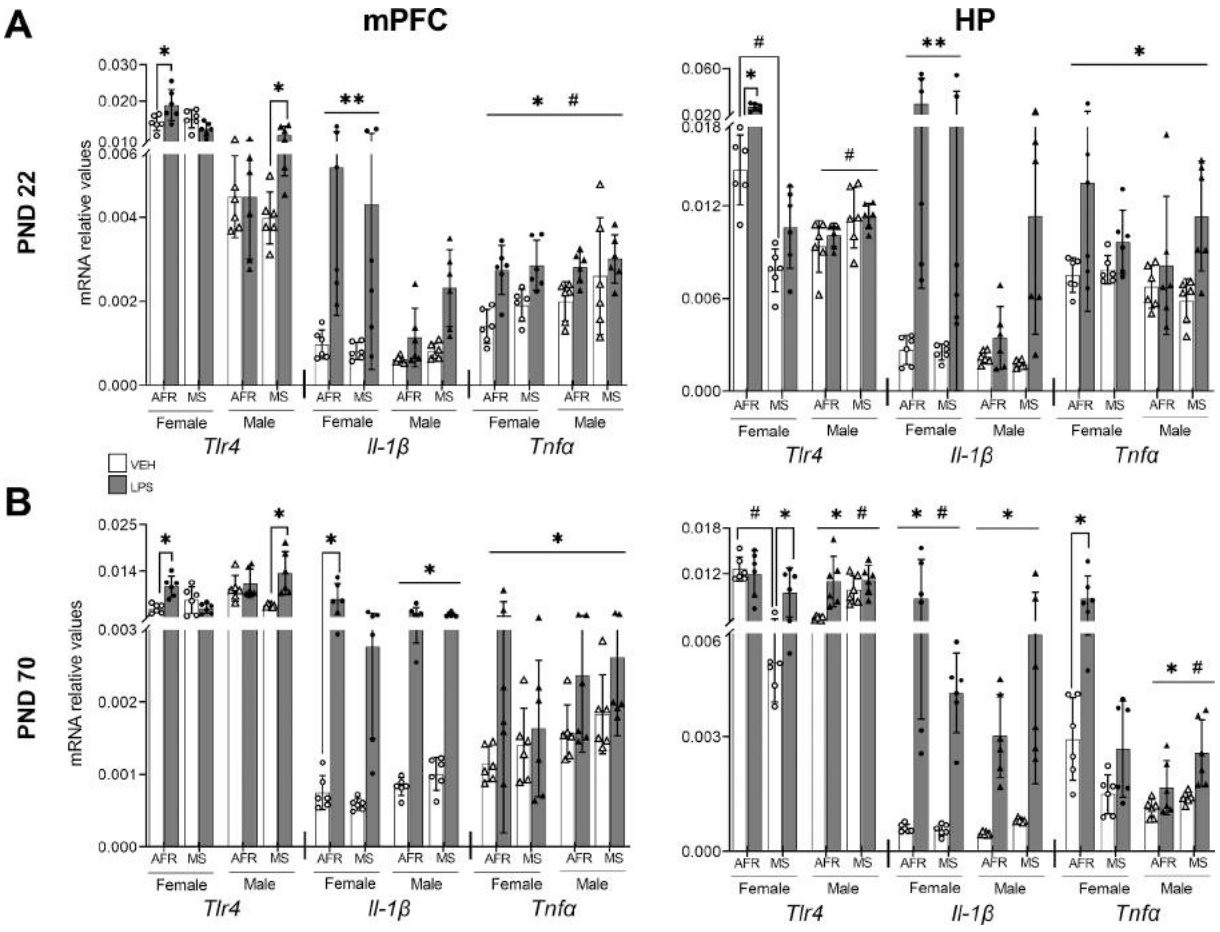

Fig. 6. The effect of MS and subsequent LPS treatment in juvenile (A) and adult rats (B) on the mRNA expression of LPS-recognizing receptor *Tlr4* and proinflammatory cytokines *Il-1β* and *Tnfα* in the mPFC (left column) and HP (right column). The mRNA expression was determined by RT–qPCR. The data are presented as the mean ± SD and expressed as relative values of mRNA levels. Circles and triangles represent individual data points ($n = 6$). *$p < 0.05$: the effect of treatment, #$p < 0.05$: the effect of RC. Lines with a single symbol * and # relate to the significance of the main effects in ANOVA, connectors indicate *post hoc* comparisons between the specific groups, and twin symbols ** relate to the effect of significant interaction between two factors in a three-way ANOVA. For clarity, detailed summary of sex differences in the basal levels of studied markers is presented in Table 4.

to immune challenge in the HP than females (Tchessalova and Tronson, 2020; Posillico et al., 2021). Our results concerning sex differences in the healthy and LPS-challenged immune systems of control rats did not fall into any of the patterns described above. However, in the present study, we applied only one time point for the analysis. Therefore, we cannot compare the dynamics of the inflammatory response between females and males. We cannot rule out that the less pronounced brain reaction to LPS challenge in juvenile AFR males may be related to a sex-specific time frame in the onset and resolution of the immune response and that LPS-induced neuroinflammation resolved earlier in juvenile males than in females. Nevertheless, our data also suggest that the prepubertal switch in sex differences in microglial reactivity reported by Schwarz et al. (2012) may occur earlier than around PND 30 in rats, i.e., at least on PND 22. However, we did not have morphological evidence for that earlier occurrence.

There is a consensus among researchers on the early genesis of sexual differentiation of the immune system and microglia. Sex differences in the immune response relate to genetic sex and develop during perinatal exposure to sex steroids (perinatal sexual differentiation) (Schwarz and Bilbo, 2012; Klein and Flanagan, 2016; Villa et al., 2018; Dudek et al., 2021). Nevertheless, gonadal hormones may also strongly modulate the immune system after puberty (Schwarz and Bilbo, 2012; Klein and Flanagan, 2016; Dudek et al., 2021). Therefore, the discrepancies in the reported results concerning immune response in postpubertal animals, especially females, are not surprising. The levels of sex hormones are not routinely measured in studies on the immune response. We also did not test them in our study and did not check the phase of the estrus cycle in adult females.

4.2. The effects of ELS and LPS-induced immune challenge on BBB permeability and the mRNA expression of Cld5 and Ocln

It has been demonstrated that systemic inflammation may contribute to BBB disruption (Varatharaj and Galea, 2017). However, in our study, we observed a lack of a consistent relationship between the intensity of the inflammatory response and changes in BBB permeability after LPS administration. For example, juvenile males showed increased BBB permeability 24 h after LPS injections, although only one proinflammatory cytokine was elevated in the periphery at this time, and many brain markers of inflammation were not affected by LPS in control males. The explanation for that specific discrepancy can be the high sensitivity of the method applied in our study to measure BBB permeability. The fluorescent tracer NaF used in our experiments is a very small molecule (376 Da) and is detectable at very low concentrations (Sun et al., 2021). Therefore, this method detects even slight BBB breakdown. Additionally, it is worth emphasizing that LPS can also directly modify TJ proteins, damage endothelial cells and basement membranes within the BBB by binding to TLR4, and consequently affect BBB permeability without any need for strong inflammatory components (Varatharaj and Galea, 2017; Peng et al., 2021).

On the other hand, the induction of neuroinflammation does not always have to be dependent on BBB disruption. LPS may produce nondisruptive changes in the BBB, e.g., activate brain endothelial cells to induce cytokines and express ICAM1, and in this way, promote transmigration of peripheral immune cells and transmit inflammatory signals into the brain. This phenomenon could explain the discrepancy between the LPS-induced increase in the expression of neuroinflammatory markers and the lack of change in BBB permeability observed in AFR adult rats. However, we cannot rule out that the lack of a correlation between the intensity of the inflammatory response and change in BBB permeability relates to a specific time point chosen for observation and implies differences in the dynamics of those two processes. Sex differences should also be considered.

LPS has been demonstrated to affect TJ integrity by altering TJ protein distribution, turnover, and expression (Varatharaj and Galea, 2017; Peng et al., 2021). Many studies have reported LPS-induced decreases in the mRNA and protein levels of TJ proteins that correlate with BBB leakage (Brooks et al., 2006; Zhou et al., 2014). However, there are also data showing an increase in the expression of TJ proteins, especially after a longer elapsed time (48–72 h) after LPS injection (Brooks et al., 2006). In our study, we mainly observed the latter situation, i.e., an LPS-triggered elevation in *Cld5* and *Ocln* expression or a lack of any changes. Moreover, an LPS-induced increase in the mRNA levels of TJ proteins was observed in the case of both enhanced (e.g., in the HP of juvenile males) and unchanged BBB permeability (in the mPFC of adults). Although we did not study the protein expression of TJ proteins or the TJ ultrastructure, we argued that the obtained results indicated compensatory or adaptive mechanisms induced after LPS challenge to protect BBB integrity. At least in males, it can be related to enhanced serum CORT levels observed 24 h after LPS injection. Glucocorticoids are well-known modulators of TJ protein expression and BBB function (Salvador et al., 2014). It has been shown that both glucocorticoids and systemic inflammation may increase the expression of TJ proteins in the cells of the neurovascular unit and in vessel-associated microglia to maintain BBB integrity, especially during the acute phase of inflammation (Kroll et al., 2009; Salvador et al., 2014; Haruwaka et al., 2019).

MS experience combined with LPS challenge and regardless of sex increased BBB permeability in the mPFC and HP of juveniles when compared to AFR rats. In the mPFC, this effect was accompanied by enhanced expression of *Cld5* and *Ocln* (only in males). The above-mentioned changes in BBB function in MS juveniles may be related to the increased neuroinflammatory response to LPS, but only in males. Interestingly, in the HP of adults, stimulatory effects of LPS on BBB permeability and mRNA expression of TJ proteins were observed only in MS rats. However, BBB permeability in MS-LPS rats altogether resembled that in AFR rats. The magnitude of the LPS effect was rather slight and mainly related to the lower basal BBB permeability observed in MS-VEH rats in the HP. This finding may suggest the occurrence of some kind of adaptive mechanisms within the BBB of MS adult rats that protect the barrier from enhanced harmful dysregulation in response to environmental insults.

4.3. Sex-dependent effects of ELS on peripheral and brain responses to immune challenge

The main finding of the present study is that the MS procedure modulated the neuroinflammatory response to LPS challenge in a sex-specific fashion. Simultaneously, we did not observe a significant impact of MS per se on the basal levels of inflammatory markers when comparing MS-VEH to AFR-VEH-treated rats, which is in line with many previous reports (Dutcher et al., 2020). Interestingly, MS females, both juvenile and adult, showed lower mRNA levels of *Tlr4* in the HP than AFR females.

Notably, MS intensified or prolonged the neuroinflammatory response to LPS challenge in juveniles. It was especially manifested in juvenile MS males. LPS enhanced the expression of many inflammatory markers, e.g., *Icam1, Tlr4, Aif1, and Itgam,* specifically in the mPFC or/and HP of MS but not AFR juvenile males. Moreover, MS generally increased CORT serum levels in juvenile males. MS-induced elevation in CORT concentration can be strongly related to a concurrent vulnerability to LPS challenge in accordance with many data showing that prior exposure to glucocorticoids or stress can sensitize or prime proinflammatory responses (Frank et al., 2010; Loram et al., 2011). MS juvenile females showed a more diverse pattern of responses to LPS challenge.

Interestingly, in adulthood, MS rats were less sensitive to LPS action than AFR rats. This finding was especially evident in females. The expression of many inflammatory markers, e.g., *Il-1β* or microglial/macrophage markers, was not triggered at all or was even decreased by LPS 24 h after its administration. This phenomenon may potentially relate not only to a less intense response to LPS challenge but also to faster resolution of neuroinflammation in MS adult females.

Stress and glucocorticoids have been historically regarded as anti-inflammatory agents (Baxter and Forsham, 1972). However, currently, a large amount of data accumulated from both animal and human studies indicate that previous stress and glucocorticoids may prime the neuroinflammatory response to subsequent proinflammatory challenge (Frank et al., 2016; Kelly et al., 2018; Barrett et al., 2021). Nevertheless, the most consistent data on this topic came from studies of stress in adulthood (Frank et al., 2010; Loram et al., 2011; Kelly et al., 2018; Barrett et al., 2021). Past results from animal studies that showed the effects of ELS on subsequent immune challenge later in life were often inconclusive, probably due to the differences in the ELS procedures, the regimen of LPS treatment and the small number of inflammatory markers under study. However, these studies often showed sex differences in the effects of ELS (Avitsur et al., 2013; Gildawie et al., 2020). It has been shown that MS intensifies some of the symptoms of sickness behavior, especially in adult males (Avitsur et al., 2013). A few studies have focused on the effect of ELS on the morphology of microglial cells in juveniles and showed that MS juvenile males (PND 15) had more microglia with large soma and thicker processes in the HP in response to LPS (Saavedra et al., 2017), and juvenile females (PND 21) with MS exposure had a greater increase in microglial soma size following LPS injection in the PFC (Gildawie et al., 2020), which suggests enhanced microglia reactivity to LPS challenge in MS subjects. To the best of our knowledge, our study is the first to show a clear pattern of sex-specific effects of ELS on subsequent neuroinflammatory challenge based on the analysis of multiple peripheral and central markers of inflammation. Sex differences in MS-triggered effects were observed in both juvenile and adult rats and were related to the impact of ELS on the perinatal phases of sexual differentiation and programming of brain and inflammatory functions.

We can only speculate about the functional consequences of MS-induced intensification or prolongation of the neuroinflammatory processes in response to common environmental factors observed in males, especially juveniles. Such intensification may imply enhanced reactivity of microglial cells, which are not only engaged in immune defense of the brain but also play essential roles in postnatal brain maturation and synaptic plasticity. Microglial cells take part in neurodevelopmental apoptosis and synapse pruning (Nikodemova et al., 2015). Therefore, aberrant function of microglia and exacerbated neuroimmune responses may strongly affect postnatal development of the brain, especially the mPFC, which shows a prolonged developmental trajectory and undergoes morphological and functional reorganization during the pre-adolescence period (Brenhouse and Andersen, 2011; Selemon, 2013). Altogether, such ELS-induced changes may underlie the dysfunctions in synaptic plasticity, fear memory and innate fear observed previously in our model in both adolescent and adult males (Chocyk et al., 2014; Majcher-Maslanka et al., 2019; Solarz et al., 2021b).

It has been postulated that the phenomenon of stress-induced sensitization of the proinflammatory response may be strongly related to the predisposition to some psychiatric and neurodegenerative

disorders (Frank et al., 2016). It is commonly accepted that ELS increases the risk of early-onset mood and anxiety disorders, cognitive impairments and adult psychopathology (Kessler et al., 2010; Reincke and Hanganu-Opatz, 2017).

Although there are no clear and consistent differences in vulnerability to the abovementioned pathologies between females and males subjected to ELS, numerous data have shown that females may be more resilient to cognitive impairments induced by early-life adversity (Loi et al., 2017; Reincke and Hanganu-Opatz, 2017). It is interesting that the present study reported that MS females (especially adults) showed blunted (or shorter) responses to immune challenge. Thus, in this context, the immune phenotype of MS females can be considered beneficial and potentially promotes resilience. In contrast to the hypothesis of stress-induced sensitization of the proinflammatory response, it has been argued that exposure to moderate amounts of stressors, especially during the perinatal period, may help to cope with other environmental challenges later in life. This phenomenon is known as stress inoculation (Parker et al., 2019; Qin et al., 2019). Our study indicates that sex may strongly modulate both stress inoculation and stress sensitization phenomena.

It is worth emphasizing that our present study showed a consistent regulation of *Tlr4* mRNA expression by ELS observed both in juveniles and adults in response to LPS. Especially in the mPFC, this regulation had the opposite direction in males and females. MS males responded to LPS administration with upregulation of *Tlr4* expression, in contrast to AFR males, which did not show such an effect. The opposite situation was revealed in the mPFC of females, where an upregulation of *Tlr4* expression was observed in control but not in MS females. Additionally, MS males showed generally higher levels of *Tlr4* expression in the HP, whereas females had the opposite trend when compared to AFR subjects. These phenomena are in line with the observed sex-specific modulation of neuroinflammatory responses to acute challenge by MS. A large amount of accumulated preclinical and clinical data have shown a potential role of TLR4 signaling not only in the pathophysiology of multiple sclerosis, AD, and ischemia but also in depression and anxiety (Femenia et al., 2018; Nie et al., 2018; Figueroa-Hall et al., 2020). Upregulation of TLR4 expression has been observed in animal models of depression based on chronic stress procedures and in postmortem tissue from major depressive disorder patients (Garate et al., 2011; Figueroa-Hall et al., 2020; Zhang et al., 2020). TLR4 belongs to the pattern recognition receptors that specifically recognize Gram-negative bacterial LPS and subsequently initiate the innate immune response. However, TLR4 may also recognize damage-associated molecular patterns (DAMPs) released from cells during injury or stress and trigger sterile inflammation. Well-known examples of DAMPs are heat shock proteins of 70 kDa (HSP70). We have recently shown that the MS procedure increased the expression of HSP70 family members in the mPFC and HP of both juvenile and adult male rats (Solarz et al., 2021b). Altogether, our results suggest that the regulation of TLR4 signaling in pathogen and nonpathogen-associated neuroinflammation can be an important mechanism that affects the susceptibility or resilience to ELS effects in a sex-specific fashion.

The limitation of our study is that we checked the response to LPS challenge only at one (late) time point. Therefore, we cannot rule out that the effects triggered by LPS administration reflect some compensatory or adaptive mechanisms, as in the case of LPS-induced upregulation of mRNA expression of TJ proteins. Another limitation is that we did not perfuse the animals with saline to remove the blood with peripheral immune cells before brain tissue collection, which could, to some degree, affect the proper separation of central and peripheral immune effects in our study. However, recent reports have shown that the mRNA levels of several cytokines measured in the brain were unaffected by prior perfusion of the tissue with saline regardless of immune status (Kvichansky et al., 2019; Walker et al., 2020). Nevertheless, it is worth underlining that AIF1 and ITGAM are not specific markers of microglial cells but they are also expressed in peripheral immune cells.

In conclusion, we showed that MS experience modulated the neuroinflammatory response to subsequent immune challenge later in life in a sex-dependent fashion. Specifically, MS males had increased and females had decreased central responses to an acute LPS injection. These results suggest that ELS may precondition individuals to other environmental factors and in this way determine their susceptibility or resilience to mental and/or neurodegenerative diseases.

Declaration of Competing Interest

The authors declare that they have no known competing financial interests or personal relationships that could have appeared to influence the work reported in this paper.

Data availability

Data will be made available on request.

Acknowledgements

This work was supported by the National Science Centre, Poland (grant numbers 2016/23/N/NZ4/01148 and 2017/25/B/NZ7/00174) and partially by statutory activity of the Maj Institute of Pharmacology, Polish Academy of Sciences, 31-343 Kraków, Smętna Street 12, Poland.

Appendix A. Supplementary data

Supplementary data to this article can be found online at https://doi.org/10.1016/j.bbi.2022.11.005.

References

Abbott, N.J., Patabendige, A.A., Dolman, D.E., Yusof, S.R., Begley, D.J., 2010. Structure and function of the blood-brain barrier. Neurobiol. Dis. 37, 13–25. https://doi.org/10.1016/j.nbd.2009.07.030.

Andersen, S.L., Teicher, M.H., 2004. Delayed effects of early stress on hippocampal development. Neuropsychopharmacology 29, 1988–1993. https://doi.org/10.1038/sj.npp.1300528.

Avitsur, R., Maayan, R., Weizman, A., 2013. Neonatal stress modulates sickness behavior: Role for proinflammatory cytokines. J. Neuroimmunol. 257, 59–66. https://doi.org/10.1016/j.jneuroim.2013.02.009.

Ballabh, P., Braun, A., Nedergaard, M., 2004. The blood-brain barrier: An overview: Structure, regulation, and clinical implications. Neurobiol. Dis. 16, 1–13. https://doi.org/10.1016/j.nbd.2003.12.016.

Barrett, T.J., Corr, E.M., van Solingen, C., Schlamp, F., Brown, E.J., Koelwyn, G.J., Lee, A.H., Shanley, L.C., Spruill, T.M., Bozal, F., de Jong, A., Newman, A.A.C., Drenkova, K., Silvestro, M., Ramkhelawon, B., Reynolds, H.R., Hochman, J.S., Nahrendorf, M., Swirski, F.K., Fisher, E.A., Berger, J.S., Moore, K.J., 2021. Chronic stress primes innate immune responses in mice and humans. Cell Rep. 36, 109595 https://doi.org/10.1016/j.celrep.2021.109595.

Baudin, A., Blot, K., Verney, C., Estevez, L., Santamaria, J., Gressens, P., Giros, B., Otani, S., Dauge, V., Naudon, L., 2012. Maternal deprivation induces deficits in temporal memory and cognitive flexibility and exaggerates synaptic plasticity in the rat medial prefrontal cortex. Neurobiol. Learn. Mem. 98, 207–214. https://doi.org/10.1016/j.nlm.2012.08.004.

Baxter, J.D., Forsham, P.H., 1972. Tissue Effects of Glucocorticoids. Am J Med 53, 573-+,Doi 10.1016/0002-9343(72)90154-4.

Bay-Richter, C., Janelidze, S., Hallberg, L., Brundin, L., 2011. Changes in behaviour and cytokine expression upon a peripheral immune challenge. Behav. Brain Res. 222, 193–199. https://doi.org/10.1016/j.bbr.2011.03.060.

Bollinger, J.L., Bergeon Burns, C.M., Wellman, C.L., 2016. Differential effects of stress on microglial cell activation in male and female medial prefrontal cortex. Brain Behav. Immun. 52, 88–97. https://doi.org/10.1016/j.bbi.2015.10.003.

Brenhouse, H.C., Andersen, S.L., 2011. Developmental trajectories during adolescence in males and females: A cross-species understanding of underlying brain changes. Neurosci. Biobehav. Rev. 35, 1687–1703. https://doi.org/10.1016/j.neubiorev.2011.04.013.

Brenhouse, H.C., Danese, A., Grassi-Oliveira, R., 2019. Neuroimmune impacts of early-life stress on development and psychopathology. Curr. Top. Behav. Neurosci. 43, 423–447. https://doi.org/10.1007/7854_2018_53.

Brooks, T.A., Ocheltree, S.M., Seelbach, M.J., Charles, R.A., Nametz, N., Egleton, R.D., Davis, T.P., 2006. Biphasic cytoarchitecture and functional changes in the BBB induced by chronic inflammatory pain. Brain Res. 1120, 172–182. https://doi.org/10.1016/j.brainres.2006.08.085.

N.M. Brydges J. Reddaway Neuroimmunological effects of early life experiences Brain Neurosci Adv 4 2020 2398212820953706 10.1177/2398212820953706.

Caley, D.W., Maxwell, D.S., 1970. Development of the blood vessels and extracellular spaces during postnatal maturation of rat cerebral cortex. J. Comp. Neurol. 138, 31–47. https://doi.org/10.1002/cne.901380104.
Catale, C., Gironda, S., Lo Iacono, L., Carola, V., 2020. Microglial function in the effects of early-life stress on brain and behavioral development. J. Clin. Med. 9 https://doi.org/10.3390/jcm9020468.
Chocyk, A., Dudys, D., Przyborowska, A., Mackowiak, M., Wedzony, K., 2010. Impact of maternal separation on neural cell adhesion molecules expression in dopaminergic brain regions of juvenile, adolescent and adult rats. Pharmacol. Rep. 62, 1218–1224. https://doi.org/10.1016/s1734-1140(10)70385-6.
Chocyk, A., Bobula, B., Dudys, D., Przyborowska, A., Majcher-Maslanka, I., Hess, G., Wedzony, K., 2013. Early-life stress affects the structural and functional plasticity of the medial prefrontal cortex in adolescent rats. Eur. J. Neurosci. 38, 2089–2107. https://doi.org/10.1111/ejn.12208.
Chocyk, A., Przyborowska, A., Makuch, W., Majcher-Maslanka, I., Dudys, D., Wedzony, K., 2014. The effects of early-life adversity on fear memories in adolescent rats and their persistence into adulthood. Behav. Brain Res. 264, 161–172. https://doi.org/10.1016/j.bbr.2014.01.040.
Chocyk, A., Majcher-Maslanka, I., Przyborowska, A., Mackowiak, M., Wedzony, K., 2015. Early-life stress increases the survival of midbrain neurons during postnatal development and enhances reward-related and anxiolytic-like behaviors in a sex-dependent fashion. Int. J. Dev. Neurosci. 44, 33–47. https://doi.org/10.1016/j.ijdevneu.2015.05.002.
Danese, A., Lewis, S.J., 2017. Psychoneuroimmunology of early-life stress: The hidden wounds of childhood trauma? Neuropsychopharmacology 42, 99–114. https://doi.org/10.1038/npp.2016.198.
Dion-Albert, L., Cadoret, A., Doney, E., Kaufmann, F.N., Dudek, K.A., Daigle, B., Parise, L. F., Cathomas, F., Samba, N., Hudson, N., Lebel, M., Signature, C., Campbell, M., Turecki, G., Mechawar, N., Menard, C., 2022. Vascular and blood-brain barrier-related changes underlie stress responses and resilience in female mice and depression in human tissue. Nat. Commun. 13, 164. https://doi.org/10.1038/s41467-021-27604-x.
C. Disdier B.S. Stonestreet Blood-Brain Barrier. Stress: Physiology, Biochemistry, and Pathology 2019 325 336.
Dudek, K.A., Dion-Albert, L., Lebel, M., LeClair, K., Labrecque, S., Tuck, E., Ferrer Perez, C., Golden, S.A., Tamminga, C., Turecki, G., Mechawar, N., Russo, S.J., Menard, C., 2020. Molecular adaptations of the blood-brain barrier promote stress resilience vs. depression. Proc. Natl. Acad. Sci. U S A 117, 3326–3336. https://doi.org/10.1073/pnas.1914655117.
Dudek, K.A., Dion-Albert, L., Kaufmann, F.N., Tuck, E., Lebel, M., Menard, C., 2021. Neurobiology of resilience in depression: Immune and vascular insights from human and animal studies. Eur. J. Neurosci. 53, 183–221. https://doi.org/10.1111/ejn.14547.
E.G. Dutcher E.A.C. Pama M.E. Lynall S. Khan M.R. Clatworthy T.W. Robbins E.T. Bullmore J.W. Dalley Early-life stress and inflammation: A systematic review of a key experimental approach in rodents Brain Neurosci Adv 4 2020 2398212820978049 10.1177/2398212820978049.
Erickson, M.A., Banks, W.A., 2011. Cytokine and chemokine responses in serum and brain after single and repeated injections of lipopolysaccharide: Multiplex quantification with path analysis. Brain Behav. Immun. 25, 1637–1648. https://doi.org/10.1016/j.bbi.2011.06.006.
Erickson, M.A., Banks, W.A., 2013. Blood-brain barrier dysfunction as a cause and consequence of Alzheimer's disease. J. Cereb. Blood Flow Metab. 33, 1500–1513. https://doi.org/10.1038/jcbfm.2013.135.
Erickson, M.A., Banks, W.A., 2018. Neuroimmune axes of the blood-brain barriers and blood-brain interfaces: Bases for physiological regulation, disease states, and pharmacological interventions. Pharmacol. Rev. 70, 278–314. https://doi.org/10.1124/pr.117.014647.
Femenia, T., Qian, Y., Arentsen, T., Forssberg, H., Heijtz, R.D., 2018. Toll-like receptor-4 regulates anxiety-like behavior and DARPP-32 phosphorylation. Brain Behav. Immun. 69, 273–282. https://doi.org/10.1016/j.bbi.2017.11.022.
Figueroa-Hall, L.K., Paulus, M.P., Savitz, J., 2020. Toll-like receptor signaling in depression. Psychoneuroendocrinology 121, 104843. https://doi.org/10.1016/j.psyneuen.2020.104843.
Frank, M.G., Miguel, Z.D., Watkins, L.R., Maier, S.F., 2010. Prior exposure to glucocorticoids sensitizes the neuroinflammatory and peripheral inflammatory responses to E. coli lipopolysaccharide. Brain Behav. Immun. 24, 19–30. https://doi.org/10.1016/j.bbi.2009.07.008.
Frank, M.G., Weber, M.D., Watkins, L.R., Maier, S.F., 2016. Stress-induced neuroinflammatory priming: A liability factor in the etiology of psychiatric disorders. Neurobiol. Stress 4, 62–70. https://doi.org/10.1016/j.ynstr.2015.12.004.
I. Garate B. Garcia-Bueno J.L.M. Madrigal L. Bravo E. Berrocoso J.R. Caso J.A. Mico J.C. Leza Origin and consequences of brain Toll-like receptor 4 pathway stimulation in an experimental model of depression J Neuroinflamm 8, Artn 151 2011 10.1186/1742-2094-8-151.
Gildawie, K.R., Orso, R., Peterzell, S., Thompson, V., Brenhouse, H.C., 2020. Sex differences in prefrontal cortex microglia morphology: Impact of a two-hit model of adversity throughout development. Neurosci. Lett. 738, 135381 https://doi.org/10.1016/j.neulet.2020.135381.
Gomez-Gonzalez, B., Escobar, A., 2009. Altered functional development of the blood-brain barrier after early life stress in the rat. Brain Res. Bull. 79, 376–387. https://doi.org/10.1016/j.brainresbull.2009.05.012.
Haruwaka, K., Ikegami, A., Tachibana, Y., Ohno, N., Konishi, H., Hashimoto, A., Matsumoto, M., Kato, D., Ono, R., Kiyama, H., Moorhouse, A.J., Nabekura, J., Wake, H., 2019. Dual microglia effects on blood brain barrier permeability induced by systemic inflammation. Nat. Commun. 10, 5816. https://doi.org/10.1038/s41467-019-13812-z.
Haseloff, R.F., Dithmer, S., Winkler, L., Wolburg, H., Blasig, I.E., 2015. Transmembrane proteins of the tight junctions at the blood-brain barrier: Structural and functional aspects. Semin. Cell Dev. Biol. 38, 16–25. https://doi.org/10.1016/j.semcdb.2014.11.004.
Hoeijmakers, L., Ruigrok, S.R., Amelianchik, A., Ivan, D., van Dam, A.M., Lucassen, P.J., Korosi, A., 2017. Early-life stress lastingly alters the neuroinflammatory response to amyloid pathology in an Alzheimer's disease mouse model. Brain Behav. Immun. 63, 160–175. https://doi.org/10.1016/j.bbi.2016.12.023.
Italia, M., Forastieri, C., Longaretti, A., Battaglioli, E., Rusconi, F., 2020. Rationale, relevance, and limits of stress-induced psychopathology in rodents as models for psychiatry research: An introductory overview. Int. J. Mol. Sci. 21 https://doi.org/10.3390/ijms21207455.
Jangula, A., Murphy, E.J., 2013. Lipopolysaccharide-induced blood brain barrier permeability is enhanced by alpha-synuclein expression. Neurosci. Lett. 551, 23–27. https://doi.org/10.1016/j.neulet.2013.06.058.
Kelly, K.A., Michalovicz, L.T., Miller, J.V., Castranova, V., Miller, D.B., O'Callaghan, J.P., 2018. Prior exposure to corticosterone markedly enhances and prolongs the neuroinflammatory response to systemic challenge with LPS. PLoS One 13, e0190546.
Kessler, R.C., McLaughlin, K.A., Green, J.G., Gruber, M.J., Sampson, N.A., Zaslavsky, A. M., Aguilar-Gaxiola, S., Alhamzawi, A.O., Alonso, J., Angermeyer, M., Benjet, C., Bromet, E., Chatterji, S., de Girolamo, G., Demyttenaere, K., Fayyad, J., Florescu, S., Gal, G., Gureje, O., Haro, J.M., Hu, C.Y., Karam, E.G., Kawakami, N., Lee, S., Lepine, J.P., Ormel, J., Posada-Villa, J., Sagar, R., Tsang, A., Ustun, T.B., Vassilev, S., Viana, M.C., Williams, D.R., 2010. Childhood adversities and adult psychopathology in the WHO world mental health surveys. Br. J. Psychiatry 197, 378–385. https://doi.org/10.1192/bjp.bp.110.080499.
Klein, S.L., Flanagan, K.L., 2016. Sex differences in immune responses. Nat. Rev. Immunol. 16, 626–638. https://doi.org/10.1038/nri.2016.90.
Krause, D., Faustmann, P.M., Dermietzel, R., 2002. Molecular Anatomy of the Blood-Brain Barrier in Development and Aging. In: de Vellis, J.S. (Ed.), Neuroglia in the Aging Brain. Humana Press, Totowa, NJ, pp. 291–303.
Kroll, S., El-Gindi, J., Thanabalasundaram, G., Panpumthong, P., Schrot, S., Hartmann, C., Galla, H.J., 2009. Control of the blood-brain barrier by glucocorticoids and the cells of the neurovascular unit. Ann. N. Y. Acad. Sci. 1165, 228–239. https://doi.org/10.1111/j.1749-6632.2009.04040.x.
Kvichansky, A.A., Volobueva, M.N., Spivak, Y.S., Tret'yakova, L.V., Gulyaeva, N.V., Bolshakov, A.P., 2019. Expression of mRNAs for IL-1beta, IL-6, IL-10, TNFalpha, CX3CL1, and TGFbeta1 cytokines in the brain tissues: Assessment of contribution of blood cells with and without perfusion. Biochemistry (Mosc) 84, 905–910. https://doi.org/10.1134/S0006297919080066.
Loi, M., Mossink, J.C., Meerhoff, G.F., Den Blaauwen, J.L., Lucassen, P.J., Joels, M., 2017. Effects of early-life stress on cognitive function and hippocampal structure in female rodents. Neuroscience 342, 101–119. https://doi.org/10.1016/j.neuroscience.2015.08.024.
Loram, L.C., Taylor, F.R., Strand, K.A., Frank, M.G., Sholar, P., Harrison, J.A., Maier, S.F., Watkins, L.R., 2011. Prior exposure to glucocorticoids potentiates lipopolysaccharide induced mechanical allodynia and spinal neuroinflammation. Brain Behav. Immun. 25, 1408–1415. https://doi.org/10.1016/j.bbi.2011.04.013.
Loria, A.S., Ho, D.H., Pollock, J.S., 2014. A mechanistic look at the effects of adversity early in life on cardiovascular disease risk during adulthood. Acta Physiol (Oxf) 210, 277–287. https://doi.org/10.1111/apha.12189.
Lumertz, F.S., Kestering-Ferreira, E., Orso, R., Creutzberg, K.C., Tractenberg, S.G., Stocchero, B.A., Viola, T.W., Grassi-Oliveira, R., 2022. Effects of early life stress on brain cytokines: A systematic review and meta-analysis of rodent studies. Neurosci. Biobehav. Rev. 139, 104746 https://doi.org/10.1016/j.neubiorev.2022.104746.
Majcher-Maslanka, I., Solarz, A., Chocyk, A., 2019. Maternal separation disturbs postnatal development of the medial prefrontal cortex and affects the number of neurons and glial cells in adolescent rats. Neuroscience 423, 131–147. https://doi.org/10.1016/j.neuroscience.2019.10.033.
Menard, C., Pfau, M.L., Hodes, G.E., Kana, V., Wang, V.X., Bouchard, S., Takahashi, A., Flanigan, M.E., Aleyasin, H., LeClair, K.B., Janssen, W.G., Labonte, B., Parise, E.M., Lorsch, Z.S., Golden, S.A., Heshmati, M., Tamminga, C., Turecki, G., Campbell, M., Fayad, Z.A., Tang, C.Y., Merad, M., Russo, S.J., 2017. Social stress induces neurovascular pathology promoting depression. Nat. Neurosci. 20, 1752–1760. https://doi.org/10.1038/s41593-017-0010-3.
Nicolas, S., McGovern, A.J., Hueston, C.M., O'Mahony, S.M., Cryan, J.F., O'Leary, O.F., Nolan, Y.M., 2022. Prior maternal separation stress alters the dendritic complexity of new hippocampal neurons and neuroinflammation in response to an inflammatory stressor in juvenile female rats. Brain Behav. Immun. 99, 327–338. https://doi.org/10.1016/j.bbi.2021.10.016.
Nie, X., Kitaoka, S., Tanaka, K., Segi-Nishida, E., Imoto, Y., Ogawa, A., Nakano, F., Tomohiro, A., Nakayama, K., Taniguchi, M., Mimori-Kiyosue, Y., Kakizuka, A., Narumiya, S., Furuyashiki, T., 2018. The innate immune receptors TLR2/4 mediate repeated social defeat stress-induced social avoidance through prefrontal microglial activation. Neuron 99 (464–479), e467.
Nikodemova, M., Kimyon, R.S., De, I., Small, A.L., Collier, L.S., Watters, J.J., 2015. Microglial numbers attain adult levels after undergoing a rapid decrease in cell number in the third postnatal week. J. Neuroimmunol. 278, 280–288. https://doi.org/10.1016/j.jneuroim.2014.11.018.
Ortega, A., Jadeja, V., Zhou, H., 2011. Postnatal development of lipopolysaccharide-induced inflammatory response in the brain. Inflamm. Res. 60, 175–185. https://doi.org/10.1007/s00011-010-0252-y.

Parker, K.J., Buckmaster, C.L., Hyde, S.A., Schatzberg, A.F., Lyons, D.M., 2019. Nonlinear relationship between early life stress exposure and subsequent resilience in monkeys. Sci. Rep. 9, 16232. https://doi.org/10.1038/s41598-019-52810-5.
Paxinos, G., Watson, C., 1998. The Rat Brain in Stereotaxic Coordinates. Academic Press.
Peng, X., Luo, Z., He, S., Zhang, L., Li, Y., 2021. Blood-brain barrier disruption by lipopolysaccharide and sepsis-associated encephalopathy. Front. Cell. Infect. Microbiol. 11, 768108 https://doi.org/10.3389/fcimb.2021.768108.
Posillico, C.K., Garcia-Hernandez, R.E., Tronson, N.C., 2021. Sex differences and similarities in the neuroimmune response to central administration of poly I:C. J Neuroinflammation 18, 193. https://doi.org/10.1186/s12974-021-02235-7.
Qin, X., He, Y., Wang, N., Zou, J.X., Zhang, Y.M., Cao, J.L., Pan, B.X., Zhang, W.H., 2019. Moderate maternal separation mitigates the altered synaptic transmission and neuronal activation in amygdala by chronic stress in adult mice. Mol Brain 12, 111. https://doi.org/10.1186/s13041-019-0534-4.
Ramirez, S.H., Potula, R., Fan, S.S., Eidem, T., Papugani, A., Reichenbach, N., Dykstra, H., Weksler, B.B., Romero, I.A., Couraud, P.O., Persidsky, Y., 2009. Methamphetamine disrupts blood-brain barrier function by induction of oxidative stress in brain endothelial cells. J Cerebr Blood F Met 29, 1933–1945. https://doi.org/10.1038/jcbfm.2009.112.
Reincke, S.A., Hanganu-Opatz, I.L., 2017. Early-life stress impairs recognition memory and perturbs the functional maturation of prefrontal-hippocampal-perirhinal networks. Sci. Rep. 7, 42042. https://doi.org/10.1038/srep42042.
Saavedra, L.M., Fenton Navarro, B., Torner, L., 2017. Early life stress activates glial cells in the hippocampus but attenuates cytokine secretion in response to an immune challenge in rat pups. NeuroImmunoModulation 24, 242–255. https://doi.org/10.1159/000485383.
Salvador, E., Shityakov, S., Forster, C., 2014. Glucocorticoids and endothelial cell barrier function. Cell Tissue Res. 355, 597–605. https://doi.org/10.1007/s00441-013-1762-z.
Santha, P., Veszelka, S., Hoyk, Z., Meszaros, M., Walter, F.R., Toth, A.E., Kiss, L., Kincses, A., Olah, Z., Seprenyi, G., Rakhely, G., Der, A., Pakaski, M., Kalman, J., Kittel, A., Deli, M.A., 2015. Restraint stress-induced morphological changes at the blood-brain barrier in adult rats. Front. Mol. Neurosci. 8, 88. https://doi.org/10.3389/fnmol.2015.00088.
Schwarz, J.M., Bilbo, S.D., 2012. Sex, glia, and development: Interactions in health and disease. Horm. Behav. 62, 243–253. https://doi.org/10.1016/j.yhbeh.2012.02.018.
Schwarz, J.M., Sholar, P.W., Bilbo, S.D., 2012. Sex differences in microglial colonization of the developing rat brain. J. Neurochem. 120, 948–963. https://doi.org/10.1111/j.1471-4159.2011.07630.x.
Selemon, L.D., 2013. A role for synaptic plasticity in the adolescent development of executive function. Transl. Psychiatry 3, e238.
Singh, A.K., Jiang, Y., 2004. How does peripheral lipopolysaccharide induce gene expression in the brain of rats? Toxicology 201, 197–207. https://doi.org/10.1016/j.tox.2004.04.015.
Solarz, A., Majcher-Maslanka, I., Chocyk, A., 2021a. Effects of early-life stress and sex on blood-brain barrier permeability and integrity in juvenile and adult rats. Dev. Neurobiol. 81, 861–876. https://doi.org/10.1002/dneu.22846.
Solarz, A., Majcher-Maslanka, I., Kryst, J., Chocyk, A., 2021b. A search for biomarkers of early-life stress-related psychopathology: Focus on 70-kDa heat shock proteins. Neuroscience 463, 238–253. https://doi.org/10.1016/j.neuroscience.2021.02.026.
Stolp, H.B., Dziegielewska, K.M., 2009. Review: Role of developmental inflammation and blood-brain barrier dysfunction in neurodevelopmental and neurodegenerative diseases. Neuropathol. Appl. Neurobiol. 35, 132–146. https://doi.org/10.1111/j.1365-2990.2008.01005.x.
Sun, H.X., Hu, H.L., Liu, C.J., Sun, N.N., Duan, C.H., 2021. Methods used for the measurement of blood-brain barrier integrity. Metab. Brain Dis. 36, 723–735. https://doi.org/10.1007/s11011-021-00694-8.
Tchessalova, D., Tronson, N.C., 2020. Enduring and sex-specific changes in hippocampal gene expression after a subchronic immune challenge. Neuroscience 428, 76–89. https://doi.org/10.1016/j.neuroscience.2019.12.019.
Varatharaj, A., Galea, I., 2017. The blood-brain barrier in systemic inflammation. Brain Behav. Immun. 60, 1–12. https://doi.org/10.1016/j.bbi.2016.03.010.
Vetulani, J., 2013. Early maternal separation: A rodent model of depression and a prevailing human condition. Pharmacol. Rep. 65, 1451–1461. https://doi.org/10.1016/s1734-1140(13)71505-6.
Villa, A., Gelosa, P., Castiglioni, L., Cimino, M., Rizzi, N., Pepe, G., Lolli, F., Marcello, E., Sironi, L., Vegeto, E., Maggi, A., 2018. Sex-specific features of microglia from adult mice. Cell Rep 23, 3501–3511. https://doi.org/10.1016/j.celrep.2018.05.048.
Walker 2nd, W.H., Bumgarner, J.R., Nelson, R.J., Courtney DeVries, A., 2020. Transcardial perfusion is not required to accurately measure cytokines within the brain. J. Neurosci. Methods 334, 108601. https://doi.org/10.1016/j.jneumeth.2020.108601.
Xu, G., Li, Y., Ma, C., Wang, C., Sun, Z., Shen, Y., Liu, L., Li, S., Zhang, X., Cong, B., 2019. Restraint stress induced hyperpermeability and damage of the blood-brain barrier in the amygdala of adult rats. Front. Mol. Neurosci. 12, 32. https://doi.org/10.3389/fnmol.2019.00032.
Yen, L.F., Wei, V.C., Kuo, E.Y., Lai, T.W., 2013. Distinct Patterns of Cerebral Extravasation by Evans Blue and Sodium Fluorescein in Rats. Plos One 8,ARTN e685951371/journal.pone.0068595.
Zhang, K., Lin, W., Zhang, J., Zhao, Y., Wang, X., Zhao, M., 2020. Effect of toll-like receptor 4 on depressive-like behaviors induced by chronic social defeat stress. Brain Behav. 10, e01525.
Zhou, T., Zhao, L., Zhan, R., He, Q., Tong, Y., Tian, X., Wang, H., Zhang, T., Fu, Y., Sun, Y., Xu, F., Guo, X., Fan, D., Han, H., Chui, D., 2014. Blood-brain barrier dysfunction in mice induced by lipopolysaccharide is attenuated by dapsone. Biochem. Biophys. Res. Commun. 453, 419–424. https://doi.org/10.1016/j.bbrc.2014.09.093.

Supplementary Table 1. Results of a three-way ANOVA investigating the effects of sex, lipopolysaccharide (LPS) treatment and rearing conditions (RC) and their interactions on circulating CORT and proinflammatory cytokines levels in juvenile and adult rats

PND	Serum level	Source of variation	$F_{1,20}$	p
22	CORT	SEX	16.42	< **0.001**
		LPS	5.89	**0.020**
		RC	2.97	0.093
		SEX_xLPS	4.58	**0.039**
		SEX_xRC	13.96	< **0.001**
		LPS_xRC	2.87	0.098
		SEX_xRC_xLPS	4.38	**0.043**
	IL-1β	SEX	3.30	0.077
		LPS	29.17	< **0.001**
		RC	3.37	0.074
		SEX_xLPS	10.63	**0.002**
		SEX_xRC	0.78	0.382
		LPS_xRC	6.93	**0.012**
		SEX_xRC_xLPS	0.01	0.906
	TNFα	SEX	0.73	0.399
		LPS	21.58	< **0.001**
		RC	0.09	0.764
		SEX_xLPS	1.15	0.290
		SEX_xRC	0.01	0.935
		LPS_xRC	0.04	0.848
		SEX_xRC_xLPS	3.19	0.081
70	CORT	SEX	0.48	0.492
		LPS	31.09	< **0.001**
		RC	2.53	0.120
		SEX_xLPS	0.15	0.702
		SEX_xRC	0.17	0.685
		LPS_xRC	0.00	0.991
		SEX_xRC_xLPS	0.47	0.496
	IL-1β	SEX	0.23	0.635
		LPS	57.61	< **0.001**
		RC	0.16	0.693
		SEX_xLPS	0.36	0.553
		SEX_xRC	2.50	0.122
		LPS_xRC	0.03	0.853
		SEX_xRC_xLPS	4.42	**0.042**

Supp. Tab. 1. continued

PND	Serum level	Source of variation	$F_{1,20}$	p
70	TNFα	SEX	0.29	0.600
		LPS	151.42	< **0.001**
		RC	4.91	**0.032**
		SEX_xLPS	2.63	0.112
		SEX_xRC	3.03	0.089
		LPS_xRC	1.14	0.293
		SEX_xRC_xLPS	0.28	0.597

Statistically significant effects are given in bold.

Supplementary Table 2. Results of a two-way ANOVA investigating the effects of lipopolysaccharide (LPS) treatment and rearing conditions (RC) and their interactions on circulating CORT and IL-1β levels

			Females		Males	
PND	Serum level	Source of variation	$F_{1,20}$	*p*	$F_{1,20}$	*p*
22	CORT	RC	2.91	0.104	11.44	**0.003**
		LPS	0.06	0.811	8.00	**0.010**
		RC_xLPS	10.28	**0.004**	0.06	0.807
70	IL-1β	RC	1.19	0.289	9.71	**0.005**
		LPS	20.38	< **0.001**	119.09	< **0.001**
		RC_xLPS	1.59	0.222	10.24	**0.004**

Statistically significant effects are given in bold.

Supplementary Table 3. Results of a three-way ANOVA investigating the effects of sex, lipopolysaccharide (LPS) treatment and rearing conditions (RC) and their interactions on the content of extravasated NaF in the mPFC and HP of juvenile and adult rats

Source of variation	PND							
	22				70			
	mPFC		HP		mPFC		HP	
	$F_{1,40}$	p	$F_{1,40}$	p	$F_{1,40}$	p	$F_{1,40}$	p
SEX	90.01	< **0.001**	91.13	< **0.001**	0.13	0.722	0.23	0.631
LPS	51.03	< **0.001**	28.04	< **0.001**	0.40	0.529	2.59	0.112
RC	6.75	**0.013**	4.82	**0.034**	0.00	0.948	4.22	**0.047**
SEX_xLPS	3.56	0.066	5.66	**0.022**	4.35	**0.043**	1.14	0.292
SEX_xRC	1.90	0.176	2.55	0.118	4.84	**0.034**	5.56	**0.023**
LPS_xRC	2.84	0.100	1.59	0.214	2.76	0.104	7.40	**0.010**
SEX_xRC_xLPS	0.01	0.935	0.72	0.403	0.36	0.550	2.14	0.155

Statistically significant effects are given in bold.

Supplementary Table 4. Results of a three-way ANOVA investigating the effects of sex, lipopolysaccharide (LPS) treatment and rearing conditions (RC) and their interactions on mRNA expression of TJ proteins and inflammatory response markers in the mPFC and HP of juvenile and adult rats

Gene	Source of variation	PND							
		22				70			
		mPFC		HP		mPFC		HP	
		$F_{1,40}$	p	$F_{1,40}$	p	$F_{1,40}$	p	$F_{1,40}$	p
Cld5	SEX	64.53	< **0.001**	4.56	**0.039**	82.97	< **0.001**	26.82	< **0.001**
	LPS	26.04	< **0.001**	22.28	< **0.001**	32.34	< **0.001**	27.89	< **0.001**
	RC	3.06	0.088	2.87	0.098	0.74	0.396	9.04	**0.005**
	SEXxLPS	1.96	0.169	3.44	0.071	14.60	< **0.001**	0.40	0.533
	SEXxRC	1.14	0.292	0.68	0.415	24.96	< **0.001**	0.03	0.863
	LPSxRC	7.15	**0.011**	2.14	0.151	3.93	0.054	4.30	**0.045**
	SEXxRCxLPS	0.59	0.445	2.10	0.155	9.88	**0.003**	2.99	0.092
Ocln	SEX	10.21	**0.003**	18.45	< **0.001**	607.14	< **0.001**	36.95	< **0.001**
	LPS	27.24	< **0.001**	27.18	< **0.001**	17.27	< **0.001**	19.98	< **0.001**
	RC	3.83	0.057	0.10	0.324	0.08	0.787	4.45	**0.041**
	SEXxLPS	2.70	0.108	1.12	0.297	9.08	**0.004**	1.79	0.188
	SEXxRC	4.07	0.050	0.30	0.585	11.05	**0.002**	0.65	0.425
	LPSxRC	2.28	0.139	1.11	0.297	0.05	0.817	7.29	**0.010**
	SEXxRCxLPS	4.31	**0.044**	1.43	0.238	8.51	**0.006**	0.93	0.342
Icam1	SEX	271.65	< **0.001**	44.59	< **0.001**	3.32	0.076	26.82	< **0.001**
	LPS	0.14	0.708	21.11	< **0.001**	100.88	< **0.001**	58.67	< **0.001**
	RC	20.49	< **0.001**	1.00	0.321	2.69	0.109	3.52	0.068
	SEXxLPS	0.09	0.767	0.05	0.817	0.02	0.877	2.39	0.130
	SEXxRC	0.82	0.370	2.53	0.120	7.19	**0.011**	2.43	0.151
	LPSxRC	12.20	**0.001**	9.72	**0.003**	0.75	0.390	1.78	0.190
	SEXxRCxLPS	49.87	< **0.001**	11.14	**0.002**	13.29	< **0.001**	0.93	0.340
Aif1	SEX	1.00	0.322	0.05	0.817	0.22	0.642	68.09	< **0.001**
	LPS	15.66	< **0.001**	40.09	< **0.001**	138.09	< **0.001**	45.21	< **0.001**
	RC	2.84	0.100	8.01	**0.007**	1.34	0.253	45.02	< **0.001**
	SEXxLPS	1.42	0.240	2.13	0.152	0.62	0.436	22.52	< **0.001**
	SEXxRC	3.14	0.084	3.22	0.080	0.76	0.389	53.73	< **0.001**
	LPSxRC	5.81	**0.021**	0.87	0.356	10.85	**0.002**	19.26	< **0.001**
	SEXxRCxLPS	3.97	0.053	4.05	0.051	1.27	0.267	3.93	0.054
Itgam	SEX	13.28	< **0.001**	8.09	**0.007**	2.21	0.145	0.86	0.358
	LPS	27.51	< **0.001**	68.53	< **0.001**	194.49	< **0.001**	218.63	< **0.001**
	RC	0.572	0.454	0.67	0.419	5.33	**0.026**	0.14	0.710
	SEXxLPS	9.81	**0.003**	5.35	**0.026**	0.98	0.324	0.28	0.601
	SEXxRC	2.27	0.140	8.77	**0.005**	1.14	0.293	0.016	0.900
	LPSxRC	0.06	0.800	0.12	0.730	6.18	**0.017**	0.036	0.852
	SEXxRCxLPS	1.74	0.194	10.62	**0.002**	1.04	0.313	0.02	0.887

Supp. Tab. 4. continued

Gene	Source of variation	PND 22 mPFC $F_{1,40}$	PND 22 mPFC p	PND 22 HP $F_{1,40}$	PND 22 HP p	PND 70 mPFC $F_{1,40}$	PND 70 mPFC p	PND 70 HP $F_{1,40}$	PND 70 HP p
Tlr4	SEX	102.59	< **0.001**	24.62	< **0.001**	14.48	< **0.001**	0.09	0.770
	LPS	4.21	**0.047**	36.43	< **0.001**	13.48	< **0.001**	14.43	< **0.001**
	RC	1.60	0.213	47.94	< **0.001**	2.11	0.154	5.48	**0.024**
	SEXxLPS	0.17	0.682	16.50	< **0.001**	2.75	0.105	0.70	0.407
	SEXxRC	9.36	**0.004**	73.55	< **0.001**	0.26	0.611	28.11	< **0.001**
	LPSxRC	3.07	0.088	11.15	**0.002**	0.04	0.843	0.41	0.523
	SEXxRCxLPS	17.77	< **0.001**	7.54	**0.009**	16.95	< **0.001**	10.84	**0.002**
*Il-1*β	SEX	8.35	**0.006**	7.01	**0.012**	1.08	0.305	2.17	0.149
	LPS	19.27	< **0.001**	17.11	< **0.001**	75.14	< **0.001**	48.76	< **0.001**
	RC	0.02	0.879	0.04	0.834	8.41	**0.006**	0.34	0.564
	SEXxLPS	6.63	**0.014**	6.03	**0.018**	2.65	0.112	2.41	0.128
	SEXxRC	1.17	0.285	1.88	0.178	7.09	**0.011**	7.67	**0.008**
	LPSxRC	0.01	0.906	0.01	0.907	8.51	**0.006**	0.63	0.430
	SEXxRCxLPS	0.59	0.447	2.00	0.164	5.09	**0.030**	6.17	**0.017**
*Tnf*α	SEX	8.94	**0.005**	2.22	0.143	0.24	0.629	36.03	< **0.001**
	LPS	10.21	**0.003**	11.50	**0.002**	7.01	**0.012**	33.06	< **0.001**
	RC	8.07	**0.007**	0.08	0.781	0.46	0.502	17.35	< **0.001**
	SEXxLPS	0.04	0.847	0.04	0.835	0.38	0.543	12.03	**0.001**
	SEXxRC	0.77	0.384	1.77	0.191	1.76	0.193	33.16	< **0.001**
	LPSxRC	0.02	0.879	0.00	0.975	1.80	0.187	6.93	**0.012**
	SEXxRCxLPS	1.32	0.257	3.68	0.062	1.74	0.194	11.96	**0.001**

Statistically significant effects are given in bold.

Supplementary Table 5. Results of a two-way ANOVA investigating the effects of lipopolysaccharide (LPS) treatment and rearing conditions (RC) and their interactions on mRNA expression of TJ proteins and inflammatory response markers in the mPFC and HP of juvenile and adult rats

PND	Gene	Source of variation	mPFC				HP			
			Female		Male		Female		Male	
			$F_{1,20}$	p	$F_{1,20}$	p	$F_{1,20}$	p	$F_{1,20}$	p
22	*Ocln*	RC	0.01	0.934	4.54	**0.046**	-	-	-	-
		LPS	24.39	< **0.001**	13.55	**0.001**	-	-	-	-
		RC_xLPS	0.61	0.443	3.70	0.069	-	-	-	-
	Icam1	RC	8.18	**0.010**	33.27	< **0.001**	0.13	0.718	4.67	**0.043**
		LPS	0.01	0.967	1.16	0.294	9.11	**0.007**	13.18	**0.002**
		RC_xLPS	30.89	< **0.001**	32.32	< **0.001**	0.012	0.892	28.88	< **0.001**
	Itgam	RC	-	-	-	-	6.94	**0.016**	2.37	0.139
		LPS	-	-	-	-	54.59	< **0.001**	18.30	< **0.001**
		RC_xLPS	-	-	-	-	6.33	**0.021**	4.36	**0.049**
	Tlr4	RC	5.84	**0.025**	4.04	0.058	111.62	< **0.001**	7.33	**0.014**
		LPS	0.84	0.370	7.61	**0.012**	47.36	< **0.001**	0.54	0.469
		RC_xLPS	11.12	**0.003**	7.61	**0.012**	17.21	< **0.001**	0.30	0.592
70	*Cld5*	RC	47.42	< **0.001**	5.23	**0.033**	-	-	-	-
		LPS	4.76	**0.041**	27.53	< **0.001**	-	-	-	-
		RC_xLPS	36.36	< **0.001**	0.41	0.528	-	-	-	-
	Ocln	RC	1.65	0.217	2.49	0.129	-	-	-	-
		LPS	20.57	< **0.001**	13.78	**0.001**	-	-	-	-
		RC_xLPS	0.86	0.366	1.93	0.1780	-	-	-	-
	Icam1	RC	7.27	**0.014**	0.76	0.394	-	-	-	-
		LPS	38.05	< **0.001**	72.75	< **0.001**	-	-	-	-
		RC_xLPS	7.93	**0.011**	5.39	**0.031**	-	-	-	-
	Tlr4	RC	3.41	0.079	0.31	0.584	25.89	< **0.001**	5.03	**0.036**
		LPS	3.58	0.073	9.91	**0.005**	3.89	0.063	12.32	**0.002**
		RC_xLPS	16.43	< **0.001**	5.35	**0.031**	6.87	**0.016**	12.32	0.059
	Il-1β	RC	8.75	**0.008**	0.12	0.735	4.44	**0.048**	3.26	0.086
		LPS	29.95	< **0.001**	107.81	< **0.001**	28.80	< **0.001**	20.05	< **0.001**
		RC_xLPS	7.56	**0.012**	0.96	0.338	4.26	0.052	1.94	0.179
	Tnfα	RC	-	-	-	-	27.33	< **0.001**	4.19	**0.020**
		LPS	-	-	-	-	23.56	< **0.001**	9.47	**0.017**
		RC_xLPS	-	-	-	-	10.29	**0.004**	0.81	0.204

Statistically significant effects are given in bold.

NEUROSCIENCE
RESEARCH ARTICLE
A. Solarz et al. / Neuroscience 463 (2021) 238–253

A Search for Biomarkers of Early-life Stress-related Psychopathology: Focus on 70-kDa Heat Shock Proteins

Anna Solarz, Iwona Majcher-Maślanka, Joanna Kryst and Agnieszka Chocyk *

Maj Institute of Pharmacology, Polish Academy of Sciences, Department of Pharmacology, Laboratory of Pharmacology and Brain Biostructure, Smętna Street 12, 31-343 Kraków, Poland

Abstract—Clinical studies clearly indicate that early-life stress (ELS) may cause physical and mental health problems later in life. Therefore, the identification of universal biomarkers of ELS-related diseases is very important. The 70-kDa heat shock proteins (HSP70s), specifically HSPA5 and HSPA1B, have been recently shown to be potentially associated with occurrence of anxiety, mood disorders, and schizophrenia; thus, we hypothesized that HSP70s are potential candidate biomarkers of ELS-induced psychopathologies. A maternal separation (MS) procedure in rats was used to model ELS, and the expression of HSPA5 and HSPA1B was investigated in the blood, medial prefrontal cortex (mPFC), and hippocampus of juvenile, preadolescent, and adult animals. We also studied the effects of MS on the long-term potentiation (LTP) and behavioral phenotypes of adult rats. We found that MS enhanced the expression of HSPA1B mRNA in the blood and mPFC of juvenile and preadolescent rats. This increase was accompanied by an increase in the HSPA1A/1B protein levels in the mPFC and hippocampus of juvenile rats that persisted in the mPFC until adulthood. MS juvenile and adult rats showed enhanced HSPA5 mRNA expression in the blood and increased HSPA5 protein expression in the mPFC (juveniles) and hippocampus (adults). Concurrently, MS adult rats exhibited aberrations in LTP in the mPFC and hippocampus and a less anxious behavioral phenotype. These results indicate that MS may produce enduring overexpression of HSPA1B and HSPA5 in the brain and blood. Therefore, both HSP70 family members may be potential candidate peripheral and brain biomarkers of ELS-induced changes in brain functioning.

Key words: anxiety, early-life stress, HSPA1B, HSPA5, long-term potentiation, mood disorders.

INTRODUCTION

Epidemiological and clinical studies clearly indicate that early-life stress (ELS) may have a profound and long-lasting impact on health outcomes. ELS increases the risk of occurrence of physical health problems, such as cardiovascular diseases and metabolic syndrome (Maniam et al., 2014; Murphy et al., 2017). ELS is also associated with appearance of mental health problems, such as anxiety, mood disorders, addiction, and dementia (Green et al., 2010; Donley et al., 2018; Hoeijmakers et al., 2018). Consequently, ELS-related disorders generate considerable social and economic costs. However, not all individuals with a history of ELS develop health problems (Teicher and Khan, 2019). Therefore, it may be very important to identify the common and consistent biomarkers of ELS-related diseases to help assess the risk of these diseases in individuals with early-life trauma as early as possible.

Based on the literature within the past decade, we hypothesized that a family of 70-kDa heat shock proteins (HSP70s) could be candidate biomarkers of ELS-related diseases. HSP70s are evolutionary conserved proteins encoded by 17 genes in humans (Brocchieri et al., 2008). These proteins are present in most cells and tissues. The most studied members of HSP70s include stress-inducible HSPA1A (also known as HSP70-1) and HSPA1B (also known as HSP70-2) that are almost identical proteins differing by two amino acids (Daugaard et al., 2007; Kampinga et al., 2009). These proteins are mainly located in the cytosol and nucleus. Initially, the expression of these proteins was considered to be enhanced after heat shock; however, it is now well known that HSPA1A and HSPA1B are induced in response to a number of various cellular stressors related to the accumulation of unfolded/misfolded proteins, hypoxia, hyperglycemia, oxidative stress, and imbalance in calcium levels (Daugaard et al., 2007; Karunanithi and Brown, 2015). HSPA5 (also known as binding

*Corresponding author.
E-mail address: chocyk@if-pan.krakow.pl (A. Chocyk).
Abbreviations: AFR, animal facility rearing; ELS, early-life stress; FST, forced swimming test; HP, hippocampus; HSP70s, 70-kDa heat shock proteins; HSPs, heat shock proteins; LTP, long-term potentiation; MDD, major depression disorder; mPFC, medial prefrontal cortex; MS, maternal separation; PND, postnatal day.

https://doi.org/10.1016/j.neuroscience.2021.02.026
0306-4522/

immunoglobulin protein (BiP) or 78-kDa glucose-regulated protein (GRP78)) is another interesting member of the HSP70s family. HSPA5 is constitutively expressed in the endoplasmic reticulum (ER). However, the expression of HSPA5 can be substantially increased under ER stress and in calcium homeostasis imbalance (Daugaard et al., 2007; Wang et al., 2017). HSPA8 (also known as HSPC70) is a typical representative of HSP70s constitutively expressed in the cytosol and nucleus (Stricher et al., 2013).

The best known role of HSP70s is acting as molecular chaperones through engagement in (i) protein folding and refolding, (ii) the degradation of unstable and misfolded proteins, and (iii) the transport of proteins between cellular compartments (Daugaard et al., 2007). HSP70s are very important regulators of cell survival and apoptosis (Arya et al., 2007). HSPA5 is one of the key player in the regulation of ER stress and unfolded protein response (UPR), which are essential cellular repair processes with strong impact of the cell death/survival decisions (Arya et al., 2007; Wang et al., 2017).

The protective effects of HSP70s in myocardial and brain ischemia and neurodegeneration have been clearly demonstrated (Tsuchiya et al., 2003; Leak, 2014; Santos-Junior et al., 2018; Song et al., 2020). Increased expression of HSP70s is commonly observed in patients with heart failure and neurodegenerative disorders (Leak, 2014; Santos-Junior et al., 2018). In contrast, decreased levels of HSP70s in the liver were detected in the animal models of diabetes and insulin resistance (Kavanagh et al., 2011; Amawi et al., 2019).

Certain HSP70s family members, such as HSPA5 and HSPA8, are localized not only inside the cells but can also be detected in the extracellular space (Tytell, 2005; Casas, 2017). Moreover, active release of these HSPA8 by the glia and uptake by the axons has been demonstrated and is associated with cytoprotective and anti-apoptotic effects of HSP70s in the nervous system (for review, see: Tytell, 2005). HSP70s, as the regulators of cell survival or death and stabilizers of cytoskeletal elements, play a crucial role in cell growth, apoptosis, and migration during neurodevelopment (Miller and Fort, 2018). HSP70s are also engaged in synaptic plasticity and memory processes (Ammon-Treiber et al., 2008; Porto and Alvares, 2019). Inducible HSP70s are present in the synapses, and synaptic activity and learning tasks augment their expression (Igaz et al., 2004; Porto et al., 2018).

Recently, it has been proposed that ER stress and UPR can be associated with pathophysiology of mood disorders (Kakiuchiet al., 2005; Le-Niculescu et al., 2011; Yang et al., 2013; Nevell et al., 2014; Yoshino and Dwivedi, 2020). Increased expression of UPR-related genes or proteins, including HSPA5, was observed in the medial prefrontal cortex (mPFC) and temporal cortex of subjects with major depression disorder (MDD) who died from suicide and in leukocytes from patients with MDD and posttraumatic stress disorder (Bown et al., 2000; Nevell et al., 2014; Yoshino and Dwivedi, 2020). Moreover, functional polymorphisms of HSPA5 were shown to have possible association with bipolar disorder in a Japanese population (Kakiuchiet al., 2005).

Recent data have also shown that HSPA1B polymorphism may be associated with schizophrenia and suicidal behavior of schizophrenic patients (Pae et al., 2005; Bosnjak et al., 2020; Kowalczyk et al., 2020). On the other hand, HSPA1B was identified as one of the candidate blood and brain biomarkers of anxiety disorders (Le-Niculescu et al., 2011; Yang et al., 2013).

Surprisingly, the expression of HSP70s has not been practically studied in animal models of ELS (Coccurello et al., 2014; Majcher-Maslanka et al., 2019a). These considerations and our experience in ELS modeling (Chocyk et al., 2013, 2014; Majcher-Maslanka et al., 2018, 2019a) prompted us to assess whether two representatives of HSP70s, HSPA5 and HSPA1B, are potential biomarkers of ELS-induced psychopathology. Initially, we investigated the developmental profiles of the expression of HSPA5 and HSPA1B mRNAs and proteins in the mPFC and hippocampus, which are the brain regions highly implicated in anxiety, mood disorders, and schizophrenia (McTeague et al., 2020). To the best of our knowledge, there are no data evaluating the developmental expression of these specific HSP70s family members in rodents. Then, we used a maternal separation (MS) procedure in rats from postnatal day (PND) 1 to 14 to model ELS and investigated the effects of ELS on HSPA5 and HSPA1B mRNA levels in the blood and HSPA5 and HSPA1B mRNA and protein expression in the mPFC and hippocampus of juvenile, preadolescent, and adult rats. We also evaluated the effect of MS on LTP in the mPFC and hippocampus of adult rats. The behavioral phenotype of adult rats was also assessed for depressive- and anxiety-like behavior and dysfunction of sensorimotor gating, that is typical for schizophrenia (Braff et al., 2001).

EXPERIMENTAL PROCEDURES

Animals

All experimental procedures were approved by the Local Ethics Committees for Animal Research in Krakow, Poland and met the requirements of the Directive 2010/63/EU of the European Parliament and of the Council of 22 September 2010 on the protection of animals used for scientific purposes. All efforts were made to minimize animal suffering.

Adult male and female Wistar rats were purchased from Charles River Laboratories (Sulzfeld, Germany). All animals were housed under controlled conditions with an artificial 12 h light/dark cycle (lights on from 07:00 to 19:00), 55% ± 10 humidity, and a temperature of 22 °C ± 2. Food and tap water were freely available. The rats were mated at the Maj Institute of Pharmacology, PAS, Krakow Animal Facility. The offspring of primiparous dams were used in this study. Before delivery, the dams were housed individually in standard plastic cages (38 × 24 × 19 cm). The day of birth was designated as PND 0. On PND 1, the litter size was standardized to eight pups per litter (four males and four females), and

the litters were assigned to one of the following rearing conditions: MS or animal facility rearing (AFR), i.e., control condition.

Maternal separation procedure

The MS procedure was performed as described previously by Majcher-Maślanka et al. (2018, 2019a, 2019b) and Chocyk et al. (2013), Chocyk et al. (2015). Briefly, on PNDs 1–14, the dams and pups were removed from the maternity cages for 3 h (09.00–12.00) daily. The mothers were placed individually in the holding cages (38 × 24 × 19 cm), while each litter was placed in a plastic container (22 × 16 × 10 cm) lined with fresh bedding material, and the containers were moved to an adjacent room and placed in an incubator that was set at a constant temperature of 34 °C mimicking the nest temperature. After the 3 h separation, the pups and dams were returned to the maternity cages. The AFR animals were left undisturbed with their mothers except during the weekly cage cleaning corresponding to a small amount of handling. The impact of the MS procedure on specific maternal and pup behaviors was described previously in detail by our group (Chocyk et al., 2013). Twenty-four hours after the last MS, i.e., on PND 15, a part of the animals was assigned to the experimental groups to investigate the effects of repeated MS in juveniles. The rest of the animals were weaned on PND 22, sexed, and randomly distributed between subsequent experimental groups to investigate the long-term effects of repeated MS. These rats were housed under the controlled conditions (as described above) in standard plastic cages (57 × 33 × 20 cm) in the same-sex groups of five unrelated subjects according to the same treatment protocol until the preadolescence period (PND 26) or adulthood (PND 70).

Experimental groups

A total of 95 AFR and 94 MS male rats originating from 24 AFR and 24 MS litters were used in the study. Female offspring was used in other scientific projects. In the case of biochemical experiments, the final experimental groups included the animals that originated from different litters and were unrelated (n = 5–8). In the case of behavioral experiments, maximum two subjects from the same litter were used (n = 9–12). The separate groups of animals of each age (PND 15, PND 26, and PND 70) were analyzed for i) gene expression in the brain and blood and ii) protein expression. Additionally, the separate groups of adult animals were used for electrophysiological measurements and behavioral tests.

RT qPCR

The RT qPCR procedure was performed as described previously by Majcher-Maślanka et al. (2018, 2019b). Briefly, on PND 15, PND 26, or PND70, the animals were sacrificed by decapitation (6 AFR and 6 MS rats in each age group). Trunk blood was collected and the brain was immediately removed from the skull. The mPFC (including the cingulate cortex 1, prelimbic cortex, and infralimbic cortex regions) was dissected from 1 mm thick coronal sections using a rodent brain matrix (Ted Pella Inc., CA, USA); whereas, the hippocampus was dissected freehand. After dissection, the brain tissue was quickly frozen in liquid nitrogen and stored at −80 °C for later use. Total RNA from the whole blood and brain tissue was extracted using the Mouse RiboPure Blood RNA Isolation Kit (Invitrogen) and RNAeasy Mini Kit (Qiagen), respectively. The total RNA concentration was measured using an Eon absorbance microplate reader and Gen 5 software (BioTek, Winooski, VT, USA). The RNA was reverse transcribed using a High-Capacity cDNA Reverse Transcription Kit (Applied Biosystems). qPCR was performed using the QuantStudio 12 K Flex (Applied Biosystems). Gene-specific primers and probes of the TaqMan® Gene Expression Assays (Applied Biosystems) were used according to the manufacturer's recommendation, including Rn02532795_s1 for Hspa1b, Rn01435769_g1 for Hspa5, and Rn99999916_s1 for Gapdh (glyceraldehyde-3-phosphate dehydrogenase). Amplification using TaqMan Gene Expression PCR Master Mix (Applied Biosystems) was performed under the following conditions: 50 °C for 2 min and 95 °C for 10 min followed by 40 cycles at 95 °C for 15 s and 60 °C for 1 min. The threshold values of the cycles were calculated automatically (QuantStudio 12 K Flex Software, Applied Biosystems). The RNA abundance was calculated theoretically according to the following equation: abundance = $2^{-(\text{threshold cycle})}$. The results of each individual sample were normalized to Gapdh expression.

Western blot

Western blot was performed as described previously by Majcher-Maślanka et al. (2018, 2019b). Briefly, on PND 15, PND 26, or PND 70, the animals were sacrificed by decapitation (6 AFR and 6 MS rats in each age group), and the brain was rapidly removed from the skull. The mPFC (including the cingulate cortex 1, prelimbic cortex and infralimbic cortex regions) was dissected from 1 mm-thick coronal sections using a rodent brain matrix (Ted Pella, CA, USA), and the hippocampus was dissected freehand. After dissection, the brain tissue was quickly frozen in liquid nitrogen and stored at − 80 °C until further use. The tissue was homogenized (TissueLyser, Retsch, Germany) in ice-cold lysis buffer (PathScan® Sandwich ELISA Lysis Buffer, Cell Signaling). The homogenates were then centrifuged for 15 min at 15,000×g at 4 °C. The total protein concentration of the supernatants was determined using the bicinchoninic acid (BCA) method (Sigma-Aldrich, USA). Samples with equal protein concentrations were loaded into each lane, run on 10% sodium dodecyl sulfate–polyacrylamide gels in a Laemmli buffer system, and transferred onto a nitrocellulose membrane (Bio-Rad, USA). The blots were probed with diluted primary antibodies as follows: mouse anti-HSPA1B antibody (1:500, Sigma-Aldrich, SAB1403949), rabbit anti-BIP antibody (1:1000, Cell Signaling Technology, #3183), and mouse anti-β-actin (1:500, Sigma-Aldrich). Then, the blots were incubated with the appropriate (anti-mouse IgG or anti-rabbit IgG)

horseradish peroxidase-conjugated secondary antibodies (Roche Diagnostics, Basel, Switzerland), and the bands were visualized by enhanced chemiluminescence (Lumi-LightPlus Western Blotting Kit, Roche Diagnostics, Switzerland). The immunoblots were evaluated using a luminescent image analyzer (LAS-4000, Fujifilm, USA). The relative levels of immunoreactivity were quantified using the Image Gauge software (Fujifilm, USA). β-Actin immunoreactivity was not influenced by MS. Therefore, the ratio of the specific protein level to the actin level was calculated for each sample to normalize for small variations in loading and transfer.

Ex vivo electrophysiology

The electrophysiological procedure has been described previously by Majcher-Maslanka et al. (2018). The procedure was performed on adult rats that reached PND 70. A total of 14 AFR and 14 MS rats were tested in a counterbalanced alternating order. Rats were anesthetized with isoflurane (Aerrane, Baxter) and decapitated. The brain was rapidly removed and immersed in an ice-cold artificial cerebrospinal fluid (ACSF) of the following composition (in mM): 130 NaCl, 5 KCl, 2.5 $CaCl_2$, 1.3 $MgSO_4$, 1.25 NaH_2PO_4, 26 $NaHCO_3$, and 10 D-glucose; ACSF was bubbled with a mixture of 95% O_2 and 5% CO_2 (pH 7.4). A block of tissue containing the mPFC or hippocampus, according to the stereotaxic atlas of the rat brain (Paxinos and Watson, 1998), was dissected and cut into 420 μm thick sections along the coronal plane using a vibratome at 1 °C (VT 1000S, Leica, Germany). The sections were transferred into a recording chamber a fluid-gas interface type and superfused at 2 ml/min with warm (32 ± 0.5 °C) modified ACSF containing (in mM): 130 NaCl, 2 KCl, 2.5 $CaCl_2$, 1.3 $MgSO_4$, 1.25 NaH_2PO_4, 26 $NaHCO_3$, and 10 D-glucose. The recordings started 2–4 h after the sections were prepared. The field potentials were evoked using square-wave stimuli (duration 0.2 ms) applied through a constant current isolation unit (WPI, Germany) at 0.016 Hz in the mPFC and 0.033 Hz in the hippocampus via a bipolar concentric Pt-Ir electrode (FHC, USA). The electrode was placed in layer II/III or in the Schaffer collaterals for the recording in the mPFC and hippocampus, respectively. A recording micropipette filled with ACSF (resistance of approximately 2–4 MΩ) was placed in the cortical layer V of the mPFC or the CA1 area of the hippocampus. The responses were amplified (500×), filtered (0.1–500 Hz), and acquired at a 10 kHz sampling rate (EXT 10-C amplifier, NPI, Germany) using a Micro1401 interface and Signal 2 software (CED, Cambridge, UK).

After stabilization of the responses, stimulus/response (input–output) curves were determined individually for each section by applying square stimuli of increasing intensities (duration of 0.0003 s; range of 0–50 μA, step 5 μA; range of 50–100 μA, step 10 μA; applied at 15 s intervals). Then, the stimulation intensity was adjusted to evoke a response corresponding to 40% of the maximum amplitude, and the stimulus was applied in the subsequent LTP experiments. When the signals became stable over a baseline period of 15 min, LTP was induced in the mPFC with a sequence of five stimulus bursts (15 s apart). A single burst consisted of 5 individual square pulses (duration of 0.3 ms, applied at 100 Hz) that were repeated ten times (0.2 s apart). In the hippocampus, LTP was induced using a single high-frequency stimulation burst of 100 square pulses (duration of 0.2 ms, applied at 100 Hz). The recording then continued for additional 90 min. The response amplitude of the individual sections was normalized to the percent change versus the baseline values. The amount of LTP was determined by comparing the data of the baseline recording averaged over the last 15 min to the data of the posttetanic recording averaged over the last 15 min.

The light/dark exploration test

On PND 70, separate groups of 12 AFR and 10 MS rats were subjected to the light/dark exploration test. The light/dark exploration test was performed as described previously by Chocyk et al. (2013), Chocyk et al. (2015). Briefly, each experimental cage included an arena (45 × 45 × 45 cm) with a light compartment made of clear acrylic and a dark compartment made of black acrylic. The black compartment covered 33% of the total cage area, and the black dividing wall was equipped with a central tunnel gate (11 × 8.4 cm). The light compartment was brightly illuminated (100 lx), whereas the dark compartment received no light at all. The animals were kept in total darkness for 30 min prior to the testing, and the entire experiment was conducted with the room lights off. The animals were individually tested in single 10 min trials. The behavioral responses during the test session were recorded using Fear Conditioning software (TSE, Bad Homburg, Germany). Specifically, the number of transitions between the compartments, time spent in each compartment, and locomotor activity (the distance traveled) were measured.

Sucrose preference test

Sucrose preference was measured in a two-bottle choice paradigm as described previously by Chocyk et al. (2015). Briefly, 9 AFR and 10 MS adult rats at PND 70 were singly housed and habituated to drink water from two bottles for 5 days. Then, the water in one of the bottles was replaced by 1% sucrose solution for 2 days to avoid neophobia. The position of the bottles (sucrose left or right) was reversed every 8 h to prevent the development of place preference. After habituation, the rats were subjected to water deprivation for 16 h before performing the sucrose preference test. During the test, two bottles, one containing tap water and another containing 1% sucrose solution, were presented to each rat for 4 h (08.00-12.00). The positioning of the water and sucrose bottles (left or right) was balanced between the experimental groups. Sucrose preference was calculated as the percentage of sucrose intake versus total liquid intake (water + sucrose) over the 4 h test period.

Forced swimming test (FST)

A total of 12 AFR and 12 MS adult rats were used in the test. The rats were placed in cylinders (height: 40 cm,

diameter: 18 cm) containing 25 cm of water (25 °C). After 15 min exposure in the water, the animals were removed, dried, and returned to their home cages. Then, 24 h later, the rats were again placed in the water, and the total duration of immobility, climbing, and swimming was measured during a 5 min test (Porsolt et al., 1978). After the test, the locomotor activity of the rats was examined as described previously by Majcher-Maślanka et al. (2019a). Briefly, the locomotor activity of each animal was recorded for 30 min and analyzed using Opto-Varimex cages (43 × 44 cm) and Auto-Track software (Columbus Instruments, OH, USA).

Sensorimotor gating

The efficacy of sensorimotor gating was assessed using a prepulse-induced inhibition of the acoustic startle response (PPI), and startle reactivity was measured using a startle apparatus (SR-LAB, San Diego Instruments, San Diego, CA, USA) as described previously by (Bator et al., 2018). The startle apparatus included individual soundproof ventilated chambers containing a nonrestrictive plexiglas cylinder (inner diameter = 9 cm). A high-frequency loudspeaker inside each chamber produced a continuous background noise of 65 dB and various acoustic stimuli. Movement of the plexiglas cylinder caused by startle response of the animal was transduced into the analog signals by a piezoelectric unit attached to the platform. These signals were then digitized and saved on a computer. One hundred readings were taken at 1 ms intervals starting from the stimulus onset, and the average amplitude was used to determine the average amplitude of startle reflex. The amplitude of the startle response was measured during the 200 ms recording window.

After habituation (5 min, background white noise, 65 dB), two types of acoustic stimuli were presented to 12 AFR and 12 MS adult rats in a random order: an acoustic stimulus alone as a pulse [(P), duration 40 ms, intensity 120 dB] or an acoustic stimulus (P) preceded by an acoustic prepulse [(PP), duration 20 ms, intensities: 70, 75, 80, and 85 dB] applied 80 ms before the stimulus (P). During each experimental session, 20 trials of each type were presented with randomized interstimulus intervals from 5 to 20 s. The amplitudes were averaged separately for each animal and for both types of trials (stimulus alone, P; or stimulus preceded by a prepulse, PP). The degree of PPI was calculated as a percentage of inhibition (% PPI) as follows: ([(P-PP)/P] × 100). The final data are presented as % PPI for each prepulse intensity.

Statistical analysis

Statistical analysis was performed using the Statistica 10 package (StatSoft, Inc., OK, USA). Data were tested for normal distribution and homogeneity of variances using Shapiro-Wilk test and Levene's test, respectively. The majority of data followed normal distribution and had equal variances among groups. In these cases, statistical differences between two groups (AFR vs. MS) in the analysis of the gene and protein expression and the most of behavioral data were evaluated by Student's *t*-test. Developmental profile of the gene and protein expression was evaluated by two-way analysis of variance (ANOVA) with developmental time and brain region as the independent variables and Bonferroni post hoc test. The electrophysiological data were analyzed by mixed-design ANOVA with rearing conditions as a between-subject factor and probe (conditions pre- and posttheta burst stimulation; data averaged over the last 15 min of baseline recording and over the last 15 min after the tetanization recording) as a within-subject factor. The data of PPI were evaluated by mixed-design ANOVA with rearing conditions as a between-subject factor and prepulse intensity as a within-subject factor. In the case of data which did not show normal distribution and homogeneity of variances, statistical differences between two groups were analyzed by Mann–Whitney *U* test. A fixed effects statistical model was used in the analysis. *P* values < 0.05 were considered significantly different. The data in the text, tables and in the line charts are presented as the group mean and standard deviation (SD).

RESULTS

Developmental profiles of HSPA1B and HSPA5 expression in the mPFC and hippocampus

HSPA1B and HSPA1A genes and proteins are highly similar (Milner and Campbell, 1990; Kampinga et al., 2009). However, these two genes have certain differences in the promoter sequences and completely divergent sequences in 3′-untranslated regions, which enable to produce a specific tools for studying mRNA expression of each gene (Milner and Campbell, 1990; Maugeri et al., 2010). By contrast, any specific antibodies designed to recognize these proteins cannot distinguish HSPA1B from HSPA1A in Western blot analysis of the tissue samples. Therefore, Western blots probed with a mouse anti-HSPA1B antibody (SAB1403949) used in our study probably detected the expression of both inducible HSP70s, HSPA1A and HSPA1B. Consequently, in the present study, the immunoreactivity of stress-induced HSP70s was termed HSPA1A/1B.

Statistical analysis of HSPA1B mRNA expression showed a significant main effect of developmental time ($p < 0.0001$) and brain region ($p < 0.0001$) and a significant effect of the interaction between these two factors ($p < 0.0001$) (Table 1, Fig. 1A). HSPA1B mRNA expression in the hippocampus at all developmental time points was higher than that in the mPFC ($p < 0.0001$ for each PND) (Fig. 1A). Juvenile (PND 15) and preadolescent (PND 26) rats showed higher levels of HSPA1B mRNA in the hippocampus than that in adults ($p < 0.0001$ for each PND) (Fig. 1A). However, an opposite profile of the changes was observed in the mPFC, i.e., HSPA1B mRNA expression was lower in juveniles ($p < 0.0001$) and preadolescents ($p < 0.0001$) compared to that in adults (Fig. 1A). Juvenile and preadolescent rats did not differ in HSPA1B mRNA levels in the hippocampus ($p = 1.00$) or mPFC ($p = 1.00$).

Table 1. Results of two-way ANOVA investigating the effects of developmental time and brain region on HSPA1B and HSPA5 expression in control rats

Parameter	Source of variation	F	p	Effect size: η^2
HSPA1B mRNA	Dev. Time	$F_{2,30} = 219.87$	**<0.0001**	0.23
	Brain area	$F_{1,30} = 959.04$	**<0.0001**	0.51
	Dev. time × brain area	$F_{2,30} = 225.01$	**<0.0001**	0.24
HSPA1A/1B protein	Dev. time	$F_{2,12} = 4.90$	**0.028**	0.27
	Brain area	$F_{1,12} = 10.33$	**0.007**	0.28
	Dev. time × brain area	$F_{2,12} = 2.05$	0.172	0.11
HSPA5 mRNA	Dev. time	$F_{2,30} = 189.14$	**<0.0001**	0.58
	Brain area	$F_{1,30} = 106.90$	**<0.0001**	0.16
	Dev. time × brain area	$F_{2,30} = 69.09$	**<0.0001**	0.21
HSPA5 protein	Dev. time	$F_{2,12} = 2.84$	0.098	0.30
	Brain area	$F_{1,12} = 0.43$	0.523	0.02
	Dev. time × brain area	$F_{2,12} = 0.36$	0.703	0.04

Statistically significant effects are given in bold. Abbreviations: Dev, developmental.

Analysis of the HSPA1A/1B protein expression revealed a significant main effect of developmental time ($p = 0.028$) and brain region ($p = 0.007$) (Table 1, Fig. 1B, Fig. S1A). There was no statistically significant effect of the interaction between time and brain region ($p = 0.172$). Adult rats had a higher level of HSPA1A/1B proteins than that in juvenile rats on PND 15 ($p = 0.046$) (Fig. 1B, Fig. S1A). HSPA1A/1B protein expression was generally higher in the hippocampus compared with that in the mPFC (Table 1, Fig. 1B, Fig. S1A).

Statistical evaluation of HSPA5 mRNA expression levels showed a significant main effect of developmental time ($p < 0.0001$) and brain region ($p < 0.0001$) and a significant effect of the interaction between these two factors ($p < 0.0001$) (Table 1, Fig. 1C). HSPA5 mRNA expression in juveniles and preadolescent rats was lower in the hippocampus than that in the mPFC ($p < 0.0001$ for both PND 15 and 26) (Fig. 1C). In contrast, HSPA5 mRNA level was higher in adult rats in the hippocampus than that in the mPFC ($p = 0.017$). A developmental increase in the level of HSPA5 mRNA in young vs. adult rats was detected in the hippocampus and mPFC (Fig. 1C) (HP: $p < 0.0001$ for both PND 15 and 26 vs. PND 70; mPFC: PND 15 vs. PND 70: $p = 0.015$; PND 26 vs. PND 70: $p = 0.004$). In contrast, juvenile and preadolescent rats did not differ in the HSPA5 mRNA levels in the hippocampus ($p = 1.00$) or mPFC ($p = 1.00$).

Analysis of HSPA5 protein expression revealed a lack of any statistically significant effects (Table 1, Fig. 1D, Fig. S1B).

The effects of MS on the expression of HSPA1B and HSPA5 in the blood, mPFC, and hippocampus of juvenile, preadolescent, and adult rats

MS procedure increased mRNA expression of HSPA1B in the blood ($p = 0.016$) and mPFC ($p = 0.041$) in juvenile rats (Table 2, Fig. 2A). There was no change in the HSPA1B mRNA levels in the hippocampus ($p = 0.999$) (Table 2, Fig. 2A). Moreover, MS rats had increased levels of HSPA1A/1B proteins in the mPFC and hippocampus compared to that in AFR rats (mPFC: $U_{6,6} = 3$, $p = 0.020$, $r = 0.67$; HP: $U_{6,6} = 5$, $p = 0.040$, $r = 0.58$) (Fig. 2B).

In the case of HSPA5 expression in juveniles, MS augmented the HSPA5 mRNA levels in the blood ($p = 0.015$) and reduced the HSPA5 mRNA levels in the hippocampus ($p = 0.016$) (Table 2, Fig. 2C). There was no concurrent change in the expression of HSPA5 mRNA in the mPFC ($p = 0.199$) (Table 2, Fig. 2C). However, MS rats showed an increase in the HSPA5 protein levels in the mPFC compared to that in AFR rats ($p = 0.039$) (Table 2, Fig. 2D). In contrast, there was no change in the expression of HSPA5 protein in the hippocampus of juveniles ($p = 0.414$) (Fig. 2D).

In preadolescent rats, MS increased the mRNA expression of HSPA1B in the blood ($p = 0.045$) and mPFC ($p = 0.001$) but there was no change in HSPA1B mRNA level in the hippocampus ($p = 0.861$) (Table 2, Fig. 3A). There were no statistically significant effects of MS on HSPA1A/1B protein expression in the hippocampus ($p = 0.843$) or mPFC; however, a trend toward an increase in the HSPA1A/1B protein level in the mPFC of MS preadolescent rats was detected ($p = 0.066$) (Table 2, Fig. 3B).

MS procedure did not affect HSPA5 mRNA expression in the blood ($p = 0.127$), mPFC ($p = 0.496$) or hippocampus ($p = 0.626$) in preadolescent rats (Table 2, Fig. 3C). Additionally, there were no differences between MS and AFR rats in the HSPA5 protein levels in the mPFC ($p = 0.504$) or hippocampus ($p = 0.164$) (Table 2, Fig. 3D).

In adult rats, MS did not influence HSPA1B mRNA expression in the blood ($p = 0.618$), mPFC ($p = 0.657$), or hippocampus ($p = 0.077$) (Table 2, Fig. 4A). However, MS adult rats had augmented levels of HSPA1A/1B proteins in the mPFC compared to that in AFR rats ($p = 0.038$) (Fig. 4B). There were no differences in the HSPA1A/1B protein levels in the hippocampus between MS and AFR rats ($p = 0.072$) (Table 2, Fig. 4B).

In the case of HSPA5 expression in adult rats, MS increased HSPA5 mRNA levels in the blood

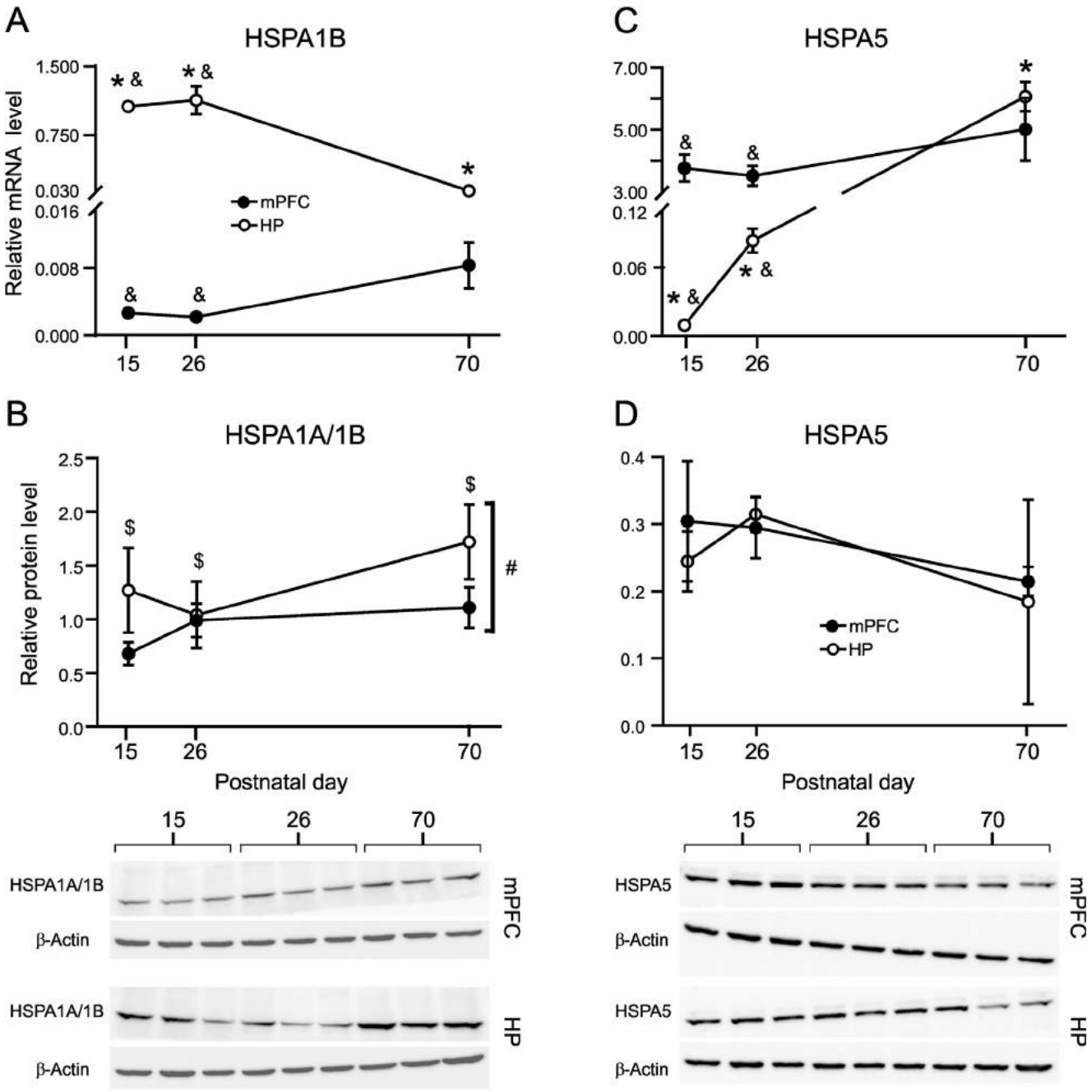

Fig. 1. Developmental time course of HSP70 family members mRNA **(A, C)** and protein **(B, D)** expression in the mPFC and hippocampus (HP) of control (AFR) rats. The data are presented as the group mean and SD (n = 3–6). $^{*}p < 0.05$ compared with the mPFC at the corresponding time points. $^{\&}p < 0.05$ compared with PND 70. $^{\#}p < 0.05$ compared with PND 15. $^{\$}p < 0.05$ vs. the mPFC, the main effect of brain region.

(p = 0.044); however, no changes were observed in HSPA5 mRNA expression in the mPFC (p = 0.937) or hippocampus (p = 0.182) (Table 2, Fig. 4C). Additionally, MS adult rats had augmented HSPA5 protein levels in the hippocampus (p = 0.011). There was no difference in the expression of HSPA5 protein in the mPFC between AFR and MS rats (p = 0.121) (Table 2, Fig. 4D).

The effects of MS on LTP in the mPFC and hippocampus of adult rats

Statistical analyses of LTP in the mPFC showed significant effects of tetanization ($p < 0.0001$) and the interaction between rearing conditions and tetanization (p = 0.002) on the field potential amplitude (Table 3, Fig. 5A). Moreover, the tetanic stimulation resulted in LTP in the mPFC of AFR rats but not in the MS rats

Table 2. Results of *t* statistic investigating the effects of MS on HSPA1B and HSPA5 expression in juvenile (PND 15), preadolescent (PND 26) and adult (PND 70) rats

PND	Parameter	Tissue	Mean ± SD		*t* statistic			Effect size
			AFR	MS	*t*	df	*p*	Cohen's *d*
15	HSPA1B mRNA	WB	0.013440 ± 0.004197	0.022117 ± 0.005970	2.91	10	**0.016**	1.7
		mPFC	0.000006 ± 0.000002	0.000010 ± 0.000004	2.44	8	**0.041**	1.3
		HP	0.010302 ± 0.000475	0.010302 ± 0.000536	0.001	10	0.999	0.0
	HSPA5 mRNA	WB	0.121701 ± 0.019435	0.148028 ± 0.010568	2.91	10	**0.015**	1.7
		mPFC	0.198379 ± 0.013772	0.187995 ± 0.012351	1.37	10	0.199	0.8
		HP	0.005211 ± 0.001364	0.003131 ± 0.001105	2.90	10	**0.016**	1.7
	HSPA5 protein	mPFC	1.482068 ± 0.544990	2.055043 ± 0.233225	2.37	10	**0.039**	1.4
		HP	1.248734 ± 0.149504	1.317162 ± 0.127778	0.85	10	0.414	0.5
26	HSPA1B mRNA	WB	0.004551 ± 0.003130	0.009282 ± 0.003653	2.32	9	**0.045**	1.4
		mPFC	0.000141 ± 0.000031	0.000226 ± 0.000037	4.36	10	**0.001**	2.0
		HP	0.011038 ± 0.001632	0.010868 ± 0.001636	0.18	10	0.861	0.1
	HSPA1A/1B protein	mPFC	0.851191 ± 0.154285	1.056956 ± 0.189658	2.06	10	0.066	1.2
		HP	5.841367 ± 1.054763	5.986220 ± 1.393591	0.20	10	0.843	0.1
	HSPA5 mRNA	WB	0.204825 ± 0.044135	0.161279 ± 0.041130	1.68	9	0.127	1.0
		mPFC	0.227392 ± 0.011945	0.240719 ± 0.044624	0.71	10	0.496	0.4
		HP	0.093412 ± 0.012814	0.101065 ± 0.034995	0.50	10	0.626	0.3
	HSPA5 protein	mPFC	0.319844 ± 0.082117	0.284359 ± 0.094896	0.69	10	0.504	0.4
		HP	1.254411 ± 0.119212	1.124680 ± 0.175003	1.50	10	0.164	0.9
70	HSPA1B mRNA	WB	0.009390 ± 0.004593	0.011125 ± 0.006553	0.52	9	0.618	0.3
		mPFC	0.000095 ± 0.000030	0.000087 ± 0.000028	0.46	10	0.657	0.3
		HP	0.000322 ± 0.000091	0.000237 ± 0.000054	1.97	10	0.077	1.1
	HSPA1A/1B protein	mPFC	0.302945 ± 0.064052	0.386947 ± 0.057637	2.39	10	**0.038**	1.4
		HP	0.486782 ± 0.050557	0.436416 ± 0.034618	2.01	10	0.072	1.2
	HSPA5 mRNA	WB	0.014335 ± 0.001052	0.016556 ± 0.002038	2.34	9	**0.044**	1.4
		mPFC	0.162172 ± 0.007128	0.161836 ± 0.007170	0.08	10	0.937	0.04
		HP	5.964062 ± 0.503036	6.486474 ± 0.736125	1.43	10	0.182	0.8
	HSPA5 protein	mPFC	2.343803 ± 0.218356	2.048353 ± 0.367613	1.69	10	0.121	0.9
		HP	0.390454 ± 0.096401	0.621727 ± 0.155253	3.10	10	**0.011**	1.8

Data (mean and SD) show relative mRNA and protein values and are presented in arbitrary units. Statistically significant effects are given in bold. Abbreviations: HP, hippocampus; PND, postnatal day, WB, whole blood.

(AFR: 150.76 ± 39.05% potentiation vs. baseline amplitude, t_{30} = 4.40, p = 0.0001, d = 1.5; MS: 121.33 ± 40.70% potentiation, t_{30} = 1.60, p = 0.119, d = 0.6) (Fig. 5A). During the last 15 min of recording, AFR rats showed higher field potential amplitude than that in MS rats (t_{30} = 2.09, p = 0.04, d = 0.7) (Fig. 5A).

Analyses of LTP in the hippocampus revealed significant effects of tetanization (p < 0.0001) and the interaction between rearing conditions and tetanization (p = 0.011) on the field potential amplitude (Table 3, Fig. 5B). Moreover, tetanic stimulation resulted in LTP in the hippocampus of both rearing conditions groups (AFR: 153.91 ± 48.43% potentiation, t_{22} = 3.34, p = 0.002, d = 1.4; MS: 187.50 ± 24.12% potentiation, t_{22} = 11.06, p < 0.0001, d = 2) (Fig. 5B). MS rats had a higher magnitude of potentiation than that in AFR rats (t_{22} = 2.15, p = 0.04, d = 0.9) (Fig. 5B).

The effects of MS on adult rat behavior

Statistical analysis of anxiety-like behavior in the light/dark exploration test revealed that MS rats traveled a greater distance in the light compartment (p = 0.005) and spent more time in the light compartment than AFR rats (p = 0.049) (Table 4, Fig. 6A, B). However, there was no difference in the number of transitions between the light and dark compartment (p = 0.115) (Table 4, Fig. 6C). There was also no difference in the total distance traveled by AFR and MS rats during the test (p = 0.170) (Table 4).

Analysis of depressive-like behaviors in the sucrose preference test showed no difference between the experimental groups (p = 0.841) (Table 4, Fig. 7A). However, during the FST, MS rats showed longer immobility time (p = 0.022) and shorter swimming time (p = 0.035) than those of the AFR rats (Table 4, Fig. 7B, C). There was no difference in climbing time between the studied groups of rats (p = 0.717) (Fig. 7D). Analysis of the locomotor activity measured after FST revealed no differences between the studied groups of rats (p = 0.527) (Table 4).

Statistical analysis of the data on the efficiency of sensorimotor gating measured in the PPI test indicated that MS did not influence the PPI level at any of the tested prepulse intensities (Table 3, Fig. 8).

DISCUSSION

The most important finding of the present study is that MS had a long-lasting impact on HSPA1B and HSPA5 expression in the mPFC, hippocampus, and blood. Specifically, MS caused the upregulation of HSPA1B

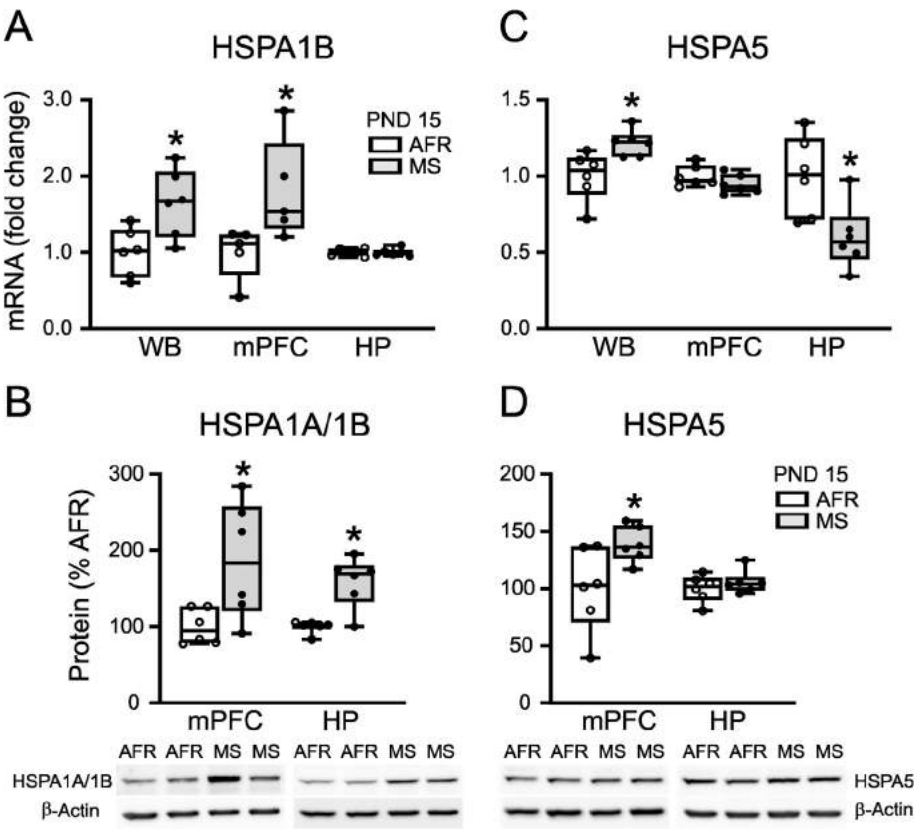

Fig. 2. The effects of MS on HSP70 family members mRNA **(A, C)** and protein **(B, D)** expression in the whole blood (WB), mPFC, and hippocampus (HP) of juvenile rats (PND 15). The data are presented as box plots and expressed as the fold-change (mRNA) or percentage (protein) relative to the values of the AFR rats. In the box plots, the box depicts the 25th and 75th quartiles, the horizontal line corresponds to the median, and the whiskers correspond to the minimum and maximum of the data. Black or white circles represent individual data points (n = 5–6). *$p < 0.05$ compared with AFR rats.

mRNA expression in the blood and mPFC of juvenile and preadolescent rats. This upregulation was accompanied by an increase in HSPA1A/1B protein levels in the mPFC and hippocampus of MS juveniles that persisted in the mPFC until adulthood. Concurrently, MS juveniles exhibited an increase in HSPA5 mRNA in the blood and an upregulation of HSPA5 protein expression in the mPFC. Adult MS rats continued to show elevated levels of HSPA5 mRNA in the blood and showed an upregulation of HSPA5 protein expression in the hippocampus. Additionally, MS adult rats exhibited aberrations in LTP in the mPFC and hippocampus and a less anxious behavioral phenotype.

Our study has several limitations that should be addressed. First, different types of measurements (mRNA vs. protein expression or biochemical vs. behavioral data in adult animals) were performed in different cohorts of rats. Therefore, we cannot directly correlate biochemical changes observed at the level of HSP70 mRNA or protein expression with electrophysiological and behavioral data. We intentionally used separate groups of rats for the measurement of HSP70s expression and behavior because many different behavioral paradigms, including the FST (Jiang et al., 2008), fear conditioning (Sirri et al., 2010), and the induction of anxiety-like behaviors (Le-Niculescu et al., 2011), have been demonstrated to influence HSP70s expression.

Second, due to the high level of similarity between HSPA1B and HSPA1A (99%) (Milner and Campbell, 1990; Kampinga et al., 2009), we were unable to investigate the specific expression of the HSPA1B protein in our Western blot analyses, and we probably measured the protein levels of both HSPA1B and HSPA1A; thus, we used the HSPA1A/1B parameter in our study. Additionally, although we used a specific assay for HSPA1B gene expression that was guaranteed by the manufacturer, we cannot completely exclude the possibility that this assay also detected HSPA1A mRNA.

Initially, the present study demonstrated that basal HSPA1B and HSPA5 mRNA levels were substantially different in the mPFC and hippocampus during development. A higher level of HSPA1B mRNA was observed in the hippocampus than in the mPFC. The opposite phenomenon was observed for HSPA5, at least during the juvenile and preadolescent periods. These results suggest that HSPA1B and HSPA5 are likely to play different roles during the development of the studied brain regions. In most cases, the level of HSP70s expression was higher in adults than in young animals. To the best of our knowledge, there are no other studies evaluating the developmental expression of these specific HSP70 family members.

Our study also demonstrated an ELS-induced increase in HSP70s mRNA and/or protein levels on PND 15, PND 26, and PND 70, i.e., 24 h, 12 days, and 56 days, respectively, after the termination of the prolonged repeated MS procedure. Limited data in the literature have shown that acute and chronic stress in adult and adolescent animals can enhance HSPA1A/1B immunoreactivity and the mRNA and protein expression of HSPA5 (GRP78) and other proteins related to UPR activation (Li et al., 2006; Ishisaka et al., 2011; Han et al., 2013; Huang et al., 2013; Timberlake and Dwivedi, 2015). For example, upregulation of HSPA5 was observed in the hippocampus 15 days after exposure to the learned helplessness paradigm (Timberlake and Dwivedi, 2015) and in the hippocampus and PFC 21 days after chronic social defeat stress (Huang et al., 2013). To the best of our knowledge, our study is the first to show

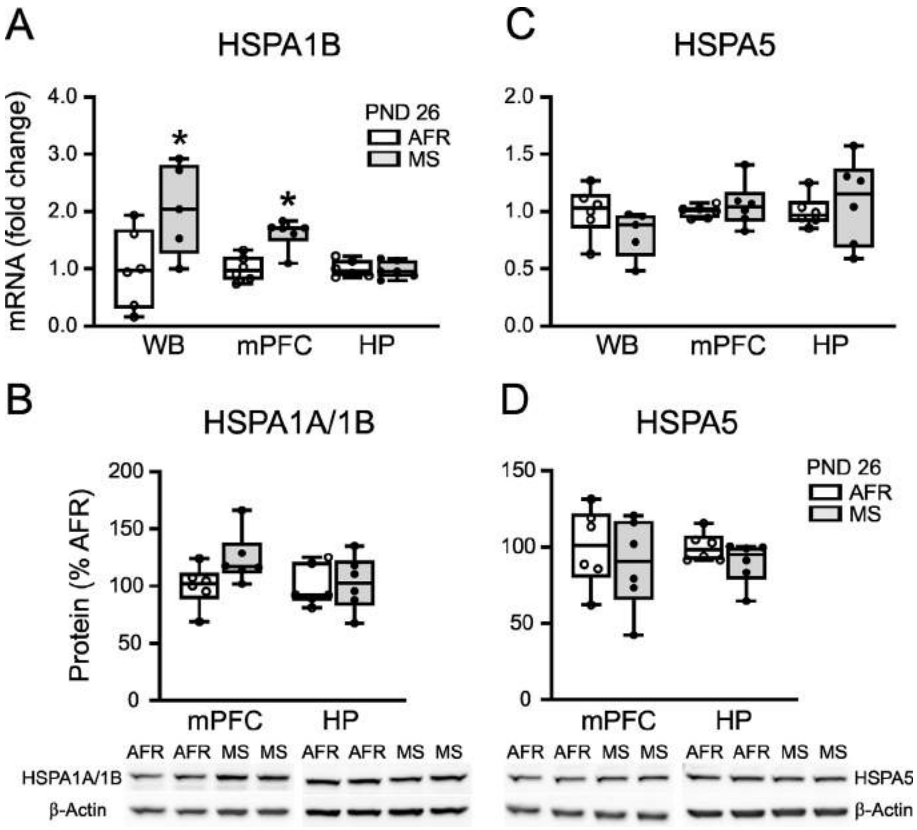

Fig. 3. The effects of MS on HSP70 family members mRNA **(A, C)** and protein **(B, D)** expression in the whole blood (WB), mPFC, and hippocampus (HP) of preadolescent rats (PND 26). The data are presented as box plots and expressed as the fold-change (mRNA) or percentage (protein) relative to the values of the AFR rats. In the box plots, the box depicts the 25th and 75th quartiles, the horizontal line corresponds to the median, and the whiskers correspond to the minimum and maximum of the data. Black or white circles represent individual data points (n = 5–6). *p < 0.05 compared with AFR rats.

prolonged stress-induced changes in HSP70s expression occurring at various stages of postnatal development.

Generally, we observed discrepancies between the effect of developmental time or MS on HSP70s mRNA and protein expression. For example, the basal protein levels of HSP70s at specific developmental time points were not considerably different compared with the developmental profile of mRNA levels. Additionally, the MS-triggered upregulation of HSP70s proteins observed in our study was not accompanied by an increase in the mRNA levels in most cases. There are many potential explanations for these differences. First, we must consider the methodological limitations discussed at the beginning. Second, the abundance and activity of HSP70s are tightly regulated initially at the transcription level and subsequently by many posttranscriptional and posttranslational mechanisms that influence the stability of mRNA and proteins, respectively (for review see: Wang et al., 2017; Casas, 2017; Nitika et al., 2020). The expression of stress-inducible HSP70s is regulated by a specific transcription factor, namely, a heat shock factor (HSF) (Abravaya et al., 1992). HSPA1A/1B proteins are direct negative regulators of their own transcription that bind and interact with HSF and block its activation (Abravaya et al., 1992). The HSPA1A/1B proteins also bind to their own mRNAs and contribute to their degradation as a self-limiting mechanism of the regulation of HSPA1A/1B expression (Balakrishnan and De, 2006).

The expression of HSPA5 is mainly regulated by ER stress and the UPR induced by the accumulation of unfolded/misfolded proteins, hypoxia and redox and calcium imbalance (Wang et al., 2017; Casas, 2017). The promoter of the HSPA5 gene contains a conserved ER stress response element (ERSE). Transcription factors related to the UPR bind to the ERSE and other elements in the HSPA5 promoter and enhance mRNA synthesis and translation (Wang et al., 2017; Casas, 2017). There is some evidence that prolonged overexpression of HSPA5 can inhibit ER stress transducers and the UPR and thus indirectly negatively regulate HSPA5 mRNA synthesis (Bertolotti et al., 2000; Casas, 2017).

The above-described phenomenon of negative and/or self-limiting regulation of HSPA1A/1B and HSPA5 expression is one of the possible explanations for MS-induced upregulation of HSP70s proteins and concurrent no change in their mRNA levels observed in our study. Alternatively, the results suggest enhanced stability or slower turnover of HSP70 proteins due to specific posttranslational modifications (Mao et al., 2013). Many well-known posttranslational modifications, including phosphorylation, acetylation, ubiquitination, and ADP-ribosylation, regulate the specific activity, location, turnover, and stability of HSP70 proteins (Concannon et al., 2005; Dai et al., 2010; Nitika et al., 2020). A vast array of posttranslational modifications enables the fulfilment of a number of various chaperone functions without the need for *de novo* protein synthesis of HSP70s.

The results of our study strongly suggest that MS may influence ER stress and the UPR throughout development. The UPR generally enhances the expression of HSPA5 and other chaperones, e.g., HSPA1A/1B (Almanza et al., 2019). Further studies are needed to validate this interesting hypothesis in the future. Recently, it has been shown that ER stress and UPR can be associated with the pathophysiology of mood disorders (Kakiuchiet al., 2005; Le-Niculescu et al., 2011; Yang et al., 2013; Nevell et al., 2014; Yoshino and Dwivedi, 2020). On the other hand, specific changes in

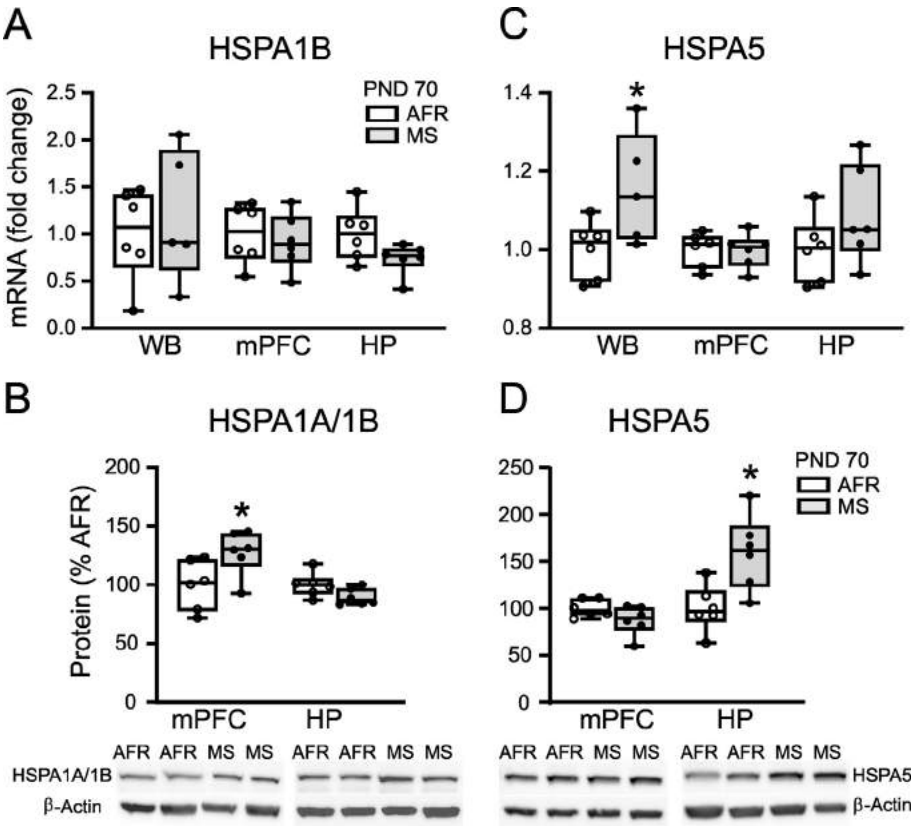

Fig. 4. The effects of MS on HSP70 family members mRNA **(A, C)** and protein **(B, D)** expression in the whole blood (WB), mPFC, and hippocampus (HP) of adult rats (PND 70). The data are presented as box plots and expressed as the fold-change (mRNA) or percentage (protein) relative to the values of the AFR rats. In the box plots, the box depicts the 25th and 75th quartiles, the horizontal line corresponds to the median, and the whiskers correspond to the minimum and maximum of the data. Black or white circles represent individual data points (n = 5–6). *p < 0.05 compared with AFR rats.

HSPA1B expression have been potentially linked with schizophrenia (Pae et al., 2005; Bosnjak et al., 2020; Kowalczyk et al., 2020) and anxiety (Le-Niculescu et al., 2011; Yang et al., 2013).

Results demonstrating the functional and behavioral consequences of ELS in animal models are very often inconsistent between laboratories, mainly due to the differences in ELS procedures (Tractenberg et al., 2016). On the other hand, neuroimaging studies in human subjects with a history of early-life trauma clearly show that although such trauma usually induces changes in brain functioning, these changes do not always correlate with the occurrence of psychopathology (Teicher and Khan, 2019). Thus, an additional aim of our study was to examine whether our ELS procedure affects functional synaptic plasticity, i.e., LTP in the mPFC and hippocampus, and produces behavioral changes resembling the symptoms of psychopathology in adult animals.

The hippocampus and mPFC and their bidirectional interactions are involved in cognitive processes and emotional regulation (Jin and Maren, 2015). LTP is considered to be a major cellular mechanism underlying learning and memory (Lisman et al., 2012). In general, data in the literature implicate that stress may have opposing effects on LTP, depending on the severity of the stress and/or the adaptive potential of the organism (Kim et al., 2015). We found that the MS procedure impaired LTP in the mPFC of adult rats. We previously showed a similar effect of MS in adolescents (Chocyk et al., 2013; Majcher-Maślanka et al., 2018). Aberrations in synaptic plasticity within the mPFC may underlie cognitive and emotional dysfunctions observed in animals subjected to ELS (Baudin et al., 2012; Yang et al., 2017). To the best of our knowledge, a very limited number of studies have focused on the effects of ELS on LTP in the mPFC (Baudin et al., 2012; Chocyk et al., 2013; Majcher-Maślanka et al., 2018). In contrast to our results, Baudin et al. (2012) revealed MS-induced enhancement of LTP in the hippocampal-mPFC pathway in adult rats. The above effect was accompanied by MS-induced cognitive deficits in mPFC-dependent tasks (Baudin et al., 2012).

Table 3. Results of mixed-design ANOVA investigating the effects of MS on LTP and efficiency of sensorimotor gating (PPI) in adult rats

Parameter	Source of variation	F	p	Effect size: η^2
Field potential amplitude in the mPFC	RC	$F_{1,30}$ = 1.58	0.219	0.037
	Tetanization	$F_{1,30}$ = 69.72	**<0.0001**	0.221
	RC × Tetanization	$F_{1,30}$ = 11.62	**0.002**	0.037
Field potential amplitude in the HP	RC	$F_{1,22}$ = 2.39	0.136	0.035
	Tetanization	$F_{1,22}$ = 136.97	**<0.0001**	0.613
	RC × Tetanization	$F_{1,22}$ = 7.73	**0.011**	0.035
PPI	RC	$F_{1,22}$ = 0.89	0.355	0.024
	Prepulse intensity	$F_{3,66}$ = 59.23	**<0.0001**	0.381
	RC × prepulse intensity	$F_{3,66}$ = 0.08	0.969	0.001

Statistically significant effects are given in bold. Abbreviations: HP, hippocampus; RC, rearing conditions.

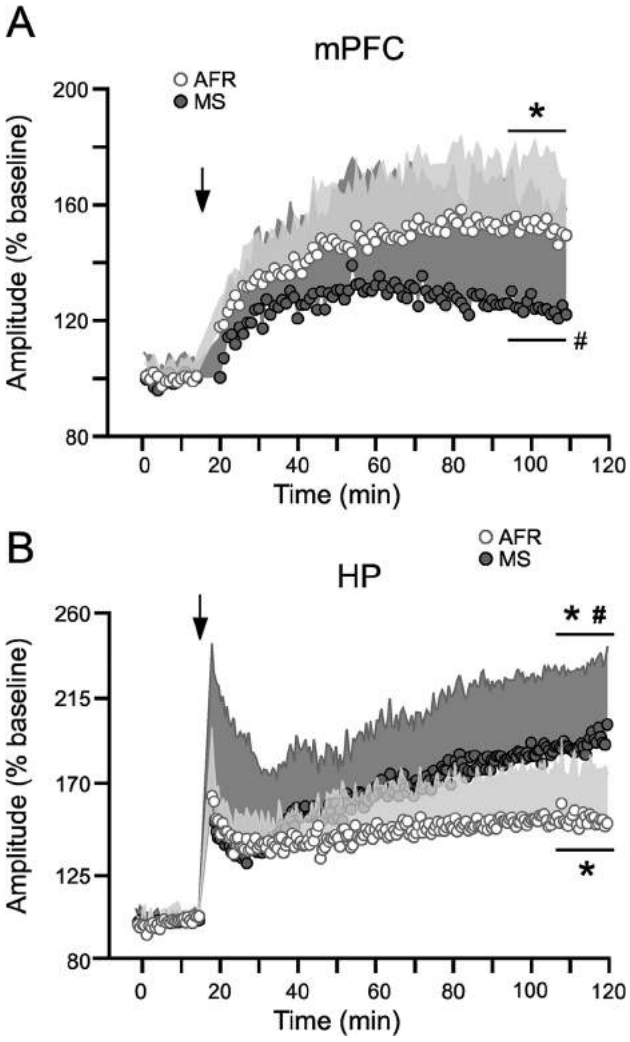

Fig. 5. The effects of MS on LTP in the mPFC **(A)** and hippocampus **(B)** of adult rats. The data are presented as the group mean (circle) and SD (shadow) (n = 12 for the hippocampus (HP) and n = 16 for the mPFC; number of brain sections from 6 and 8 animals, respectively). The data are expressed as percentage of the baseline amplitude values for each time point. $^{*}p < 0.05$ compared with the last 15 min of pretetanization recording (for values averaged over the last 15 min of recording); $^{\#}p < 0.05$ compared with AFR animals (for values averaged over the last 15 min of recording). Arrows indicate time of delivery of tetanic stimulation.

On the other hand, the present study revealed that MS enhanced LTP in the hippocampus of adults. Our results are in line with the results of other laboratories (Derks et al., 2016; Wang et al., 2018). However, there are also studies that demonstrate ELS-induced impairment or no change in LTP in the hippocampus (Brunson et al., 2005; Cao et al., 2014). Interestingly, transgenic mice with lifelong overexpression of inducible HSP70s have increased LTP in the hippocampus (Ammon-Treiber et al., 2008). Generally, HSP70s are known to be involved in synaptic plasticity and memory processes (Porto and Alvares, 2019). We can only speculate whether MS-induced changes in LTP are related to the increased protein expression of HSPA1A/1B and HSPA5 observed in MS adults.

Clinical studies have shown that ELS increases the risk of anxiety and mood disorders (Green et al., 2010). Numerous animal studies have demonstrated that ELS influences anxiety-like behavior in many different tests (Millstein and Holmes, 2007; Uchida et al., 2010; Llorente-Berzalet al., 2011; Kember et al., 2012; Wang et al., 2020). The most common behavioral outcome observed in ELS models is an enhancement in anxiety levels (Uchida et al., 2010; Kember et al., 2012; Cui, et al., 2020; Wang et al., 2020). We previously showed that our MS procedure increased anxiety-like behavior in adolescents (Chocyk et al., 2013; Majcher-Maślanka et al., 2019a). In contrast, the present study and our previous results in adult rats consistently showed reduced anxiety-like behaviors in MS rats (Chocyk et al., 2015). Changes in anxiety level are the most reproducible and persistent behavioral effects observed in our ELS model. MS-induced anxiolytic-like behaviors were also observed by others and can be associated with enhanced novelty-seeking and risk-taking behaviors (Millstein and Holmes, 2007; Llorente-Berzal et al., 2011; Kember et al., 2012). Interestingly, Huttenrauch et al. (2016) showed that reduced anxiety in mice is accompanied by enhanced expression of HSPA1B mRNA in the brain (especially in the mPFC). Moreover, Bobkova et al. (2015) demonstrated that intranasal administration of exogenous HSP70s (HSPA1A/1B) decreases anxiety and increases curiosity in aging mice. HSPA1B was recently proposed as one of the possible candidate brain and blood biomarkers of anxiety disorders (Le-Niculescu et al., 2011; Yang et al., 2013).

Table 4. Results of t statistic investigating the effects of MS on anxiety- and depressive-like behavior of adult rats

Parameter	Mean ± SD		t statistic			Effect size
	AFR	MS	t	df	p	Cohen's d
Total distance traveled (cm)	6166.436 ± 1009.367	6953.913 ± 1567.716	1.42	22	0.170	0.6
Distance in light (cm)	2135.067 ± 663.159	3147.356 ± 835.832	3.17	20	**0.005**	1.3
Time in light (s)	151.833 ± 62.320	205.706 ± 57.088	2.10	20	**0.049**	0.9
Number of transitions	8.906 ± 2.644	11.100 ± 3.604	1.65	20	0.115	0.7
Sucrose preference (%)	77.011 ± 20.880	75.200 ± 17.787	0.20	17	0.841	0.1
Immobility time in FST (s)	74.000 ± 31.351	117.583 ± 52.785	2.46	22	**0.022**	1.0
Swimming time in FST (s)	133.250 ± 52.917	91.727 ± 35.947	2.25	22	**0.035**	0.9
Climbing time in FST (s)	92.750 ± 51.498	84.667 ± 56.203	0.37	22	0.717	0.1
Distance traveled after FST (cm)	3388.167 ± 1231.562	3139.792 ± 525.979	0.64	22	0.527	0.2

The first four parameters relate to rat behavior in light/dark exploration test. Statistically significant effects are given in bold.

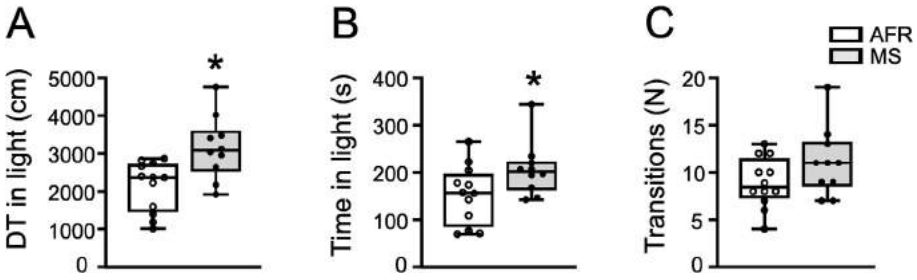

Fig. 6. The effects of MS on adult rat behavior in the light/dark exploration test. Intensity of anxiety-like behavior was assessed as the distance traveled (DT) in the light side (A), time spent in the light side **(B)**, and a number of transitions between the light and dark sides **(C)**. The data are presented as box plots. In the box plots, the box depicts the 25th and 75th quartiles, the horizontal line corresponds to the median, and the whiskers correspond to the minimum and maximum of the data. Black or white circles represent individual data points (n = 10–12). *p < 0.05 compared with AFR rats.

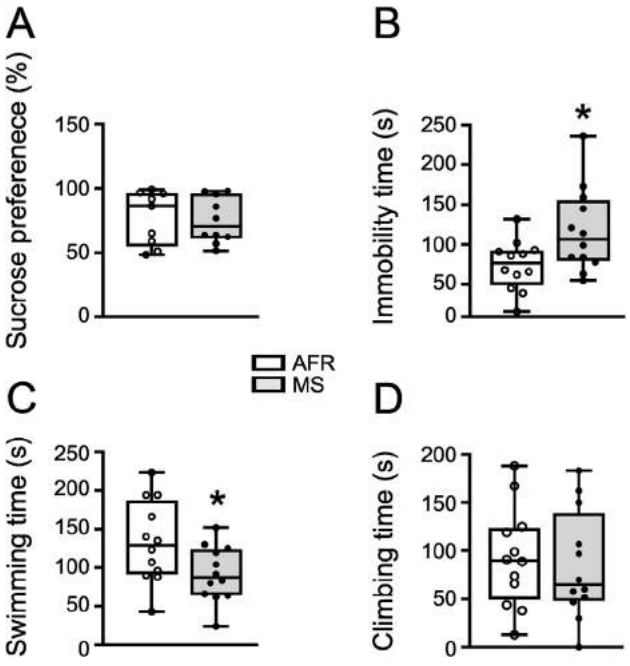

Fig. 7. The effects of MS on depressive-like behaviors in the sucrose preference test **(A)** and forced swim test **(B–D)** in adult rats. The data are presented as box plots. In the box plots, the box depicts the 25th and 75th quartiles, the horizontal line corresponds to the median and, the whiskers correspond to the minimum and maximum of the data. Black or white circles represent individual data points (n = 9–12). *p < 0.05 compared with AFR rats.

Chronic stress, including ELS, is known to induce depressive-like behaviors in animals (Willner, 2016; Cui, et al., 2020). However, not all studies in ELS models show this trend (Millstein and Holmes, 2007; Bogdanova et al., 2013; Goodwill et al., 2019). Anhedonia, which is measured by the sucrose preference test, is considered a sensitive indicator of depressive-like behaviors in animals (Liu et al., 2018). The present study showed that MS did not influence sucrose preference in adult rats. Moreover, we previously observed similar effects in adolescents (Majcher-Maślanka et al., 2019a). On the other hand, MS increased immobility time and decreased swimming time in the FST, which may indicate depressive-like symptoms in MS adults. However, it was recently argued that animal behavior in the FST (swimming vs. immobility) should instead be considered a behavioral adaptation or switch from active to passive coping strategies in the face of an inescapable acute stressor, which promotes survival (Molendijk and de Kloet, 2019). In summary, our MS adult rats did not show an unambiguous depressive-like behavioral phenotype.

Animal studies within the last two decades have not conclusively shown whether ELS produces the deficits in sensorimotor gating that are typical of schizophrenia (Lehmann et al., 2000; Ellenbroek et al., 2004; Garner et al., 2007; Niwa et al., 2011). The present study joins many other studies that have shown a lack of effect of MS on the efficiency of sensorimotor gating, as evaluated using the PPI test (Lehmann et al., 2000; Niwa et al., 2011).

In conclusion, we found that MS produced long-lasting upregulation of HSPA1B and HSPA5 in the brain and blood. Additionally, MS affected synaptic plasticity and induced anxiolytic-like behavior in adult rats. The results suggest that both HSP70 family members can be potential candidate peripheral and brain biomarkers of ELS-related changes in brain functioning. However, further studies are needed to confirm this hypothesis and extend the search to other organs and health problems related to ELS.

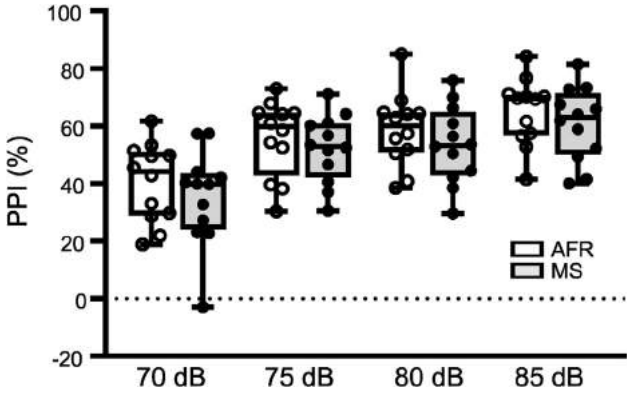

Fig. 8. The effects of MS on the process of sensorimotor gating in adult rats. The data are presented as box plots and expressed as the percentage of prepulse-induced inhibition (PPI) of acoustic startle response for each prepulse intensity. In the box plots, the box depicts the 25th and 75th quartiles, the horizontal line corresponds to the median, and the whiskers correspond to the minimum and maximum of the data. Black or white circles represent individual data points (n = 12). Mixed-design ANOVA revealed no significant effect of the rearing conditions.

ACKNOWLEDGMENTS

The authors thank Dr. Natalia Nowak for her expertise in RNA isolation from the whole blood and the analysis of gene expression in the blood.

This work was supported by grant Opus 2017/25/B/NZ7/00174 from the National Science Centre, Poland.

REFERENCES

Abravaya K, Myers MP, Murphy SP, Morimoto RI (1992) The human heat shock protein hsp70 interacts with HSF, the transcription factor that regulates heat shock gene expression. Genes Dev 6:1153–1164.

Almanza A, Carlesso A, Chintha C, Creedican S, Doultsinos D, Leuzzi B, Luis A, McCarthy N, Montibeller L, More S, Papaioannou A, Puschel F, Sassano ML, Skoko J, Agostinis P, de BJ, Eriksson LA, Fulda S, Gorman AM, Healy S, Kozlov A, Munoz-Pinedo C, Rehm M, Chevet E, Samali A (2019) Endoplasmic reticulum stress signalling - from basic mechanisms to clinical applications. FEBS J 286:241-278.

Amawi KF, Al-Mazari IS, Alsarhan A, Alhamad HQM, Alkhatib AJ (2019) Diabetes upregulates the expression of HSP90 and downregulates HSP70 in the liver of diabetic rats. Comp Clin Path 28:473–478.

Ammon-Treiber S, Grecksch G, Angelidis C, Vezyraki P, Hollt V, Becker A (2008) Emotional and learning behaviour in mice overexpressing heat shock protein 70. Neurobiol Learn Mem 90:358–364.

Arya R, Mallik M, Lakhotia SC (2007) Heat shock genes - integrating cell survival and death. J Biosci 32:595–610.

Balakrishnan K, De MA (2006) Heat shock protein 70 binds its own messenger ribonucleic acid as part of a gene expression self-limiting mechanism. Cell Stress Chaperones 11:44–50.

Bator E, Latusz J, Wedzony K, Mackowiak M (2018) Adolescent environmental enrichment prevents the emergence of schizophrenia-like abnormalities in a neurodevelopmental model of schizophrenia. Eur Neuropsychopharmacol 28:97–108.

Baudin A, Blot K, Verney C, Estevez L, Santamaria J, Gressens P, Giros B, Otani S, Daugé V, Naudon L (2012) Maternal deprivation induces deficits in temporal memory and cognitive flexibility and exaggerates synaptic plasticity in the rat medial prefrontal cortex. Neurobiol Learn Mem 98:207–214.

Bertolotti A, Zhang Y, Hendershot LM, Harding HP, Ron D (2000) Dynamic interaction of BiP and ER stress transducers in the unfolded-protein response. Nat Cell Biol 2:326–332.

Bobkova NV, Evgen'ev M, Garbuz DG, Kulikov AM, Morozov A, Samokhin A, Velmeshev D, Medvinskaya N, Nesterova I, Pollock A, Nudler E (2015) Exogenous Hsp70 delays senescence and improves cognitive function in aging mice. Proc Natl Acad Sci U S A 112:16006-16011.

Bogdanova OV, Kanekar S, D'Anci KE, Renshaw PF (2013) Factors influencing behavior in the forced swim test. Physiol Behav 118:227–239.

Bosnjak KD, Bozina N, Ganoci L, Makaric P, Kekin I, Prpic N, Bozina T, Rojnic KM (2020) Association of HSPA1B genotypes with psychopathology and neurocognition in patients with the first episode of psychosis: a longitudinal 18-month follow-up study. Pharmacogenomics J 20:638–646.

Bown C, Wang JF, MacQueen G, Young LT (2000) Increased temporal cortex ER stress proteins in depressed subjects who died by suicide. Neuropsychopharmacology 22:327–332.

Braff DL, Geyer MA, Swerdlow NR (2001) Human studies of prepulse inhibition of startle: normal subjects, patient groups, and pharmacological studies. Psychopharmacology (Berl) 156:234–258.

Brocchieri L, Conway de ME, Macario AJ (2008) hsp70 genes in the human genome: Conservation and differentiation patterns predict a wide array of overlapping and specialized functions. BMC Evol Biol 8:19.

Brunson KL, Kramár E, Lin B, Chen Y, Colgin LL, Yanagihara TK, Lynch G, Baram TZ (2005) Mechanisms of late-onset cognitive decline after early-life stress. J Neurosci 25:9328–9338.

Cao X, Huang S, Cao J, Chen T, Zhu P, Zhu R, Su P, Ruan D (2014) The timing of maternal separation affects morris water maze performance and long-term potentiation in male rats. Dev Psychobiol 56:1102–1109.

Casas C (2017) GRP78 at the centre of the stage in cancer and neuroprotection. Front Neurosci 11:177.

Chocyk A, Bobula B, Dudys D, Przyborowska A, Majcher-Maslanka I, Hess G, Wedzony K (2013) Early-life stress affects the structural and functional plasticity of the medial prefrontal cortex in adolescent rats. Eur J Neurosci 38:2089–2107.

Chocyk A, Majcher-Maslanka I, Przyborowska A, Mackowiak M, Wedzony K (2015) Early-life stress increases the survival of midbrain neurons during postnatal development and enhances reward-related and anxiolytic-like behaviors in a sex-dependent fashion. Int J Dev Neurosci 44:33–47.

Chocyk A, Przyborowska A, Makuch W, Majcher-Maslanka I, Dudys D, Wedzony K (2014) The effects of early-life adversity on fear memories in adolescent rats and their persistence into adulthood. Behav Brain Res 264:161–172.

Coccurello R, Bielawski A, Zelek-Molik A, Vetulani J, Kowalska M, D'Amato FR, Nalepa I (2014) Brief maternal separation affects brain alpha1-adrenoceptors and apoptotic signaling in adult mice. Prog Neuropsychopharmacol Biol Psychiatry 48:161–169.

Concannon CG, FitzGerald U, Holmberg CI, Szegezdi E, Sistonen L, Samali A (2005) CD95-mediated alteration in Hsp70 levels is dependent on protein stabilization. Cell Stress Chaperones 10:59–65.

Cui Y, Cao K, Lin H, Cui S, Shen C, Wen W, Mo H, Dong Z, Bai S, Yang L, Shi Y, Zhang R (2020) Early-life stress induces depression-like behavior and synaptic-plasticity changes in a maternal separation rat model: gender difference and metabolomics study. Front Pharmacol 11:102.

Dai RY, Chen SK, Yan DM, Chen R, Lui YP, Duan CY, Li J, He T, Li H (2010) PI3K/Akt promotes GRP78 accumulation and inhibits endoplasmic reticulum stress-induced apoptosis in HEK293 cells. Folia Biol (Praha) 56:37–46.

Daugaard M, Rohde M, Jaattela M (2007) The heat shock protein 70 family: Highly homologous proteins with overlapping and distinct functions. FEBS Lett 581:3702–3710.

Derks NA, Krugers HJ, Hoogenraad CC, Joëls M, Sarabdjitsingh RA (2016) Effects of early life stress on synaptic plasticity in the developing hippocampus of male and female rats. PLoS One 11.

Donley GAR, Lonnroos E, Tuomainen TP, Kauhanen J (2018) Association of childhood stress with late-life dementia and Alzheimer's disease: the KIHD study. Eur J Public Health 28:1069–1073.

Ellenbroek BA, de Bruin NM, van Den Kroonenburg PT, van Luijtelaar EL, Cools AR (2004) The effects of early maternal deprivation on auditory information processing in adult Wistar rats. Biol Psychiatry 55:701–707.

Garner B, Wood SJ, Pantelis C, van den Buuse M (2007) Early maternal deprivation reduces prepulse inhibition and impairs spatial learning ability in adulthood: no further effect of post-pubertal chronic corticosterone treatment. Behav Brain Res 176:323–332.

Goodwill HL, Manzano-Nieves G, Gallo M, Lee HI, Oyerinde E, Serre T, Bath KG (2019) Early life stress leads to sex differences in development of depressive-like outcomes in a mouse model. Neuropsychopharmacology 44:711–720.

Green JG, McLaughlin KA, Berglund PA, Gruber MJ, Sampson NA, Zaslavsky AM, Kessler RC (2010) Childhood adversities and adult psychiatric disorders in the national comorbidity survey replication I: associations with first onset of DSM-IV disorders. Arch Gen Psychiatry 67:113–123.

Han F, Yan S, Shi Y (2013) Single-prolonged stress induces endoplasmic reticulum-dependent apoptosis in the hippocampus in a rat model of post-traumatic stress disorder. PLoS One 8 e69340.

Hoeijmakers L, Lesuis SL, Krugers H, Lucassen PJ, Korosi A (2018) A preclinical perspective on the enhanced vulnerability to Alzheimer's disease after early-life stress. Neurobiol Stress 8:172–185.

Huang GB, Zhao T, Muna SS, Bagalkot TR, Jin HM, Chae HJ, Chung YC (2013) Effects of chronic social defeat stress on behaviour, endoplasmic reticulum proteins and choline acetyltransferase in adolescent mice. Int J Neuropsychopharmacol 16:1635–1647.

Huttenrauch M, Salinas G, Wirths O (2016) Effects of long-term environmental enrichment on anxiety, memory, hippocampal plasticity and overall brain gene expression in C57BL6 mice. Front Mol Neurosci 9:62.

Igaz LM, Bekinschtein P, Izquierdo I, Medina JH (2004) One-trial aversive learning induces late changes in hippocampal CaMKIIalpha, Homer 1a, Syntaxin 1a and ERK2 protein levels. Brain Res Mol Brain Res 132:1–12.

Ishisaka M, Kudo T, Shimazawa M, Kakefuda K, Oyagi A, Hyakkoku K, Tsuruma K, Hara H (2011) Restraint-induced expression of endoplasmic reticulum stress-related genes in the mouse brain. Pharmacol Pharma 2:10–16.

Jiang H, Li Y, Liu DX, Zhang Q, Ji YJ, Pan F (2008) Effects of gradual hypoxia stress and forced swimming on HSP70 expression in the CA3 subfield of hippocampus and behavior of different aged mice. Clinical Molecular Medicine 1:11–16.

Jin J, Maren S (2015) Prefrontal-hippocampal interactions in memory and emotion. Front Syst Neurosci 9:170.

Kakiuchi C, Ishiwata M, Nanko S, Kunugi H, Minabe Y, Nakamura K, Mori N, Fujii K, Umekage T, Tochigi M, Kohda K, Sasaki T, Yamada K, Yoshikawa T, Kato T (2005) Functional polymorphisms of HSPA5: possible association with bipolar disorder. Biochem Biophys Res Commun 336:1136-1143.

Kampinga HH, Hageman J, Vos MJ, Kubota H, Tanguay RM, Bruford EA, Cheetham ME, Chen B, Hightower LE (2009) Guidelines for the nomenclature of the human heat shock proteins. Cell Stress Chaperones 14:105–111.

Karunanithi S, Brown IR (2015) Heat shock response and homeostatic plasticity. Front Cell Neurosci 9:68.

Kavanagh K, Flynn DM, Jenkins KA, Zhang L, Wagner JD (2011) Restoring HSP70 deficiencies improves glucose tolerance in diabetic monkeys. Am J Physiol Endocrinol Metab 300: E894–E901.

Kember RL, Dempster EL, Lee TH, Schalkwyk LC, Mill J, Fernandes C (2012) Maternal separation is associated with strain-specific responses to stress and epigenetic alterations to Nr3c1, Avp and Nr4a1 in mouse. Brain Behav 2:455–467.

Kim EJ, Pellman B, Kim JJ (2015) Stress effects on the hippocampus: a critical review. Learn Mem 22:411–416.

Kowalczyk M, Kucia K, Owczarek A, Suchanek-Raif R, Merk W, Fila-Danilow A, Paul-Samojedny M, Choreza P, Kowalski J (2020) Association of HSPA1B polymorphisms with paranoid schizophrenia in a polish population. Neuromolecular Med 22:159–169.

Le-Niculescu H, Balaraman Y, Patel SD, Ayalew M, Gupta J, Kuczenski R, Shekhar A, Schork N, Geyer MA, Niculescu AB (2011) Convergent functional genomics of anxiety disorders: translational identification of genes, biomarkers, pathways and mechanisms. Transl Psychiatry 1.

Leak RK (2014) Heat shock proteins in neurodegenerative disorders and aging. J Cell Commun Signal 8:293–310.

Lehmann J, Pryce CR, Feldon J (2000) Lack of effect of an early stressful life event on sensorimotor gating in adult rats. Schizophr Res 41:365–371.

Li Q, Pan F, Chen XY, Jiang H, Zhang HJ, Yu HL, Lu CY (2006) HSP70 expression in the hippocampal CA3 subfield in different chronic stress models. Chin J Physiol 49:119–125.

Lisman J, Yasuda R, Raghavachari S (2012) Mechanisms of CaMKII action in long-term potentiation. Nat Rev Neurosci 13:169–182.

Liu MY, Yin CY, Zhu LJ, Zhu XH, Xu C, Luo CX, Chen H, Zhu DY, Zhou QG (2018) Sucrose preference test for measurement of stress-induced anhedonia in mice. Nat Protoc 13:1686–1698.

Llorente-Berzal A, Fuentes S, Gagliano H, Lopez-Gallardo M, Armario A, Viveros MP, Nadal R (2011) Sex-dependent effects of maternal deprivation and adolescent cannabinoid treatment on adult rat behaviour. Addict Biol 16:624–637.

Majcher-Maslanka I, Solarz A, Chocyk A (2019a) Maternal separation disturbs postnatal development of the medial prefrontal cortex and affects the number of neurons and glial cells in adolescent rats. Neuroscience 423:131–147.

Majcher-Maslanka I, Solarz A, Chocyk A (2019b) The impact of early-life stress on corticosteroid carrier protein levels and 11beta-hydroxysteroid dehydrogenase 1 expression in adolescent rats. Pharmacol Rep 71:347–350.

Majcher-Maslanka I, Solarz A, Wedzony K, Chocyk A (2018) Previous early-life stress modifies acute corticosterone-induced synaptic plasticity in the medial prefrontal cortex of adolescent rats. Neuroscience 379:316–333.

Maniam J, Antoniadis C, Morris MJ (2014) Early-life stress, HPA axis adaptation, and mechanisms contributing to later health outcomes. Front Endocrinol (Lausanne) 5:73.

Mao RF, Rubio V, Chen H, Bai L, Mansour OC, Shi ZZ (2013) OLA1 protects cells in heat shock by stabilizing HSP70. Cell Death Dis 4.

Maugeri N, Radhakrishnan J, Knight JC (2010) Genetic determinants of HSP70 gene expression following heat shock. Hum Mol Genet 19:4939–4947.

McTeague LM, Rosenberg BM, Lopez JW, Carreon DM, Huemer J, Jiang Y, Chick CF, Eickhoff SB, Etkin A (2020) Identification of common neural circuit disruptions in emotional processing across psychiatric disorders. Am J Psychiatry 177:411–421.

Miller DJ, Fort PE (2018) Heat shock proteins regulatory role in neurodevelopment. Front Neurosci 12:821.

Millstein RA, Holmes A (2007) Effects of repeated maternal separation on anxiety- and depression-related phenotypes in different mouse strains. Neurosci Biobehav Rev 31:3–17.

Milner CM, Campbell RD (1990) Structure and expression of the three MHC-linked HSP70 genes. Immunogenetics 32:242–251.

Molendijk ML, de Kloet ER (2019) Coping with the forced swim stressor: current state-of-the-art. Behav Brain Res 364:1–10.

Murphy MO, Cohn DM, Loria AS (2017) Developmental origins of cardiovascular disease: Impact of early life stress in humans and rodents. Neurosci Biobehav Rev 74:453–465.

Nevell L, Zhang K, Aiello AE, Koenen K, Galea S, Soliven R, Zhang C, Wildman DE, Uddin M (2014) Elevated systemic expression of ER stress related genes is associated with stress-related mental disorders in the Detroit Neighborhood Health Study. Psychoneuroendocrinology 43:62–70.

Nitika PCM, Truman AW, Truttmann MC (2020) Post-translational modifications of Hsp70 family proteins: Expanding the chaperone code. J Biol Chem 295:10689–10708.

Niwa M, Matsumoto Y, Mouri A, Ozaki N, Nabeshima T (2011) Vulnerability in early life to changes in the rearing environment plays a crucial role in the aetiopathology of psychiatric disorders. Int J Neuropsychopharmacol 14:459–477.

Pae CU, Kim TS, Kwon OJ, Artioli P, Serretti A, Lee CU, Lee SJ, Lee C, Paik IH, Kim JJ (2005) Polymorphisms of heat shock protein 70 gene (HSPA1A, HSPA1B and HSPA1L) and schizophrenia. Neurosci Res 53:8–13.

Paxinos G, Watson C (1998) Rat brain in stereotactic coordinates. San Diego CA, USA: Academic Press.

Porsolt RD, Anton G, Blavet N, Jalfre M (1978) Behavioural despair in rats: a new model sensitive to antidepressant treatments. Eur J Pharmacol 47:379–391.

Porto RR, Alvares LO (2019) Role of HSP70 in plasticity and memory. Heat shock proteins in neuroscience 20:53-67 Springer Nature Switzerland AG.

Porto RR, Dutra FD, Crestani AP, Holsinger RMD, Quillfeldt JA, Homem de Bittencourt Jr PI, de Oliveira AL (2018) HSP70 facilitates memory consolidation of fear conditioning through MAPK pathway in the hippocampus. Neuroscience 375:108–118.

Santos-Junior VA, Lollo PCB, Cantero MA, Moura CS, Amaya-Farfan J, Morato PN (2018) Heat shock proteins: protection and potential

biomarkers for ischemic injury of cardiomyocytes after surgery. Braz J Cardiovasc Surg 33:291–302.
Sirri A, Bianchi V, Pelizzola M, Mayhaus M, Ricciardi-Castagnoli P, Toniolo D, D'Adamo P (2010) Temporal gene expression profile of the hippocampus following trace fear conditioning. Brain Res 1308:14–23.
Song N, Ma J, Meng XW, Liu H, Wang H, Song SY, Chen QC, Liu HY, Zhang J, Peng K, Ji FH (2020) Heat shock protein 70 protects the heart from ischemia/reperfusion injury through inhibition of p38 MAPK signaling. Oxid Med Cell Longev 2020:3908641.
Stricher F, Macri C, Ruff M, Muller S (2013) HSPA8/HSC70 chaperone protein: structure, function, and chemical targeting. Autophagy 9:1937–1954.
Teicher MH, Khan A (2019) Childhood maltreatment, cortical and amygdala morphometry, functional connectivity, laterality, and psychopathology. Child Maltreat 24:458–465.
Timberlake MA, Dwivedi Y (2015) Altered expression of endoplasmic reticulum stress associated genes in hippocampus of learned helpless rats: relevance to depression pathophysiology. Front Pharmacol 6:319.
Tractenberg SG, Levandowski ML, de Azeredo LA, Orso R, Roithmann LG, Hoffmann ES, Brenhouse H, Grassi-Oliveira R (2016) An overview of maternal separation effects on behavioural outcomes in mice: Evidence from a four-stage methodological systematic review. Neurosci Biobehav Rev 68:489–503.
Tsuchiya D, Hong S, Matsumori Y, Kayama T, Swanson RA, Dillman WH, Liu J, Panter SS, Weinstein PR (2003) Overexpression of rat heat shock protein 70 reduces neuronal injury after transient focal ischemia, transient global ischemia, or kainic acid-induced seizures. Neurosurgery 53:1179–1187.
Tytell M (2005) Release of heat shock proteins (Hsps) and the effects of extracellular Hsps on neural cells and tissues. Int J Hyperthermia 21:445–455.
Uchida S, Hara K, Kobayashi A, Funato H, Hobara T, Otsuki K, Yamagata H, McEwen BS, Watanabe Y (2010) Early life stress enhances behavioral vulnerability to stress through the activation of REST4-mediated gene transcription in the medial prefrontal cortex of rodents. J Neurosci 30:15007–15018.
Wang RH, Chen YF, Chen S, Hao B, Xue L, Wang XG, Shi YW, Zhao H (2018) Maternal deprivation enhances contextual fear memory via epigenetically programming second-hit stress-induced reelin expression in adult rats. Int J Neuropsychopharmacol 21:1037–1048.
Wang J, Lee J, Liem D, Ping P (2017) HSPA5 Gene encoding Hsp70 chaperone BiP in the endoplasmic reticulum. Gene 618:14–23.
Wang D, Levine JLS, Avila-Quintero V, Bloch M, Kaffman A (2020) Systematic review and meta-analysis: effects of maternal separation on anxiety-like behavior in rodents. Transl Psychiatry 10:174.
Willner P (2016) The chronic mild stress (CMS) model of depression: History, evaluation and usage. Neurobiol Stress 6:78–93.
Yang Y, Cheng Z, Tang H, Jiao H, Sun X, Cui Q, Luo F, Pan H, Ma C, Li B (2017) Neonatal maternal separation impairs prefrontal cortical myelination and cognitive functions in rats through activation of Wnt signaling. Cereb Cortex 27:2871–2884.
Yang R, Daigle Jr BJ, Muhie SY, Hammamieh R, Jett M, Petzold L, Doyle III FJ (2013) Core modular blood and brain biomarkers in social defeat mouse model for post traumatic stress disorder. BMC Syst Biol 7:80.
Yoshino Y, Dwivedi Y (2020) Elevated expression of unfolded protein response genes in the prefrontal cortex of depressed subjects: Effect of suicide. J Affect Disord 262:229–236.

APPENDIX A. SUPPLEMENTARY DATA

Supplementary data to this article can be found online at https://doi.org/10.1016/j.neuroscience.2021.02.026.

(Received 9 July 2020, Accepted 21 February 2021)
(Available online 2 March 2021)

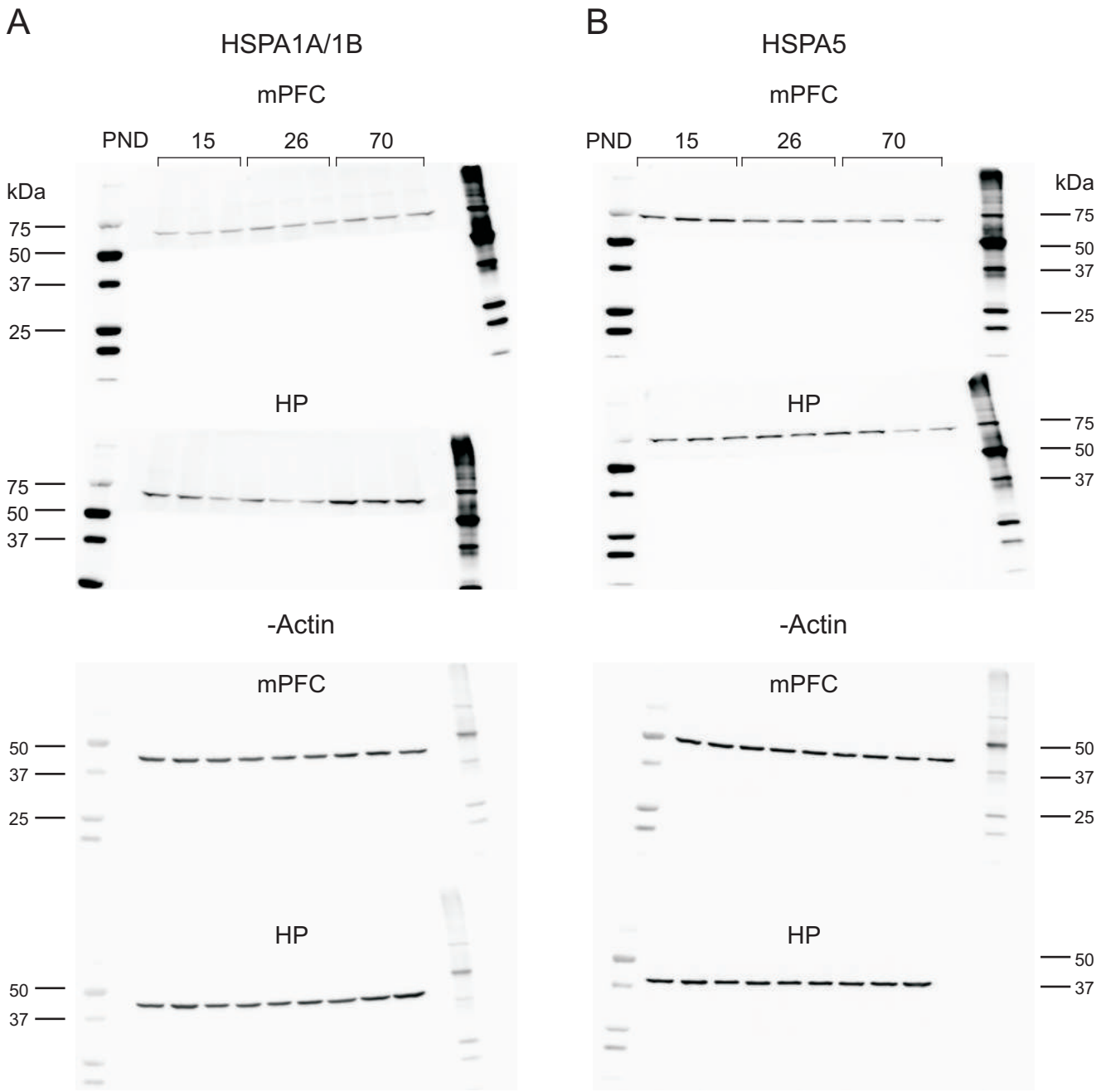

Fig. S1. Original blots presenting HSPA1A/1B (A) and HSPA5 (B) expression during postnatal development (upper panels) and respective -actin blots as control of gel loading and transfer (lower panels). Each lane was loaded with a sample of equal protein concentration (8 µg). Samples of the mPFC and hippocampus were loaded according to the same pattern. After a transfer the blots were cut into pieces slightly above the level of 50 kDa molecular weight standard to separately evaluate HSPA70s and corresponding -actin immunoreactivity from the same samples. The blots of mPFC, HP and molecular weight standards were exposed together; therefore they constitute one image for each protein.

Pharmacological Reports (2023) 75:293–319
https://doi.org/10.1007/s43440-023-00456-6

ARTICLE

Modulation of the endoplasmic reticulum stress and unfolded protein response mitigates the behavioral effects of early-life stress

Anna Solarz-Andrzejewska[1] · Iwona Majcher-Maślanka[1] · Joanna Kryst[1,2] · Agnieszka Chocyk[1]

Received: 10 November 2022 / Revised: 25 January 2023 / Accepted: 29 January 2023 / Published online: 27 February 2023

Abstract

Background Early-life stress (ELS) affects brain development and increases the risk of mental disorders associated with the dysfunction of the medial prefrontal cortex (mPFC). The mechanisms of ELS action are not well understood. Endoplasmic reticulum (ER) stress and the unfolded protein response (UPR) are cellular processes involved in brain maturation through the regulation of pro-survival or proapoptotic processes. We hypothesized that ER stress and the UPR in the mPFC are involved in the neurobiology of ELS.

Methods We performed a maternal separation (MS) procedure from postnatal days 1 to 14 in rats. Before each MS, pups were injected with an inhibitor of ER stress, salubrinal or a vehicle. The mRNA and protein expression of UPR and apoptotic markers were evaluated in the mPFC using RT-qPCR and Western blot methods, respectively. We also estimated the numbers of neurons and glial cells using stereological methods. Additionally, we assessed behavioral phenotypes related to fear, anhedonia and response to psychostimulants.

Results MS slightly enhanced the activation of the UPR in juveniles and modulated the expression of apoptotic markers in juveniles and preadolescents but not in adults. Additionally, MS did not affect the numbers of neurons and glial cells at any age. Both salubrinal and vehicle blunted the expression of UPR markers in juvenile and preadolescent MS rats, often in a treatment-specific manner. Moreover, salubrinal and vehicle generally alleviated the behavioral effects of MS in preadolescent and adult rats.

Conclusions Modulation of ER stress and UPR processes may potentially underlie susceptibility or resilience to ELS.

Keywords Endoplasmic reticulum stress · Unfolded protein response · Maternal separation · Apoptosis, Salubrinal · Medial prefrontal cortex

Abbreviations

AFC	Auditory fear conditioning
AFR	Animal facility rearing
ATF6	Activating transcription factor 6
BD	Bipolar disorder
CFC	Contextual fear conditioning
Cg1	Cingulate cortex 1
eIF2α	Eukaryotic translation initiation factor 2α
Eif2ak3	Eukaryotic translation initiation factor 2 α kinase 3
alias: PERK	RNA-activated protein kinase (PRK)-like endoplasmic reticulum kinase
ELS	Early-life stress
ER	Endoplasmic reticulum
Ern1	Endoplasmic reticulum to nucleus signaling 1
alias: IRE1α	Inositol-requiring enzyme 1
FC	Fear conditioning
GFAP	Glial fibrillary acidic protein
Hspa5	Heat shock protein family A member 5
alias: GRP78	Glucose-regulated protein 78 kDa
IBA1	Ionized calcium-binding adapter molecule
ILC	Infralimbic cortex
IR	Immunoreactive
MDD	Major depressive disorder

✉ Agnieszka Chocyk
chocyk@if-pan.krakow.pl

[1] Laboratory of Pharmacology and Brain Biostructure, Department of Pharmacology, Maj Institute of Pharmacology, Polish Academy of Sciences, Smętna Street 12, 31-343 Kraków, Poland

[2] Department of Chemistry and Biochemistry, Institute for Basics Sciences, Faculty of Physiotherapy, University of Physical Education, Jana Pawła II Av. 78, 31-571 Kraków, Poland

mPFC	Medial prefrontal cortex
MS	Maternal separation
PLC	Prelimbic cortex
PND	Postnatal day
SAL	Salubrinal
SAL-MS	MS with salubrinal injections
SD	Standard deviation
UPR	Unfolded protein response
VEH-MS	MS with vehicle injections

Introduction

Clinical and epidemiological studies have clearly indicated that early-life stress (ELS) increases the risk of mental health problems, such as mood and anxiety disorders, substance use disorder and cognitive deficits. Moreover, ELS accelerates the early onset of the abovementioned mental disorders in children and adolescents [1]. Thanks to animal studies and advances in neuroimaging techniques in humans, it is evident that ELS interferes with brain development [2, 3]. Although psychobiological consequences of ELS have been extensively explored in the past decade (for review see: [3–5]), the specific mechanisms of ELS action on brain development and maturation are still poorly understood and, thus, require intensive study.

One of the widely used and popular model of ELS and human psychopathology with a high construct validity is the repeated maternal separation procedure (MS) in rodents during the first two weeks of life [6, 7]. Our previous studies based on such MS procedure in rats have shown that this early-life experience affects the process of neurodevelopmental apoptosis in the midbrain and medial prefrontal cortex (mPFC) in males [8–10]. Specifically, we observed a sustained increase in the survival of midbrain neurons and a specific delay in neuronal apoptosis during adolescence in the mPFC, manifested as an increase in the number of neuronal cells, which could potentially affect proper neuronal network building and functioning [8, 10].

One of the key cellular processes affecting the decision of cells to survive or die in response to different environmental insults is endoplasmic reticulum (ER) stress and, closely related to it, the unfolded protein response (UPR) [11]. The ER governs the synthesis, folding, modification and transport of over one-third of cellular proteins and, thus, plays a central role in maintaining protein homeostasis (proteostasis). Many conditions, such as nutrient deprivation, hypoxia, loss of redox and calcium balance and increased protein load, may disturb proteostasis and lead to accumulation of unfolded or misfolded proteins and, consequently, to the induction of ER stress and the UPR [11, 12]. These processes, in general protective and adaptive, act to restore ER homeostasis by attenuating general translation, inducing chaperones and eliminating misfolded proteins. However, if cellular stress exceeds the pro-survival capability of the UPR, the ER induces cell death pathways through the proapoptotic component of the UPR [13, 14].

ER stress is sensed by three ER transmembrane proteins, i.e., inositol-requiring enzyme 1 (IRE1α), RNA-activated protein kinase (PKR)-like endoplasmic reticulum kinase (PERK) and activating transcription factor 6 (ATF6). Under resting conditions, these UPR sensors are bound to heat shock 70 kDa protein A 5 (HSPA5), also known as glucose-regulated protein 78 (GRP78). Upon ER stress and accumulation of unfolded or misfolded proteins, HSPA5 dissociates from these sensor molecules and allows their activation. During activation, IRE1α, also known as endoplasmic reticulum to nucleus signaling 1 and encoded by the Ern1 gene, undergoes autophosphorylation at serine 724 and then induces cleavage of X box-binding protein 1 (XBP1) mRNA and production of spliced XBP1 mRNA and protein. The spliced XBP1 protein is a highly active transcription factor that regulates genes involved in the UPR. Release of HSPA5 from ATF6 induces its translocation to the Golgi apparatus, where it is cleaved (activated). Active forms of ATF6 migrate into the nucleus, where they act as transcription factors that are also engaged in the regulation of UPR-related genes. The third sensor, PERK, also known as eukaryotic translation initiation factor 2 alpha kinase 3 and encoded by the Eif2ak3 gene, undergoes autophosphorylation at threonine 980 during its activation. Next, PERK phosphorylates (at serine 51), and in this way inactivates eukaryotic translation initiation factor 2α (eIF2α, encoded by the Eif2a gene), which causes an inhibition of general protein synthesis. Concurrently, some specific mRNA translation is allowed to further regulate UPR processes [11, 14, 15].

ER stress and UPR processes have been implicated in the pathophysiology of numerous diseases, such as cancer, diabetes, atherosclerosis and autoimmune and neurodegenerative diseases [15, 16]. However, in recent years, there has been an accumulation of data showing the involvement of ER stress and the UPR in the mechanisms of mental disorders [17–22]. Increased expression levels of UPR-related genes or proteins have been observed in the mPFC and temporal cortex of subjects with major depressive disorder (MDD) who died from suicide and in leukocytes from patients with MDD and posttraumatic stress disorder [20, 21, 23]. In contrast, an impaired ER stress response was observed in leukocytes from patients with bipolar disorder (BD) [24–26]. Additionally, functional polymorphisms in the promoter regions of XBP1 and HSPA5 were shown to have a possible association with BD in a Japanese population [17, 25]. Enhanced ER stress and activation of the UPR have also been observed in animal models of depression based on chronic restraint and chronic social defeat stress paradigms [27–29]. Surprisingly, although ELS is considered a relevant

factor in the etiology of mental and neurodegenerative disorders, ER stress and UPR processes in the brain have not been well studied in animal models of ELS. We have recently shown that the repeated MS procedure in rats produces long-lasting upregulation of HSPA5 and another chaperone belonging to the 70-kDa heat shock protein family, HSPA1B, in the brain and blood, which suggests that ELS may influence ER stress and UPR processes throughout development [30]. Dynamic regulation of the UPR has been implicated in cell fate acquisition, cortical neurogenesis, cell maturation, apoptosis and neuritogenesis during prenatal development of the central nervous system [31]. However, the role of ER stress and UPR processes in postnatal brain maturation is poorly explored. Therefore, in the present study, we investigated whether MS enhances ER stress and the UPR and consequently affects cell fate, particularly the pro-survival or apoptotic processes during postnatal maturation of the mPFC. We focused on this specific brain region because the mPFC shows a prolonged developmental trajectory, characterized by waves of postnatal neurodevelopmental apoptosis and intensive structural and functional reorganization during preadolescence and adolescence periods, which makes it especially vulnerable to the effects of stress [32–35]. Moreover, the mPFC is highly implicated in the pathophysiology of mood and anxiety disorders [36]. Simultaneously, to further evaluate the potential role of ER stress and the UPR in the mechanisms of ELS, we also studied the short- and long-term effects of transient early-life inhibition of ER stress processes by salubrinal (SAL), a selective inhibitor of eIF2α dephosphorylation, on MS-induced biochemical changes and behavioral phenotypes related to anxiety, fear memory, anhedonia and response to psychostimulants.

Materials and methods

Animals

All experimental procedures were approved by the Local Ethics Committees for Animal Research in Krakow, Poland (permit no. 186/2018 issued 07/06/2018 and 136/2019 issued 27/06/2019) and met the requirements of the Directive 2010/63/EU of the European Parliament and of the Council of 22 September 2010 on the protection of animals used for scientific purposes. All efforts were made to minimize animal suffering.

Adult male and female Wistar rats were purchased from Charles River Laboratories (Sulzfeld, Germany). All animals were housed under controlled conditions with an artificial 12-h light/dark cycle (lights on from 07:00 to 19:00), 55% ± 10 humidity, and a temperature of 22 ºC ± 2. Food and tap water were freely available. The rats were mated at the Maj Institute of Pharmacology, PAS, Krakow Animal Facility. The offspring of primiparous dams were used in this study. Before delivery, the dams were housed individually in standard plastic cages (38 × 24 × 19 cm). The day of birth was designated as postnatal day (PND) 0. On PND 1, the litter size was standardized to eight pups per litter (four males and four females), and the litters were randomly assigned to one of the following early-life treatment: animal facility rearing (AFR), i.e., control condition, MS procedure, MS with salubrinal injections (SAL-MS) or MS with vehicle injections (VEH-MS).

Repeated maternal separation and salubrinal injections

The MS procedure was performed as described previously by Solarz et al. and Chocyk et al. [8, 9, 30, 37–41]. Briefly, on PNDs 1–14, the dams and pups were removed from the maternity cages for 3 h (09.00–12.00) daily. The mothers were placed individually in the holding cages (38 × 24 × 19 cm), while each litter was placed in a plastic container (22 × 16 × 10 cm) lined with fresh bedding material, and the containers were moved to an adjacent room and placed in an incubator that was set at a constant temperature of 34 °C mimicking the nest temperature (a basic MS group). Additionally, before each daily separation, the pups from SAL-MS group received a single injection of salubrinal (1 mg/kg/5 ml *sc*, PNDs 1–14, Tocris), whereas VEH-MS group was injected with respective vehicle, i.e., 2.5% dimethyl sulfoxide (DMSO) in PBS (5 ml/kg, *sc*, PNDs 1–14, Sigma). SAL dose was chosen based on the data from literature which showed that SAL in a dose of 1 mg/kg can modulate ER stress processes in the brain and promotes neuroprotection [42, 43]. Moreover, such dose of SAL in repeated injections has been also safely administered to juvenile mice [44].

After the 3-h separation, the pups and dams were returned to the maternity cages. The AFR animals were left undisturbed with their mothers except during the weekly cage cleaning corresponding to a small amount of handling. Twenty-four hours after the last MS, i.e., on PND 15, a part of the animals was assigned to the experimental groups to investigate the effects of repeated MS and SAL in juveniles (Fig. 1). The rest of the animals were weaned on PND 22, sexed, and randomly distributed between subsequent experimental groups to investigate the long-term effects of repeated MS and SAL. These rats were housed under the controlled conditions (as described above) in standard plastic cages (57 × 33 × 20 cm) in the same-sex groups of five unrelated subjects according to the same treatment protocol until the preadolescence period (PND 26) or adulthood (PND 70) (Fig. 1). An exception was made in the case of sucrose preference test, when animals were singly housed in plastic cages (38 × 24 × 19 cm) from PND 22 to PND 26. The

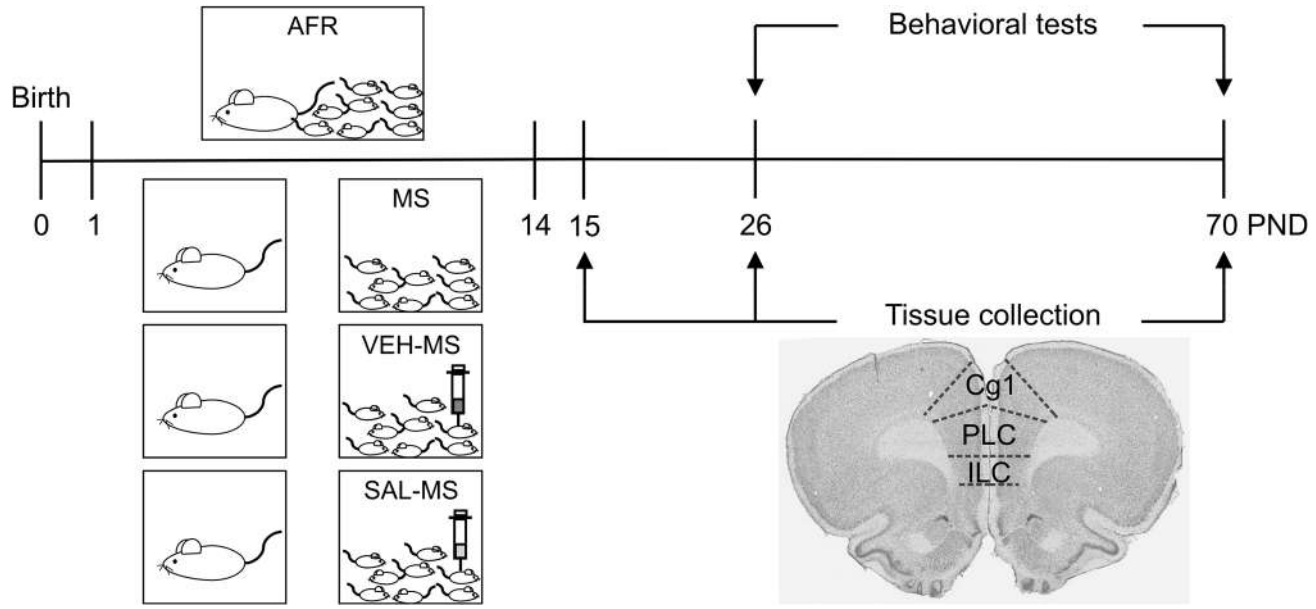

Fig. 1 Scheme of the experimental paradigm applied in the study. On PNDs 1–14, the dams and pups were separated for 3 h daily. Before each daily separation, the pups from SAL-MS group received a single injection of salubrinal (SAL, 1 mg/kg *sc*), whereas VEH-MS group was injected with respective vehicle (2.5% DMSO in PBS, 5 ml/kg *sc*). On PND 26 and PND 70, behavioral phenotype of rats was assessed in the battery of tests, such as, the light/dark exploration, fear conditioning, sucrose preference and novelty- and amphetamine-induced locomotor activity. On PNDs 15, 26 and 70, the mPFC samples were also collected for biochemical analyses. Included photomicrograph shows a cresyl violet-stained rat brain section with marked subregions of the mPFC. *AFR* animal facility rearing, *Cg1* cingulate cortex 1, *ILC* infralimbic cortex, *MS* maternal separation, *mPFC* medial prefrontal cortex, *PLC* prelimbic cortex, *PND* postnatal day, *SAL* salubrinal, *VEH* vehicle

body weights of animals were measured daily from PND 1 to PND 15 and on PND 26 and PND 70 with a Kerm PCB electronic precision scale (Balingen, Germany).

Experimental groups

A total number of 291 male rats were used in the study: 80 AFR, 68 MS, 71 VEH-MS and 72 SAL-MS rats. Female offspring was used in other scientific projects. In the case of biochemical experiments, the final experimental groups included the animals that originated from different litters and were unrelated ($n = 5$–6). In the case of behavioral experiments, maximum two subjects from the same litter were used ($n = 9$–15). The separate groups of animals were analyzed for (1) gene expression (on PND 15 and PND 26), (2) protein expression (on PND 15 and PND 26), and (3) different behavioral test (part of animals from that cohort was also used for immunohistochemistry and gene expression on PND 70).

RT-qPCR

The RT-qPCR procedure was performed as described previously by Solarz et al. [30, 40, 41]. Briefly, on PND 15, PND 26, or PND70, the animals were sacrificed by decapitation (6 rats in each treatment and age group) and the brain was immediately removed from the skull. The mPFC (including the cingulate cortex 1 (Cg1), prelimbic cortex (PLC), and infralimbic cortex (ILC) regions) was dissected from 1 mm thick coronal sections using a rodent brain matrix (Ted Pella Inc., CA, USA). After dissection, the brain tissue was quickly frozen in liquid nitrogen and stored at − 80 ºC for later use. Total RNA from the brain tissue was extracted using the RNAeasy Mini Kit (Qiagen). The total RNA concentration was measured using an Eon absorbance microplate reader and Gen 5 software (BioTek, Winooski, VT, USA). RNA was reverse transcribed using a High-Capacity cDNA Reverse Transcription Kit (Thermo Fisher Scientific, MA). Quantitative real-time PCR was performed in duplicate with TaqMan® Gene Expression Assays (Thermo Fisher Scientific, MA; Table 1) using TaqMan™ Universal Master Mix II, no UNG (Thermo Fisher Scientific, MA) and the QuantStudio 12 K Flex System (Thermo Fisher Scientific, MA). Real-time PCR was conducted under the following conditions: 50 °C for 2 min and 95 °C for 10 min followed by 40 cycles of 95 °C for 15 s and 60 °C for 1 min. The abundance of RNA was calculated according to the following equation: abundance $= 2^{-(\text{threshold cycle})}$ [45]. The results were normalized to glyceraldehyde-3-phosphate dehydrogenase (Gapdh*)* expression levels.

Table 1 The list of TaqMan® Gene Expression Assays used in the study

Gene product	Gene name	Assay ID
Heat shock protein family A member 5 alias: glucose-regulated protein GRP 78kD	Hspa5	Rn01435769_g1
Endoplasmic reticulum to nucleus signaling 1 alias: inositol-requiring enzyme 1(IRE1α)	Ern1	Rn01471008_m1
Eukaryotic translation initiation factor 2 α kinase 3 alias: RNA-activated protein kinase (PRK)-like endoplasmic reticulum kinase (PERK)	Eif2ak3	Rn00581002_m1
Activating transcription factor 6	Atf6	Rn01490844_m1
Eukaryotic initiation factor 2	Eif2a	Rn01494813_m1
Caspase-12	Casp12	Rn00590440_m1
Caspase-9	Casp9	Rn00581212_m1
Caspase-3	Casp3	Rn00563902_m1
Apoptosis regulator Bcl2	Bcl2	Rn99999125_m1
Apoptosis regulator Bax	Bax	Rn01480161_g1
Glyceraldehyde-3-phosphate dehydrogenase	Gapdh	Rn99999916_s1

Western blot

Western blot was performed as described previously by Majcher-Maślanka et al. [46, 47] and Solarz et al. [30]. Briefly, on PND 15 or PND 26, the animals were sacrificed by decapitation (6 rats in each treatment and age group), and the brain was rapidly removed from the skull. The mPFC (including Cg1, PLC and ILC regions) was dissected from 1 mm thick coronal sections using a rodent brain matrix (Ted Pella, CA, USA). After dissection, the brain tissue was quickly frozen in liquid nitrogen and stored at − 80 °C until further use. The tissue was homogenized (TissueLyser, Retsch, Germany) in ice-cold lysis buffer (PathScan® Sandwich ELISA Lysis Buffer, Cell Signaling). The homogenates were then centrifuged for 15 min at 15,000 g at 4 °C. The total protein concentration of the supernatants was determined using the bicinchoninic acid (BCA) method (Sigma-Aldrich, USA). Samples with equal protein concentrations were loaded into each lane, run on 10% sodium dodecyl sulfate–polyacrylamide gels in a Laemmli buffer system, and transferred onto a nitrocellulose membrane (Bio-Rad, USA). The blots were probed with diluted primary antibodies listed in Table 2. Then, the blots were incubated with the appropriate (anti-mouse IgG or anti-rabbit IgG) horseradish peroxidase-conjugated secondary antibodies (Roche Diagnostics, Basel, Switzerland), and the bands were visualized by enhanced chemiluminescence (Lumi-LightPlus Western Blotting Kit, Roche Diagnostics, Switzerland). The immunoblots were evaluated using a luminescent image analyzer (LAS-4000, Fujifilm, USA). Immunoblot images were acquired using exposure time increment option. Representative, unprocessed images were presented in Online Resource ESM_11-14. The relative levels of immunoreactivity were quantified using the Image Gauge software (Fujifilm, USA). The ratio of the specific protein level to the actin level was calculated for each sample to normalize for small variations in loading and transfer.

Table 2 List of primary antibodies used in the study

Specificity	Host	Dilution	Supplier	Product #
GRP78/HSPA5	Rabbit	1:1000	Cell Signaling Tech	3183
IRE1α	Rabbit	1:1000	Abcam	ab37073
p-IRE1α (S724)	Rabbit	1:1000	Abcam	ab48187
PERK	Rabbit	1:1000	Cell Signaling Tech	3192
p-PERK (Thr980)	Rabbit	1:1000	Cell Signaling Tech	3179
ATF6	Rabbit	1:1000	Proteintech	24169–1-AP
eIF2α	Rabbit	1:2000	Cell Signaling Tech	5324
p-eIF2α (S51)	Rabbit	1:1000	Cell Signaling Tech	3398
Bax	Mouse	1:500	Santa Cruz Biotech	sc-7480
Bcl2	Mouse	1:500	Santa Cruz Biotech	sc-7382
Caspase-3 (cleaved)	Rabbit	1:500	Cell Signaling Tech	9661
Caspase-9	Mouse	1:500	Cell Signaling Tech	9508
Caspase-12	Rabbit	1:500	Abcam	ab62484
NeuN	Mouse	1:1000	Millipore	MAB377
GFAP	Goat	1:250	Santa Cruz Biotech	sc-6170
IBA1	Rabbit	1:500	Proteintech	10904–1-AP

Immunohistochemistry

Immunohistochemistry was performed as previously described by Chocyk et al. [8, 39] and Majcher-Maślanka et al. [10]. Briefly, on PND 26 and PND 70, the animals (6 rats in each treatment and age group) were deeply anesthetized and transcardially perfused with saline followed by 4% paraformaldehyde in 0.1 M PBS (pH 7.4). The brains were removed from the skulls, postfixed in 4% paraformaldehyde in PBS for 24 h at 4 °C, and sectioned using a vibratome (VT1000S, Leica, Wetzlar, Germany) into 50-µm thick coronal slices at the level of the mPFC (Bregma = 3.70 to 2.20 mm) according to a stereotaxic atlas of the rat brain [48]. Every fourth section was preserved for further processing (10–11 sections from each subject).

Free-floating sections were washed in 0.01 M PBS (pH 7.4) and incubated for 30 min in PBS containing 0.3% H_2O_2 and 0.2% Triton X-100. The sections were then rinsed and transferred to a blocking buffer (5% solution of appropriate normal serum (goat, horse or rabbit) in 0.2% Triton X-100 in PBS) for 1 h. After the blocking procedure, the sections were incubated for 48 h at 4 °C with a mouse anti-NeuN antibody (1:1000; Millipore), a goat anti-glial fibrillary acidic protein (GFAP) antibody (1:250; Santa Cruz Biotechnology), or a rabbit anti-ionized calcium-binding adapter molecule (IBA1), also known as allograft inflammatory factor 1 (AIF-1), antibody (1:500; Proteintech) (Table 2). The antibodies were diluted with 3% normal serum and 0.2% Triton X-100 in PBS. After being washed in PBS, the sections were incubated for 1 h with an appropriate solution of biotinylated secondary antibodies (goat anti-rabbit, horse anti-mouse or rabbit anti-goat IgG, 1:500; Vector Laboratories), followed by a 1 h incubation with an avidin–biotin-peroxidase complex (1:200, 1 h; Vectastain ABC Kit, Vector Laboratories). The immunochemical reaction was developed in a diaminobenzidine (DAB)-nickel solution containing 0.02% DAB, 0.01% H_2O_2 and 0.06% $NiCl_2$ in TBS, which stained the immunoreactive material black. The sections were mounted onto gelatin-coated slides, air-dried and coverslipped using Permount (Fisher Scientific) as the mounting medium.

Cell counting

The number of immunoreactive (IR) cells was estimated by unbiased stereological methods [49], as described previously by Chocyk et al. [8, 39] and Majcher-Maślanka et al. [10]. Briefly, every fourth section, selected by systematic random sampling along the rostrocaudal axis of the mPFC, was chosen for analysis (10–11 sections per animal). Optical fractionator sampling was performed using a Leica DM 6000 B microscope equipped with a motorized stage (Ludl Electronic Products, Hawthorne, NY, USA) connected to a controller (MAC 5000, Ludl) and a digital camera (MBF C × 9000, Williston, VT, USA). Sampling was performed using Stereo Investigator 8.0 software (MBF Bioscience, Williston, VT, USA) by experimenters unaware of treatment group allocation to the specific slides. The studied regions of the mPFC, i.e., the Cg1, PLC and ILC, were outlined under low magnification (2.5×) according to a stereotaxic atlas of the rat brain [48] (Fig. 1). Sampling was performed bilaterally under high magnification (63×, oil-immersion objective) using counting frames with areas of 2500 μm^2 and heights of 15 µm. The sampling parameters resulted in the mean of 1277 NeuN-IR cell counted (range 724–2161), 471 IBA1-IR cells counted (range 228–723) and 642 GFAP-IR cells counted (range 397–995) in each subregion of the mPFC. The total number of immunoreactive (IR) cells per region was estimated from the number of cells sampled within the optical dissectors and calculated by multiplying the numerical density of the cells (the number of IR cells/mm^3) by the regional volume occupied by the cells within the studied region. The regional volumes of the studied mPFC areas in each animal were determined using the Cavalieri method [50]. The final results are presented as the estimated total number of cells within the specific regions.

The light/dark exploration test

On PND 26, separate groups of rats (10 rats per experimental group) were subjected to the light/dark exploration test to assess anxiety-like behaviors. The light/dark exploration test was performed as described previously by Chocyk et al. [8, 37] and Solarz et al. [30]. Briefly, each experimental cage included an arena (45 × 45 × 45 cm) with a light compartment made of clear acrylic and a dark compartment made of black acrylic. The black compartment covered 33% of the total cage area, and the black dividing wall was equipped with a central tunnel gate (11 × 8.4 cm). The light compartment was brightly illuminated (100 lx), whereas the dark compartment received no light at all. The animals were kept in total darkness for 30 min prior to the testing, and the entire experiment was conducted with the room lights off. The animals were individually tested in single 10 min trials. Six weeks later, the same groups of rats were retested for anxiety-like behaviors when they approached adulthood (PND 70), together with additional 5 AFR, 2 VEH-MS and 2 SAL-MS adult rats. The behavioral responses during the test sessions were recorded using Fear Conditioning (FC) software (TSE, Bad Homburg, Germany). Specifically, the number of transitions between the compartments, time spent in each compartment, and locomotor activity (the distance traveled) were measured.

Fear conditioning

Behavioral tests were performed and analyzed using a computer-controlled FC system (TSE, Bad Homburg, Germany) as described previously by Chocyk et al. [38] and Bialon et al. [51]. Each FC unit consisted of sound-attenuating housing with a loudspeaker, camera, ventilation fan and 4 symmetrically mounted lamps in the ceiling construction and test box. The test box comprised the test arena and a base construction containing integrated infrared animal detection sensors in the X, Y (horizontal) and Z (vertical) axes. The sensor frames along the axes were equipped with 32 sensor pairs mounted 14 mm apart. All sensors were scanned at a sampling rate of 100 Hz, i.e., the position of the animal was checked 100 times per second. Several pilot experiments were run that compared automatic and manual scoring of freezing behavior; the data obtained from each method were highly correlated.

During the experimental procedure, the animals were tested in two different arenas and contexts (A and B). For the first context (Context A), the arena (46 × 46 × 47 cm) was made of transparent acrylic and had a floor made up of stainless steel rods (4 mm in diameter) spaced 8.9 mm apart (center to center). The floor was connected to a shocker-scrambler unit for delivering shocks of defined duration and intensity. The arena was cleaned with 1% acetic acid solution. A ventilation fan provided background noise (65 dB), and lamps provided uniform illumination of 60 lx inside the fear conditioning housing. During tests in Context A, the room lights remained on. Animals were transported to this context with transparent plastic boxes. Experimenters wore white clothes and gloves.

For the second context (Context B), the arena (46 × 46 × 47 cm) was made of black acrylic (permeable to infrared light) with a gray plastic floor. The arena was cleaned with 70% ethanol solution and faintly illuminated (4 lx). The tests in Context B were conducted with the room light off. Animals were transported to this context with black plastic boxes. Experimenters wore blue clothes and gloves.

Fear conditioning (FC) and memory were assessed using the Pavlovian paradigm. The schedule of FC procedures is presented in Table 3. On day 1 of experiment (PND 26), the animals (14 AFR rats and 10 rats in each other treatment group) were subjected to FC procedure in Context A (acquisition/training). Animals were placed in Context A and allowed to habituate for 180 s. Next, the animals received five tone-shock pairings in which the tone (amplitude: 80 dB; frequency: 2 kHz; duration: 10 s) was co-terminated with foot shock (intensity: 0.7 mA; duration: 1 s). The intertrial interval was 60 s. Animals were removed from Context A 60 s after the last trial.

On day 2, all animals were once again exposed to Context A and were left undisturbed for 6 min (expression of contextual fear conditioning, CFC), then returned to their home cages. Two hours later, the animals were placed in a new context (Context B) and, after 180 s of habituation, received five presentations of tone-alone with 61-s intertrial intervals (expression of auditory fear conditioning, AFC). Animals were removed from Context B 60 s after the last trial.

Table 3 A schedule of FC procedures

PND	Procedure
26	FC acquisition/training (Context A)
27	CFC expression (Context A) AFC expression (Context B)
70	CFC memory test (recall) in adulthood (Context A)
71	AFC memory test (recall) in adulthood (Context B)
77	FC retraining in adulthood (Context A)
78	CFC expression after retraining in adulthood (Context A) AFC expression after retraining in adulthood (Context B)

AFC auditory fear conditioning, *CFC* contextual fear conditioning, *FC* fear conditioning, *PND* postnatal day

Six weeks after the FC training (on PND 70), the same animals were once again tested in both Context A and B for recall of fear memories. First, they were placed and left undisturbed for 6 min in Context A, and 24 h later, they were exposed to five presentations of tone-alone in Context B (Table 3). Seven days later, all animals were subjected to a session of retraining of fear conditioning in Context A; retraining followed the same procedure as training during preadolescence (Day 1). On the following day, fear memory was tested both in Context A and B (the same sessions as on Day 2 during preadolescence) (Table 3).

Behavioral responses during all sessions were recorded and automatically analyzed using FC software (TSE, Bad Homburg, Germany). Freezing (i.e., immobility) was taken as the behavioral measure of fear and was defined as the absence of all non-respiratory movements for at least 2 s. The cumulative duration of freezing was calculated for each session and expressed as percentage of entire session time, excluding habituation time.

Sucrose preference test

To assess anhedonic-like behavior, a sucrose preference was measured in a two-bottle choice paradigm as described previously by Chocyk et al. [8] and Solarz et al. [30]. Briefly, on PND 22 separate groups of rats (10 rats per experimental group) were singly housed and habituated to drink water from two bottles for 2 days. Then, the water in one of the bottles was replaced by 1% sucrose solution for 2 days to avoid neophobia. The position of the bottles (sucrose left or right) was reversed every 8 h to prevent the development of place preference. After habituation, the rats were subjected

to water deprivation for 16 h before performing the sucrose preference test. During the test, two bottles, one containing tap water and another containing 1% sucrose solution, were presented to each rat for 4 h (from 8 a.m. to 12 p.m.). The positioning of the water and sucrose bottles (left or right) was balanced between the experimental groups. Six weeks later, the same groups of rats were retested for anhedonic-like behavior when they approached adulthood (PND 70). Sucrose preference was calculated as the percentage of sucrose intake versus total liquid intake (water + sucrose) over the 4-h test period.

Measurement of novelty- and amphetamine-induced locomotor activity

On PND 26, a separate group of animals was subjected to the locomotor activity test ($n = 9$–12). Locomotor activity was recorded and analyzed individually for each animal using Opto-Varimex cages (43 × 44 cm) and Auto-Track software (Columbus Instruments, OH, USA), as described previously by Majcher-Maślanka et al. [10, 52]. The rats were placed into the test cages without previous habituation and were free to explore the environment for 20 min (novelty-induced locomotion, session 1). Next, the rats received vehicle injections (saline, 1 ml/kg *sc*) and were left in test cages for 50 min (session 2). Finally, the same rats were injected with amphetamine (1 mg/kg) and left in test cages for another 50 min (session 3). Six weeks later, the same groups of rats were retested for locomotor activity when they approached adulthood (PND 70). Locomotor activity of the animals was recorded for each session separately. The data are presented as the average distance traveled over the entire session.

Statistical analysis

Statistical analysis of the data was performed using Statistica 13.3 software (TIBCO Software Inc., USA). Initially, data were tested for normal distribution and homogeneity of variances using Shapiro–Wilk test and Levene's test, respectively. In the case of data that followed normal distribution and had equal variances among groups, they were further analyzed by one-way analysis of variance (ANOVA) with early-life treatment (AFR, MS, VEH-MS and SAL-MS) as independent variable followed by Tukey's HSD post hoc test. Amphetamine-induced locomotor activity was specifically analyzed by mixed-design ANOVA with early-life treatment as a between-subject factor and saline and amphetamine injections as within-subject factor. In the case of data which did not show normal distribution and homogeneity of variances, statistical differences between experimental groups were analyzed by Kruskal–Wallis test followed by Dunn's test for multiple comparisons. P values < 0.05 were considered significantly different. The data are presented as the group mean and standard deviation (SD, parametric statistics) or as the median and interquartile range (IQR, nonparametric statistics).

Results

The effects of MS and early-life SAL/VEH injections on body weight

To examine whether specific early-life treatment, such as repeated MS and SAL/VEH injections, affected the body weight of juvenile rats, a body weight gain index between PND 1 and PND 15 was calculated. Statistical analysis revealed that early-life treatment significantly affected body weight gain in juvenile rats ($F_{3,220} = 5.21$, $p = 0.002$, one-way ANOVA followed by Tukey's test). Specifically, VEH-MS rats showed a slightly higher body weight gain index in comparison to AFR and MS rats (Fig. 2).

Body weight was also assessed during the preadolescence and adulthood periods. However, Kruskal–Wallis test did not show any significant differences between the experimental groups (PND 26: $H_3 = 2.64$, $N_1 = 31$, $N_2 = 29$, $N_3 = 26$, $N_4 = 30$, $p = 0.450$; PND 70: $H_3 = 1.46$, $N_1 = 34$, $N_2 = 25$, $N_3 = 25$, $N_4 = 26$, $p = 0.690$) (Table 4).

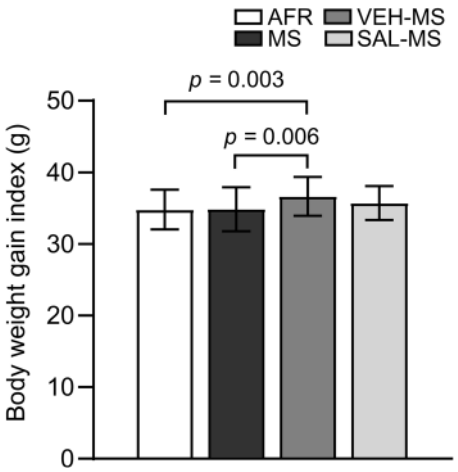

Fig. 2 The effects of MS and early-life SAL/VEH injections on a body weight gain in juvenile rats. The data are presented as the mean ± SD ($n = 48$–64) and expressed as a body weight gain index calculated as the body weight difference between PND 15 and PND 1. Connectors indicate statistically significant differences between specific experimental groups (one-way ANOVA followed by Tukey's HSD post hoc analysis). *AFR* animal facility rearing, *MS* maternal separation, *SAL* salubrinal, *VEH* vehicle

Table 4 The effects of MS and early-life SAL/VEH treatment on body weight of preadolescent and adult rats

PND	Group	Body weight
26	AFR	90.0 (11.5)
	MS	92.5 (13.8)
	VEH-MS	93.2 (15.0)
	SAL-MS	93.0 (19.1)
70	AFR	440.5 (63.0)
	MS	449.0 (26.0)
	VEH-MS	442.0 (82.0)
	SAL-MS	449.5 (87.0)

Data are presented as the median (IQR) ($n = 25$–34) and expressed in grams. *AFR* animal facility rearing, *IQR* interquartile range, *MS* maternal separation, *PND* postnatal day, *SAL* salubrinal, *VEH* vehicle

The effects of MS and early-life SAL/VEH injections on ER stress and UPR processes in juvenile rats (PND 15)

To study the early effects of repeated MS and SAL/VEH injections on ER stress and UPR processes, we examined the gene and protein expression of ER stress and UPR markers in the mPFC of rats on PND 15, which was 24 h after the last MS procedure.

Statistical analysis of Hspa5 mRNA expression in the mPFC showed a significant effect of early-life treatment (Kruskal–Wallis test, $H_3 = 17.02$, $N_{1-4} = 6$, $p = 0.0007$). Specifically, VEH-MS rats had lower Hspa5 mRNA levels than AFR and MS rats (Dunn's test) (Fig. 3A).

The analysis of HSPA5 (GRP 78) protein levels in the mPFC of juveniles also revealed a significant effect of early-life treatment (one-way ANOVA, $F_{3,20} = 3.35$, $p = 0.039$). In this case, MS rats showed enhanced expression of HSPA5 protein in comparison to AFR rats (Tukey's test) (Fig. 3B).

Next, we examined the effect of MS and SAL/VEH on the mRNA and protein expression of the ER stress sensors Eif2ak3 (PERK), Ern1 (IRE1α) and ATF6 in the mPFC.

In the case of all ER stress sensors, analysis of their mRNA expression showed no significant differences between experimental groups (one-way ANOVA, Online Resource ESM_1: Table S1; ESM_2: Fig. S1A) (Fig. 4A, D). Moreover, we did not observe an effect of MS and SAL/VEH on the total protein levels of PERK, IRE1α and ATF6 (one-way ANOVA, Table S1) (Fig. 4B, E; ESM_2: Fig. S1B). However, we did find a significant effect of early-life treatment on activation by phosphorylation of PERK at residue Thr980 ($F_{3,20} = 5.93$, $p = 0.005$, one-way ANOVA followed by Tukey's test). Specifically, VEH-MS rats showed increased levels of p-PERK (Thr980) protein in comparison to AFR rats (Fig. 4C). A similar trend was also observed

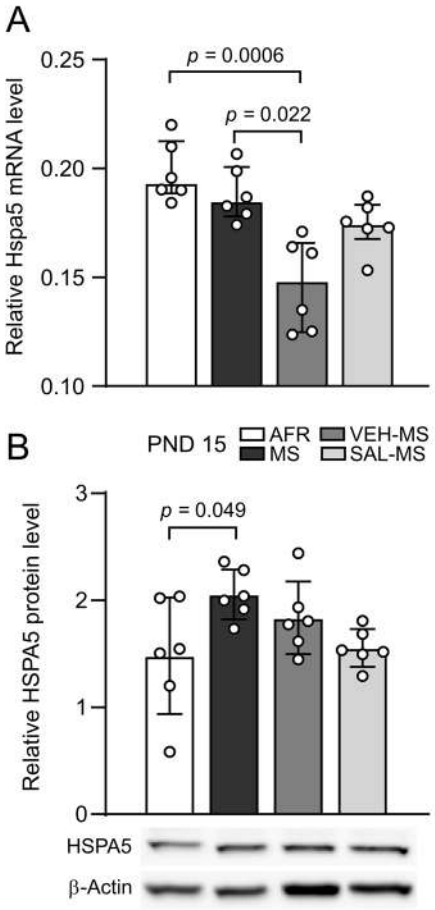

Fig. 3 The effects of MS and early-life SAL/VEH injections on HSPA5 mRNA (**A**) and protein (**B**) expression in the mPFC of juvenile rats. The data are presented as the median and IQR (**A**) or mean ± SD (**B**) and were analyzed by Kruskal–Wallis test or one-way ANOVA, respectively ($n = 6$). Circles represent individual data points. Connectors indicate statistically significant differences between specific experimental groups in Dunn's post hoc test (**A**) or Tukey's HSD post hoc test (**B**). *AFR* animal facility rearing, *MS* maternal separation, *PND* postnatal day, *SAL* salubrinal, *VEH* vehicle

in the case of the MS group, though it did not reach statistical significance ($p = 0.051$). Nevertheless, when a single comparison between AFR and MS groups was performed, the effect was observed to be statistically significant ($U = 2$, $N_{1-2} = 6$, $p = 0.013$, Mann−Whitney U test). Analysis of the phosphorylation of IRE1α at residue S724 also showed a significant effect of early-life treatment (one-way ANOVA, $F_{3,20} = 3.88$, $p = 0.024$). In this case, MS increased the phosphorylation of IRE1α at S724 in comparison to AFR rats (Tukey's test) (Fig. 4F).

Because SAL acts as an inhibitor of eIF2α dephosphorylation at residue S51, we also investigated how repeated MS and SAL/VEH injections impacted the expression and phosphorylation of eIF2α in the mPFC of juveniles. We observed that SAL-MS rats showed lower levels of

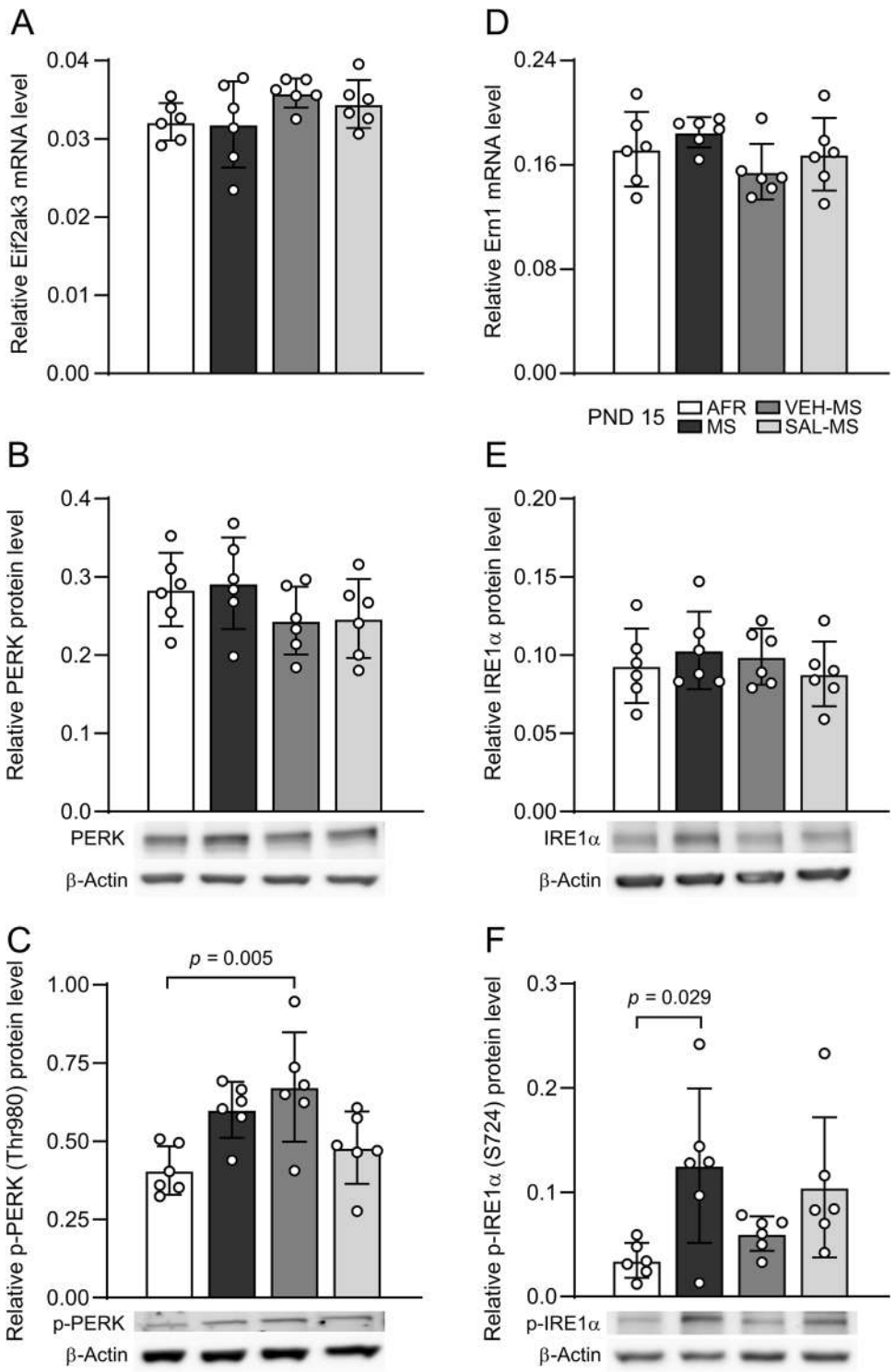

Fig. 4 The effects of MS and early-life SAL/VEH injections on mRNA expression and protein expression and phosphorylation of ER stress sensors PERK (**A**–**C**) and IRE1α (**D**–**F**) in the mPFC of juvenile rats. The data are presented as the mean ± SD ($n = 6$) and were analyzed by one-way ANOVA. Circles represent individual data points. Connectors indicate statistically significant differences between specific experimental groups in Tukey's HSD post hoc test. *AFR* animal facility rearing, *MS* maternal separation, *PND* postnatal day, *SAL* salubrinal, *VEH* vehicle

Eif2a mRNA than MS and AFR rats ($H_3 = 18.83$, $N_{1\text{-}4} = 6$, $p = 0.003$, Kruskal–Wallis test followed by Dunn's test) (Fig. 5A). We also observed a similar effect in total protein of eIF2α ($F_{3,20} = 6.10$, $p = 0.004$, ANOVA followed by Tukey's test) (Fig. 5B). However, one-way ANOVA of eIF2α phosphorylation did not reveal any differences in the level of p-eIF2α (S51) between the experimental groups ($F_{3,20} = 4.97$, $p = 0.050$) (Fig. 5C).

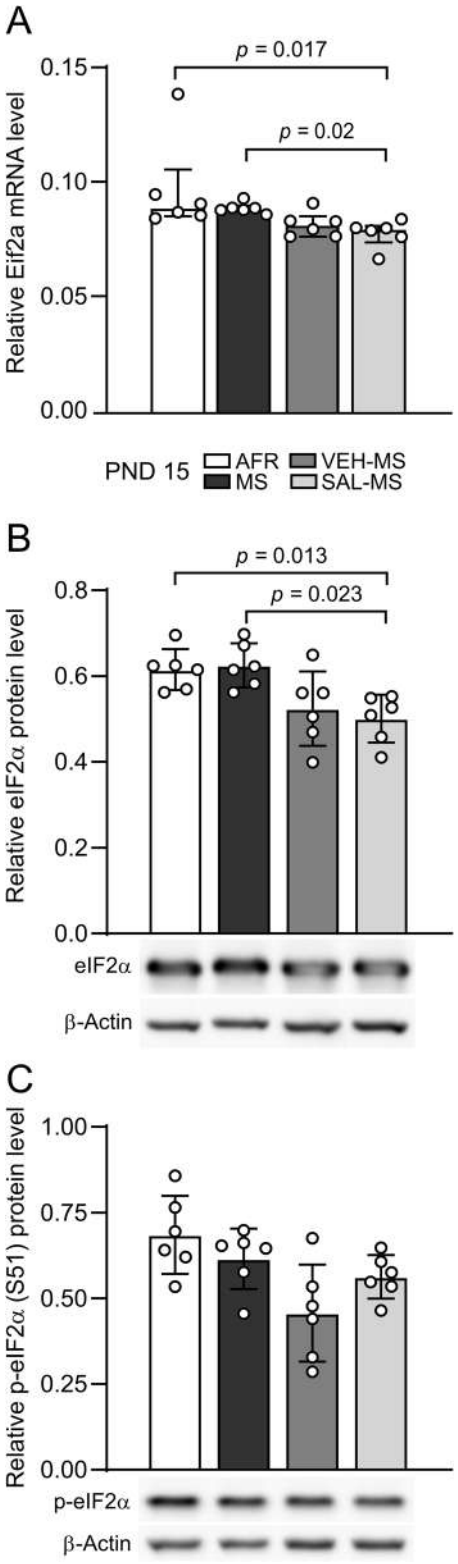

Fig. 5 The effects of MS and early-life SAL/VEH injections on mRNA expression (**A**) and protein expression and phosphorylation (**B**–**C**) of eIF2α in the mPFC of juvenile rats. The data are presented as the median and IQR (**A**) or mean ± SD (**B**, **C**) and were analyzed by Kruskal–Wallis test or one-way ANOVA, respectively ($n = 6$). Circles represent individual data points. Connectors indicate statistically significant differences between specific experimental groups in Dunn's post hoc test (**A**) or Tukey's HSD post hoc test (**B**). The same immunoblot of β-Actin was used for normalization of both p-eIF2α (**C**) and p-IRE1α immunoblots (Fig. 4F). After protein electrotransfer the blots were horizontally cut into two pieces to separately evaluate p-eIF2α and p-IRE1α protein levels from the same samples. Next, after membrane stripping procedure, appropriate blot was reprobed with β-Actin antibody. *AFR* animal facility rearing, *MS* maternal separation, *PND* postnatal day, *SAL* salubrinal, *VEH* vehicle

The effects of MS and early-life SAL/VEH injections on apoptotic processes in the mPFC of juvenile rats (PND 15)

Since ER stress and UPR processes are known to affect cell death and survival decisions, the next goal of our study was to examine the gene and protein expression of the main apoptotic markers in the mPFC.

Statistical analysis showed that early-life MS and SAL/VEH treatment affected the mRNA expression of a few apoptotic markers but not their protein levels (Online Resource ESM_1: Table S1; ESM_2: Fig. S2; Fig. S3) (Fig. 6). Notably, we observed that MS rats subjected to SAL treatment had lower levels of caspase-9 mRNA in comparison to that of VEH-MS and AFR rats ($F_{3,20} = 5.11$, $p = 0.009$, one-way ANOVA followed by Tukey's test) (Fig. 6A). A trend toward reduced expression of caspase-9 was also observed in the SAL-MS group compared to MS rats, though it did not reach statistical significance ($p = 0.051$). On the other hand, we did not observe any differences between the experimental groups in caspase-3 mRNA expression, a key effector caspase involved in a mitochondrial pathway of apoptosis (Kruskal–Wallis test, $H_3 = 7.13$, $N_{1-4} = 6$, $p = 0.068$) (Fig. 6B).

Interestingly, our study also revealed a statistically significant effect of early-life treatment on the mRNA expression of caspase-12, a specific caspase that is localized in the ER membrane and engaged in the ER stress-induced pathway of apoptosis (one-way ANOVA, $F_{3,20} = 5.36$, $p = 0.007$). The MS procedure increased caspase-12 mRNA expression compared to that in the AFR group (Fig. 6C). Moreover, VEH-MS rats had a significantly lower level of caspase-12 mRNA than MS rats (Tukey's test).

As described above, we did not observe a statistically significant effect of early-life treatment on procaspase-9 or procaspase-12 protein expression or cleaved (active) caspase-9, -12 or cleaved caspase-3 protein levels (one-way ANOVA, Table S1) (ESM_2: Fig. S2). Nevertheless, in the case of cleaved caspase-9, when a single comparison between AFR and MS groups was performed using a Student's *t*-test, statistical significance was observed, and MS rats showed increased cleaved caspase-9 protein levels in the mPFC ($t_{10} = 2.56$, $p = 0.023$) (Fig. S2B).

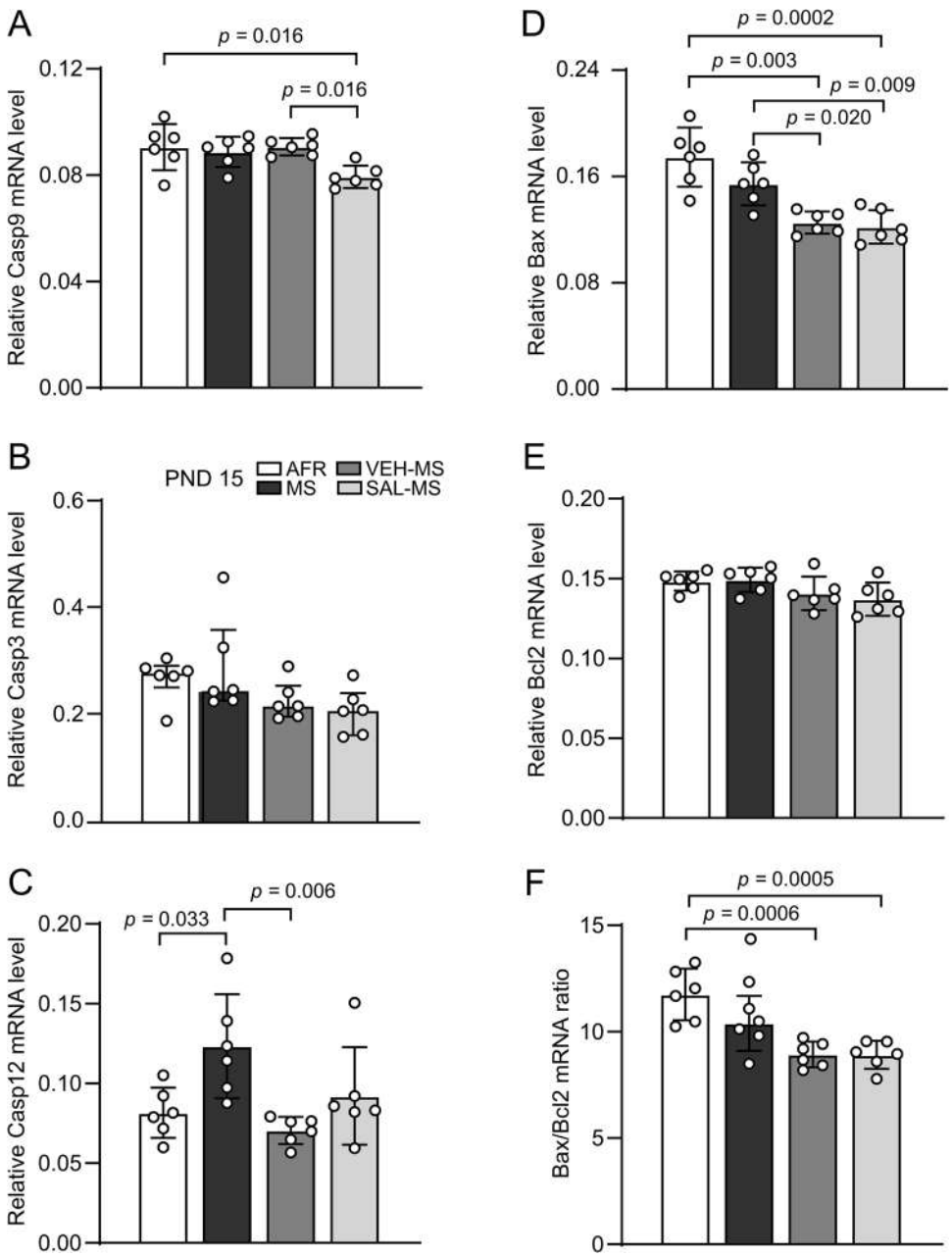

Fig. 6 The effects of MS and early-life SAL/VEH injections on mRNA expression of apoptotic markers in the mPFC of juvenile rats: Casp9 (**A**), Casp3 (**B**), Casp12 (**C**), Bax (**D**), Bcl2 (**E**), and Bax/Bcl2 mRNA ratio (**F**). The data are presented as the mean ± SD (**A**, **C**–**F**) or median and IQR (**B**) and were analyzed by one-way ANOVA or Kruskal–Wallis test, respectively ($n = 6$). Circles represent individual data points. Connectors indicate statistically significant differences between specific experimental groups in Tukey's HSD post hoc test. *AFR* animal facility rearing, *MS* maternal separation, *PND* postnatal day, *SAL* salubrinal, *VEH* vehicle

Next, we examined Bax and Bcl2 expression and the Bax/Bcl2 ratio and observed a significant effect of early-life treatment on Bax mRNA levels ($F_{3,20} = 15.34$, $p < 0.0001$, ANOVA) and the Bax/Bcl2 mRNA ratio ($F_{3,20} = 11.29$, $p < 0.0001$) (Fig. 6D–F). Specifically, both SAL- and VEH-injected MS rats showed lower levels of Bax mRNA compared to MS and AFR rats (Tukey's test) (Fig. 6D). The Bax/Bcl2 mRNA ratio was decreased in SAL-MS and VEH-MS rats compared to AFR rats only (Tukey's test) (Fig. 6F). There was no statistically significant effect of early-life treatment on the protein expression of Bax or Bcl2 or the Bax/Bcl2 protein ratio (one-way ANOVA, ESM_1: Table S1; ESM_2: Fig. S3). Nevertheless, in the case of Bax protein expression, when a single comparison between AFR and MS groups was performed using a Student's *t*-test, statistical significance was observed, and the MS rats showed increased Bax protein levels in the mPFC ($t_{10} = 3.08$, $p = 0.012$) (Fig. S3A).

The effects of MS and early-life SAL/VEH injections on ER stress and UPR processes in preadolescent rats (PND 26)

Preadolescence and adolescence are crucial periods in mPFC postnatal maturation. During the preadolescence period, neurodevelopmental apoptosis starts to progress.

The next goal of our study was to determine whether early-life MS and SAL/VEH treatment affect ER stress and UPR processes specifically in preadolescent rats (on PND 26) and in this way influence neurodevelopmental apoptosis in the mPFC.

Statistical analysis showed that in preadolescent rats, early-life treatment only affected mRNA expression of Hspa5 ($F_{3,20}=11.23$, $p<0.0001$) and two ER stress sensors, Ern1 ($F_{3,20}=11.15$, $p=0.0002$) and Atf6 ($F_{3,20}=4.42$, $p=0.015$) (one-way ANOVA) (Fig. 7). We did not observe differences between experimental groups in protein expression or activation (phosphorylation) of any of the ER stress or UPR markers we examined (ESM_1: Table S1) (ESM_3: Fig S4; Fig S5). Post hoc analysis of mRNA expression showed that both SAL- and VEH-injected MS rats had lower levels of Hspa5 mRNA compared to MS and AFR rats (Tukey's test) (Fig. 7A). A similar effect of early-life treatment was also observed in the case of Ern1 (Fig. 7C). However, analysis of Atf6 mRNA levels showed that only SAL-injected MS rats had reduced Atf6 mRNA expression compared to MS and AFR (Tukey's test) (Fig. 7D).

Next, we examined Eif2a mRNA and protein expression and eIF2α phosphorylation at residue S51. Statistical analysis revealed a lack of any significant differences between experimental groups in all these parameters (Table S1) (ESM_3: Fig. S5).

The effects of MS and early-life SAL/VEH injections on apoptotic processes in the mPFC of preadolescent rats (PND 26)

Statistical analysis of the mRNA expression of the analyzed caspases showed a significant effect of early-life treatment on caspase-3 ($H_3=10.82$, $N_{1-4}=6$, $p=0.013$, Kruskal–Wallis test) and caspase-12 ($F_{3,20}=5.26$, $p=0.008$, ANOVA) but not caspase-9 mRNA levels ($H_3=6.76$, $N_{1-4}=6$, $p=0.080$) (Online Resource ESM_1: Table S1) (Fig. 8). VEH-injected MS rats showed a lower level of caspase-3 mRNA than AFR rats (Dunn's test) (Fig. 8B). Both MS and MS-VEH rats showed reduced caspase-12 mRNA expression compared to AFR rats (Tukey's test) (Fig. 8C). However, statistical analysis did not reveal any significant differences between experimental groups in protein levels of procaspase-12 or -9 or cleaved forms of caspase-12, -9 or -3 (Table S1) (ESM_3: Fig. S6A–E).

Next, we investigated the effects of MS and SAL/VEH injections on the expression of Bcl-2 family members. Statistical analysis revealed that early-life treatment significantly affected Bcl2 mRNA expression ($F_{3,20}=12.02$, $p=0.0001$, ANOVA) and the Bax/Bcl2 mRNA ratio ($H_3=16.61$, $N_{1-4}=6$, $p=0.0009$) but not Bax mRNA levels ($H_3=1.32$, $N_{1-4}=6$, $p=0.724$, Kruskal–Wallis test) (Fig. 8). Specifically, MS increased Bcl2 mRNA expression compared to

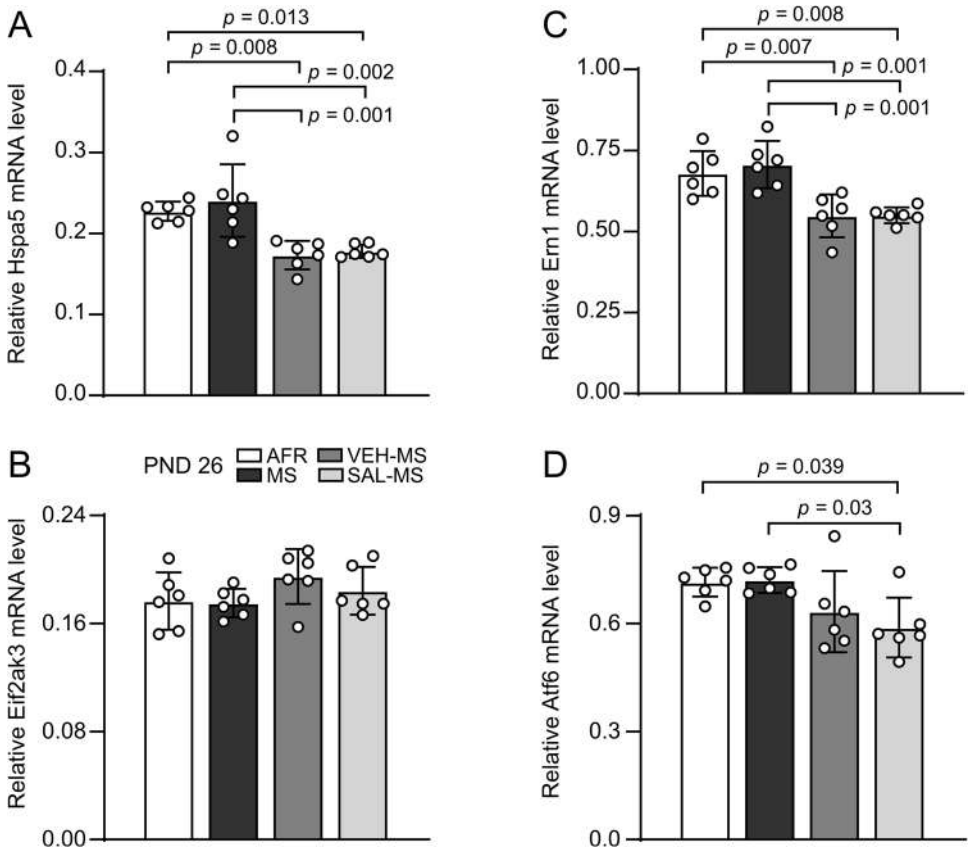

Fig. 7 The effects of MS and early-life SAL/VEH injections on mRNA expression of Hspa5 (**A**) and ER stress sensors Eif2ak3 (**B**), Ern1 (**C**), Atf6 (**D**) in the mPFC of preadolescent rats. The data are presented as the mean ± SD ($n=6$) and were analyzed by one-way ANOVA. Circles represent individual data points. Connectors indicate statistically significant differences between specific experimental groups in Tukey's HSD post hoc test. *AFR* animal facility rearing, *MS* maternal separation, *PND* postnatal day, *SAL* salubrinal, *VEH* vehicle

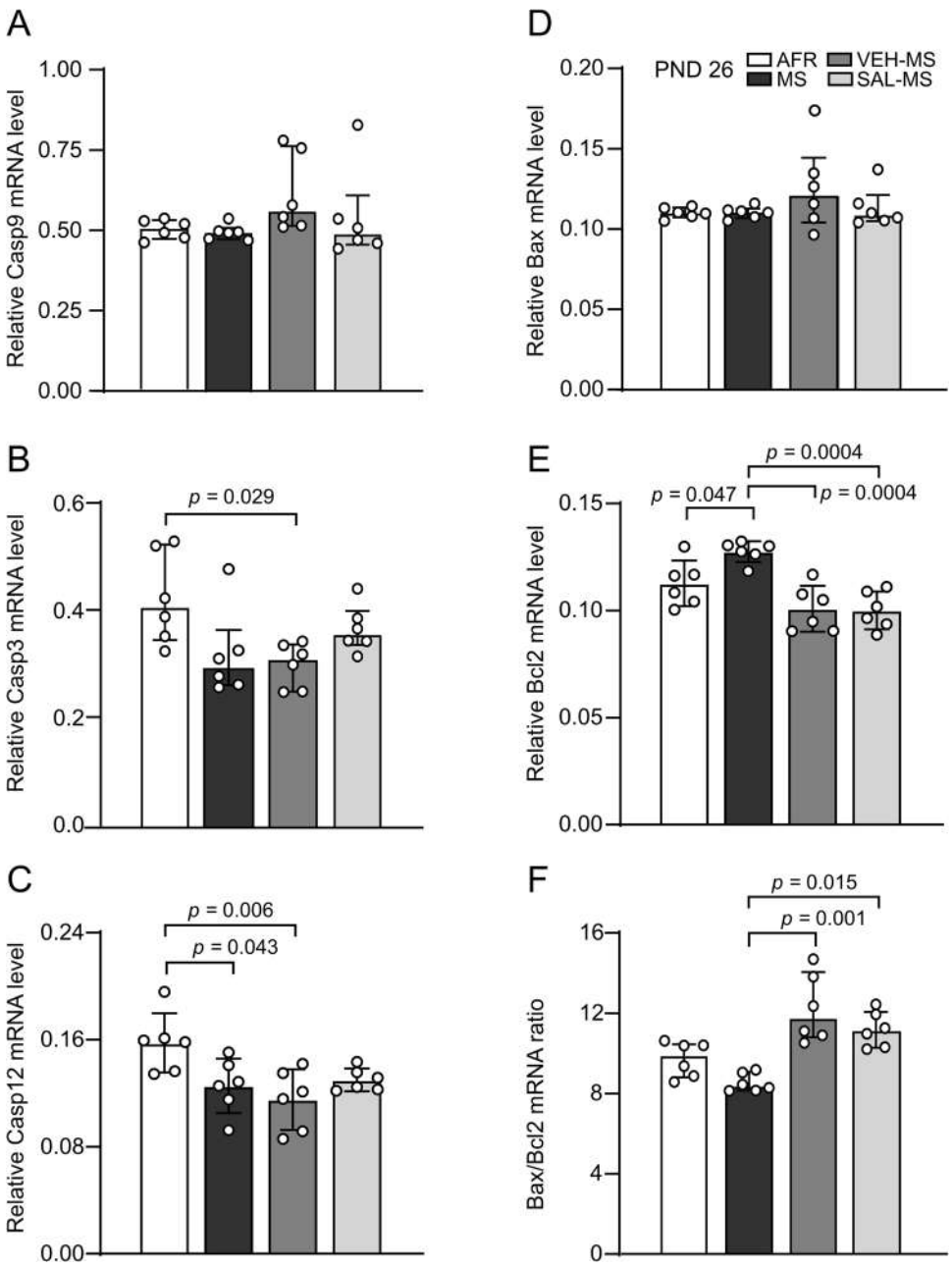

Fig. 8 The effects of MS and early-life SAL/VEH injections on mRNA expression of apoptotic markers in the mPFC of preadolescent rats: Casp9 (**A**), Casp3 (**B**), Casp12 (**C**), Bax (**D**), Bcl2 (**E**), and Bax/Bcl2 mRNA ratio (**F**). The data are presented as the median and IQR (**A**, **B**, **D**, **F**) or mean ± SD (**C**, **E**) and were analyzed by Kruskal–Wallis test or one-way ANOVA, respectively ($n = 6$). Circles represent individual data points. Connectors indicate statistically significant differences between specific experimental groups in Dunn's post hoc test (**B**, **F**) or Tukey's HSD post hoc test (**C**, **E**). *AFR* animal facility rearing, *MS* maternal separation, *PND* postnatal day, *SAL* salubrinal, *VEH* vehicle

that in AFR rats, and this effect was prevented in MS rats by both VEH and SAL injections (Tukey's test) (Fig. 8E). On the other hand, post hoc analysis of the Bax/Bcl2 mRNA ratio revealed that this parameter was similar in AFR and MS rat, but both VEH- and SAL-injected MS rats showed an increased Bax/Bcl2 mRNA ratio compared to MS rats (Dunn's test) (Fig. 8F). However, analysis of the Bax/Bcl2 protein ratio revealed a different effect, namely that both MS and VEH-MS rats showed a lower level of this parameter compared to AFR rats (Kruskal–Wallis test, $H_3 = 11.29$, $N_{1-4} = 6$, $p = 0.010$, followed by Dunn's test) (ESM_3: Fig. S7C). No change in the protein levels of Bax and Bcl2 was observed between the treatment groups (Online Resource ESM_1: Table S1) (Fig. S7A–B).

Finally, we investigated whether repeated MS and SAL/VEH treatment affected the number of neurons and glial cells in specific subregions of the mPFC in preadolescent rats. Statistical analysis revealed that early-life treatment did not have any significant impact on the number of neurons (NeuN-IR), astrocytes (GFAP-IR) or microglial cells (IBA1-IR) in the mPFC of preadolescent rats (results and statistics are presented in Table 5). Representative photomicrographs showing neuronal and glial cells in the subregions of the mPFC of preadolescent rats are presented in Online Resource ESM_5-7.

Table 5 The effects of MS and early-life SAL/VEH treatment on the number of neurons astrocytes and microglial cells in the mPFC of preadolescent rats

Cell marker	mPFC region	Group	Number of IR cells	Statistic
NeuN	Cg1	AFR	685,481.1 ± 59,206.6	$F_{3,18} = 0.20$, $p = 0.896$
		MS	698,794.9 ± 45,376.6	
		VEH-MS	681,216.5 ± 28,241.7	
		SAL-MS	684,556.8 ± 35,757.5	
	PLC	AFR	1,250,600.6 ± 132,051.7	$F_{3,18} = 0.27$, $p = 0.844$
		MS	1,281,136.8 ± 57,292.6	
		VEH-MS	1,252,841.1 ± 64,980.4	
		SAL-MS	1,291,928.6 ± 103,713.6	
	ILC	AFR	288,312.2 (35,984.3)	$H_3 = 0.88$, $p = 0.830$
		MS	275,936.1 (29,923.8)	
		VEH-MS	275,092.7 (7595.9)	
		SAL-MS	281,630.6 (24,893.4)	
GFAP	Cg1	AFR	204,453.6 ± 29,435.2	$F_{3,18} = 0.80$, $p = 0.510$
		MS	200,720.3 ± 37,443.2	
		VEH-MS	189,177.3 ± 11,617.8	
		SAL-MS	181,914.7 ± 26,710.8	
	PLC	AFR	374,166.3 ± 67,722.5	$F_{3,18} = 0.48$, $p = 0.700$
		MS	359,114.3 ± 34,219.7	
		VEH-MS	347,362.8 ± 46,345.4	
		SAL-MS	338,200.3 ± 55,135.5	
	ILC	AFR	120,888.7 ± 18,295.7	$F_{3,18} = 0.47$, $p = 0.704$
		MS	118,740.8 ± 17,268.8	
		VEH-MS	114,362.4 ± 18,440.6	
		SAL-MS	108,330.1 ± 21,168.5	
IBA1	Cg1	AFR	212,681.4 ± 26,186.8	$F_{3,18} = 0.61$, $p = 0.616$
		MS	202,346.7 ± 13,552.4	
		VEH-MS	197,790.9 ± 19,641.8	
		SAL-MS	200,501.6 ± 15,313.6	
	PLC	AFR	319,342.3 ± 29,654.3	$F_{3,18} = 0.23$, $p = 0.872$
		MS	323,430.3 ± 31,567.8	
		VEH-MS	310,514.0 ± 46,495.7	
		SAL-MS	326,914.1 ± 30,180.7	
	ILC	AFR	73,607.2 ± 9470.6	$F_{3,18} = 0.19$, $p = 0.902$
		MS	76,013.2 ± 6420.1	
		VEH-MS	73,424.5 ± 5295.1	
		SAL-MS	73,042.3 ± 6925.9	

Data indicate the numbers of IR cells per region estimated by stereological method (the mean ± SD or median (IQR), $n = 5$–6). *AFR* animal facility rearing, *Cg1* cingulate cortex, *ILC* infralimbic cortex, *IQR* interquartile range, *IR* immunoreactive, *mPFC* medial prefrontal cortex, *MS* maternal separation, *PLC* prelimbic cortex, *PND* postnatal day, *SAL* salubrinal, *VEH* vehicle

The effects of MS and early-life SAL/VEH injections on the anxiety-like behavior of preadolescent and adult rats in the light/dark box test

The next goal of our study was to investigate the effects of early-life MS and SAL/VEH treatment on the behavioral phenotypes of both preadolescent and adult rats. We started by assessing anxiety-like behaviors in the light/dark box test. The experimental procedure for the light/dark exploration applied in the present study has been previously tested in adolescent (PND 35) [10] and adult rats [30]. Nevertheless, this specific procedure when performed on PND 26 in preadolescent rats induced a very high level of anxiety in the light compartment. For example, preadolescent AFR rats on average spent only 2.4% of a trial time (14.5 s) in the light compartment, and the distance traveled in the light compartment represented only 5.7% of the total distance traveled during the entire session (Fig. 9A–B). The average number of transitions between dark and light compartments was 2.6 for AFR rats (Fig. 9C). However,

Kruskal–Wallis test followed by Dunn's test revealed that VEH- and SAL-injected MS rats were significantly less fearful during this light/dark exploration procedure than AFR rats (Online Resource ESM_1: Table S2) (Fig. 9). Specifically, VEH-MS and SAL-MS preadolescent rats spent more time in the light compartment than AFR rats ($H_3 = 11.97$, $N_{1-4} = 10$, $p = 0.007$) (Fig. 9A). Additionally, they traveled a longer distance in the light compartment than the AFR rats ($H_3 = 12.87$, $N_{1-4} = 10$, $p = 0.005$) (Fig. 9B). There was also a trend toward a greater number of transitions between light and dark compartments for VEH-MS rats compared to AFR rats ($H_3 = 8.58$, $N_{1-4} = 10$, $p = 0.035$, post hoc: $p = 0.084$) (Fig. 9C).

In adulthood, statistical analysis also revealed a significant effect of early-life treatment on the time spent in the light compartment ($F_{3,45} = 4.51$, $p = 0.007$, ANOVA) and the distance traveled in the light compartment ($H_3 = 12.83$, $p = 0.005$) but not on the number of transitions between compartments ($H_3 = 6.0$, $N_1 = 15$, $N_2 = 10$, $N_{3-4} = 12$, $p = 0.112$, Kruskal–Wallis test) (Fig. 9D–F). Adult MS rats showed a trend toward less fearful behavior during the light/dark exploration test than AFR rats (Fig. 9D–E), which is in agreement with our previous studies [8, 30]. However, in

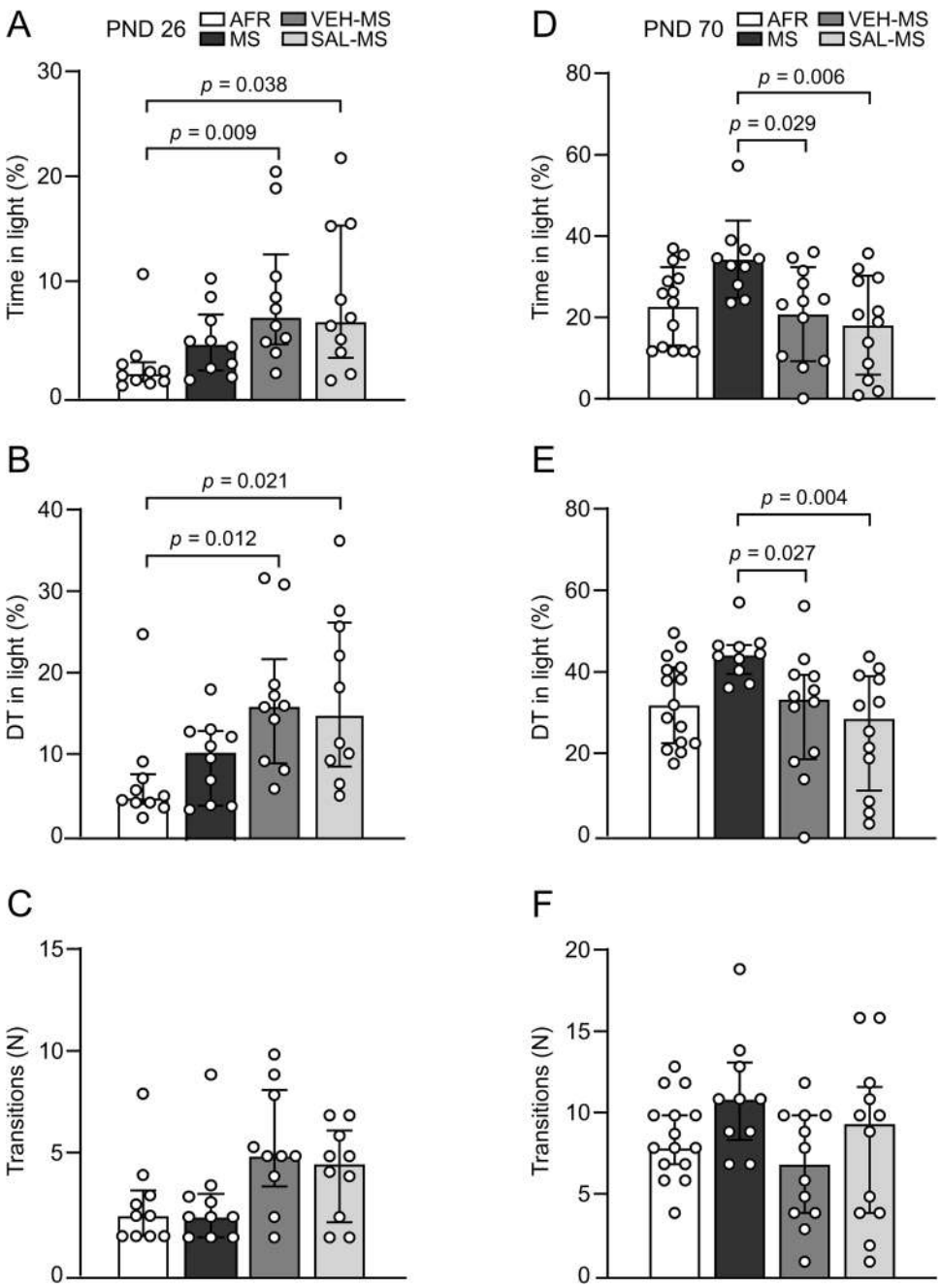

Fig. 9 The effects of MS and early-life SAL/VEH injections on anxiety-like behavior of preadolescent (**A**–**C**) and adult rats (**D**–**F**) in the light/dark box test. Intensity of anxiety-like behavior was assessed as the time spent in the light side (**A**, **D**) and distance traveled in the light side (**B**, **E**) (both expressed as the percentage of the entire session) and the number of transitions between the dark and light sides (**C**, **F**). The data are presented as the median and IQR (**A**–**C**, **E**, **F**) or mean ± SD (**D**) and were analyzed by Kruskal–Wallis test or one-way ANOVA, respectively ($n = 10 - 15$). Circles represent individual data points. Connectors indicate statistically significant differences between specific experimental groups in Dunn's post hoc test (**A**, **B**, **E**) or Tukey's HSD post hoc test (**D**). *AFR* animal facility rearing, *DT* distance traveled, *MS* maternal separation, *PND* postnatal day, *SAL* salubrinal, *VEH* vehicle

this experiment we did not observe statistical significance in a post hoc analysis (for the time in light: $p = 0.093$; for the distance traveled: $p = 0.082$). Nevertheless, we did observe a statistically significant effect when we performed a single comparison between the AFR and MS groups (for the time in light: $t_{23} = 2.65$, $p = 0.014$; for the distance traveled: $U = 31$, $N_1 = 15$, $N_2 = 10$, $p = 0.016$). Interestingly, both VEH-MS and SAL-MS adult rats showed more fearful behavior compared to MS rats but not AFR rats. Notably, they spent less time in the light compartment than MS rats (Tukey's test) (Fig. 9D). They also traveled a shorter distance in the light compartment than the MS rats (Dunn's test) (Fig. 9E).

The effects of MS and early-life SAL/VEH injections on fear conditioning and memory in preadolescent and adult rats

On PND 26, preadolescent rats underwent the FC procedure. Statistical analysis of freezing behavior during the acquisition/training session (Day 1, context A) revealed a lack of a significant effect of early-life treatment (one-way ANOVA, $F_{3,40} = 1.82$, $p = 0.160$) (Online Resource ESM_1: Table S2) (Fig. 10A). However, when the expression of CFC was analyzed (Day 2, context A), we observed that MS rats showed reduced freezing in response to context A compared to AFR rats ($F_{3,40} = 4.20$, $p = 0.011$, ANOVA followed by Tukey's test) (Fig. 10B). The behavior of VEH-MS and SAL-MS rats did not differ significantly from MS rats (for VEH-MS: $p = 0.162$; for SAL-MS: $p = 0.654$) or AFR rats (for VEH-MS: $p = 0.689$; for SAL-MS: $p = 0.156$, Tukey's test). Additionally, there was no significant effect of early-life treatment on the expression of AFC (Day 2, context B) in preadolescent rats ($H_3 = 2.91$, $N_1 = 14$, $N_{2-4} = 10$, $p = 0.405$, Kruskal–Wallis test) (Fig. 10C).

Six weeks after the FC training, the same animals were once again tested in both contexts A and B for the recall of fear memories in adulthood (Table 3). Statistical analysis of freezing behavior revealed a lack of a significant effect of early-life treatment on CFC ($H_3 = 4.14$, $p = 0.246$) and AFC memory recall in adult rats ($H_3 = 1.63$, $N_1 = 14$, $N_{2-4} = 10$, $p = 0.653$, Kruskal–Wallis test) (Online Resource ESM_4: Fig. S8A–B).

Seven days later, all animals underwent a session of retraining of FC in context A. Retraining followed the same procedure as training during preadolescence (Day 1 of experiment) (Table 3). On the following day, fear memory was tested both in contexts A and B (the same sessions as on Day 2 during preadolescence). One way ANOVA of freezing behavior during retraining of FC did not show any differences between experimental groups ($F_{3,40} = 0.99$, $p = 0.406$) (Fig. 10D). Interestingly, in our analysis of the CFC expression after retraining in adulthood we observed that MS rats showed increased freezing in response to context A compared to AFR rats ($F_{3,40} = 3.28$, $p = 0.031$, ANOVA followed by Tukey's test) (Table S2) (Fig. 10E). Additionally, VEH injections significantly reduced freezing behavior in MS rats. The SAL-MS rats did not differ significantly from the MS rats ($p = 0.115$), VEH-MS ($p = 0.979$) or AFR rats ($p = 0.996$) in their CFC expression after retraining in adulthood (Tukey's test) (Fig. 10E). Additionally, there was no significant effect of early-life treatment on the expression of AFC after retraining in adulthood (in context B) ($F_{3,40} = 1.92$, $p = 0.141$, ANOVA) (Fig. 10F).

The effects of MS and early-life SAL/VEH injections on sucrose preference in preadolescent and adult rats

To study anhedonic-like behaviors, we first applied the sucrose preference test in preadolescent rats, and then, six weeks later, the same animals were retested for sucrose preference when they approached adulthood (PND 70).

Statistical analysis of sucrose preference during the preadolescence period revealed a significant effect of early-life treatment (one-way ANOVA, $F_{3,36} = 3.82$, $p = 0.018$) (Online Resource ESM_1: Table S2). Specifically, MS rats showed reduced sucrose preference compared to AFR rats (Fig. 11A) (Tukey's test). The behavior of VEH-MS and SAL-MS rats did not differ significantly from MS rats (for VEH-MS: $p = 0.770$; for SAL-MS: $p = 0.743$) or AFR rats (for VEH-MS: $p = 0.117$; for SAL-MS: $p = 0.129$, Tukey's test) (Fig. 11A). There was no difference in sucrose preference between the treatment groups in adulthood (Kruskal–Wallis test, $H_3 = 0.21$, $N_{1-4} = 10$, $p = 0.996$) (Fig. 11B).

The effects of MS and early-life SAL/VEH injections on novelty- and amphetamine-induced locomotor activity in preadolescent and adult rats

The next goal of the study was to determine whether early-life treatment affected the locomotor activity of rats in response to novelty and amphetamine injections. Analysis of novelty-induced locomotion in preadolescent rats revealed that VEH-injected MS rats traveled a greater distance than MS rats ($F_{3,36} = 2.91$, $p = 0.047$, ANOVA followed by Tukey's test) (Online Resource ESM_1: Table S2) (Fig. 12A). A mixed-design ANOVA of amphetamine-induced locomotion during preadolescence showed the significant effects of early-life treatment ($F_{3,36} = 3.53$, $p = 0.024$) and amphetamine injection ($F_{1,36} = 338.20$, $p < 0.0001$) on PND 26 and a significant interaction between these factors ($F_{3,36} = 3.68$, $p = 0.021$). In all experimental groups, amphetamine injection enhanced locomotor activity compared to VEH injection (Tukey's test) (Fig. 12B). Moreover, MS rats showed greater amphetamine-induced locomotor activity than AFR

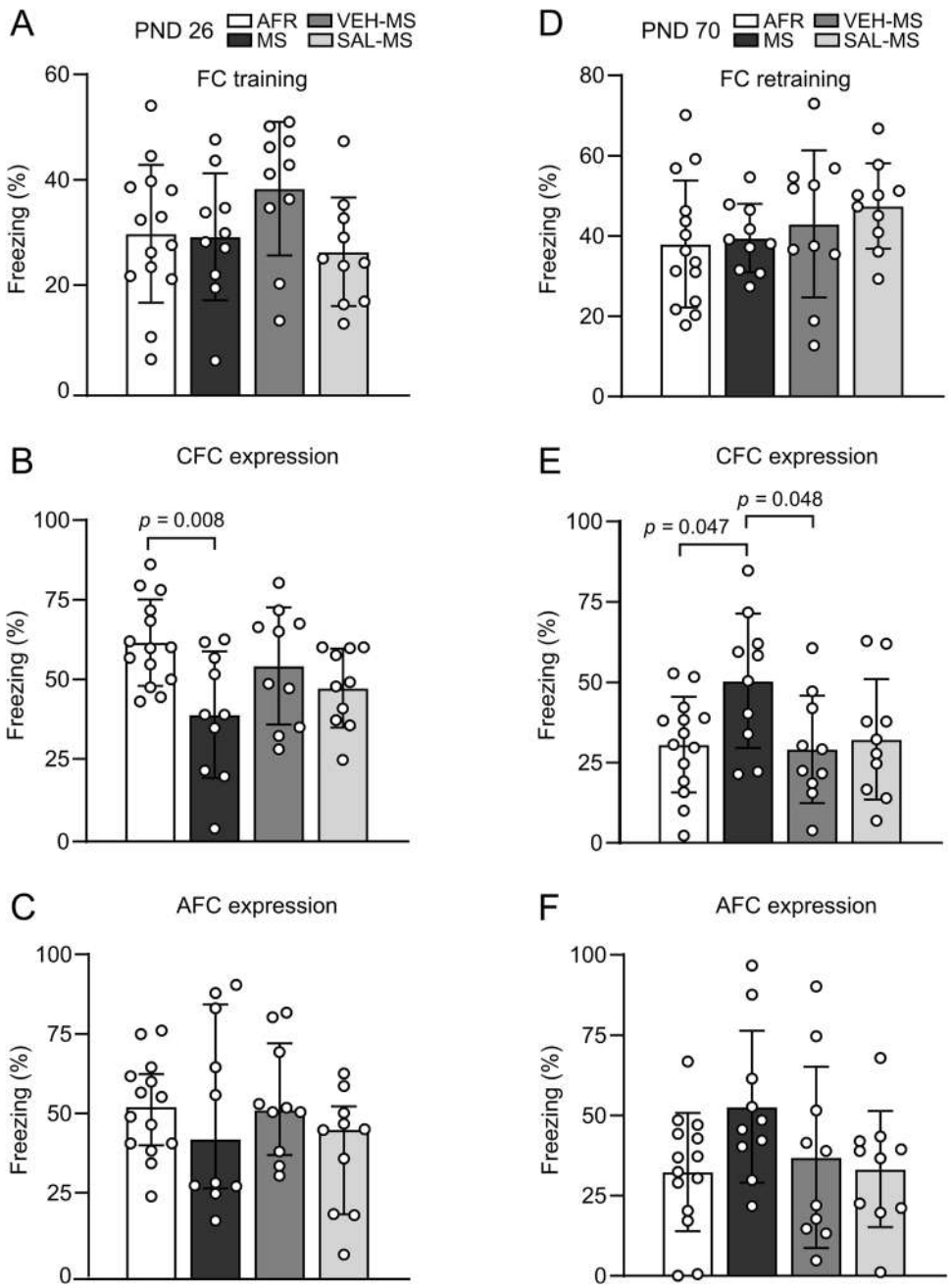

Fig. 10 The effects of MS and early-life SAL/VEH injections on fear conditioning and memory in preadolescent (**A**–**C**) and adult rats (**D**–**F**). The data are presented as the mean ± SD (**A**, **B**, **D**–**F**) or median and IQR (**C**) and expressed as a percentage of the session time ($n = 10$–14). Results were analyzed by one-way ANOVA or Kruskal–Wallis test, respectively. Circles represent individual data points. Connectors indicate statistically significant differences between specific experimental groups in Tukey's HSD post hoc test. *AFC* auditory fear conditioning, *AFR* animal facility rearing, *CFC* contextual fear conditioning, *FC* fear conditioning, *MS* maternal separation, *PND* postnatal day, *SAL* salubrinal, *VEH* vehicle

rats, and this effect was prevented by early-life VEH and SAL treatment (Tukey's test) (Fig. 12B).

After six weeks, the same groups of rats were retested for locomotor activity when they approached adulthood (PND 70) (Fig. 12C). A mixed-design ANOVA of amphetamine-induced locomotion during adulthood also revealed statistically significant effects of early-life treatment ($F_{3,36} = 7.17$, $p = 0.0007$) and amphetamine injection ($F_{1,36} = 203.27$, $p < 0.0001$) as well as a significant interaction between these factors ($F_{3,36} = 7.96$, $p = 0.0003$). In all experimental groups, amphetamine injection enhanced locomotor activity compared to VEH injection (Tukey's test) (Fig. 12C). Additionally, MS and VEH-MS rats showed greater amphetamine-induced locomotion than AFR rats. Moreover, SAL injections reduced amphetamine-triggered locomotor activity in MS rats (Tukey's test) (Fig. 12C).

A search for a permanent imprint of MS and early-life SAL/VEH treatment on ER stress, the UPR and apoptosis in the mPFC

To determine whether MS and early-life SAL/VEH treatment left a permanent imprint on the expression of ER stress, UPR and apoptosis markers in the mPFC, we measured expression levels of relevant mRNA in adult rats.

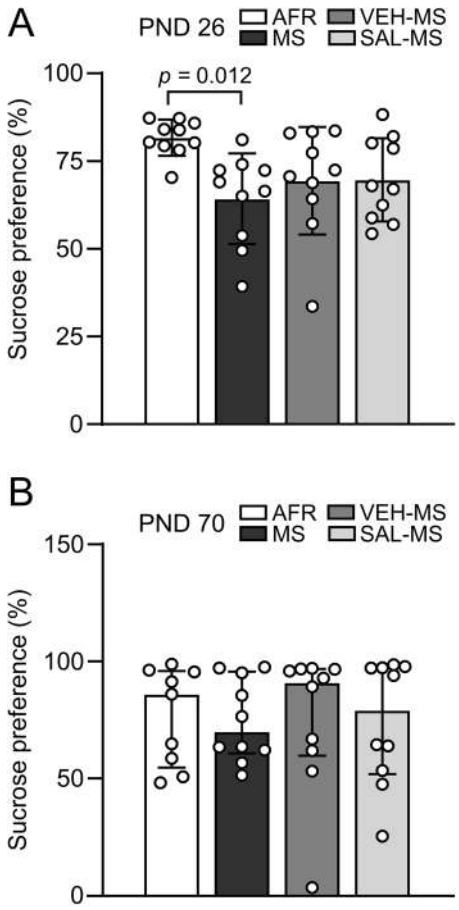

Fig. 11 The effects of MS and early-life SAL/VEH injections on sucrose preference in preadolescent (**A**) and adult rats (**B**). The data are presented as the mean ± SD (**A**) or median and IQR (**B**) and were analyzed by one-way ANOVA or Kruskal–Wallis test, respectively ($n = 10$). Circles represent individual data points. Connector indicates statistically significant difference between specific experimental groups in Tukey's HSD post hoc test. *AFR* animal facility rearing, *MS* maternal separation, *PND* postnatal day, *SAL* salubrinal, *VEH* vehicle

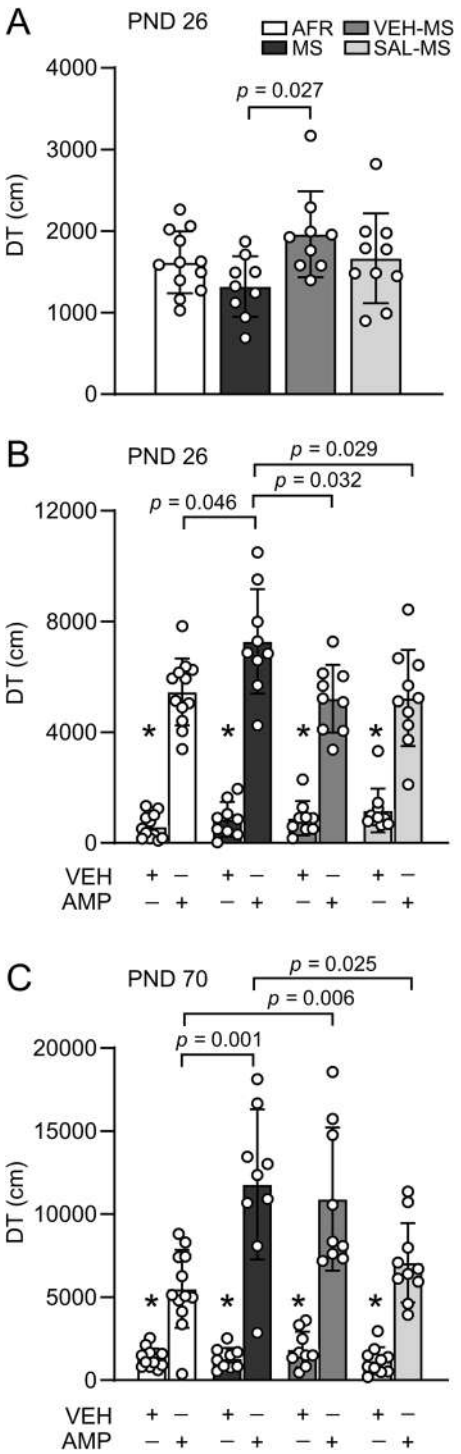

Fig. 12 The effects of MS and early-life SAL/VEH injections on locomotor activity: novelty-induced locomotion in preadolescents (**A**), amphetamine (AMP)-induced locomotor activity in preadolescents (**B**) and adults (**C**). The data are presented as the mean ± SD ($n = 10$–14) and expressed as distance traveled during the specific session. Results were analyzed by mixed-design ANOVA. Circles represent individual data points. *$p < 0.01$ vs. AMP in corresponding early-life treatment group (Tukey's HSD post hoc test). Connectors indicate other statistically significant differences between specific experimental groups in Tukey's test. *AFR* animal facility rearing, *AMP* amphetamine, *DT* distance traveled, *MS* maternal separation, *PND* postnatal day, *SAL* salubrinal, *VEH* vehicle

Statistical analysis revealed that among ER stress and UPR markers, only the expression of Eif2a was significantly affected by early-life treatment (one-way ANOVA: $F_{3,20} = 4.07$, $p = 0.021$) (all results and statistics are presented in Table 6). Specifically, SAL-injected MS rats showed lower Eif2a mRNA levels than AFR rats. A similar trend was also observed in VEH-injected MS rats, though it was not statistically significant ($p = 0.059$) (Tukey's test) (Table 6).

Analysis of the effect of early-life treatment on the expression of apoptotic markers showed statistical significance only in the case of caspase-9 ($F_{3,20} = 4.20$, $p = 0.019$) and Bcl2 mRNA expression ($F_{3,20} = 4.71$, $p = 0.012$, ANOVA) (Table 6). Specifically, both SAL- and VEH-injected MS rats had greater levels of caspase-9 mRNA compared to AFR rats (Tukey's test). Additionally, SAL-MS rats showed increased

Table 6 The effects of MS and early-life SAL/VEH treatment on mRNA expression of ER stress, UPR and apoptosis markers in the mPFC of adult rats

Gene	Group	Relative mRNA level	Statistic
Hspa5	AFR	0.1622 ± 0.0071	$F_{3,20} = 1.74$, $p = 0.190$
	MS	0.1618 ± 0.0072	
	VEH-MS	0.1534 ± 0.0134	
	SAL-MS	0.1512 ± 0.0127	
Eif2ak3	AFR	0.0222 ± 0.0019	$F_{3,20} = 3.00$, $p = 0.055$
	MS	0.0206 ± 0.0012	
	VEH-MS	0.0211 ± 0.0016	
	SAL-MS	0.0231 ± 0.0014	
Ern1	AFR	0.00420 (0.0005)	$H_3 = 3.99$, $p = 0.262$
	MS	0.00440 (0.0004)	
	VEH-MS	0.00404 (0.0004)	
	SAL-MS	0.00463 (0.0008)	
Atf6	AFR	0.0312 (0.0074)	$H_3 = 4.73$, $p = 0.193$
	MS	0.0305 (0.0015)	
	VEH-MS	0.0307 (0.0022)	
	SAL-MS	0.0324 (0.0032)	
Eif2a	AFR	0.0116 ± 0.0010	**$F_{3,20} = 4.07$, $p = 0.021$**
	MS	0.0106 ± 0.0009	
	VEH-MS	0.0091 ± 0.0013	
	SAL-MS	0.0088 ± 0.0025*	
Casp9	AFR	0.0161 ± 0.0011	**$F_{3,20} = 4.20$, $p = 0.019$**
	MS	0.0175 ± 0.0009	
	VEH-MS	0.0181 ± 0.0018*	
	SAL-MS	0.0182 ± 0.0005*	
Casp3	AFR	0.00105 (0.0002)	$H_3 = 3.85$, $p = 0.278$
	MS	0.00093 (0.0004)	
	VEH-MS	0.00093 (0.0001)	
	SAL-MS	0.00104 (0.0001)	
Casp12	AFR	0.00010 (0.00011)	$H_3 = 5.93$, $p = 0.115$
	MS	0.00010 (0.00003)	
	VEH-MS	0.00008 (0.00002)	
	SAL-MS	0.00015 (0.00012)	
Bax	AFR	0.0506 (0.0028)	$H_3 = 7.43$, $p = 0.069$
	MS	0.0474 (0.0018)	
	VEH-MS	0.0406 (0.0048)	
	SAL-MS	0.0463 (0.0040)	
Bcl2	AFR	0.0042 ± 0.0002	**$F_{3,20} = 4.71$, $p = 0.012$**
	MS	0.0043 ± 0.0004	
	VEH-MS	0.0039 ± 0.0004	
	SAL-MS	0.0046 ± 0.0002$^{\#}$	

The mRNA expression was determined by RT-qPCR and presented as relative values of mRNA levels in arbitrary units. The data are presented as the mean ± SD or median (IQR), $n = 6$. Statistically significant effects are given in bold. *$p < 0.05$ vs. AFR, $^{\#}p < 0.05$ vs. VEH-MS (Tukey's HSD post hoc test). *AFR* animals facility rearing, *ER* endoplasmic reticulum, *IQR* interquartile range, *mPFC* medial prefrontal cortex, *MS* maternal separation, *SAL* salubrinal, *UPR* unfolded protein response, *VEH* vehicle

Bcl2 expression compared with VEH-MS rats (Tukey's test) (Table 6).

Finally, we analyzed the effect of early-life MS and SAL/VEH treatment on the number of neurons and glial cells in the mPFC of adult rats. Representative photomicrographs showing NeuN-IR neurons, GFAP-IR astrocytes and IBA1-IR microglial cells in the subregions of the mPFC of adult rats are presented in Online Resource ESM_8–10. Statistical analysis revealed that early-life treatment significantly affected the number of microglial cells but not the other populations of analyzed cells (all results and statistics are presented in Table 7). Notably, SAL-injected MS rats had a lower number of IBA1-IR microglial cells than MS and AFR rats in the PLC region ($F_{3,20} = 4.01$, $p = 0.022$, one-way ANOVA followed by Tukey's test). Moreover, in the Cg1 region of the mPFC, SAL-MS rats also had a lower number of microglial cells than AFR rats ($F_{3,20} = 3.47$, $p = 0.035$, ANOVA followed by Tukey's test) (Table 7).

Discussion

The main goal of the present study was to investigate whether ER stress and UPR processes are affected by the MS procedure and thereby underlie the cellular and behavioral consequences of ELS. We found that MS enhanced the activation of the UPR in juveniles to a small degree and modulated the mRNA expression of a few apoptotic markers in the mPFC of juveniles and preadolescents but not in adults. However, MS did not affect the numbers of neurons or glial cells in the mPFC at any age. Both early-life SAL and VEH injections (often in a treatment-specific manner) affected the expression of UPR and apoptotic markers, especially in juvenile and preadolescent MS rats, and in some cases prevented MS-induced effects at the biochemical level. Moreover, SAL/VEH generally mitigated the behavioral effects of MS.

The effects of MS procedure on ER stress and UPR processes and apoptosis in the mPFC

Enhanced expression and activation of ER stress and UPR markers have been observed in animal models of depression based on chronic stress procedures in adults [27–29] and in different acute stress models [53, 54]. Moreover, the infusion of tunicamycin, an activator of the UPR, into the hippocampus produces a depressive-like phenotype in rats [55]. We have recently shown that MS produces long-lasting upregulation of chaperones HSPA5 and HSPA1B in the brain and blood, which suggests that ELS may influence ER stress and UPR processes throughout development [30]. To the best of our knowledge, the present study is the first to comprehensively examine the role of ER stress and UPR processes

Table 7 The effects of MS and early-life SAL/VEH treatment on the number of neurons astrocytes and microglial cells in the mPFC of adult rats

Cell marker	mPFC region	Group	Number of IR cells	Statistic
NeuN	Cg1	AFR	610,968.1 ± 29,926.0	$F_{3,20} = 1.54$, $p = 0.236$
		MS	573,292.1 ± 50,768.4	
		VEH-MS	573,422.1 ± 28,788.9	
		SAL-MS	585,200.9 ± 24,677.5	
	PLC	AFR	1,164,797.7 ± 77,242.8	$F_{3,20} = 1.06$, $p = 0.386$
		MS	1,148,378.2 ± 69,778.6	
		VEH-MS	1,123,820.5 ± 48,786.8	
		SAL-MS	1,100,882.2 ± 66,967.7	
	ILC	AFR	225,567.6 ± 11,134.5	$F_{3,20} = 0.94$, $p = 0.442$
		MS	221,745.4 ± 13,552.3	
		VEH-MS	215,989.6 ± 16,123.5	
		SAL-MS	214,057.7 ± 12,151.9	
GFAP	Cg1	AFR	173,806.4 (22,206.7)	$H_3 = 6.31$, $p = 0.097$
		MS	175,147.5 (57,261.2)	
		VEH-MS	208,999.4 (50,311.9)	
		SAL-MS	177,485.1 (22,710.1)	
	PLC	AFR	350,950.1 (46,224.9)	$H_3 = 3.39$, $p = 0.335$
		MS	387,533.7 (126,461.1)	
		VEH-MS	379,827.4 (77,912.9)	
		SAL-MS	373,984.3 (33,948.9)	
	ILC	AFR	104,831.6 ± 10,104.6	$F_{3,20} = 2.88$, $p = 0.061$
		MS	118,909.7 ± 18,272.5	
		VEH-MS	124,738.9 ± 13,458.0	
		SAL-MS	107,309.7 ± 11,342.5	
IBA1	Cg1	AFR	103,190.2 ± 5918.0	**$F_{3,20} = 3.47$, $p = 0.035$**
		MS	98,219.3 ± 7121.3	
		VEH-MS	94,696.7 ± 9686.7	
		SAL-MS	88,517.6 ± 9156.4*	
	PLC	AFR	175,265.5 ± 7211.8	**$F_{3,20} = 4.01$, $p = 0.022$**
		MS	173,557.7 ± 16,899.1	
		VEH-MS	165,775.0 ± 12,457.6	
		SAL-MS	154,006.0 ± 8281.9*#	
	ILC	AFR	40,693.6 ± 3630.7	$F_{3,20} = 3.06$, $p = 0.052$
		MS	40,061.2 ± 3470.1	
		VEH-MS	37,174.0 ± 4103.3	
		SAL-MS	35,219.0 ± 3023.6	

Data indicate the numbers of IR cells per region estimated by stereological method (the mean ± SD or median (IQR), $n = 6$). Statistically significant effects are given in bold. $^{*}p < 0.05$ vs. AFR, $^{\#}p < 0.05$ vs. MS (Tukey's HSD post hoc test). *AFR* animal facility rearing, *Cg1* cingulate cortex, *ILC* infralimbic cortex, *IQR* interquartile range, *IR* immunoreactive, *mPFC* medial prefrontal cortex, *MS* maternal separation, *PLC* prelimbic cortex, *PND* postnatal day, *SAL* salubrinal, *VEH* vehicle

in ELS-induced effects. We once again confirmed that MS increased the protein expression of HSPA5 in the mPFC of juveniles on PND 15, which is 24 h after the last MS. MS also increased the phosphorylation (activation) of one of the ER stress sensors, IRE1α, in juveniles. These effects were temporal, and we generally did not observe any MS-induced changes in the expression of ER stress or UPR markers in the mPFC of preadolescents and adults. Concurrently, in this study, we observed subtle changes in the mRNA expression of apoptotic markers in MS juveniles and preadolescents but not in adults. Specifically, the expression of Casp12 was increased in juveniles and decreased in preadolescent MS rats. Casp12 is a specific caspase that is localized in the ER membrane and engaged in the ER stress-induced pathway of apoptosis [56]. We also observed an MS-induced increase in the mRNA expression of Bcl2 in preadolescents. These subtle changes in the expression of UPR and apoptotic markers were not accompanied by any changes in the numbers

of neurons, astrocytes or microglial cells in the mPFC of preadolescent or adult MS rats. These results are in contrast to our previous observations in adolescent rats (on PND 35), in which we found a clear delay in neurodevelopmental apoptosis, manifested as increased numbers of neurons in the mPFC and antiapoptotic trends in the expression and activation of apoptotic markers [10]. Thus, our results suggest that adolescence is a developmental period that specifically unveils the effects of ELS on neurodevelopmental apoptosis of the mPFC [10, 37]. This is not surprising, because during adolescence, the mPFC undergoes intensive structural and functional reorganization [32, 34]. Nevertheless, we expected that the effects of MS would be manifested even earlier, in preadolescence period, but our biochemical results did not support that hypothesis. However, in the present study we did observe some behavioral effects of MS in the preadolescence period, such as a decrease in sucrose preference (anhedonia-like behavior) and an impairment in CFC expression. Moreover, MS-triggered enhancement of the locomotor response to psychostimulant drugs, a typical behavioral phenotype observed in ELS models [39, 57, 58], was also observed in preadolescents. This behavioral effect was the only enduring effect observed also in adult MS rats. Additionally, MS rats showed an increased CFC expression after retraining in adulthood. It is worth noting that the mPFC is highly implicated both in the expression of FC [59] and psychostimulant-induced hyperlocomotion [60]. Taken together, the results showed that, although we did not detect a strong impact of MS on ER stress, the UPR and apoptosis in the mPFC of juveniles and preadolescents, MS did produce long-lasting functional consequences observed at behavioral level even during preadolescence period. Our study implicates that MS procedure may influence ER stress and the UPR in an age-specific manner and manifest its strongest effects on the abovementioned processes in different developmental time points than that chosen for the present experiment. However, we should bear in mind that the studied behaviors are also regulated by many other cellular mechanisms and brain regions.

The effects of early-life modulation of ER stress and the UPR by SAL/VEH treatment on biochemical and behavioral phenotype of MS rats

To modulate ER stress and UPR processes in MS rats, we applied repeated early-life treatment with SAL before each MS procedure. SAL is a small-molecule inhibitor of eIF2α phosphatases that prolongs eIF2α phosphorylation at residue S51 and thereby its inactivation, which causes an inhibition of general protein synthesis. SAL has been shown to reduce cell death and have neuroprotective properties in animal models of neurodegenerative disorders [13, 61], cerebral ischemia [43] and traumatic brain injury [42, 62]. In the present study, we also used conventional solvent/vehicle injections (VEH) to adequately control experimental conditions. Interestingly, early-life VEH treatment by itself affected the studied parameters and sometimes produced similar effects to SAL treatment. This phenomenon greatly complicated understanding and interpretation of the results. Both VEH and SAL treatments prevented some MS-induced effects. For example, SAL treatment decreased Bcl2 mRNA levels in preadolescent rats and dampened amphetamine-induced hyperlocomotion in preadolescents and adults (SAL-MS vs. MS rats). VEH injections prevented the effects of MS at the level of Casp12 and Bcl2 transcription in juveniles and preadolescents, respectively. At behavioral level, VEH treatment also reduced amphetamine-triggered locomotor activity in preadolescent MS rats and CFC expression in MS adult rats (VEH-MS vs. MS rats). In many cases, when MS rats resembled AFR rats at the biochemical level, SAL or VEH significantly modulated the mRNA expression of ER stress, UPR and apoptosis markers especially in juvenile and preadolescent MS rats. For example, SAL- and/or VEH-MS rats generally showed reduced mRNA expression of many ER stress and UPR markers when compared to MS rats. The results suggest that both VEH and SAL treatment exerted inhibitory influence on ER stress and UPR processes in MS rats.

At the behavioral level, in sucrose preference or CFC tests, SAL- and VEH-MS preadolescent rats exhibited intermediate behavioral phenotypes between AFR and MS rats (not significantly different from either AFR and MS rats), and those phenotypes turned out to be advantageous in the specific experimental conditions of this study.

The effect of SAL/VEH on anxiety-like behaviors in the light/dark box test is also worth noting. Interestingly, preadolescent SAL-MS and VEH-MS rats were less anxious than AFR rats. On the other hand, in adulthood, SAL and VEH normalized the behavior of MS rats, which showed a statistically insignificant trend toward less fearful (impulsive-like) behavior. However, when a single comparison between the AFR and MS groups was performed, the analysis revealed that MS significantly enhanced impulsive-like behavior in adults, which is in line with our previous studies [8, 30]. Interestingly, Logstdon et al. reported that SAL treatment reduced impulsive-like behaviors in adult rats subjected to traumatic brain injury [42, 62]. Whereas, Jangra et al. showed that other ER stress inhibitor, the chemical chaperone sodium phenylbutyrate, abrogated anxiety- and depressive-like behaviors in adult mice subjected to chronic restraint stress [27]. It is worth emphasizing that, in contrast to the abovementioned studies, we injected SAL/VEH during the early-life period, and the behavioral consequences of that treatment were observed at later developmental stages, even in adulthood.

Our results concerning SAL/VEH action in our experimental paradigm lead to the question of whether SAL treatment exerted a specific biological effect as an inhibitor of eIF2α dephosphorylation, promoting the inhibition of global translation. Some data evidently supported the specific action of SAL in our experiment. Namely, 24 h after the last separation in juveniles, the mRNA and protein expression of eIF2α was significantly lower in SAL-MS rats than in MS rats. These results may indicate that some kind of compensation or adaptation to repeated SAL injections and to an inhibition of eIF2α activity occurred. Interestingly, in adulthood, SAL-MS rats still showed low levels of Eif2a expression, though this effect was statistically significant only when compared to AFR rats. Although we did not observe an increase in eIF2α phosphorylation after SAL treatment in MS juveniles, this result was not surprising because MS by itself did not induce activation/phosphorylation of PERK or eIF2α. However, it is important to note that PERK is not the only kinase that phosphorylates eIF2α [63]. Additionally, although eIF2α phosphorylation attenuates general translation, it simultaneously promotes translation of specific proteins, such as activating transcription factor 4 (ATF4). ATF4 is known to activate the transcription of the regulatory subunit of protein phosphatase 1, also known as growth arrest and DNA damage-inducible protein GADD34, to generate active eIF2α phosphatase and initiate a feedback loop to dephosphorylate eIF2α and consequently restore general protein synthesis. This feedback loop in the regulation of eIF2α phosphorylation is the main concern associated with the use of SAL and other eIF2α phosphatase inhibitors in the clinic and in animal models because it limits the duration of their action [13]. Searching for another evidence for the specific action of SAL, it is worth noting a decrease in the number of microglial cells in the PLC of SAL-MS adult rats compared to MS and AFR rats. This interesting observation needs further studies. It is well known that ER stress and the UPR are key regulators of inflammation and function of immune cells in the periphery and brain [11, 14, 15]. Early-life SAL treatment could potentially influence the rate of postnatal proliferation and/or apoptosis of microglial cells.

Enduring biological action of early-life VEH injections: a pitfall and challenge for controlling of experimental conditions

It is well known that routine laboratory procedures such as animal handling and injections involve some level of mild to moderate physical and psychological stress. Acute procedures usually activate the hypothalamic–pituitary–adrenal axis and increase the levels of glucocorticoids, whereas chronic interventions lead to a desensitization of this response with time [64–66]. Therefore, in pharmacological studies, solvent/vehicle injections are commonly used to control experimental conditions. However, growing amount of data has accumulated and shown that both acute and chronic VEH injections not only modulate serum glucocorticoids levels but also affect animal behavior [64, 65, 67]. For example, single *ip* injections of saline produced anxiogenic effect in mice [66]. A recent study also demonstrated that repeated saline injections for 6 weeks (starting during the adolescent period) increased anxiety-like behaviors, decreased systemic inflammation, and increased corticosterone reactivity and microglial activation in the dentate gyrus of the hippocampus [67]. However, when saline treatment was combined with additional stress (social isolation), it did not worsen and even improved some effects produced by chronic stress [67]. A similar trend was observed in our study. It has been argued that exposure to moderate but not minimal or substantial amounts of stressors, especially during the perinatal period, may facilitate coping with other environmental challenges later in life. This phenomenon is known as stress inoculation [68, 69]. In the case of our study, we have a combination of two early-life stressors (MS and VEH/SAL injections) that turned out to be beneficial for MS rats and produced a more resilient phenotype in preadolescents and adults. Our study suggests that a modulation of ER stress and UPR processes may underlie the injection-triggered changes in animal behavior, especially when injections are applied during a critical period of early-life development. However, it is worth underlining that we studied the effects of VEH treatment only in stressed subjects and not in control (AFR) animals.

We cannot also overlook in our discussion a potential biological action of the solvent/vehicle used in our experiments, 2.5% DMSO diluted in PBS and given in a dose of 0.125 µl of DMSO per gram of body weight. We chose DMSO as a vehicle for SAL based on a large amount of previous data in the literature [42, 43, 70]. DMSO is routinely used in biological research as a solvent and a cryopreservative in bone marrow and organ transplants. However, data have accumulated showing that DMSO may produce both adverse and beneficial effects on brain tissue [71–75]. A small dose of 0.2 µl/g given for 5 days to juvenile rats has been shown to lead to global changes in the brain metabolome and increase oxidative stress and proteolysis markers. However, only higher doses of DMSO (2 and 4 µl/g) have been shown to affect rat behavior, i.e., decreased social habits [75]. Another group demonstrated that DMSO (0.3–10 µl/g) produced widespread apoptosis in the developing brain [73]. Nevertheless, in the above-cited studies, DMSO was injected in undiluted form (~ 100%) and at higher doses than our VEH treatment. On the other hand, DMSO has also been shown to have neuroprotective and procognitive properties in animal models of ischemia, cerebral hypoperfusion and Alzheimer's disease [71, 72, 74]. It has been argued that the neuroprotective effects of DMSO may be linked to its anti-inflammatory

and free radical scavenging activities [72, 76]. To the best of our knowledge, only one study showed that DMSO modulated (increased) the expression of UPR genes, including Hspa5, though in mouse embryos and in the context of the cytotoxic effects of DMSO [77].

Unfortunately, based on the results presented in our study, we cannot explicitly determine whether the effects produced by VEH/SAL treatments in MS rats are specifically related to the action of SAL or DMSO or the procedure of repeated injections during the early-life period. The results show how unpredictable the effects of repeated VEH injections can be in the early-life period. However, we can at least state that early-life VEH/SAL treatment modulated ER stress and UPR processes in MS rats to some extent. Although, SAL/VEH treatment did not leave a permanent imprint on the expression of ER stress and UPR markers in the mPFC of MS adults, it promoted resilience at the behavioral level in both preadolescent and adult rats.

Recently, it has been argued that ER stress and the UPR, next to oxidative stress and hormonal regulation, may play a role in mediating inter- and intraspecific variations in response to different environmental conditions and, in this way, may shape susceptibility or resilience to stressors [78]. ER stress and the UPR are evolutionarily conserved and heritable cellular processes. There are also considerable individual variations in ER stress and UPR phenotypes in humans and nonhuman animals, suggesting that these phenotypes can be subjected to natural selection [78, 79]. Strong individual variations in ER stress and UPR phenotypes may be, to some degree, responsible for the relatively small changes in the expression of ER stress and UPR markers observed in our experimental paradigm, which involved Wistar outbred rats. Nevertheless, these small changes may better reflect the situation in naturally existing populations.

The main limitation of the present study was that we did not include female subjects in the whole experiment and analysis and not explore sex differences in ER stress and UPR signaling. However, our pilot study of the mRNA expression of UPR and apoptotic markers showed that females were less affected by MS procedure and early-life SAL/VEH treatment than males. It is generally in line with our previous reports showing that in many aspects female rats are more resilient to MS procedure conducted in our laboratory [8, 9, 40].

The role of ER stress and UPR signaling in the pathophysiology of ELS-related diseases: potential clinical implications

Epidemiological and clinical studies clearly show that ELS not only increases the risk of mental disorders but also physical health problems, such as metabolic syndrome that may lead to cardiovascular diseases and type 2 diabetes [80, 81]. Recently, broadscale attempts to identify causative mechanisms linking ELS to psycho-cardio-metabolic multimorbidity have been started [82]. We hypothesize that ER stress and UPR processes may potentially represent shared molecular pathways and mechanisms by which ELS affects both mental and physical health. ER stress and UPR signaling acts in most cells and tissues and has been implicated in the pathophysiology of numerous diseases, such as cancer, diabetes, atherosclerosis, neurodegenerative diseases [15, 16, 83], as well as MDD and BD [17–22]. Interestingly, all the above mentioned diseases have evident inflammatory components and ER stress and UPR processes are known to regulate inflammatory response [11, 14, 15, 84–86]. In the present study we applied a systemic SAL administration, therefore this inhibitor of ER stress could potentially affect not only the brain but also other organs and systems. Further multiorgan studies are needed to confirm the hypothesis that ER stress and UPR signaling can be implicated in the pathophysiology of ELS-related diseases or the phenomenon of resilience.

Many pharmacological strategies targeting different components of UPR signaling for disease intervention have been tested in preclinical and clinical studies [12, 87]. They include chemical chaperones and small-molecule activators or inhibitors of the UPR, such as SAL [13, 87] The most promising strategies concern the treatment of cancer and cardiovascular and neurodegenerative disorders [87, 88]. However, UPR-targeting drugs are non-selective and their potential administration to the patients with a history of ELS and multimorbidity is rather unlikely. Nevertheless, the key players in ER stress and the UPR can be at least potential candidate biomarkers of ELS-related changes, measured in blood or peripheral organ biopsy samples and help to diagnose ELS-induced multimorbidity [12]. UPR biomarkers have been already used to monitor progression of cancer, kidney disease, neurodegenerative diseases [12, 89]. It is worth mentioning that we previously showed that MS procedure caused enduring upregulation of Hspa5 expression in the blood that was accompanied by impulsive- and depressive-like behavior in male adult rats [30].

Conclusions

We found that MS did not exert a strong impact on ER stress and UPR processes or apoptosis at developmental stages under study. However, both early-life SAL and VEH treatment (often in an injection-specific manner) influenced the expression of UPR and apoptotic markers, especially in juvenile and preadolescent MS rats, and in some cases prevented MS-induced effects at the biochemical level. Moreover, SAL and/or VEH alleviated some behavioral effects of MS in both preadolescent and adult rats. These results suggest that a

regulation of ER stress and UPR processes may play a potential role in the mechanisms of susceptibility or resilience to ELS and other environmental factors. Further multiorgan studies are needed to validate this interesting hypothesis in future.

Supplementary Information The online version contains supplementary material available at https://doi.org/10.1007/s43440-023-00456-6.

Author contributions ASA: conception and design, acquisition of data, analysis and interpretation of data, drafting the manuscript, final approval of the version to be published; IMM: acquisition of data, analysis and interpretation of data, critical revision, final approval of the version to be published; JK: acquisition of data, analysis and interpretation of data, critical revision, final approval of the version to be published; AC: conception and design, acquisition and interpretation of data, critical revision, final approval of the version to be published.

Funding This work was supported by grant Opus 2017/25/B/NZ7/00174 from the National Science Centre, Poland to AC.

Data availability statement The datasets generated during and/or analyzed during the current study are available from the corresponding author on reasonable request.

Declarations

Conflict of interest The authors declare that the research was conducted in the absence of any commercial or financial relationships that could be construed as a potential conflict of interest.

References

1. Green JG, McLaughlin KA, Berglund PA, Gruber MJ, Sampson NA, Zaslavsky AM, et al. Childhood adversities and adult psychiatric disorders in the national comorbidity survey replication I: associations with first onset of DSM-IV disorders. Arch Gen Psychiatry. 2010;67:113–23.
2. Smith KE, Pollak SD. Early life stress and development: potential mechanisms for adverse outcomes. J Neurodev Disord. 2020;12:34.
3. Teicher MH, Samson JA, Anderson CM, Ohashi K. The effects of childhood maltreatment on brain structure, function and connectivity. Nat Rev Neurosci. 2016;17:652–66.
4. Agorastos A, Pervanidou P, Chrousos GP, Baker DG. Developmental trajectories of early life stress and trauma: a narrative review on neurobiological aspects beyond stress system dysregulation. Front Psychiatry. 2019;10:118.
5. Noll JG, Shalev I. The biology of early life stress, understanding child maltreatment and trauma. Berlin: Springer; 2018.
6. Italia M, Forastieri C, Longaretti A, Battaglioli E, Rusconi F. Rationale, relevance, and limits of stress-induced psychopathology in rodents as models for psychiatry research: an introductory overview. Int J Mol Sci. 2020;21:7455.
7. Vetulani J. Early maternal separation: a rodent model of depression and a prevailing human condition. Pharmacol Rep. 2013;65:1451–61.
8. Chocyk A, Majcher-Maslanka I, Przyborowska A, Mackowiak M, Wedzony K. Early-life stress increases the survival of midbrain neurons during postnatal development and enhances reward-related and anxiolytic-like behaviors in a sex-dependent fashion. Int J Dev Neurosci. 2015;44:33–47.
9. Chocyk A, Dudys D, Przyborowska A, Majcher I, Mackowiak M, Wedzony K. Maternal separation affects the number, proliferation and apoptosis of glia cells in the substantia nigra and ventral tegmental area of juvenile rats. Neuroscience. 2011;173:1–18.
10. Majcher-Maslanka I, Solarz A, Chocyk A. Maternal separation disturbs postnatal development of the medial prefrontal cortex and affects the number of neurons and glial cells in adolescent rats. Neuroscience. 2019;423:131–47.
11. Hetz C, Papa FR. The unfolded protein response and cell fate control. Mol Cell. 2018;69:169–81.
12. Almanza A, Carlesso A, Chintha C, Creedican S, Doultsinos D, Leuzzi B, et al. Endoplasmic reticulum stress signaling—from basic mechanisms to clinical applications. FEBS J. 2019;286:241–78.
13. Fullwood MJ, Zhou W, Shenolikar S. Targeting phosphorylation of eukaryotic initiation factor-2alpha to treat human disease. Prog Mol Biol Transl Sci. 2012;106:75–106.
14. Kitamura M. The unfolded protein response triggered by environmental factors. Semin Immunopathol. 2013;35:259–75.
15. Chaudhari N, Talwar P, Parimisetty A, Lefebvre d'Hellencourt C, Ravanan P. A molecular web: endoplasmic reticulum stress, inflammation, and oxidative stress. Front Cell Neurosci. 2014;8:213.
16. Tabas I. The role of endoplasmic reticulum stress in the progression of atherosclerosis. Circ Res. 2010;107:839–50.
17. Kakiuchi C, Ishiwata M, Nanko S, Kunugi H, Minabe Y, Nakamura K, et al. Functional polymorphisms of HSPA5: possible association with bipolar disorder. Biochem Biophys Res Commun. 2005;336:1136–43.
18. Le-Niculescu H, Balaraman Y, Patel SD, Ayalew M, Gupta J, Kuczenski R, et al. Convergent functional genomics of anxiety disorders: translational identification of genes, biomarkers, pathways and mechanisms. Transl Psychiatry. 2011;1: e9.
19. Yang R, Daigle BJ Jr, Muhie SY, Hammamieh R, Jett M, Petzold L, et al. Core modular blood and brain biomarkers in social defeat mouse model for post traumatic stress disorder. BMC Syst Biol. 2013;7:80.
20. Nevell L, Zhang K, Aiello AE, Koenen K, Galea S, Soliven R, et al. Elevated systemic expression of ER stress related genes is associated with stress-related mental disorders in the Detroit Neighborhood Health Study. Psychoneuroendocrinology. 2014;43:62–70.
21. Yoshino Y, Dwivedi Y. Elevated expression of unfolded protein response genes in the prefrontal cortex of depressed subjects: effect of suicide. J Affect Disord. 2020;262:229–36.
22. Kowalczyk M, Kowalczyk E, Kwiatkowski P, Lopusiewicz L, Talarowska M, Sienkiewicz M. Cellular response to unfolded proteins in depression. Life (Basel). 2021;11:1376.
23. Bown C, Wang JF, MacQueen G, Young LT. Increased temporal cortex ER stress proteins in depressed subjects who died by suicide. Neuropsychopharmacology. 2000;22:327–32.

24. Pfaffenseller B, Wollenhaupt-Aguiar B, Fries GR, Colpo GD, Burque RK, Bristot G, et al. Impaired endoplasmic reticulum stress response in bipolar disorder: cellular evidence of illness progression. Int J Neuropsychopharmacol. 2014;17:1453–63.
25. Bengesser SA, Fuchs R, Lackner N, Birner A, Reininghaus B, Meier-Allard N, et al. Endoplasmic reticulum stress and bipolar disorder—almost forgotten therapeutic drug targets in the unfolded protein response pathway revisited. CNS Neurol Disord Drug Targets. 2016;15:403–13.
26. Suliman M, Schmidtke MW, Greenberg ML. The role of the UPR pathway in the pathophysiology and treatment of bipolar disorder. Front Cell Neurosci. 2021;15: 735622.
27. Jangra A, Sriram CS, Dwivedi S, Gurjar SS, Hussain MI, Borah P, et al. Sodium phenylbutyrate and edaravone abrogate chronic restraint stress-induced behavioral deficits: implication of oxido-nitrosative, endoplasmic reticulum stress cascade, and neuroinflammation. Cell Mol Neurobiol. 2017;37:65–81.
28. Tang J, Yu W, Chen S, Gao Z, Xiao B. Microglia polarization and endoplasmic reticulum stress in chronic social defeat stress induced depression mouse. Neurochem Res. 2018;43:985–94.
29. Li MX, Li Q, Sun XJ, Luo C, Li Y, Wang YN, et al. Increased Homer1-mGluR5 mediates chronic stress-induced depressive-like behaviors and glutamatergic dysregulation via activation of PERK-eIF2alpha. Prog Neuropsychopharmacol Biol Psychiatry. 2019;95: 109682.
30. Solarz A, Majcher-Maslanka I, Kryst J, Chocyk A. A search for biomarkers of early-life stress-related psychopathology: focus on 70-kDa heat shock proteins. Neuroscience. 2021;463:238–53.
31. Godin JD, Creppe C, Laguesse S, Nguyen L. Emerging roles for the unfolded protein response in the developing nervous system. Trends Neurosci. 2016;39:394–404.
32. Selemon LD. A role for synaptic plasticity in the adolescent development of executive function. Transl Psychiatry. 2013;3: e238.
33. Willing J, Juraska JM. The timing of neuronal loss across adolescence in the medial prefrontal cortex of male and female rats. Neuroscience. 2015;301:268–75.
34. Caballero A, Granberg R, Tseng KY. Mechanisms contributing to prefrontal cortex maturation during adolescence. Neurosci Biobehav Rev. 2016;70:4–12.
35. Juraska JM, Drzewiecki CM. Cortical reorganization during adolescence: What the rat can tell us about the cellular basis. Dev Cogn Neurosci. 2020;45: 100857.
36. Myers-Schulz B, Koenigs M. Functional anatomy of ventromedial prefrontal cortex: implications for mood and anxiety disorders. Mol Psychiatry. 2012;17:132–41.
37. Chocyk A, Bobula B, Dudys D, Przyborowska A, Majcher-Maslanka I, Hess G, et al. Early-life stress affects the structural and functional plasticity of the medial prefrontal cortex in adolescent rats. Eur J Neurosci. 2013;38:2089–107.
38. Chocyk A, Przyborowska A, Makuch W, Majcher-Maslanka I, Dudys D, Wedzony K. The effects of early-life adversity on fear memories in adolescent rats and their persistence into adulthood. Behav Brain Res. 2014;264:161–72.
39. Chocyk A, Przyborowska A, Dudys D, Majcher I, Mackowiak M, Wedzony K. The impact of maternal separation on the number of tyrosine hydroxylase-expressing midbrain neurons during different stages of ontogenesis. Neuroscience. 2011;182:43–61.
40. Solarz A, Majcher-Maslanka I, Kryst J, Chocyk A. Early-life stress affects peripheral, blood-brain barrier, and brain responses to immune challenge in juvenile and adult rats. Brain Behav Immun. 2022;108:1–15.
41. Solarz A, Majcher-Maslanka I, Chocyk A. Effects of early-life stress and sex on blood-brain barrier permeability and integrity in juvenile and adult rats. Dev Neurobiol. 2021;81:861–76.
42. Logsdon AF, Turner RC, Lucke-Wold BP, Robson MJ, Naser ZJ, Smith KE, et al. Altering endoplasmic reticulum stress in a model of blast-induced traumatic brain injury controls cellular fate and ameliorates neuropsychiatric symptoms. Front Cell Neurosci. 2014;8:421.
43. Nakka VP, Gusain A, Raghubir R. Endoplasmic reticulum stress plays critical role in brain damage after cerebral ischemia/reperfusion in rats. Neurotox Res. 2010;17:189–202.
44. Li B, Zani A, Lee C, Zani-Ruttenstock E, Zhang Z, Li X, et al. Endoplasmic reticulum stress is involved in the colonic epithelium damage induced by maternal separation. J Pediatr Surg. 2016;51:1001–4.
45. Livak KJ, Schmittgen TD. Analysis of relative gene expression data using real-time quantitative PCR and the 2(-Delta Delta C(T)) Method. Methods. 2001;25:402–8.
46. Majcher-Maslanka I, Solarz A, Wedzony K, Chocyk A. Previous early-life stress modifies acute corticosterone-induced synaptic plasticity in the medial prefrontal cortex of adolescent rats. Neuroscience. 2018;379:316–33.
47. Majcher-Maslanka I, Solarz A, Chocyk A. The impact of early-life stress on corticosteroid carrier protein levels and 11beta-hydroxysteroid dehydrogenase 1 expression in adolescent rats. Pharmacol Rep. 2019;71:347–50.
48. Paxinos G, Watson C. The rat brain in stereotaxic coordinates. Cambridge: Academic Press; 1998.
49. West MJ, Slomianka L, Gundersen HJ. Unbiased stereological estimation of the total number of neurons in thesubdivisions of the rat hippocampus using the optical fractionator. Anat Rec. 1991;231:482–97.
50. West MJ. Estimating volume in biological structures. Cold Spring Harb Protoc. 2012;2012:1129–39.
51. Bialon M, Chocyk A, Majcher-Maslanka I, Zarnowska M, Michalski K, Antkiewicz-Michaluk L, et al. 1MeTIQ and olanzapine, despite their neurochemical impact, did not ameliorate performance in fear conditioning and social interaction tests in an MK-801 rat model of schizophrenia. Pharmacol Rep. 2021;73:490–505.
52. Majcher-Maslanka I, Solarz A, Wedzony K, Chocyk A. The effects of early-life stress on dopamine system function in adolescent female rats. Int J Dev Neurosci. 2017;57:24–33.
53. Ishisaka M, Kudo T, Shimazawa M, Kakefuda K, Oyagi A, Hyakkoku K, et al. Restraint-induced expression of endoplasmic reticulum stress-related genes in the mouse brain. Pharmacol Pharm. 2011;2:10–6.
54. Xie J, Han F, Shi Y. The unfolded protein response is triggered in rat neurons of the dorsal raphe nucleus after single-prolonged stress. Neurochem Res. 2014;39:741–7.
55. Timberlake Ii M, Roy B, Dwivedi Y. A novel animal model for studying depression featuring the induction of the unfolded protein response in hippocampus. Mol Neurobiol. 2019;56:8524–36.
56. Szegezdi E, Fitzgerald U, Samali A. Caspase-12 and ER-stress-mediated apoptosis: the story so far. Ann N Y Acad Sci. 2003;1010:186–94.
57. Rentesi G, Antoniou K, Marselos M, Syrrou M, Papadopoulou-Daifoti Z, Konstandi M. Early maternal deprivation-induced modifications in the neurobiological, neurochemical and behavioral profile of adult rats. Behav Brain Res. 2013;244:29–37.
58. Anier K, Malinovskaja K, Pruus K, Aonurm-Helm A, Zharkovsky A, Kalda A. Maternal separation is associated with DNA methylation and behavioural changes in adult rats. Eur Neuropsychopharmacol. 2014;24:459–68.
59. Sierra-Mercado D, Padilla-Coreano N, Quirk GJ. Dissociable roles of prelimbic and infralimbic cortices, ventral hippocampus, and basolateral amygdala in the expression and extinction of conditioned fear. Neuropsychopharmacology. 2011;36:529–38.

60. Tzschentke TM. Pharmacology and behavioral pharmacology of the mesocortical dopamine system. Prog Neurobiol. 2001;63:241–320.
61. Saxena S, Cabuy E, Caroni P. A role for motoneuron subtype-selective ER stress in disease manifestations of FALS mice. Nat Neurosci. 2009;12:627–36.
62. Logsdon AF, Lucke-Wold BP, Nguyen L, Matsumoto RR, Turner RC, Rosen CL, et al. Salubrinal reduces oxidative stress, neuroinflammation and impulsive-like behavior in a rodent model of traumatic brain injury. Brain Res. 2016;1643:140–51.
63. Moon SL, Sonenberg N, Parker R. Neuronal regulation of eif2alpha function in health and neurological disorders. Trends Mol Med. 2018;24:575–89.
64. Deutsch-Feldman M, Picetti R, Seip-Cammack K, Zhou Y, Kreek MJ. Effects of handling and vehicle injections on adrenocorticotropic and corticosterone concentrations in Sprague-Dawley compared with Lewis rats. J Am Assoc Lab Anim Sci. 2015;54:35–9.
65. Freiman SV, Onufriev MV, Stepanichev MY, Moiseeva YV, Lazareva NA, Gulyaeva NV. The stress effects of a single injection of isotonic saline solution: systemic (blood) and central (frontal cortex and dorsal and ventral hippocampus). Neurochem J. 2016;10:115–9.
66. Lapin IP. Only controls: effect of handling, sham injection, and intraperitoneal injection of saline on behavior of mice in an elevated plus-maze. J Pharmacol Toxicol Methods. 1995;34:73–7.
67. Du Preez A, Law T, Onorato D, Lim YM, Eiben P, Musaelyan K, et al. The type of stress matters: repeated injection and permanent social isolation stress in male mice have a differential effect on anxiety- and depressive-like behaviours, and associated biological alterations. Transl Psychiatry. 2020;10:325.
68. Parker KJ, Buckmaster CL, Hyde SA, Schatzberg AF, Lyons DM. Nonlinear relationship between early life stress exposure and subsequent resilience in monkeys. Sci Rep. 2019;9:16232.
69. Qin X, He Y, Wang N, Zou JX, Zhang YM, Cao JL, et al. Moderate maternal separation mitigates the altered synaptic transmission and neuronal activation in amygdala by chronic stress in adult mice. Mol Brain. 2019;12:111.
70. Gao B, Liu X, Yan Q, Yang R, Jiang T, Zhang X. DMSO-mediated difunctionalization of electron-deficient olefins to access β-hydroxysulfides with high chemoselectivity. Synthesis. 2022;54:2258–66.
71. Farkas E, Institoris A, Domoki F, Mihaly A, Luiten PG, Bari F. Diazoxide and dimethyl sulphoxide prevent cerebral hypoperfusion-related learning dysfunction and brain damage after carotid artery occlusion. Brain Res. 2004;1008:252–60.
72. Bardutzky J, Meng X, Bouley J, Duong TQ, Ratan R, Fisher M. Effects of intravenous dimethyl sulfoxide on ischemia evolution in a rat permanent occlusion model. J Cereb Blood Flow Metab. 2005;25:968–77.
73. Hanslick JL, Lau K, Noguchi KK, Olney JW, Zorumski CF, Mennerick S, et al. Dimethyl sulfoxide (DMSO) produces widespread apoptosis in the developing central nervous system. Neurobiol Dis. 2009;34:1–10.
74. Penazzi L, Lorengel J, Sundermann F, Golovyashkina N, Marre S, Mathis CMB, et al. DMSO modulates CNS function in a preclinical Alzheimer's disease model. Neuropharmacology. 2017;113:434–44.
75. Rabow Z, Morningstar T, Showalter M, Heil H, Thongphanh K, Fan S, et al. Exposure to DMSO during infancy alters neurochemistry, social interactions, and brain morphology in long-evans rats. Brain Behav. 2021;11: e02146.
76. Elisia I, Nakamura H, Cederberg R, Lee L, Lam V, Adomat H, et al. DMSO represses inflammatory cytokine production from human blood cells and reduces autoimmune arthritis. FASEB J. 2015;29:282.
77. Kang M-H, Das J, Gurunathan S, Park H-W, Song H, Park C, et al. The cytotoxic effects of dimethyl sulfoxide in mouse preimplantation embryos: a mechanistic study. Theranostics. 2017;7:4735.
78. Yap KN, Yamada K, Zikeli S, Kiaris H, Hood WR. Evaluating endoplasmic reticulum stress and unfolded protein response through the lens of ecology and evolution. Biol Rev Camb Philos Soc. 2021;96:541–56.
79. Dombroski BA, Nayak RR, Ewens KG, Ankener W, Cheung VG, Spielman RS. Gene expression and genetic variation in response to endoplasmic reticulum stress in human cells. Am J Hum Genet. 2010;86:719–29.
80. Murphy MO, Cohn DM, Loria AS. Developmental origins of cardiovascular disease: impact of early life stress in humans and rodents. Neurosci Biobehav Rev. 2017;74:453–65.
81. Womersley JS, Nothling J, Toikumo S, Malan-Muller S, van den Heuvel LL, McGregor NW, et al. Childhood trauma, the stress response and metabolic syndrome: a focus on DNA methylation. Eur J Neurosci. 2022;55:2253–96.
82. Mariani N, Borsini A, Cecil CAM, Felix JF, Sebert S, Cattaneo A, et al. Identifying causative mechanisms linking early-life stress to psycho-cardio-metabolic multi-morbidity: the EarlyCause project. PLoS ONE. 2021;16: e0245475.
83. Mohan S, Brown L, Ayyappan P. Endoplasmic reticulum stress: a master regulator of metabolic syndrome. Eur J Pharmacol. 2019;860:172553.
84. Miller AH. Beyond depression: the expanding role of inflammation in psychiatric disorders. World Psychiatry. 2020;19:108–9.
85. Hasheminasabgorji E, Jha JC. Dyslipidemia, diabetes and atherosclerosis: role of inflammation and ros-redox-sensitive factors. Biomedicines. 2021;9:1602.
86. Guzman-Martinez L, Maccioni RB, Andrade V, Navarrete LP, Pastor MG, Ramos-Escobar N. Neuroinflammation as a common feature of neurodegenerative disorders. Front Pharmacol. 2019;10:1008.
87. Gonzalez-Teuber V, Albert-Gasco H, Auyeung VC, Papa FR, Mallucci GR, Hetz C. Small molecules to improve ER proteostasis in disease. Trends Pharmacol Sci. 2019;40:684–95.
88. Zhang G, Wang X, Gillette TG, Deng Y, Wang ZV. Unfolded protein response as a therapeutic target in cardiovascular disease. Curr Top Med Chem. 2019;19:1902–17.
89. Li C, Krothapalli S, Chen YM. Targeting endoplasmic reticulum for novel therapeutics and monitoring in acute kidney injury. Nephron. 2022;147:1–4.

Table S1. Results of one-way ANOVA or Kruskal-Wallis test investigating the effects of MS and early-life SAL/VEH treatment on mRNA and protein expression of ER stress, UPR and apoptosis markers in the mPFC of juvenile and preadolescent rats

Parameter	**PND 15** **Statistic**	**PND 26** **Statistic**
Hspa5 mRNA	$\boldsymbol{H_3 = 17.02, p = 0.0007}$	$\boldsymbol{F_{3,20} = 11.23, p < 0.0001}$
HSPA5 protein	$\boldsymbol{F_{3,20} = 3.35, p = 0.039}$	$H_3 = 0.99$, $p = 0.803$
Eif2ak3 mRNA	$F_{3,20} = 1.78$, $p = 0.183$	$F_{3,20} = 1.51$, $p = 0.242$
PERK protein	$F_{3,20} = 1.47$, $p = 0.253$	$F_{3,20} = 0.26$, $p = 0.850$
p-PERK (Thr980) protein	$\boldsymbol{F_{3,20} = 5.93, p = 0.005}$	$H_3 = 0.67$, $p = 0.879$
Ern1 mRNA	$F_{3,20} = 1.70$, $p = 0.200$	$\boldsymbol{F_{3,20} = 11.15, p = 0.0002}$
IRE1α protein	$F_{3,20} = 0.52$, $p = 0.672$	$H_3 = 3.18$, $p = 0.365$
p-IRE1α (S724) protein	$\boldsymbol{F_{3,20} = 3.88, p = 0.024}$	$F_{3,20} = 2.88$, $p = 0.061$
Atf6 mRNA	$F_{3,20} = 1.49$, $p = 0.248$	$\boldsymbol{F_{3,20} = 4.42, p = 0.015}$
ATF protein	$F_{3,20} = 1.57$, $p = 0.229$	$F_{3,20} = 0.90$, $p = 0.459$
Eif2a mRNA	$\boldsymbol{H_3 = 18.83, p = 0.003}$	$H_3 = 1.67$, $p = 0.643$
eIF2α protein	$\boldsymbol{F_{3,20} = 6.10, p = 0.004}$	$F_{3,20} = 1.10$, $p = 0.373$
p-eIF2α (S51) protein	$F_{3,20} = 4.97$, $p = 0.050$	$H_3 = 1.63$, $p = 0.652$
Casp9 mRNA	$\boldsymbol{F_{3,20} = 5.11, p = 0.009}$	$H_3 = 6.76$, $p = 0.080$
Caspase-9 protein	$F_{3,20} = 1.59$, $p = 0.222$	$F_{3,20} = 0.56$, $p = 0.647$
Cleaved caspase-9 protein	$F_{3,20} = 2.09$, $p = 0.135$	$F_{3,20} = 0.49$, $p = 0.693$
Casp3 mRNA	$H_3 = 7.13$, $p = 0.068$	$\boldsymbol{H_3 = 10.82, p = 0.013}$
Cleaved caspase-3 protein	$F_{3,20} = 1.06$, $p = 0.389$	$H_3 = 9.53$, $p = 0.0500$
Casp12 mRNA	$\boldsymbol{F_{3,20} = 5.36, p = 0.007}$	$\boldsymbol{F_{3,20} = 5.26, p = 0.008}$
Caspase-12 protein	$F_{3,20} = 0.62$, $p = 0.061$	$F_{3,20} = 0.47$, $p = 0.708$
Cleaved caspase-12 protein	$F_{3,20} = 0.52$, $p = 0.670$	$F_{3,20} = 0.36$, $p = 0.785$
Bax mRNA	$\boldsymbol{F_{3,20} = 15.34, p < 0.0001}$	$H_3 = 1.32$, $p = 0.724$
Bax protein	$F_{3,20} = 2.72$, $p = 0.072$	$F_{3,20} = 1.79$, $p = 0.189$
Bcl2 mRNA	$F_{3,20} = 2.67$, $p = 0.075$	$\boldsymbol{F_{3,20} = 12.02, p = 0.0001}$
Bcl2 protein	$F_{3,20} = 1.60$, $p = 0.221$	$F_{3,20} = 1.91$, $p = 0.160$
Bax/Bcl2 mRNA	$\boldsymbol{F_{3,20} = 11.29, p < 0.0001}$	$\boldsymbol{H_3 = 16.61, p = 0.0009}$
Bax/Bcl2 protein	$F_{3,20} = 0.51$, $p = 0.679$	$\boldsymbol{H_3 = 11.29, p = 0.010}$

Statistically significant differences are given in bold. *Abbreviations:* mPFC, medial prefrontal cortex; MS, maternal separation; PND, postnatal day; SAL, salubrinal; VEH, vehicle.

Table S2. Results of ANOVA or Kruskal-Wallis test investigating the effects of MS and early-life SAL/VEH treatment on behavioral phenotype of preadolescent and adult rats

Parameter	**PND 26** **Statistic**	**PND 70** **Statistic**
Light/dark box:		
% Time in light	$\boldsymbol{H_3 = 11.97, p = 0.007}$	$\boldsymbol{F_{3,45} = 4.51, p = 0.007}$
% Distance traveled in light	$\boldsymbol{H_3 = 12.87, p = 0.005}$	$\boldsymbol{H_3 = 12.83, p = 0.005}$
Transitions (N)	$\boldsymbol{H_3 = 8.58, p = 0.035}$	$H_3 = 6.0, p = 0.112$
Fear memory:		
FC acquisition	$F_{3,40} = 1.82, p = 0.160$	$F_{3,40} = 0.99, p = 0.406$
CFC expression	$\boldsymbol{F_{3,40} = 4.20, p = 0.011}$	$\boldsymbol{F_{3,40} = 3.28, p = 0.031}$
AFC expression	$H_3 = 2.91, p = 0.405$	$F_{3,40} = 1.92, p = 0.141$
CFC recall	N.A.	$H_3 = 4.14, p = 0.246$
AFC recall	N.A.	$H_3 = 1.63, p = 0.653$
Sucrose preference	$\boldsymbol{F_{3,36} = 3.82, p = 0.018}$	$H_3 = 0.21, p = 0.996$
Novelty-induced locomotion	$\boldsymbol{F_{3,36} = 2.91, p = 0.047}$	N/A
Amphetamine-induced locomotion:		
Effect of early-life treatment	$\boldsymbol{F_{3,36} = 3.53, p = 0.024}$	$\boldsymbol{F_{3,36} = 7.17, p = 0.0007}$
Effect of amphetamine	$\boldsymbol{F_{1,36} = 338.20, p < 0.0001}$	$\boldsymbol{F_{1,36} = 203.27, p < 0.0001}$
Effect of early-life x amphetamine	$\boldsymbol{F_{3,36} = 3.68, p = 0.021}$	$\boldsymbol{F_{3,36} = 7.96, p = 0.0003}$

Statistically significant differences are given in bold. *Abbreviations:* AFC, auditory fear conditioning; CFC, contextual fear conditioning; FC, fear conditioning; MS, maternal separation; N/A; not assessed; PND, postnatal day; SAL, salubrinal; VEH, vehicle.

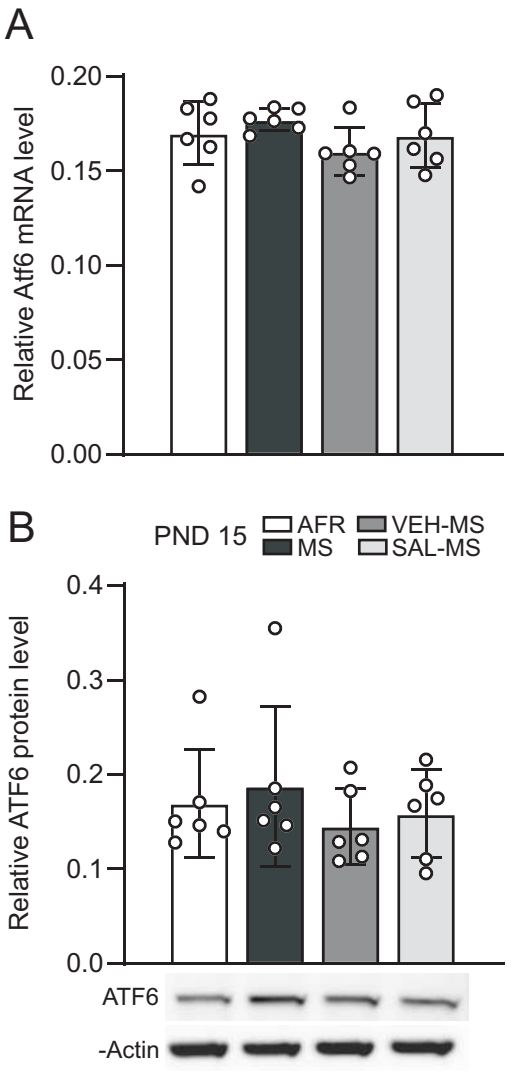

Fig. S1. The effects of MS and early-life SAL/VEH injections on mRNA (A) and protein expression (B) of ER stress sensor ATF6 in the mPFC of juvenile rats. The data are presented as the mean ± SD (*n* = 6) and were analyzed by one-way ANOVA. Circles represent individual data points. Statistical analysis showed no significant differences between experimental groups. *Abbreviations:* AFR, animal facility rearing; MS, maternal separation; PND, postnatal day; SAL, salubrinal; VEH, vehicle.

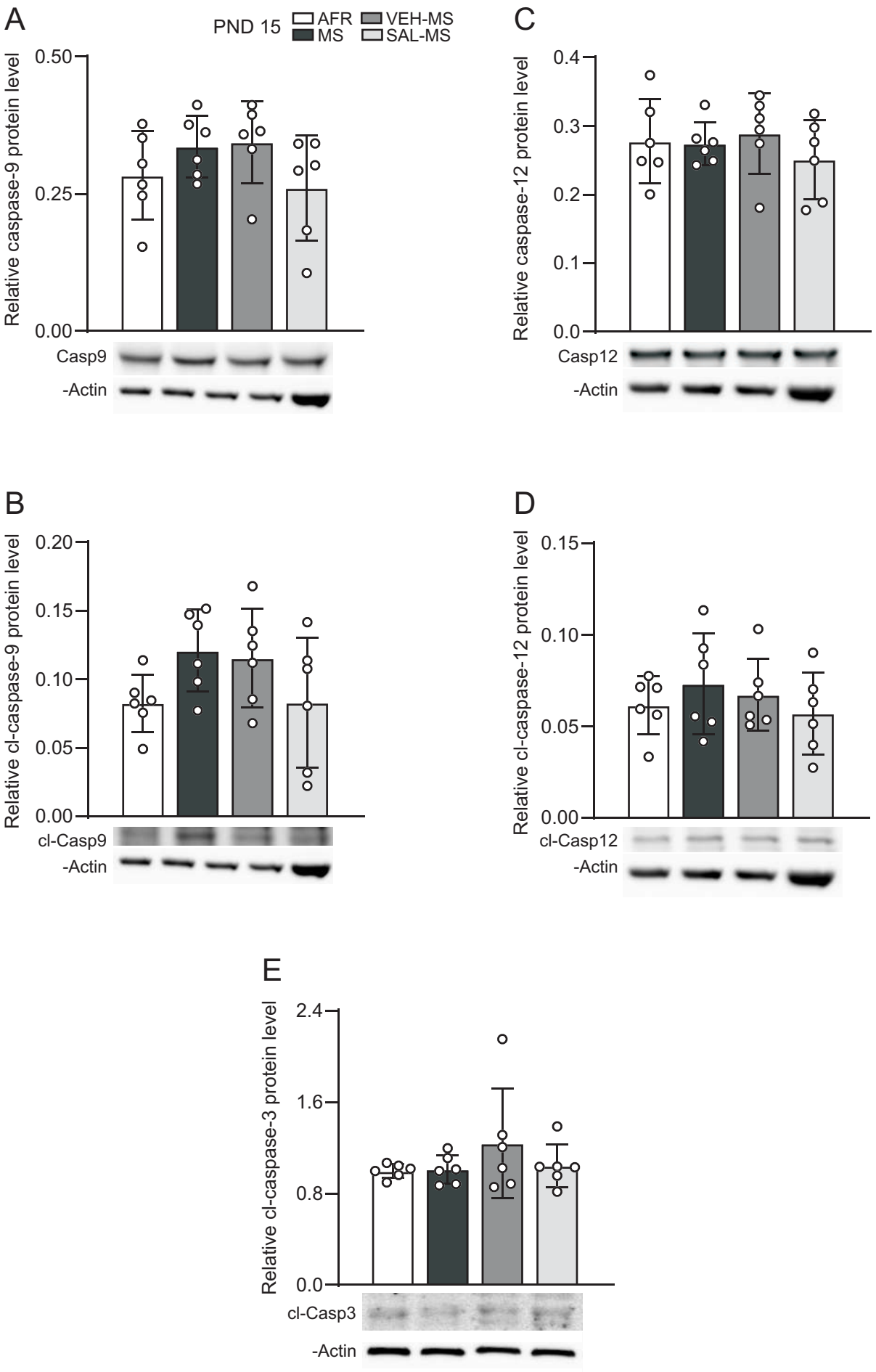

Fig. S2. The effects of MS and early-life SAL/VEH injections on protein expression and cleavage of caspase-9 (A-B), caspase-12 (C-D) and cleavage of caspase-3 (E) in the mPFC of juvenile rats. The data are presented as the mean ± SD (*n* = 6) and were analyzed by one-way ANOVA. Circles represent individual data points. Statistical analysis showed no significant differences between experimental groups. *Abbreviations:* AFR, animal facility rearing; cl, cleaved; MS, maternal separation; PND, postnatal day; SAL, salubrinal; VEH, vehicle.

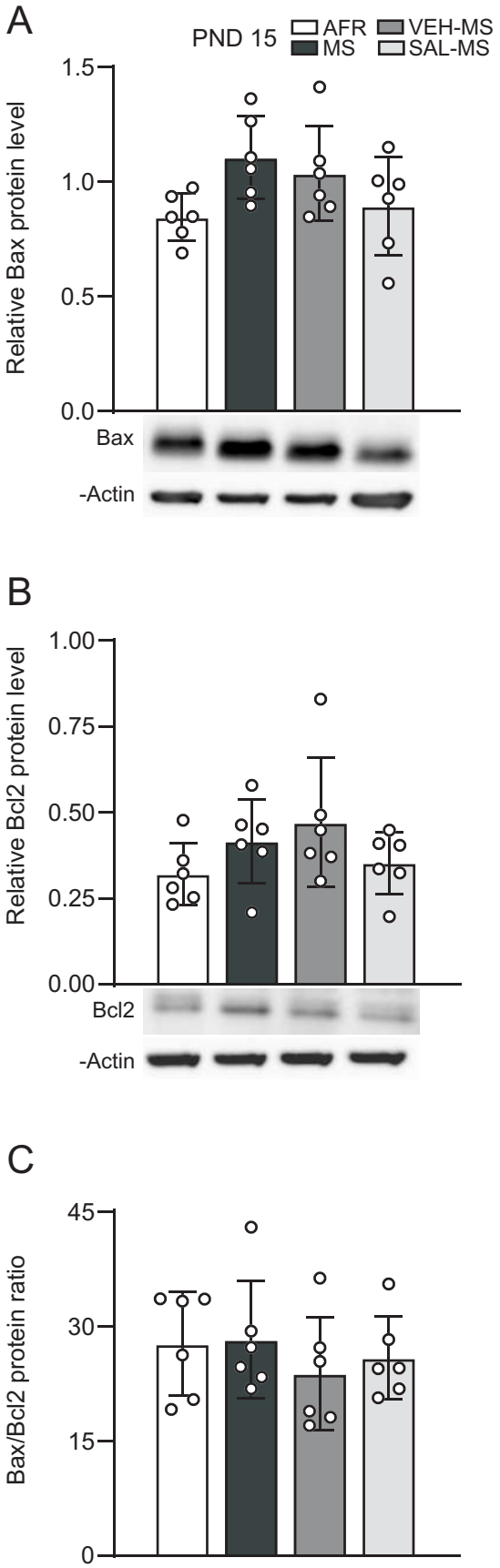

Fig. S3. The effects of MS and early-life SAL/VEH injections on Bax (A) and Bcl2 (B) protein levels and Bax/Bcl2 protein ratio (C) in the mPFC of juvenile rats. The data are presented as the mean ± SD (n = 6) and were analyzed by one-way ANOVA. Circles represent individual data points. Statistical analysis showed no significant differences between experimental groups. The same immunoblot of -Actin was used for normalization of both Bcl2 (B) and ATF6 immunoblots (Fig. S1B). After protein electrotransfer the blots were horizontally cut into appropriate pieces to separately evaluate ATF, -Actin and Bcl2 protein levels from the same samples. *Abbreviations:* AFR, animal facility rearing; MS, maternal separation; PND, postnatal day; SAL, salubrinal; VEH, vehicle.

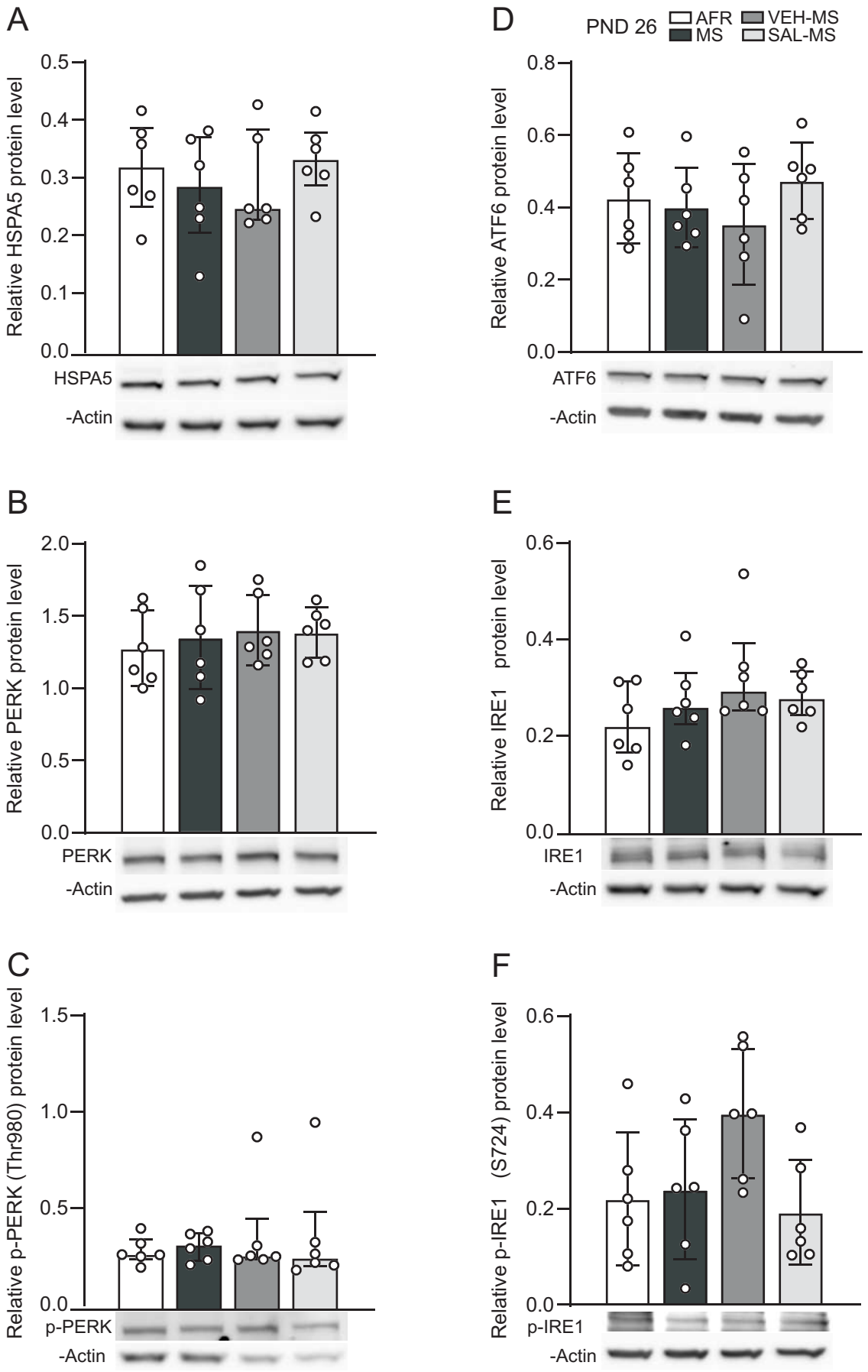

Fig. S4. The effects of MS and early-life SAL/VEH injections on protein expression and activation of ER stress markers in the mPFC of preadolescent rats. (A) HSPA5, (B-C) PERK and p-PERK, (D) ATF6, (E-F) IRE1 and p-IRE1 . The data are presented as the mean ± SD (B, D, F) or median and IQR (A, C, E) and were analyzed by one-way ANOVA or Kruskal-Wallis test, respectively (n = 6). Circles represent individual data points. Statistical analysis showed no significant differences between experimental groups. *Abbreviations:* AFR, animal facility rearing; IQR, interquartile range; MS, maternal separation; PND, postnatal day; SAL, salubrinal; VEH, vehicle.

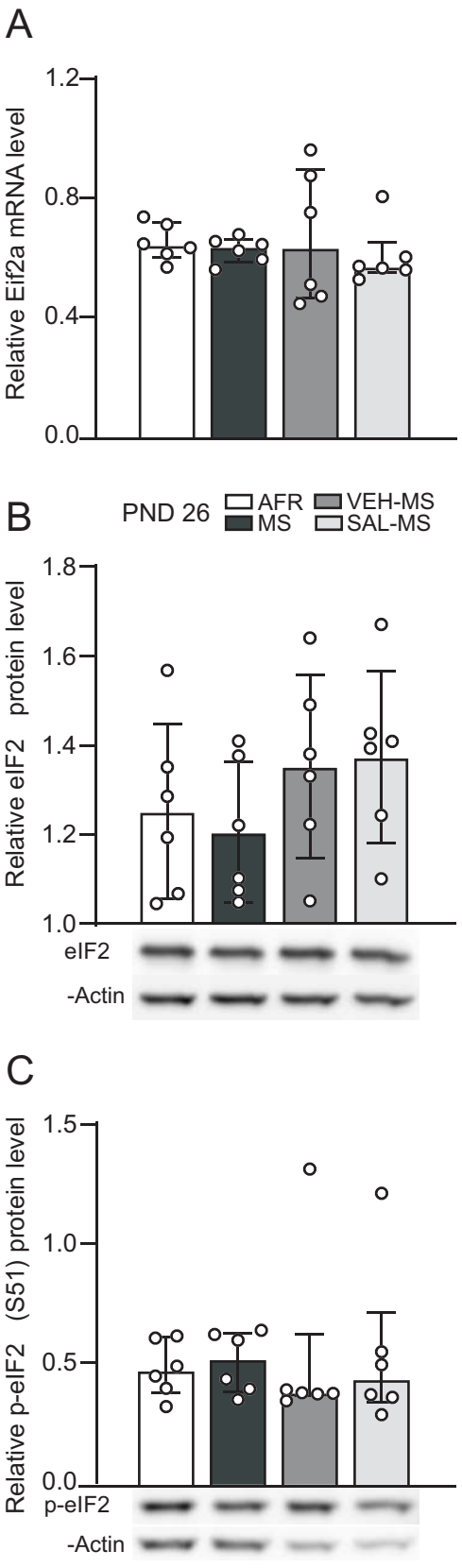

Fig. S5. The effects of MS and early-life SAL/VEH injections on mRNA expression (A) and protein expression and phosphorylation (B-C) of eIF2 in the mPFC of preadolescent rats. The data are presented as the median and IQR (A, C) or mean ± SD (B) and were analyzed by Kruskal-Wallis test or one-way ANOVA, respectively (n = 6). Circles represent individual data points. Statistical analysis showed no significant differences between experimental groups. The same immunoblot of -Actin was used for normalization of both p-eIF2 (C) and p-PERK immunoblots (Fig. S4C). After protein electrotransfer the blots were horizontally cut into two pieces to separately evaluate p-eIF2 and p-PERK protein levels from the same samples. Next, after membrane stripping procedure, appropriate blot was reprobed with -Actin antibody. *Abbreviations:* AFR, animal facility rearing; IQR, interquartile range; MS, maternal separation; PND, postnatal day; SAL, salubrinal; VEH, vehicle.

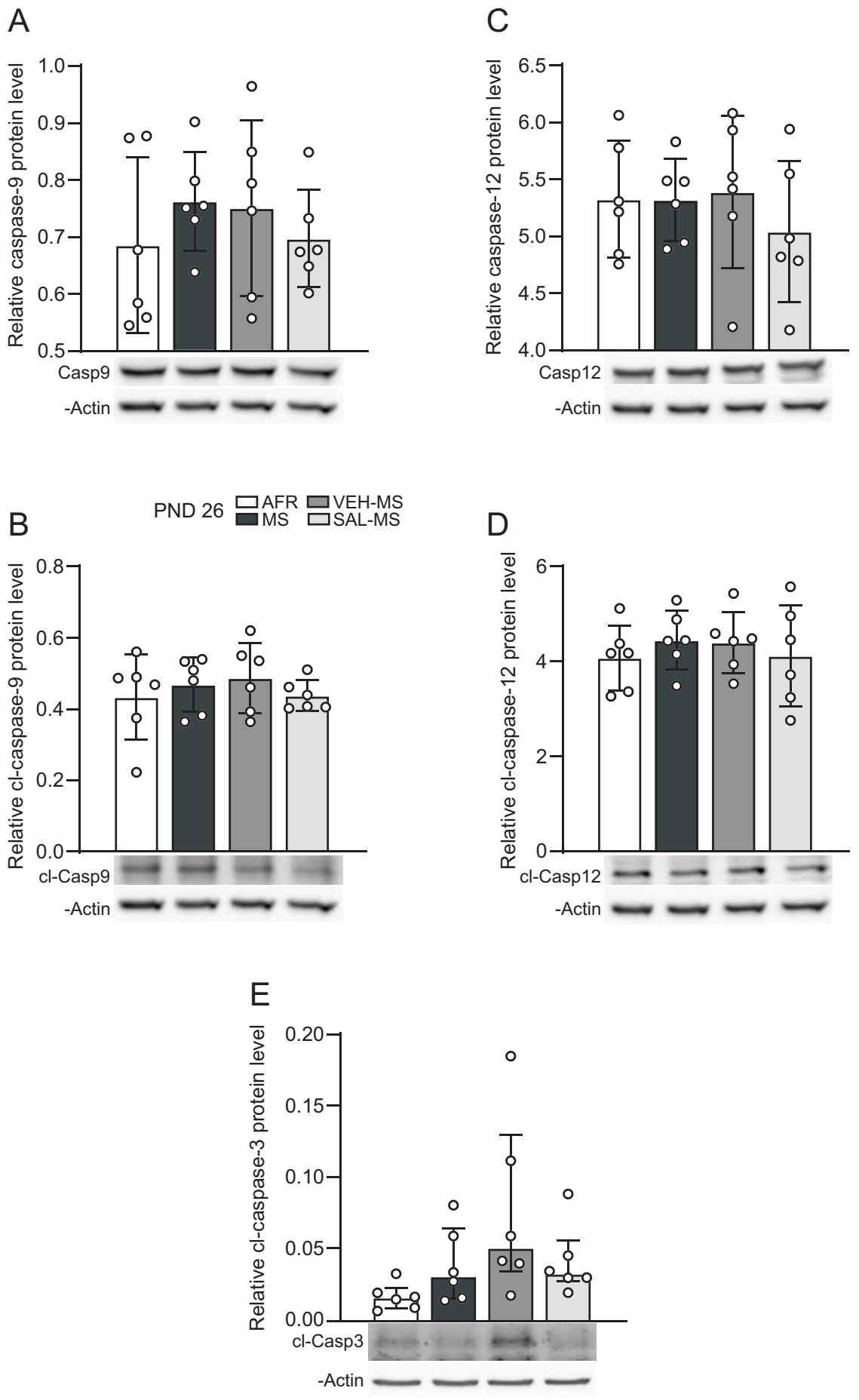

Fig. S6. The effects of MS and early-life SAL/VEH injections on protein expression and cleavage of caspase-9 (A-B), caspase-12 (C-D) and cleavage of caspase-3 (E) in the mPFC of preadolescent rats. The data are presented as the mean ± SD (A-D) or median and IQR (E) and were analyzed by one-way ANOVA or Kruskal-Wallis test, respectively (n = 6). Circles represent individual data points. The same immunoblots of -Actin was used for normalization of specific procaspases and their cleaved forms. Additionally, -Actin blots presented in A, B and C, D served also for normalization of IRE1 (Fig. S4E) and HSPA5 (Fig. S4A) immunoblots, respectively (membrane cutting after protein transfer, stripping and reprobing with -Actin antibody). *Abbreviations:* AFR, animal facility rearing; IQR, interquartile range; MS, maternal separation; PND, postnatal day; SAL, salubrinal; VEH, vehicle.

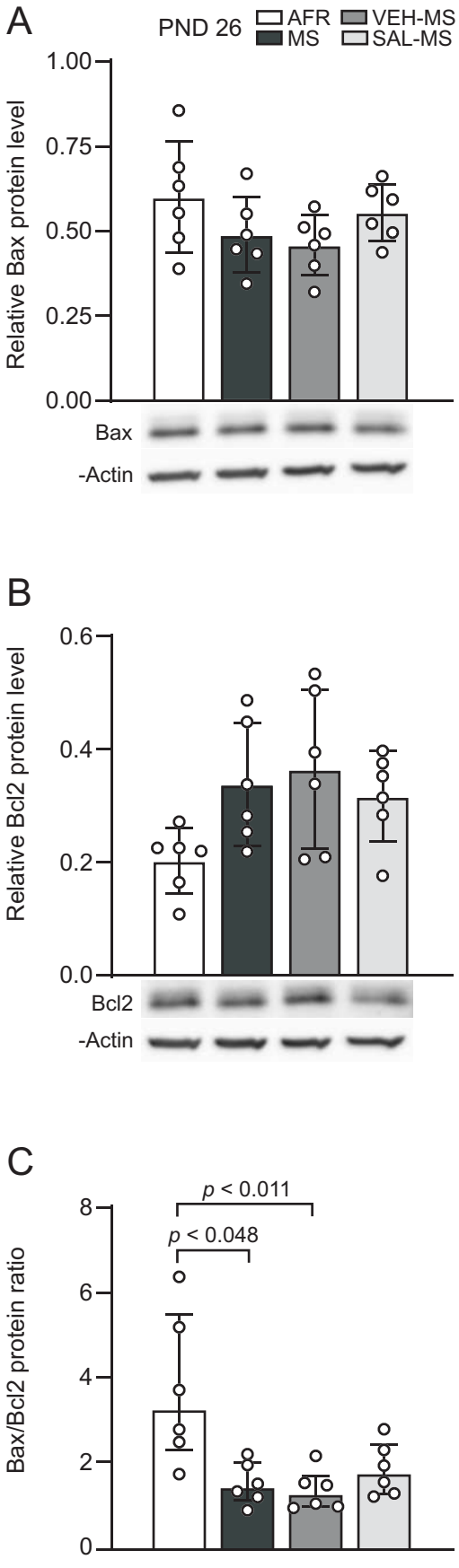

Fig. S7. The effects of MS and early-life SAL/VEH injections on Bax (A) and Bcl2 (B) protein levels and Bax/Bcl2 protein ratio (C) in the mPFC of preadolescent rats. The data are presented as the mean ± SD (A, B) or median and IQR (C) and were analyzed by one-way ANOVA or Kruskal-Wallis test, respectively (n = 6). Circles represent individual data points. Connectors indicate statistically significant difference between specific experimental groups in Dunn's test *post hoc* analysis, $p < 0.05$. -Actin blots presented in A and B served also for normalization of PERK (Fig. S4B) and p-IRE1 (Fig. S4F) immunoblots, respectively (membrane cutting after protein transfer and separate evaluation of specific proteins expression from the same samples). *Abbreviations:* AFR, animal facility rearing; IQR, interquartile range; MS, maternal separation; PND, postnatal day; SAL, salubrinal; VEH, vehicle.

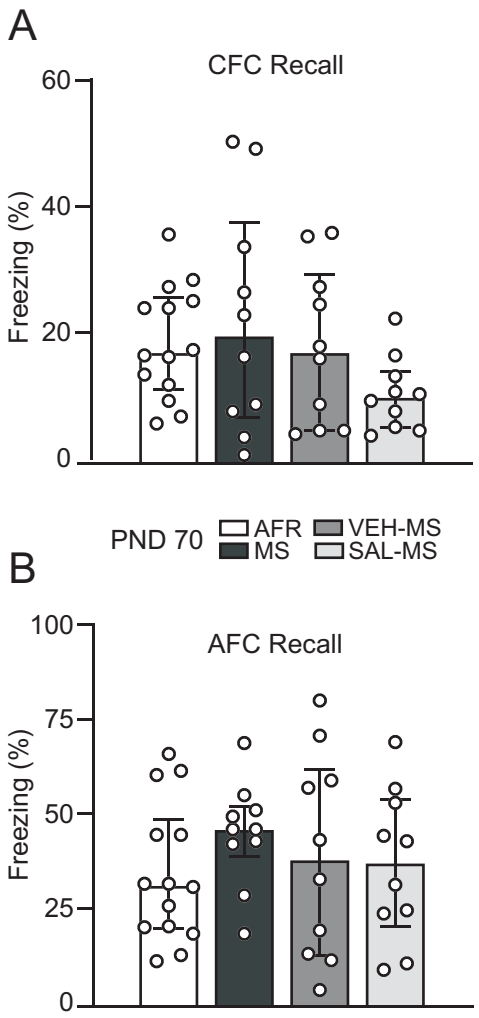

Fig. S8. The effects of MS and early-life SAL/VEH injections on the recall of contextual (A) and auditory (B) fear memories in adulthood. The data are presented as the median and IQR (n = 10-14) and expressed as a percentage of the session time. Circles represent individual data points. Kruskal-Wallis test showed no significant differences between experimental groups. *Abbreviations:* AFC, auditory fear conditioning; AFR, animal facility rearing; CFC, contextual fear conditioning; IQR, interquartile range; MS, maternal separation; PND, postnatal day; SAL, salubrinal; VEH, vehicle.

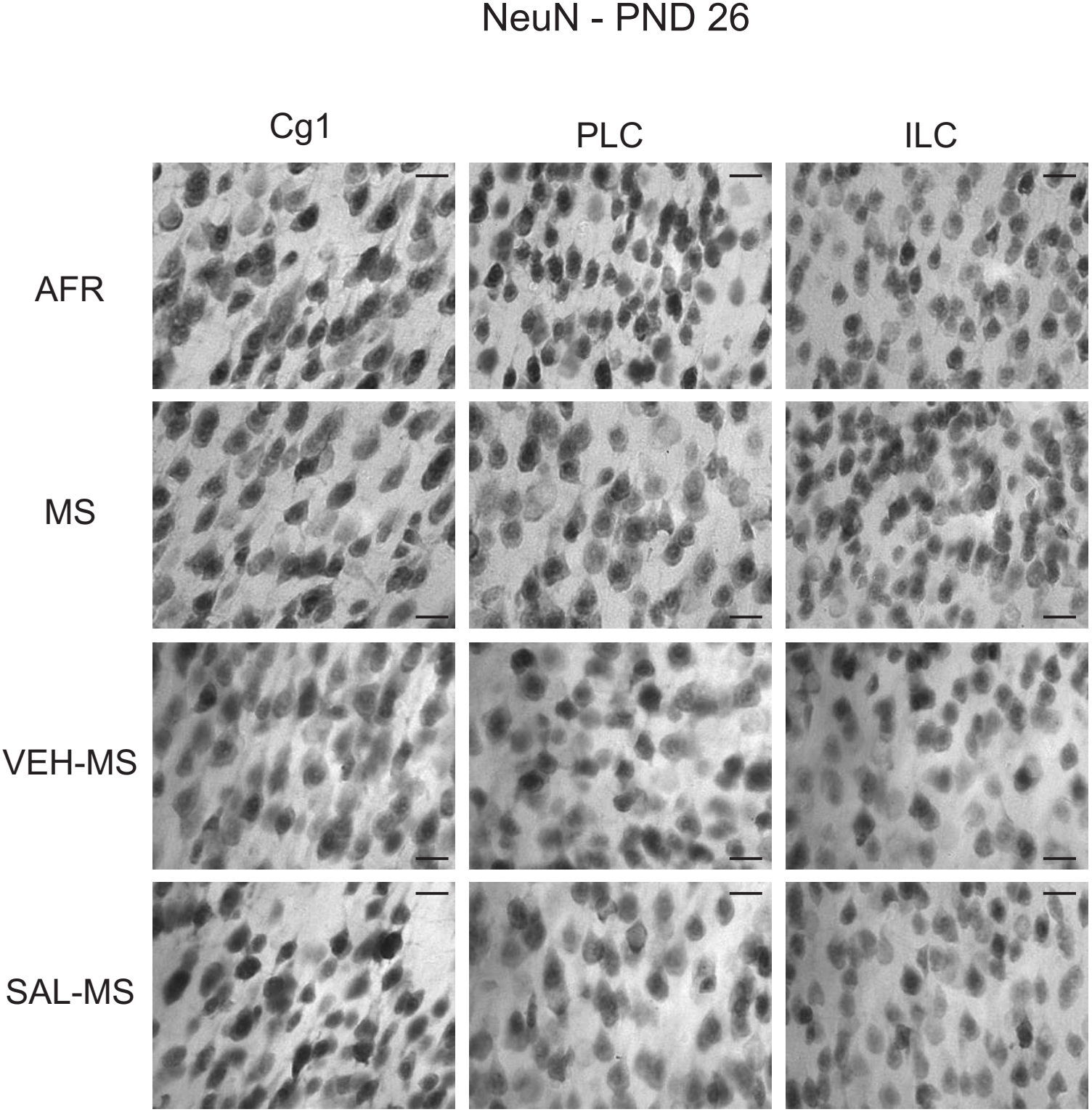

ESM_5. Representative photomicrographs showing NeuN-IR neurons in the subregions of the mPFC (columns) of preadolescent rats. Photomicrographs of the specific experimental groups are presented in rows. *Abbreviations:* AFR, animal facility rearing; Cg1, cingulate cortex 1; ILC, infralimbic cortex; IR, immunoreactive; MS, maternal separation; mPFC, medial prefrontal cortex; PLC, prelimbic cortex; PND, postnatal day; SAL, salubrinal; VEH, vehicle. Scale bar: 20 μm.

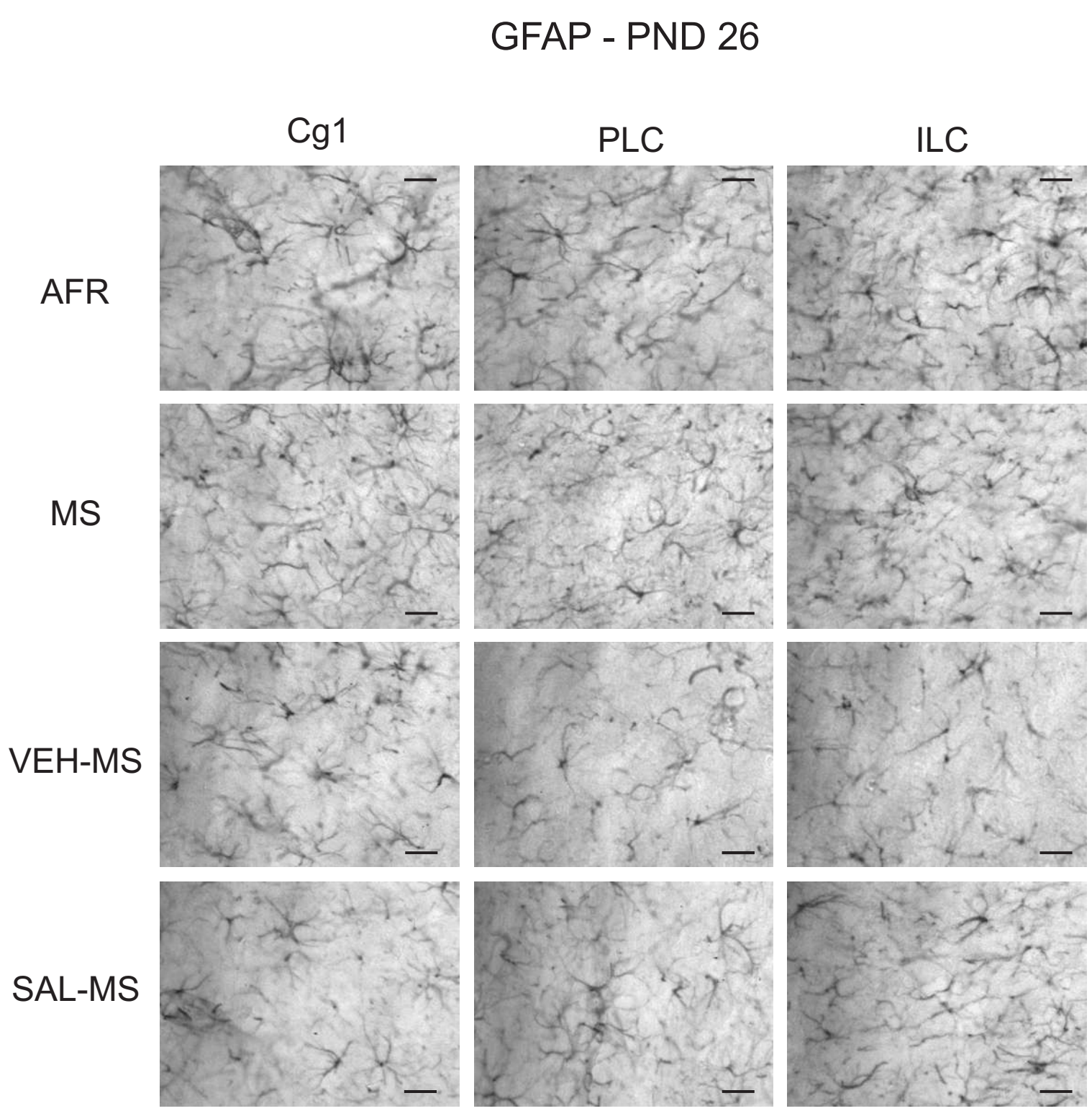

ESM_ 6. Representative photomicrographs showing GFAP-IR astrocytes in the subregions of the mPFC (columns) of preadolescent rats. Photomicrographs of the specific experimental groups are presented in rows. *Abbreviations:* AFR, animal facility rearing; Cg1, cingulate cortex 1; GFAP, glial fibrillary acidic protein; ILC, infralimbic cortex; IR, immunoreactive; MS, maternal separation; mPFC, medial prefrontal cortex; PLC, prelimbic cortex; PND, postnatal day; SAL, salubrinal; VEH, vehicle. Scale bar: 20 μm.

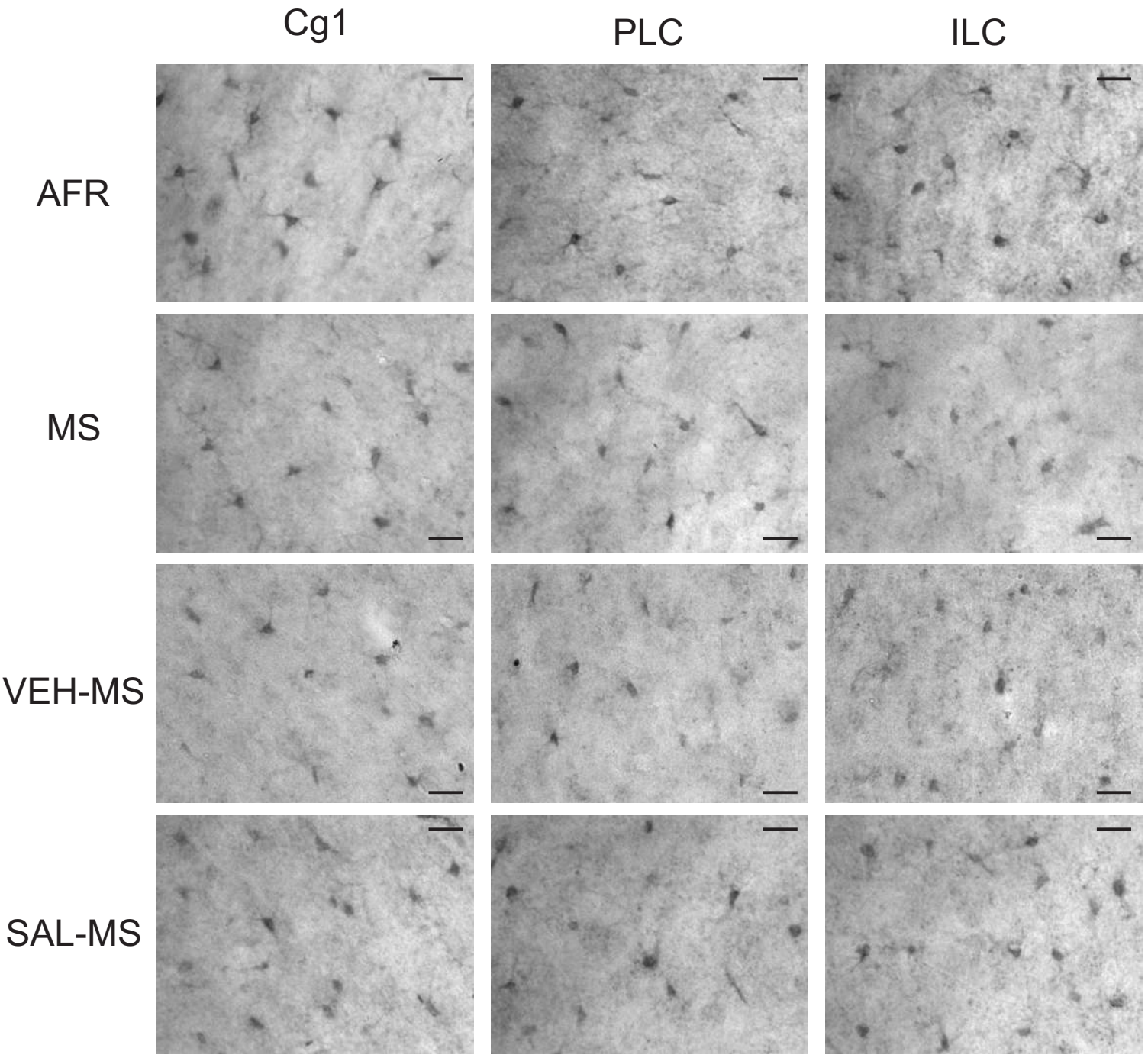

ESM_7. Representative photomicrographs showing IBA1-IR microglial cells in the subregions of the mPFC (columns) of preadolescent rats. Photomicrographs of the specific experimental groups are presented in rows. *Abbreviations:* AFR, animal facility rearing; Cg1, cingulate cortex 1; IBA1, ionized calcium-binding adapter molecule, ILC, infralimbic cortex; IR, immunoreactive; MS, maternal separation; mPFC, medial prefrontal cortex; PLC, prelimbic cortex; PND, postnatal day; SAL, salubrinal; VEH, vehicle. Scale bar: 20 μm.

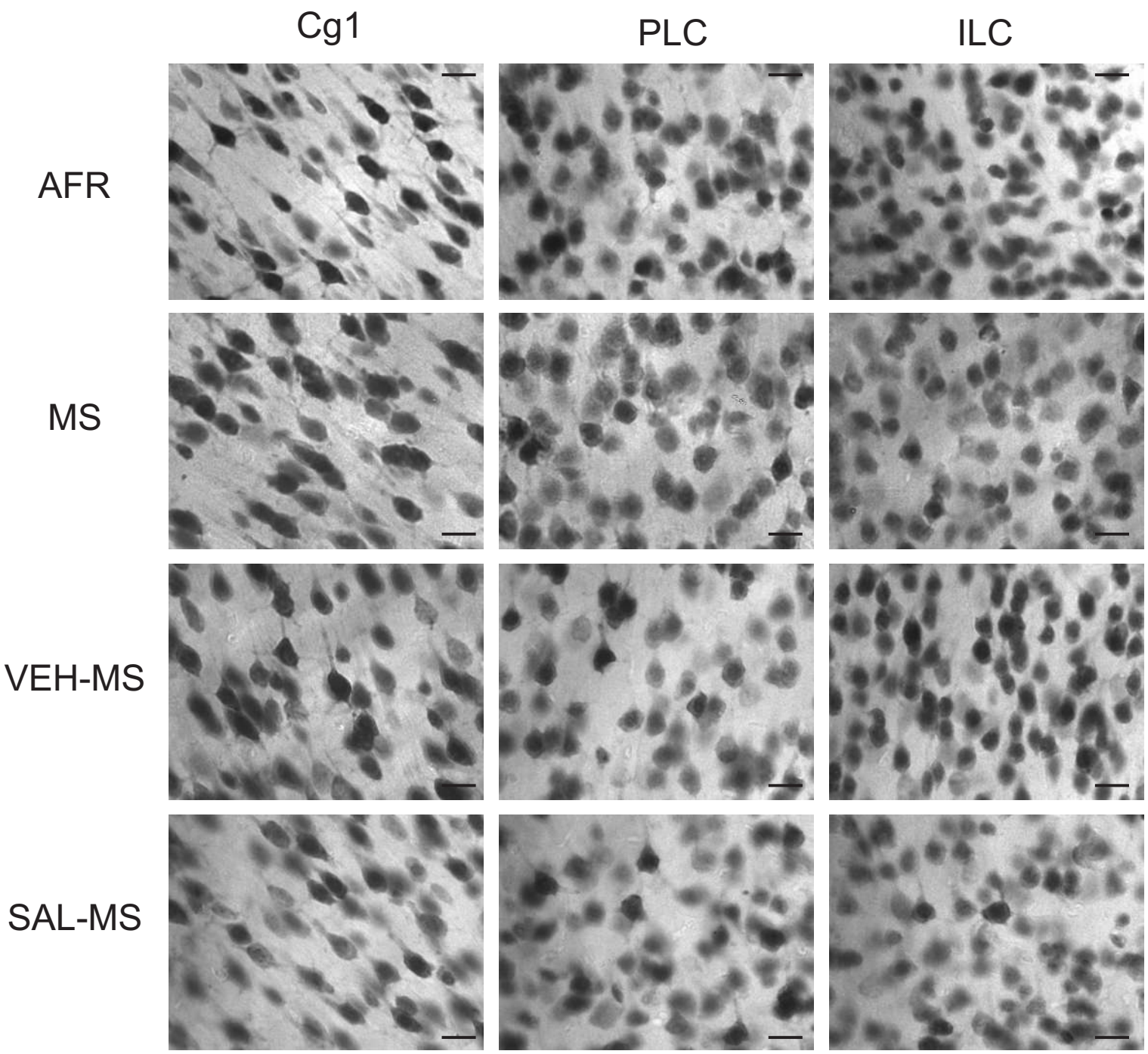

ESM_8. Representative photomicrographs showing NeuN-IR neurons in the subregions of the mPFC (columns) of adult rats. Photomicrographs of the specific experimental groups are presented in rows. *Abbreviations:* AFR, animal facility rearing; Cg1, cingulate cortex 1; ILC, infralimbic cortex; IR, immunoreactive; MS, maternal separation; mPFC, medial prefrontal cortex; PLC, prelimbic cortex; PND, postnatal day; SAL, salubrinal; VEH, vehicle. Scale bar: 20 μm.

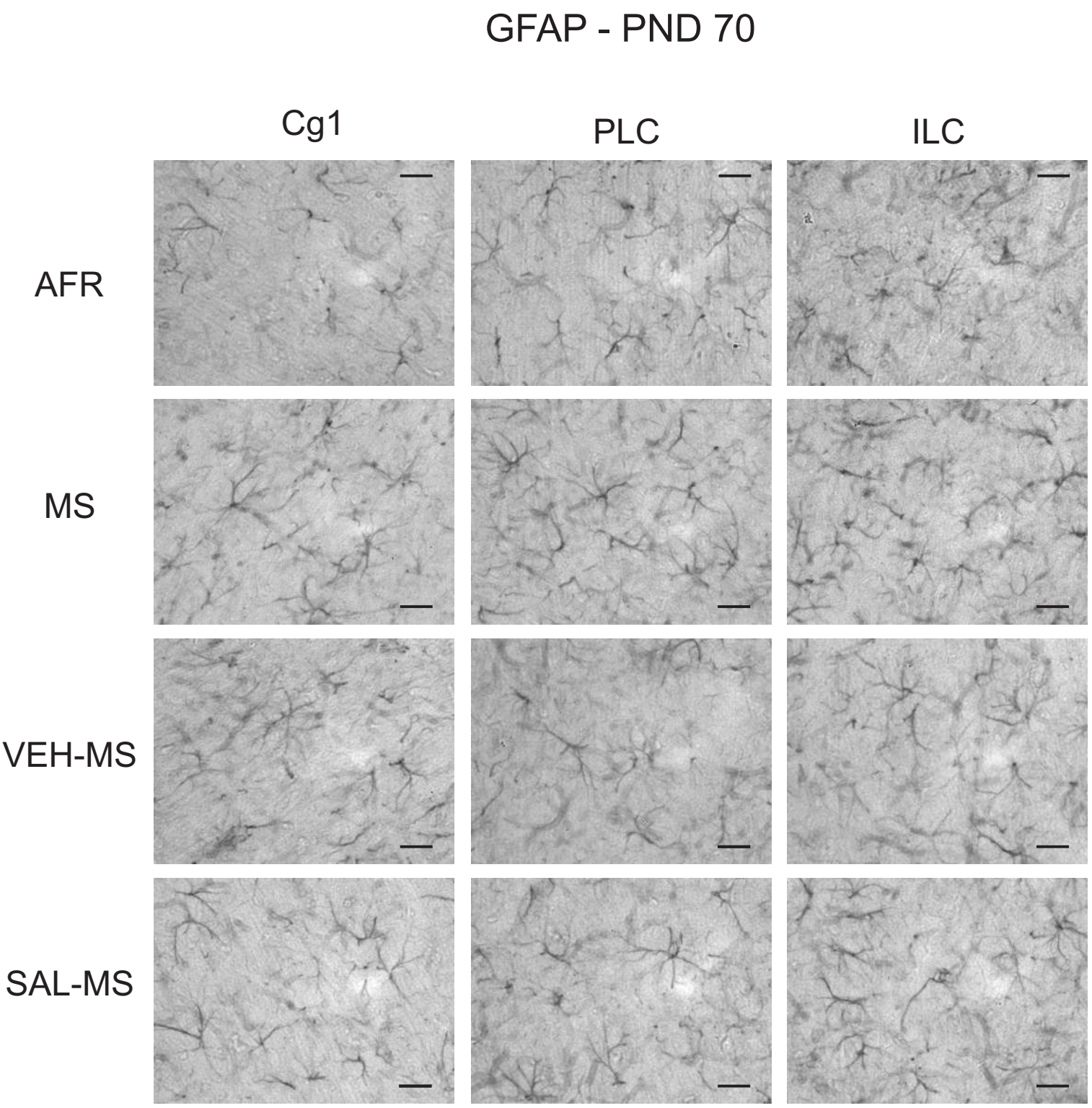

ESM_9. Representative photomicrographs showing GFAP-IR astrocytes in the subregions of the mPFC (columns) of adult rats. Photomicrographs of the specific experimental groups are presented in rows. *Abbreviations:* AFR, animal facility rearing; Cg1, cingulate cortex 1; GFAP, glial fibrillary acidic protein; ILC, infralimbic cortex; IR, immunoreactive; MS, maternal separation; mPFC, medial prefrontal cortex; PLC, prelimbic cortex; PND, postnatal day; SAL, salubrinal; VEH, vehicle. Scale bar: 20 μm.

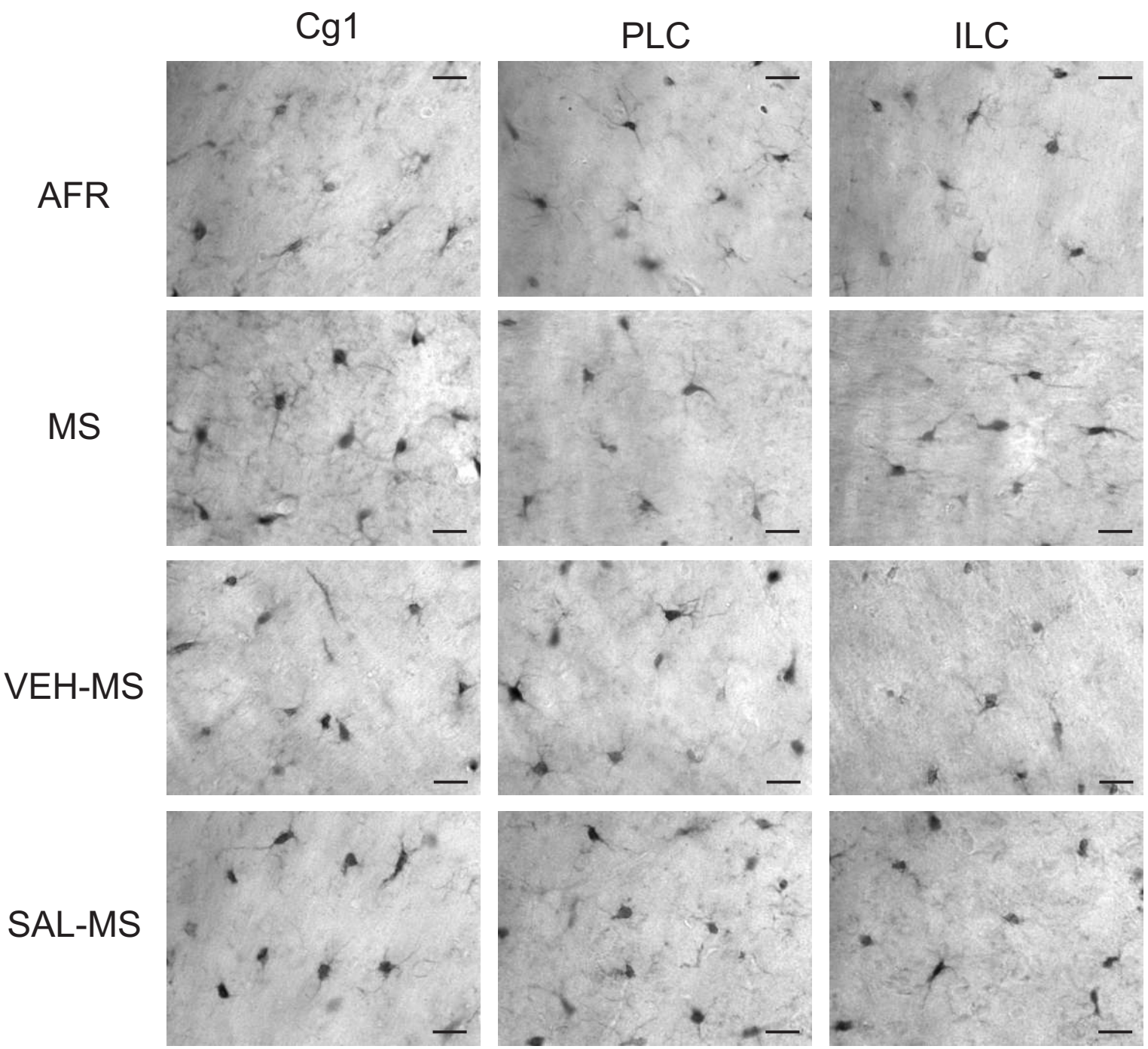

ESM_10. Representative photomicrographs showing IBA1-IR microglial cells in the subregions of the mPFC (columns) of adult rats. Photomicrographs of the specific experimental groups are presented in rows. *Abbreviations:* AFR, animal facility rearing; Cg1, cingulate cortex 1; IBA1, ionized calcium-binding adapter molecule; ILC, infralimbic cortex; IR, immunoreactive; MS, maternal separation; mPFC, medial prefrontal cortex; PLC, prelimbic cortex; PND, postnatal day; SAL, salubrinal; VEH, vehicle. Scale bar: 20 µm..

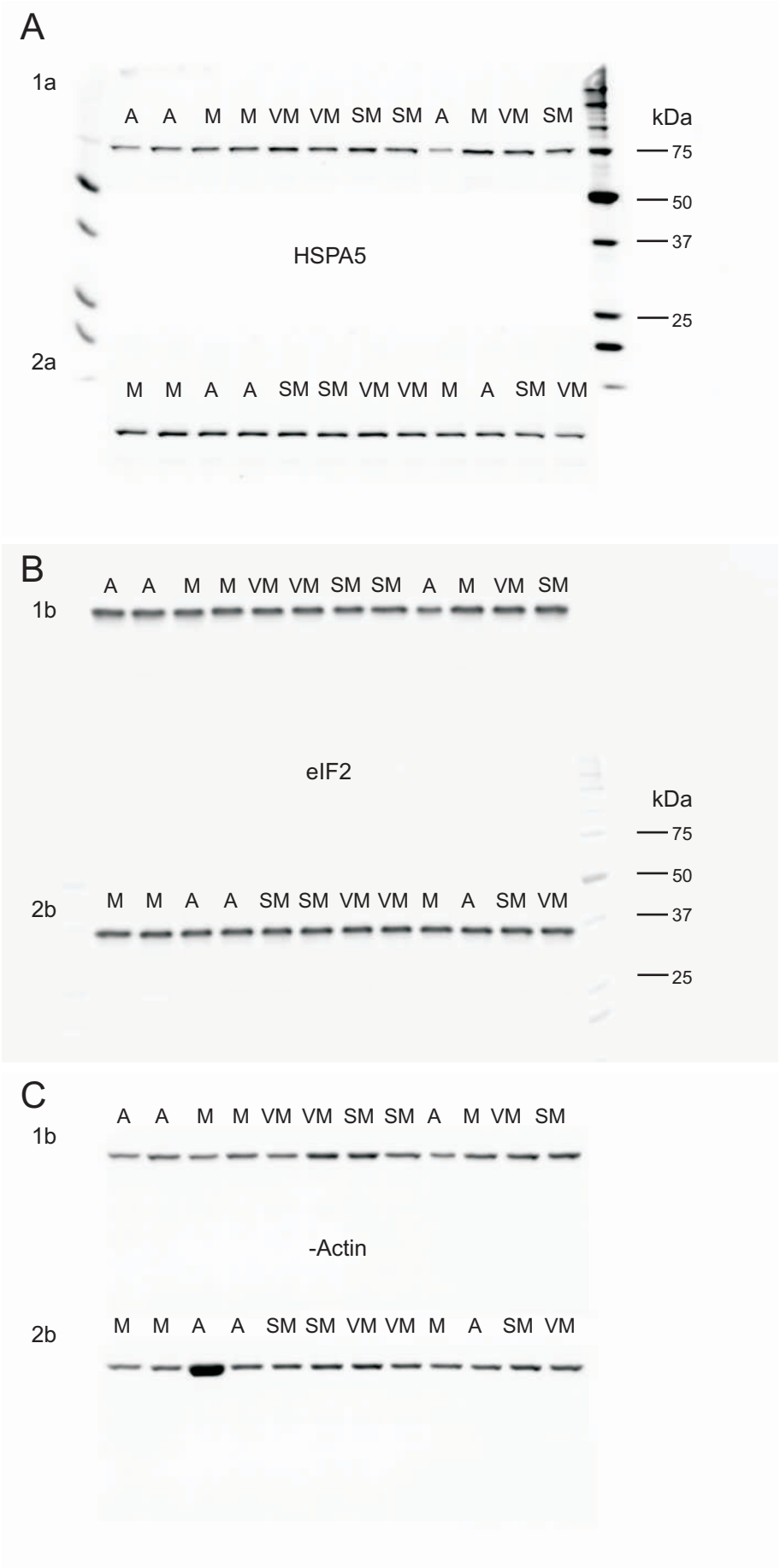

Fig. S9. Original blots presenting HSPA5 (A) and eIF2 (B) expression in juvenile rats and -Actin immunoreactivity as control of gel loading and transfer (C). After a transfer, two distinct blots (1 and 2) were cut into pieces (a and b) slightly above the level of 50 kDa to separately evaluate HSPA5 (1a, 2a) and eIF2 (1b, 2b). Next, after membrane stripping, blots 1b and 2b were reprobed with anti- -Actin antibody. The blots 1a, 2a and 1b, 2b, respectively, were exposed together, therefore they constitute one image. Molecular weight standards were matched only with blot 1a and 2b (B), respectively. *Abbreviations:* A (AFR), animal facility rearing; M (MS), maternal separation; VM (VEH-MS); SM (SAL-MS); SAL, salubrinal; VEH, vehicle.

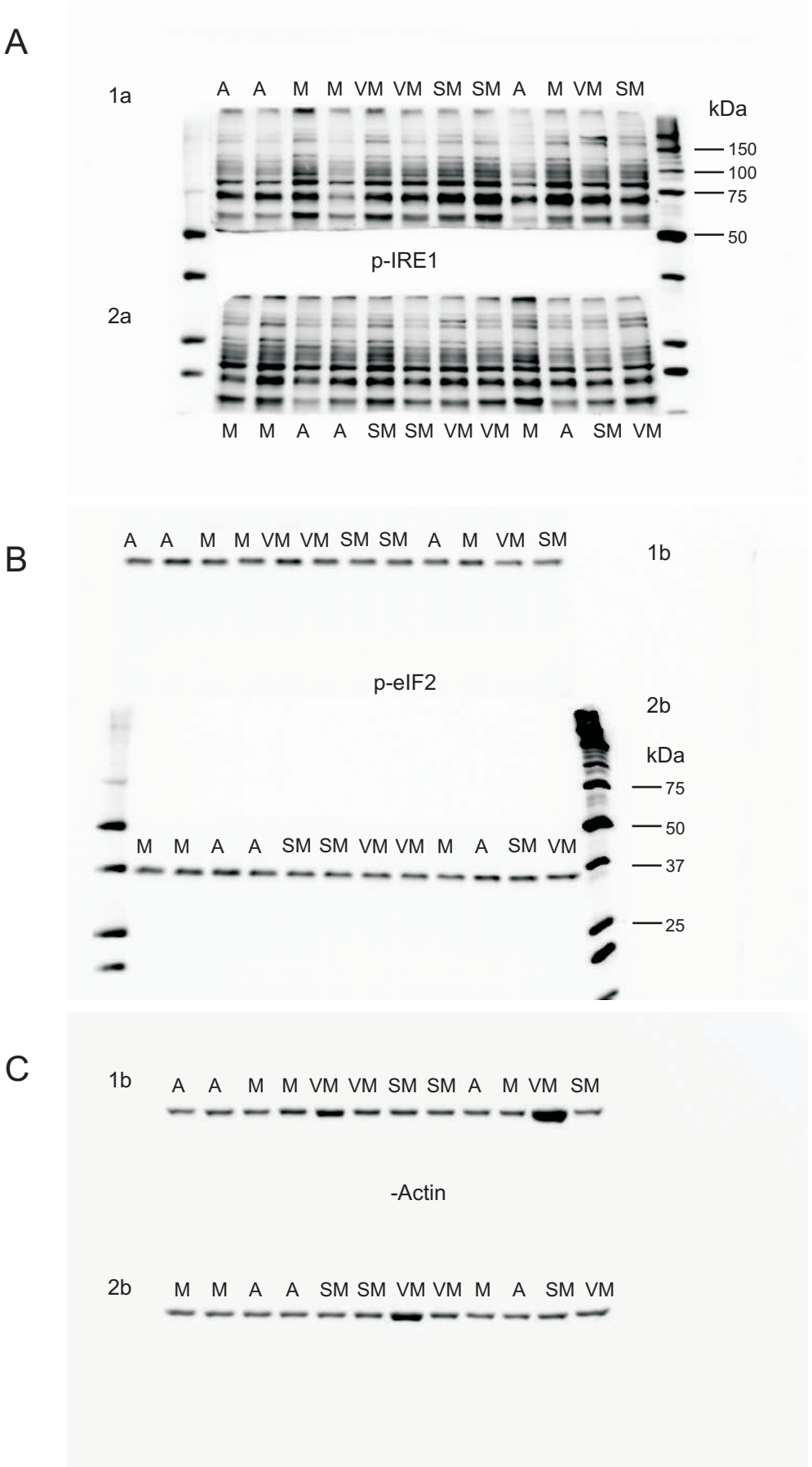

Fig. S10. Original blots presenting p-IRE1 (A) and p-eIF2 (B) expression in juvenile rats and -Actin immunoreactivity as control of gel loading and transfer (C). After a transfer, two distinct blots (1 and 2) were cut into pieces (a and b) slightly above the level of 50 kDa to separately evaluate p-IRE1 (1a, 2a) and p-eIF2 (1b, 2b). Next, after membrane stripping, blots 1b and 2b were reprobed with anti- -Actin antibody. The blots 1a, 2a and 1b, 2b, respectively, were exposed together, therefore they constitute one image. Molecular weight standards were matched only with blot 1a and 2b (B), respectively. Red arrows indicate the band subjected to the analysis. *Abbreviations:* A (AFR), animal facility rearing; M (MS), maternal separation; VM (VEH-MS); SM (SAL-MS); SAL, salubrinal; VEH, vehicle.

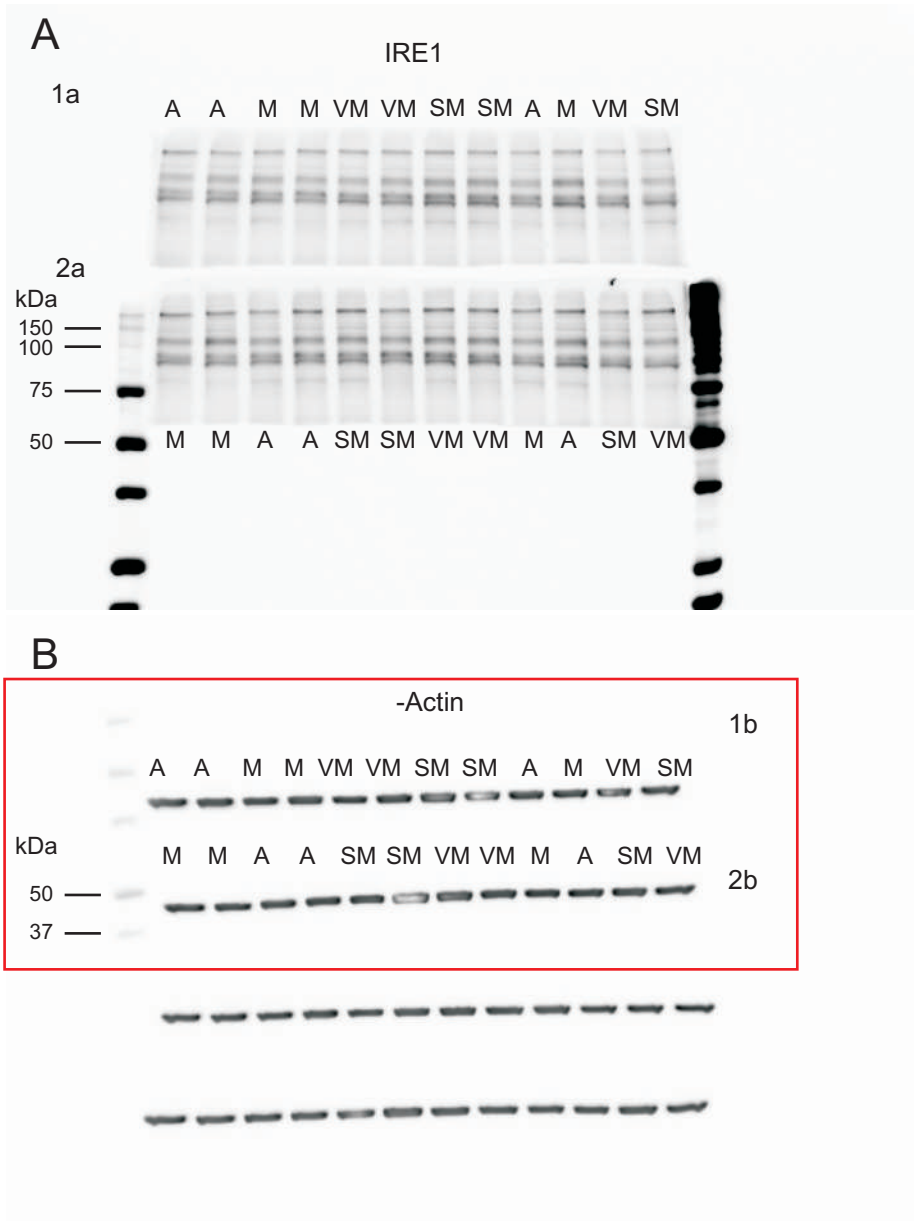

Fig. S11. Original blots presenting IRE1 expression (A) in juvenile rats and -Actin immunoreactivity as control of gel loading and transfer (B). After a transfer, two distinct blots (1 and 2) were cut into pieces (a and b) slightly above the level of 50 kDa to separately evaluate IRE1 (1a, 2a) and -Actin (1b, 2b). The blots 1a, 2a and 1b, 2b, respectively, were exposed together, therefore they constitute one image. Molecular weight standards were matched only with blot 2a and 2b, respectively. Red arrows indicate the band subjected to the analysis. *Abbreviations:* A (AFR), animal facility rearing; M (MS), maternal separation; VM (VEH-MS); SM (SAL-MS); SAL, salubrinal; VEH, vehicle.

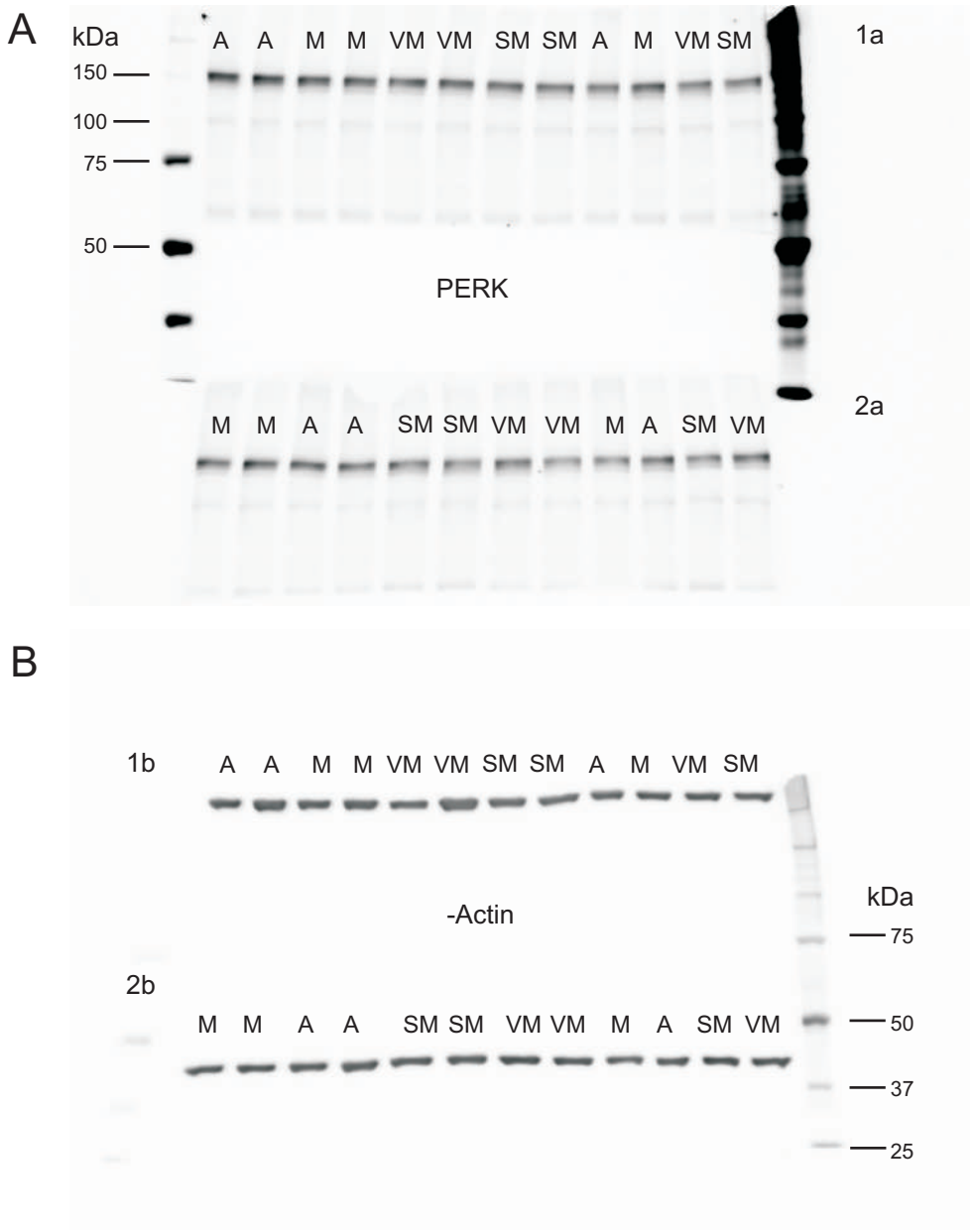

Fig. S12. Original blots presenting PERK expression (A) in juvenile rats and -Actin immunoreactivity as control of gel loading and transfer (B). After a transfer, two distinct blots (1 and 2) were cut into pieces (a and b) slightly above the level of 50 kDa to separately evaluate PERK (1a, 2a) and -Actin (1b, 2b). The blots 1a, 2a and 1b, 2b, respectively, were exposed together, therefore they constitute one image. Molecular weight standards were matched only with blot 1a and 2b, respectively. *Abbreviations:* A (AFR), animal facility rearing; M (MS), maternal separation; VM (VEH-MS); SM (SAL-MS); SAL, salubrinal; VEH, vehicle.

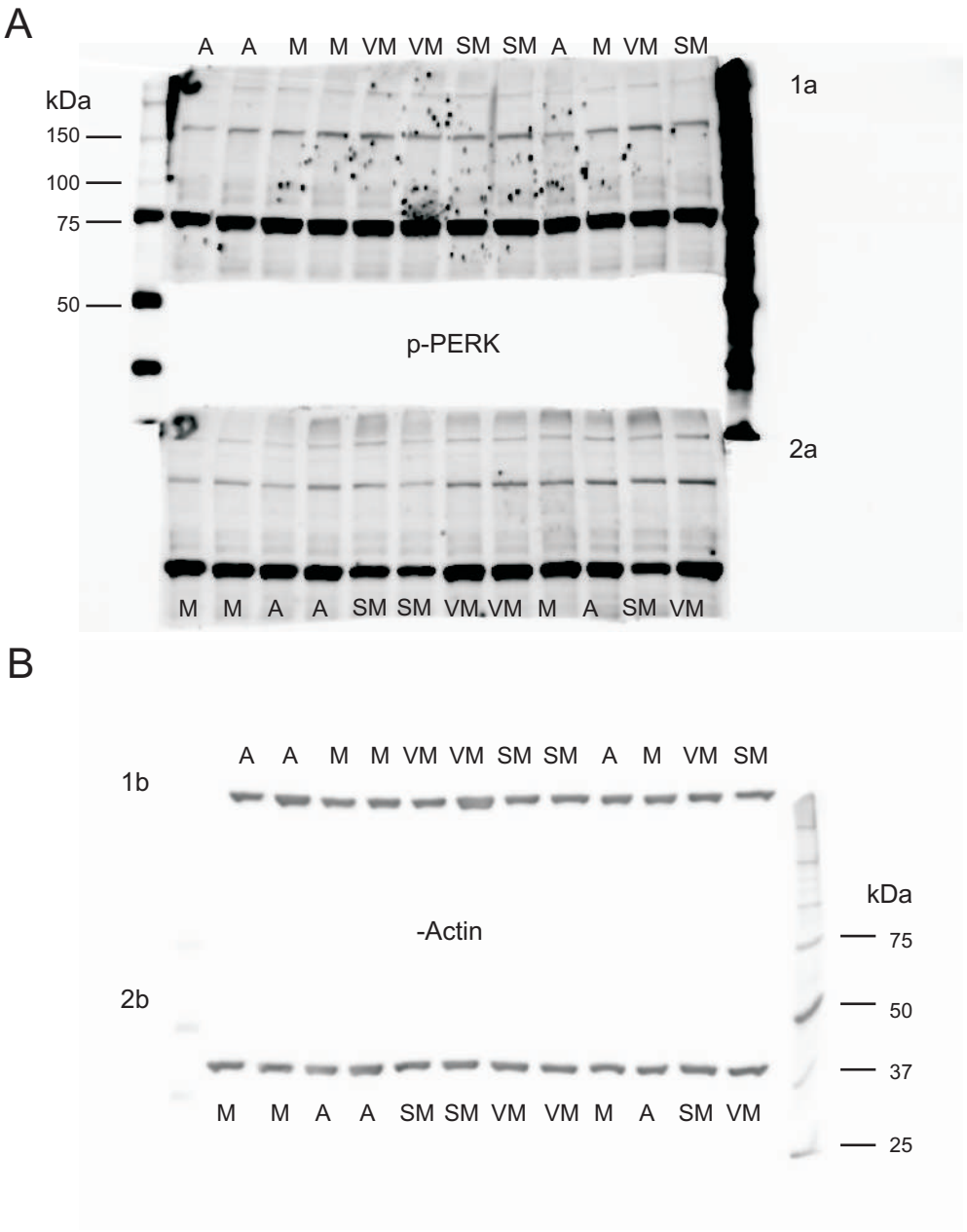

Fig. S13. Original blots presenting p-PERK expression (A) in juvenile rats and -Actin immunoreactivity as control of gel loading and transfer (B). After a transfer, two distinct blots (1 and 2) were cut into pieces (a and b) slightly above the level of 50 kDa to separately evaluate p-PERK (1a, 2a) and -Actin (1b, 2b). The blots 1a, 2a and 1b, 2b, respectively, were exposed together, therefore they constitute one image. Molecular weight standards were matched only with blot 1a and 2b, respectively. Red arrows indicate the band subjected to the analysis. *Abbreviations:* A (AFR), animal facility rearing; M (MS), maternal separation; VM (VEH-MS); SM (SAL-MS); SAL, salubrinal; VEH, vehicle.

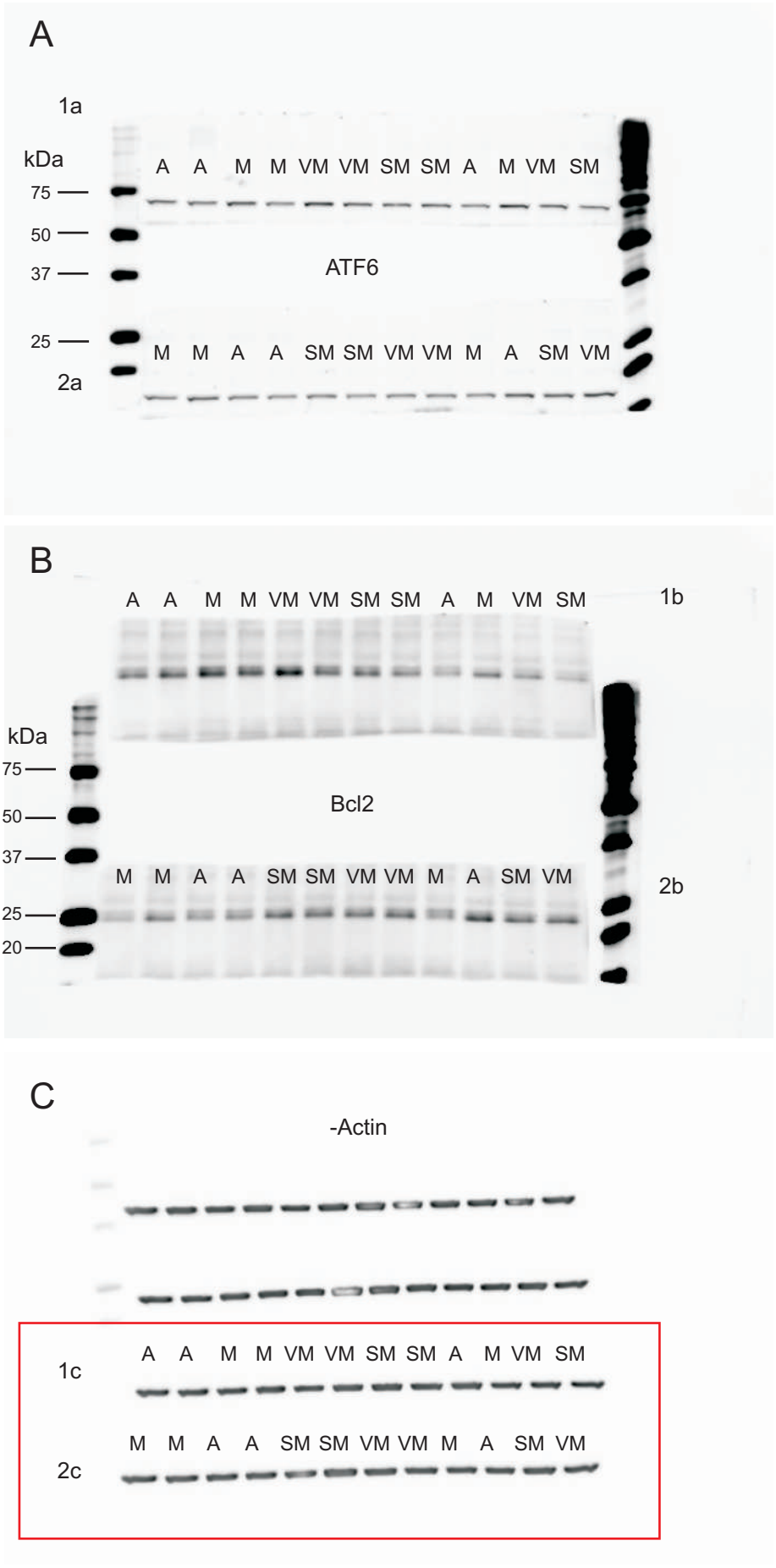

Fig. S14. Original blots presenting ATF6 (A) and Bcl2 (B) expression in juvenile rats and -Actin immunoreactivity as control of gel loading and transfer (C). After a transfer, two distinct blots (1 and 2) were cut into pieces (a, b and c) slightly above the level of 50 kDa and below 37 kDa to separately evaluate ATF6 (1a, 2a), Bcl2 (1b, 2b) and -Actin (1c, 2c). The blots 1a, 2a and 1b, 2b and 1c, 2c, respectively, were exposed together, therefore they constitute one image. Molecular weight standards were matched only with blot 1a and 2b. *Abbreviations:* A (AFR), animal facility rearing; M (MS), maternal separation; VM (VEH-MS); SM (SAL-MS); SAL, salubrinal; VEH, vehicle.

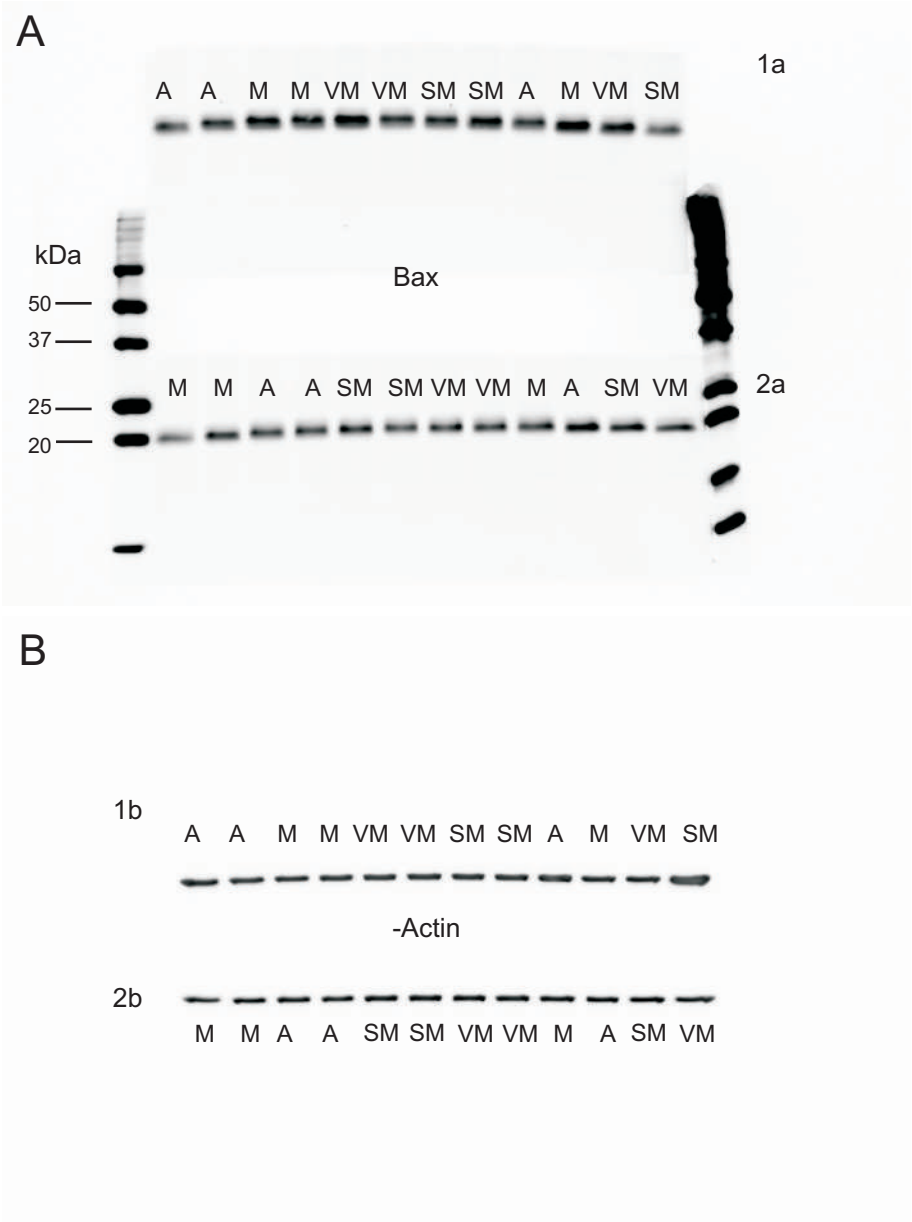

Fig. S15. Original blots presenting Bax expression (A) in juvenile rats and -Actin immunoreactivity as control of gel loading and transfer (B). After a transfer, two distinct blots (1 and 2) were cut into pieces (a and b) slightly below the level of 37 kDa to separately evaluate Bax (1a, 2a) and -Actin (1b, 2b). The blots 1a, 2a and 1b, 2b, respectively, were exposed together, therefore they constitute one image. Molecular weight standards were matched only with blot 2a. *Abbreviations:* A (AFR), animal facility rearing; M (MS), maternal separation; VM (VEH-MS); SM (SAL-MS); SAL, salubrinal; VEH, vehicle.

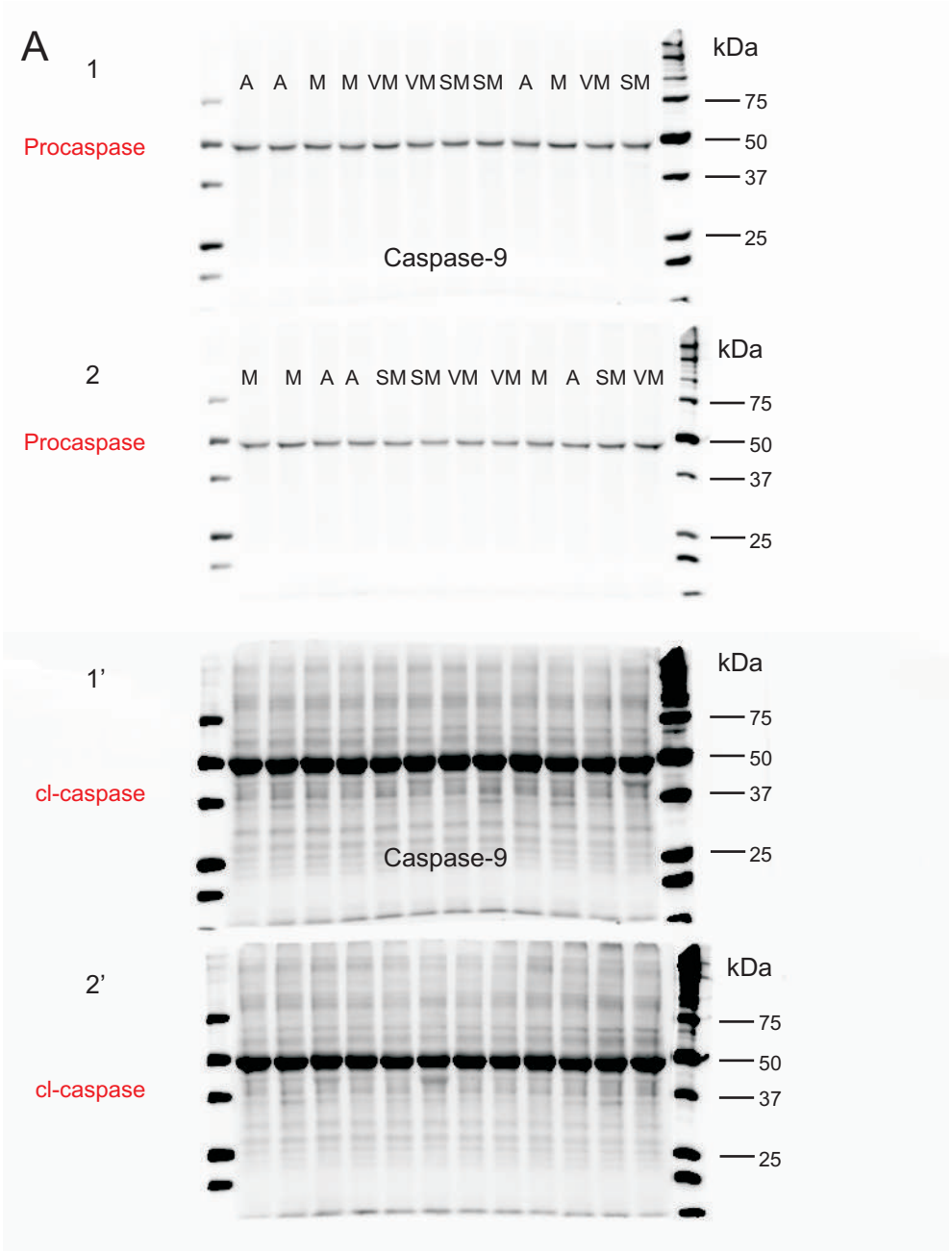

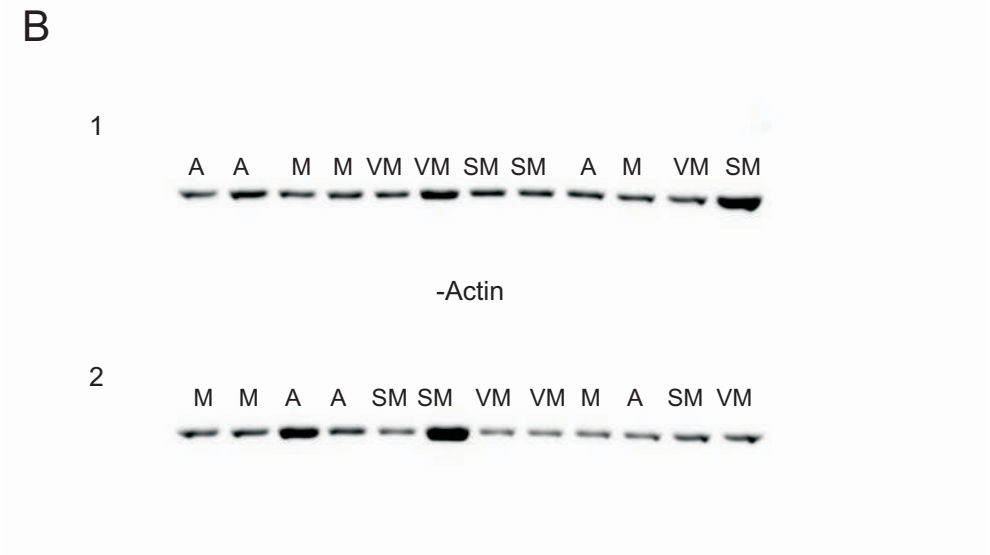

Fig. S16. Original blots presenting caspase-9 expression in juvenile rats (A). After membrane stripping, blots 1 and 2 were reprobed with anti- -Actin antibody to control gel loading and transfer (B). The blots 1, 2 were exposed together, therefore they constitute one image. Lower image in A (1', 2') was subjected to a higher exposure time than upper image (the same blots) to evaluate cl-caspase levels. Red arrows indicate the bands subjected to the analysis. *Abbreviations:* A (AFR), animal facility rearing; cl, cleaved; M (MS), maternal separation; VM (VEH-MS); SM (SAL-MS); SAL, salubrinal; VEH, vehicle.

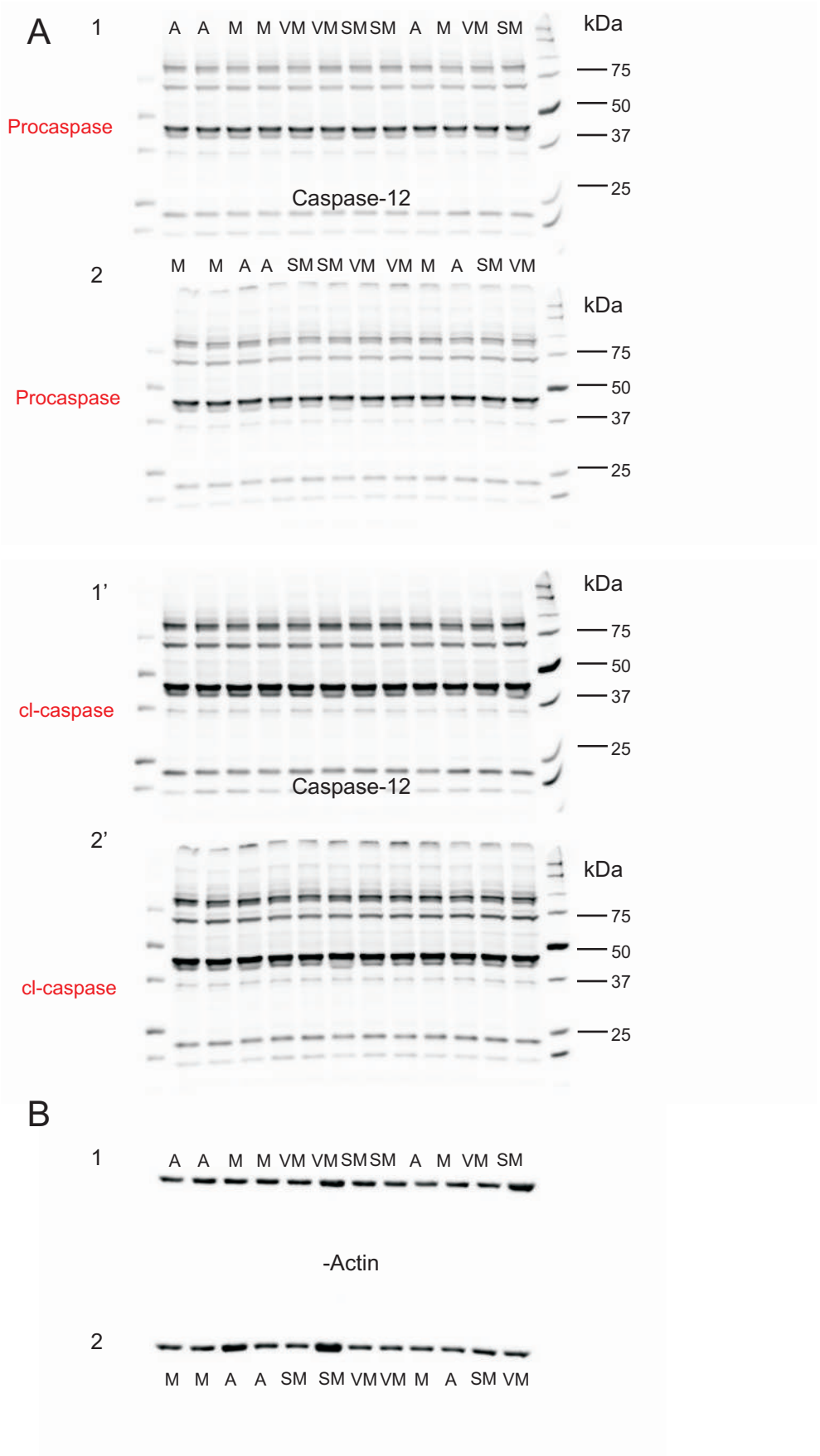

Fig. S17. Original blots presenting caspase-12 expression in juvenile rats (A). After membrane stripping, blots 1 and 2 were reprobed with anti- -Actin antibody to control gel loading and transfer (B). The blots 1, 2 were exposed together, therefore they constitute one image. Lower image in A (1', 2') was subjected to a higher exposure time than upper image (the same blots) to evaluate cl-caspase levels. Red arrows indicate the bands subjected to the analysis. *Abbreviations:* A (AFR), animal facility rearing; cl, cleaved; M (MS), maternal separation; VM (VEH-MS); SM (SAL-MS); SAL, salubrinal; VEH, vehicle.

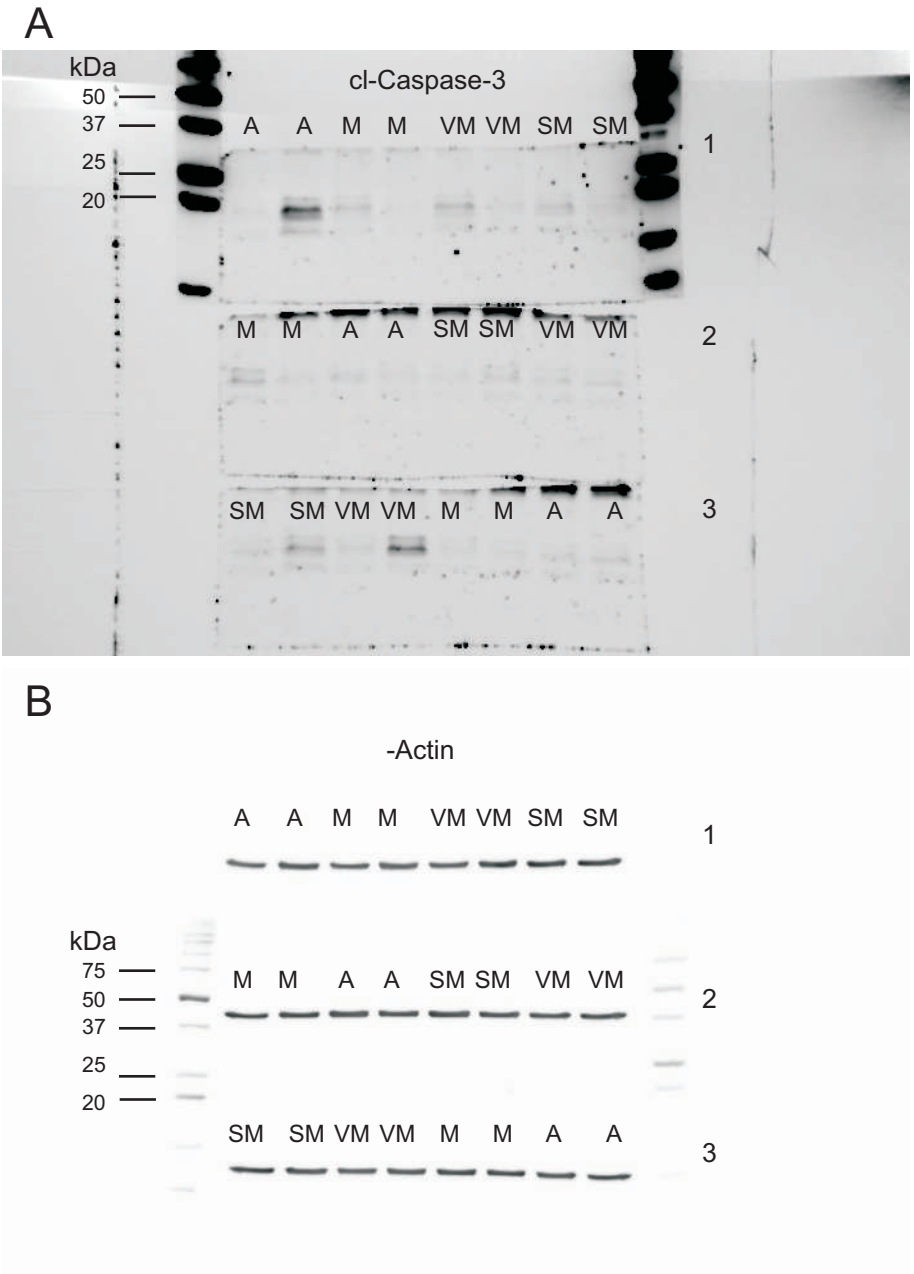

Fig. S18. Original blots presenting cl-caspase-3 expression in juvenile rats (A). After membrane stripping, blots 1, 2 and 3 were reprobed with anti- -Actin antibody to control gel loading and transfer (B). The blots 1, 2, 3 were exposed together, therefore they constitute one image. Red arrows indicate the band subjected to the analysis. Molecular weight standards were matched only with blot 1 (A) and 2 (B). *Abbreviations:* A (AFR), animal facility rearing; cl, cleaved; M (MS), maternal separation; VM (VEH-MS); SM (SAL-MS); SAL, salubrinal; VEH, vehicle,

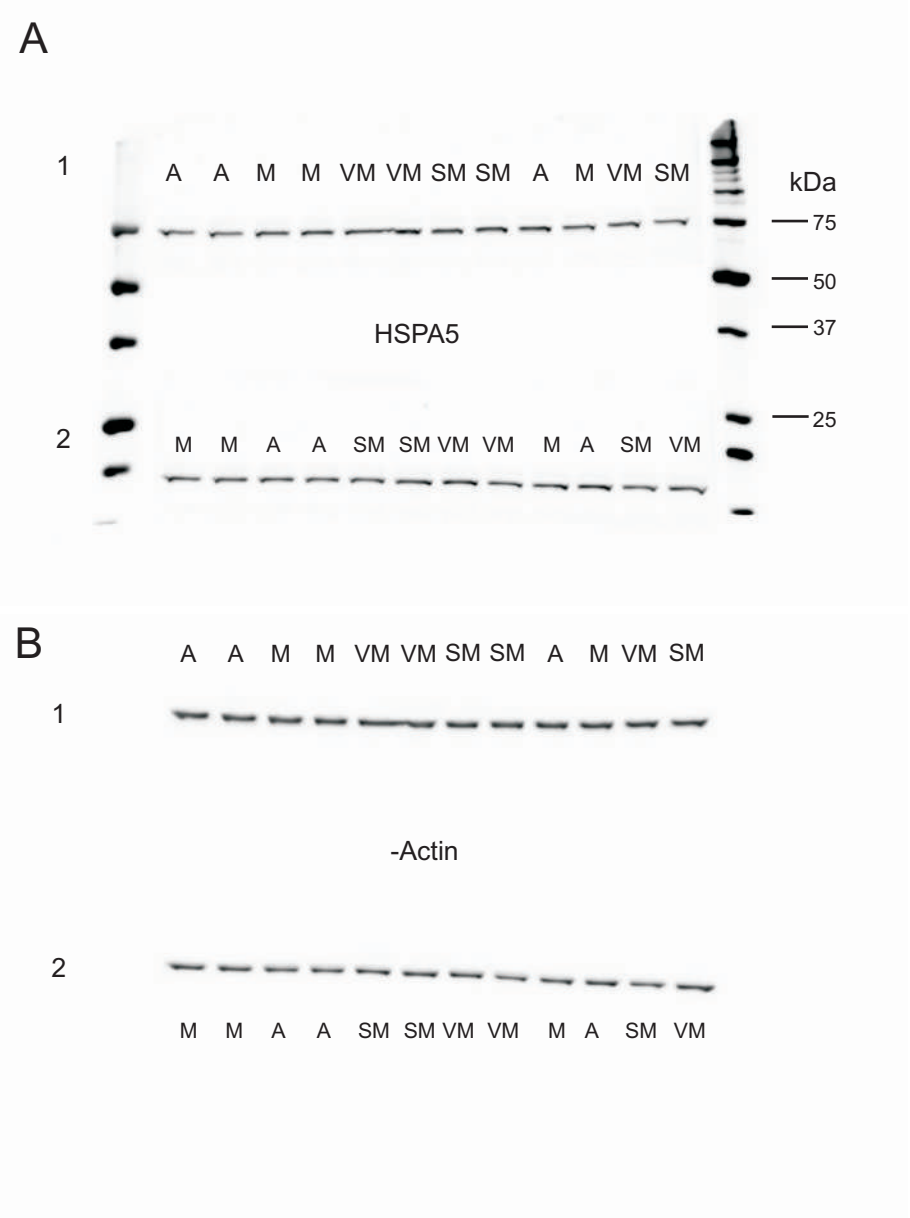

Fig. S19. Original blots presenting HSPA5 expression (A) in preadolescent rats and -Actin immunoreactivity as control of gel loading and transfer (B). After a transfer, two distinct blots (1 and 2) were cut into pieces above the level of 50 kDa to separately evaluate HSPA5, caspase-12 and finally -Actin (after membrane stripping), therefore -Actin blot served also for normalization of caspas-12 blot (Fig. S27). The blots 1 and 2, respectively, were exposed together, therefore they constitute one image. Molecular weight standards were matched only with blot 1 (A). *Abbreviations:* A (AFR), animal facility rearing; M (MS), maternal separation; VM (VEH-MS); SM (SAL-MS); SAL, salubrinal; VEH, vehicle.

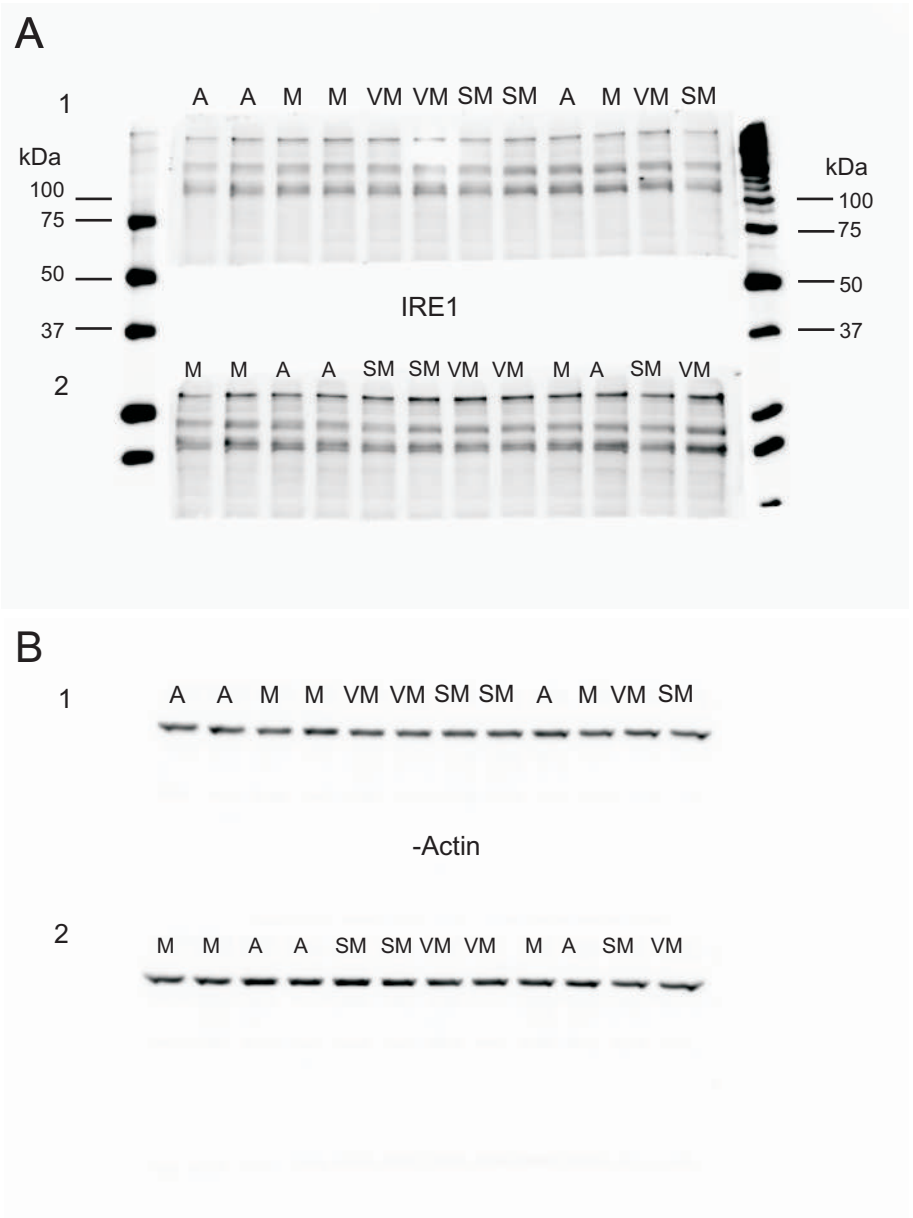

Fig. S20. Original blots presenting IRE1 expression (A) in preadolescent rats and -Actin immunoreactivity as control of gel loading and transfer (B). After a transfer, two distinct blots (1 and 2) were cut into pieces above the level of 50 kDa to separately evaluate IRE1 , caspase-9 and finally -Actin (after membrane stripping), therefore -Actin blot served also for normalization of caspas-9 blot (Fig. S26). The blots 1 and 2, respectively, were exposed together, therefore they constitute one image. Molecular weight standards were matched only with blot 1 (A). Red arrows indicate the band subjected to the analysis. *Abbreviations:* A (AFR), animal facility rearing; M (MS), maternal separation; VM (VEH-MS); SM (SAL-MS); SAL, salubrinal; VEH, vehicle.

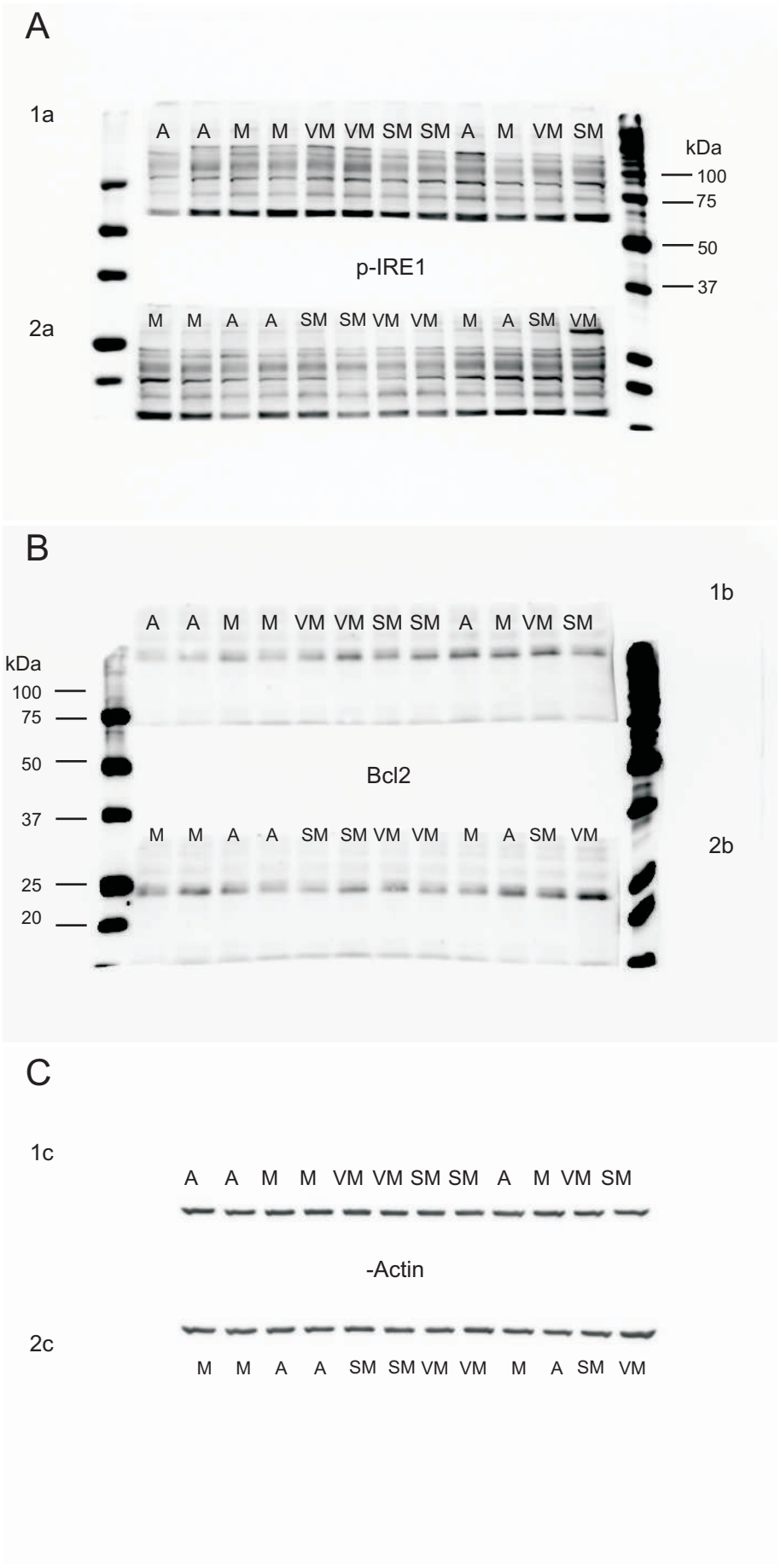

Fig. S21. Original blots presenting p-IRE1 (A) and Bcl2 (B) expression in preadolescent rats and -Actin immunoreactivity as control of gel loading and transfer (C). After a transfer, two distinct blots (1 and 2) were cut into pieces (a, b and c) slightly above the level of 50 kDa and below 37 kDa to separately evaluate p-IRE1 (1a, 2a), Bcl2 (1b, 2b) and -Actin (1c, 2c). The blots 1a, 2a and 1b, 2b and 1c, 2c, respectively, were exposed together, therefore they constitute one image. Molecular weight standards were matched only with blot 1a and 2b. Red arrows indicate the band subjected to the analysis. *Abbreviations:* A (AFR), animal facility rearing; M (MS), maternal separation; VM (VEH-MS); SM (SAL-MS); SAL, salubrinal; VEH, vehicle.

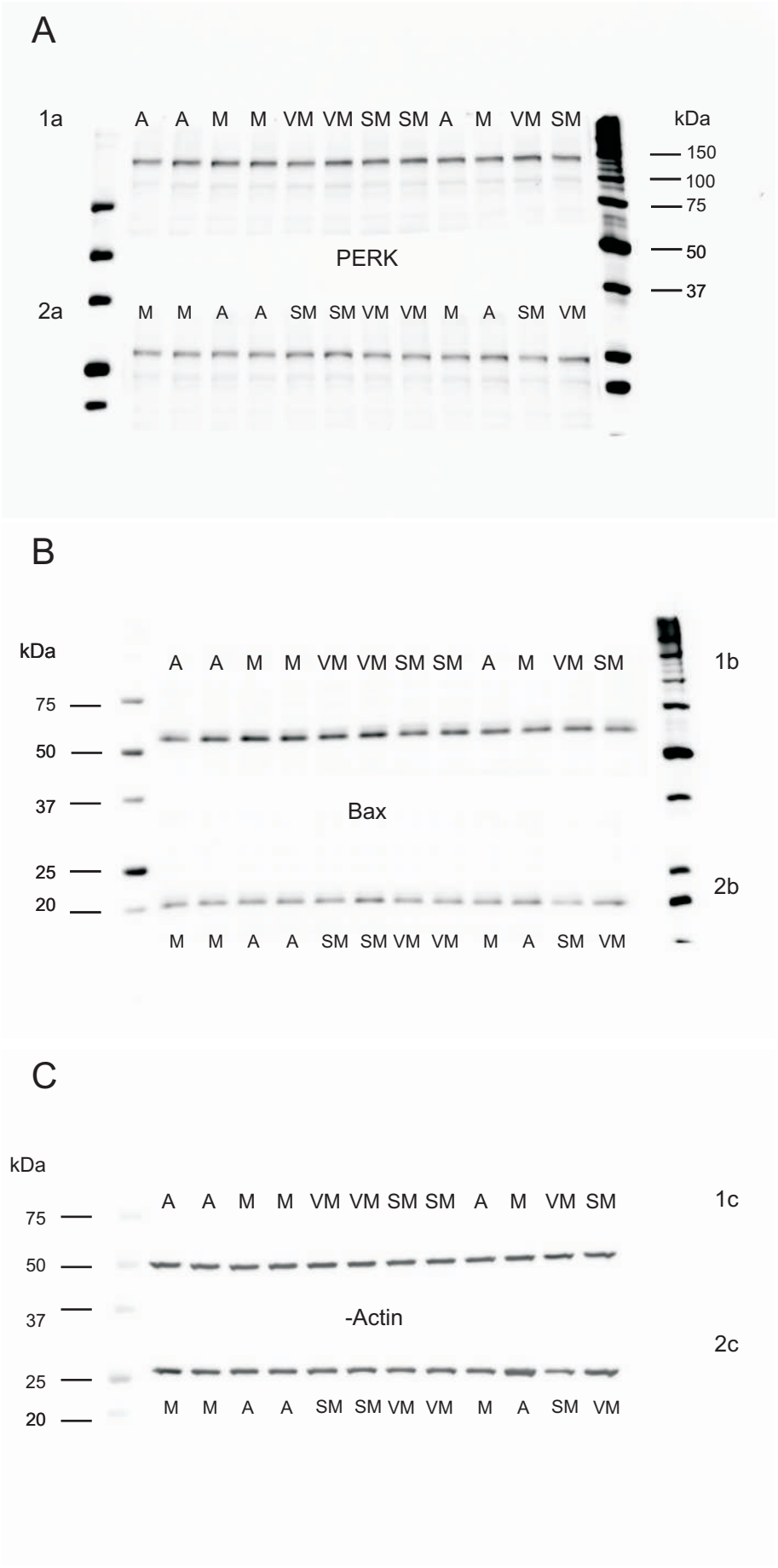

Fig. S22. Original blots presenting PERK (A) and Bax (B) expression in preadolescent rats and -Actin immunoreactivity as control of gel loading and transfer (C). After a transfer, two distinct blots (1 and 2) were cut into pieces (a, b and c) slightly above the level of 50 kDa and below 37 kDa to separately evaluate PERK (1a, 2a), Bax (1b, 2b) and -Actin (1c, 2c). The blots 1a, 2a and 1b, 2b and 1c, 2c, respectively, were exposed together, therefore they constitute one image. Molecular weight standards were matched only with blot 1a, 2b and 1c . *Abbreviations:* A (AFR), animal facility rearing; M (MS), maternal separation; VM (VEH-MS); SM (SAL-MS); SAL, salubrinal; VEH, vehicle.

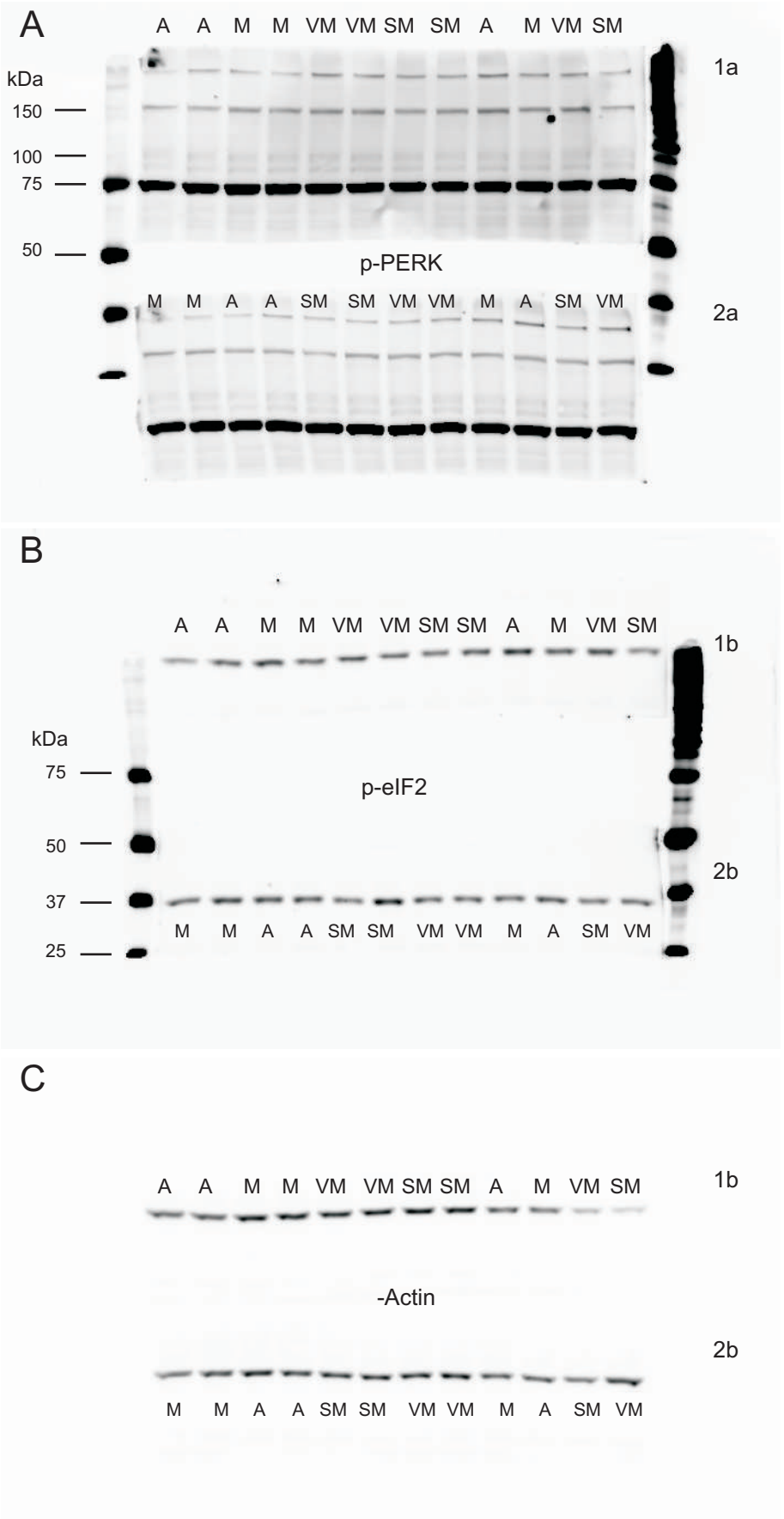

Fig. S23. Original blots presenting p-PERK (A) and p-eIF2 (B) expression in preadolescent rats and -Actin immunoreactivity as control of gel loading and transfer (C). After a transfer, two distinct blots (1 and 2) were cut into pieces (a and b) slightly above the level of 50 kDa to separately evaluate p-PERK (1a, 2a) and p-eIF2 (1b, 2b). Next, after membrane stripping, blots 1b and 2b were reprobed with anti- -Actin antibody. The blots 1a, 2a and 1b, 2b, respectively, were exposed together, therefore they constitute one image. Molecular weight standards were matched only with blot 1a and 2b (B), respectively. Red arrows indicate the band subjected to the analysis. *Abbreviations:* A (AFR), animal facility rearing; M (MS), maternal separation; VM (VEH-MS); SM (SAL-MS); SAL, salubrinal; VEH, vehicle.

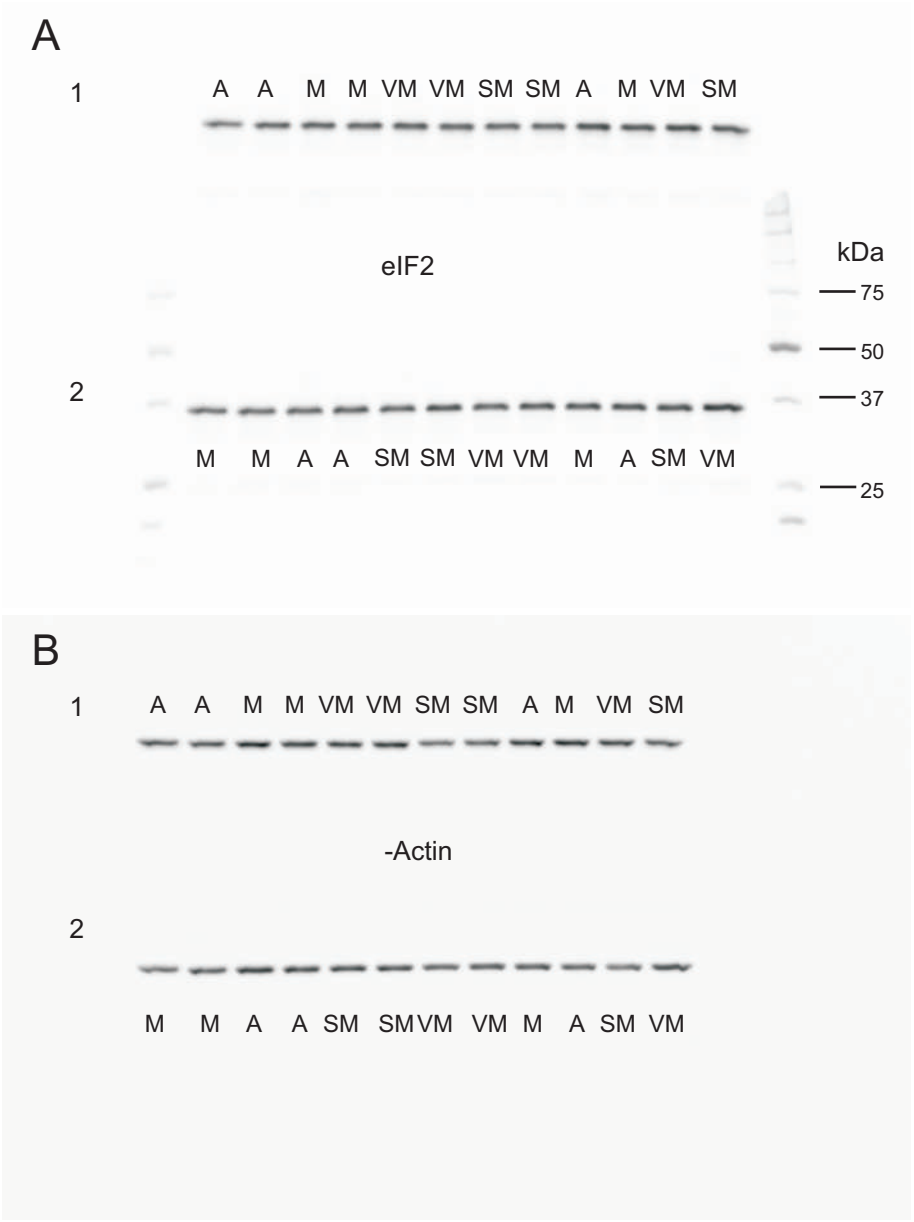

Fig. S24. Original blots presenting eIF2 expression in preadolescent rats (A). After membrane stripping, blots 1 and 2 were reprobed with anti- -Actin antibody to control gel loading and transfer (B). The blots 1 and 2 were exposed together, therefore they constitute one image. Molecular weight standards were matched only with blot 2 (A). *Abbreviations:* A (AFR), animal facility rearing; M (MS), maternal separation; VM (VEH-MS); SM (SAL-MS); SAL, salubrinal; VEH, vehicle.

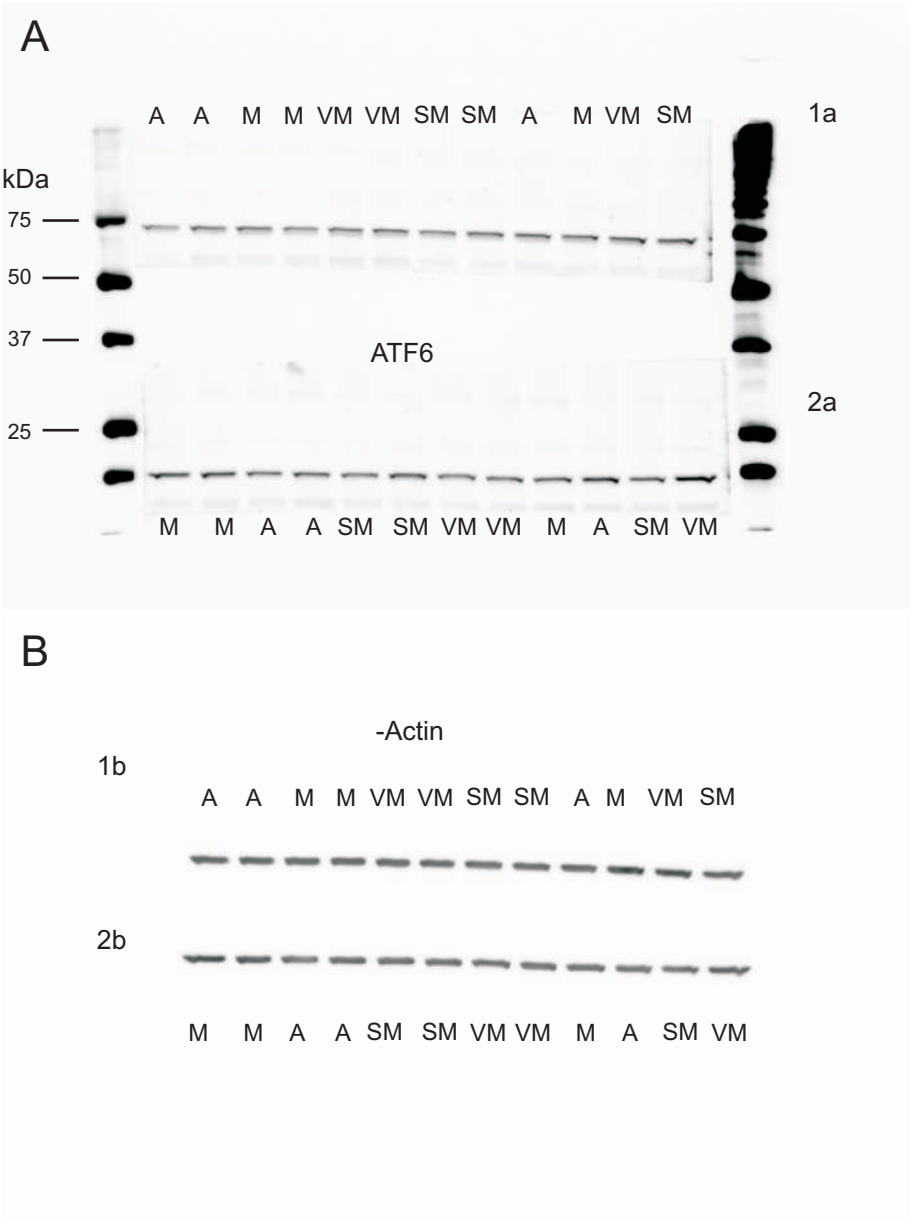

Fig. S25. Original blots presenting ATF6 expression in preadolescent rats (A) and -Actin immunoreactivity as control of gel loading and transfer (B). After a transfer, two distinct blots (1 and 2) were cut into pieces (a and b) slightly above the level of 50 kDa to separately evaluate ATF6 (1a, 2a) and -Actin (1b, 2b). The blots 1a, 2a and 1b, 2b, respectively, were exposed together, therefore they constitute one image. Molecular weight standards were matched only with blot 1a. *Abbreviations:* A (AFR), animal facility rearing; M (MS), maternal separation; VM (VEH-MS); SM (SAL-MS); SAL, salubrinal; VEH, vehicle.

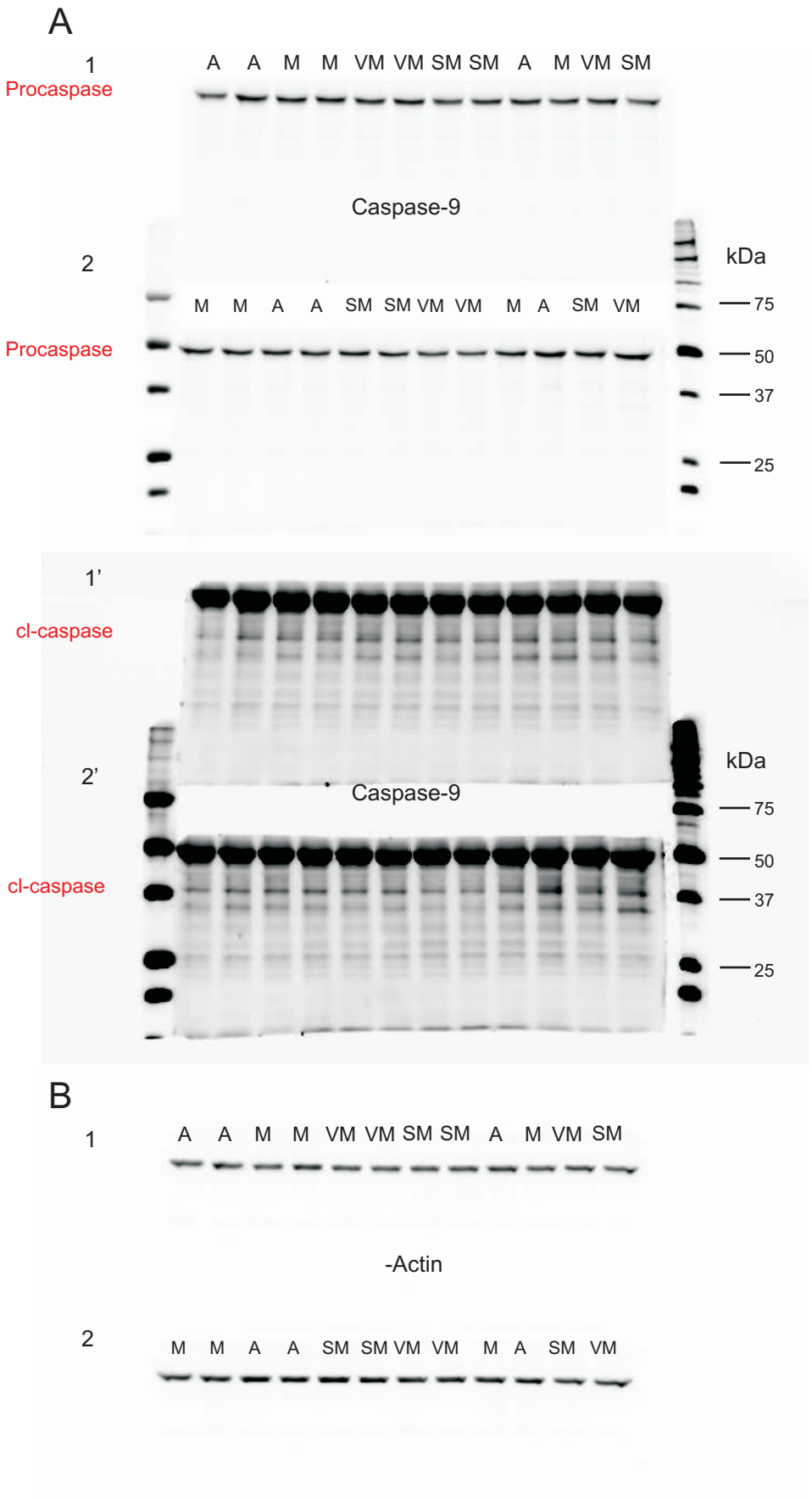

Fig. S26. Original blots presenting caspase-9 expression in preadolescent rats (A). After membrane stripping, blots 1 and 2 were reprobed with anti- -Actin antibody to control gel loading and transfer (B). The blots 1, 2 were exposed together, therefore they constitute one image. Lower image in A (1', 2') was subjected to a higher exposure time than upper image (the same blots) to evaluate cl-caspase levels. Molecular weight standards were matched only with blot 2. Red arrows indicate the bands subjected to the analysis. *Abbreviations:* A (AFR), animal facility rearing; cl, cleaved; M (MS), maternal separation; VM (VEH-MS); SM (SAL-MS); SAL, salubrinal; VEH, vehicle.

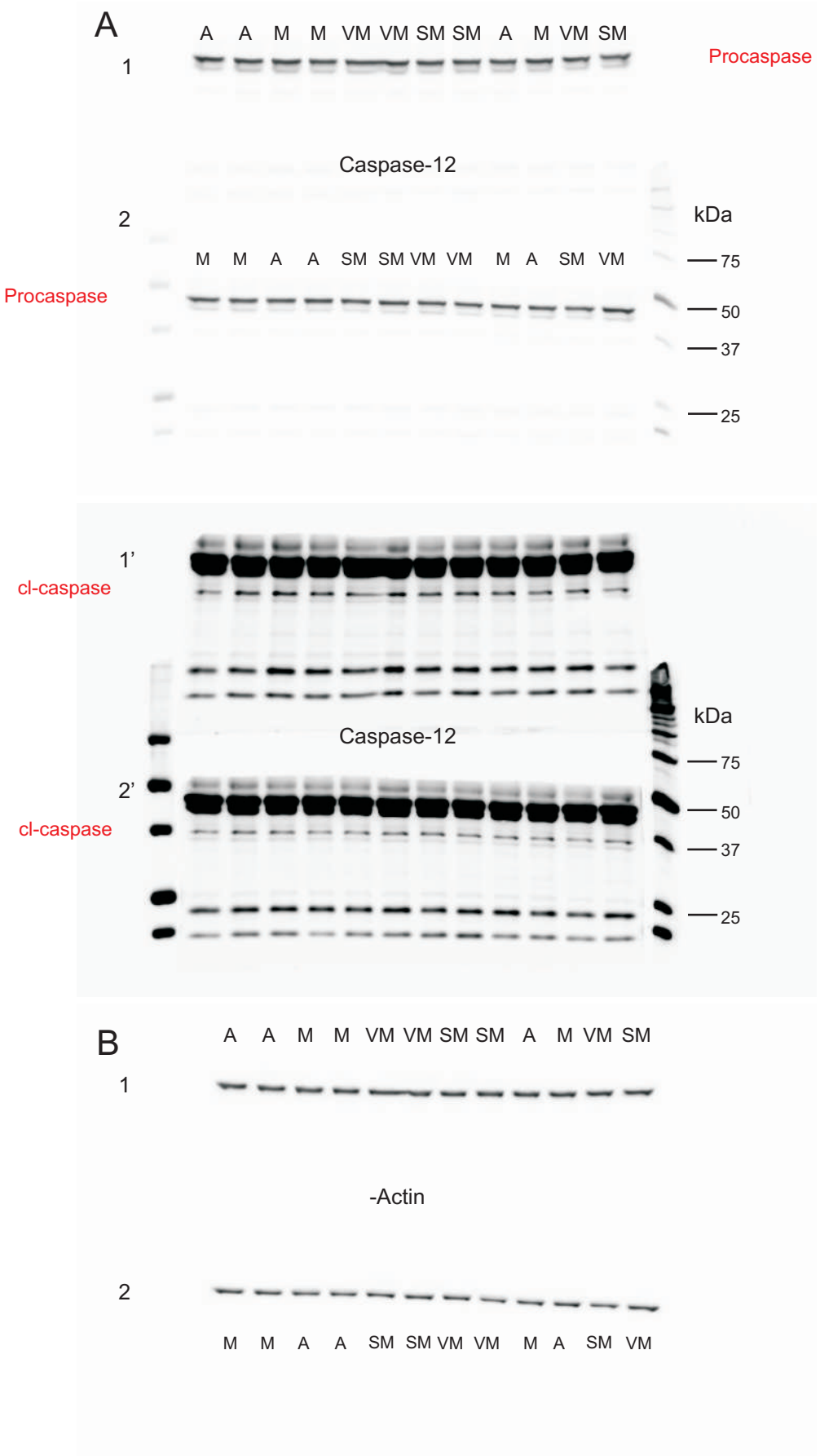

Fig. S27. Original blots presenting caspase-12 expression in preadolescent rats (A). After membrane stripping, blots 1 and 2 were reprobed with anti- -Actin antibody to control gel loading and transfer (B). The blots 1, 2 were exposed together, therefore they constitute one image. Lower image in A (1', 2') was subjected to a higher exposure time than upper image (the same blots) to evaluate cl-caspase levels. Molecular weight standards were matched only with blot 2. Red arrows indicate the bands subjected to the analysis. *Abbreviations:* A (AFR), animal facility rearing; cl, cleaved; M (MS), maternal separation; VM (VEH-MS); SM (SAL-MS); SAL, salubrinal; VEH, vehicle.

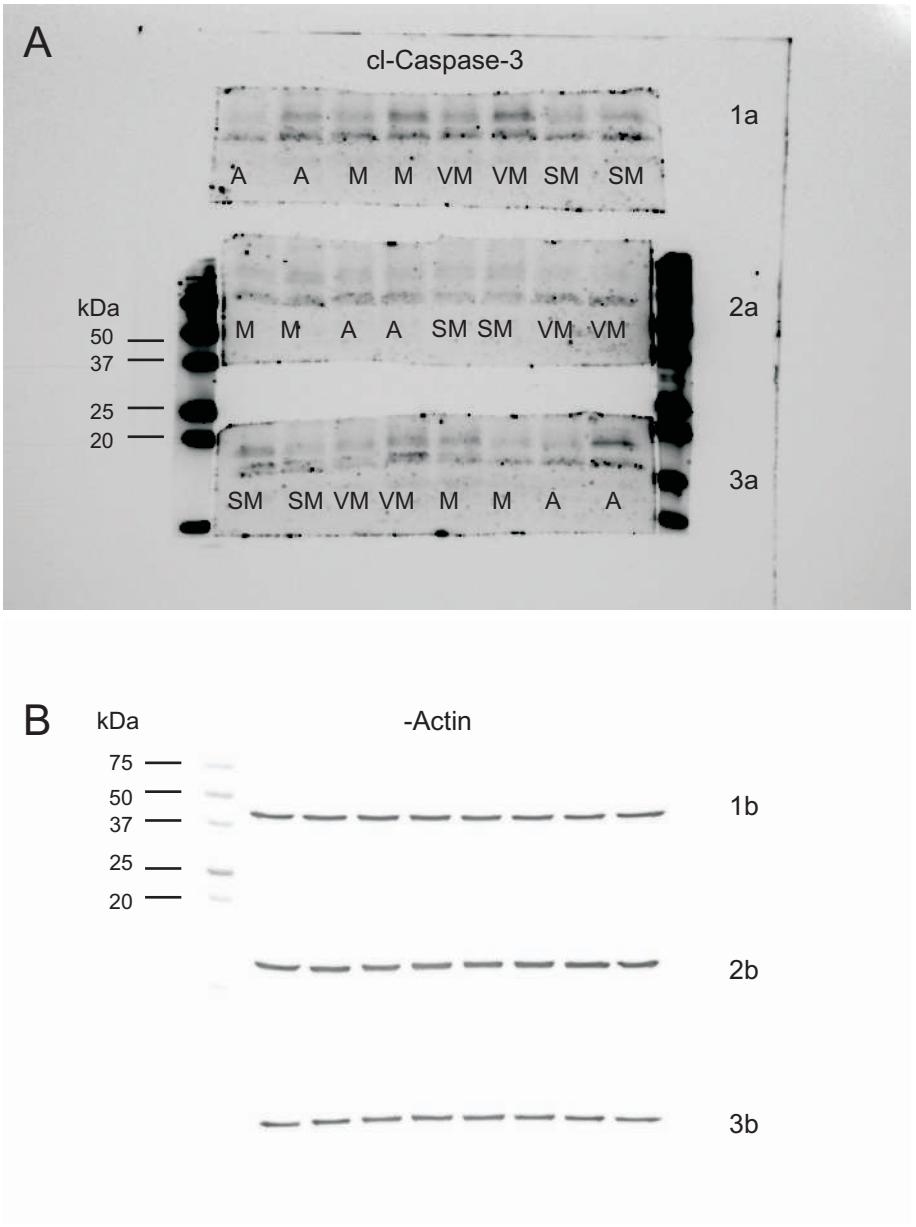

Fig. S28. Original blots presenting cl-caspase-3 expression in preadolescent rats (A) and -Actin immunoreactivity as control of gel loading and transfer (B). After a transfer, three distinct blots (1, 2, 3) were cut into pieces (a and b) at the level of 25 kDa to separately evaluate cl-caspase-3 (1a, 2a, 3a) and -Actin (1b, 2b, 3b). The blots 1a, 2a, 3a and 1b, 2b, 3b were exposed together, therefore they constitute one image. Red arrows indicate the band subjected to the analysis. Molecular weight standards were matched only with blot 3a and 1b, respectivelly. *Abbreviations:* A (AFR), animal facility rearing; cl, cleaved; M (MS), maternal separation; VM (VEH-MS); SM (SAL-MS); SAL, salubrinal; VEH, vehicle.